The effect of the intervertebral disc microenvironment on disc cell and mesenchymal stem cell behaviour: implications for disc degeneration and regeneration

A thesis submitted to The University of Manchester for the degree of

Doctor of Philosophy in the Faculty of Medical and Human Sciences

2013

Shahnaz Khan

Institute of Inflammation and Repair

School of Medicine

Contents

Total word count= 70,481

I. List of Figures

II. List of Tables

III. Abstract

Intervertebral disc (IVD) degeneration is associated with low back pain (LBP). It has been suggested that changes in the IVD physio-chemical microenvironment (i.e. hypoxia, reduced nutrient and acidic conditions) may lead to disc degeneration. Studying the response of human nucleus pulposus (NP) cells to these conditions could establish the causal relationship between IVD microenvironment and aberrant cellular behaviour, characteristic of disc degeneration. Human bone marrow mesenchymal stem cells (BM-MSCs) are a promising cell population for disc regeneration. However, knowledge of their survival and functioning in the microenvironment of the IVD is still lacking. Moreover, *in vitro* co-culture model studies that are used to study MSC/disc cell interaction, also need to consider the effect of the microenvironment on cellular responses. BM-MSCs and degenerate NP cells were cultured alone or co-cultured in monolayer under hypoxia ($2\%O_2$), reduced nutritional (2% serum or/and 5mM glucose) and acidic (moderate pH 6.8 or severe pH 6.5) conditions alone or in combination for 7 days. Cell viability, proliferation, gene and protein expression was assessed. Degenerate NP cells and BM-MSCs maintained good cell viability under all conditions. Both cell types demonstrated overall similar proliferation and gene and protein responses under the majority of the conditions and combinations studied. Hypoxia promoted aggrecan and versican matrix biosynthesis in both cell types. Nutrient deprived and moderate acidic conditions (pH 6.8) inhibited proliferation of both cell types. Interestingly the combination of hypoxia with these conditions showed a protective effect in modulating cell proliferation. These results imply that hypoxia may be beneficial in some instances. Nutrient deprived conditions had a relatively minor effect on degenerate NP cell gene and protein expression but these conditions specifically inhibited VCAN expression in BM-MSCs. The combination of hypoxia with these conditions increased or restored VCAN expression. Interestingly the combination of hypoxia with reduced glucose conditions increased aggrecan and versican matrix biosynthesis in both NP cells and BM-MSCs. The combination of hypoxia and complete nutrient deprived conditions (both reduced serum and reduced glucose) impaired ACAN, VCAN and PAX-1 gene and aggrecan and versican protein expression in degenerate NP cells implicating disc hypoxia and complete nutrient deprived combined microenvironment in accelerating degenerate changes in NP cells. In contrast, these conditions showed no such detrimental effects on BM-MSC gene and protein expression. pH 6.5 was critical for both cell types proliferation and ACAN and VCAN gene expression suggesting that severe acidic conditions may exacerbate degenerative changes and be inhibitory for implanted MSCs. Finally, a combination of hypoxia, complete nutrient deprived and moderate acidic conditions, reduced cell proliferation without affecting the gene expression profile of both cell types. IVD-like physio-chemical microenvironmental conditions also appeared to influence differentiation of BM-MSC and modulation of degenerate NP cell phenotype observed during co-culture. Noticeably hypoxia, reduced serum or reduced glucose conditions stimulated BM-MSC differentiation and modulation of degenerate NP cell phenotype. Hypoxia also increased or recovered changes at gene expression level in both BM-MSCs and degenerate NP cells under nutrient deprived (reduced serum or/and reduced glucose) conditions during co-culture. Degenerate NP cell and BM-MSC co-culture also showed noticeable increase in aggrecan and versican biosynthesis under hypoxia and reduced glucose combine conditions, implicating these in improving the co-culture responses. Severe pH condition alone, pH 6.8 in combination with hypoxia and finally all IVD-like physio-chemical conditions together compromised co-culture responses. Such results imply that IVD-like physio-chemical microenvironmental conditions may influence MSC based regenerative outcomes. This work has increased our understanding about the influence of disc harsh microenvironment on degeneration and regeneration processes.

IV. Declaration

No portion of the work referred to in the thesis has been submitted in support of an application for another degree or qualification of this or any other university or other institute of learning.

V. Copyright statement

i. The author of this thesis (including any appendices and/or schedules to this thesis) owns certain copyright or related rights in it (the "Copyright") and she has given The University of Manchester certain rights to use such Copyright, including for administrative purposes.

ii. Copies of this thesis, either in full or in extracts and whether in hard or electronic copy, may be made only in accordance with the Copyright, Designs and Patents Act 1988 (as amended) and regulations issued under it or, where appropriate, in accordance with licensing agreements which the University has from time to time. This page must form part of any such copies made.

iii. The ownership of certain Copyright, patents, designs, trade marks and other intellectual property (the "Intellectual Property") and any reproductions of copyright works in the thesis, for example graphs and tables ("Reproductions"), which may be described in this thesis, may not be owned by the author and may be owned by third parties. Such Intellectual Property and Reproductions cannot and must not be made available for use without the prior written permission of the owner(s) of the relevant Intellectual Property and/or Reproductions.

iv. Further information on the conditions under which disclosure, publication and commercialisation of this thesis, the Copyright and any Intellectual Property and/or Reproductions described in it may take place is available in the University IP Policy (seehttp://www.campus.manchester.ac.uk/medialibrary/policies/intellectualproperty.pdf), in any relevant Thesis restriction declarations deposited in the University Library, The University Library's regulations (see http://www.manchester.ac.uk/library/aboutus/regulations) and in The University's policy on presentation of Theses

VI. Acknowledgement

My thanks go firstly to my supervisor Prof. Judith Hoyland, who gave me this opportunity in the first place. I am grateful for her constant support and encouragement she provided throughout this doctoral project. I highly appreciate her dedication and commitment in prompt processing of thesis drafts to easily meet my target deadline for submission.

I would also like to thank my second supervisor, Dr. Stephen Richardson for his support and inspiration. He motivated me to think independently and take initiative in the lab. I would also like to thank him, for answering many of my questions and giving me confidence especially during times of less hope.

I am also thankful to my advisor, Prof. Tony Freemont for his guidance and constructive feedback during the progress meetings.

I would like to thank to Mrs Pauline Baird and Mr Andy Fotheringham for their support during learning of lab skills and providing everything I needed for my experiments. I would also like to thank all of my colleagues from the postgrad study room, lab and tea room, including Hamish, Matt, Jude, Fran, Jo, Kim, Sonal, Chris, Ricardo, Louisa, Jane and Christine for all of their friendly chats and advice. Thanks to everyone in the tea room for plenty of cakes and biscuits.

Many thanks especially go to Mike Jackson for FACS support during this project.

I would like to express deep appreciation to my family especially my Husband (Hanif) and my Sisters (Gulnaz and Farah) and my Parents for their unbelievable encouragement. I could not have been where I am now without their love and support.

Finally many thanks to ALLAH the most gracious and the most merciful, for giving me the strength to go through. Quite simply I could not have done it without His blessings.

1 Introduction

1.1 Overview

Lower back pain (LBP) is a major public health problem associated with huge socioeconomic burden worldwide (Dagenais et al., 2008, Hoy et al., 2010). In many cases, intervertebral disc (IVD) degeneration has been identified as a significant contributing factor to the LBP (Hughes et al., 2012). The IVD limited nutritional and acidic harsh microenvironmental conditions have been associated with disc degenerative changes (Horner and Urban, 2001, Razaq et al., 2003). Investigations into the effect of this microenvironment on human disc cell physiology can contribute to our understanding about the pathogenesis of disc degeneration and LPB. The growing field of cell based regenerative medicine brings the promise of stem cells particularly human bone marrow mesenchymal stem cells (BM-MSCs) in the treatment of disc degeneration. Studying the influence of disc harsh microenvironment on BM-MSCs is equally important in order to fully understand their potential before clinical translation for IVD regeneration.

1.1.1 Division of the thesis

The thesis has been divided into six main chapters which are as follows:

Chapter 1 – Introduction: The reader will be introduced to the IVD biology in health and disease, IVD nutrition/metabolism, IVD microenvironment and its link with degeneration, repair of IVD, use of MSCs in disc repair and potential challenges.

Chapter 2 – Materials and methods: Full details of the equipment, reagents and methodologies used during the PhD project will be disclosed.

Chapter 3 – 'Effect of an intervertebral disc-like physio-chemical microenvironment on human degenerate nucleus pulposus cell behaviour'.

The IVD centre namely the nucleus pulposus (NP) has a hypoxic, nutrient deprived and acidic microenvironment (termed as IVD-like physio-chemical microenvironment) that has been implicated in disc degeneration. However, the effect of these conditions on the survival and function of human NP cells is largely unknown. This study will investigate the effects of these conditions on human NP cells to identify factors that may influence cell behaviour that may lead to the processes characteristic of disc degeneration.

Chapter 4 – 'The effect of an intervertebral disc-like physio-chemical microenvironment on human bone marrow derived mesenchymal stem cell behaviour'

The response of an ideal cell population for disc regeneration i.e. the BM-MSCs, to the harsh IVD-like physio-chemical microenvironmental conditions is largely unknown. This study will investigate the effects of these conditions on human BM-MSCs behaviour to identify factors beneficial or detrimental to these cells.

Chapter 5 – 'Impact of an intervertebral disc-like physio-chemical microenvironment on co-culture of human bone marrow derived mesenchymal stem cell with degenerate nucleus pulposus cell: Implication for disc regeneration'

MSCs and NP cells co-culture studies suggest that MSC based disc repair may be due to both MSC differentiation and modulatory effects on degenerate NP cell phenotype. However, limited importance has been given to the effect of the IVD-like physio-chemical microenvironmental conditions on these responses. This study will investigate the effects of these conditions on MSC differentiation towards NP-like cells (discogenic differentiation) and modulation of degenerate NP cell phenotype during co-culture to identify their impact on possible regenerative processes.

Chapter 6 – Conclusions and Future Work

1.2 The intervertebral disc (IVD)

The human spine consists of four major zones starting from the cervical vertebrae (C1-C7) followed by the thoracic (T1-T12), the lumbar (L1-L5) and ending in the fused sacral vertebrae (S1-S5) (Figure 1.1 A). The cervical, thoracic and lumbar vertebrae are interconnected by a specialized fibrocartilaginous structure called the intervertebral disc (IVD). Each IVD and its upper and lower vertebrae constitute a spinal unit (Figure 1.1B). The IVD makes movement between the various vertebrae possible, provides stability to the rigid spine, and enables load transfer between individual vertebrae.

1.2.1 Structure and function of the IVD

The unique anatomy of the IVD enables it to perform these functions. The IVD is composed of three interrelated tissues (Figure 1.1 B); a central gelatinous nucleus pulposus (NP), and a dense outer connective tissue layer, the annulus fibrosus (AF) and the end plate (EP) which provides the connection to the vertebral bodies (Freimark and Czermak, 2009, Hughes et al., 2012). These all are critical to the proper functioning of the disc.

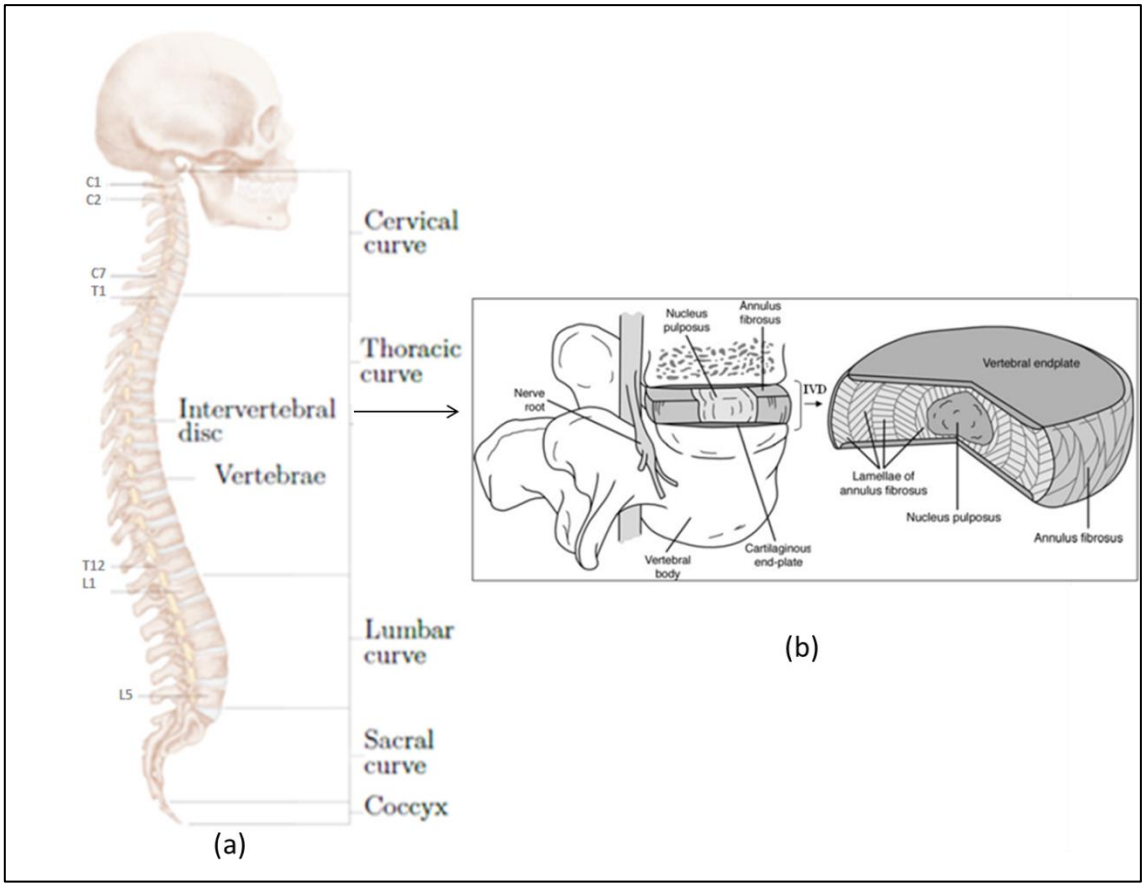

Figure 1.1 A schematic view of the spine and intervertebral disc. (A) four major zones of the spine (adapted from http://www.martianpictures.com/portfolio/spine-illustration/) (B) spinal unit comprises of two adjacent vertebrae and an intervertebral disc sandwiched between them; consist of nucleus pulposus in the centre surrounded by the lamellae of the annulus fibrosus and separated from the vertebral bodies by the end-plate adapted from (Raj, 2008).

1.2.1.1 End plate (EP)

The EP is a thin layer of tissue that borders the disc space superiorly and inferiorly. It forms an interface between the IVD and the vertebral bodies (Roberts et al., 1989). The healthy EP is comprised of an osseous and a cartilaginous part; when referring to the latter, the term cartilaginous end plate (CEP) is generally used. Osseous or bony EP is also known as vertebral subchondral bone (VSB). It is defined as the vascularized cortical and trabecular bone layer located between the CEP and vertebral body (Nguyen et al., 2012) (Figure 1.2).

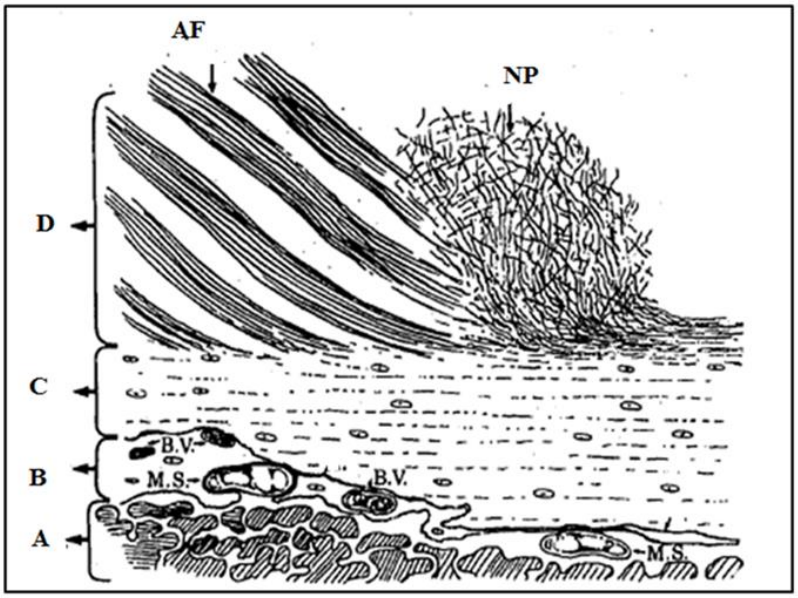

Figure 1.2 Schematic representation of the normal disc histology with elaborated structure of EP. (A) (bone), (B) osseous or bony EP with marrow spaces and blood vessels (BV), (C) cartilaginous EP and (D) disc consist of AF and NP [modified from (Roberts et al., 1989)]

VSB is an important part of the EP. VSB vessels ensure IVD nutrition by diffusion of dissolved molecules through marrow contact channels (also known as vascular buds) (Nachemson et al., 1970, Ogata and Whiteside, 1981, Roberts et al., 1989). Capillary buds emerge from marrow contact channels; penetrate the VSB and terminate at the CEP without penetrating into it (Benneker et al., 2005, Nguyen et al., 2012). Nutrients required for energy metabolism diffuse from the capillaries across the thin layer of cartilage and through the dense disc matrix to the cells which lie in the disc centre as much as 8 mm from the blood supply (Urban et al., 2004). Metabolic waste products are removed from the tissue by the reverse route.

1.2.1.2 Annulus fibrosus (AF)

The AF consists of lamellar collagen fibres surrounding the NP. Based on structural and cellular differences, the AF can be divided into an inner and an outer part. The outer AF is composed of highly ordered concentric layers (lamellae) composed mainly of collagen type 1 fibres (Inoue and Takeda, 1975, Eyre and Muir, 1976, Marchand and Ahmed, 1990, Roberts et al., 1991). Fibres in each lamella run parallel to each other; they are orientated obliquely with respect to the fibres of the adjacent lamellae (Inoue and Takeda, 1975). The inner AF is a broad transition zone between the highly organised collagenous structure of the outer AF and the highly hydrated NP and consists of a mixture of both type I and type II collagen (Eyre

et al., 2002, Bron et al., 2009, Pattappa et al., 2012). The highly organized architecture of the collagen network in AF confers resistance to tensile loads across the disc and constrains the expanding NP upon compression, facilitating mobility between the spinal segments (Bron et al., 2009).

1.2.1.3 Nucleus pulposus (NP)

The NP is the gelatinous core of the IVD. It is composed of two major macromolecular components: collagen (mainly type II and XI) and proteoglycan (PG) predominantly aggrecan (Chelberg et al., 1995, Eyre et al., 2002, Singh et al., 2009). PGs are negatively charged and create an osmotic pressure that causes water attraction in the NP and gives it a hydrogel like consistency. The hydrated NP functions as a shock absorber and provides resistance to compressive loads. The expanded NP pushes out against the surrounding AF preventing it from buckling and so maintaining its strength. The fine balance between expansion of the hydrated NP and tension in the AF enables the IVD to resist compression under load (Sztrolovics et al., 1997, Pattappa et al., 2012).

1.2.2 Cells of the IVD

The human IVD is a cell sparse tissue with mean cell density of about 6000 cells/mm^3 (Maroudas et al., 1975). Cell density decreases from the EP or from peripheral parts of the AF, inwards towards the NP (Maroudas et al., 1975, Liebscher et al., 2011). In the adult IVD the cell density of the EP, AF and NP is approximately 15000, 9000 and 4000 cells/mm^3 respectively. In all regions of the disc, cell density also decreases from new-born age to adolescence with no significant change afterwards (Liebscher et al., 2011).

1.2.2.1 Cells of the EP

The EP is populated by rounded chondrocyte-like cells embedded in a matrix consisting primarily of water, PGs, and type II collagen (Maroudas et al., 1975, Roberts et al., 1989, Roberts et al., 1991).

1.2.2.2 Cells of the AF

Cells in the outer AF have a morphology and phenotype similar to that of elongated, thin fibroblast-like cells (Maroudas et al., 1975) whereas inner AF contains chondrocyte-like cells (Roberts et al., 2006b) both of which align parallel to collagen fibres.

1.2.2.3 Cells of the NP

The NP tissue of the new-born contains large vacuolated notochordal cells (Chen et al., 2006) that rapidly decline with age, leaving the smaller chondrocyte-like NP cells as the dominant cell population in adults (Liebscher et al., 2011). NP cells have small rounded morphology and are classically described as chondrocytes or chondrocyte-like cells owing to similarities with articular cartilage chondrocytes and synthesis of cartilage components including aggrecan, type II collagen and the transcription factor SOX-9 (SRY (Sex determining region Y)-Box-9) (Sive et al., 2002). However, recently detailed phenotypic investigation of NP cells has identified unique markers of NP cells, distinguishing them from articular cartilage chondrocytes. In addition to classical articular cartilage chondrocytes markers, these cells show differential expression of a panel of genes including PAX-1, FOXF1 and CA12 (Minogue et al., 2010a, Minogue et al., 2010b, Power et al., 2011). Differential expression of these genes has been confirmed in independent studies using bovine and human NP cells (Minogue et al., 2010a, Minogue et al., 2010b, Power et al., 2011).

1.3 Development of IVD

Formation of the embryonic IVD is a highly coordinated multi-step process, that begins during the process of gastrulation, whereby the embryo develops into three layers; an outer ectoderm, inner endoderm and middle mesoderm layer (Kaplan et al., 2005). The notochord is one of the first axial structures to appear in the embryo derived from mesoderm and occupies the central axis of developing vertebrae (Risbud and Shapiro, 2011). During the development of the neural tube from ectoderm, mesoderm adjacent to the developing neural tube forms a thickened column of cells, the paraxial mesoderm that undergoes segmentation to form somites (Rawls and Fisher, 2010). Most components of the axial skeleton, the associated musculature, and the overlying dermis derive from these somites. Each somite is divided into: 1) dermomyotome, which gives rise to muscles and dermis and 2) sclerotome, which gives rise to vertebral structures (Figure 1.2). Sclerotome cells migrate towards notochord and form a uniform continuous column of mesenchymal cells, the peri-notochordal sheath, which completely surrounds the notochord (Pourquie, 2000, Rawls and Fisher, 2010) (Figure 1.3). Initially cells within the notochord synthesize PGs that generates osmotic pressures that further induce elongation and straightening of the notochord (Adams et al., 1990). The mesenchymal cells of the peri-notochordal sheath condense around the notochord and exhibit metameric pattern of less condensed and more condensed regions (Peacock, 1951, Kaplan et al., 2005, Rawls and Fisher, 2010) (Figure 1.3). Occupying the most central part

along the axis of the foetus is still a continuous row of large vacuolated notochordal cells. The less dense regions form the cartilaginous primordial of the vertebral bodies while the more condense regions develop into AF (Peacock, 1951, Aszodi et al., 1998). The notochord within the vertebral body regresses and in contrast persists and expands within the AF region that leads to formation of the NP (Choi et al., 2008, Choi and Harfe, 2011, Smith et al., 2011). The chronological transition from a notochordal cell population to the adult NP cell origin is debatable. Some investigators argue that migration of chondrocytes from EPs to NP is responsible for the notochordal to fibrocartilaginous NP transition (Kim et al., 2003, Kim et al., 2009b), while others, using definitive markers of notochord and lineage mapping studies, suggest that despite morphological differences, adult NP cells are descended from the notochordal cell population (Choi et al., 2008, Choi and Harfe, 2011). However, these studies were conducted using mouse models and conclusive evidence is still lacking in humans. A significant overlapping gene expression profile (e.g. SHH, brachyury, KRT8, 18, 19) between notochord and human NP cells does however provide some support to the theory of a common ancestry (Choi et al., 2008, Risbud et al., 2010a, Minogue et al., 2010b, Weiler et al., 2010, Ludwinski et al., 2013, Rodrigues-Pinto et al., 2013).

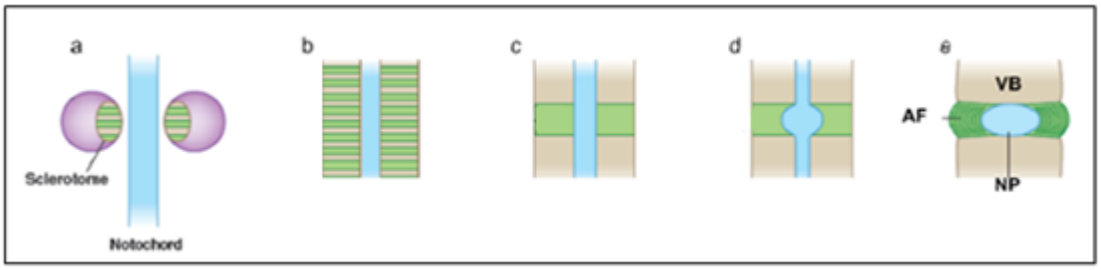

Figure 1.3 Schematic view of the foetal IVD development. a) At the beginning, the notochord occupies the central axis of developing vertebrae with rows of somites on each side. b) sclerotome cells condense around the notochord and c) adopt a metameric pattern of more condensed (green) and less condensed (brown) regions that give rise to the disc and vertebral bodies (VB) respectively. At this stage, the notochord is a continuous structure along the foetal axis d) notochord contracts within the future vertebral bodies and expands within the future AF e) notochord completely disappears from the VB anlagen, occupying the centre of the IVD, encircled by the lamellar AF fibres (Adapted from (Smith et al., 2011)).

1.4 Extracellular matrix (ECM) composition in the normal (non-degenerate) IVD

Phenotypically distinct cells of the IVD secrete and organise an ECM whose molecular composition plays a central role in the normal functioning of the IVD. Collagens and PGs are

secreted locally and assemble into an organized meshwork. Catabolic enzymes and their specific inhibitors play important role in regulating IVD matrix homeostasis.

1.4.1 Collagens

Collagens are proteins found in the ECM and comprise approximately 70 % of the dry weight of the disc (Eyre et al., 2002). The IVD ECM collagen network is composed mostly of type I and type II collagen fibrils. Their proportion varies across the disc with the NP containing mainly type II collagen and AF mainly type I collagen. Other collagens, in particular types III, V, VI, IX, XI, XI1 and XIV are also present in small quantities and contribute to the organization and mechanical stability of ECM (Eyre and Muir, 1976, Roberts et al., 1991). In addition to collagens, other matrix proteins such as cartilage oligomeric matrix protein (COMP) have been found in the disc (Ishii et al., 2006). COMP contributes in collagen assembly by binding to collagen fibres and aligning them in a close parallel orientation (Feng et al., 2006). The collagen network provides tensile strength to the disc and constrains expanding NP to resist compressive forces.

1.4.2 Proteoglycans (PGs)

PGs represent a special class of glycoproteins subdivided into two distinct groups: large aggregating and small, leucine-rich PGs (SLRPs) (Iozzo and Murdoch, 1996). Large aggregating PGs are heavily glycosylated. Aggrecan and versican are the main large aggregating PGs present in the disc with aggrecan being by far the most abundant. They share a tri-domain structure. Both have a hyaluronan-binding globular domain and a C-type lectin motif for binding to other proteins; this allows them to form large aggregates with hyaluronan and other proteins in the ECM (Iozzo and Murdoch, 1996, Wu et al., 2005). The glycosaminoglycan (GAG) chains are covalently attached to the central region (Figure 1.4).

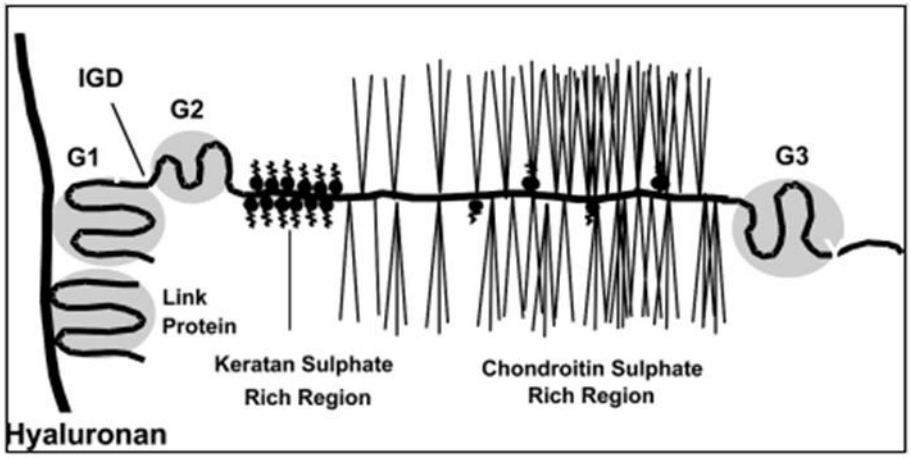

Figure 1.4 Illustration of an aggrecan molecule. It contains two N-terminal globular domains, G1 and G2, separated by an IGD (interglobular domain), followed by a GAG-attachment region and a C-terminal globular domain, G3 [Adapted from (Porter et al., 2005).

GAG chains are linear polysaccharides consist of repeating disaccharide that contain negatively charged sulphate group. Chondroitin and keratan sulphate chains are the most common GAGs with the former dominating in the normal IVD (Iozzo and Murdoch, 1996, Feng et al., 2006). Sulphation confers a strong negative charge on the GAGs which allows them to bind water and provides viscoelastic properties to disc tissues (Feng et al., 2006). The family of SLRPs is characterized by a leucine-rich core protein substituted by a few GAGs side chains (Iozzo, 1997). Biglycan, decorin, fibromodulin and lumican are SLRPs found in disc affecting the assembly of collagen network (Hedbom and Heinegard, 1993, Sztrolovics et al., 1999, Wiberg et al., 2002).

1.4.3 Catabolic enzymes

In the normal IVD, the ECM is remodelled by metalloproteinases and their inhibitors. There are two main families of metalloproteinases: (1) the matrix metalloproteinases (MMPs) and (2) the disintegrin and metalloproteinase with thrombospondin motifs (ADAMTSs) (Vo et al., 2013). Sub-groups of MMPs and ADAMTS cleave different ECM components, with some sub-groups favouring certain families such as MMPs-1, -8 and -13 which are termed ‘collagenases’ and cleave collagens. ADAMTS-4 and ADAMTS -5 are termed aggrecanases and show strong affinity for the degradation of aggrecan (Sivan et al., 2013). MMPs and ADAMTS activity is regulated by a family of proteins called tissue inhibitors of metalloproteinases (TIMPs) that bind covalently to these molecules and inhibit their actions.

TIMPs-1 and -2 inhibits MMPs whereas TIMPs-3 is a potent inhibitor of ADAMTS-4 and -5 (Kashiwagi et al., 2001).

1.5 IVD nutrition

The blood supply of the IVD is impaired markedly with increasing age. Hassler found that the IVD of the foetus and infant, had a more ample vascular supply, with vessels penetrating deeply into the disc, than those of the adult (Hassler, 1969). The adult disc is the largest avascular tissue in the adult human (Hassler, 1969). But like other types of cells, disc cells also require nutrients to remain viable. The adult disc relies on two routes for transport of nutrients (Figure 1.5): a) Annular route which supplies nutrients to the outer AF cells through diffusion from the vessels around AF periphery and b) The EP route which supplies nutrients to inner AF and NP cells by long diffusion through the marrow contact channels (vascular buds) in the vertebral EP (Nachemson et al., 1970, Urban et al., 1977, Ogata and Whiteside, 1981, Urban et al., 1982, Selard et al., 2003, Rajasekaran et al., 2004, van der Werf et al., 2007).

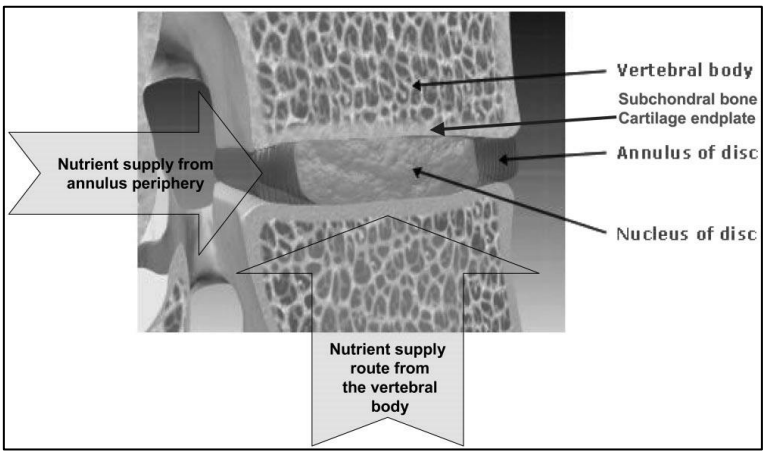

Figure 1.5 Schematic view of the routes supplying nutrients to the avascular IVD. (Adapted from (Urban et al., 2004)

Diffusion appears to be the primary process for transport of small solutes such as glucose and O_2 to satisfy the nutritional needs of cells in the disc centre and removal of metabolic waste (lactic acid) (Urban et al., 1982, Urban et al., 2004, Grunhagen et al., 2006). A concentration gradient establishes depend on the balance between the rate of supply from blood source to the disc and the rate of cellular metabolism in the disc centre. For solutes such as glucose and O_2 and lactic acid which are used and produced respectively at a high rate, the gradients are steep (Figure 1.6) (Grunhagen et al., 2006).

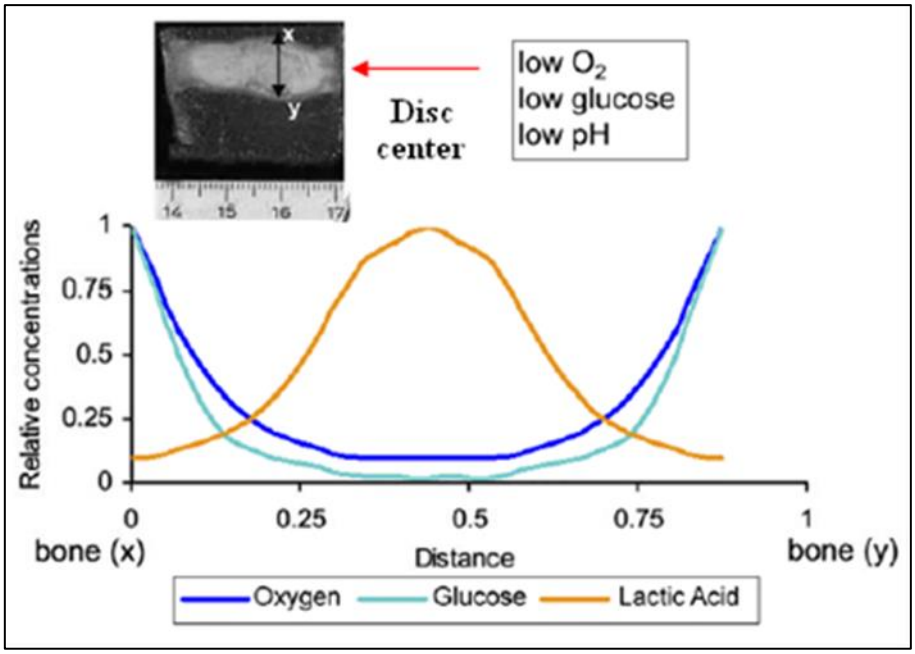

Figure 1.6 A sagittal section through a human intervertebral disc illustrating the dimensions of disc and levels of oxygen, glucose and lactic acid (relative to 1 as highest concentration) across the disc from EP (x) to EP (y) [Modified from (Urban et al., 2004)]

It has been shown that transport of small solutes does not occur through fluid flow (movement of the fluid in and out of the disc as a result of diurnal loading pattern) (Katz et al., 1986, O'Hara et al., 1990, Ferguson et al., 2004). However, changes in disc height during loading may affect diffusion distances and in turn affect transport of small solute (Urban et al., 2004). The properties of the solute i.e. size, shape and charge also appear to affect the degree of solute penetration through cartilage matrix (Roberts et al., 1996). A solute that is high molecular weight or negative charge diffuses slowly into the disc matrix (expected from the polyanionic nature of the disc matrix) than a solute that has a relatively low molecular weight and is positively charge or neutral. Long-chain polymers are able to penetrate the matrix less readily than the more globular molecules (Urban et al., 2004, Grunhagen et al., 2006).

1.6 Disc metabolism

At low O_2 concentrations cells rely on O_2 independent-anaerobic metabolism such as glycolysis (Karp, 1996). Previous studies have suggested that glycolysis is the major pathway for energy generation in the NP (Holm et al., 1981, Holm et al., 1982, Ishihara and Urban, 1999) even in the presence of high O_2 tensions (19.9% O_2) (Holm et al., 1981). Nevertheless, the effect of O_2 concentration on disc metabolism is still not clearly understood (Grunhagen

et al., 2006). It has been suggested that the rate of O_2 utilization and lactic acid production depends ultimately on the O_2 concentration. A steep increase in glycolysis rate was observed at low O_2 tensions when O_2 consumption rates fall (Holm et al., 1981, Ishihara and Urban, 1999). Holm *et al* have shown a 40% increase in production of lactic acid as the O_2 tension decreased below 9.5%. Ishihara and Urban have also reported similar findings by showing a 50% higher lactate production at 1% O_2 than 21% O_2 (Holm et al., 1981, Ishihara and Urban, 1999). These studies, hence suggest a positive Pasteur effect by disc cells in low O_2 concentrations. In contrast, other studies have demonstrated no significant effect of O_2 tension on lactic acid production (Bibby and Urban, 2004) or a decrease in lactic acid production (a negative Pasteur effect) with a decrease in O_2 concentration (Bibby et al., 2005). Whatever mechanism is involved, it appears that in the disc, glucose as the main substrate for glycolysis may be a critical nutrient for disc cell metabolism.

In addition to the Pasteur effect, a few investigators have also attempted to study the Crabtree effect in disc cells (Huang et al., 2007). The Crabtree effect is described as the inhibition of cellular respiration by glycolysis or conversely, when glucose decreases, glycolysis is inhibited and oxidative phosphorylation increases. To date, the Crabtree effect has been mainly described in chondrocytes where it serves as a potential survival mechanism by which chondrocytes initiate oxidative energy metabolism in order to supply their basal ATP requirements in conditions of critically limited glucose supply (Heywood et al., 2006). It has been suggested that in contrast to chondrocytes, disc cells may not demonstrate the Crabtree effect as the oxygen consumption rates in disc cells were found to be insensitive to glucose levels (Bibby et al., 2005, Huang et al., 2007).

Although cellular energy metabolism in the disc is dominated by glycolysis, there are indications that disc cells also exhibit mitochondrial oxidative phosphorylation. Previous reports suggest O_2 utilization of disc cells and production of carbon dioxide (Holm et al., 1981). Oxidative phosphorylation uncoupler 2,4-dinitrophenol, and the oxidative phosphorylation inhibitor sodium azide markedly reduced matrix synthesis that correlated with decrease in ATP concentration (Ishihara and Urban, 1999). Furthermore functioning of mitochondria (oxidation of fatty acids) has been observed in the NP cells (Agrawal et al., 2007). These findings together with carbon dioxide measurements, reinforce the hypothesis

that the disc can also produce ATP through oxidative phosphorylation (Bibby et al., 2001, Urban et al., 2004, Risbud et al., 2010b).

1.7 Aetiology of disc degeneration

The exact aetiology of disc degeneration has not been clearly defined yet. However, many factors, including environmental factors (exposure of discs to abnormal mechanical forces), genetic influences (predisposition of an individual to degeneration) and a limited nutritional and acidic microenvironment have been frequently associated with disc degeneration.

1.7.1 Mechanical load

The disc is always under load from body weight and muscle activity. Excessive loading or trauma may result in tissue damage. Injury may influence the disc structure and mechanics in a manner that accelerates the degenerative process (Hancock et al., 2010). Studies suggest that mechanical forces depending on frequency, magnitude and duration have profound influences on disc matrix turnover (Walsh and Lotz, 2004, Setton and Chen, 2006, Gilbert et al., 2010). It has been suggested that loading at physiological levels acts as an anabolic factor for stimulation of collagen II, PG synthesis and TIMPs production (Handa et al., 1997, Maclean et al., 2004) whereas non-physiological high mechanical stresses result in decreases in anabolic proteins and an increase in catabolic matrix degrading enzymes (Lotz et al., 1998, Walsh and Lotz, 2004, Maclean et al., 2004, Neidlinger-Wilke et al., 2006, Gilbert et al., 2010, Paul et al., 2013). A few recent studies link increased magnitude of loading with matrix anabolism and prolonged periods of loading with disc matrix catabolism (Wuertz et al., 2009b, Sowa et al., 2011).

1.7.2 Genetic influences

Numerous studies have suggested that heredity is also responsible for the development of disc degeneration (Varlotta et al., 1991, Matsui et al., 1998, Battie et al., 2007, Battie et al., 2009). This has led to the well justified search for specific genetic risk factors in various ethnic populations and advanced our understanding of the aetiology of IVD degeneration. Allelic diversity in 1) structural [collagen type IX alpha 2/3 (COL9A2/3) (Paassilta et al., 2001, Jim et al., 2005), vitamin D receptor (VDR) (Videman et al., 1998) and aggrecan (ACAN) (Kim et al., 2011)]; 2) matrix-modifying molecules [MMP-3 (Takahashi et al., 2001)] and 3) inflammatory [IL-1 (Videman et al., 2009)] encoding genes have been frequently linked with disc degeneration [as review in (Kepler et al., 2013).

1.7.3 The microenvironment of the IVD

As the nutritional situation of cells in the disc centre is already critical, any loss in blood vessel contact or reduction in blood flow to the capillary beds adjacent to the EP could lead to decreased nutritional supply and an increased acidic microenvironment (due to the inefficient removal of lactic acid). This could have profound effects on the viability and functioning of the cells that will ultimately affect tissue composition and disc mechanics.

Blood flow to the EP can be altered by environmental factors, such as exposure to nicotine that is associated with reduction in the density of vascular buds and narrowing of the vascular lumen that supplies nutrients to the disc (Iwahashi et al., 2002). Systemic diseases may also alter the delivery of blood to the EP capillary beds and retard disc nutrition. For example, atherosclerosis of the lumbar arteries has been associated with disc degeneration and LBP (Kauppila, 1997, Kauppila et al., 2004). Loss in nutrient supply also appears to arise because of calcification of EP or because of the EP sclerosis. Calcification of EP occludes the vascular openings within it, depriving the cells of nutrients, leading to insufficient maintenance of the ECM and disc degeneration (Nachemson et al., 1970, Roberts et al., 1996, Benneker et al., 2005). In particular, calcification of the EP in scoliotic patients has been correlated with the loss in nutrients and cell death (Urban et al., 2001, Bibby et al., 2002) .

Determining the *in vivo* concentrations of nutrients and metabolites in human IVD is invasive and difficult. Therefore knowledge regarding their specific concentration in human IVD is still limited. Due to the difficulty of *in vivo* measurement, finite element modelling is often used to complement practical experiments and provide further insights into disc nutrition and degeneration issues. Few attempts have been made to measure O_2 concentration profile *in vivo*. O_2 concentration ranging from 0.5-1.3% has been measured in animal discs (Holm et al., 1981) whilst Bartels and colleagues measured O_2 concentration ranging from 2-12% in human degenerate disc (Bartels et al., 1998). Disc cells respond to growth factors *in vitro* (Gruber et al., 2000, Zhang et al., 2006a, Cho et al., 2013).

Growth factors have been found in both normal and degenerated discs (Murakami et al., 2006). However, there are no quantitative data exist on the endogenous expression of growth factors in the disc tissue. As diffusion of nutrients to the disc centre through disc matrix depends on their size and shape (Roberts et al., 1996, Urban et al., 2004), it can be envisaged that due to the large, globular structure of growth factors, their transport to the disc centre by

diffusion may be limited (Johnson et al., 2008). There are no direct measurements of glucose concentration *in vivo*. However, various *in vitro* nutrient transport models have predicted low glucose concentration in both normal and degenerated discs (Selard et al., 2003, Soukane et al., 2007, Jackson et al., 2011a). For example as high as 1.7 mM and as low as 0.345 mM glucose has been predicted in normal and impermeable EP (degenerated) discs respectively (Jackson et al., 2011a). Lactate concentration ranging from 2-6 mM has been measured in discs of patients with LBP (Bartels et al., 1998). The predicted lactic acid concentration also appears to fall within this measured range (Soukane et al., 2007, Mokhbi Soukane et al., 2009). It has been shown that lactate concentration directly correlates with pH of the disc (Diamant et al., 1968). Nachemson in 1969 measured intradiscal pH of patients with lumbar rhizopathies. He reported pH values from 7.5 to 5.7 inside lumbar discs and found a significant negative correlation (r= -0.41*) between pH and degeneration (i.e. the lower pH, the more degenerate changes in the disc) (Diamant et al., 1968, Nachemson, 1969). Increased lactic acid production at low O_2 concentration coupled with abundance of free cations (H+, K+ Na+) due to high negative PG content of IVD tissue may account for lower pH values (Nachemson, 1969, Razaq et al., 2000). pH values from 7.0-7.3 and 6.65 have been predicted in models of normal and degenerate discs (Soukane et al., 2007). Disc cells reside in an osmotic environment resulting from attraction of water due to sulfated GAGs. It has been suggested that NP cells of the normal disc experience extracellular osmotic pressure that cycles between 400 milliosmole (mOsm) (iso-osmotic) to 500 mOsm (hyper-osmotic) being the outcome of daily loading pattern (Takeno et al., 2007, Wuertz et al., 2007). Three hundred mOsm represents hypo-osmotic condition for disc cells and characterized degenerated disc (Mavrogonatou and Kletsas, 2010). Table 1.1 shows both the *in vivo* measured and finite element model predicted values of physio-chemical microenvironment components of both normal and degenerated disc.

Table 1.1 IVD physio-chemical microenvironmental conditions measured in vivo and predicted by finite element modelling

IVD-like physio-chemical microenvironmental Conditions	***In vivo* measurement**		**Computational analysis**		**References**
	Normal	**Degenerate**	**Normal (EP permeable)**	**Degenerate (EP impermeable)**	
Oxygen (%)	X	2-12%	0.5%	0.5%	(Bartels et al., 1998, Soukane et al., 2007)
Glucose (mM)	X	x	1.7	0.34	(Jackson et al., 2011a)
Lactic acid (mM)	X	2-6	5.29	5.3	(Bartels et al., 1998, Soukane et al., 2007)
pH	X	5.7-7.4	7.0–7.3	6.65	(Nachemson, 1969, Soukane et al., 2007)
Osmotic pressure (defined as osmolarity (mOsm/L of solution) or osmolality (mOsm/kg of solvent)	400	300	x	X	(Wuertz et al., 2007, Mavrogonatou and Kletsas, 2010)

X= value not measured/predicted

A number of investigators have examined the effects of IVD-like physio-chemical conditions on NP cell survival and functioning to determine the relationship between disc microenvironment and aberrant cellular behaviour (Bibby et al., 2002, Razaq et al., 2003, Bibby and Urban, 2004, Johnson et al., 2008, Illien-Junger et al., 2010). In these studies, degenerate disc nutritional conditions were represented by using ≤ 10mM glucose or/and ≤ 6% serum compare to 25mM glucose or/and 10% serum used in standard culture conditions (Bibby et al., 2002, Bibby and Urban, 2004, Johnson et al., 2008, Illien-Junger et al., 2010). Acidic pH of 6.8 or less has been used to represent reduced acidic microenvironment of degenerate disc compared to pH 7.4 in standard culture conditions (Ohshima and Urban, 1992, Horner and Urban, 2001, Razaq et al., 2003). O_2 of ≤ 5% used to represent disc hypoxic condition compared to 20% O_2 used in standard culture conditions (Agrawal et al., 2007, Feng et al., 2013). These investigations have shown that reduced nutrient and acidic conditions may induce detrimental effects on survival and the appropriate functioning of disc cells. These attempts have established the causal relationship linking the disc microenvironment to altered behaviour of NP cells characteristic of disc degeneration

(Horner and Urban, 2001, Razaq et al., 2003, Bibby and Urban, 2004). (These studies will be reviewed in more detail in the introduction of chapter 3). Such studies have predominantly focused on animal IVD cells and the effect of these conditions on human NP cell survival and function still need to be explored which is the aim of chapter 3 of this thesis.

1.8 IVD degeneration

IVD degeneration is thought to involve a number of sequential events that cause significant modifications in matrix composition and integrity which not only affect the disc but also the behaviour of associated spinal tissues such as muscles and ligaments leading to LBP (Smith et al., 2011). The balance between synthesis, breakdown, and accumulation of matrix macromolecules determine the quality and integrity of the matrix and ultimately the mechanical behaviour of the disc. Importantly, the imbalance between biosynthesis and breakdown of matrix molecules, especially of collagen and aggrecan, is implicated in disc degeneration. Such modifications have been reported to be the consequence of changes in cell number, physiology and up-regulation of inflammatory cytokines and catabolic enzymes.

1.8.1 Characteristic features of disc degeneration

1.8.1.1 Changes in cell density

At the cellular level, cell death has been observed to increase with degeneration (Trout et al., 1982, Gruber and Hanley, 1998). Both necrosis and apoptotic cell death mechanisms have been observed during degeneration (Sitte et al., 2009, Bertram et al., 2009), however, apoptosis appears to be a more common mechanism (Gruber and Hanley, 1998, Zhang et al., 2008, Bertram et al., 2009, Haschtmann et al., 2008). This is usually linked with diminished nutrient supply (Horner and Urban, 2001, Bibby and Urban, 2004) caused by calcification of EPs (containing vascular supply) (Roberts et al., 1996).

In addition to cell death, increased cell proliferation is also a feature of disc degeneration (Johnson et al., 2001). It has been suggested that cell proliferation is the likely cause of cell cluster formation in regions of marked matrix disorganisation, e.g. near clefts or fissures in degenerate discs (Johnson et al., 2001, Boos et al., 2002, Zhao et al., 2007, Ciapetti et al., 2012). It has been shown that growth factors (platelet-derived growth factor (PDGF), transforming growth factor-β (TGF-β) and insulin-like growth factor (IGF)) (Gruber et al., 1997, Pratsinis and Kletsas, 2007) and nutrient (glucose and serum) (Johnson et al., 2008, Stephan et al., 2011) supply increases NP cell proliferation. These findings suggest that the

increased proliferation of disc cells may be related to the elevation of some nutritional factors in specific areas of the degenerate disc. For example, it has been proposed that the increased proliferation and cell clusters near cleft and fissures may be the result of localised areas of increased nutrients due to neovascularisation occurring adjacent to these regions (Kauppila, 1995, Zhao et al., 2007)

1.8.1.2 Cellular senescence

Cellular senescence is defined as the point at which a cell stops dividing. There are two mechanisms for cellular senescence: replicative senescence which is caused by cell division induced telomere shortening (Campisi, 1997) or stress-induced premature senescence resulting from various stresses including mechanical load, high level of cytokines such as interleukin-1 (IL-1) and reactive O_2 species which disrupt cellular function and replication [reviewed in (Zhao et al., 2007)]. These two kinds of cell senescence may differently contribute to disc aging and degeneration. Cells present in clusters in degenerate discs have shown expression of cell senescence markers (Roberts et al., 2006a, Gruber et al., 2007). It is assumed that increased cell proliferation seen in cell clusters observed during aging and degeneration may lead to replicative senescence (Johnson et al., 2001, Roberts et al., 2006a, Gruber et al., 2007). However, stress induced premature senescence may occur specifically during disc degeneration as opposed to chronological aging. It has been suggested that the hostile microenvironment of the degenerate disc (e.g. high levels of pro-inflammatory cytokines seen in degenerate IVDs) may lead to stress induced premature senescence (Le Maitre et al., 2005, Le Maitre et al., 2007a).

1.8.1.3 Changes in IVD ECM composition

During disc degeneration a number of changes in synthesis, composition and breakdown of the ECM may contribute to the pathogenesis of the disease (Le Maitre et al., 2007d). During degeneration PG synthesis, particularly aggrecan decreases (Buckwalter, 1995). Additionally a change in the relative proportions of GAGs, from chondroitin sulphate to keratan sulphate, occurs (Scott et al., 1994). Keratan sulphate chains are less hydrophilic than chondroitin sulphate (Choi, 2009). Decreased and altered synthesis of aggrecan ultimately leads to dehydration of the IVD matrix.

Along with PG, a change in the ratio of type I to type II collagen has also been observed during degeneration i.e. types I and II collagen increased and decreased in the NP, respectively, and types II and I collagen increased and decreased in the AF, respectively

(Nerlich et al., 1997, Zhang et al., 2009). In the NP increased type I collagen confers a more fibrous nature to this tissue. Increased type X collagen (usually associated with ossification of hypertrophic chondrocytes) has also been observed in advanced degenerate discs, signifying abnormal cellular activity (Boos et al., 1997). This increase may contribute to the decrease in EP porosity observed in degenerate disc.

During degeneration, abnormal cellular physiology also evidenced by increased production of matrix degrading enzymes, namely MMP-1, -3, -7, -9, -10 and -13 and ADAMTS-1, -4, -5, -9 and -15 (Roberts et al., 2000, Le Maitre et al., 2004, Pockert et al., 2009, Richardson et al., 2009, Vo et al., 2013). During degeneration TIMP-1 and -2 expression increases along with MMPs (Roberts et al., 2000). However TIMPs-3 expression does not correlate with ADAMTS during degeneration (Le Maitre et al., 2004, Pockert et al., 2009) suggesting an imbalance between ADAMTS and TIMP-3 in degeneration in favour of ADAMTS expression and aggrecan breakdown (Le Maitre et al., 2004, Pockert et al., 2009).

The pro-inflammatory cytokine IL-1 (both α and β isoforms) appears to be an important regulator for the normal function of the disc cells, with a balanced production of its natural inhibitor, IL-1 receptor antagonist (IL-1Ra). During degeneration increased production of IL-1α and IL-1β has been reported without a concomitant up-regulation in IL-1Ra. This imbalance has been associated with many changes seen during degeneration i.e. up regulation of MMPs and ADAMTSs and down regulation of ECM genes (Le Maitre et al., 2005, Le Maitre et al., 2007b). The importance of IL-1 up-regulation in the IVD is further confirmed by the fact that exogenous applications of IL-1Ra inhibited ECM degradation and expression of MMPs and ADAMTS in degenerate discs (Le Maitre et al., 2007c). Increased expression of tumour necrosis factor α (TNFα) has also been seen in disc degeneration (Weiler et al., 2005, Le Maitre et al., 2007b). TNFα has been shown to increase MMP-1, -3, and -12 (Vo et al., 2013) and decrease expression of aggrecan and collagen types II (Studer et al., 2007).

1.8.1.4 Neovascularisation and neoinnervation

Disc degeneration is associated with neovascularisation and neoinnervation of the previously avascular and anueral disc and is coupled with increased pain (Kauppila, 1995, Freemont et al., 2002, Ratsep et al., 2013). It has been shown that nerve fibres grow into the IVD under stimulation of the neurotrophic factors such as nerve growth factor (NGF) and brain-derived neurotrophic factor (BDNF). Increased production of these factors has been demonstrated in

degenerate discs (Purmessur et al., 2008). IL-1β has been shown to increase production of NGF and BDNF in disc cells (Purmessur et al., 2008). Experiments have shown that during degeneration the microvessels that populate the avascular disc also show increased expression of NGF (Freemont et al., 2002). It has been suggested that this increased production of neurotrophic factors may influence and enhance innervation in the degenerate IVD. There is also evidence to suggest that the decrease of aggrecan during degeneration may also play an important role in the vascularisation and innervation of the disc. Aggrecan from normal disc has been shown to inhibit the growth of neurites and endothelial cells *in vitro*. These findings suggest that the reduction of aggrecan may allow the previously inhibited structures to form (Johnson et al., 2005, Johnson et al., 2002). It has been shown that penetrating nerves express the nociceptive neurotransmitter substance P (Freemont et al., 1997). Treatment with TNFα has also been shown to upregulate substance P expression (Purmessur et al., 2008). Substance P may contribute to nociceptive processes within the degenerate IVD (Freemont et al., 1997, Purmessur et al., 2008).

Neoinervation may be associated with pain in the disc while neovascularization may improve nutritional status of the degenerated disc. However, studies that link affected nutrient supplies with disc degeneration need to explain the effect of neovascularization of the IVD.

1.8.2 Consequences of disc degeneration

The IVD mechanical function of distributing axial loads and absorbing shock while providing flexibility relies heavily on the hydrodynamic capabilities of the NP. Loss of PG and matrix disorganization results in a serious loss of disc mechanical function. A less hydrated, more fibrous NP is unable to evenly distribute compressive forces between the vertebral bodies. The forces are instead transferred to the surrounding AF, which experiences change in forces from tensile (exerted by the hydrated NP) to compressive (exerted by the vertebral bodies) forces (Adams et al., 1996). This results in altered AF mechanical properties and progressive structural deterioration, including the bulging of the NP and annular tears that may lead to NP herniation which is implicated in painful symptoms (Adams and Roughley, 2006). Figure 1.7 shows a healthy IVD with the NP in the centre and the surrounding AF and illustrates a degenerate IVD with no distinction between NP and AF. Due to degeneration the spacing effect of the normal NP is lost and the vertebral bodies approximate to one another resulting in abnormal movement and loading throughout the entire motion segment causing traumatic damage to the facet joints and other structures leading to LBP (Freemont, 2009).

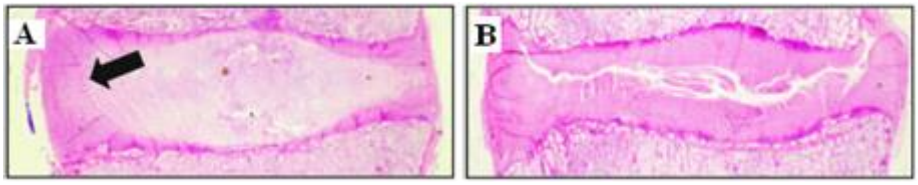

Figure 1.7 Degenerative changes of IVD. Comparison of healthy (A) and degenerated (B) discs illustrates alterations in all anatomical regions of disc. Presence of slit and loss of distinction (arrow) between AF and NP are obvious changes in degenerate disc (B) (Sive et al., 2002)

1.9 Repair of IVD

Currently the mainstay of treatment for LBP is either symptomatic medical therapy or surgery, both of which have limited long term success. Physical therapy and different forms of exercise are usually the first choices to improve core stability, motion and muscles strength but the relief effect is only short term (Shen et al., 2006).

A wide range of surgical treatments aimed at removing degenerate tissue are currently being performed in clinical practice. Fusion of assumed symptomatic segments in patients with LBP has been used widely (Deyo et al., 2005). However, there is still controversy regarding its effectiveness. Some studies have shown signs of improvements (Fritzell et al., 2002) while others demonstrate no significant improvement (Fairbank et al., 2005, Brox et al., 2010). Additionally it has been shown that lumber fusion may accelerate degeneration in adjacent discs (Levin et al., 2007). A range of new non-fusion surgical treatments including artificial discs and NP prostheses designed to improve disc mobility in cases of severe IVD degeneration are currently being developed. However further research is required to overcome associated complications including migration, prolapse, extrusion and device failure (van den Eerenbeemt et al., 2010).

1.9.1 Biological treatments

A range of novel regenerative and tissue engineering strategies targeting at regeneration and repair of degenerate IVD/NP have been proposed. Unlike the above mentioned treatments these strategies address the underlying disease pathology to both alleviate the painful symptoms and to restore mechanical function (Smith et al., 2011, Hughes et al., 2012).

Regenerative strategies focus on either stimulating existing native tissue cells (through administration of growth factors, use of cytokine inhibitors and gene manipulation), or

transplantation of exogenous cells to either provide signalling cues that ameliorate the effects of disc degeneration, or to adopt and/or maintain disc-like phenotypes themselves, producing appropriate ECM needed to re-establish healthy disc function (Smith et al., 2011, Zhang et al., 2011).

The therapeutic potential of growth factor (e.g. bone morphogenetic protein (BMP), TGF-β, IGF and PDGF) injection for the treatment of disc degeneration can be found both in *in vitro* and *in vivo* preclinical studies (Gruber et al., 2000, Chujo et al., 2006, Miyamoto et al., 2006, Imai et al., 2007, Abbott et al., 2012, Cho et al., 2013). However, despite the encouraging results the clinical utility of this molecular based therapy is limited for a number of reasons: 1) the presence of a low number of healthy endogenous cells in the degenerate disc able to respond to exogenous stimulus; 2) the lack of understanding of the response of uncontrolled release of growth factors on various regulatory mechanisms functioning within the disc; and 3) the short term effect of this form of stimulation. Nevertheless a phase 1 safety trial testing the efficacy of BMP-7 and growth differentiation factor-5 (GDF-5) has started in the USA (Zhang et al., 2011), but it will take several years to determine whether intradiscal injection of these growth factors will have therapeutic responses in patients with LBP.

Targeting the proinflammatory cytokines (e.g IL-1) that deplete the matrix content through stimulation of catabolic processes and block anabolism is another approach for treating degenerative changes. Injection of IL-1Ra transfected NP cells into degenerate NP explants inhibited IL-mediated MMP production (Le Maitre et al., 2007c).

Gene therapy for the treatment of disc degeneration has also been proposed. Genetic delivery of various activators such as anti-inflammatory molecules: IL-1Ra (Le Maitre et al., 2006, Le Maitre et al., 2007c); transcription factors and growth factors: SOX-9, BMPs (Paul et al., 2003, Zhang et al., 2006b), TGF-β3 (Nishida et al., 1999); protease inhibitor: TIMP-1 (Wallach et al., 2003) and intracellular regulator: LMP1 (latent membrane protein 1) (Kuh et al., 2008) led to the restoration of IVD structure and increased synthesis of PG and collagens. However safety concerns such as ectopic transfection, patient-specific dose responses or immune reactions to viral proteins are the main barrier to the clinical use of gene therapy (Wallach et al., 2006, Maerz et al., 2013).

1.9.2 Cell based therapies for disc regeneration

Cell based therapies provide a rational cellular approach to restore the IVD cell population, structure and function through introduction of suitable cells and/or biomaterials. Proposed sources of cells include disc derived cells (NP cells, Notochordal cells) and MSCs.

1.9.2.1 Disc derived cells

Disc derived cell therapy focuses on utilizing cells of a committed phenotype to halt the process of degeneration and in some instances, rejuvenate endogenous cells that have been damaged by degeneration (Maerz et al., 2013). Activation of autologous NP cells by co-culture with AF cells and reinsertion into animal models of disc degeneration has shown that these cells may be implanted with long term cell survival and improved ECM synthesis in experimentally induced disc degeneration models (Okuma et al., 2000, Watanabe et al., 2003). These results support the hypothesis that the transplantation of *in vitro* cultivated disc cells from autologous disc tissue (autologous disc cell transplantation - ADCT) might be an appropriate therapeutic approach to repair disc damage and inhibit degeneration. Additionally, the *EuroDisc* study, a multicenter clinical trial, gave further confidence in this ADCT approach. Here patients who had ADCT (disc cells harvested through discectomy), experienced more pain relief and had greater IVD fluid content two years after the procedure than patients who had discectomy alone (Meisel et al., 2007, Hohaus et al., 2008). However, re-implantation of autologous disc cells includes disadvantages because there is a need for two separate invasive surgeries (to harvest and implant cells) thus increasing risks of infection and nerve root damage (Maidhof et al., 2012). Furthermore, genetic predisposition for these autologous cells to undergo degeneration also raises concerns about their regenerative capacity (Lewis, 2012). Moreover NP cells isolated from degenerate discs show features of cellular senescence (Roberts et al., 2006a, Gruber et al., 2007, Le Maitre et al., 2007a) and altered cell physiology (Le Maitre et al., 2004, Le Maitre et al., 2005) that would preclude normal cell function.

An alternative to autologous NP cells would be the use of allogenic cells. Nomura *et al* showed that implantation of allogenic NP cells into a rabbit model of disc degeneration was effective in reducing degeneration without significant immunogenic response (Nomura et al., 2001). By using an allogenic cell population it is possible to escape the genetic predisposition issue related to the use of autologous NP cells. However, such an approach requires an

abundant supply of healthy human disc samples, which is difficult to achieve. Additionally the acquisition of allogenic cells may initiate degeneration at the donor site.

Co-culturing of notochordal cells with NP cells results in significant increase in PG content in NP cells (Aguiar et al., 1999). Notochordal cell conditioned media also protects cells from the catabolic effects of IL-1, causing a decreased expression of matrix catabolic factors and increased expression of genes associated with matrix anabolism in bovine and human degenerate NP cells (Erwin et al., 2011, Abbott et al., 2012). Harnessing the restorative powers of the notochordal cell could lead to novel cellular and molecular strategies in the treatment of DDD. However, as it has been suggested that notochordal cells are lost from the human NP with aging (Risbud et al., 2010a), availability of abundant notochordal cell supply seems difficult.

1.9.2.2 Mesenchymal stem cells (MSCs)

Stem cells are defined as a population of unspecialized cells capable of long term self-renewal and differentiation into specialized cells. MSCs are found in numerous anatomic locations such as BM (Pittenger et al., 1999), adipose tissue (Gimble and Guilak, 2003), umbilical cord (Trivanovic et al., 2013), muscle (Bosch et al., 2000) and dermis (Zong et al., 2012). Additionally, many investigators have identified the presence of progenitor/stem cells population in normal animal (Henriksson et al., 2009a, Erwin et al., 2013) and human degenerate disc tissue (Risbud et al., 2007, Blanco et al., 2010, Liu et al., 2011, Brisby et al., 2013). These cells have been defined as MSCs and showed morphology, immunophenotype, gene expression and differentiation capacities comparable with BM-MSCs (Blanco et al., 2010, Liu et al., 2011).

MSCs were first identified more than 40 years ago by Friedenstein and colleagues, who showed that in BM there is a population of adherent non-haematopoeitic cells that have a fibroblast shape and have ability to differentiate into bone and cartilage cells (Friedenstein et al., 1968). Caplan popularized the term mesenchymal stem cell in the early 1990s (Caplan, 1991). The term “mesenchymal stem cells” (with the acronym MSCs) has been reserved for the population of cells that demonstrate stem cell activity by clearly stated criteria that: (1) MSCs must be plastic-adherent when maintained in standard culture conditions; (2) express cluster of differentiation (CD) 73, CD90, and CD105 and lack expression of CD45, CD34,

CD14 or CD11b, CD79α, or CD19 and human leukocyte antigen-DR (HLA-DR) and (3) differentiate to osteoblasts, adipocytes and chondrocytes *in vitro* (Dominici et al., 2006).

MSCs provide a reservoir of regenerative cells for mature tissues of mesenchymal origin including bone, cartilage, fat, muscle and tendon (Pittenger et al., 1999, Tuan et al., 2003) (Figure 1.8). MSCs differentiation potential, their easy accessibility and expansion make them an attractive source of cells to regenerate the degenerate disc. In the past decade, MSCs, especially derived from BM tissue (BM-MSCs) have been explored extensively for their discogenic differentiation potential and feasibility in the repair of degenerate disc.

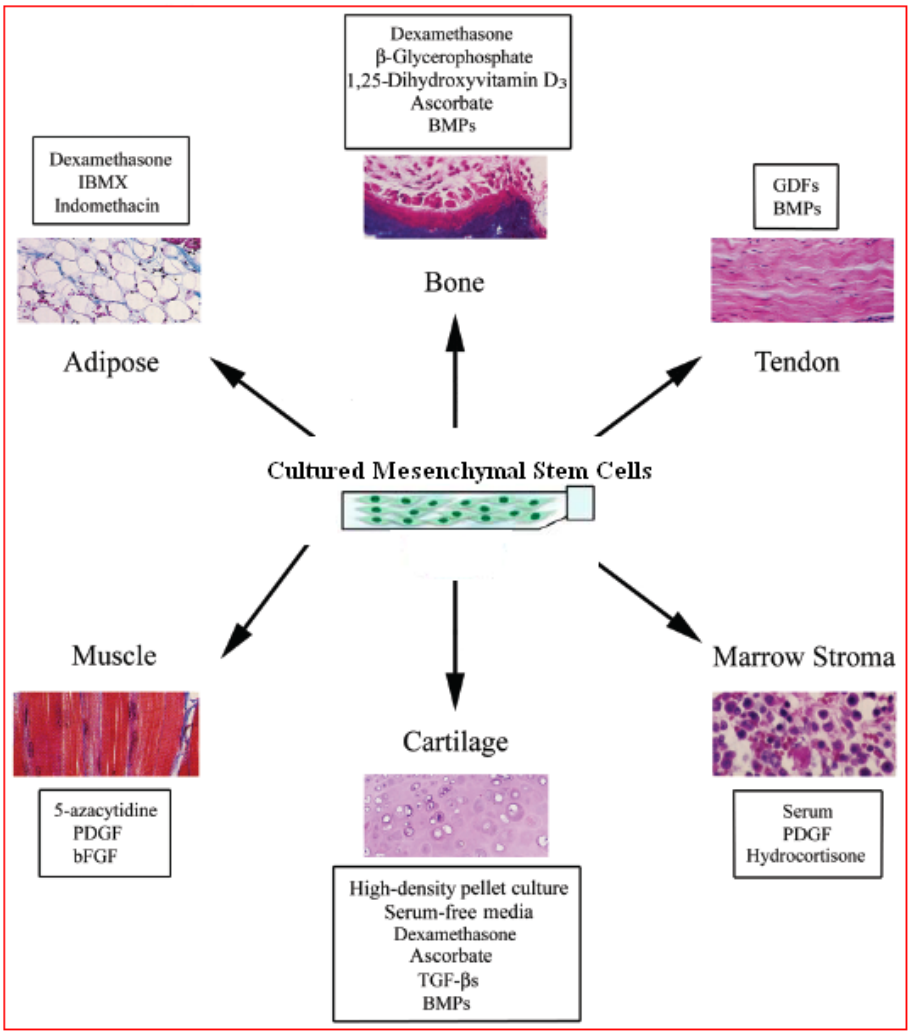

Figure: 1.8 Differentiation potential of MSCs. This figure depicts some of the *in vitro* culture conditions (boxed) that promote the respective differentiation process into bone, cartilage, adipose tissue, muscle, tendon, and marrow stroma. Modified from (Tuan et al., 2003).

1.10 The use of MSCs for IVD repair

A number of *in vitro* studies have demonstrated that MSCs are capable of differentiating towards a NP-like phenotype (Risbud et al., 2004a, Steck et al., 2005, Richardson et al., 2008, Fang et al., 2013). These investigations concluded that MSCs may have the potential to regenerate the degenerate IVD and provided rational for *in vivo* transplantation of MSCs.

In vivo studies with implantation of MSCs into the IVD have shown encouraging results with long-term viability of the implanted cells and functionality to slow the process of IVD degeneration and regenerate the matrix. In 2004, Crevensten *et al* was the first to study the viability of BM-MSCs injected into rat IVD using hyaluronan gel as a scaffold (Crevensten et al., 2004). They showed that BM-MSCs were able to survive, proliferate and contribute to increased disc height (indicative of restoration of disc tissue). Sakai and colleagues also explored the use of BM-MSCs in degenerate disc repair *in vivo* using a rabbit model of IVD degeneration. They embedded BM-MSCs in Atelocollagen matrix and then injected into experimentally induced degenerated discs. BM-MSCs survived and demonstrated an anti-degenerative effect by improving disc height and increasing PG synthesis and expression of matrix molecules in degenerate discs (Sakai et al., 2003, Sakai et al., 2005, Sakai et al., 2006). Many other investigators have used small animal (i.e. rabbit and rat) models and have confirmed the effectiveness of the use of BM-MSC for disc regeneration (Crevensten et al., 2004, Zhang et al., 2005, Sobajima et al., 2008, Wei et al., 2009, Yang et al., 2009, Jeong et al., 2009, Yang et al., 2010, Feng et al., 2011). In addition to BM-MSCs, MSCs isolated from other sources such as synovial derived MSCs (SD-MSCs) have also been used in small animal models with promising potential for regeneration of the disc (Miyamoto et al., 2010).

While small animal models have yielded universally positive results, the results of large animal studies (whose discs more closely mimic the human IVD) have been mixed and require more work for definitive conclusion. Hiyama *et al* found that BM-MSCs injected into a canine degenerate disc model increased PG content and effectively diminished degeneration (Hiyama et al., 2008). Similarly Henriksson *et al* injected human BM-MSCs into porcine degenerate disc model and showed MSC survival, differentiation and matrix production (Henriksson et al., 2009b). Recently Ghosh *et al* injected ovine BM-MSCs into an ovine degenerate disc model and showed that MSC transplantation into a degenerate IVD can contribute to the regeneration of a new ECM. Adipose derived MSCs (AD-MSCs) injected into a canine disc injury model were also effective in promoting disc regeneration (Ganey et

al., 2009). While these results were encouraging, one recent large animal study casts doubt on the potential of MSCs to treat IVD degeneration clinically. Acosta *et al* injected injured porcine discs with BM-MSCs but found no viable cells or improved PG synthesis at follow up (3, 6 and 12 months) (Acosta et al., 2011). In this study it was hypothesized that the disc microenvironment may compromise survival and regenerative effects of implanted MSCs. It has been postulated that large animal IVDs may more closely mimic the adult human disc size (Acosta et al., 2011). A large disc size and long distance diffusion transport between the disc blood supply and disc centre, may result in steep gradients of nutrients and metabolic wastes and ultimately a more hostile microenvironment than that found in the discs of small animals (Drazin et al., 2012). As such the difference in nutrient transport in the disc centre may result in different outcomes following implantation of cells. Recently a small human trial has investigated the efficacy of MSC based therapy for the treatment of LBP in 10 patients (Orozco et al., 2011). Although this study reported improvement in clinical symptoms (pain and disability) and disc water content, it failed to report any improvement in disc height after 1 year follow up. A longer follow-up period to fully evaluate the anatomical and functional changes after MSCs injection was suggested. Nevertheless the lack of improvement in disc height raises concerns about the functionality of injected cells which could be compromised due to the harsh microenvironment found in the human degenerate disc.

1.11 Potential challenges in MSC based disc repair

For the purpose of regenerating a degenerate disc with MSCs, the most important question to address is whether MSCs can survive, proliferate, differentiate and produce PGs in the inhospitable microenvironment of the disc in a satisfactory manner to contribute to disc repair.

The effect of the complex microenvironment of the disc on the survival and function of MSCs has received limited attention. Recently few investigators have studied the effects of disc-like microenvironmental conditions on survival, proliferation and matrix synthesis of rat BM-MSCs and human AD-MSCs (Wuertz et al., 2008, Wuertz et al., 2009a, Liang et al., 2012a, Li et al., 2012). These pioneering *in vitro* studies highlighted that some conditions of the disc microenvironment may impair MSC behaviour and consequently regenerative outcomes. However, the effects of disc microenvironmental conditions on human BM-MSCs which are considered the main candidate for regeneration therapy, are still unknown which is

the main aim of chapter 4 of this thesis. This will enhance our understanding about survival and functioning of BM-MSCs in degenerate microenvironmental conditions.

MSC and NP cell co-culture model systems have been increasingly utilized to study MSC based disc repair (Richardson et al., 2006, Strassburg et al., 2010, Watanabe et al., 2010). These model systems suggest that disc repair after MSC implantation may be due to both differentiation of MSCs and modulation of degenerate NP cell phenotype. But as it is increasingly emphasized that disc microenvironmental conditions influence both NP cells and MSCs, it is possible that these conditions could also affect MSC differentiation and modulation of degenerate NP cell phenotype during co-culture. Therefore it is equally important to incorporate disc-like microenvironmental conditions in to the co-culture model system to evaluate their possible stimulatory or inhibitory effects on the co-culture responses. This may enhance our understanding about the possible impact of disc microenvironmental conditions during regenerative interaction of implanted MSCs with resident cells and will reveal factors crucial for modulation of both MSC differentiation and degenerate NP cell phenotype for ultimate disc repair. This is the aim of chapter 5 of this thesis.

1.12 Aims of the project

LBP is a major health problem strongly associated with degeneration of the IVD with changes initially occurring in the NP. The underlying causes of disc degeneration are considered to be multifactorial including changes to IVD microenvironment. Various investigations have attempted to correlate these changes e.g. limited nutritional and acidic conditions with the features that characterise disc degeneration. However, the response of human NP cells to these conditions is largely unknown. BM-MSCs are considered a promising cell population to regenerate IVD structure and functions. However, hostile microenvironment of the degenerated IVD may pose a potential challenge in their use. Therefore, it is important to understand whether they can survive and function in the degenerate disc microenvironment. Co-culture model studies that suggest that BM-MSC based disc repair may be due to both MSC differentiation and modulation of degenerated NP cell phenotype also need to consider the influence of these conditions on proposed regenerative responses.

The aims of this thesis are:

i) To investigate the stimulatory or inhibitory influences of IVD-like physio-microenvironmental conditions particularly hypoxia, reduced nutrients, moderate and severe acidic pH on human NP cells behaviour in terms of survival, proliferation, gene and protein synthesis, to ascertain conditions modulating or accelerating processes characteristic of IVD degeneration (Chapter 3).

ii) To study the stimulatory or inhibitory influences of IVD-like physio-chemical microenvironmental conditions on human BM-MSC behaviour in terms of survival, proliferation, IVD gene and protein synthesis, to determine conditions beneficial or critical for BM-MSC survival and functioning (Chapter 4).

iii) To incorporate IVD-like physio-chemical microenvironmental conditions in an *in vitro* co-culture model system to investigate the stimulatory or inhibitory influences of disc microenvironmental conditions on MSC differentiation and modulation of degenerate NP cell phenotype (Chapter 5).

2 Chapter 2 Materials and methods

2A Materials and methods

All reagents were obtained from Sigma unless otherwise stated

2A.1 Cell extraction and culture

Degenerate NP cells and BM-MSCs used in this study were isolated from human IVD and BM tissue samples respectively obtained with consent during surgery in accordance with university and ethical committee policies and Human tissue Act (HTA) legislation. All cell culture was conducted aseptically in class II laminar flow cell line culture hoods at room temperature. Cells were cultured in an incubator (Galaxy S-Wolf Laboratories) at 37^{o}C with ventilation of 5% CO_2 and 20% O_2 in air unless otherwise stated.

NP tissue was dissected from AF tissue macroscopically, cut into small pieces and placed in a shaking incubator at 37ºC in pronase solution (Calbiochem) (300-350PUK/ml) for 30 minutes. Following this, the tissue was enzymatically digested with 0.25% (w/v) collagenase type II and 0.1% (w/v) hyaluronidase in serum-free medium containing antibiotics until almost all tissue was digested. The digested tissue/cell suspension was filtered through a 40µm cell strainer to remove tissue debris. Cells were then centrifuged at 400g for 5min, counted and cultured to confluence in a 75 cm^2 flask in Dulbecco's Modified Eagle Medium (DMEM) (Gibco) supplemented with 10% v/v fetal calf serum (FCS), 50µg/ml ascorbate, 100U/ml penicillin, 100µg/ml streptomycin and 250 µg/ml amphotericin B (DMEM standard medium). Representative IVD tissue samples were also embedded in paraffin wax for histological assessment/grading on the basis of morphological changes (assessed by Professor Anthony Freemont). Graded tissue was given a score between 0-12 with 0-3 classed as non-degenerate, 4-7 classed as mildly degenerate and 8-12 classed as severely degenerate (Sive et al., 2002).

BM-MSCs were isolated by Histopaque-1077 density gradient method with simultaneous application of RosetteSep to negatively sort for unwanted blood cells. The sample was spun at 500g for 10 minutes and the fatty supernatant removed. The pellet was resuspended in 5ml Minimum Essential Medium α-modification (α-MEM) supplemented with antibiotics and antimycotics (100U/ml penicillin, 100µg/ml streptomycin and 250µg/ml amphotericin B). Two hundred and fifty microliters of RosetteSep (Stem Cell Technologies) was added per 2.5ml sample and incubated for 20 minutes at room temperature. Subsequently, the sample

was diluted with 5ml Hank´s Buffered Salt Solution (HBSS) containing 2% (v/v) FCS and 1mM EDTA (buffer for RosetteSep). Using a plugged Pasteur pipette 5ml Histopaque (density: 1.077g/ml) was carefully pipette into the bottom of the sample tube and centrifuged at 500g for 30 minutes without applying the brakes in order not to destroy the gradient. Mononuclear cells from the cloudy interface were removed and cultured to confluence in a 75 cm^2 flask with 12ml of α-MEM (Gibco) supplemented with 10% v/v FCS (Gibco), 25µg/ml ascorbate, 100U/ml penicillin, 100µg/ml streptomycin and 0.25µg/ml amphotericin B (α-MEM standard medium).

2A.2 Passaging of cells

Upon reaching 70-90% confluence, as estimated by phase contrast microscopy (Leitz), the cells were passaged. During passaging media was removed and the cell monolayer was washed with 10ml Dulbecco's phosphate buffer saline (PBS) (PAA Laboratories) and incubated with 5ml of 0.25% (w/v) trypsin/EDTA for 2-3 minutes. Flasks were gently tapped to dislodge the cells and viewed under the microscope to ensure complete detachment of the cells. An equal amount of fresh pre-warmed standard media was added to inactivate the trypsin solution.

The cell suspension was collected in 50ml centrifuge tubes and centrifuged at 400g for 5 minutes. Supernatant was discarded and cells were washed with PBS. Finally cells were resuspended in an adequate volume of fresh standard medium for cell counting. A 10µl aliquot of the resuspended cell solution was pipetted into the chamber of a haemocytometer. Cells were counted within the 4 corner squares including cells touching two of the four bordering grid lines and excluding cells touching the other two lines under a phase contrast light microscope. Each square has a surface area of $1mm^2$ with depth of the chamber 0.1mm representing a total volume of 0.1 mm^3 or 10^{-4} cm^3 ($1000mm^3=1cm^3$). 10^{-4} cm^3 is usually expressed as 10^{-4} ml since 1 cm^3 =1 ml. To calculate the number of cells per ml an average cell count from 4 corner squares was multiplied by the conversion factor 10^4 (based on the fact that each large square represents a total volume of 10^{-4} cm^3) to give the cell number/ml. To obtain the total cell number, the cell number/ml was multiplied by the total volume of the cell suspension. Using this calculation 3000-5000 cells/cm^2 were seeded into new flasks for cell expansion. Cells were passaged until sufficient numbers for experimentation were obtained.

2A.3 Culture under IVD-like physio-chemical microenvironmental conditions

Cells were cultured in four DMEM media formulations [1) DMEM 4.5mg/ml glucose, 2) DMEM 1mg/ml glucose, 3) DMEM-F12 3.5 mg/ml glucose and 4) DMEM 1mg/ml glucose without HEPES and $NaHCO_3$] supplemented with various components to mimic different IVD-like physio-chemical microenvironmental conditions (Table 2.1).

Table 2.1 Media formulations used to represent IVD-like physio-chemical microenvironmental conditions

Component	Standard Medium	Reduced serum medium	Reduced glucose medium	Reduced serum and reduced glucose medium	Standard medium for pH work (pH 7.4)	pH 6.8/6.5 medium	All condition combined standard medium pH 7.4 (M1)	All condition combined experimental medium pH 6.8 (M2)
Type of media used								
DMEM (4.5mg/ml) glucose	✓	✓	x	x	x	X	x	x
DMEM (1mg/ml) glucose	X	X	✓	✓	x	X	x	x
DMEM-F12 (3.5mg/ml) glucose	X	X	x	x	✓	✓	x	x
DMEM-low glucose (1mg/ml) no HEPES/ $NaHCO_3$	X	X	x	x	x	X	✓	✓
Additional components added								
Glucose (mg/ml)	-	-	-	-	-	-	3.5	-
FCS (% v/v)	10	2	10	2	10	10	10	2
Ascorbate (µg/ml)	25	25	25	25	25	25	25	25
Penicillin (U/ml)	100	100	100	100	100	100	100	100
Streptomycin (µg/ml)	100	100	100	100	100	100	100	100
Amphotericin B (µg/ml)	0.25	0.25	0.25	0.25	0.25	0.25	0.25	0.25
HEPES (mM)	-	-	-	-	-	-	15	15
$NaHCO_3$ (mg/ml)	-	-	-	-	2	0.58/ 0.34	2	0.58

✓ / x = medium type used/ not used

– = Nutrient was already present in basal media and not further added

Cells were cultured for 7 days (with media change twice a week) to allow sufficient time for any phenotypic change to occur. Cells were seeded in triplicate in 6 well culture plates for hypoxia, reduced serum and reduced glucose conditions. For all pH conditions (i.e. pH 7.4, pH 6.8, pH 6.5 alone and in combination with other conditions) cells were seeded in 25cm^2 culture flasks to avoid pH fluctuations during incubation (Refer to section 2B.1 for optimization of pH monitoring and maintenance).

2A.3.1 Cell culture under hypoxia

For cell culture under hypoxia, standard medium (Table 2.1 column 1) was equilibrated with 2% O_2 by filtering using a bottle top 0.2µm filter system in a HEPA-filtered hypoxic chamber (Coy Laboratories) set at 2% O_2. Cells were incubated in a hypoxia incubator (Binder CB150) at 37°C with 2% O_2 and 5% CO_2. Medium was changed twice a week in a hypoxic chamber to ensure cells were not exposed to atmospheric O_2 concentrations at any point during the culture period.

2A.3.1.1 Hypoxia detection assay

For hypoxic work, it was of paramount importance to determine that cells had a constant exposure to reduced oxygen levels. Pimonidazole is a hypoxia marker that is routinely used to detect hypoxia in tissues. In hypoxic cells pimonidazole reduces and binds to thiol containing proteins, peptides and amino acids (Arteel et al., 1995, Arteel et al., 1998). To confirm hypoxic exposure of the cells, 3000 cells/cm^2 were seeded on 8 well culture slides. BM-MSCs were incubated under normoxia (20% O_2) and hypoxia (2% O_2) for 24 hours with 200µM of pimonidazole (Hypoxyprobe, Inc) dissolved in the culture medium. After incubation cells were washed with PBS and fixed with 4% (w/v) paraformaldehyde (PFA) for 20 minutes at room temperature. After fixation cells were washed 3 x 5 minutes in PBS. Cells were blocked in 10% normal goat serum in PBS for 60 minutes. Cells were then incubated overnight at 4°C in monoclonal mouse anti-pimonidazole antibody (Hypoxyprobe, Inc) diluted 1:100 in 10% normal goat serum in PBS with 0.1% Triton X-100. After primary antibody incubation, cells were washed and incubated with goat Alexa 488 anti-mouse antibody (stock concentration 2mg/ml) (Invitrogen, A11001) diluted 1:300 in 10% normal goat serum in PBS with 0.1% Triton X-100 for 60 minutes at room temperature in the dark. Cells were washed with PBS and one drop of mounting medium with DAPI (Vector Labs) was added to cells. Cover slips were placed on the slides and cells were observed using upright fluorescence microscope (Olympus BX51) with QCapture software. Positive

pimonidazole staining following culture in hypoxic conditions confirmed that cells were indeed exposed to hypoxia (Figure 2.1).

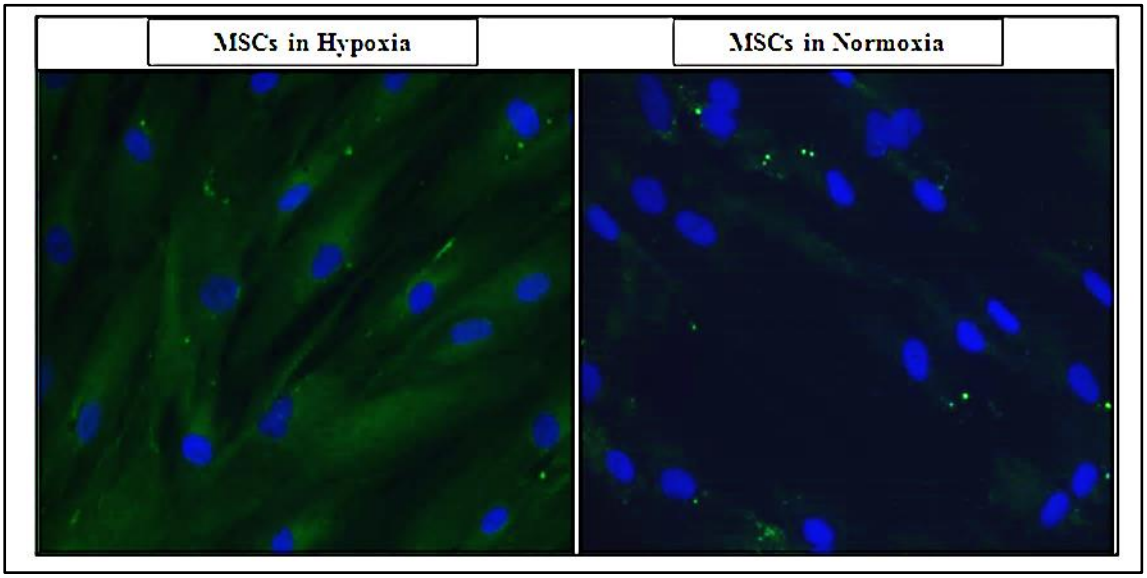

Figure 2.1 Immunofluorescent detection of pimonidazole, a marker of cellular hypoxia in MSCs. Cells were incubated for 24 hours with 200µM pimonidazole under normoxia and hypoxia. Positive staining was observed in cells incubated under hypoxic (2%) but not in normoxic (20%) conditions. Magnification x200.

2A.3.2 Cell culture under reduced serum

Cell culture under reduced serum was conducted using standard medium supplemented with 2% v/v FCS instead of normal 10% v/v FCS (Table 2.1 column 2). Cells were seeded in a Class II tissue culture hood and incubated in an incubator at 37°C with 5% CO_2 and 20% O_2 with medium changed twice a week.

2A.3.3 Cell culture under reduced serum and hypoxia

For cell culture under reduced serum combined with hypoxia, reduced serum medium (Table 2.1 column 2) was equilibrated with 2% O_2 in a hypoxic chamber. Cells were incubated in a hypoxia incubator with appropriate medium changed twice a week in a hypoxic chamber.

2A.3.4 Cell culture under reduced glucose

For cell culture under reduced glucose conditions, DMEM with glucose content of only 1 mg/ml instead of 4.5 mg/ml was supplemented with all components used in DMEM standard medium (Table 2.1 column 3). Cells was seeded in a Class II tissue culture hood and incubated in an incubator at 37°C with 5% CO_2 and 20% O_2 with medium changed twice a week.

2A.3.5 Cell culture under reduced glucose and hypoxia

For cell culture under reduced glucose condition combined with hypoxia, reduced glucose medium (Table 2.1 column 3) was equilibrated with 2% O_2 in a hypoxic chamber. Cells were incubated in a hypoxia incubator with appropriate medium changed twice a week in a hypoxic chamber.

2A.3.6 Cell culture under reduced serum and reduced glucose

For cell culture under reduced serum and reduced glucose, reduced glucose medium was supplemented with 2% v/v instead of 10% v/v FCS (Table 2.1 column 4). Cells were incubated in an incubator at 37°C with 5% CO_2 and 20% O_2 with medium changed twice a week.

2A.3.7 Cell culture under reduced serum, reduced glucose and hypoxia

For cell culture under reduced serum and reduced glucose condition combined with hypoxia, reduced serum and reduced glucose medium (Table 2.1 column 4) was equilibrated with 2% O_2 in a hypoxic chamber. Cells were incubated in a hypoxia incubator with appropriate medium changed twice a week in a hypoxic chamber.

2A.3.8 Cell culture under reduced pH

For the control of pH in cell culture, one simulates the conditions found in blood. In the natural system, a blood HCO_3^- concentration of 24 mM (corresponding to about 2mg/ml $NaHCO_3$) is in equilibrium with a lung CO_2 partial pressure of 40 mm Hg (corresponding to about 5% CO_2) implying the physiological pH 7.4. *In vitro* cell culture takes advantage of this system i.e. addition of 2mg/ml $NaHCO_3$ in medium and incubation in 5% CO_2 results in pH 7.4. Based on available literature, to study the effect of reduced pH on cells, three different pH values 7.4, 6.8 and 6.5 were selected (Nachemson, 1969). The Nomogram scale (Figure 2.2) (Esser, 2010) and Henderson-Hasselbalch equation (Eq-1) were used to identify and confirm $NaHCO_3$ concentrations respectively to achieve different pHs. Initially the Nomogram scale was used to identify $NaHCO_3$ concentrations to achieve pH 7.4 and 6.8. It showed that pH 7.4 and 6.8 can be achieved using 2 and 0.58mg/ml $NaHCO_3$ respectively at 5% CO_2. These estimated values were then inserted into Henderson-Hasselbalch equation (Eq-1). This version of Henderson-Hasselbalch equation has been suggested to estimate $NaHCO_3$ values satisfying different pHs (Esser, 2010). Calculations below Eq-1 show that Henderson-Hasselbalch equation confirms Nomogram scale recommendations.

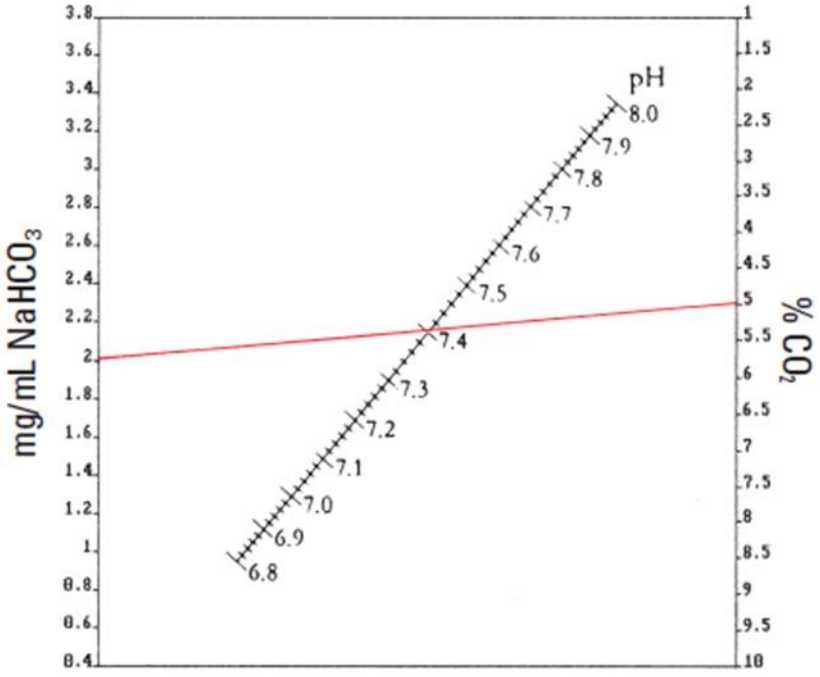

Figure 2.2 Nomogram for estimation of $NaHCO_3$ at 5% CO_2 to get required pH values according to the Henderson-Hasselbalch equation given in the text. With any two values, the third value can be determined easily by connecting the known values with a ruler. For example, the red interpolation indicates that at 5% CO_2 to achieve physiological pH 7.4, 2mg/ml $NaHCO_3$ is required. Adapted from (Esser, 2010).

Eq-1 $pH = 6.1+\log [52(\textbf{?}\ mg/ml\ NaHCO_3/5\%\ CO_2)-1]$

Calculations for pH 7.4

$pH = 6.1+ \log [52(2mg/ml\ NaHCO_3/5\%\ CO_2)-1]$

$pH= 6.1+ 1.3$

pH = 7.4

Calculations for pH 6.8

$pH = 6.1+ \log [52(0.58mg/ml\ NaHCO_3/5\%\ CO_2)-1]$

$pH = 6.1+ 0.70$

pH =6.8

As shown in figure 2.2 the Nomogram pH scale ends at pH 6.8, therefore, this scale was not used to find out $NaHCO_3$ concentration to achieve pH 6.5. Various concentrations of $NaHCO_3$ (0.2-0.34) were inserted into Henderson-Hasselbalch equation (Eq-1) and it was found that 0.34mg/ml $NaHCO_3$ would give pH 6.5. Correspondences of Henderson-

Hasselbalch equation (Eq-1) with Nomogram scale on pH 7.4 and 6.8, gave confidence to use Henderson-Hasselbalch equation (Eq-1) suggested concentration of 0.34mg/ml of $NaHCO_3$ to achieve pH 6.5.

To achieve these different pHs it was important to use a cell culture media without $NaHCO_3$ supplement. DMEM (4.5mg/ml glucose) media used above is supplied with added $NaHCO_3$ to achieve pH 7.4, therefore basal media DMEM-F12 was selected as a close alternate to DMEM as it contains most nutrients present in DMEM and importantly it was without $NaHCO_3$.

DMEM-F12 medium (7.8g/l) was initially supplemented with 10% v/v FCS, 50µg/ml ascorbate, 100U/ml penicillin, 100µg/ml streptomycin and 250µg/ml amphotericin B. Two, 0.58 and 0.34 mg/ml of $NaHCO_3$ were added separately to supplemented media to achieve pH 7.4, 6.8 and 6.5 respectively (Table 2.1 column 6-7).

One molar HCL or 1M NaOH was added drop wise to supplemented media to set the pH. pH change was confirmed using pH microelectrode (Cole Parmer). Prepared media were incubated overnight to allow pH equilibrium (5% CO_2 dependent). On the same day cells were seeded in $25cm^2$ flask in triplicate in standard medium. After overnight incubation, equilibrated pH was measured again to confirm pH stability after incubation. Standard medium was replaced by adjusted pH medium with each culture set being incubated under 3 different pH conditions 7.4, 6.8 and 6.5. Cells incubated in pH 7.4 DMEM-F12 standard medium served as control. Optimization of pH work is discussed in detail in section 2B.l.

2A.3.9 Cell culture under reduced pH 6.8 and hypoxia

For cell culture under reduced pH 6.8 and hypoxia, pH 6.8 DMEM-F12 medium (Table 2.1 column 7) was equilibrated with 2% O_2 in a hypoxic chamber and equilibrated overnight in a hypoxia incubator (5% CO_2). Cells were incubated in a hypoxia incubator with appropriate medium changed twice a week in a hypoxic chamber.

2A.3.10 Cell culture under all IVD-like physio-chemical microenvironmental conditions

To conduct a cell culture mimicking all IVD-like physio-chemical microenvironmental conditions combined (2%O_2, 2% FCS, 1mg/ml glucose and pH6.8) it was important to select a media without glucose or with low glucose concentration and without $NaHCO_3$. DMEM

low glucose medium without $NaHCO_3$ and HEPES was selected because: 1) It had 1mg/ml of glucose and 2) was also without $NaHCO_3$. Initially the media was supplemented with ascorbate, penicillin, streptomycin, amphotericin B (concentrations similar as in DMEM standard medium). DMEM low glucose medium is devoid of HEPES in addition to $NaHCO_3$. Therefore it was supplemented with 15mM HEPES which is the same concentration as in DMEM-F12. It was then divided into two portions labelled as M1 (all condition combined standard medium pH 7.4) and M2 (all conditions combined experimental medium pH 6.8).

To M1 medium an additional 3.5mg/ml of D-glucose (Fisher scientific) was added to obtain a final concentration of 4.5 mg/ml glucose, followed by addition of 10% (v/v) FCS (Table 2.1 column 8). Finally M1 medium was supplemented with 2mg/ml of $NaHCO_3$ and equilibrated as mentioned in section 2A.3.8 to achieve pH 7.4. M1 medium served as control for all IVD-like physio-chemical conditions combined experiments.

M2 medium was supplemented with 2% (v/v) FCS to represent reduced serum and reduced glucose condition. To achieve pH 6.8 under hypoxia 0.58mg/ml of $NaHCO_3$ was added to supplemented medium (Table 2.1 column 8) followed by equilibrium under hypoxic condition as mentioned in section 2A.3.9.

On the day of media preparation, cells were seeded in $25cm^2$ flask in duplicate in DMEM standard medium. Following incubation, standard medium was replaced with prepared media with each culture set being cultured with M1 and M2 medium. Cells cultured in M1 (pH 7.4) medium served as controls. Cells were incubated in normoxia and hypoxia with appropriate media changed twice a week in Class II tissue culture hood and hypoxic chamber respectively.

2A.4 Immunofluorescence

Cells were cultured in 8 well chamber slides (Falcon) for immunofluorescence staining of aggrecan and versican under all IVD-like physio-chemical microenvironmental conditions, excluding those in which pH was reduced. Plastic coverslips (Thermanox^{TM}) placed in $25cm^2$ flask were used as an alternative to 8 well chamber slides in all pH conditions but unfortunately it was found that these coverslips exhibited autofluorescence which interfered with, and compromised, the fluorescence signal from cells. Therefore images from pH conditions could not be processed.

For immunofluorescence cultured cells were fixed in 4% (PFA) in PBS at room temperature for 20 minutes and washed with PBS for 10 minutes (total of 3 washes). In order to block non-specific binding of secondary antibody, cells were incubated with 10% normal goat serum in PBS for 1 hour at room temperature. The serum type corresponded to the host species of the secondary antibody. After blocking, cells were incubated with primary antibodies i.e. monoclonal mouse anti-human aggrecan antibody (Cat No: MCA1451, AbD Serotec) (stock concentration 25µg/ml) diluted 1:20 or monoclonal mouse anti-human versican antibody (Cat No: 12C5, Developmental Studies Hybridoma Bank) (stock concentration 30µg/ml) diluted 1:300 in 10% (v/v) normal goat serum in PBS with 0.1% (v/v) Triton X-100. Cells were then washed with PBS for 10 minutes at room temperature (3 times). Following washing, cells were incubated with appropriate secondary antibodies (goat anti mouse Alexa 488 (stock concentration 2mg/ml) (Invitrogen, A11001) for chapter 3 or goat anti mouse Alexa 555 (stock concentration 2mg/ml) (Invitrogen, A21422) for chapters 4 and 5) diluted 1:300 in 10% normal goat serum in PBS with 0.1% Triton X-100 for 60 minutes at room temperature in the dark. Cells were then washed with PBS for 10 minutes at room temperature (3 times). After washing excess liquid was blotted and cells mounted in ProLong Gold antifade reagent mounting media containing 4$^{/}$, 6-diamidino- 2-phenylindole (DAPI) (Invitrogen). Images were acquired using an upright fluorescence microscope (Olympus BX51) with QImaging RETIGA-SRV camera and QCapture software. Finally black and white images were assigned false colours (blue for DAPI and green for aggrecan/versican in chapter 3; blue for DAPI and red for aggrecan/versican in chapter 4; or blue for DAPI, green for CFDA labelled BM-MSCs and red for aggrecan/versican in chapter 5).

2A.5 Cell viability

Cell viability was assessed using Live/Dead Viability/cytotoxicity fluorescence based assay (Invitrogen Cat # L3224). It simultaneously determined live and dead cells using two probes that measure known parameters of cell viability: intracellular esterase activity and cell membrane integrity. In live cells ubiquitous intracellular esterase activity enzymatically cleaves non-fluorescent cell-permeable calcein AM to intensely fluorescent calcein. It is retained well within live cells, producing an intense uniform green fluorescence (ex/em ~495 nm/~515 nm). Ethidium-1 (EthD-1) selectively enters cells with damaged membranes and produces bright red fluorescence upon binding to nucleic acids (ex/em~495 nm/~635 nm).

Cells were seeded under IVD-like physio-chemical conditions in triplicate. After 7 days of culture, phase contrast microscopy showed that in addition to plastic adherent cells, some dead floating cells were also present in the culture. To get an accurate representation of cell viability both adherent and floating cell populations were included in the analysis, thus media from all cultures was removed and centrifuged to pellet floating cells. Remaining adherent cells were washed with PBS. Floating cell pellets were also washed with PBS and resuspended in staining solution consisted of 2µM calcein-AM and 2µM EthD-1 in PBS which was then applied to adherent cells. Labelling was performed for 30-35 minutes at 37^{o}C. Green and red cells were imaged in the same field of view at appropriate focal planes under the AxioVision dieter inverted fluorescence microscope with AxioVison software to qualitatively assessed cell viability.

2A.6 Cell proliferation

Cell proliferation was assessed by quantifying lactate dehydrogenase (LDH) release from lysis of adherent cells in culture over time. LDH release was quantified using the Cytotoxicity Detection Kit^{plus} (Roche Cat# 04744926001) according to manufacturer's instructions.

LDH is a stable cytoplasmic enzyme ubiquitously present in all cells. Upon substantial cell membrane damage during cell death or cell lysis it is released into supernatant medium. LDH quantification assay is based on a 2-step colorimetric reaction. In the first step, NAD^+ is reduced to $NADH/H^+$ through LDH-catalysed conversion of lactate to pyruvate. In the second step the catalyst (diaphorase) transfers H/H^+ from $NADH/H^+$ to the tetrazolium salt INT, which is then reduced to formazan red. The degree of colour change can be measured using a spectrophotometer and directly correlates to the number of lysed cells

2A.6.1 Proliferation assay for cells cultured under hypoxia, reduced serum and reduced glucose conditions

To determined cell proliferation under hypoxia, reduced serum and reduced glucose conditions alone or in combinations, 3000 cell/cm^2 were seeded in triplicate in five 96 well plates labelled as day 0 control (baseline), day 1 control/test and day 7 control/test plates. Cells were allowed to adhere for 4 hours in DMEM standard medium. After 4 hours incubation, DMEM standard medium was aspirated from all seeded wells and washed with PBS to remove floating or loosely attached cells. Remaining adherent cells in Day 0 labelled

plate were lysed to release LDH by adding 105µl lysis solution (5µl of kit lysis solution in 100µl of PBS) to each well and incubating at 37^{o}C for 15 minutes. Day 1 and day 7 control/test plates were further incubated in DMEM standard and test media (Table 2.1 column 1) for 1 and 7 days respectively. Day 7 plates were fed twice a week with fresh media. At the end of day 1 and 7, seeded wells in both control and test plates were washed with PBS to remove medium and dead floating cells. Residual adherent cells were lysed to release LDH. Following lysis, LDH release was measured according to the manufacturer instructions.

A working solution of LDH assay reaction mixture was prepared by dissolving lyophilized cofactors in bottle 1 (blue cap – catalyst) in 1ml distilled water (dH_2O) for 10 minutes**.** One hundred microliters of reaction mixture was added to the lysed cell solution. Plates were incubated at room temperature for 15 minutes. After incubation 50µl of stop solution was added to each well. Plates were shaken using a plate reader and absorbance was measured at 492nm. In each plate 3 empty wells were set for negative control (lysis solution + 100µl reaction mixture + 50µl stop solution). Absorbance in each well was subtracted from the average absorbance in the negative controls.

For direct comparison of the amount of LDH release to the amount of lysed cells, a standard curve was constructed that involved lysing known numbers of cells. Four dilutions of cells were prepared: $1.5x10^4$, $3x10^4$, $6x10^4$ and $1.2x10^5$cells/ml of PBS. One hundred microliters of each cell dilution ($1.5x10^3$, $3x10^3$, $6x10^3$ and $1.2x10^4$ cells) was transferred to a 96 well plate in triplicate. These cells were lysed with the addition of 5µl of lysis solution and processed to measure LDH release. The absorbance was plotted against the known number of cells to give a standard curve. The cell numbers in the control and test groups was derived by plotting the absorbance against the known cell numbers from the standard curve using linear regression analysis in excel. Day 0 cell numbers were used as starting cell density (baseline) for both day 1 and 7 control and test samples.

2A.6.2 Proliferation assay of cells cultured under reduced pH 6.8/6.5, pH 6.8 combined with hypoxia and all IVD microenvironmental conditions

To measure proliferation under reduced pH 6.8/6.5, pH 6.8 combined with hypoxia and all IVD-like physio-chemical microenvironmental conditions combined, 3000 cell/cm^2 cells were seeded in five 25cm^2 flasks labelled as day 0 control (baseline), day 1 control/test and

day7 control/test flask. Cells were allowed to adhere for 4 hours in DMEM standard medium. After 4 hours incubation, DMEM standard medium was aspirated from all flasks and cells were washed with PBS to remove floating or loosely attached cells. Remaining adherent cells in Day 0 flasks were lysed to release LDH. For cell lysis, cells were incubated in 1.5ml of 2% v/v triton X-100 in PBS (enough to cover cells in flask) at 37^{o}C for 60 minutes. Day 1 and 7 control/test flasks were further incubated in DMEM standard and test media for 1 and 7 days respectively. Day 7 flasks were fed twice with fresh media. At the end of day 1 and day 7, both control and test flasks were washed with PBS to remove medium and dead floating cells. Remaining cells were lysed with 2% v/v triton X-100 in PBS. To quantify LDH release 100µl (1:15 dilution) of lysed sample was transfered to 96 well plate in triplicate and processed as mentioned previously in section 2A.6.1. The final absorbance value was multiplied by 15 (dilution factor) to get actual absorbance for each time point. A standard curve for this set of the experiment was produced as previously described in 2A.6.1 but using 2% v/v triton X as lysis solution.

2A.7 Molecular biology

2A.7.1 Cell lysis for RNA extraction

Cells were incubated with 1ml of Trizol® (Invitrogen) for approximately 5 minutes and pipetted repeatedly to ensure full cell lysis and RNA dispersion. Cell lysates were stored at -80°C.

2A.7.2 RNA extraction

Cell lysates in Trizol® were removed from -80°C, defrosted in a fume cupboard, and centrifuged at 12,000g for 15 minutes at 4°C. Supernatant was transferred to labelled microcentrifuge tubes. Two hundred microliters of chloroform was added to each sample in a fume cupboard. Tubes were shaken vigorously by hand for 20 seconds and incubated at room temperature for 3 minutes. The samples were spun at 12,000g for 15 minutes at 4°C, separating the RNA into an upper aqueous phase from the other components (i.e DNA and protein, which were in the interface and lower organic phase). The upper aqueous phase (~500µl) was transferred to a new tube without disturbing the interface. Two microliters glycoblue (Ambion) and 500µl of isopropanol were added to each sample to precipitate total RNA. The tubes were inverted and incubated at room temperature for 10 minutes followed by centrifugation at 12,000g for 15 minutes at 4°C to form a blue RNA pellet. The supernatant was carefully discarded and the pellet was washed with ice cold 75% v/v ethanol. Samples

were then centrifuged at 7,500g for 5 minutes at 4°C. Ethanol was removed, pellets were air dried and re-suspended in 21.2µl Tris EDTA buffer solution (TE buffer) (10mM Tris HCl and 1mM EDTA, pH 7.5).

2A.7.3 RNA quantification

From 21.1µl of each RNA sample solution, 1.2µl was used to quantify RNA using a Nanodrop ND 1000 Spectrophotometer with the ND-1000 V3 1.0 software. Absorbance at 260nm (absorbance for nucleic acids) and 280nm (absorbance for proteins) were used to identify concentration and purity of nucleic acid in the samples.

2A.7.4 Purity of RNA samples

Some RNA samples showed enhanced absorption at 270 nm, which was most likely due to carryover of phenol. Those samples were considered impure and purified using a published method (Krebs et al., 2009). Twenty microliters of RNA solution was thoroughly mixed with 500µl of water-saturated 1-butanol (top layer of 1:1 mixture of butanol and dH_2O) and centrifuged at 12,000g. The upper organic phase was carefully removed and discarded except for a thin layer on the top of the aqueous phase. A single extraction was sufficient to remove contaminating phenol. However, before using the purified RNA for downstream applications, residual 1-butanol was completely removed by extraction with 500µl of water-saturated diethylether (top layer of 1:1 mixture of diethylether and dH_2O). After centrifugation at 12, 000g for 1 minute the upper phase was carefully aspirated and discarded, leaving a thin organic layer on the top of the aqueous phase. Residual ether was evaporated by incubating the open tubes in a fume hood for 10 minutes at 37^oC (hot plate). RNA concentration and purity was quantified as mentioned in section 2A.7.3.

2A.7.5 Reverse transcription of RNA (cDNA synthesis)

cDNA was synthesised from pure RNA samples using the High Capacity Reverse Transcription Kit (Applied Biosystems). For cDNA synthesis RNA samples were diluted to 200ng/µl final concentration. Where samples had small quantities of RNA (i.e. < 200ng/µl) the maximum possible volume was added. A sufficient 2X master mix was prepared on ice using the reagents quantities shown in table 2.2.

Table 2.2 RT PCR master mix

Master Mix reagents X1	Volumes added (µl)
10X RT Buffer	2
25X dNTP mix (100mM)	0.8
10X RT Random Primers	2
MultiScribe™ Reverse Transcriptase	1
RNAse Inhibitor	1
Molecular biology grade H_2O	3.2

Ten microliters of master mix was mixed with 10µl of diluted RNA solution in labelled 0.5ml tubes. Tubes were placed in a thermocycler under the temperature/time settings: 25°C for 10 minutes, 37°C for 120 minutes, 85°C for 5 seconds and rapidly chilled to 4°C. After reverse transcription, cDNA samples were diluted in molecular biology grade H_2O to 5ng/µl. cDNA samples were stored at -20°C until used.

2A.7.6 Quantitative Real-Time Polymerase Chain Reaction

Quantitative Real-Time Polymerase Chain Reaction (QRT-PCR) was performed to analyse Col2A1 (collagen type II alpha 1), SOX-9, ACAN, VCAN (versican), PAX-1 (paired box-1), FOXF1 (Forkhead box F1), CA9 (carbonic anhydrase 9) and CA12 expression with MRPL19 (mitochondrial ribosomal protein L19) and EIF2B1 (eukaryotic translation initiation factor 2B, subunit 1 alpha) as housekeeping genes (HK genes). Forward and reverse primer and probe (FAM-MGB) sequences are shown in Table 2.3. Optimization of HK genes is discussed in detail in section 2B.2).

Table 2.3 Primers and probe set used in QRT PCR

Target Gene	Accession No	Primer/Probe	Sequence 5'-3'	Amplicon size (bp)
Col2A1	NM_033150	Forward Primer	GGAAGAGTGGAGACTACTGGATTGAC	75
		Reverse primer	TCCATGTTGCAGAAAACCTTCA	
		Probe	AGGCTGCACCTTGGA	
SOX-9	NM_000346	Forward Primer	CAGTACCCGCACTTGCACAAC	144
		Reverse primer	ACTTGTAATCCGGGTGGTCCTT	
		Probe	AGCTCTGGAGACTTCTGAA	
ACAN	NM_001135	Forward Primer	TCCGGAATGGAAACGTGAAT	99
		Reverse primer	CGGGAAGTGGCGGTAACAGT	
		Probe	AACTGCTGCAGACCAGG	
VCAN	NM_004385	Forward Primer	TGTGAGCAAGATACCGAGACATGT	63
		Reverse primer	ATTTGTAGCACTGCCCTTGGA	
		Probe	ACTATGGCTGGCACAAA	
PAX-1	NM_006192	Forward Primer	ACCCCCGCAGTGAATGG	65
		Reverse primer	GGCCGACTGAGTGTATTTAATGTCT	
		Probe	CTAGAGAAACCTGCCTTAGA	
FOXF1	NM_001451	Forward Primer	GCCGTATCTGCACCAGAACA	115
		Reverse primer	CGTTGAAAGAGAAGACAAACTCCTT	
		Probe	CTGCAAGGCATCCCG	
CA9	NM_001216	Forward Primer	AGGGTGTCATCTGGACTGTGTTT	62
		Reverse primer	GGGTGTGGAGCTGCTTAGCA	
		Probe	ACCAGACAGTGATGCTG	
CA12	NM_001218	Forward Primer	CGTGCTCCTGCTGGTGATCT	69
		Reverse primer	AGTCCACTTGGAACCGTTCACT	
		Probe	AAAGGAACAGCCTTCCAG	
MRPL19	NM_014763	Forward Primer	CACCGCCCCGTGGAA	59
		Reverse primer	TCCCCTTCGAGGAATGAATTC	
		Probe	AACGCAGGTTCTTGAGTC	
EIF2B1	NM_001414	Forward Primer	TCATCAAAGATGGAGCGACAATA	62
		Reverse primer	CCAGGACTCTCAGGACCACTCT	
		Probe	TGACTCACGCCTACTC	

The QRT-PCR simultaneously amplifies and quantifies a targeted DNA molecule after each amplification cycle in real time through the use of fluorogenic probes. The basis of QRT-PCR is summarized in Figure 2.3.

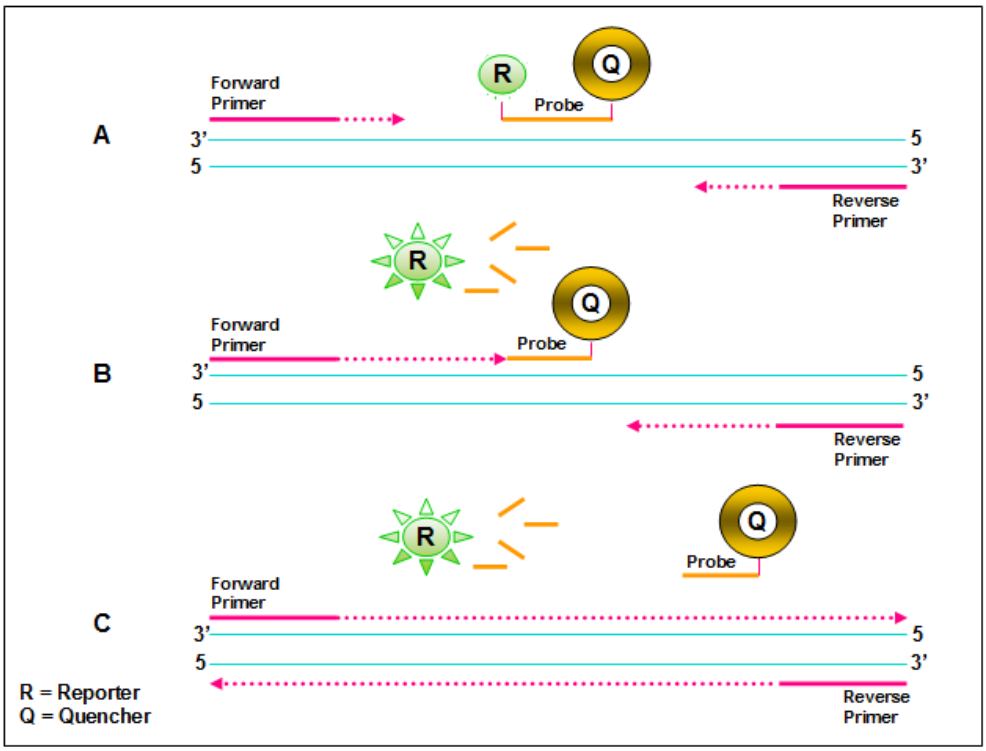

Figure 2.3 QRT-PCR. It is based on the same principle as conventional PCR. (A) Forward and reverse primers and target gene sequence specific probe bind to the target DNA. The probe contains two fluorescent labels, a reporter (at 5'end) and a quencher dye (at 3' end). When the probe is intact, the quencher suppresses the fluorescence of the reporter by the use of fluorescence resonance energy transfer (FRET). (B) When Taq-polymerase enzyme creates a complementary strand it cleaves the probe due to its 5'-3' exonuclease activity. (C) The reporter dye releases from the double stranded DNA being created. Once separated from the quencher, the reporter dye emits light in its excited state and this then quantified by the computer.

For QRT-PCR sufficient volume of master mix (Table 2.4) was prepared to run each sample in triplicate.

Table 2.4 QRT PCR master mix

Master Mix reagents X1	**Volumes added µl**
2X ABI FAST Universal Taqman mastermix	5
Molecular biology-grade H_20	0.5
Forward primer (90µM stock) (diluted 1:10 to form a working stock)	1 (900nM final concentration)
Reverse primer (90µM stock) (diluted 1:10 to form a working stock)	1 (900nM final concentration)
FAM-MBG Probe (100µM stock) (diluted 1:20 to form a working stock)	0.5 (250nM final concentration)
cDNA (5ng/µl)	2

Two microliters of cDNA sample was added to 8µl of master mix in a 96-well plate to make a final volume of 10µl per well. The plate was sealed with optical adhesive film (Applied Biosystems) and spun for 1 minute. The reactions were carried out in Applied Biosystems Step One Plus PCR system. PCR cycle was consisted of initial denaturation step at 50ºC for 2 minutes, a Taq activation step at 95ºC for 10 minutes, then amplification with 40 PCR cycles of denaturation at 95ºC for 15 seconds followed by annealing and extension at 60ºC for 1 minute.

Once the reaction was completed a Ct value was assigned to each sample by the computer software which represents the number of cycles needed until an exponential increase in fluorescence from reporter dye was detected. QRT-PCR data of BM-MSCs and degenerate NP cells cultured alone (chapter 3 and 4 respectively) was normalized to average of HK genes MRPL19 and EIF2B1 using the 2-ΔCt method. However, QRT-PCR data of BM-MSCs and degenerate NP cells co-cultured was normalized to average of HK genes MRPL19 and EIF2B1 and gene expression in BM-MSCs and degenerate NP cells co-cultured under control conditions (baseline control) respectively using the 2-ΔΔCt method (Livak and Schmittgen, 2001) (Table 2.5).

Table 2.5 Calculations for QRT-PCR data analysis

Step	**Calculations for 2-ΔCt**	**Calculation for 2-ΔΔCt**
1	Average of triplicate Ct of average MRPL19 & EIF2B1 (Av MRPL19 & EIF2B1)	Average of triplicate Ct of average MRPL19 & EIF2B1 (Av MRPL19 & EIF2B1)
2	ΔCt=Ct (target gene)-Ct (Av MRPL19 & EIF2B1)	ΔCt=Ct (target gene)-Ct (Av MRPL19 & EIF2B1)
3	ΔCt average	ΔCt average
4		ΔΔCt = (ΔCt average sample)-(ΔCt average control)
5	**2-**ΔCt=2^- (ΔCt average)	2-ΔΔCt=2^- (ΔΔCt average)
6	Standard error of the mean (SE)= [STDEV(ΔCt)/SQRT(n)]	SE= [STDEV(ΔCt)/SQRT(n)]
7	**+ Error**=(2-ΔCt-SE)-(2-ΔCt) **– Error**=(2-ΔCt)-(2-ΔCt+SE)	**+ Error**=(2-ΔΔCt-SE)-(2-ΔΔCt) **– Error**=(2-ΔΔCt)-(2-ΔΔCt+SE)

2A.7.7 Statistical analysis

Mann-Whitney statistical analysis was performed using GraphPad InStat software to compare the level of expression of target genes in BM-MSCs and NP cells cultured alone and co-cultured under IVD-like physio-chemical microenvironmental conditions with cells cultured under control conditions. A p value of ≤ 0.05 was considered as significant.

Chapter 2B: Optimization of methodology

2B.1 Optimization of pH monitoring and maintenance

It was acknowledged that monitoring and maintenance of specific pHs during the course of the experiment was challenging. Therefore the pH work was optimised to ensure a reproducible methodology.

Use of an appropriate cell culture system (i.e. well plate or tissue culture flask) to maintain adjusted pH is an important step during pH work. Initially 6 well plates were used. Three millilitres of pre-adjusted pH medium (equilibrated overnight as mention in 2A.3.8) was added to each well and incubated overnight. To measure pH stability, a pH meter microelectrode probe was placed in each well separately. Due to the small volume of medium in each well, it was difficult to fully submerge the probes electrode and directly measure accurate pH in the 6 well plate after incubation. In the following attempt, medium from each well was aspirated using 5 ml plastic pipettes and transferred to 7ml bijous tubes. The pH meter microelectrode probe was then placed in those tubes and pH was measured. However it was found that all pH values were slightly higher than equilibrated (Table 2.6).

Table 2.6 pH values of medium incubated in 6 well plate and aspirated into bijous

Adjusted pH	After incubation
Well-1 pH7.4	7.53
Well-2 pH7.4	7.55
Well-3 pH 6.8	7.13
Well-4 pH 6.8	6.89
Well-5 pH 6.5	6.63
Well-6 pH 6.5	6.63

It was assumed that this increase in pH values was due to the loss of CO_2 from the culture system during the measuring procedure which directly affected pH of the medium. It was thus hypothesised that a more appropriate method would be to immediately check the pH without allowing time for the media sample to lose CO_2. With this initial experiment two things were realised; use of a large volume of pH medium and less time for pH measurement would help to stabilise the pH. To avoid these problems, 25cm^2 flasks were utilized which permitted the use of a large volume of pH medium. Six millilitres of pre-adjusted pH medium

was added to seeded cells and flasks were incubated overnight. Following incubation, media from flasks was directly poured into bijous and the pH microprobe was inserted quickly. It was found that this procedure was faster than the previous method and all pHs were stable after overnight incubation. Based on this, it was decided to use 25cm^2 flask for pH related work.

During cell culture, cells were fed with fresh medium twice a week. For the pH work it was also decided to optimize feeding time for both BM-MSCs and NP cells because cellular metabolic end products can alter adjusted pH of the medium. For this purpose BM-MSC (n=1) and NP cells (n=1) were seeded in duplicate in 25cm^2 flasks. Cells were incubated in pH adjusted media for 48 and 72 hours followed by pH measurement. It was found that until 48 hours of incubation all pH media showed slight changes in adjusted pH, but after 72 hours larger changes were observed (Table 2.7). Based upon this finding it was decided to feed cells every 48 hours.

Table 2.7 pH monitoring after 48 and 72 hours to optimize cell feeding time

Adjusted pH	**pH change after 48 hours**		**pH change after 72 hours**	
	BM-MSCs	**NP cells**	**BM-MSCs**	**NP cells**
pH 7.4	7.42 & 7.43	7.44 & 7.45	7.45 & 7.43	7.36 & 7.38
pH 6.8	6.77 & 6.80	6.77 & 6.79	6.72 & 6.70	6.71 & 6.72
pH 6.5	6.48 & 6.49	6.46 & 6.49	6.43 & 6.41	6.41 & 6.42

Based on this optimization work, for all pH related experiments cells were seeded in 25cm^2 flask with 6 ml of pH adjusted media with feeding every 48 hours.

2B.2 Housekeeping gene (HKGs) identification and validation

QRT-PCR is a commonly used tool to quantify gene expression changes with respect to the specific biological conditions. However, sample to sample variations in reaction efficiency and errors in sample quantification during the workflow of a PCR assay can obscure real changes. To offset these technical issues, normalization with a stably expressed endogenous control referred to as a housekeeping (HK) gene is usually practiced in QRT-PCR analysis (Bustin, 2000, Wong and Medrano, 2005). One of the main requirements of a HK gene is that its expression must not be affected by any experimental treatment to avoid misinterpretations of the study findings (Radonic et al., 2004). However, increasing evidence suggests that many frequently used HK genes can modify their expression under different experimental conditions [(e.g. a change in serum concentration affected beta actin (β-actin) and glyceraldehyde 3-phosphate dehydrogenase (GAPDH) expression in fibroblasts (Schmittgen and Zakrajsek, 2000), static compression affected β-actin expression in NP cells (Yurube et al., 2011) and hypoxia affected GAPDH expression in MSCs] (reviewed in depth by (Bustin, 2000). Therefore it is of utmost importance to verify the expression stability of a HK gene in an individual experiment prior to its use for normalization to obtain reliable biological effect. This study aimed to identify stably expressed HK genes in each cell type and experimental condition used here.

2B.2.1 Use of human endogenous control 96 well plates and initial identification of the most appropriate HK genes

Fortunately several biotech companies provide panels of HK genes to simplify the selection of endogenous controls from a large panel of available potential HK genes. Initially the TaqMan® Array Human Endogenous Control 96 well Plate (Life technologies Cat # 4426700) was used to identify stably expressed genes under normoxia and hypoxia in both BM-MSCs and NP cells.

BM-MSC (n=1) and degenerate NP cells (n=2) were cultured under normoxia and hypoxia for 7 days. RNA was extracted and reverse transcribed as detail previously (section 2A 7.1-7.5). The human endogenous control 96 well plate contains 32 HK genes, plated in triplicate. These genes are lyophilised and reconstituted when liquid is added. To each well 2µl of cDNA (1-100ng), 8µl of mastermix (2X ABI FAST Universal Taqman mastermix) and 10µl of Molecular biology-grade H_20 was added to make up 20µl final reaction mixture. QRT-PCR was then performed using cycling conditions detailed previously (section 2A 7.6).

For data analysis, differences in Ct expression (ΔCt) of each gene in BM-MSCs and NP cells under normoxia and hypoxia were determined. These differences were then averaged and genes showing ≤0.5 ΔCt with smaller standard deviations were selected as most stable HK genes in both BM-MSCs and NP cells under changing O_2 tension (Figure 2.4). Additionally it was further decided to include genes which were sufficiently expressed i.e. Ct values between 20-27 and in the range of most target genes. The selection criteria identified that classical HK genes 18S, GAPDH and β-actin were least stable and most influenced genes by hypoxia. This suggests that ideal and universal HK genes do not exist and warrants validation of HK genes in each experimental condition. B2M (beta-2-microglobulin), RPLPO (ribosomal protein, large, P0), UBC (ubiquitin C), POLR2A (polymerase (RNA) II (DNA directed) polypeptide A, 220kDa), CASC3 (cancer susceptibility candidate 3), CDKN1B (cyclin-dependent kinase inhibitor 1B (p27, Kip1)), PSMC4 (proteasome (prosome, macropain) 26S subunit, ATPase, 4), EIF2B1, PES1 (pescadillo homolog 1, containing BRCT domain (zebrafish)), ABL1 (v-abl Abelson murine leukemia viral oncogene homolog 1), MRPL19, POP4 (processing of precursor 4, ribonuclease P/MRP subunit (S. cerevisiae), and RPS17 (ribosomal protein S17) with ≤0.5 ΔCt and Ct values between 20-27 fulfilled the stable gene validation criteria (Table 2.8). However, it was not practical to further validate all these genes together due to high cost and time issues; therefore it was decided to initially shortlist 4 genes and validate their expression. Firstly B2M was selected based on demonstrated results of stability in NP cells in a recent investigation i.e. identified as best HK gene during static compression (Yurube et al., 2011). Of the remaining short listed genes, 3 genes (RPLPO, MRPL19 and RPS17) encode ribosomal proteins. From this set, RPLPO and MRPL19 were selected as they better match the selection criteria. PubMed gene database identified involvement of PES1 in cell proliferation and ABL1 in cell differentiation and stress responses. It was assumed that genes involved in these functions may be affected by microenvironmental conditions studied here and therefore may be inappropriate for normalization purposes. From the remaining genes EIF2B1 was selected as the fourth best gene to further validate.

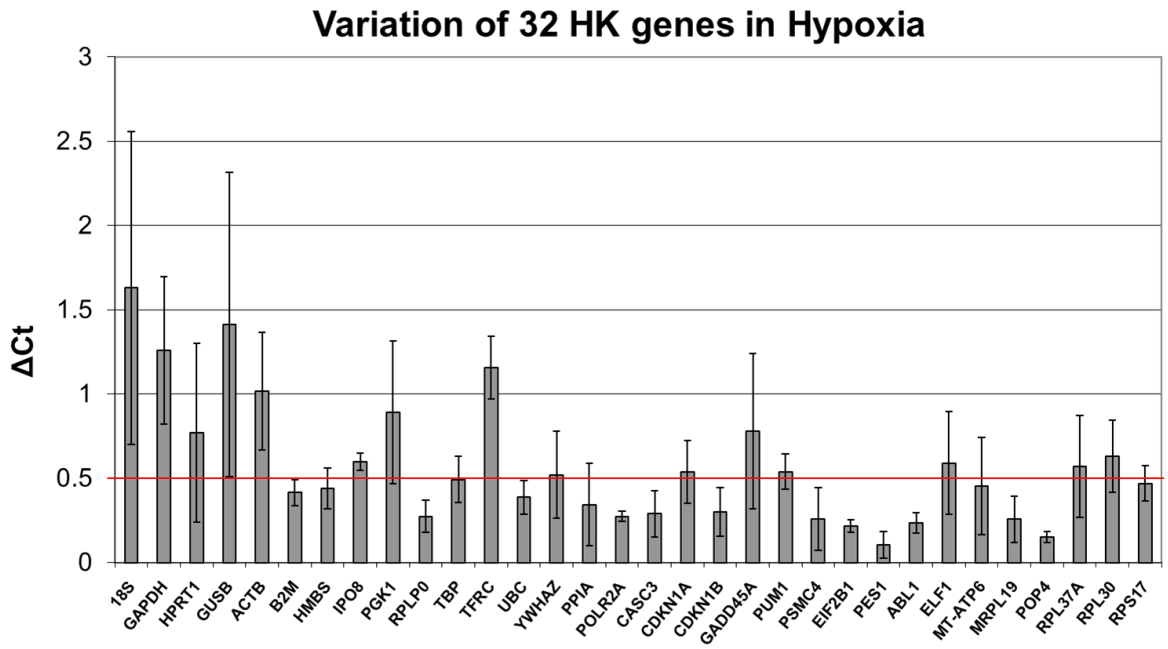

Figure 2.4 Initial identification of stable HK genes in MSCs and NP cells culture under hypoxia. Red lines shows gene showing ≤0.5 ΔCt with smaller SD. These genes were short listed as best stable genes under hypoxia.

Table 2.8 Ct values in BM-MSC and NP cells cultured under normoxia and hypoxia. Ct expression between 20-27 was used as second criteria to short list best stable genes under hypoxia

HK genes	BM-BM-MSCs		NP sample 1		NP sample 2		ΔCt ≤ 0.5
	Normoxia	Hypoxia	Normoxia	Hypoxia	Normoxia	Hypoxia	
18S	9	11	10	10	10	6	No
GAPDH	20	19	20	20	20	18	No
HPRT1	27	27	28	28	28	27	No
GUSB	26	26	29	26	26	25	No
ACTB	20	21	23	22	22	21	No
B2m	22	22	22	23	23	22	**Yes**
HMBS	28	28	29	28	29	28	No
IPO8	28	27	28	28	28	28	No
PGK1	24	23	24	24	25	24	No
RPLP0	21	22	22	22	22	22	**Yes**
TBP	30	30	30	29	30	29	No
TFRC	26	27	26	27	27	28	No
UBC	22	22	23	23	23	22	**Yes**
YWHAZ	30	30	31	31	31	30	No
PPIA	22	22	23	23	23	22	No
POLR2A	26	27	27	27	27	27	**Yes**
CASC3	26	25	26	26	26	25	**Yes**
CDKN1A	23	24	25	25	25	25	No
CDKN1B	26	26	27	27	27	26	**Yes**
GADD45A	26	27	29	27	28	28	No
PUM1	26	25	26	26	26	25	No
PSMC4	27	27	27	27	28	27	No
EIF2B1	27	27	28	27	28	27	**Yes**
PES1	26	26	26	26	26	26	**Yes**
ABL1	26	26	26	27	26	26	**Yes**
ELF1	27	27	27	27	28	27	No
MT-ATP6	20	21	21	21	20	20	No
MRPL19	27	27	27	27	27	27	**Yes**
POP4	26	27	27	27	28	27	**Yes**
RPL37A	22	23	23	23	23	23	No
RPL30	29	29	29	29	29	28	No
RPS17	22	22	23	22	23	22	**Yes**

2B.2.2 Validation of the most appropriate HK genes under hypoxia and reduced serum

Expression of initially selected 4 candidate HK genes was validated in both BM-MSCs and NP cells cultured alone and co-cultured under hypoxia and reduced serum alone and in combination. β-actin a commonly used HK gene which was shown to have poor stability, was also used as a comparator. A freely available Microsoft excel based software package NormFinder was used for data analysis (Andersen et al., 2004, Andersen et al., 2010, Seol et al., 2011).

NormFinder identifies the optimal HK genes among a set of candidate genes. It ranks the set of candidate reference genes according to their expression stability in given sample subgroups such as untreated/treatment1/treatment2 or sick/healthy. It estimates both the intra- and the intergroup expression variation in the sample set, and calculates gene "stability" value. This represents a practical measure of the systematic error that will be introduced using the investigated gene. Stability value is a direct measure for the estimated expression variation; lower value implies a higher stability in gene expression (least variable gene) and vice versa (Andersen et al., 2004, Andersen et al., 2010).

Human BM-MSCs (TH092 and TH094) and degenerate NP cells (HH0446 and HH0454) were cultured alone or co-cultured under hypoxia or/and reduced serum for 7 days. RNA was extracted and reverse transcribed as mentioned previously. QRT-PCR for each sample was performed in triplicate using 5µl of 2x ABI FAST Universal Taqman mastermix, 2.5µl of molecular biology-grade H_20, 0.5µl of primer/probe set of each HK gene and 2µl of target cDNA. QRT-PCR was performed using cycling conditions described in section 2A.7.6. As primer and probe set of B2M, RPLPO MRPL19, EIF2B1 and β-actin genes were pre-designed (applied biosystem) (B2M part no: 4333766F, RPLPO part no: 4333761F. β-actin part no: 401846, EIF2B1 assay ID: Hs01106484_m1, MRPL19 assay ID Hs00608519_m1) therefore no sequence information is available.

For data analysis QRT-PCR Ct data was transformed onto linear scale as required for Normfinder software. Ct values of each sample run in triplicates were averaged and transformed to linear scale relative quantities (Q) using **2-**ΔCt= 2^- (ΔCt average) formula where ΔCt = Ct of the highest abundant sample - Ct of the each sample. These quantities were then imported into NormFinder software which were processed as described in its manual (Andersen et al., 2010).

Normfinder analysis identified that MRPL19 and EIF2B1 showed lower stability values alone as a pair in BM-MSCs and degenerate NP cells cultured alone and co-cultured under hypoxia and reduced serum (Figure: 2.5). Lower stability value means that these genes will introduce the least systematic error when used as normalization genes.

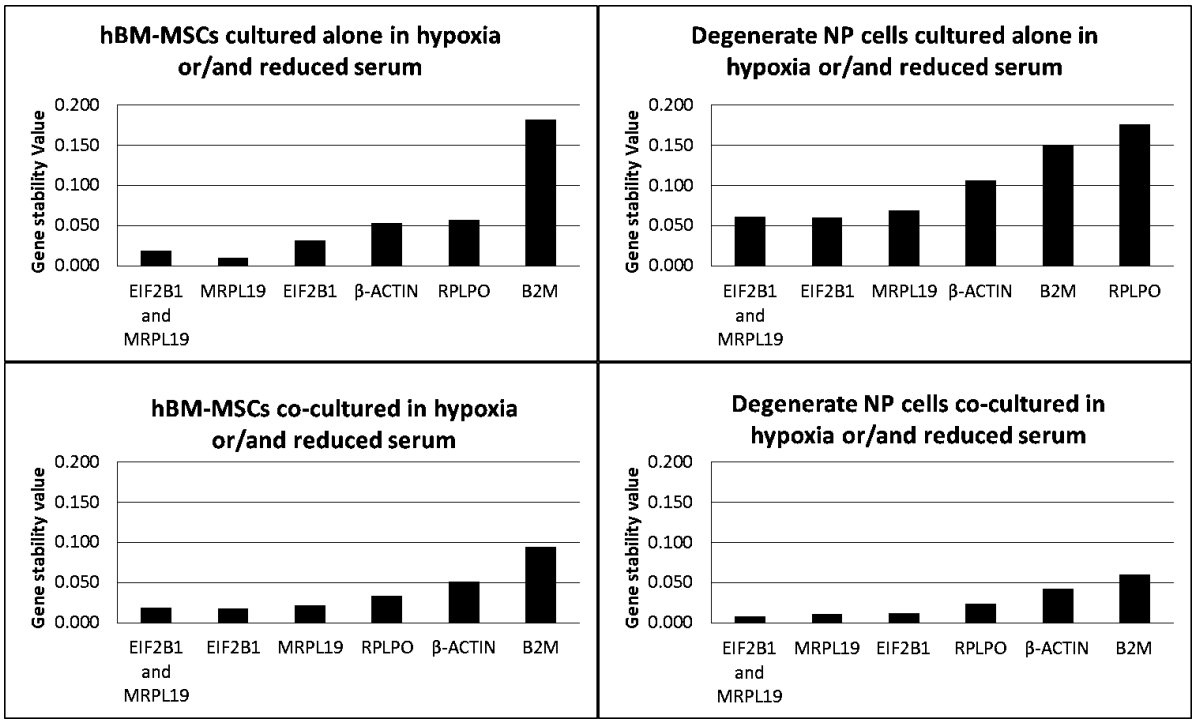

Figure 2.5 Stability values of B2M, EIF2B1, RPLPO, MRPL19 and β-ACIN calculated by Normfinder. EIF2B1 and MRPL19 pair combination showed lower stability value in human BM-MSCs and degenerate NP cells cultured under hypoxia or/and reduced serum.

Based on the findings of this work it was decided to use the average of this pair of HK genes (MRPL19 and EIF2B1) to normalize gene expression during all BM-MSCs and NP culture experiments under hypoxia or/and reduced serum conditions.

2B.2.3 MRPL19 and EIF2B1 are the most appropriate HK genes under all test conditions

Expression of MRPL19 and EIF2B1 was also studied under all other test condition combinations in both BM-MSCs and NP cells. The average of this pair of HK genes showed less than 1Ct difference in all conditions compared to control conditions. Therefore these genes were selected as stable HK genes. Gene expression under all tested conditions in this thesis was normalized to average of MRPL19 and EIF2B1.

3 Chapter 3 Effect of an intervertebral disc-like physio-chemical microenvironment on degenerate NP cell behaviour

3.1 Introduction

LBP is a debilitating, and economically important disorder. Although, its exact aetiology is not yet fully elucidated, there is an association between LBP and IVD degeneration in the majority of cases (Hughes et al., 2012). Reduction in nutrient transport and accumulation of acidic waste products in the disc centre is believed to be one of the main factors contributing to disc degeneration (Nachemson et al., 1970, Holm and Nachemson, 1988, Kauppila et al., 1994, Horner and Urban, 2001, Razaq et al., 2003, Benneker et al., 2005).

The IVD is the largest avascular structure in the body. NP cells rely on long distance EP diffusion route for supply of nutrients and removal of metabolic waste products (Brodin, 1955, Nachemson et al., 1970, Urban et al., 1977, Ogata and Whiteside, 1981, van der Werf et al., 2007). Thus, they experience steep gradients of nutrients (low O_2 and glucose) and metabolite concentration (high lactic acid producing an acidic pH) (Maroudas et al., 1975, Holm et al., 1981, Stairmand et al., 1991, Bartels et al., 1998, Johnson et al., 2008). It has been proposed that conditions that affect the EP nutritional route such as EP calcification may further disturb the transport of nutrients and removal of metabolic waste resulting in a hostile microenvironment (Roberts et al., 1996, Benneker et al., 2005, Soukane et al., 2007, Jackson et al., 2011a, Jackson et al., 2011b).

The lowest values of O_2, glucose and high levels of lactic acid and low pH measured or predicted in degenerate discs are evidences for disturb transport (Maroudas et al., 1975, Holm et al., 1981, Stairmand et al., 1991, Bartels et al., 1998, Johnson et al., 2008). NP cells may be susceptible to degenerative consequences of these hostile conditions (Horner and Urban, 2001, Razaq et al., 2003, Bibby and Urban, 2004).

It is believed that disc degeneration starts at the cellular level which then progressively cascade into structural tissue abnormalities (Ponnappan et al., 2011). A number of studies using animal discs or isolated IVD cells have been conducted to study the influence of reduced nutrient and acidic conditions on NP cell viability and functioning in an attempt to establish an indirect link between IVD harsh microenvironmental conditions and degenerative changes. These studies indicate that disc cell density is regulated by nutritional constraints and acidic conditions. It was shown that NP cells can survive glucose deprivation

for 1 day (Bibby and Urban, 2004) but die within 3 days without glucose (Horner and Urban, 2001). Using animal discs, decreased cell viability was shown under reduced glucose (10mM) compared to 25mM glucose in control conditions (Illien-Junger et al., 2010, Junger et al., 2009). These studies suggest that glucose may be an important nutrient for NP cell viability. In another study it was suggested that disc cells also require serum or serum derived growth factors for normal functioning as serum withdrawal induced growth arrest and cell senescence (Johnson et al., 2008).

It was shown that disc acidic pH levels also have profound effects on disc cell viability. Acidic pHs as low as pH 6.2 and 6.0 compared to pH 7.4 were shown to cause cell death (Horner and Urban, 2001, Bibby and Urban, 2004). It was also found that a combination of acidic pH (6.7 and 6.2) with reduced glucose (0.5mM and 0mM) induced more cell death compared to each factor acting alone suggesting that combination of harsh nutritional and acidic conditions may be more detrimental to disc cell survival (Bibby and Urban, 2004). Cells were shown to survive under hypoxic (0% O_2) and normoxic (20% O_2) conditions, suggesting that O_2 may have limited effect on cell survival (Horner and Urban, 2001, Bibby and Urban, 2004).

Apart from cell viability, the effect of disc microenvironment on ECM synthesis has also been reported using animal discs or isolated NP cells. The effect of hypoxia on synthesis of ECM has generated conflicting results. Using isolated NP cells beneficial effects of hypoxia (1-5% O2) on ECM genes and GAG synthesis has been reported (Risbud et al., 2005, Mwale et al., 2011, Pei et al., 2012, Neidlinger-Wilke et al., 2012). However, using animal discs increased GAG synthesis was shown at 5% O_2 that then decreased at 1% O_2. More work is required to establish the exact effect of hypoxia on disc matrix production. However, these studies may be complicated by the variation in the O_2 levels reported in the disc. It was shown that glucose deprivation (i.e. concentrations of 0.5 and 0mM) down regulated ACAN and COL2A1 gene (Rinkler et al., 2010, Neidlinger-Wilke et al., 2012) and collagen II protein expression (Johnson et al., 2008) in NP cells. Acidic pH levels were detrimental to ECM genes (ACAN, COL2A1), protein and PG synthesis in discs and isolated NP cells (Ohshima and Urban, 1992, Razaq et al., 2003, Neidlinger-Wilke et al., 2012). There was also down regulation in the synthesis of TIMPs with some increase in MMPs involved in matrix turnover (Razaq et al., 2003). It is suggested that acidic pH is potentially detrimental to disc function and can negatively impact disc architecture and biomechanics. All the above

studies indicate that IVD-like microenvironmental conditions influence NP cell behaviour that may cascade into pathological processes observed within the IVD.

To date only a few investigators have reported the response of human disc cells to disc microenvironmental conditions. Rinkler and colleagues, in addition to bovine NP cells, also studied the effect of glucose reduction (0.5mM and 0mM) on the gene expression of human degenerate NP cells. They showed that similar to animal disc cells, glucose reduction also decreased ACAN and COL2A1 gene expression in human degenerate NP cells. It was suggested that glucose deprivation may be detrimental to disc cell gene expression (Rinkler et al., 2010). More recently two independent studies from Feng *et al* and Yang *et al* have studied the effect of hypoxia on human degenerate NP cells gene expression (Yang et al., 2013, Feng et al., 2013). Both groups were investigating the potential of transplantation of autologous IVD cells for cell based disc therapies. They cultured human NP cells under hypoxia with the aim to increase their regenerative potential. Feng *et al* showed that hypoxia increased COL2A1, ACAN and SOX-9 gene expression along with GAG and collagen II synthesis in degenerate NP cells (Feng et al., 2013). Yang *et al* showed higher production of PGs and collagen II by human degenerative NP cells isolated and expanded in hypoxic conditions compared to normoxic conditions (Yang et al., 2013). These limited studies indicate that similar to animal disc cells, human disc cells also show response to the changing microenvironmental conditions. However, these studies were limited as only a small number of conditions mimicking the disc microenvironment were investigated. To fully understand the impact of the disc microenvironmental conditions on resident cell behaviour, it is important to investigate all factors representing the disc microenvironment in different possible combinations. As such this will increase our understanding of disc cell biology/ pathology. As availability of normal healthy human disc tissue is very limited for research purposes, this study will investigate the effects of IVD-like physio-chemical microenvironmental conditions on NP cells isolated from human degenerate disc.

3.1.1 Aims

This work aimed to study the effect of the IVD-like physio-chemical microenvironment on human NP cell behaviour (i.e. cell viability, proliferation and gene and protein expression). Hypoxia (2% O_2), limited nutrients [reduced glucose (1mg/ml or 5mM) and reduced serum (2% FCS) and acidic pHs (6.8 & 6.5 representative of moderate & severely degenerated discs

respectively (Wuertz et al., 2009a))] conditions alone and in combination were used to represent the IVD-like physio-chemical microenvironment.

For this work it was hypothesized that the IVD-like physio-chemical microenvironmental conditions would affect degenerate NP cell survival, proliferation, gene expression and protein synthesis.

The specific aims were to:

1. Evaluate the stimulatory or inhibitory effects of IVD-like physio-chemical microenvironmental conditions on degenerate NP cell survival and proliferation
2. Assess the stimulatory or inhibitory effects of IVD-like physio-chemical microenvironmental conditions on degenerate NP cell gene (COL2A1, SOX-9, ACAN, VCAN, PAX-1, FOXF-1, CA9 and CA12) and (aggrecan and versican) protein expression.

3.2 Materials and methods:

3.2.1 NP cell culture

NP cells used in this study were isolated from human degenerate NP tissue samples listed in (Table 3.1). NP cells were extracted and maintained as mentioned previously (Chapter 2, section 2A.1-2). To determine the effect of *in vitro* expansion in monolayer on degenerate NP cell gene profile, expression of COL2A1, SOX-9, ACAN and VCAN was analysed at passage 1 (First passage after extraction) and passage 3-4 (passage used in experiments). The NP cells used in the *in vitro* expansion analysis are detailed in table 3.2.

Table 3.1 Details of degenerate NP tissues used in this study

Sample No	Patient ID	Sex	Age (years)	Disc Level	Grade
1	HH0498	F	27	L4/5	7
2	HH0513	M	54	L4/5	7
3	HH0515	M	45	L5/S1	7
4	HH0409	F	47	L5/S1	9
5	HH0422	M	25	L4/5	6
6	HH0428	M	37	L5/S1	8
7	HH0083	M	48	L5/S1	5
8	HH0450	F	54	L1/2	4
9	HH0527	M	19	L5/S1	6
10	HH0446	M	31	L5/S1	6
11	HH0454	F	78	L4/5	Unknown
12	HH0447	F	41	L5/S1	8
13	HH0373	F	33	L4/5	9
14	HH0360	F	26	L5/S1	6
15	HH0445	F	37	L5/S1	7
16	HH0482	F	42	L4/5	8
17	HH0440	M	31	L4/5	9
18	HH0397	M	37	L4/5	5
19	HH0403	M	53	L5/S1	5
20	HH0489	M	60	L4/5	8

Table 3.2 Details of degenerate NP samples used in *in vitro* expansion study

Sample No	Patient ID	Sex	Age (years)	Disc Level	Grade	Days in culture
1	HH0070	M	59	L4/5	7	47 days
2	HH0081	Unknown	47	L5/S1	6	47 days
3	HH0083	M	48	L5/S1	5	47 days
4	HH0331	F	56	L4/5	9	33 days
5	HH0324	F	47	L5/S1	8	33 days

3.2.2 Degenerate NP cell culture under IVD-like physio-chemical microenvironmental conditions

Degenerate NP cells at passage 3-4 were seeded at a density of $1.2x10^4$cells/cm^2 in 6 well plate or 25cm^2 flask and cultured under IVD-like physio-chemical microenvironmental conditions for 7 days using media formulations (Table 2.1) and methodology detailed previously (chapter 2, section 2A.3).

3.2.3 Cell viability

Cell viability was assessed after 7 days of culture under IVD-like physio-chemical microenvironmental conditions using a Live/Dead viability/cytotoxicity fluorescence-based assay, following the protocol described previously (chapter 2, section 2A.5). Samples listed in table 3.3 were used in cell viability analysis.

Table 3.3 Degenerate NP samples used in cell viability assay

IVD-like conditions	**NP tissue samples**
1- Hypoxia (n=3) 2- Reduced serum (n=3) 3- Reduced serum & hypoxia (n=3) 4- Reduced glucose (n=3) 5- Reduced glucose & Hypoxia (n=3) 6- Reduced serum & reduced glucose (n=3) 7- Reduced serum, reduced glucose & hypoxia (n=3)	HH0498 HH0513 HH0515
8- Reduced pH 6.8 and 6.5 (n=3)	HH0409 HH0422 HH0428
9- Reduced pH 6.8 and Hypoxia (n=1) 10-All environmental conditions combined (n=1)	HH0083

3.2.4 Cell proliferation

The proliferation of degenerate NP cell cultured under IVD-like physio-chemical microenvironmental conditions was assessed at day 1 and day 7 utilising the LDH proliferation assay protocol detailed previously (chapter 2, section 2A.6). NP cells isolated from sample number HH0083 (n=1) were used in this assay. As only one NP cell sample was used for this assay, the student t test was performed to obtain statistical significance. It is important to highlight that any statistical significance observed is the difference between technical replicates and does not represent biological sample variation.

3.2.5 Gene expression

For gene expression degenerate NP cells cultured under IVD-like physio-chemical microenvironmental conditions were incubated with 1ml of Trizol®. RNA was extracted and reverse transcribed as previously detailed (Chapter 2, section 2A.7.1-7.5). QRT-PCR was then conducted with primers and probes for NP classical and novel markers with HK genes mentioned in Table 2.3 (chapter 2, section 2A7.6-7). NP cells isolated from tissues samples listed in table 3.4 were used in gene expression analysis.

Table 3.4 Degenerate NP samples used for the separate experiments analysing gene expression following culture in the differing conditions

IVD-like conditions	NP tissue samples
1- Hypoxia (n=8)	HH0446 HH0454 HH0447 HH0373 HH0360 HH0445 HH0482 HH0440
2- Reduced serum (n=5) 3- Reduced serum and hypoxia (n=5)	HH0446 HH0454 HH0447 HH0373 HH0360
4- Reduced Glucose (n=3) 5- Reduced glucose & Hypoxia (n=3) 6- Reduced serum and reduced glucose (n=3) 7- Reduced serum and reduced glucose and hypoxia (n=3)	HH0445 HH0482 HH0440
8- Reduced pH 6.8 & 6.5 (n=3)	HH0409 HH0422 HH0428
9- pH 6.8 & Hypoxia (n=3) 10- All IVD conditions combined (n=3)	HH0083 HH0450 HH0527

3.2.6 Assessment of ECM protein synthesis by immunofluorescence in degenerate NP cells cultured under IVD-like physio-chemical microenvironmental conditions

An immunofluorescence assay was used to assess aggrecan and versican protein expression under IVD-like physio-chemical microenvironmental conditions (i.e. hypoxia, reduced

serum, reduced glucose alone and in combinations). Cells were cultured in 8 well chamber slides using respective media formulations (Chapter 2, section 2A.3). Immunofluorescence staining was performed as previously reported (chapter 2, section 2A.4). Samples listed in Table 3.5 were used in immunofluorescence analysis.

As stated in chapter 2, section 2A.4 due to autofluorescence issues, images from all pH conditions were not analysed and included in this study.

Table 3.5 Degenerate NP samples used for the separate experiments analysing aggrecan and versican expression by immunefluorescence analysis following culture in the differing conditions

IVD-like conditions	**NP cells used for ACAN staining**	**NP cells used for VCAN staining**
1- Hypoxia 2- Reduced serum 3- Reduced glucose 4- Reduced serum & reduced glucose 5- Reduced serum & hypoxia 6- Reduced glucose & hypoxia 7- Reduced serum, reduced glucose & hypoxia	HH0397 HH0489	HH0397 HH0403 HH0489

3.3 Results

Degenerate NP cells expanded in monolayer for approximately 40 ± 4.427 days (passage 3-4) showed a significant decrease in COL2A1 (p<0.05) with no change in SOX-9, ACAN and VCAN gene expression (Figure 3.3.1).

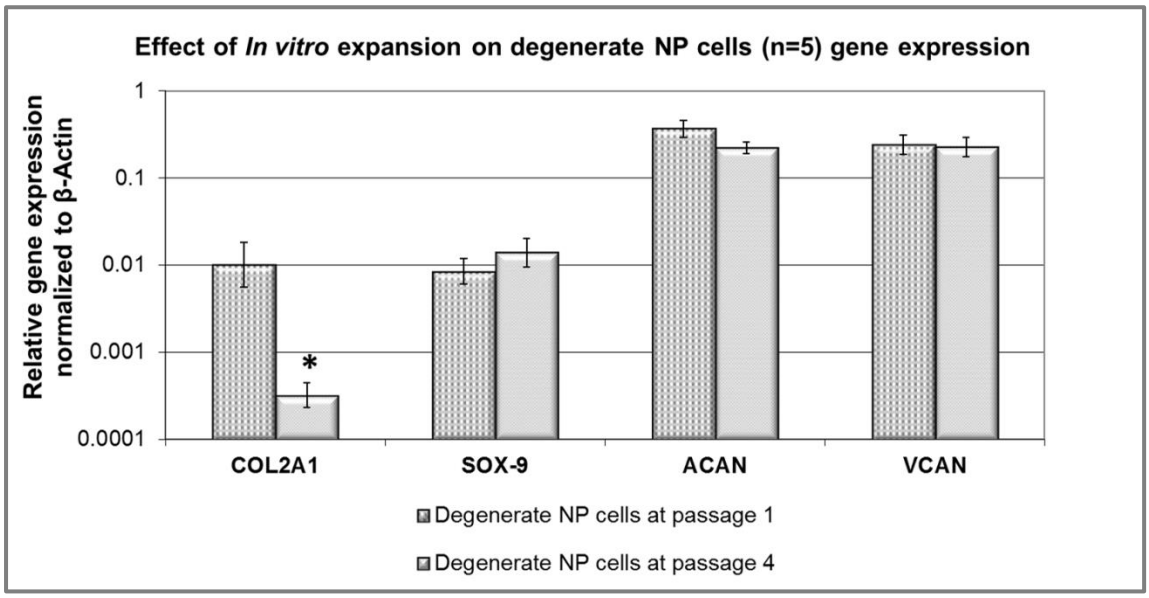

Figure 3.3.1 Relative gene expression of SOX-9, COL2A1, ACAN and VCAN in degenerate NP cells (n=5) after *in vitro* expansion in monolayer (passage 3-4). Gene expression normalized to β-actin and plotted on a log scale. * Statistical significance (p≤0.05) compared to passage 1. (β-actin expression was stable in this experiments and therefore used for normalization).

3.3.1 Influence of hypoxia on degenerate NP cell behaviour

3.3.1.1 Cell viability and proliferation

Viability analysis using Live/dead staining indicated that the majority of degenerate NP cells cultured in control conditions stained green (viable) with few red stained (dead) cells after 7 days. Degenerate NP cells cultured in hypoxia also showed similar staining pattern i.e. majority of cells stained green (viable) with very few red stained (dead) cells (Figure 3.3.2).

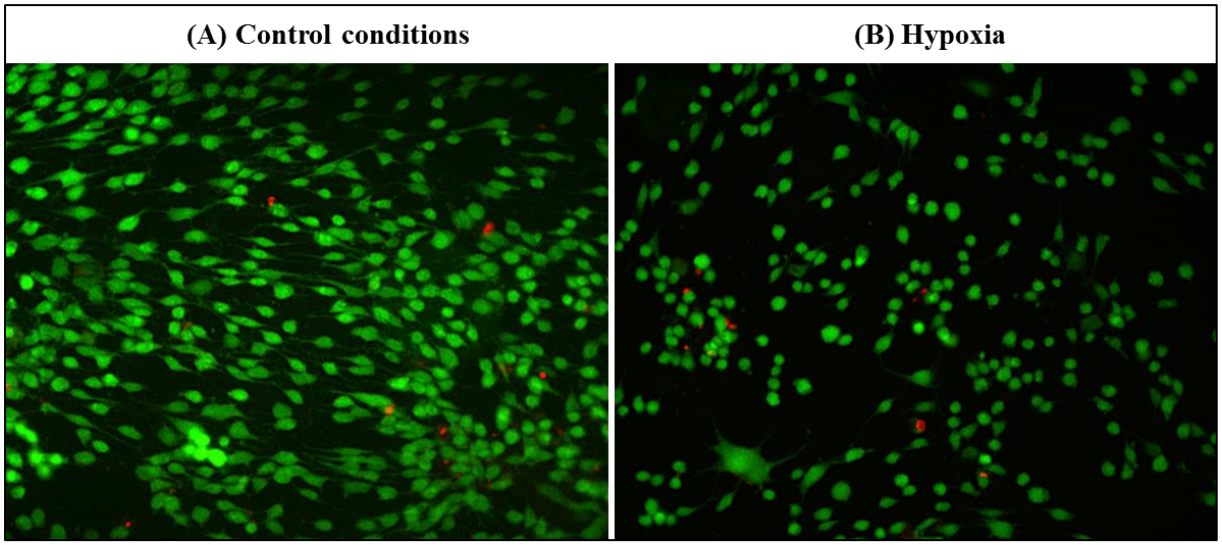

Figure 3.3.2 Effect of hypoxia on degenerate NP cell viability. Degenerate NP cells (n=3) were cultured in (A) control conditions and (B) hypoxia for 7 days and labelled with live-dead stain. Representative fluorescence microscope images indicating viable (stained green) and dead (stained red) populations under both conditions (magnification x100).

Proliferation analysis showed that by day 7 of culture, NP cells in hypoxic conditions proliferated to 12973±721 which was significantly higher (p<0.05) compared to control conditions (7390±29) (Figure 3.3.3).

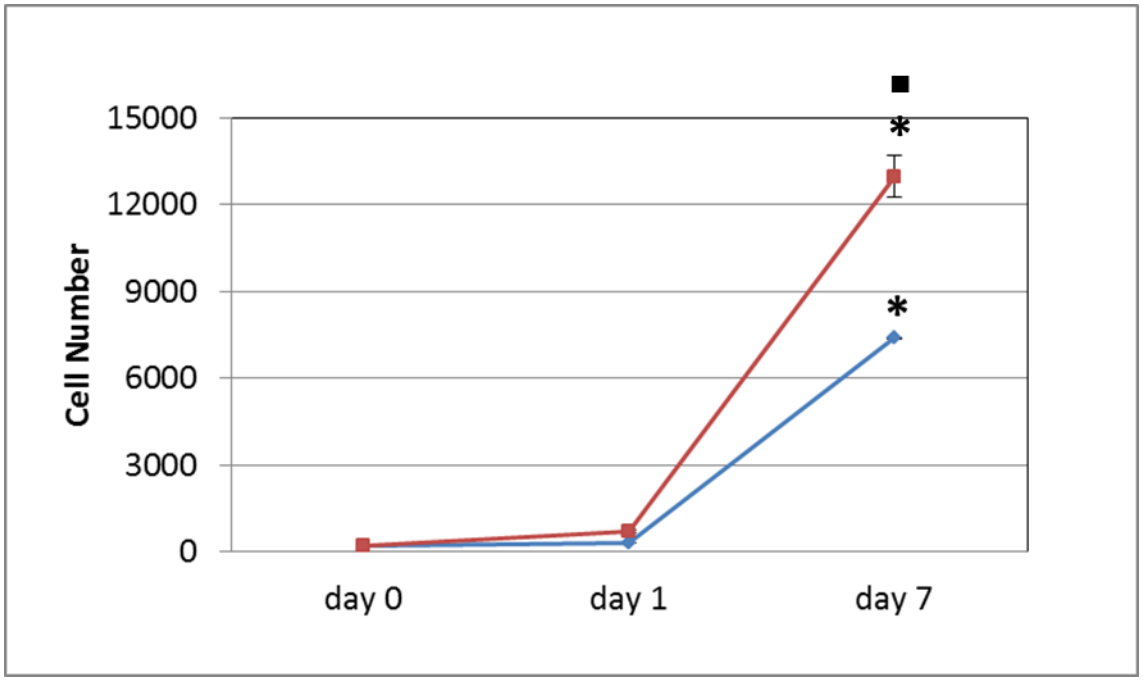

Figure 3.3.3 Effect of hypoxia on degenerate NP cell (n=1) proliferation over the course of 7 days. Total cell number was determined for degenerate NP cell cultured under hypoxia (red line) compared to control conditions (blue line). Day 0 cell number was used as baseline for each condition. Data was expressed as mean ± standard error mean (SEM) of triplicates of 1 patient sample. Significant differences ($p \leq 0.05$) * compared to day 0 and ■ day 7 control conditions.

3.3.1.2 Gene expression

Degenerate NP cells cultured under hypoxia showed no changes in SOX-9 and COL2A1 expression compared to cells cultured under control conditions (Figure 3.3.4 A). Significant increases were seen in ACAN ($p<0.05$) and VCAN ($p<0.05$) expression under hypoxia (Figure 3.3.4 B). There was no change in PAX-1 and FOXF-1 expression compared to control conditions (Figure 3.3.4 C).

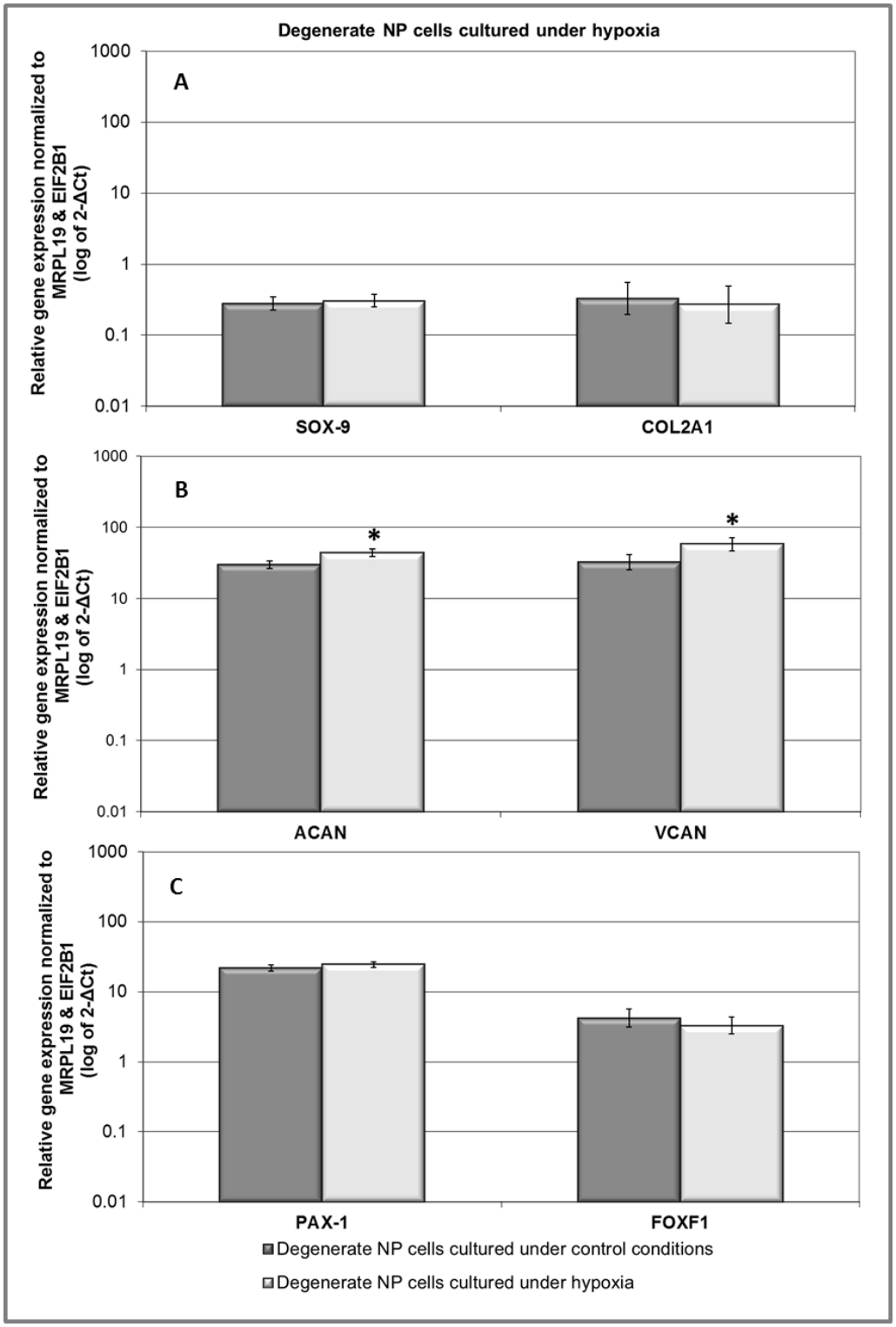

Figure 3.3.4 Relative gene expression of (A) SOX-9, COL2A1 (B) ACAN, VCAN and (C) PAX-1, FOXF1 in degenerate NP cells cultured under hypoxia (n=8) compare to control conditions. Gene expression normalized to average of HK genes MRPL19 and EIF2B1 and plotted on a log scale. * Statistical significance ($p \leq 0.05$) compared to culture in control conditions.

3.3.1.3 ECM protein expression

Degenerate NP cells cultured under hypoxia showed increased staining intensity for both aggrecan and versican compared to degenerate NP cells cultured under control conditions (Figure 3.3.5 & 3.3.6 respectively). Aggrecan staining was predominantly localized in the cytoplasm and had a similar staining pattern to that observed under control conditions. However, with versican there was a strong intracellular punctate/granular staining pattern in cells cultured under hypoxia that differed from the staining pattern seen in control conditions. Degenerate NP cells cultured under control conditions showed diffuse intra and extracellular staining pattern with fibers running between cells. Representative primary antibody controls (both for aggrecan and versican) were negative (Figure 3.3.7).

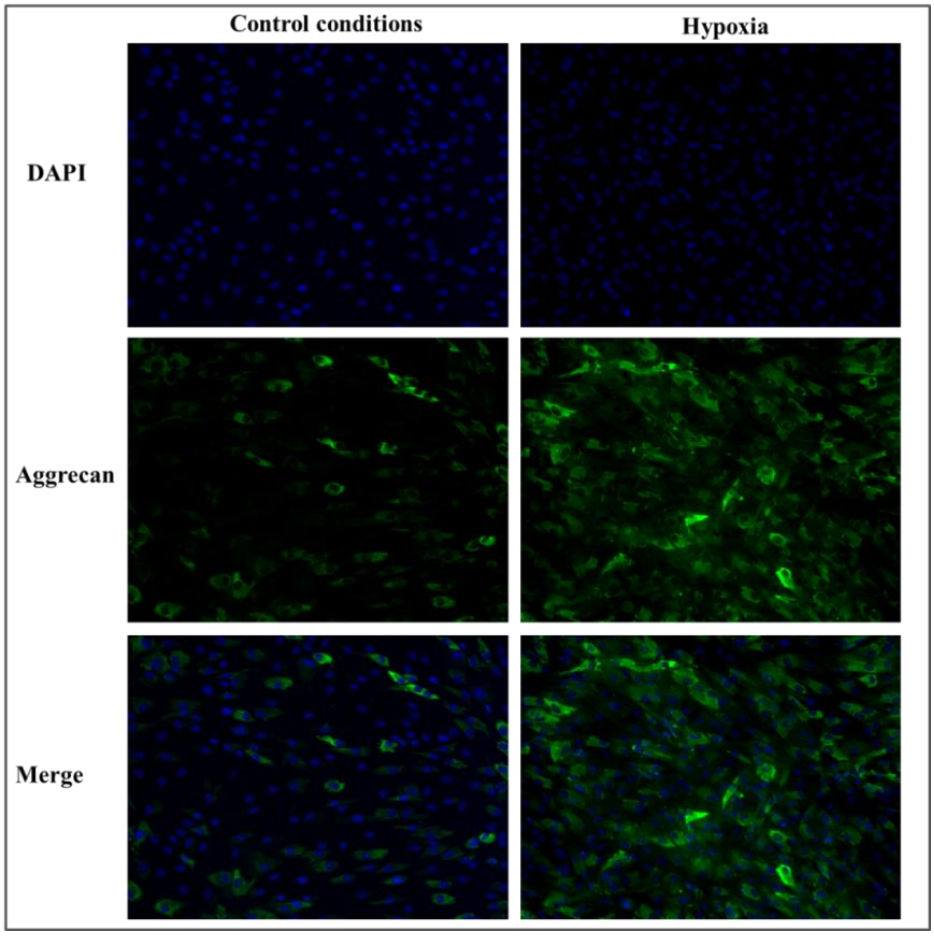

Figure 3.3.5 Representative images of aggrecan immunofluorescence staining of degenerate NP cells (n=2) cultured in control conditions (left panels) and hypoxia (right panels) for 7 days. Immunofluorescence staining was performed using anti-aggrecan primary antibody followed by Alexa Fluor 488 conjugated secondary antibody (green). DAPI (blue) was used for nucleus staining. Top row: DAPI, middle row: same field of view with aggrecan staining, bottom row: merge of above two rows (magnification x200).

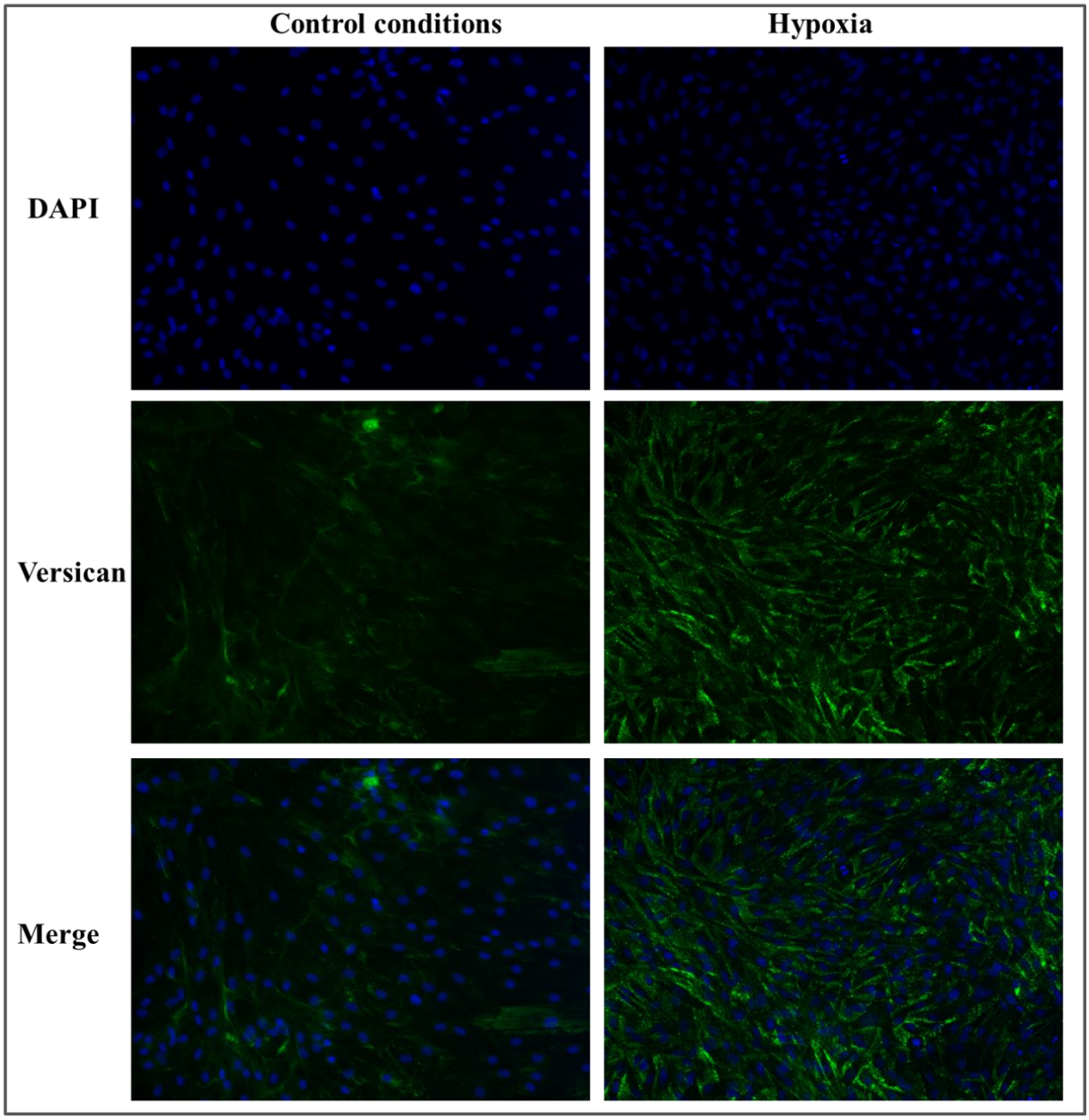

Figure 3.3.6 Representative images of versican immunofluorescence staining of degenerate NP cells (n=3) cultured in control conditions (left panels) and hypoxia (right panels) for 7 days. Immunofluorescence staining was performed using anti-versican primary antibody followed by Alexa Fluor 488 conjugated secondary antibody (green). DAPI (blue) was used for nucleus staining. Top row: DAPI, middle row: same field of view with versican staining, bottom row: merge of above two rows (magnification x200).

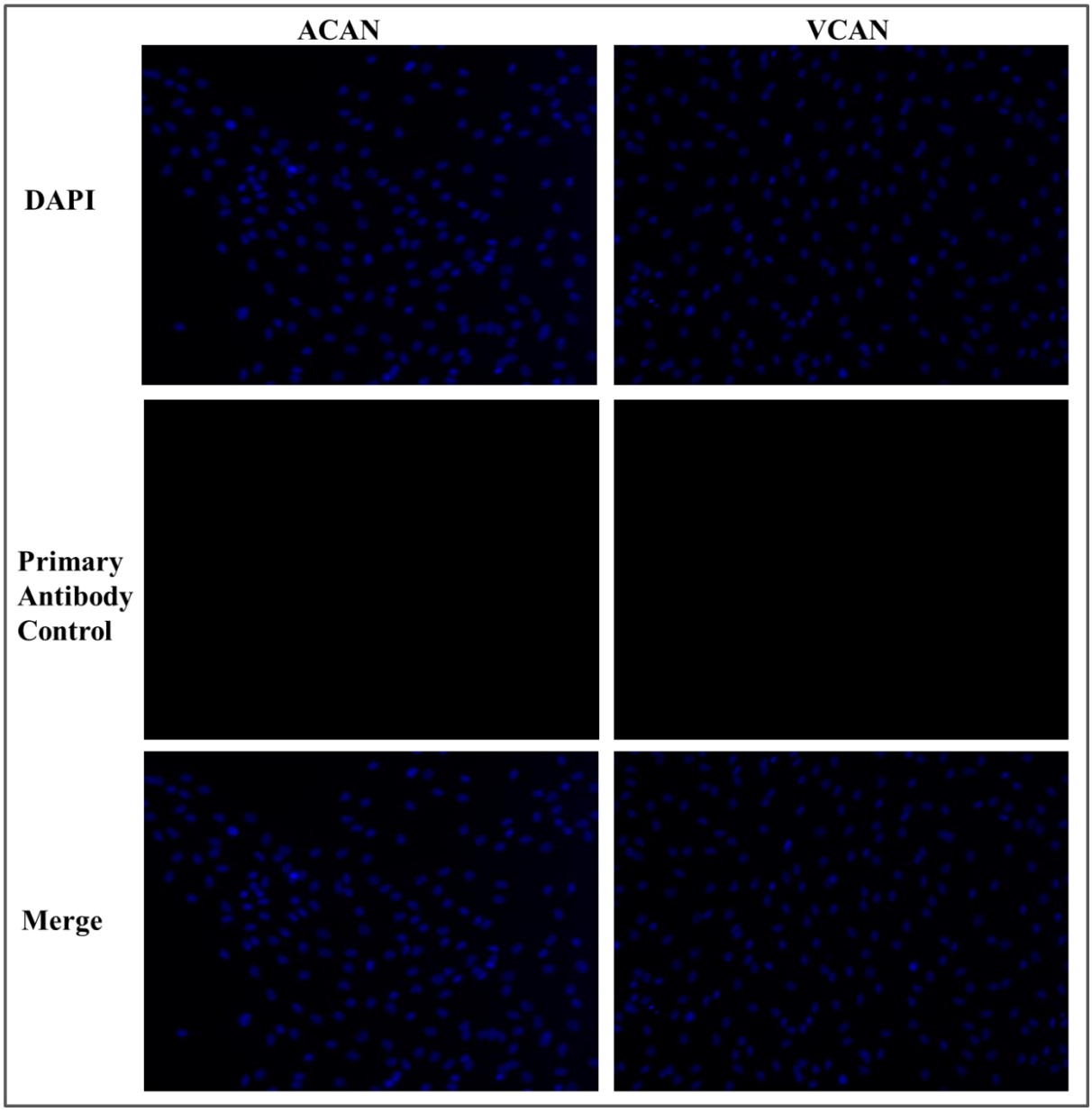

Figure 3.3.7 Representative primary antibody IgG controls for aggrecan (left panels) and versican (right panels) in degenerate NP cell culture. Immunofluorescence staining was performed using IgG control primary antibody followed by Alexa Fluor 488 conjugated secondary antibody (green). IgG controls show no non-specific IgG staining (magnification x200). Top row: DAPI, middle row: same field of view with IgG staining, bottom row: merge of above two rows (magnification x200).

3.3.2 Influence of reduced serum on degenerate NP cell behaviour

3.3.2.1 Cell viability and proliferation

Live/dead staining displayed that majority of degenerate NP cells cultured in reduced serum conditions were stained green (viable) (Figure 3.3.8).

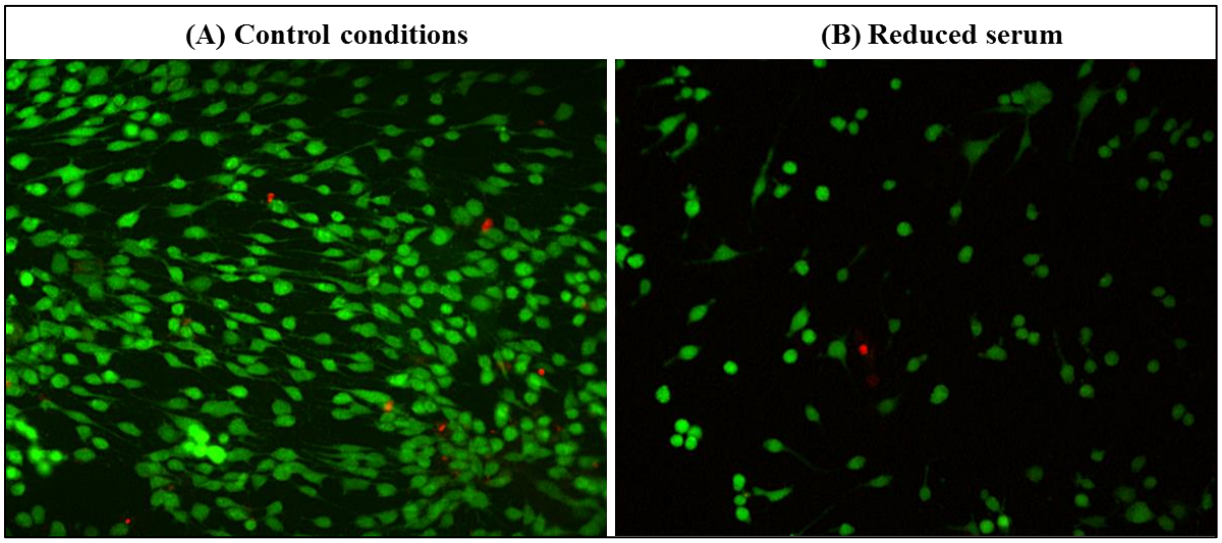

Figure 3.3.8: Effect of reduced serum on degenerate NP cell viability. Degenerate NP cells (n=3) were cultured in (A) control conditions and (B) reduced serum for 7 days and labelled with live-dead stain. Representative fluorescence microscope images indicating viable (stained green) and dead (stained red) populations under both conditions (magnification x100).

Proliferation analysis demonstrated that by day 7 of culture, the increase in cell number in reduced serum condition was significantly less (p>0.05) compared to the increase in control conditions (1710±150 versus 7390±29) (Figure 3.3.9).

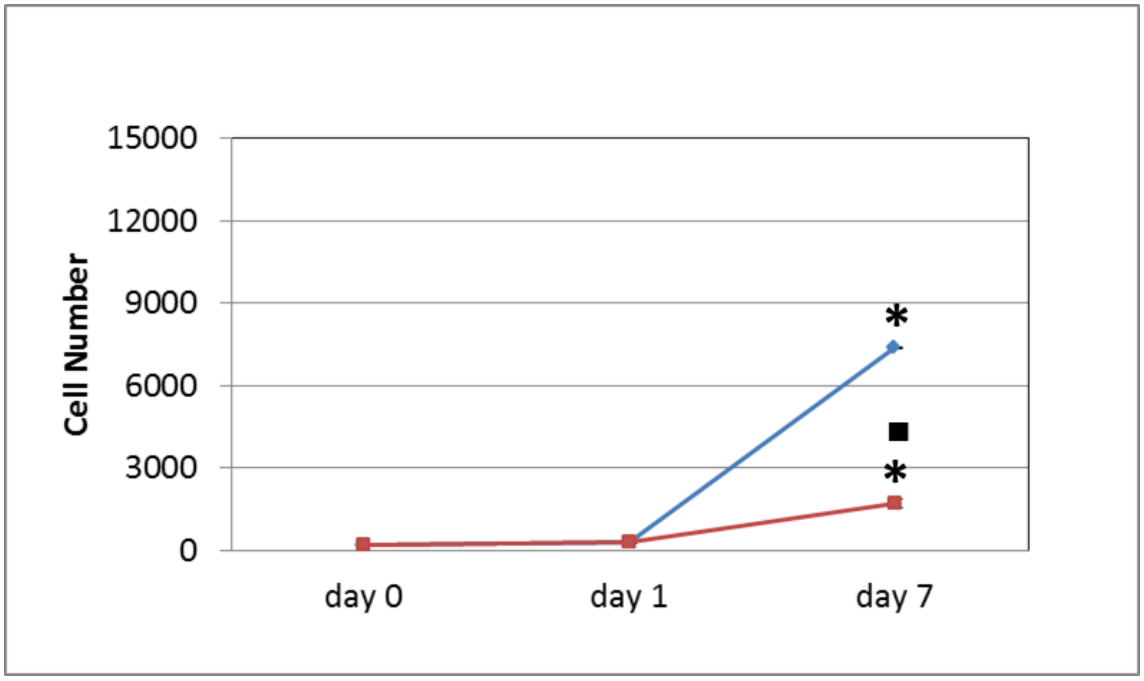

Figure 3.3.9 Effect of reduced serum on degenerate NP cell (n=1) proliferation over the course of 7 days. Total cell number was determined for degenerate NP cell cultured under reduced serum (red line) compared to control conditions (blue line). Day 0 cell number was used as baseline for each condition. Data was expressed as mean ± SEM of triplicates of 1 patient sample. Significant differences ($p \leq 0.05$) * compared to day 0 and ■ day 7 control conditions.

3.3.2.2 Gene expression

Degenerate NP cells cultured in reduced serum showed no changes in NP conventional and novel gene markers compared to control conditions (Figure 3.3.10).

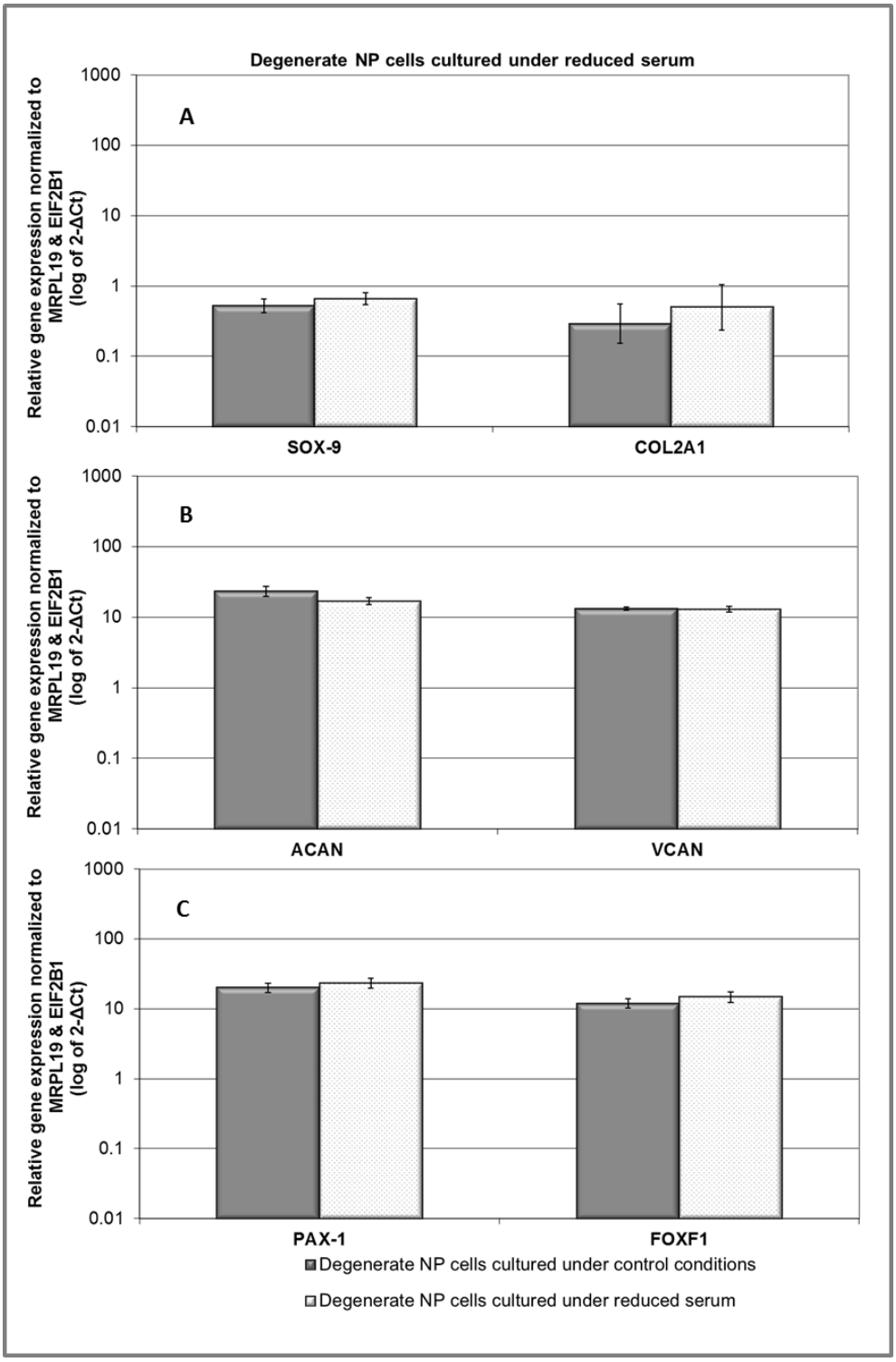

Figure 3.3.10 Relative gene expression of (A) SOX-9, COL2A1, (B) ACAN, VCAN and (C) PAX-1, FOXF1 in degenerate NP cells cultured under reduced serum (n=5) compared to control conditions. Gene expression normalized to average of HK genes MRPL19 and EIF2B1 and plotted on a log scale. * Statistical significance ($p \leq 0.05$) compared to culture in control conditions.

3.3.2.3 ECM protein expression

Degenerate NP cells cultured in reduced serum showed no prominent change in aggrecan staining intensity and pattern compare to control conditions. Due to a decrease in proliferation in reduced serum conditions aggrecan staining intensity was less intense. However, the proportion of cells positive for aggrecan appeared comparable to control conditions (Figure 3.3.11). No prominent change in versican staining intensity was seen in reduced serum conditions compared to control conditions. Staining pattern indicated few randomly dispersed thick granules (Figure 3.3.12).

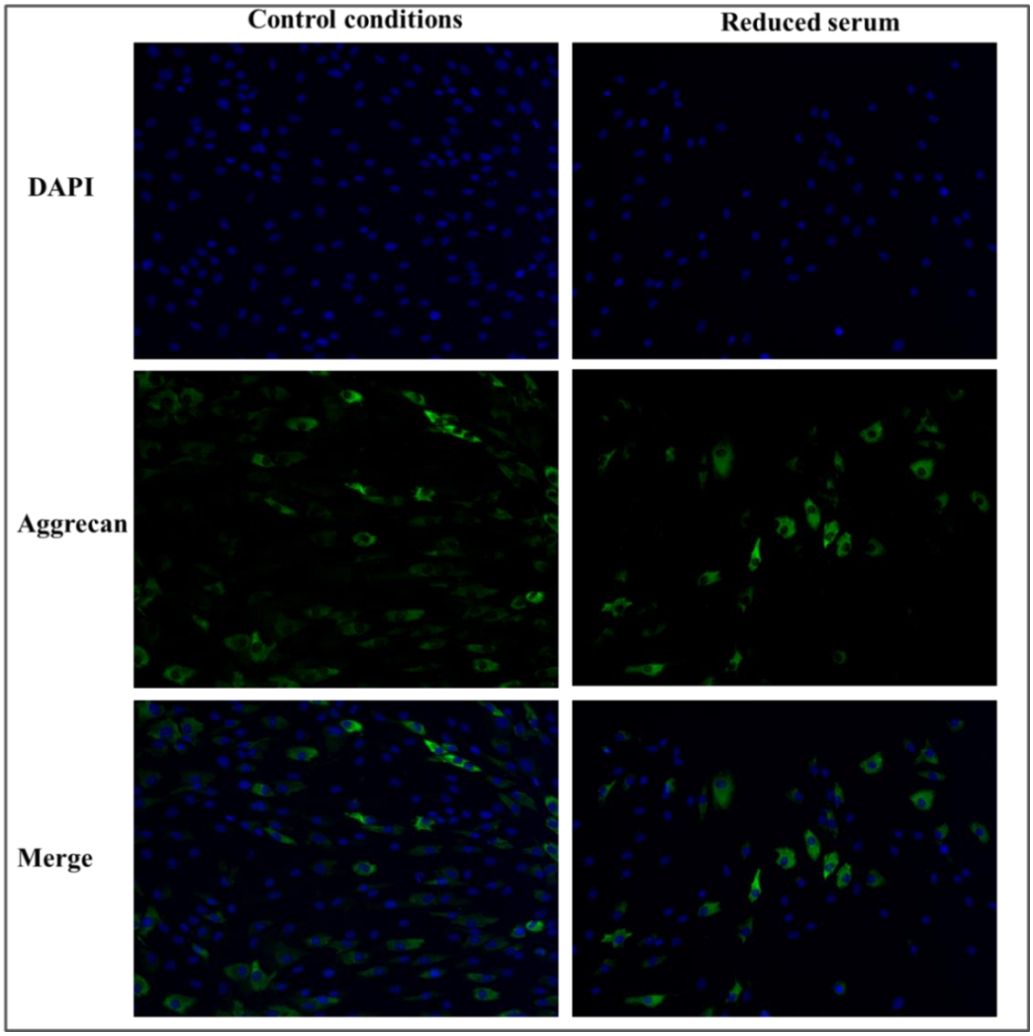

Figure 3.3.11 Representative images of aggrecan immunofluorescence staining of degenerate NP cells (n=2) cultured in control conditions (left panels) and reduced serum (right panels) for 7 days. Immunofluorescence staining was performed using anti-aggrecan primary antibody followed by Alexa Fluor 488 conjugated secondary antibody (green). DAPI (blue) was used for nucleus staining. Top row: DAPI, middle row: same field of view with aggrecan staining, bottom row: merge of above two rows (magnification x200).

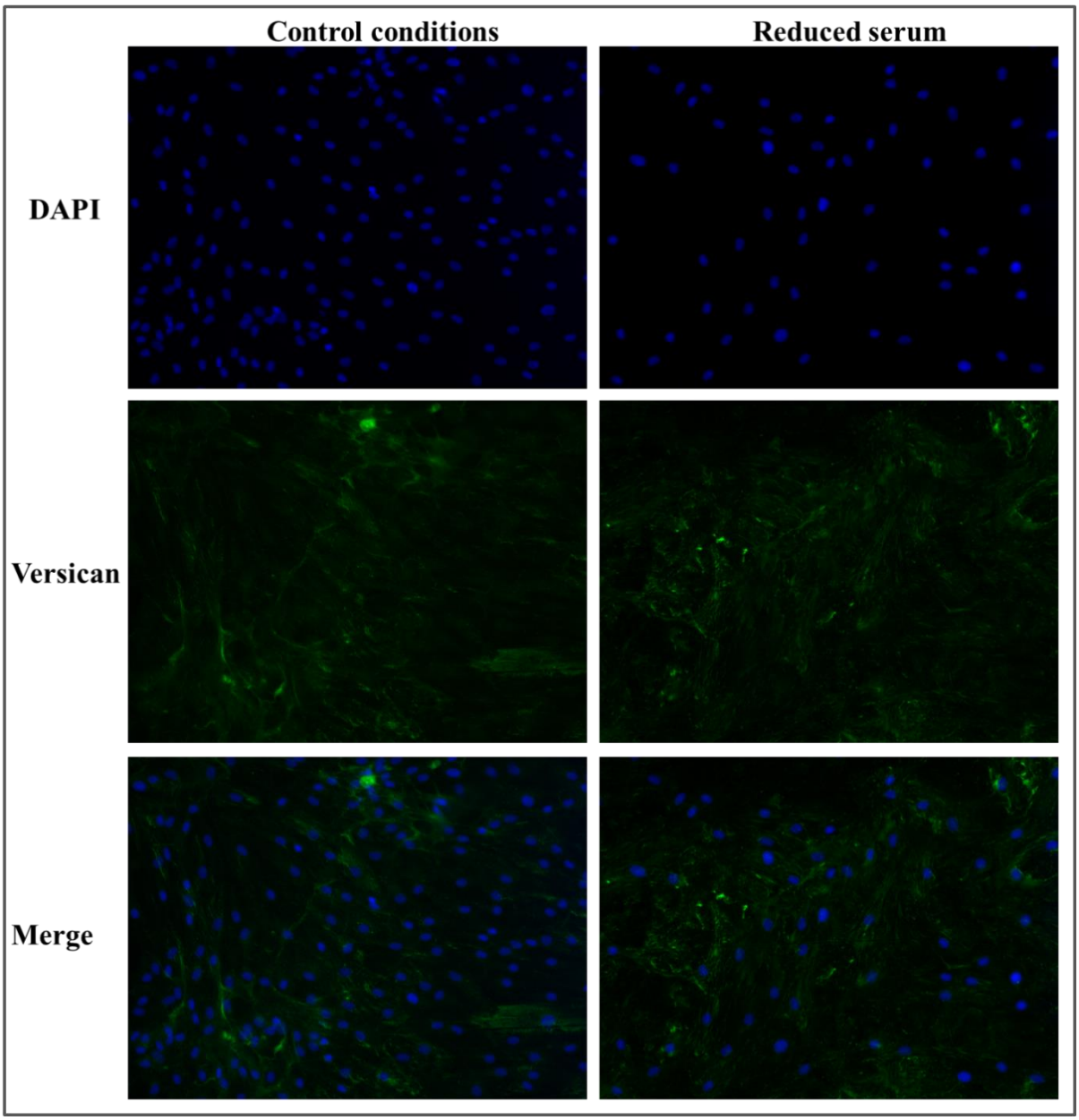

Figure 3.3.12 Representative images of versican immunofluorescence staining of degenerate NP cells (n=3) cultured in control conditions (left panels) and reduced serum (right panels) for 7 days. Immunofluorescence staining was performed using anti-versican primary antibody followed by Alexa Fluor 488 conjugated secondary antibody (green). DAPI (blue) was used for nucleus staining. Top row: DAPI, middle row: same field of view with versican staining, bottom row: merge of above two rows (magnification x200).

3.3.3 Influence of reduced glucose on degenerate NP cell behaviour

3.3.3.1 Cell viability and proliferation

Degenerate NP cells cultured in reduced glucose conditions showed live/dead staining similar to control condition i.e. majority of cells were stained green (viable) with few red stained cells (dead) (Figure 3.3.13)

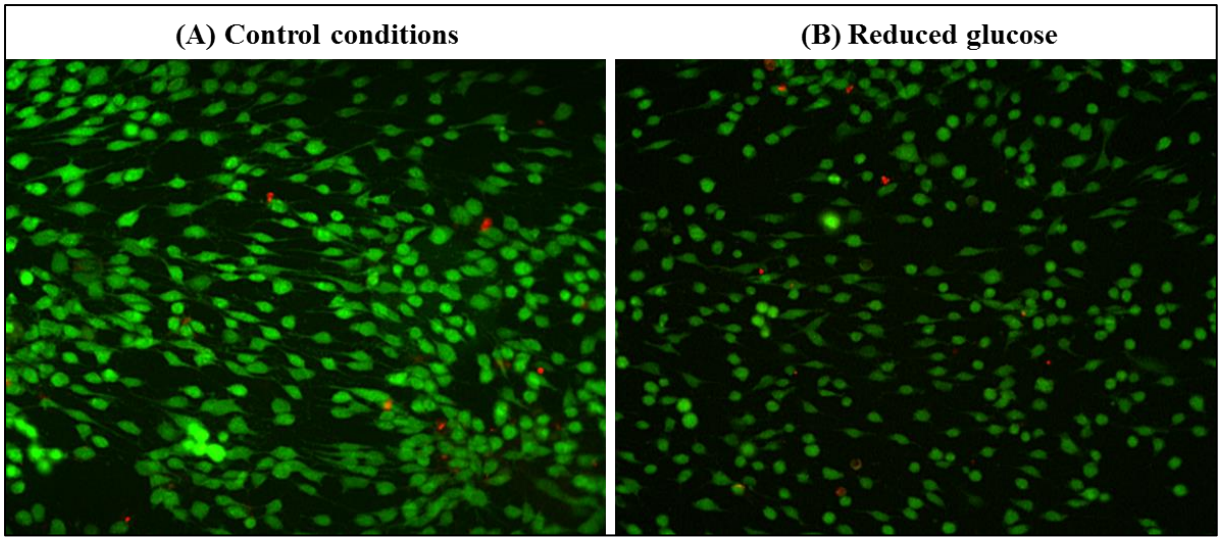

Figure 3.3.13 Effect of reduced glucose on degenerate NP cell viability. Degenerate NP cells (n=3) were cultured in (A) control conditions and (B) reduced glucose for 7 days and labelled with live-dead stain. Representative fluorescence microscope images indicating viable (stained green) and dead (stained red) populations under both conditions (magnification x100).

Proliferation analysis demonstrated that by day 7 of culture, NP cell number in reduced glucose condition (5668±220) was significantly less (p>0.05) compared to control conditions (7390±29) (Figure 3.3.14).

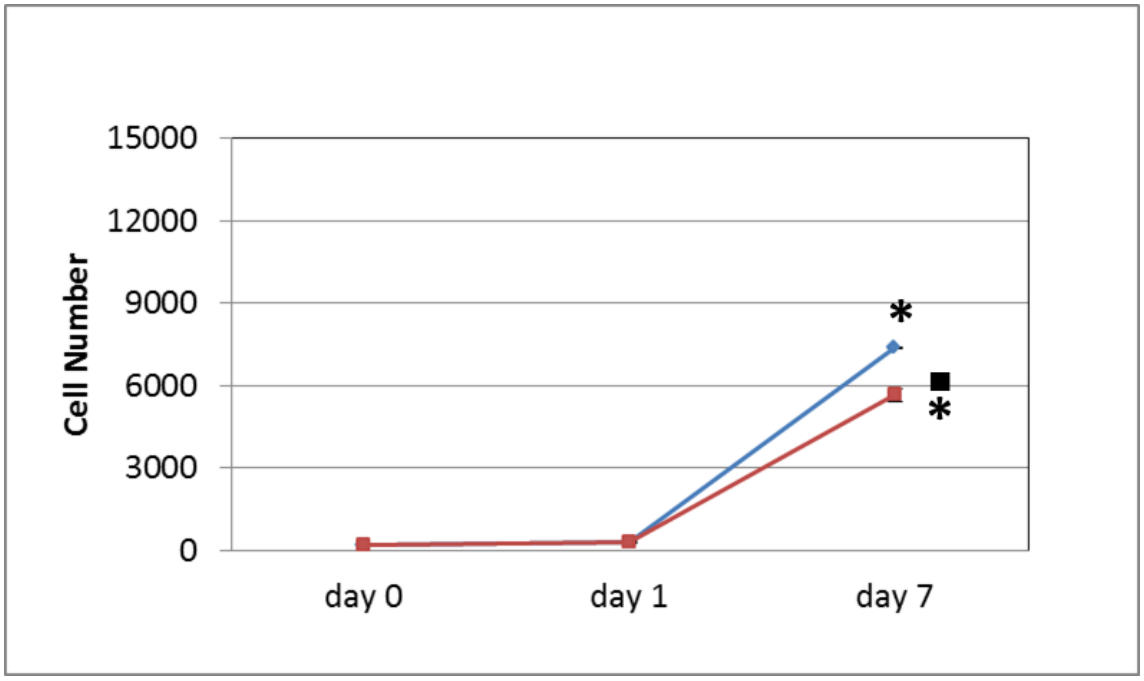

Figure 3.3.14 Effect of reduced glucose on degenerate NP cell (n=1) proliferation over the course of 7 days. Total cell number was determined for degenerate NP cell cultured under reduced glucose (red line) compared to control conditions (blue line). Day 0 cell number was used as baseline for each condition. Data was expressed as mean ± SEM of triplicates of 1 patient sample. Significant differences ($p \leq 0.05$) * compared to day 0 and ■ day 7 control conditions.

3.3.3.2 Gene expression

Degenerate NP cells cultured under reduced glucose showed no changes in NP conventional marker genes compared to control conditions (Figure 3.3.15 A & B). There was a significant decrease ($p=0.05$) in PAX-1 with no change in FOXF1 expression under reduced glucose (Figure 3.3.15 C).

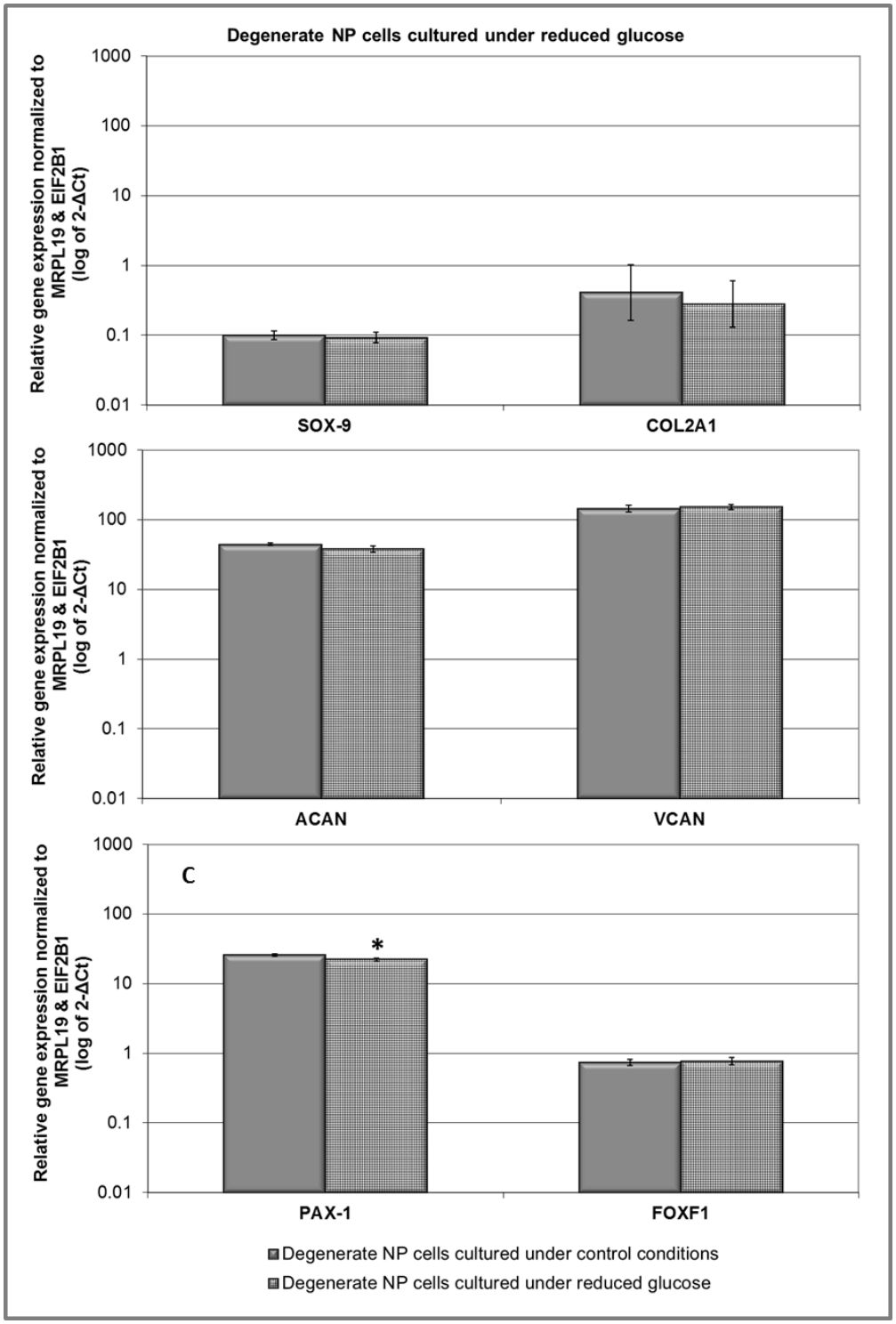

Figure 3.3.15 Relative gene expression of (A) SOX-9, COL2A1, (B) ACAN, VCAN and (C) PAX-1, FOXF1 in degenerate NP cells cultured under reduced glucose (n=3) compared to control conditions. Gene expression normalized to average of HK genes MRPL19 and EIF2B1 and plotted on a log scale. * Statistical significance ($p \leq 0.05$) compared to culture in control conditions.

3.3.3.3 ECM protein expression

Degenerate NP cells cultured under reduced glucose showed no prominent change in aggrecan and versican staining intensity compare to control conditions (Figure 3.3.16 & 3.3.17 respectively).

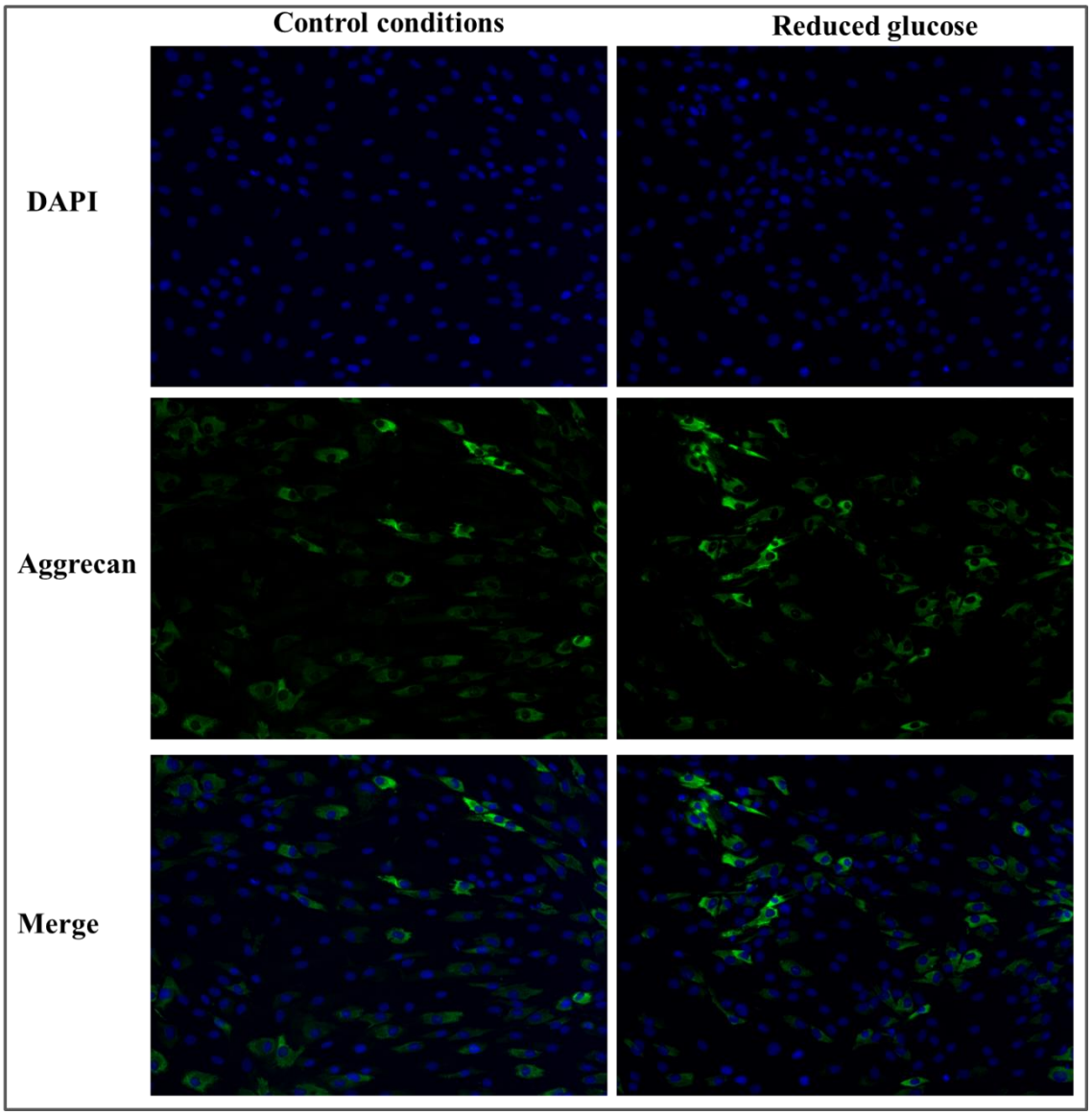

Figure 3.3.16 Representative images of aggrecan immunofluorescence staining of degenerate NP cells (n=2) cultured in control conditions (left panels) and reduced glucose (right panels) for 7 days. Immunofluorescence staining was performed using anti-aggrecan primary antibody followed by Alexa Fluor 488 conjugated secondary antibody (green). DAPI (blue) was used for nucleus staining. Top row: DAPI, middle row: same field of view with aggrecan staining, bottom row: merge of above two rows (magnification x200).

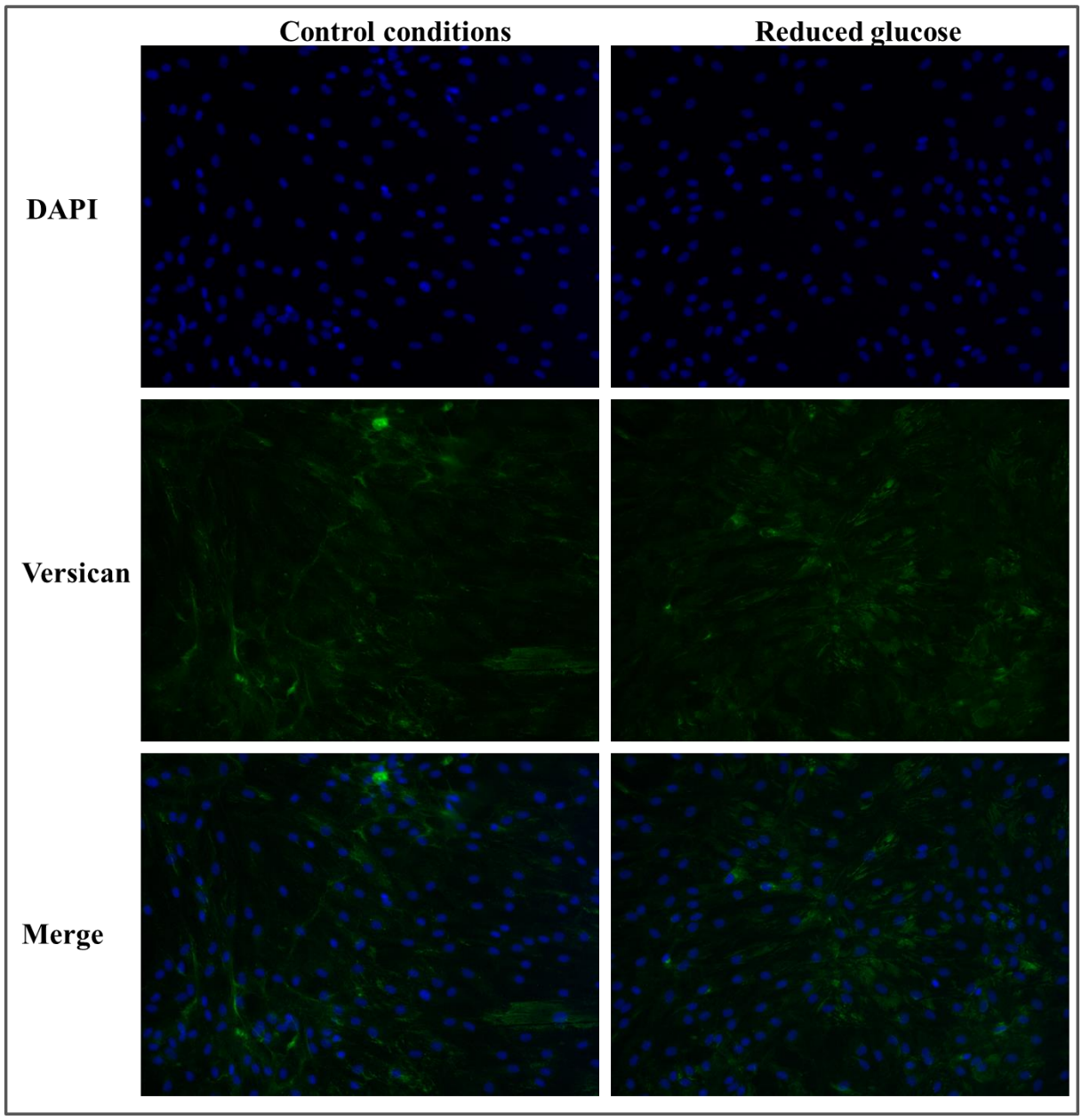

Figure 3.3.17 Representative images of versican immunofluorescence staining of degenerate NP cells (n=3) cultured in control conditions (left panels) and reduced glucose (right panels) for 7 days. Immunofluorescence staining was performed using anti-versican primary antibody followed by Alexa Fluor 488 conjugated secondary antibody (green). DAPI (blue) was used for nucleus staining. Top row: DAPI, middle row: same field of view with versican staining, bottom row: merge of above two rows (magnification x200).

3.3.4 Influence of reduced serum and reduced glucose on degenerate NP cell behaviour

3.3.4.1 Cell viability and proliferation

Degenerate NP cells cultured under reduced serum and glucose showed that after live/dead assay majority of cells stained green with few red stained cells (dead) (Figure 3.3.18).

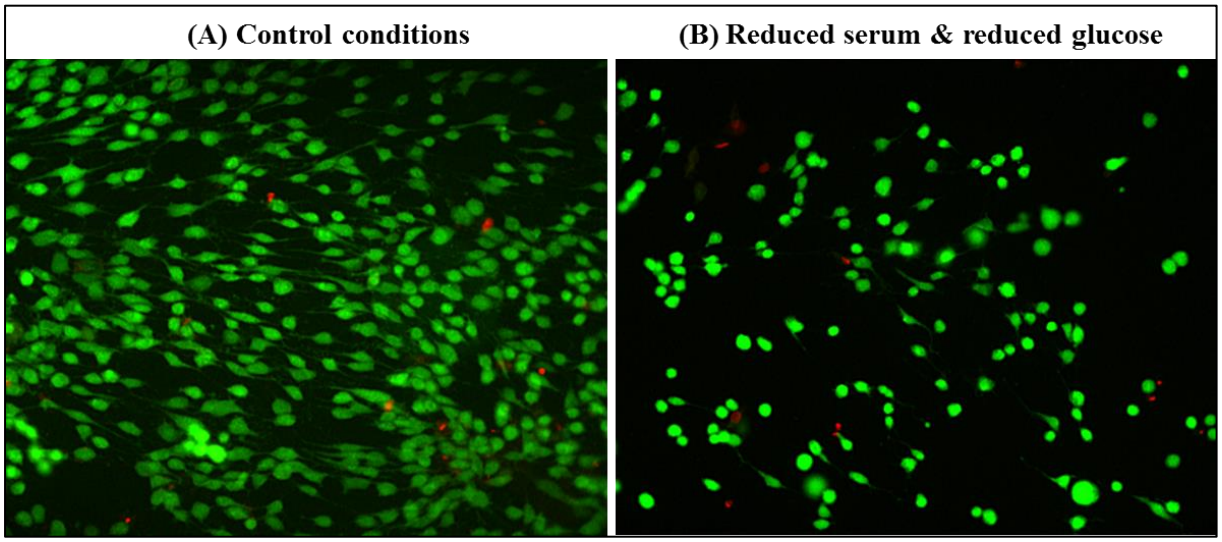

Figure 3.3.18 Effect of reduced serum and glucose on degenerate NP cell viability. Degenerate NP cells (n=3) were cultured in (A) control conditions and (B) reduced serum and glucose for 7 days and labelled with live-dead stain. Representative fluorescence microscope images indicating viable (stained green) and dead (stained red) populations in both conditions (magnification x100).

Proliferation analysis showed that at day 7 the increase in cell number under reduced serum and reduced glucose was significantly less ($p \leq 0.05$) compared to control conditions (2942±359 versus 7390±29) (Figure 3.3.19).

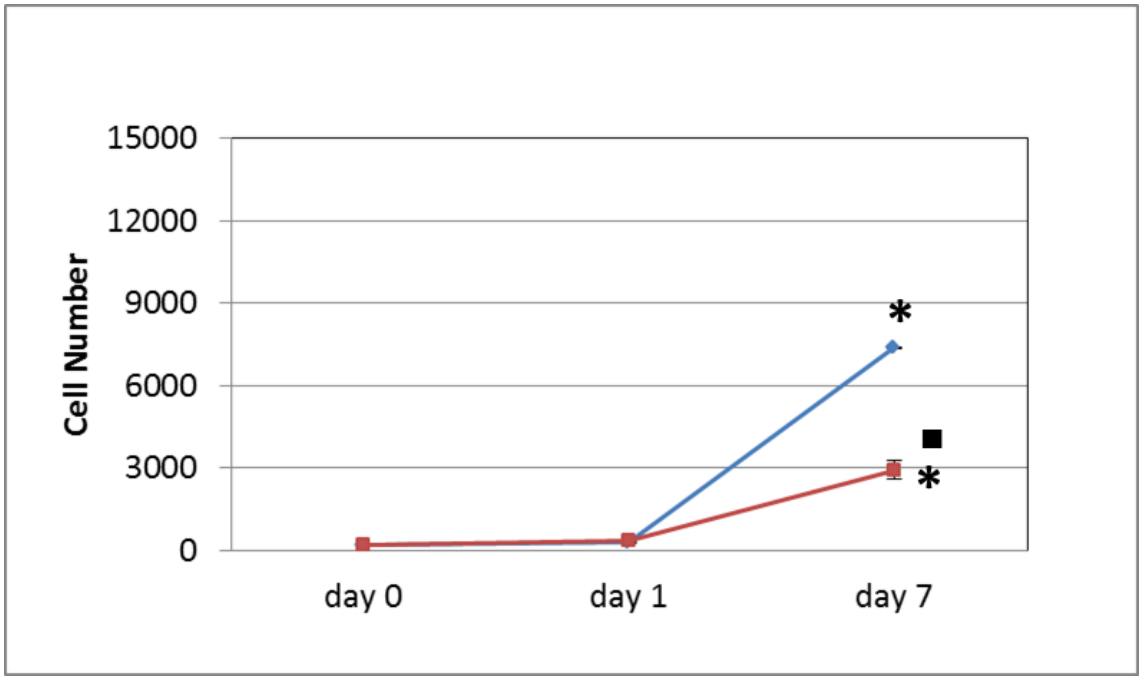

Figure 3.3.19 Effect of reduced serum and reduced glucose on degenerate NP cell (n=1) proliferation over the course of 7 days. Total cell number was determined for degenerate NP cell cultured under reduced serum and reduced glucose (red line) compared to control conditions (blue line). Day 0 cell number was used as baseline for each condition. Data was expressed as mean ± SEM of triplicates of 1 patient sample. Significant differences ($p \leq 0.05$) * compared to day 0 and ■ day 7 control conditions.

3.3.4.2 Gene expression

Degenerate NP cells cultured under reduced serum combined with reduced glucose showed a significant ($p<0.05$) increase in SOX-9 gene expression with no change in COL2A1 expression compare to control conditions (Figure 3.3.20 A). A significant down regulation ($p<0.05$) in ACAN with no change in VCAN expression was seen compared to control conditions (Figure 3.3.20 B). A significant increase in PAX-1 was seen with no change in FOXF1 expression under reduced serum combined with reduced glucose compared to control conditions (Figure 3.3.20 C)

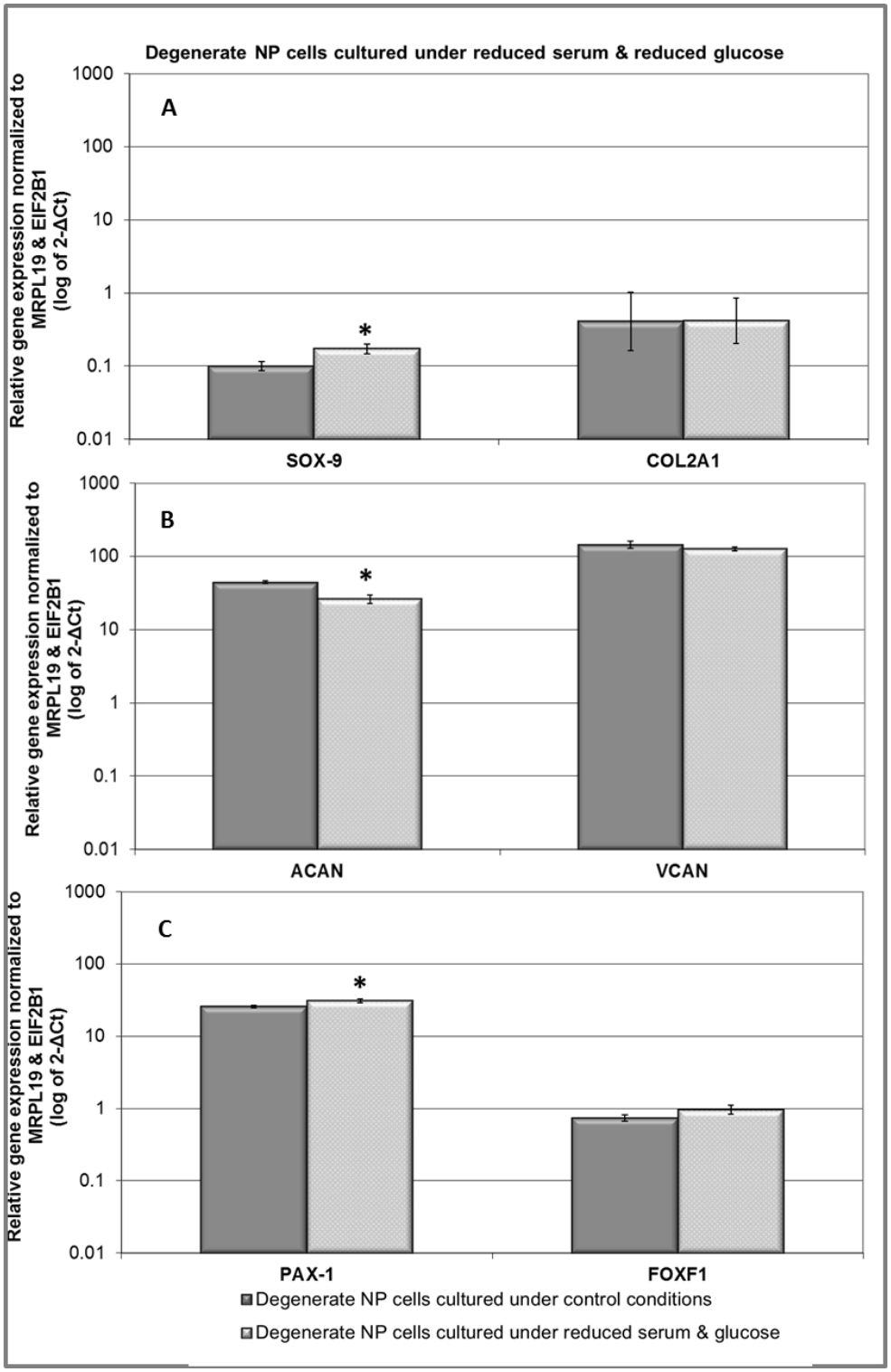

Figure 3.3.20 Relative gene expression of (A) SOX-9, COL2A1, (B) ACAN, VCAN and (C) PAX-1, FOXF1 in degenerate NP cells cultured in reduced serum combined with reduced glucose (n=3) compared to control conditions. Gene expression normalized to average of HK genes MRPL19 and EIF2B1 and plotted on a log scale. * Statistical significance ($p \leq 0.05$) compared to culture in control conditions.

3.3.4.3 ECM protein expression

Taking reduced proliferation into account degenerate NP cells cultured under reduced serum and reduced glucose showed no noticeable change in aggrecan and versican staining intensity compared to degenerate NP cells cultured under control conditions (Figure 3.3.21 & 3.3.22).

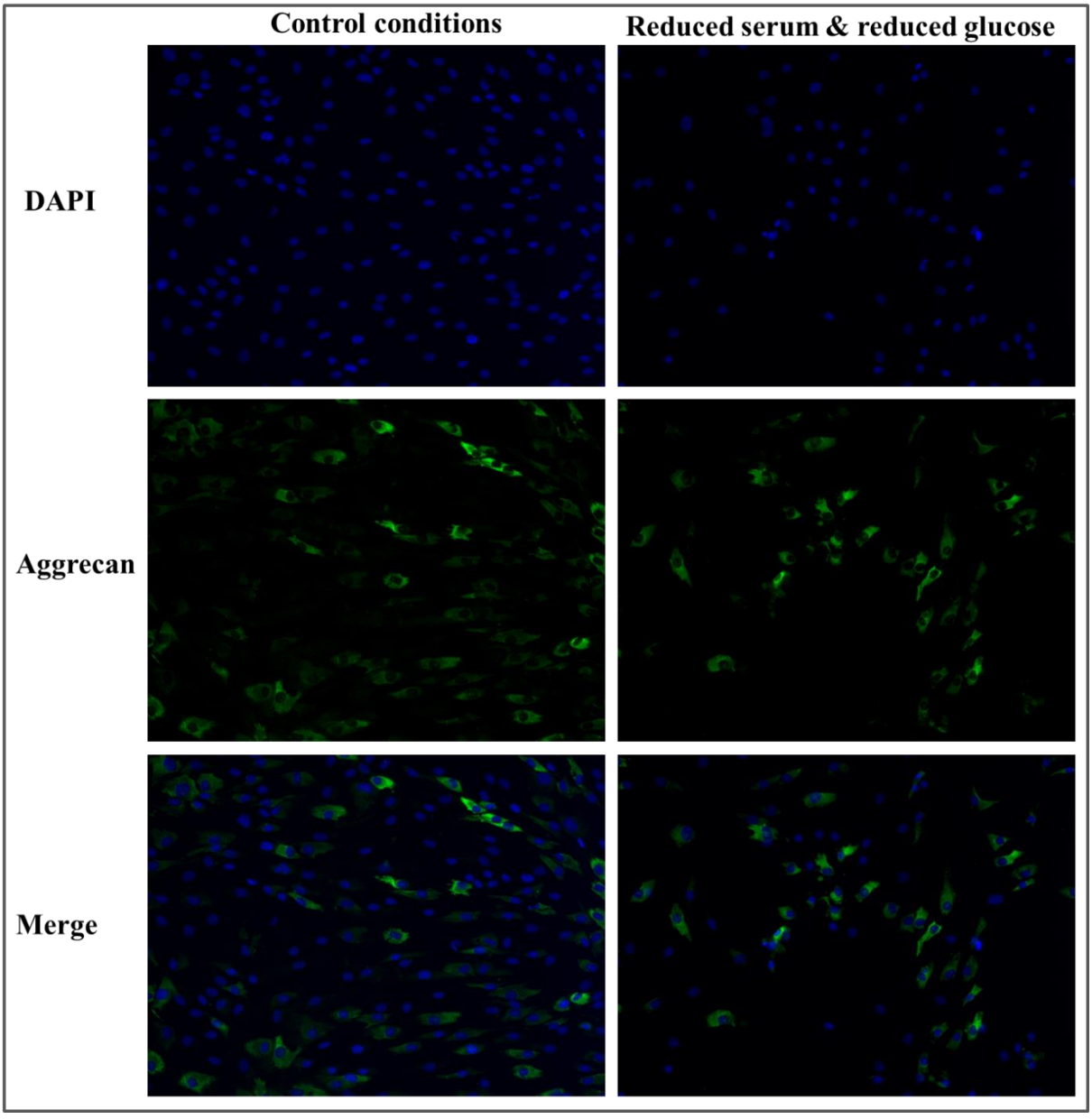

Figure 3.3.21 Representative images of aggrecan immunofluorescence staining of degenerate NP cells (n=2) cultured in control conditions (left panels) and reduced serum combined with reduced glucose (right panels) for 7 days. Immunofluorescence staining was performed using anti-aggrecan primary antibody followed by Alexa Fluor 488 conjugated secondary antibody (green). DAPI (blue) was used for nucleus staining. Top row: DAPI, middle row: same field of view with aggrecan staining, bottom row: merge of above two rows (magnification x200).

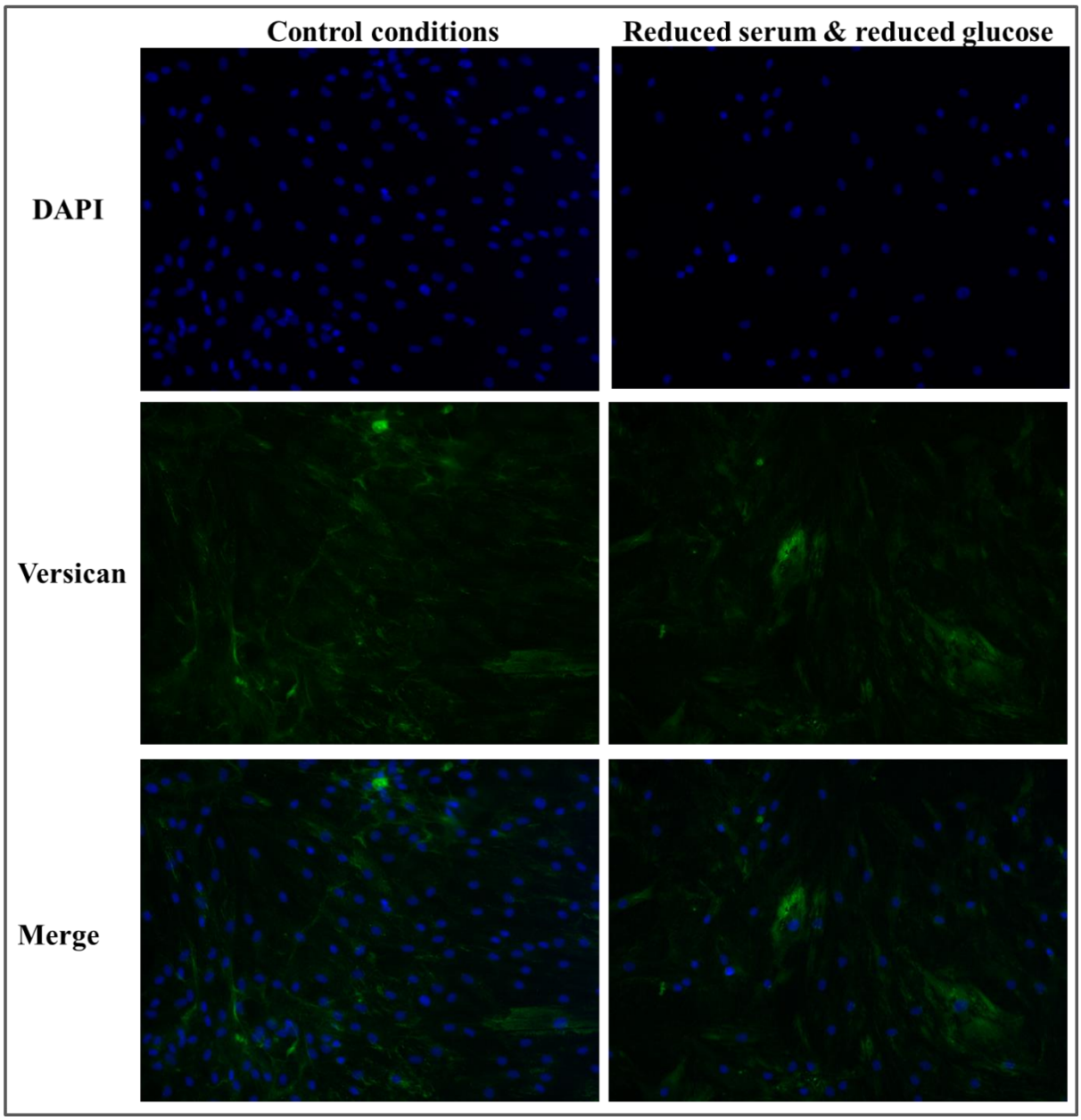

Figure 3.3.22 Representative images of versican immunofluorescence staining of degenerate NP cells (n=3) cultured in control conditions (left panels) and reduced serum combined with reduced glucose (right panels) for 7 days. Immunofluorescence staining was performed using anti-versican primary antibody followed by Alexa Fluor 488 conjugated secondary antibody (green). DAPI (blue) was used for nucleus staining. Top row: DAPI, middle row: same field of view with versican staining, bottom row: merge of above two rows (magnification x200).

3.3.5 Influence of reduced serum and hypoxia on degenerate NP cell behaviour

3.3.5.1 Cell viability and proliferation

Live/dead staining of degenerate NP cells cultured under reduced serum combined with hypoxia displayed green stained cells (live) comparable with control conditions (Figure 3.3.23).

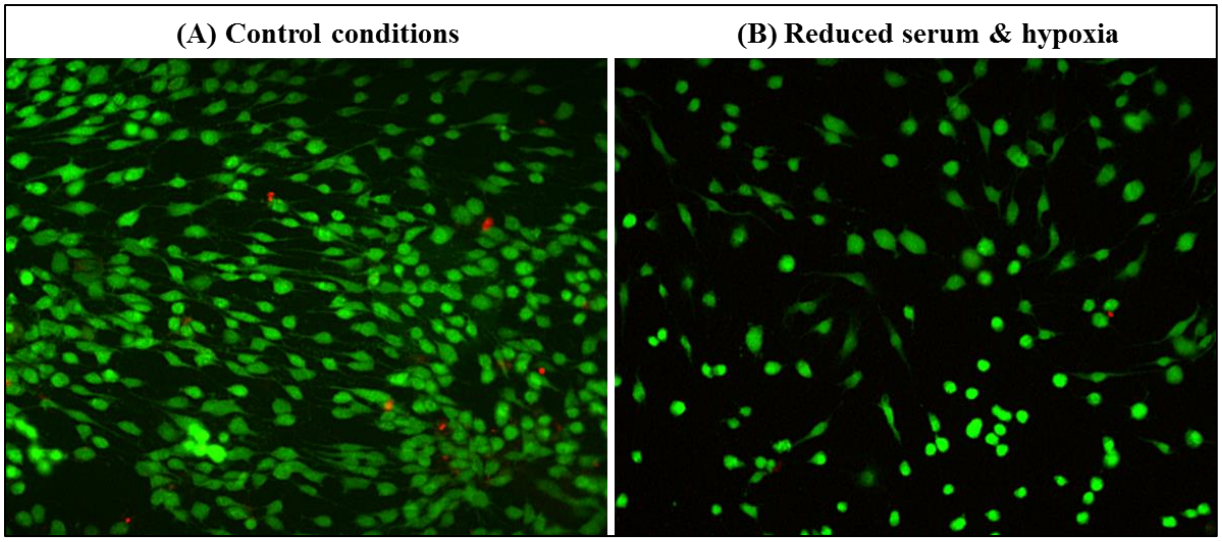

Figure 3.3.23 Effect of reduced serum and hypoxia on degenerate NP cell viability. Degenerate NP cells (n=3) were cultured in (A) control conditions and (B) reduced serum and hypoxia for 7 days and labelled with live-dead stain. Representative fluorescence microscope images indicating viable (stained green) and dead (stained red) populations under both conditions (magnification x100).

Proliferation analysis showed that at day 7 the increase in degenerate NP cell number (5519±299) under reduced serum and hypoxia condition was significantly less ($p \leq 0.05$) compared to control conditions (7390±29) (Figure 3.3.24).

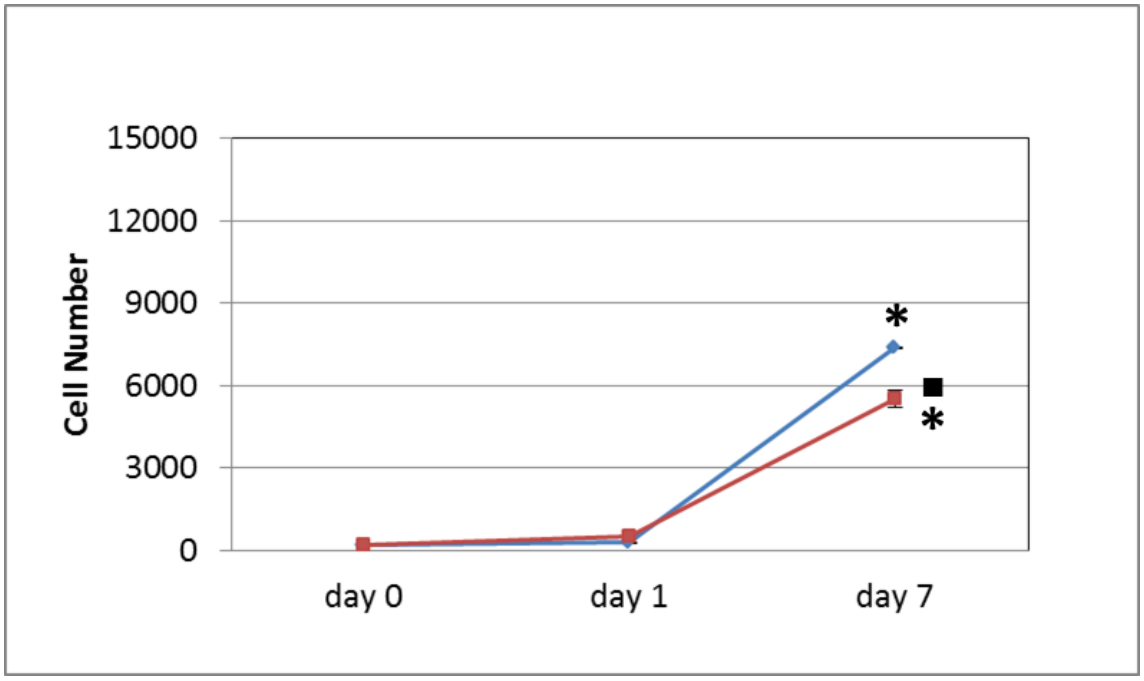

Figure 3.3.24 Effect of reduced serum and hypoxia on degenerate NP cell (n=1) proliferation over the course of 7 days. Total cell number was determined for degenerate NP cell cultured under reduced serum and hypoxia (red line) compared to control conditions (blue line). Day 0 cell number was used as baseline for each condition. Data was expressed as mean ± SEM of triplicates of 1 patient sample. Significant differences ($p \leq 0.05$) * compared to day 0 and ■ day 7 control conditions.

3.3.5.2 Gene expression

Degenerate NP cells cultured under reduced serum combined with hypoxia showed no change in SOX-9 and COL2A1 (Figure 3.3.25 A). There was no significant change ($p=0.06$) in ACAN expression while, VCAN expression was significantly up regulated ($p<0.05$) under reduced serum and hypoxia (Figure 3.3.25 B). No change in PAX-1 and FOXF1 expression was seen under reduced serum combined with hypoxia compared to control conditions (Figure 3.3.25 C).

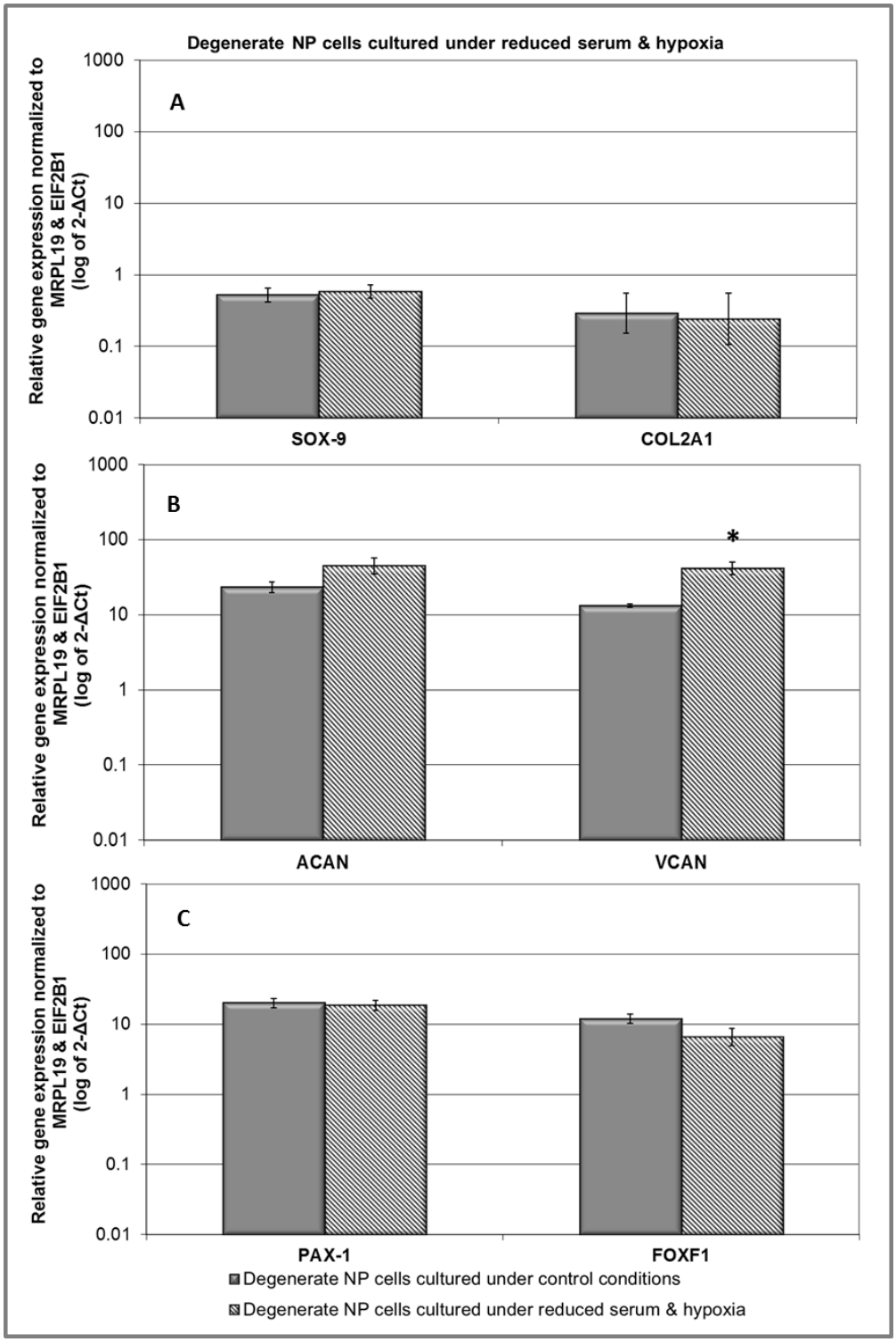

Figure 3.3.25 Relative gene expression of (A) COL2A1, SOX-9, (B) ACAN, VCAN and (C) PAX-1, FOXF1 in degenerate NP cells cultured in reduced serum combined with hypoxia (n=5) compared to control conditions. Gene expression normalized to average of HK genes MRPL19 and EIF2B1 and plotted on a log scale. * Statistical significance ($p \leq 0.05$) compared to culture in control conditions.

3.3.5.1 ECM protein expression

Degenerate NP cells cultured under reduced serum and hypoxia showed increased staining intensity of aggrecan compared to control conditions (Figure 3.3.26). Few degenerate NP cells showed strong versican staining intensity but overall there was no prominent change compare to control conditions (Figure 3.3.27).

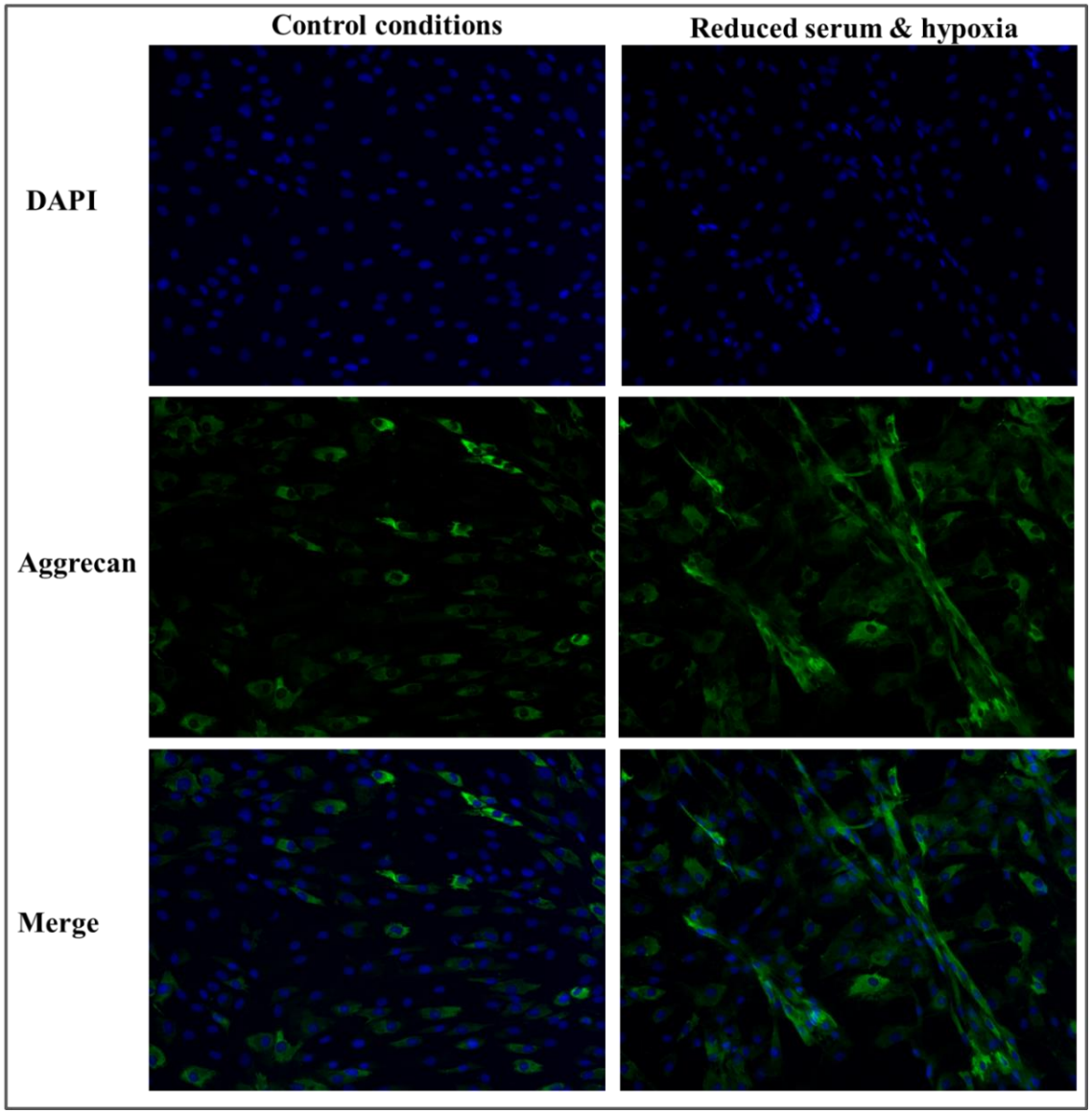

Figure 3.3.26 Representative images of aggrecan immunofluorescence staining of degenerate NP cells (n=2) cultured in control conditions (left panels) and reduced serum and hypoxia (right panels) for 7 days. Immunofluorescence staining was performed using anti-aggrecan primary antibody followed by Alexa Fluor 488 conjugated secondary antibody (green). DAPI (blue) was used for nucleus staining. Top row: DAPI, middle row: same field of view with aggrecan staining, bottom row: merge of above two rows (magnification x200).

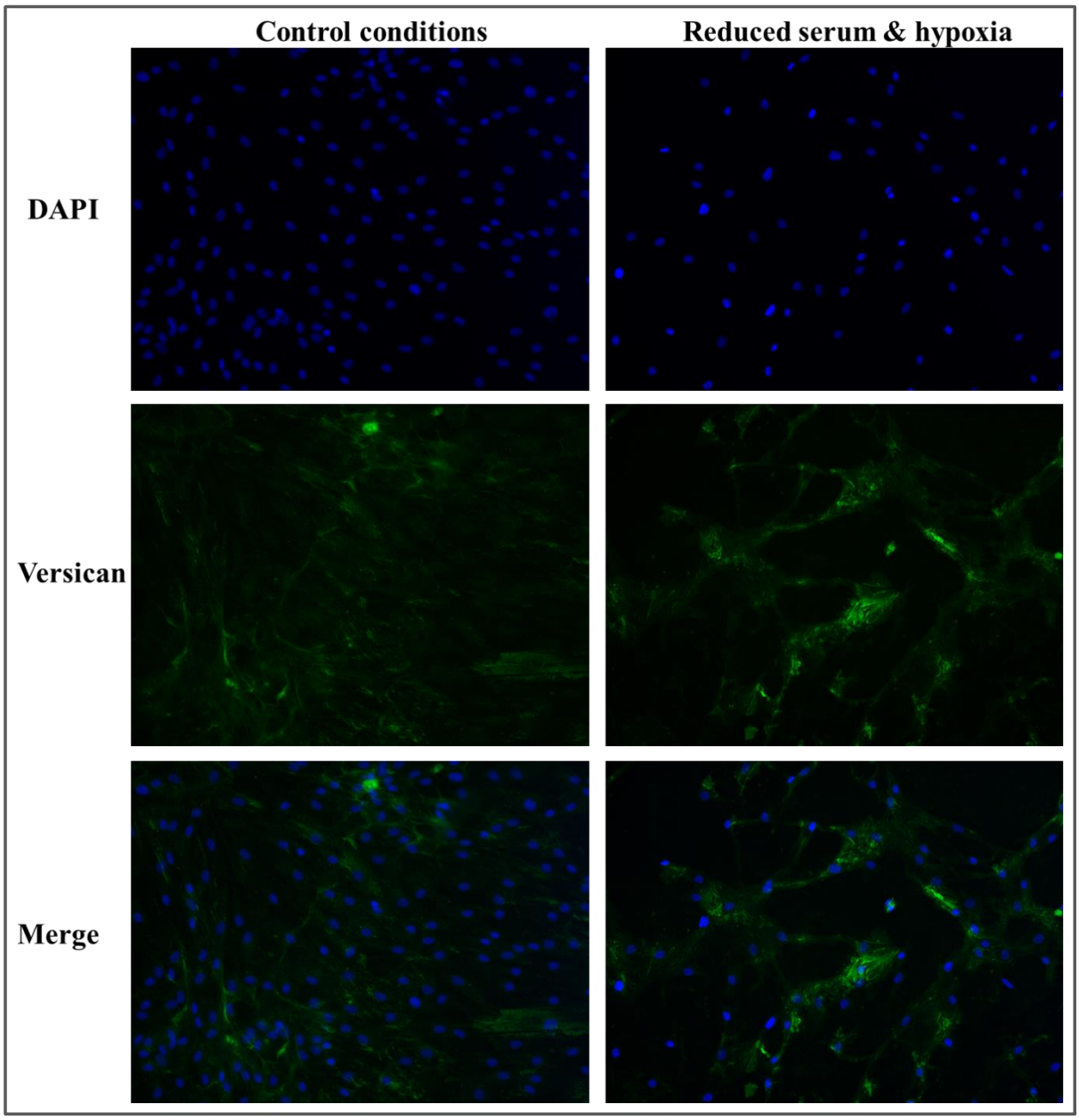

Figure 3.3.27 Representative images of versican immunofluorescence staining of degenerate NP cells (n=3) cultured in control conditions (left panels) and reduced serum and hypoxia (right panels) for 7 days. Immunofluorescence staining was performed using anti-versican primary antibody followed by Alexa Fluor 488 conjugated secondary antibody (green). DAPI (blue) was used for nucleus staining. Top row: DAPI, middle row: same field of view with versican staining, bottom row: merge of above two rows (magnification x200).

3.3.6 Influence of reduced glucose and hypoxia on NP cells (n=3) behaviour

3.3.6.1 Cell Viability and proliferation

Live/dead staining of degenerate NP cells cultured under reduced glucose and hypoxia displayed that majority of cells were stained green (viable) with few red stained (dead) cells (Figure 3.3.28).

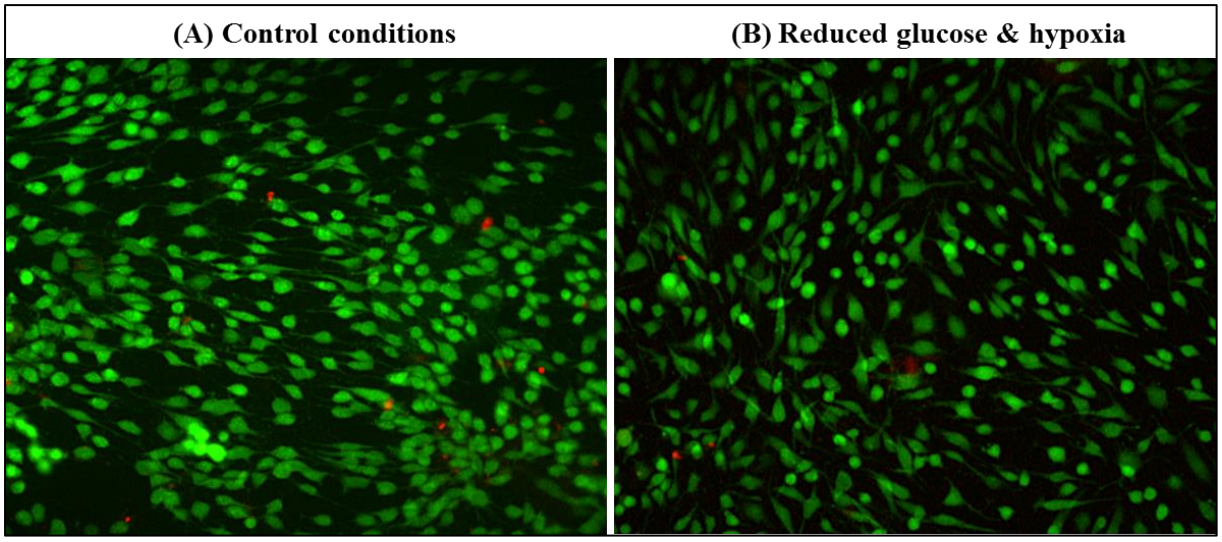

Figure 3.3.28 Effect of reduced glucose and hypoxia on degenerate NP cell viability. Degenerate NP cells (n=3) were cultured in (A) control conditions and (B) reduced glucose and hypoxia for 7 days and labelled with live-dead stain. Representative fluorescence microscope images indicating viable (stained green) and dead (stained red) populations under both conditions (magnification x100).

Proliferation analysis demonstrated that at day 7 the increase in cell number under reduced glucose and hypoxic condition was significantly high ($p \leq 0.05$) compared to the increase under control conditions (12488±256 versus 7390±29) (Figure 3.3.29).

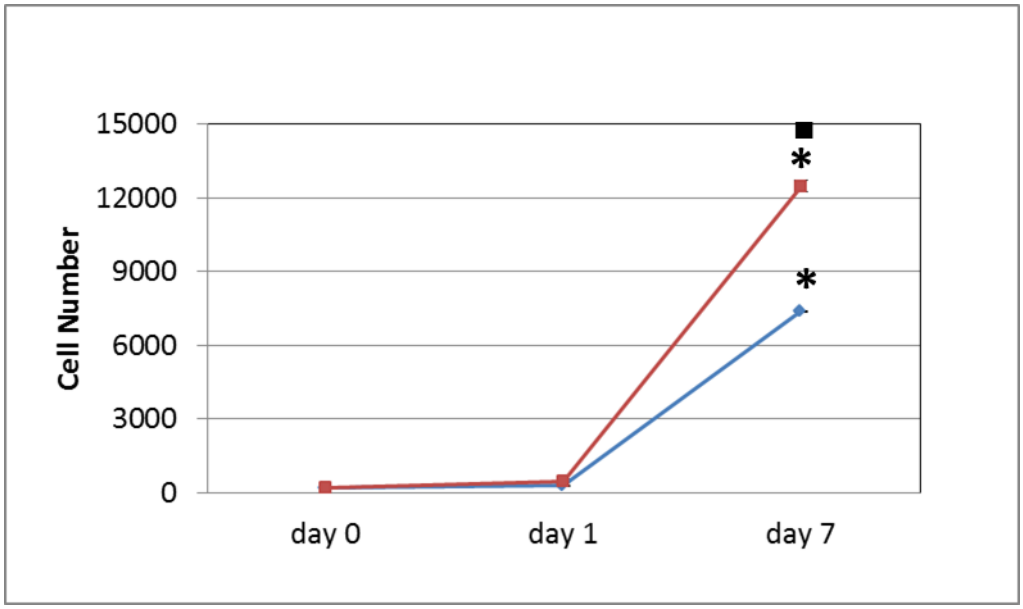

Figure 3.3.29 Effect of reduced glucose and hypoxia on degenerate NP cell (n=1) proliferation over the course of 7 days. Total cell number was determined for degenerate NP cell cultured under reduced glucose and hypoxia (red line) compared to control conditions (blue line). Day 0 cell number was used as baseline for each condition. Data was expressed as mean ± SEM of triplicates of 1 patient sample. Significant differences ($p \leq 0.05$) * compared to day 0 and ■ day 7 control conditions.

3.3.6.2 Gene expression

Degenerate NP cells cultured under reduced glucose combined with hypoxia showed no change in SOX-9 with a significant decrease in COL2A1 expression ($p<0.05$) (Figure 3.3.30 A). There was no change in ACAN expression while a significant decrease in VCAN expression ($p<0.05$) was observed under reduced glucose combined with hypoxia (Figure 3.3.30 B). A significant decrease ($p<0.05$) in PAX-1 was seen while FOXF1 expression was significantly increased ($p<0.05$) compared to control conditions (Figure 3.3.30 C).

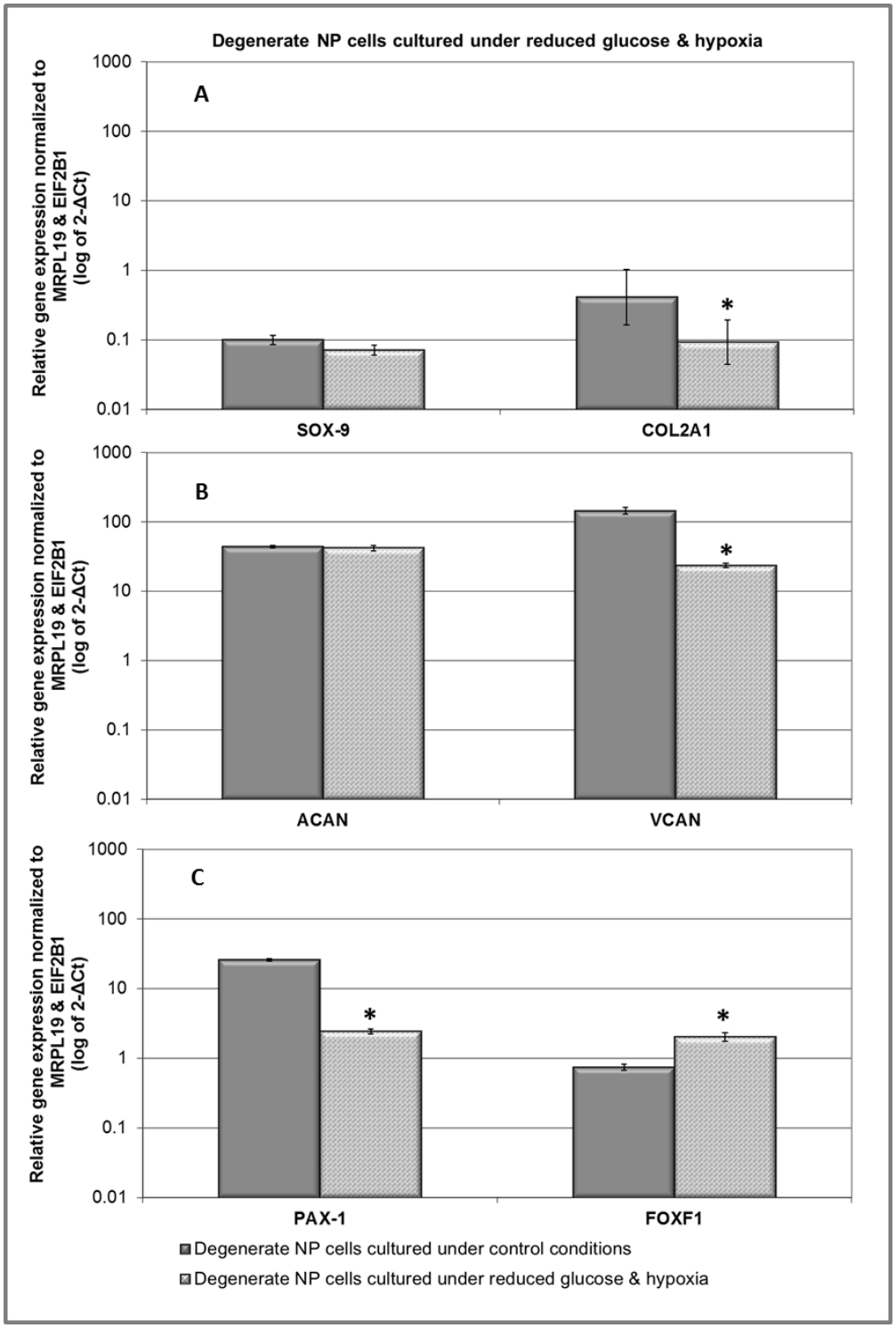

Figure 3.3.30 Relative gene expression of (A) SOX-9, COL2A1 (B) ACAN, VCAN and (C) PAX-1, FOXF-1 in degenerate NP cells cultured under reduced glucose and hypoxia (n=3). Gene expression normalized to average of HK genes MRPL19 and EIF2B1 and plotted on a log scale. * Statistical significance ($p \leq 0.05$) compared to culture in control conditions.

3.3.6.3 ECM protein expression

Degenerate NP cells cultured under reduced glucose combined with hypoxia showed increase staining intensity for both aggrecan and versican proteins (Figure 3.3.31 & 3.3.32 respectively). Versican displayed similar staining pattern seen previously under hypoxic conditions (Figure 3.3.32).

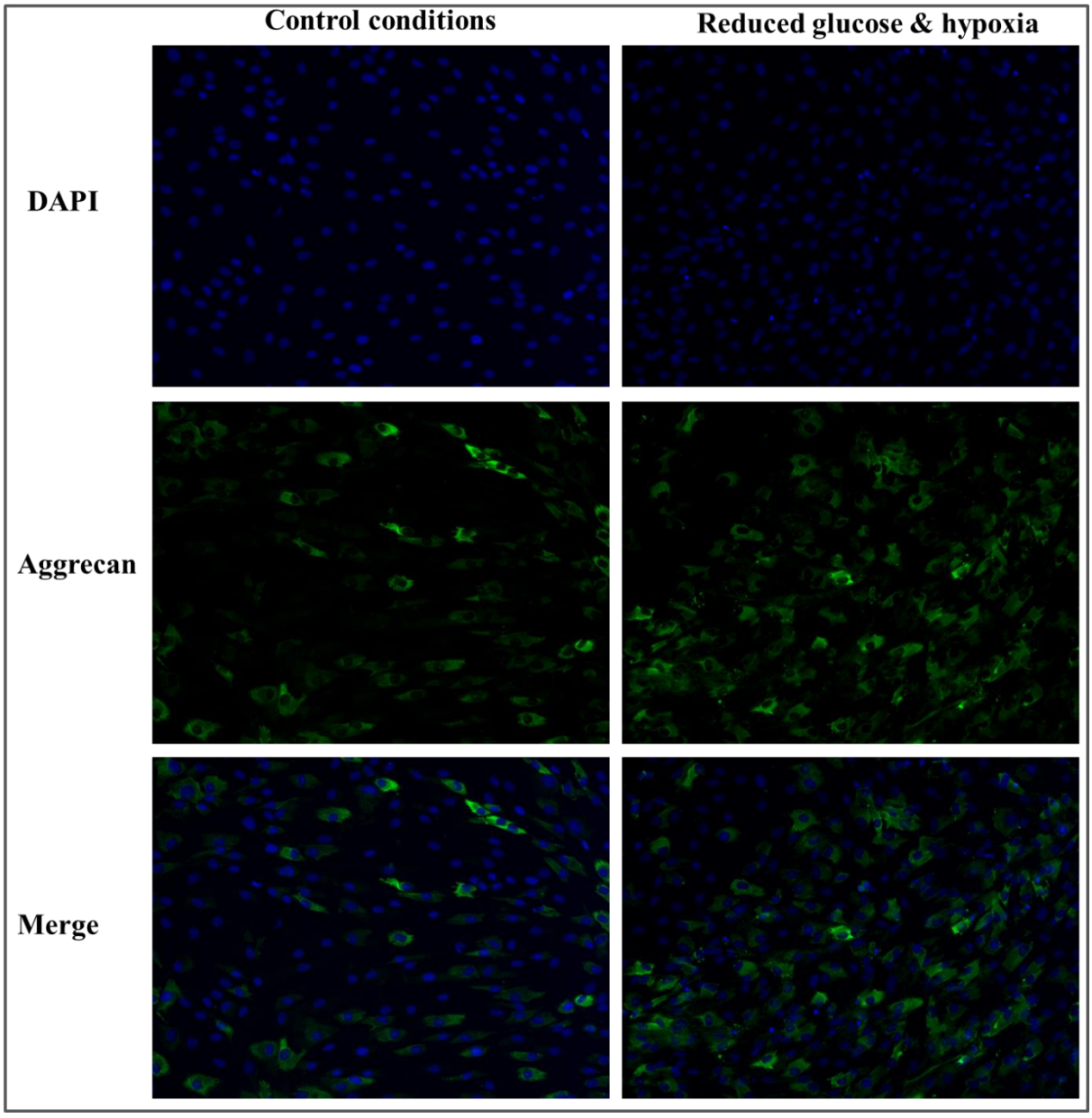

Figure 3.3.31 Representative images of aggrecan immunofluorescence staining of degenerate NP cells (n=2) cultured in control conditions (left panels) and reduced glucose and hypoxia (right panels) for 7 days. Immunofluorescence staining was performed using anti-aggrecan primary antibody followed by Alexa Fluor 488 conjugated secondary antibody (green). DAPI (blue) was used for nucleus staining. Top row: DAPI, middle row: same field of view with aggrecan staining, bottom row: merge of above two rows (magnification x200).

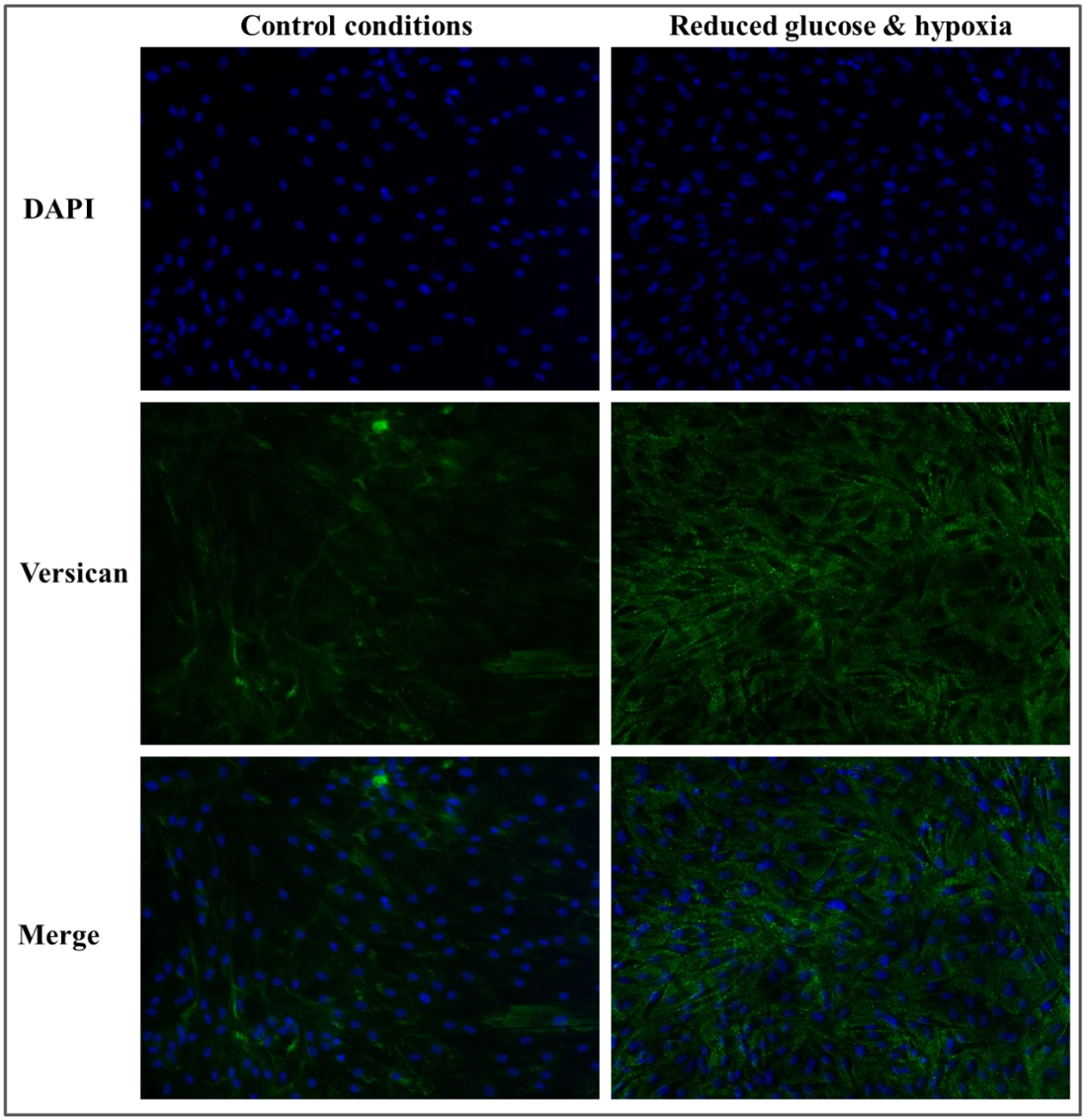

Figure 3.3.32 Representative images of versican immunofluorescence staining of degenerate NP cells (n=3) cultured in control conditions (left panels) and reduced glucose and hypoxia (right panels) for 7 days. Immunofluorescence staining was performed using anti-versican primary antibody followed by Alexa Fluor 488 conjugated secondary antibody (green). DAPI (blue) was used for nucleus staining. Top row: DAPI, middle row: same field of view with versican staining, bottom row: merge of above two rows (magnification x200).

3.3.7 Influence of reduced serum, reduced glucose and hypoxia on NP cell behaviour

3.3.7.1 Cell viability and proliferation

Live/dead assay of degenerate NP cell culture under reduced serum, glucose and hypoxia displayed that majority of cells were stained green (viable) with few red stained (dead) cells (Figure 3.3.33).

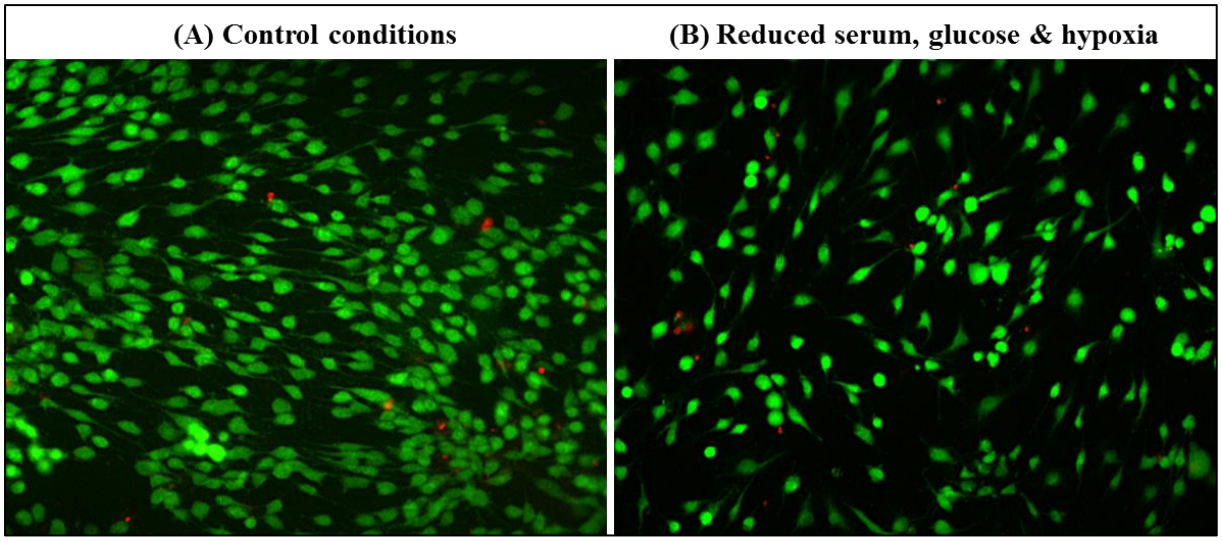

Figure 3.3.33 Effect of reduced serum, glucose and hypoxia on degenerate NP cell viability. Degenerate NP cells (n=3) were cultured in (A) control conditions and (B) reduced serum, glucose and hypoxia for 7 days and labelled with live-dead stain. Representative fluorescence microscope images indicating viable (stained green) and dead (stained red) populations under both conditions (magnification x100).

Proliferation assay indicated that at day 7 the change in degenerate NP cell number cultured under reduced serum, reduced glucose and hypoxia (8425 ±345) was not significantly different compared to control conditions (7390±29) (Figure 3.3.34).

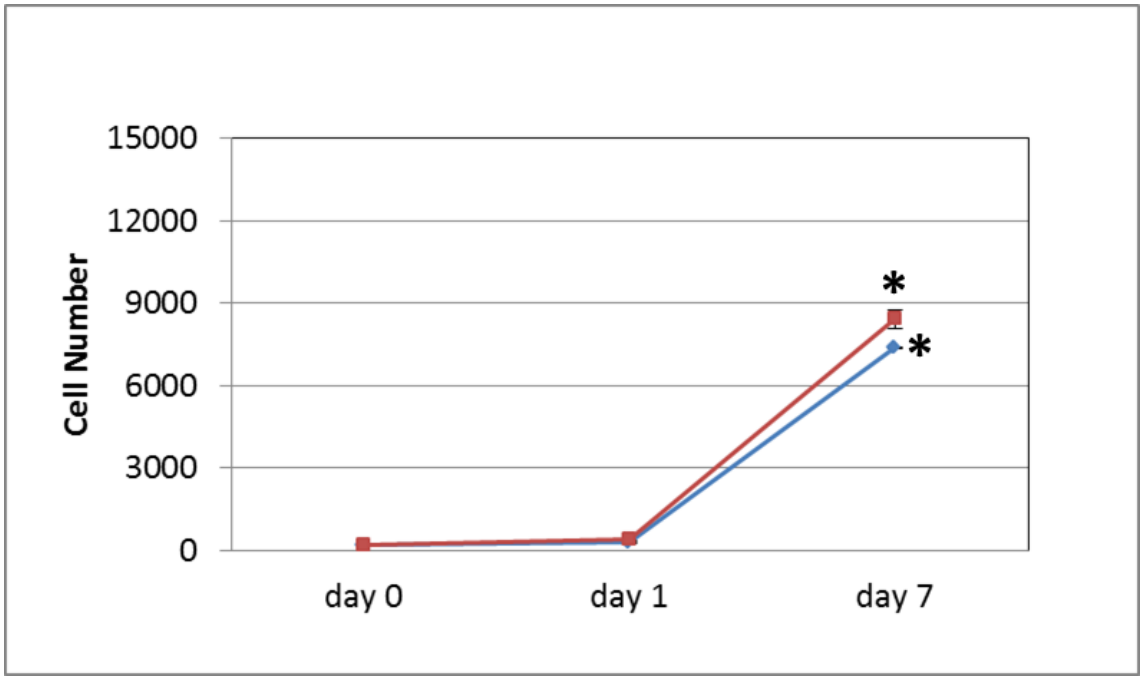

Figure 3.3.34 Effect of reduced serum, glucose and hypoxia on degenerate NP cell (n=1) proliferation over the course of 7 days. Total cell number was determined for degenerate NP cell cultured under reduced serum, reduced glucose and hypoxia (red line) compared to control conditions (blue line). Day 0 cell number was used as baseline for each condition. Data was expressed as mean ± SEM of triplicates of 1 patient sample. Significant differences ($p \leq 0.05$) * compared to day 0 control conditions.

3.3.7.2 Gene expression

Degenerate NP cells cultured under reduced serum, reduced glucose and hypoxia showed no change in SOX-9 and COL2A1 expression (Figure 3.3.35 A). A significant decrease in both ACAN and VCAN ($p<0.05$ for both) was seen compared to control conditions (Figure 3.3.35 B). PAX-1 expression was significantly decreased ($p<0.05$) while FOXF1 expression was significantly increased ($p<0.05$) under reduced serum, reduced glucose and hypoxia (Figure 3.3.35 C).

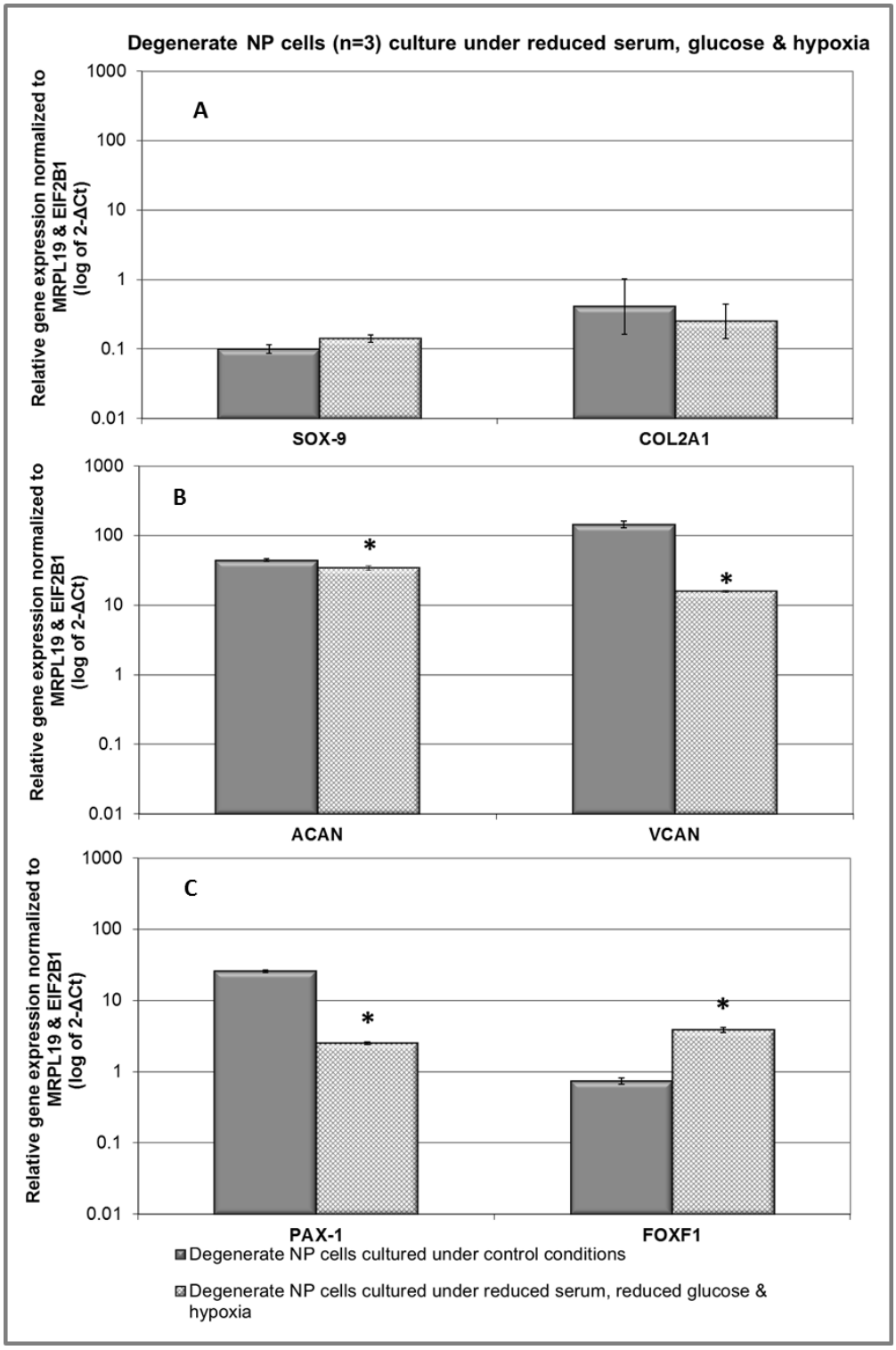

Figure 3.3.35 Relative gene expression of (A) SOX-9, COL2A1, (B) ACAN, VCAN and (C) PAX-1, FOXF1 in degenerate NP cells cultured under reduced serum, reduced glucose and hypoxia (n=3) compared to control conditions. Gene expression normalized to average of HK genes MRPL19 and EIF2B1 and plotted on a log scale. * Statistical significance ($p \leq 0.05$) compared to culture in control conditions

3.3.7.3 ECM protein expression

A decrease in aggrecan and versican staining intensity was seen in degenerate NP cells cultured under reduced serum, reduced glucose and hypoxia compare to degenerate NP cells cultured under control conditions (Figure 3.3.36 & 3.3.37 respectively).

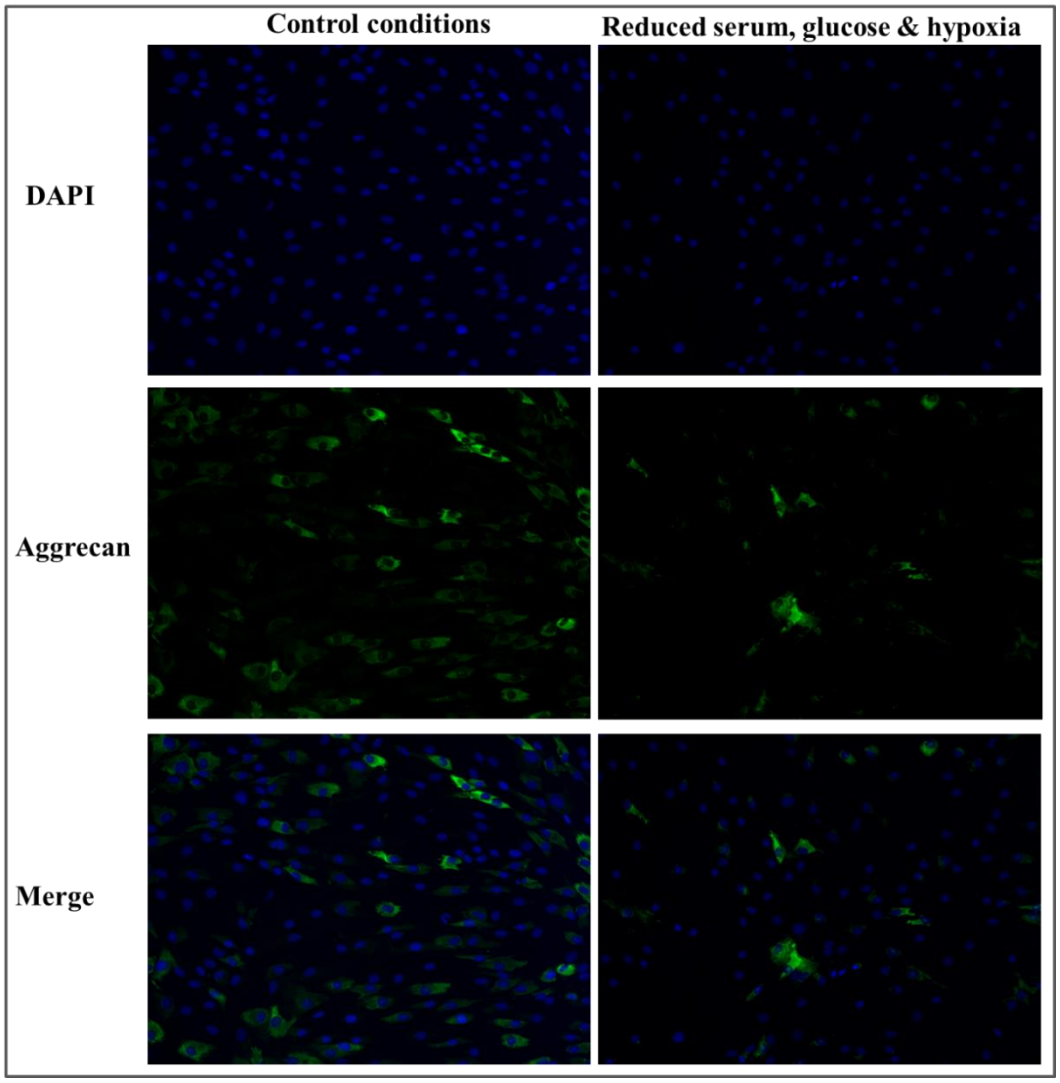

Figure 3.3.36 Representative images of aggrecan immunofluorescence staining of degenerate NP cells (n=2) cultured in control conditions (left panels) and reduced serum, reduced glucose and hypoxia (right panels) for 7 days. Immunofluorescence staining was performed using anti-aggrecan primary antibody followed by Alexa Fluor 488 conjugated secondary antibody (green). DAPI (blue) was used for nucleus staining. Top row: DAPI, middle row: same field of view with aggrecan staining, bottom row: merge of above two rows (magnification x200).

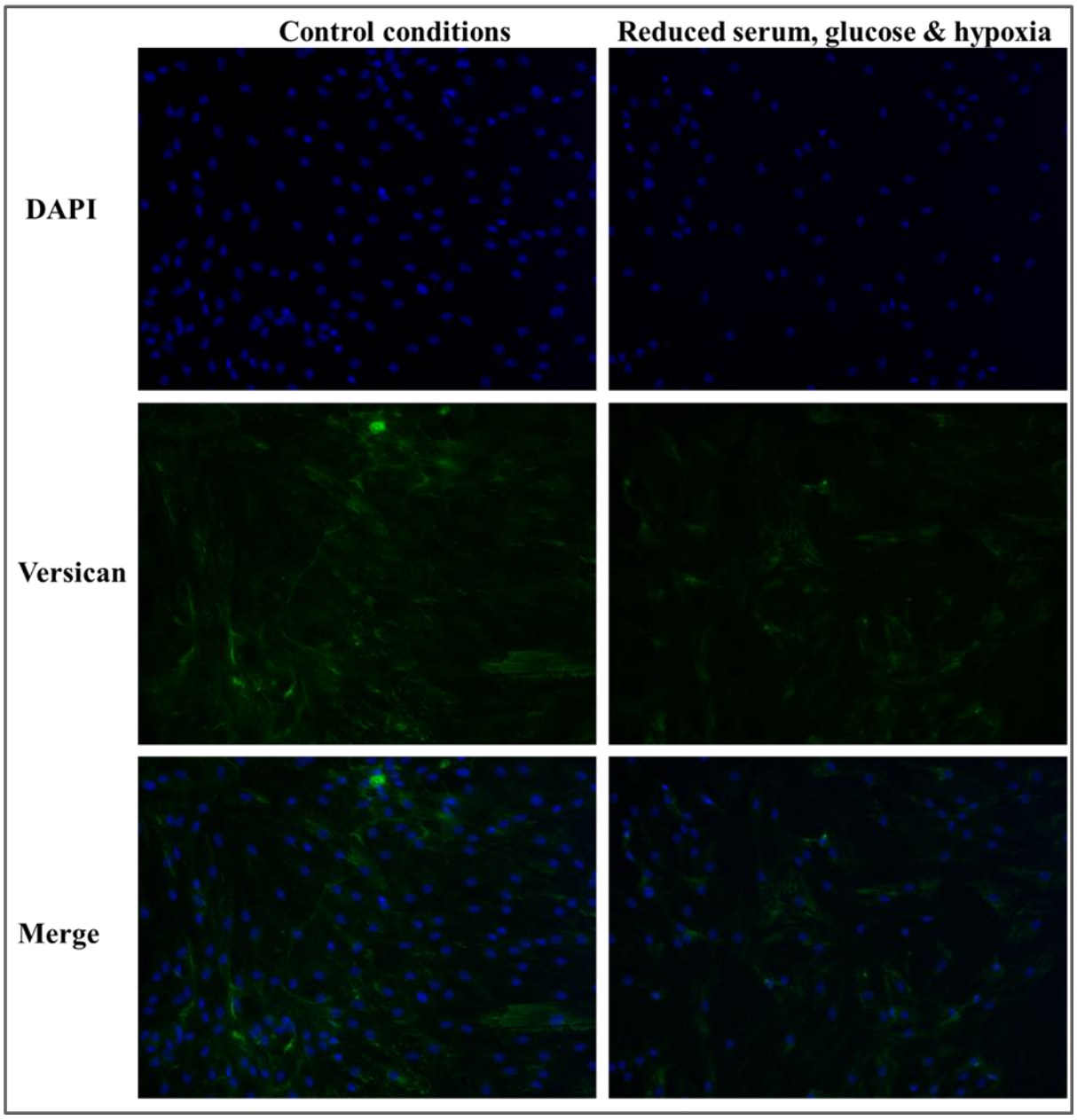

Figure 3.3.37 Representative images of versican immunofluorescence staining of degenerate NP cells (n=3) cultured in control conditions (left panels) and reduced serum, reduced glucose and hypoxia (right panels) for 7 days. Immunofluorescence staining was performed using anti-versican primary antibody followed by Alexa Fluor 488 conjugated secondary antibody (green). DAPI (blue) was used for nucleus staining. Top row: DAPI, middle row: same field of view with versican staining, bottom row: merge of above two rows (magnification x200).

3.3.8 Influence of reduced pH on degenerate NP cells behaviour

3.3.8.1 Cell viability and proliferation

Live/dead staining of degenerate NP cells culture under reduced pH 6.8 and 6.5 showed green stained cells as seen in pH 7.4. Degenerate NP cells did not display shrinkage of cytoplasm as seen for human BM-MSCs cultured alone under reduced pH conditions (Chapter 4, section 4.3.8) (Figure 3.3.38).

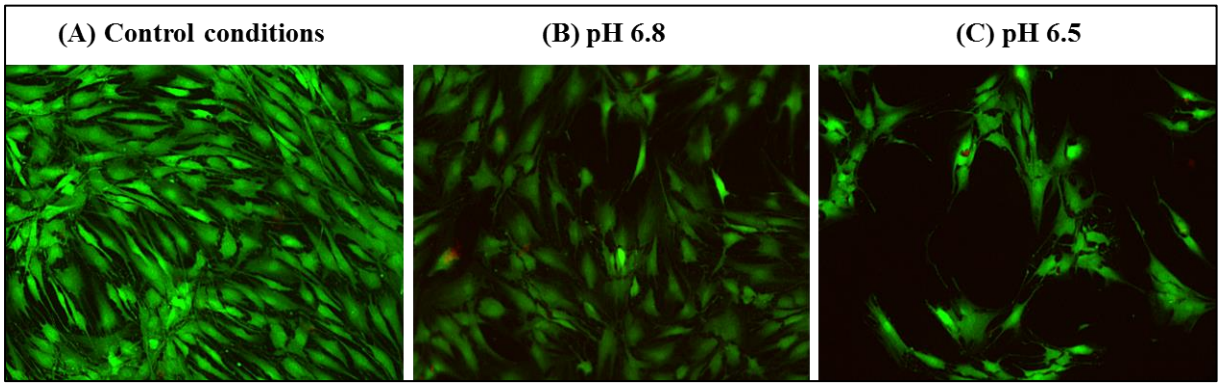

Figure 3.3.38 Effect of reduced pH (6.8 and 6.5) on degenerate NP cells viability. Degenerate NP cells (n=3) were cultured under (A) control conditions pH 7.4 (left), (B) pH 6.8 (middle) and (C) pH 6.5 (right) for 7 days and labelled with live-dead stain. Representative fluorescence microscope images indicate viable (stained green) and dead (stained red) populations under both conditions (magnification x200).

Proliferation analysis showed that at day 7 the increase in cell number under pH 6.8 was not significantly different from control conditions (323807±1640 versus 307727±1226) (Figure 3.3.39). However, the increase in cell number (126185±2829) under pH 6.5 was significantly less compared to pH 6.8 (323807±1640) and control conditions (307727±1226) ($p > 0.05$ for both) (Figure 3.3.39).

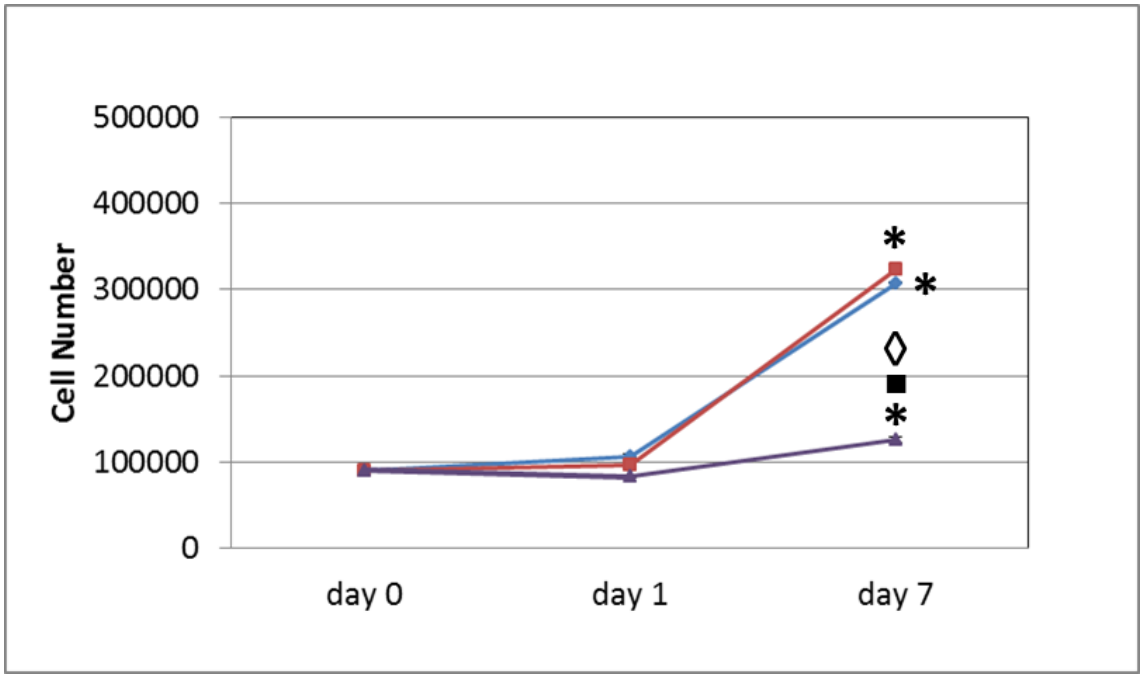

Figure 3.3.39 Effect of reduced pH 6.8 and 6.5 on degenerate NP cell (n=1) proliferation over the course of 7 days. Total cell number was determined for degenerate NP cell culture under pH 6.8 (red line), pH 6.5 (purple) and control conditions pH 7.4 (blue line). Day 0 cell number was used as baseline for each condition. Data was expressed as mean ± SEM of triplicates of 1 patient sample. Significant differences ($p \leq 0.05$) * compared to day 0 and day 7 ■ control and ◊ pH 6.8 conditions.

3.3.8.2 Gene expression

Degenerate NP cells cultured under pH 6.8 and 6.5 showed a significant increase in SOX-9 expression ($p<0.05$) compared to control conditions (Figure 3.3.40 A). There was no change in COL2A1 expression under both pH 6.8 and 6.5 (Figure 3.3.40) No significant change in ACAN and VCAN expression was seen under pH 6.8 but gene expression for both decreased significantly ($p<0.05$) under pH 6.5 compared to control and pH 6.8 (Figure 3.3.40 B). PAX-1 expression remained unaffected under pH 6.8 and 6.5 compared to control conditions but it was significantly down regulated ($p<0.05$) under pH 6.5 compared to pH 6.8. A significant increase ($p<0.05$) was seen in FOXF1 expression under both pH 6.8 and 6.5 (Figure 3.3.40). Degenerate NP cells cultured under pH 6.8 showed significant increase ($p<0.05$) in CA9 and CA12 expression. Under pH 6.5 significant up regulation in CA9 ($p<0.05$) was observed. CA12 showed significantly decreased ($p<0.05$) expression under pH 6.5 compared to pH 6.8 (Figure 5.3.32 D).

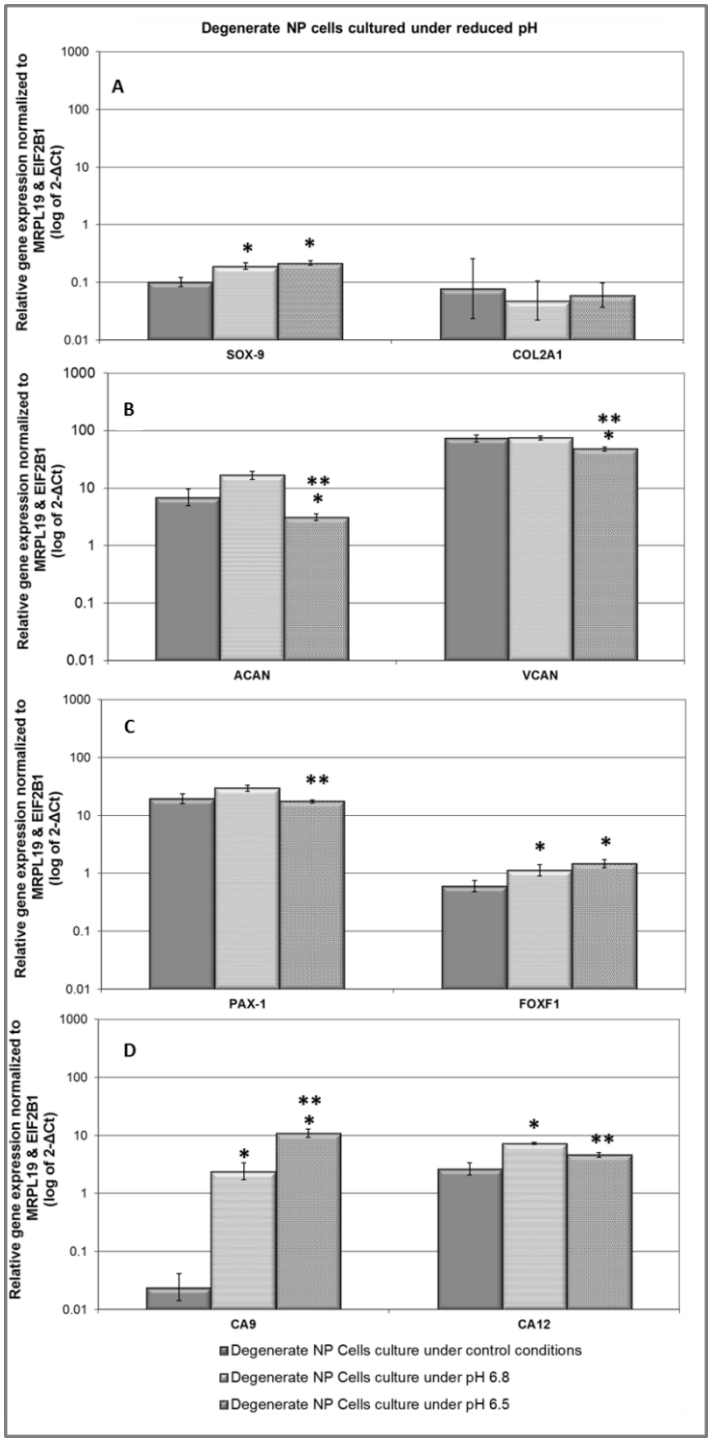

Figure 3.3.40 Relative gene expression of (A) SOX-9, Col2A1 (B) ACAN, VCAN, (C) PAX-1, FOXF1 and (D) CA9, CA12 in degenerate NP cells cultured under reduced pH 6.8 and 6.5 (n=3). Gene expression normalized to average of HK genes MRPL19 and EIF2B1 and plotted on a log scale. * Statistical significance ($p \leq 0.05$) compared to culture under control conditions and ** culture under pH 6.8.

3.3.9 Influence of reduced pH 6.8 and hypoxia on degenerate NP cell behaviour

3.3.9.1 Cell viability and proliferation

Live/dead staining of degenerate NP cells cultured under pH 6.8 combined with hypoxia showed green stained (viable) cells similar to control conditions (Figure 3.3.41)

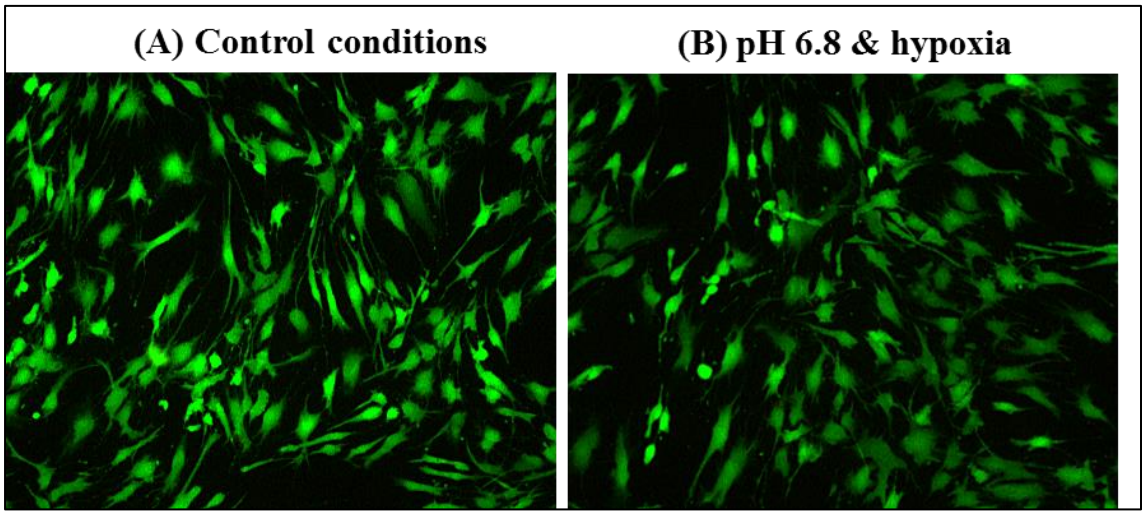

Figure 3.3.41 Effect of pH 6.8 and hypoxia on degenerate NP cell viability. Degenerate NP cells (n=1) were cultured in (A) control conditions and (B) pH 6.8 and hypoxia for 7 days and labelled with live-dead stain. Representative fluorescence microscope images indicating viable (stained green) and dead (stained red) populations under both conditions (magnification x200).

Proliferation analysis showed that at day 7 the increase in cell number under pH 6.8 combined with hypoxia was significantly high (p>0.05) compared to control conditions (441849±3554 versus 307727±1226) (Figure 3.3.42).

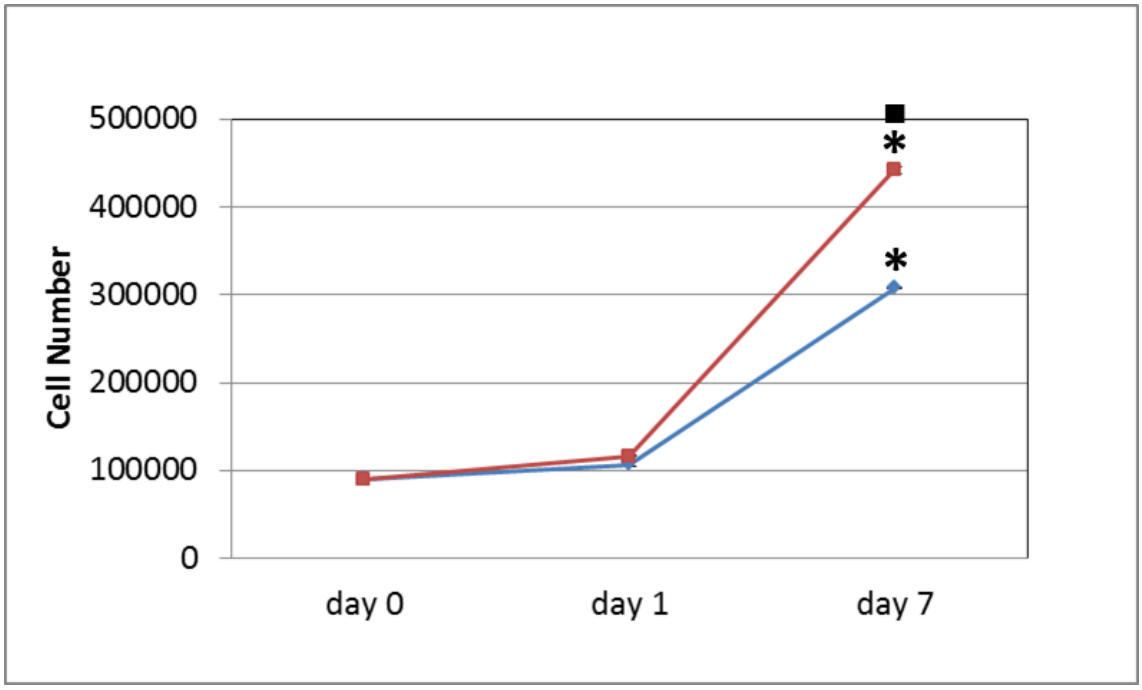

Figure 3.3.42 Effect of pH 6.8 and hypoxia on degenerate NP cell (n=1) proliferation over the course of 7 days. Total cell number was determined for degenerate NP cell cultured under pH 6.8 and hypoxia (red line) compared to control conditions (blue line). Day 0 cell number was used as baseline for each condition. Data was expressed as mean ± SEM of triplicates of 1 patient sample. Significant differences ($p \leq 0.05$) * compared to day 0 and ■ day 7 control conditions.

3.3.9.2 Gene expression

Degenerate NP cells cultured under reduced pH 6.8 combined with hypoxia showed no changes in SOX-9, COL2A1 and ACAN expression compared to degenerate NP cells cultured under control conditions (Figure 3.3.43 A). VCAN expression was significantly increased ($p<0.05$) under reduced pH 6.8 and hypoxia (Figure 3.3.43 B). PAX-1 expression was significantly decreased ($p<0.05$) while FOXF1 expression remain unchanged (Figure 3.3.43 C). A significant up regulation was seen in CA9 ($p<0.05$) with no change in CA12 expression under reduced pH and hypoxia compared to control conditions (Figure 3.3.43 D).

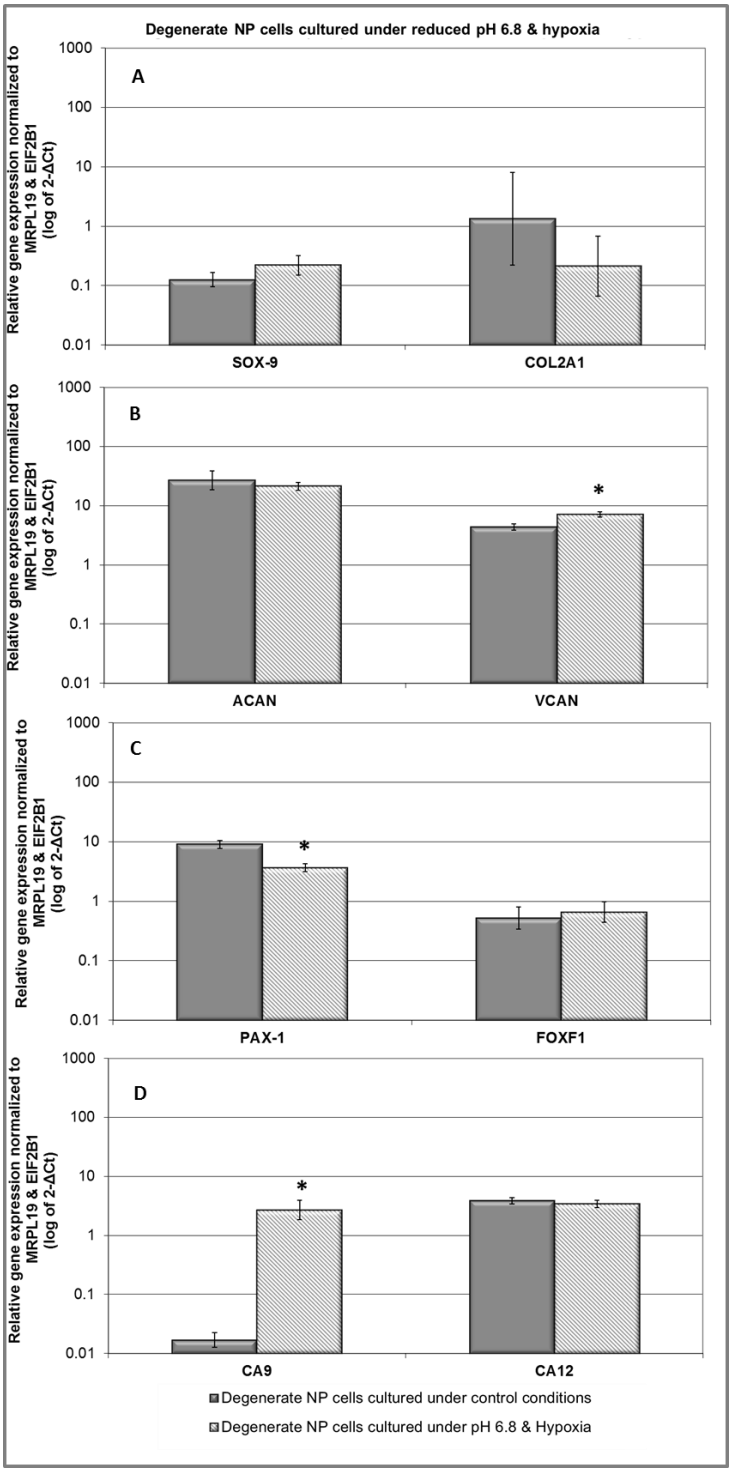

Figure 3.3.43 Relative gene expression of (A) SOX-9, COL2A1 (B) ACAN, VCAN (C) PAX-1 and FOXF-1 and (D) CA9, CA12 in degenerate NP cells cultured under reduced pH 6.8 and hypoxia (n=3). Gene expression normalized to average of HK genes MRPL19 and EIF2B1 and plotted on a log scale. * Statistical significance ($p \leq 0.05$) compared to culture in control conditions.

3.3.10 Influence of all IVD-like physio-chemical microenvironmental conditions (hypoxia, reduced serum, reduced glucose and pH 6.8) on degenerate NP cell behaviour

3.3.10.1 Cell viability and proliferation

Live/dead assay of degenerate NP cells cultured under all IVD-like physio-chemical microenvironmental conditions combined showed green stained (viable) cells similar to control conditions (Figure 3.3.44)

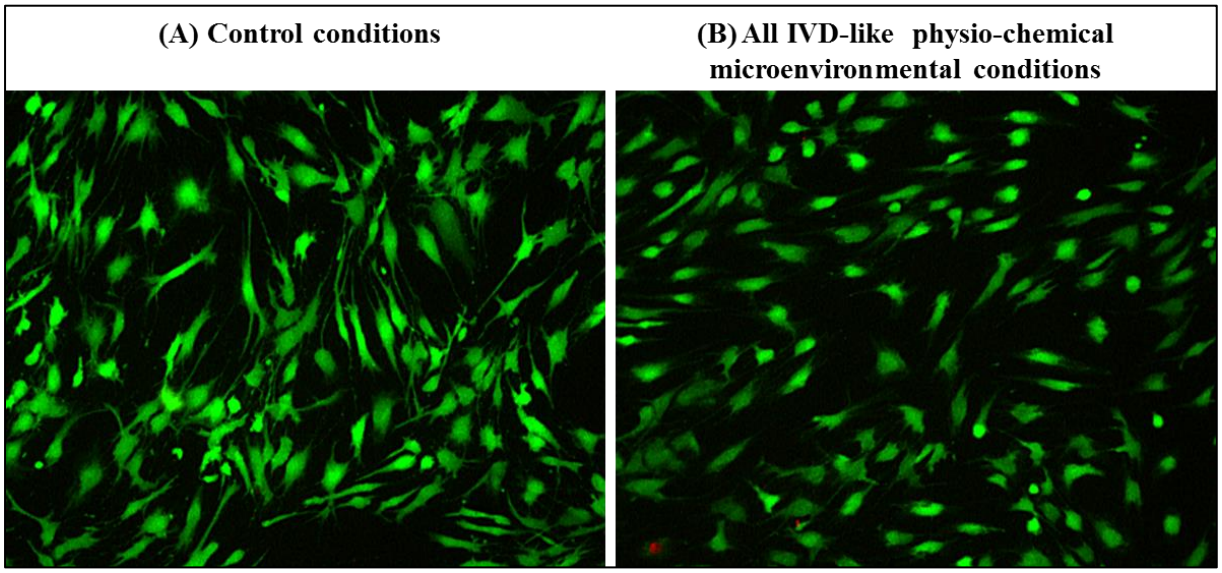

Figure 3.3.44 Effect of all IVD-like physio-chemical microenvironmental conditions combined on degenerate NP cell viability. Degenerate NP cells (n=1) were cultured in (A) control conditions and (B) all IVD-like physio-chemical microenvironmental conditions combined for 7 days and labelled with live-dead stain. Representative fluorescence microscope images indicating viable (stained green) and dead (stained red) populations in both conditions (magnification x200).

Proliferation analysis showed that at day 7 increase in cell number under all IVD-like physio-chemical conditions was significantly less (p>0.05) compared to control conditions (190433±3302 versus 307727±1226) (Figure 3.3.42).

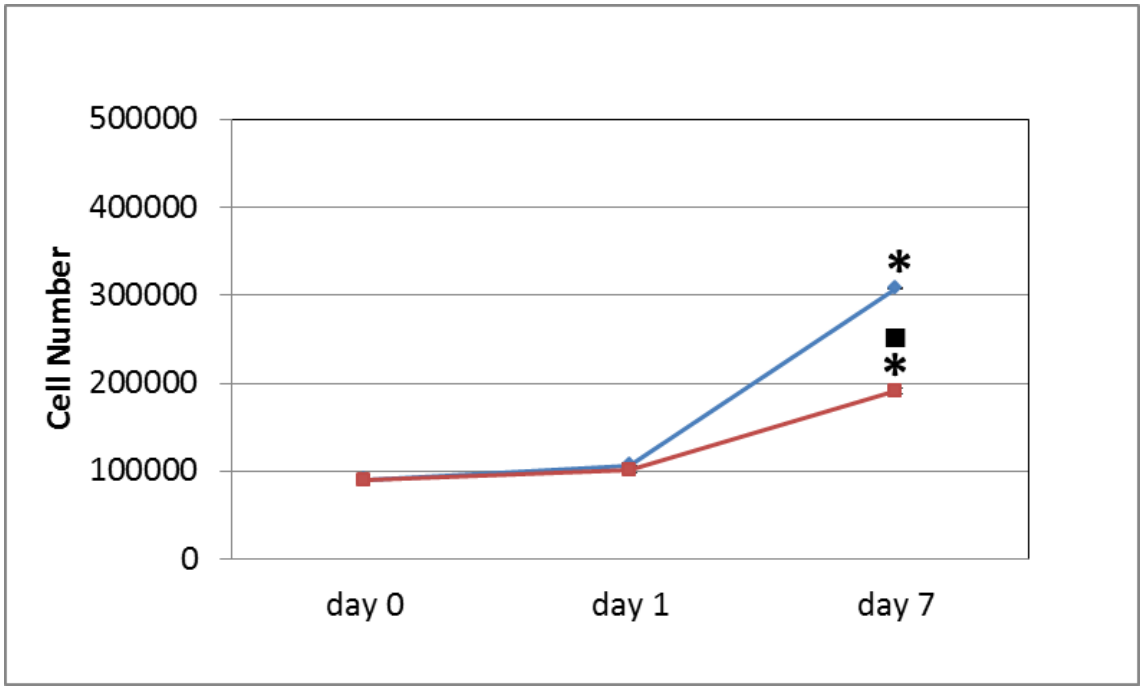

Figure 3.3.45 Effect of all IVD-like physio-chemical microenvironmental conditions combined on degenerate NP cell (n=1) proliferation over the course of 7 days. Total cell number was determined for degenerate NP cell cultured under all IVD-like physio-chemical microenvironmental conditions combined (red line) compared to control conditions (blue line). Day 0 cell number was used as baseline for each condition. Data was expressed as mean ± SEM of triplicates of 1 patient sample. Significant differences ($p \leq 0.05$) * compared to day 0 and ■ day 7 control conditions.

3.3.10.2 Gene expression

Degenerate NP cells cultured under all IVD-like physio-chemical microenvironmental conditions combined showed no significant difference in SOX-9 and COL2A1 expression (Figure 3.3.46 A). There was no change in ACAN expression with a significant increase in VCAN expression ($p<0.05$) compared to control conditions (Figure 3.3.46 B). PAX-1 showed significant decrease ($p<0.05$) while FOXF1 remained unchanged (Figure 3.3.46 C). A significant increase in CA9 ($p<0.05$) with no change in CA12 was observed compared to control conditions (Figure 3.3.46 D).

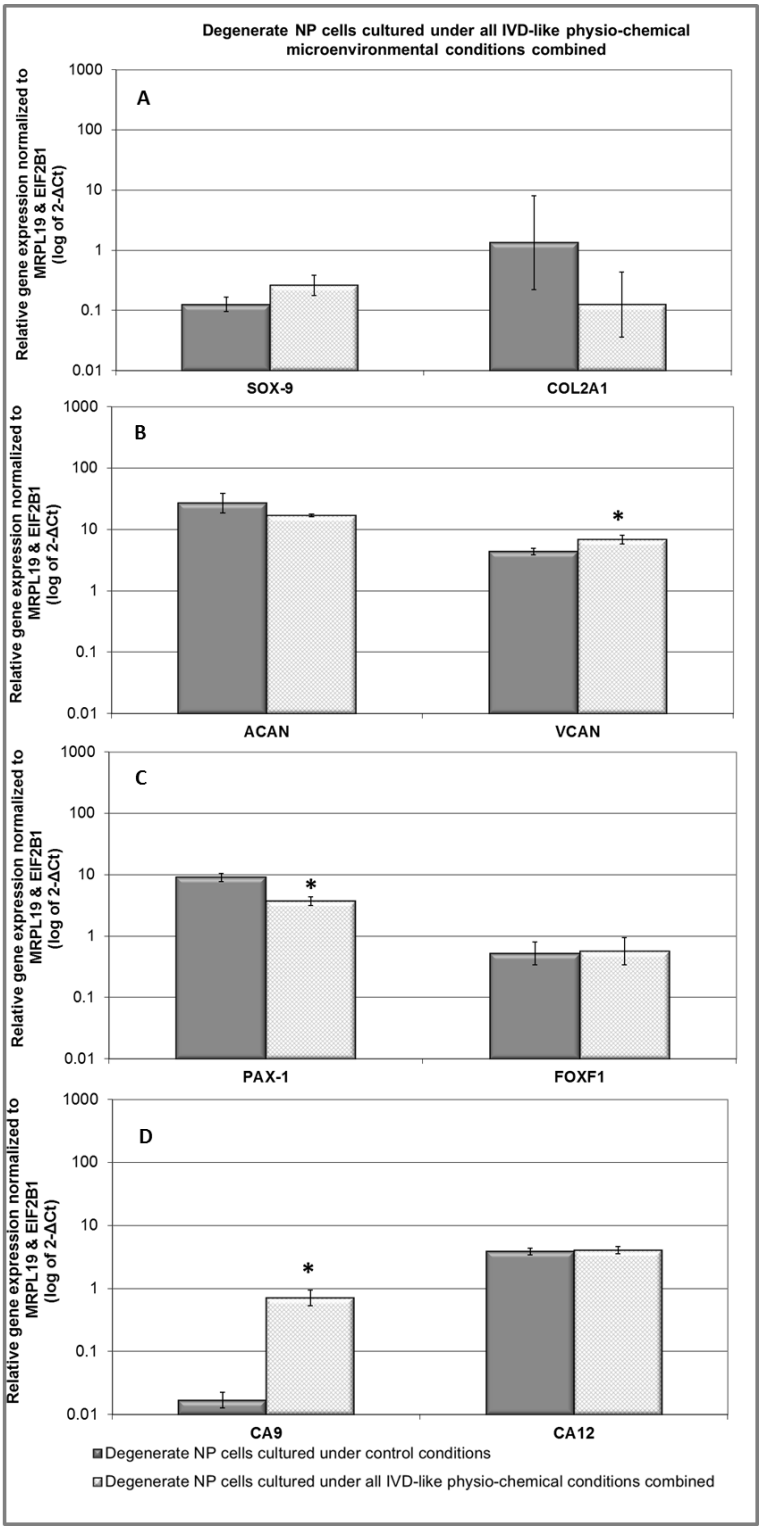

Figure 3.3.46 Relative gene expression of (A) SOX-9, COL2A1, (B) ACAN, VCAN, (C) PAX-1, FOXF1 and (D) CA9, CA12 in degenerate NP cells cultured in IVD-like physio-chemical microenvironmental conditions combined (n=3) compare to control conditions. Gene expression normalized to average of HK genes MRPL19 and EIF2B1 and plotted on a log scale. * Statistical significance ($p \leq 0.05$) compared to culture in control conditions.

Table 3.6 Summary of changes in gene and ECM protein expressions under all test conditions compared to degenerate NP cells cultured under control conditions

Condition / Genes	Hyp	Nutrient limited conditions			Nutrient limited & hypoxic conditions			Acidic conditions		Acidic & hypoxic conditions	All
		RS	RG	RS+ RG	RS +H	RG +H	RS+ RG+ H	pH 6.8	pH 6.5	pH 6.8+ H	
SOX-9	↔	↔	↔	↑	↔	↔	↔	↑	↑	↔	↔
Col2A1	↔	↔	↔	↔	↔	↓	↔	↔	↔	↔	↔
ACAN	↑	↔	↔	↓	↔	↔	↓	↔	↓	↔	↔
VCAN	↑	↔	↔	↔	↑	↓	↓	↔	↓	↑	↑
PAX-1	↔	↔	↓	↑	↔	↓	↓	↔	↓	↓	↓
FOXF1	↔	↔	↔	↔	↔	↑	↑	↑	↑	↔	↔
CA9	−−	−−	−−	−−	−−	−−	−−	↑	↑	↑	↑
CA12	−−	−−	−−	−−	−−	−−	−−	↑	↔	↔	↔

↔ = no significant change

↑= significant increase

↓= significant decrease

−− = expression was not studied

Hyp = Hypoxia, **RS** = Reduced serum, **RG** = Reduced glucose, **RS+RG** = Reduced serum, reduced glucose, **RS+H** = Reduced serum & hypoxia, **RG+ H** = Reduced glucose & hypoxia, **RS+RG+H** = Reduced serum, reduced glucose & hypoxia, **pH 6.8 + H** = pH 6.8 & hypoxia, **All** = All IVD-like physio-chemical microenvironmental conditions combined

Table 3.7 Summary of changes in ECM protein expression in degenerate NP cells under all test conditions compared to degenerate NP cells cultured under control conditions

Condition / Genes	Hyp	Nutrient limited conditions			Nutrient limited & hypoxic conditions			Acidic conditions		Acidic & hypoxic conditions
		RS	RG	RS+ RG	RS +H	RG +H	RS+ RG+ H	pH 6.8	pH 6.5	pH 6.8+ H
Aggrecan staining intensity	↑	↔	↔	↔	↑	↑	↓	––	––	––
Versican staining intensity	↑	↔	↔	↔	↔	↑	↓	––	––	––

↔ = no change

↑= increase

↓= decrease

–– = expression was not studied

Hyp = Hypoxia, **RS** = Reduced serum, **RG** = Reduced glucose, **RS+RG** = Reduced serum, reduced glucose, **RS+H** = Reduced serum & hypoxia, **RG+ H** = Reduced glucose & hypoxia, **RS+RG+H** = Reduced serum, reduced glucose & hypoxia, **pH 6.8 + H** = pH 6.8 & hypoxia, **All** = All IVD-like physio-chemical microenvironmental conditions combined

Table 3.8 Summary of changes in degenerate NP cell number under all test conditions at day 7 compared to cells cultured under control conditions

Condition		Day-7 cell number
Control Conditions (Day-0 cell number = 204±26)		7390±28
Hypoxia		12973±721
Nutrient limited conditions	Reduced serum	1710±150
	Reduced glucose	5668±220
	Reduced serum & reduced glucose	2942±359
Nutrient limited & hypoxic conditions	Reduced serum & hypoxia	5519±299
	Reduced glucose & hypoxia	12488±256
	Reduced serum, reduced glucose & hypoxia	8425 ±345
Control for pH conditions (Day-0 cell number =90172±246)		307727±1226
pH 6.8		323807±1640
pH 6.5		126185±2829
pH 6.8 & hypoxia		441849±3554
All		190433±3302

3.4 Discussion

Investigations of NP cell behaviour/biology are of great importance to our understanding of the processes involved in disc degeneration. Reports suggest that limited nutrition and acidic conditions affect NP cell viability and function which may be associated with the characteristic changes seen in disc degeneration (Ohshima and Urban, 1992, Horner and Urban, 2001, Razaq et al., 2003, Bibby and Urban, 2004, Johnson et al., 2008, Rinkler et al., 2010, Gawri et al., 2011, Neidlinger-Wilke et al., 2012). However, these studies are limited as the impact of only a small number of conditions akin to the *in vivo* microenvironment were investigated. It is important to study the effect of all conditions mimicking the disc physio-chemical microenvironment in different combinations to understand their effects on human disc cell behaviour. This is the first study to investigate the effect of the IVD-like physio-chemical microenvironmental conditions [i.e. hypoxia (2% O_2), reduced nutrient (5mM glucose and 2% FCS) and acidic pH (6.8 & 6.5)] alone and in combinations on human degenerate NP cell behaviour. Cellular behaviour was assessed in terms of cell viability, proliferation and expression of NP conventional (SOX-9, COL2A1, ACAN and VCAN) and novel (PAX-1 and FOXF1) marker genes along with aggrecan and versican protein synthesis. Expression of CA9 and CA12 was assessed under acidic conditions.

Based on the available literature O_2, glucose, serum and pH factors were chosen as representative physio-chemical parameters of IVD to vary in this study. 2% O_2 concentration was utilized to represent the hypoxic disc microenvironment as used previously (Agrawal et al., 2007, Agrawal et al., 2008, Feng et al., 2013). Conventional media used for cell isolation and expansion include supplementation of serum usually FCS at 10% (v/v). Serum contains high content of growth factors (e.g. IGF, PDGF) as well as nutritional (e.g. glucose, amino acids, vitamins) compounds required for cell maintenance and growth (Jung et al., 2012). It is not known whether this high concentration is experienced by disc cells *in vivo*. During *in vitro* culture, a serum starvation approach has been used to simulate IVD nutrient deprived conditions (Johnson et al., 2008, Liang et al., 2012c, Sudo et al., 2013). Complete serum withdrawal induces NP cell death (Risbud et al., 2005, Liang et al., 2012c, Sudo et al., 2013) suggesting that serum or serum derived growth factors may be important for survival of disc cells. In this study, instead of lowering to extremely low values, FCS concentration was limited to 2% for cell maintenance and survival. Based on previous investigations (Bibby and Urban, 2004, Wuertz et al., 2008, Liang et al., 2012a) 5mM glucose concentration was used to represent disc reduced glucose microenvironment compared to 25mM glucose

concentration. Based on previous investigations (Razaq et al., 2003, Wuertz et al., 2008, Wuertz et al., 2009a, Li et al., 2012, Liang et al., 2012a) pH 6.8 and 6.5 were used to represent moderate and severe disc pH microenvironment compared to pH 7.4 in control conditions.

Use of a model system that can retain cellular characteristics and phenotype is a critical step for better understanding the biology of cells. In this study NP cells were cultured using 2D monolayer culture system. A few reports suggest that monolayer culture alters expression of ECM genes (COL2A1 and ACAN) in NP cells (Kluba et al., 2005, Preradovic et al., 2005, Yuan et al., 2011). In this study degenerate NP after *in vitro* expansion showed maintained expression of the majority of ECM related genes SOX-9, ACAN and VCAN with a decrease in only COL2A1 which may be due to monolayer passaging. This finding is common with previous reports of monolayer culture system (Kluba et al., 2005, Preradovic et al., 2005, Yuan et al., 2011). 2D culture system is considered a basic approach to culture and study NP cells and has been utilized by many investigators (Risbud et al., 2005, Le Maitre et al., 2007a, Johnson et al., 2008, Hiyama et al., 2011, Liang et al., 2012c) suggesting that it is a valid system to use. It offers many advantages. It is economical and technically simple. It allowed high cell yield required to study different conditions alone and in different combination. Furthermore, it allows easy modification and monitoring of culture conditions mimicking *in vivo* physio-chemical microenvironment while facilitating equal distribution of nutrients to all cells in the culture. Additionally it permits easy recovery of cells following culture.

3.4.1 The effect of the IVD-like physio-chemical microenvironmental conditions on human degenerate NP cell viability

This study found no detrimental effects of any IVD-like physio-chemical condition alone or in combination on degenerate NP cell viability. A decrease in NP cell viability has been reported previously under harsh nutritional and acidic conditions (Horner and Urban, 2001, Bibby and Urban, 2004). The difference in findings may be due to two possible reasons: differences in source of cells and/or difference in the nutrients and pH levels employed. Firstly, in previous studies, cells were isolated from normal animal (rat or bovine) discs (Horner and Urban, 2001, Bibby and Urban, 2004) whereas, in this study, cells were isolated from human degenerate IVD tissue. It can be proposed that cells isolated from degenerate tissue may be the cells that had managed to survive in decreasing nutrient and acidic conditions during degeneration and due to this adaptation they may not show any further

detrimental effects. Secondly in previous investigations 0% FCS induced NP cell death, growth arrest and senescence (Risbud et al., 2005, Johnson et al., 2008) and 5mM glucose showed no effect (Bibby and Urban, 2004) while 0mM glucose induced cell death after 3 days of culture (Horner and Urban, 2001). Increased cell death was reported in decreased acidic conditions i.e. pH 6.7 and 6.2 especially without glucose (Bibby and Urban, 2004). In contrast to these investigations in this study the effect of 2% FCS, 5mM glucose and pH 6.8 and 6.5 was tested. It may be possible that more harsh nutritional and acidic conditions induce similar effects on human degenerate NP cells. However, whether these extremely harsh conditions realistically represent the *in vivo* situation is still unknown. As previously mentioned no study has determined the concentration of serum derived growth factors in the disc. Numerical studies to predict levels of glucose in the disc have shown that the disc cells are not completely deprived of glucose; as low as 0.345 glucose have been predicted in the disc (Selard et al., 2003, Soukane et al., 2007, Jackson et al., 2011a). pH 6.2 and 5.7 were the lowest pH levels seen in human disc (Nachemson, 1969). To further understand nutritional and acidic conditions related mechanisms of cell death and subsequent disc degenerative future work should be done using these ultra-low predicted values.

In this study, the live dead assay showed that degenerate NP cells cultured under the majority of the microenvironmental conditions displayed a few morphological alterations e.g. cells were spherical in shape with less processes compared to cells cultured under control conditions. Quantifying these changes may aid in our understandings about potential influences on cell survival and behaviour under harsh microenvironmental conditions. In future image analysis software packages such as Image J could be used to produce more quantitative measurements (Girish and Vijayalakshmi, 2004).

3.4.2 The effect of IVD-like physio-chemical microenvironmental conditions on human degenerate NP cells proliferation

To date few studies have investigated the direct role of disc microenvironmental factors on animal NP cell proliferation (Johnson et al., 2008, Stephan et al., 2011). This study revealed that IVD-like physio-chemical conditions influence human degenerate NP cell proliferation. It was found that hypoxia may increase proliferation of degenerate NP cells. In contrast nutrient deprived conditions (noticeably reduced serum) and severe acidic conditions (pH 6.5) inhibit proliferation of degenerate NP cells. Decreased proliferation under reduced serum supports previous observations in bovine NP cells (Johnson et al., 2008). Such results may be due to the reduction of cytokines and growth factors normally present in the serum which are

involved in cell proliferation. Inhibition of proliferation under severe acidic conditions may be due to cell cycle arrest at the G1 phase (Taylor and Hodson, 1984, Musgrove et al., 1987).

Interestingly this study found an interaction between factors when combined in different combinations. Reducing serum supply combined with reduced glucose conditions appear to reduce degenerate NP cell proliferation. Serum supplement in culture media provides growth factors and glucose (~0.6-1.2mg/ml) (Jung et al., 2012). It can be assumed that reduction of serum under reduced glucose conditions also deprived the cells from glucose and growth factors supply contributed from 10% (v/v) serum concentration that may affect their proliferation. This suggests that interaction of glucose and of other serum-derived factors may play an important role in regulating NP cell proliferation. Interestingly, the combination of hypoxia with reduced glucose alone, reduced glucose plus reduced serum and acidic condition (pH 6.8) seem to resume or improve proliferation of degenerate NP cells. Although combination of hypoxia with reduced serum also positively influenced degenerate NP cells cell proliferation, it was still lower than that of control conditions. These results overall indicate that hypoxia may be a protective factor to modulate degenerate NP cells proliferation under nutrient and acidic stress conditions.

Decreased proliferation of degenerate NP cells under combination of all IVD-like physio-chemical conditions suggest that combination of hypoxic, reduced nutrient and acidic microenvironmental conditions may have alimited role in increased cell proliferation seen in degenerated tissue. It is important to mention that this study did not include other conditions representing degenerated disc microenvironment such as hypo-osmolality which has been shown to increase NP cell proliferation with possible involvement in cluster formation during degeneration (Mavrogonatou and Kletsas, 2010). It will be interesting to perform proliferation experiments under all possible conditions closely mimicking the *in vivo* microenvironment to understand their impact on NP cell proliferative during degeneration. Although this study improves on existing knowledge of the effect of different microenvironmental conditions on degenerate NP cell proliferation, it is limited due to the use of only one degenerate NP sample. Future work is required with a larger sample size to obtain statistical significance conclusions.

3.4.3 The effect of IVD-like physio-chemical microenvironmental conditions on human degenerate NP cell gene and protein biosynthesis

Previous reports suggest that hypoxia, nutrient deprived and acidic conditions affect NP cell gene expression and PG synthesis (Ishihara and Urban, 1999, Razaq et al., 2003, Johnson et al., 2008, Illien-Junger et al., 2010, Rinkler et al., 2010, Mwale et al., 2011). However, these studies were conducted using animal NP cells and for the most part altering one variable alone. In contrast, this study for the first time, has examined the effect of hypoxia, reduced serum, reduced glucose and acidic conditions alone as well as in different combinations on human degenerate NP cells gene expression profile. It was found that IVD-like physio-chemical microenvironmental conditions have variable influences on degenerate NP cell gene and protein expression alone and in different combinations.

Hypoxia was found to up-regulate ACAN and VCAN at both gene and protein level. Beneficial effects of hypoxia on ECM genes and GAG synthesis in animal NP cells has already been reported (Risbud et al., 2005, Mwale et al., 2011, Pei et al., 2012, Neidlinger-Wilke et al., 2012). Recently Feng *et al* and Yang *et al* have also reported positive effects of hypoxia on human degenerate NP cells gene expression and collagen II and PGs synthesis (Feng et al., 2013, Yang et al., 2013). Positive effects of hypoxia seen in this study add to previous findings and indicate that hypoxia present in disc microenvironment may be a positive factor that contributes to modulate degenerate NP cell phenotype.

Reduced serum or reduced glucose alone conditions did not affect degenerated NP cells gene and protein expression. So far, only one study has investigated the effect of serum on bovine NP cells. It was reported that serum withdrawal had no influence on collagen II synthesis (Johnson et al., 2008). However, influence of glucose reduction on NP cell gene expression has received little attention. It was found that glucose reduction decreases anabolic gene (COL2A1, ACAN) expression in bovine NP cell (Johnson et al., 2008, Rinkler et al., 2010, Neidlinger-Wilke et al., 2012, Mietsch et al., 2012). In contrast glucose reduction has been shown to have no effect on human degenerated NP cells anabolic gene expression (Rinkler et al., 2010). Human degenerate NP cells maintained gene expression observed under reduced glucose in this study adds to the findings by Rinkler *et al.* Combination of reduced serum and reduced glucose induced no detrimental effect on degenerate NP cells gene expression. Only ACAN gene expression was decreased with no change at protein level. SOX-9 and PAX-1 expression increased under these conditions. These results suggest that reduced serum and

reduced glucose microenvironment may not impair degenerate NP cells gene and protein expression.

As NP cells experience low O_2 concentration together with reduced nutrient concentration it is important to study NP cells gene and protein expression under this microenvironment which is still unknown. This study found that a combination of hypoxia with reduced serum appeared to increase ACAN (though not reaching level of significance) and VCAN at gene and aggrecan at protein level in degenerate NP cells. Moreover, hypoxia combined with reduced glucose condition appeared to down regulate relatively few genes in degenerate NP cells. Importantly at the protein level this combination showed noticeable increase of both aggrecan and versican. In contrast to this hypoxia combined with both reduced serum and reduced glucose combined conditions appeared to inhibit both matrix gene and protein expression. These findings indicate that hypoxia differentially affects matrix synthesis under different reduced nutrient conditions. Under reduced serum and reduced glucose alone conditions hypoxia may have an anabolic effect on matrix synthesis which is lost when these nutrient reduced conditions were combined. It appears that under complete nutrient deprived conditions hypoxia combination may induce detrimental effects at both matrix gene and protein synthesis level. It is possible that the complex cellular metabolism under different combinations of hypoxic and nutrient deprived conditions may govern these changes. There are suggestions that NP cells may show a positive Pasteur effect under low O_2 tension, i.e. with fall in O_2 concentration NP tissue show increase in glycolysis (Holm et al., 1981, Ishihara and Urban, 1999) that increases ATP production coupled with matrix synthesis (Lee et al., 2002, Bibby et al., 2005). However, it may also increase rates of glucose depletion (Holm et al., 1981, Ishihara and Urban, 1999, Bibby et al., 2005). It can be assumed that under reduced serum and reduced glucose alone conditions cells may have more supply of glucose compared to both reduced serum and reduced glucose combined conditions. It is possible that positive Pasteur effect under these conditions lead to significant depletion of glucose that result in reduction of ATP and ultimately reduced matrix. However, there are also reports of no (Bibby and Urban, 2004) or negative Pasteur effect (Bibby et al., 2005) in NP cells. Whatever Pasteur effect NP cells show there are limited nutrient supply under reduced serum and reduced glucose combined conditions for glycolysis which may have a direct role in reduced matrix synthesis. However, all these assumptions need to be verified at experimental level. Nevertheless these findings suggest that combination of hypoxia and

nutrient deprived conditions (reduced serum and reduced glucose combined) which is more indicative of *in vivo* microenvironment may possibly accelerate degenerate changes in degenerate NP cells.

Previously in bovine NP cells PG synthesis and ECM gene expression was found to decrease at both pH 6.8 and 6.5 (representing moderate and severe acidic conditions) with more pronounced decrease at the lower pH value (Razaq et al., 2003, Neidlinger-Wilke et al., 2012). This study found that compared to pH 7.4, pH 6.8 had no negative effect on degenerate NP cell ECM gene expression. In contrast pH 6.5 induced a deleterious effect on both ACAN and VCAN gene expression in degenerate NP cells. The different response of animal and human degenerate NP cells to pH 6.8 may be due to difference in their sources i.e. animal versus human, or phenotype i.e. normal versus degenerate. Nevertheless results of this study indicate that the increasing acidic microenvironment during disc degeneration may impair matrix genes expression by human degenerate NP cells leading to an exacerbation of disc degenerative changes. However, these findings need to be verified at protein level in future studies.

Human degenerate NP cells showed minor changes in their gene expression under combined hypoxia and moderate acidic conditions. Hypoxia appeared to regulate VCAN expression under pH 6.8. These results indicate that combined hypoxic and moderate acidic conditions in disc microenvironment may not promote degenerate changes in degenerate NP cells.

There is little available information about the pH regulation in degenerate NP cells. Although it is believed that lactic acid produced by glycolysis may be a significant contributor to the acidic pH found in the disc tissue (Holm et al., 1981, Ishihara and Urban, 1999), reports also suggest production of carbon dioxide in the disc (Holm et al., 1981, Ishihara and Urban, 1999) thereby indicating the role of carbonic anhydrases (CAs) in regulating pH in disc cell. CA9 and CA12 gene and protein expression have been observed in NP cells of the IVD (Liao et al., 2009, Minogue et al., 2010a, Power et al., 2011). CAs catalyse the reversible hydration of carbon dioxide into protons and bicarbonate to maintain intracellular pH. Cell membrane associated CA9 and CA12 have been shown to promote tumour cell survival and growth through maintenance of the intracellular pH (Potter and Harris, 2003, Svastova et al., 2004, Swietach et al., 2007). Recently Power *et al* suggested that CA12 inhibition impairs lactate

release in bovine NP cells suggesting their role in pH regulation in NP cells (Power et al., 2011). In this study degenerate NP cells showed noticeably increased expression of CA9 under both decreasing acidic conditions alone and in combination with hypoxia. CA12 expression was only increased under pH 6.8. These results suggests that in degenerate NP cells CA9 may be more relevant in regulating intracellular pH along with other known acid extrusion mechanisms under both acidic and hypoxic microenvironment (Razaq et al., 2000, Potter and Harris, 2003, Uchiyama et al., 2007, Chiche et al., 2009, Wojtkowiak et al., 2012). Although expression at protein level needs to be confirmed in future studies.

Finally this study found that degenerate NP cells cultured under hypoxia, reduced serum, reduced glucose and pH 6.8 combined showed no detrimental effects on their gene expression. It may be possible that combination of reduced pH 6.8 with hypoxia and reduced nutrient conditions may have different effect on cellular metabolism that maintained their phenotype. Previously it has been shown that a fall in pH (7.4 - 6.2) lead to a decrease in glucose consumption in bovine NP cells under low concentration conditions (below 1mM) (Bibby et al., 2005). Based on this report, it may be possible that pH 6.8 may slow down the depletion of glucose under hypoxia and complete nutrient deprived conditions to maintain glycolysis rate and ultimately matrix synthesis. However, this link needs to be verified in future studies. Overall these results imply that IVD hypoxia and a nutrient deprived and moderate acidic microenvironment may not deteriorate the degenerate NP cell gene profile. Influences of other microenvironmental conditions of disc niche i.e. hypo-osmolality, load, high amount of cytokines requires future work to elucidate their contribution in developing and accelerating disc degeneration.

3.4.4 Conclusion

In summary, this study showed that IVD-like physio-chemical microenvironmental conditions thought to occur during degeneration alone and in combination influences degenerate NP cell proliferation and gene and protein expression. It was found that degenerate NP cells could survive hypoxic (2% O_2), nutrient limited (2% FCS and 5mM glucose) and moderate (pH 6.8) and severe (pH 6.5) acidic conditions. This survival may be due to their adaptation to the degenerated microenvironment. Hypoxia alone appeared to be a positive factor to modulate degenerate NP cell phenotype by improving proliferation and matrix synthesis. Reduced nutrient conditions impaired degenerate NP cell proliferation but

had no prominent negative the influence on their gene and protein expression. Interestingly this study found that interaction between different microenvironmental conditions influences degenerate NP cell phenotype. Interaction of reduced serum with reduced glucose inhibited degenerate NP cell proliferation suggesting that interaction of glucose and serum derived growth factors may be important for degenerate NP cell proliferation under reduced nutrient conditions. Combination of hypoxia with reduced glucose alone, reduced serum and reduced glucose both combined and acidic conditions were found to resume or improve degenerate NP cell proliferation suggesting that hypoxia may have a protective effect on modulation of degenerate NP cell proliferation under nutrient deprived and acidic stress conditions. Combination of hypoxia with reduced nutrient and acidic conditions also influenced ECM gene and protein expression. Combination with reduced serum increased ECM gene and with reduced glucose ECM proteins synthesis. In contrast combination of hypoxia with complete nutrient deprived conditions (reduced serum and reduced glucose) decreased degenerate NP cells in terms of ECM gene and protein expression. These results imply that hypoxic and complete nutrient deprived conditions in disc microenvironment may accelerate disc degeneration. Limited effect of moderate acidic conditions and inhibitory effects of severe acidic conditions on proliferation and matrix gene expression indicate the importance of increasing acidity in exacerbating disc degeneration. Combination of hypoxic and moderate acidic conditions also had limited effects on degenerate NP cell behaviour. Finally combination of hypoxia, nutrient deprived and moderate acidic conditions reduced degenerate NP cell proliferation but induced no detrimental effect on gene expression indicating that hypoxic, reduced nutrient and acidic conditions of disc microenvironment together may not accelerate degenerative changes. The differences observed in gene and protein expression under different combinations may be due to differences in cell metabolism under different microenvironmental conditions. Though this study has improved our understanding about impact of different microenvironmental conditions on degenerate NP cells, it is limited due to the use of already degenerated cells. To clearly establish the link between different disc conditions and degeneration use of the normal NP cells is desirable.

4 Chapter 4: The effect of intervertebral disc-like physio-chemical microenvironmental conditions on human bone marrow derived mesenchymal stem cell behaviour

4.1 Introduction

Recent advances in understanding the pathogenesis of disc degeneration combined with the advent of cell therapies utilising stem cells have provided a practical approach for the regeneration of the IVD. MSCs have attracted wide spread attention in this field because of their proliferative capacity and their ability to differentiate into several cell types of mesenchymal origin (Pittenger et al., 1999). As such MSCs aim to either provide signalling cues to endogenous cells to replenish the lost matrix, or differentiate /and maintain a disc-like phenotype themselves, to re-establish healthy disc function (Risbud et al., 2004b, Richardson et al., 2010, Longo et al., 2012)

Growth factors, gene therapy and specific culture conditions are being actively researched to maximize the regenerative potential of MSC (Risbud et al., 2004a, Richardson et al., 2010, Allon et al., 2012, Liang et al., 2012b) with limited importance placed on studying the aspect of the challenging microenvironment of the disc which could hamper the survival and function of MSCs. Recent reports of limited cell survival and PG production in a porcine degenerated disc model following MSC implantation (Acosta et al., 2011) and no height improvement in the human degenerate disc after MSC transplantation (Orozco et al., 2011) may reinforce the argument that the IVD microenvironmental conditions and their effect on cell behaviour needs to be considered.

Recently few investigators have explored the effects of the harsh microenvironmental factors of the disc on MSC behaviour in terms of survival, proliferation and matrix synthesis to identify how these cells would respond when implanted into native biological conditions (Wuertz et al., 2008, Wuertz et al., 2009a, Liang et al., 2012a, Li et al., 2012). Wuertz *el al* examined the effect of IVD-like reduced glucose (5mM), reduced acidic pH (6.8) and hyper-osmolarity (485mOsm compared to 280mOsm in control conditions) on survival, proliferation and matrix gene (ACAN and COL1) expression in rat BM-MSCs (Wuertz et al., 2008). They found that reduced glucose conditions stimulated proliferation and matrix gene expression in BM-MSC. In contrast acidic pH 6.8 and hyper-osmolarity significantly inhibited proliferation and matrix gene expression with more pronounced effects under

hyper-osmolarity. Combination of the three conditions also significantly inhibited proliferation and matrix gene expression. They concluded that reduced glucose may be a positive factor for BM-MSC but acidic pH and hyper-osmolarity appears to dominate the positive effects of reduced glucose and may be critical factors that must be overcome for MSC cell and tissue engineering therapies. They suggested that as degeneration progresses, osmolarity decreases and acidity increases, and as such acidity may be the major limitation for MSC based IVD repair. This was further enforced in their second investigation of rat BM-MSCs behaviour under four different pH conditions, representative of the healthy (pH 7.4, pH 7.1), mildly (pH 6.8) or severely degenerated discs (pH 6.5) for 5 days (Wuertz et al., 2009a). It was found that increasing acidity caused an inhibition of ACAN, COL1, TIMP3 expression, as well as a decrease in proliferation and cell viability. BM-MSC proliferation, matrix synthesis and survival were severely compromised at pH 6.5. It was concluded that severe acidic conditions are detrimental to MSC functionality, phenotype, and viability suggesting a likelihood of failure for MSC based regeneration in severely degenerate discs.

Following these studies, Liang *et al* studied the behaviour of human AD-MSCs for 2 weeks (Liang et al., 2012a) under the exact same conditions used by Wuertz *el al* (Wuertz et al., 2008). They studied AD-MSC viability, proliferation and matrix gene (ACAN and COL1) along with protein expression. Interestingly they reported overall similar findings to those of Wuertz *et al* (Wuertz et al., 2008). Reduced glucose increased expression of ACAN gene and protein expression whereas hyper-osmolarity, reduced pH and the combined conditions inhibited cell viability, proliferation, matrix gene and protein synthesis (Liang et al., 2012a). Further to this work, AD-MSCs were cultured under increasing acidic conditions (Li et al., 2012). It was found that AD-MSCs viability, proliferation and gene and protein expression (ACAN, COL1, COL2 and TIMP3) decreased along with the acidity from pH 7.4 to 6.5 suggesting that similar to BM-MSCs, extracellular acidity may also limit the success of AD-MSC-based IVD regeneration.

Although the above mentioned studies raised awareness as to the importance of IVD-like microenvironmental conditions, these studies were limited because of the use of a few conditions and combinations. For a detailed understanding of the effect of IVD microenvironment on MSC behaviour, it is important to investigate the effect of all possible conditions and combined effects thus mimicking the IVD microenvironment to identify factors that may be beneficial or detrimental to cell survival and function. Additionally in

order to develop a successful human IVD regeneration strategy it is extremely important to study the behaviour of human BM-MSCs under IVD-like microenvironmental conditions.

4.1.1 Aims

This study was designed to investigate the effects of the IVD-like physio-chemical microenvironmental conditions namely hypoxia (2%O_2), limited nutrients [reduced glucose (5mM) and reduced serum (2% FCS)] and acidic pH (6.8 & 6.5 representative of moderate & severely degenerate discs respectively) alone and in combination on human BM-MSCs behaviour through assessment of viability, proliferation and gene and protein synthesis.

For this work it was hypothesized that the IVD-like physio-chemical microenvironmental conditions will affect human BM-MSC survival, proliferation, and matrix gene and protein synthesis.

The specific aims were to:

1. Evaluate the stimulatory or inhibitory effects of IVD-like physio-chemical microenvironmental conditions on human BM-MSC survival and proliferation
2. Assess the stimulatory or inhibitory effects of IVD-like physio-chemical microenvironmental niche on human BM-MSC synthesis of IVD gene (SOX-9, COL2A1, ACAN, VCAN, CA9 and CA12) and protein (aggrecan and versican).

4.2 Materials and methods

4.2.1 BM-MSC culture

BM-MSCs used in this study were isolated from human BM samples listed in Table 4.1. BM-MSCs were isolated and maintained as described in chapter 2 section 2A.1-2.

Table 4.1 Details of human BM tissue samples used to isolate BM-MSCs

Sr. No	Tissue ID	Sex	Age (years)	Operation site	Reason for surgery
1	WH023	M	40	Hip/knee	OA
2	WH027	F	54	Hip	OA
3	WH028	M	50	Hip	OA
4	TH090	F	62	Knee	OA
5	TH092	M	77	Hip	OA
6	TH094	M	55	knee	OA
7	TH107	F	73	Hip	OA
8	TH109	M	41	Hip	OA
9	TH148	M	41	Hip	OA
10	WH047	M	47	Hip	OA
11	WH051	M	71	Hip	OA
12	WH053	F	24	Hip	OA
13	TH108	M	63	Knee	OA
14	TH110	F	76	Hip	OA
15	TH106	M	64	Knee	OA
16	TH209	F	59	Hip	OA
17	TH171	M	74	Knee	OA
18	TH172	M	72	Knee	OA
19	TH180	F	89	Hip	OA
20	WH042	M	51	Hip	OA
21	WH046	F	27	Hip	AVN

OA= Osteoarthritis

AVN = Avascular necrosis

4.2.2 BM-MSC culture under IVD-like physio-chemical microenvironmental conditions

BM-MSCs at passage 4-6 were seeded at a density of $1.2x10^4$cells/cm^2 in 6 well plate or 25cm^2 flask and cultured under IVD-like physio-chemical microenvironmental conditions for 7 days using media formulations (Table 2.1) and methodology detailed previously (chapter 2, section 2A.3).

4.2.3 Cell viability

Cell viability was assessed after 7 days of culture under IVD-like physio-chemical microenvironmental conditions using a Live/Dead viability/cytotoxicity fluorescence-based assay, following the protocol described previously (chapter 2, section 2A.5). BM-MSCs listed in Table 4.2 were used in cell viability analysis.

Table 4.2 BM-MSCs used in cell viability assay

IVD conditions	BM-MSCs
1. Hypoxia (n=3) 2. Reduced serum (n=3) 3. Reduced glucose (n=3) 4. Reduced serum & reduced glucose (n=3) 5. Reduced serum & hypoxia (n=3) 6. Reduced glucose & hypoxia (n=3) 7. Reduced serum, reduced glucose & hypoxia (n=3)	WH023 WH027 WH028
8. Reduced pH 6.8 & 6.5 (n=3)	TH106 TH108 TH110
9. Reduced pH 6.8 & hypoxia (n=3) 10. All IVD-like physio-chemical conditions combined (n=3)	WH047 WH051 WH053

4.2.4 Cell proliferation

The proliferation of BM-MSCs cultured under IVD-like physio-chemical microenvironmental conditions was assessed at day 1 and day 7 utilising the LDH proliferation assay protocol detailed previously (chapter 2, section 2A.6). BM-MSCs TH209, TH171 and TH172 were used for this assay

4.2.5 Gene expression

BM-MSCs used for gene expression studies are listed in Table 4.3. Cells cultured under IVD-like physio-chemical microenvironmental conditions were lysed with 1ml of Trizol®. RNA was subsequently extracted and reverse transcribed as previously detailed (Chapter 2, section 2A.7.1-7.5). QRT-PCR was then conducted for COL2A1, SOX-9, ACAN, VCAN, CA9 and CA12 with HK genes (MRPL19 and EIF2B1) using primers and probes detailed in Table 2.3 (chapter 2, section 2A.7.6-7.7).

Table 4.3 BM-MSCs used for the separate experiments analysing gene expression following culture in the differing conditions

IVD conditions	BM-MSCs
1. Hypoxia (n=6)	TH090 TH092 TH094 TH107 TH109 TH148
2. Reduced serum (n=3)	TH090 TH092 TH094
3. Reduced glucose (n=3) 4. Reduced serum & reduced glucose (n=3)	TH107 TH109 TH148
5. Reduced serum & hypoxia (n=3)	TH090 TH092 TH094
6. Reduced glucose & hypoxia (n=3)	TH107 TH109 TH148
7. Reduced serum, reduced glucose & hypoxia (n=3)	TH107 TH109 TH148
8. Reduced pH 6.8 & 6.5 (n=3)	TH146 TH163 TH165
9. Reduced pH 6.8 & hypoxia (n=3) 10. All IVD-like physio-chemical microenvironmental conditions combined (n=3)	WH047 WH051 WH053

4.2.6 Assessment of ECM protein synthesis by immunofluorescence in BM-MSC culture under IVD-like physio-chemical microenvironmental conditions

Aggrecan and versican protein expression under IVD-like physio-chemical microenvironmental conditions (i.e. hypoxia, reduced serum, and reduced glucose alone and in combinations) was assessed by immunofluorescence. Cells were cultured in 8 well chamber slides using respective media formulations (Chapter 2, section 2A.3). Immunofluorescence staining was performed as previously reported (chapter 2, section 2A.4). BM-MSCs TH180, WH042 and WH046 were used in immunofluorescence analysis.

As stated in chapter 2 (section 2A.4) due to autofluorescence issues, images from all pH conditions were not analysed and included in this study.

4.3 Results

4.3.1 Influence of hypoxia on BM-MSC behaviour

4.3.1.1 Cell viability and proliferation

Live/dead staining of BM-MSCs cultured under control conditions showed that majority of cells stained green (viable) with few cells staining red (dead). BM-MSCs cultured under hypoxia also showed that majority of cells stained green (viable) with very few red stained (dead) cells (Figure 4.3.1).

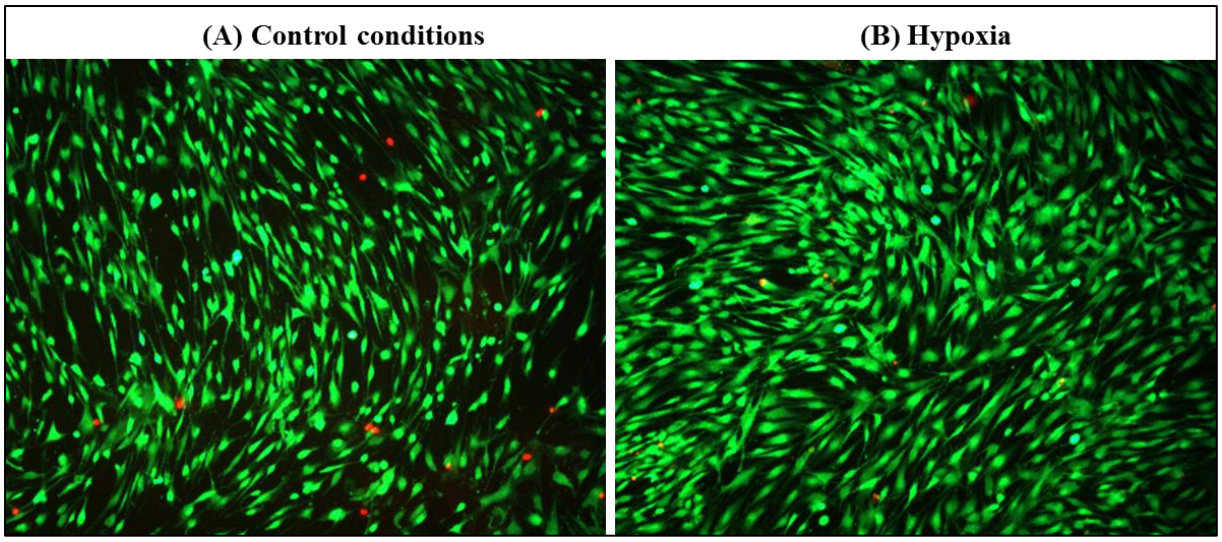

Figure 4.3.1 Effect of hypoxia on BM-MSCs viability. BM-MSCs (n=3) were cultured under (A) control conditions and (B) hypoxia for 7 days and labelled with live-dead stain. Representative fluorescence microscope images indicating viable (stained green) and dead (stained red) cell populations under both conditions (magnification x100).

Proliferation analysis showed that at day 7 the increase in BM-MSCs number under hypoxic condition was not significantly different compared to control conditions (9718±1064 versus 8299±882) (Figure 4.3.2).

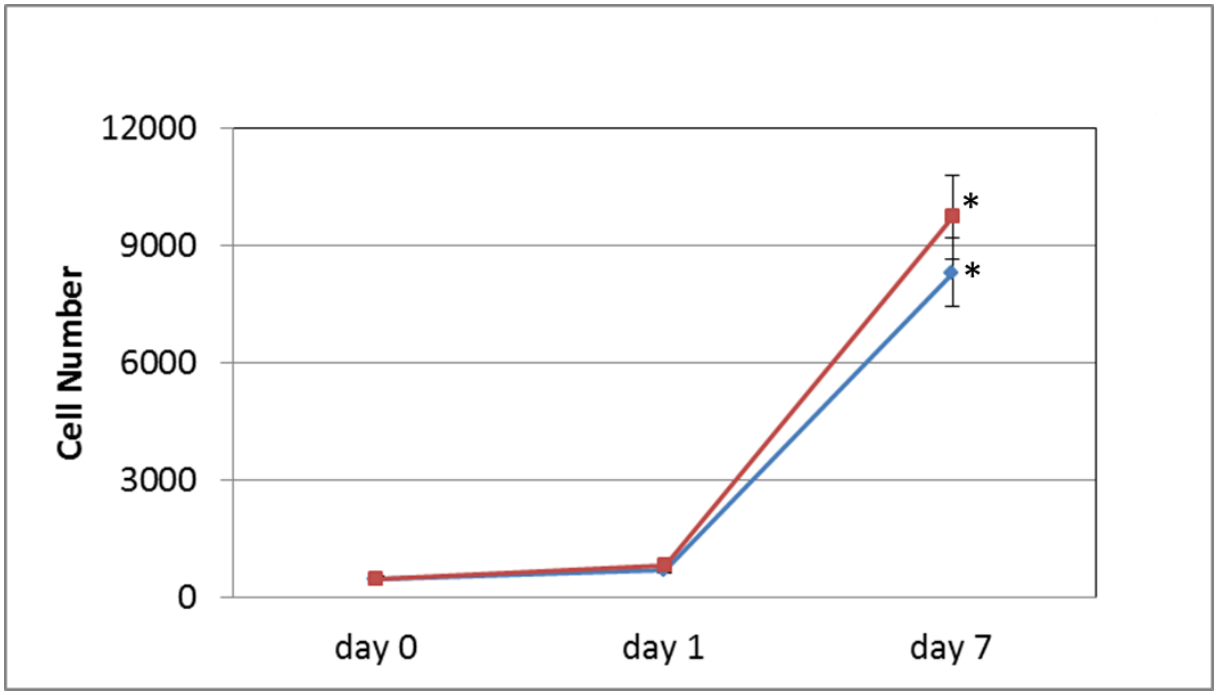

Figure 4.3.2 Effect of hypoxia on BM-MSCs (n=3) proliferation over the course of 7 days. Total cell number was determined for BM-MSCs cultured under hypoxia (red line) compared to control conditions (blue line). Day 0 cell number was used as baseline for each condition. Data was expressed as mean ± SEM of triplicates of 3 patient samples. Significant differences ($p \leq 0.05$) * compared to day 0.

4.3.1.2 Gene expression

BM-MSCs following culture under hypoxia showed no changes in SOX-9, COL2A1 and ACAN expression, but a significant increase in VCAN gene expression (p<0.05) was observed compared to BM-MSCs cultured under control conditions (Figure 4.3.3 A & B).

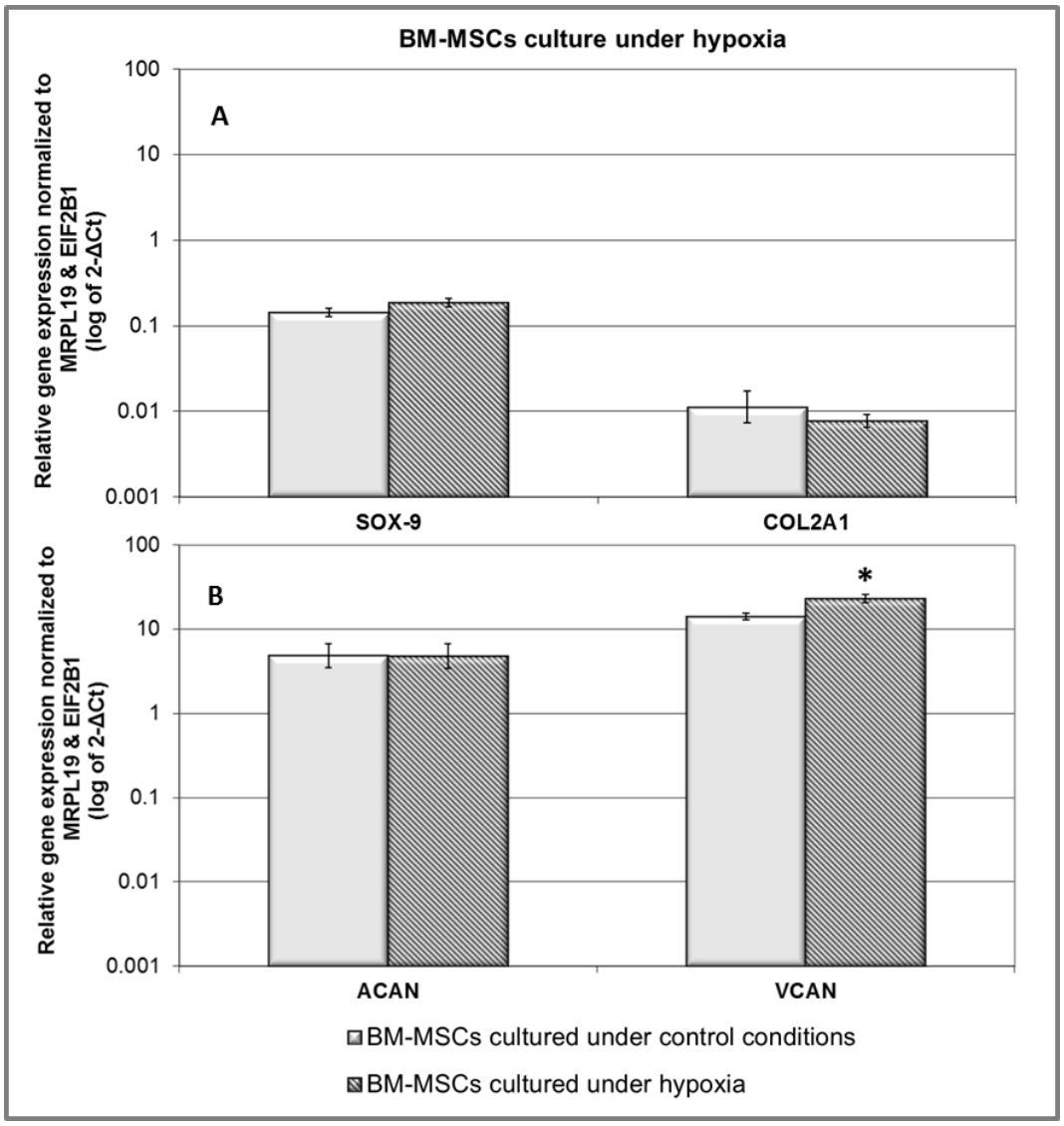

Figure 4.3.3 Relative gene expression of (**A**) SOX-9, COL2A1 and (**B**) ACAN, VCAN in BM-MSCs cultured under hypoxia (n=6) compared to control conditions. Gene expression normalized to average of HK genes MRPL19 and EIF2B1 and plotted on a log scale. * Statistical significance (p≤0.05) compared to culture under control conditions.

4.3.1.3 ECM protein expression

BM-MSCs cultured under hypoxia showed a slight increase in staining intensity for aggrecan and versican protein compared to control conditions (Figure 4.3.4 & Figure 4.3.5). Under both control and hypoxic conditions, aggrecan staining was predominantly localized in the

cytoplasm (intracellular) whereas versican staining was both intra and extracellular. Primary antibody IgG controls for both aggrecan and versican were negative (Figure 4.3.6).

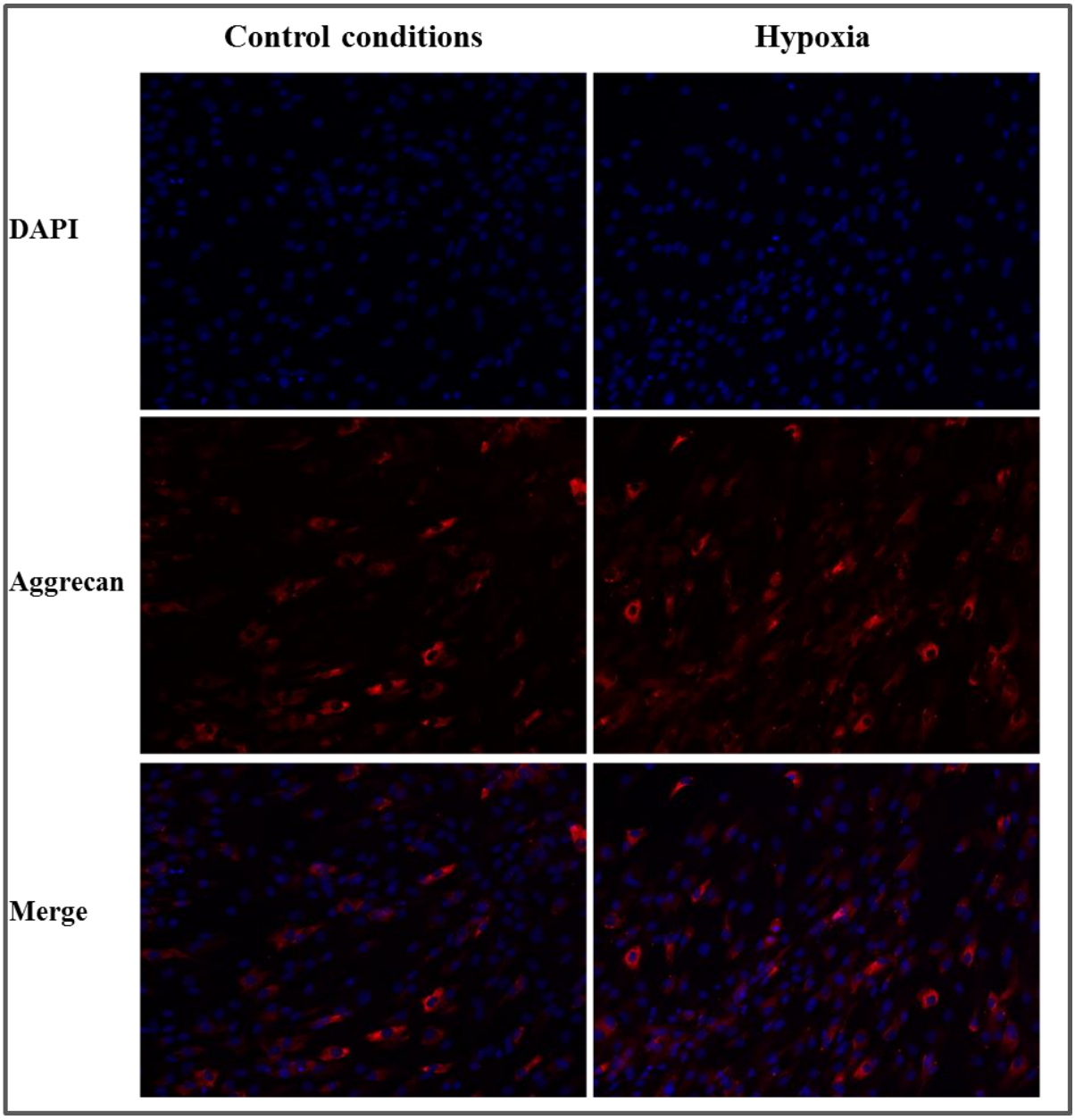

Figure 4.3.4 Representative images of aggrecan immunofluorescence staining of BM-MSCs (n=3) cultured under control conditions (left panels) and hypoxia (right panels) for 7 days. Immunofluorescence staining was performed using anti-aggrecan primary antibody followed by Alexa Fluor 555 conjugated secondary antibody (red). DAPI (blue) was used for nucleus staining. Top row: DAPI, middle row: same field of view with aggrecan staining, bottom row: merge of above two rows (magnification x200).

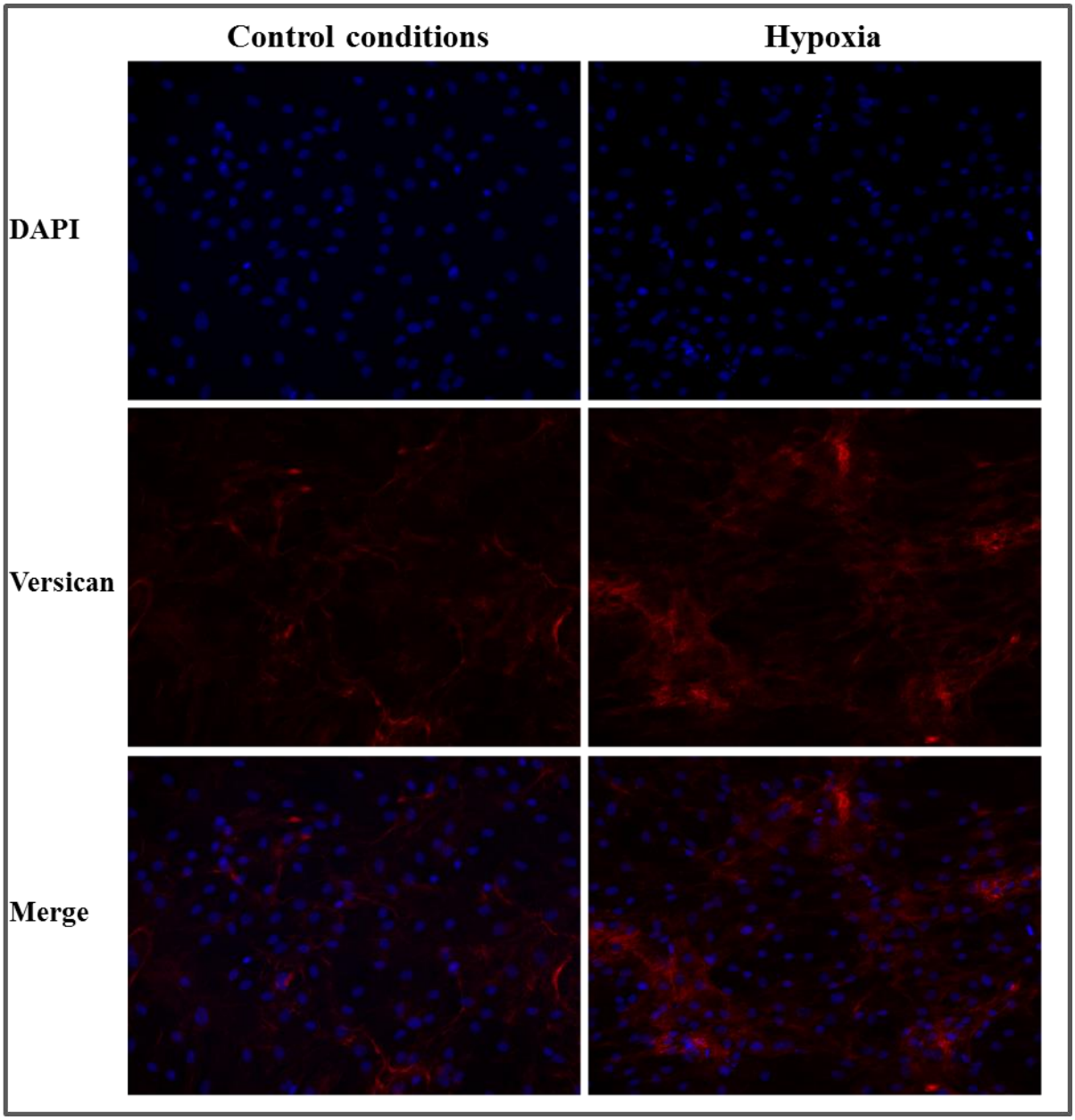

Figure 4.3.5 Representative images of versican immunofluorescence staining of BM-MSCs (n=3) cultured under control conditions (left panels) and hypoxia (right panels) for 7 days. Immunofluorescence staining was performed using anti-versican primary antibody followed by Alexa Fluor 555 conjugated secondary antibody (red). DAPI (blue) was used for nucleus staining (magnification x200). Top row: DAPI, middle row: same field of view with versican staining, bottom row: merge of above two rows (magnification x200).

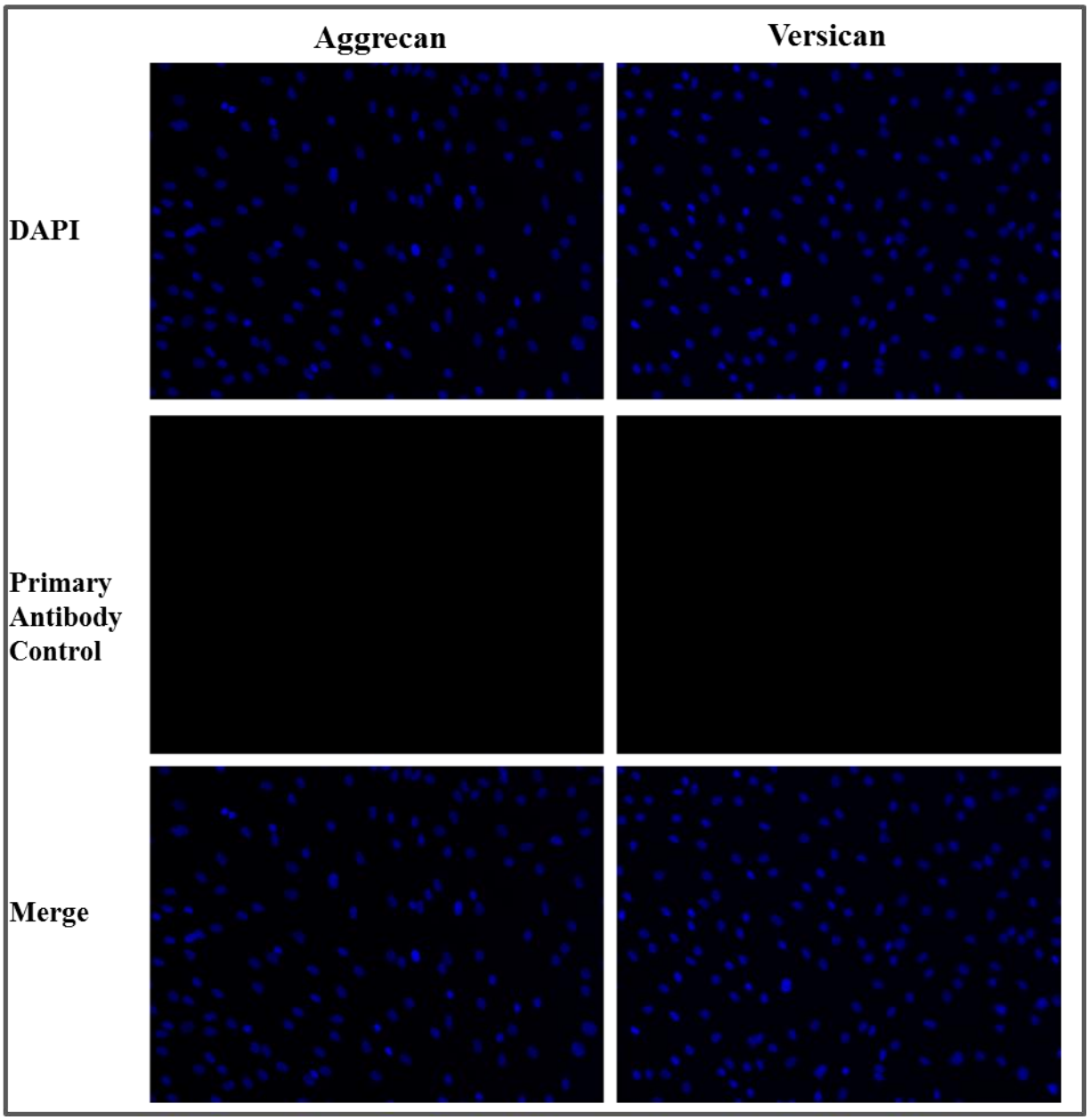

Figure 4.3.6 Representative primary antibody IgG controls for aggrecan (left panels) and versican (right panels) in BM-MSCs culture. Immunofluorescence staining was performed using IgG control primary antibody followed by Alexa Fluor 555 conjugated secondary antibody (red). IgG controls show no non-specific IgG staining. Top row: DAPI, middle row: same field of view with IgG staining, bottom row: merge of above two rows (magnification x200).

4.3.2 Influence of reduced serum on BM-MSC behaviour

4.3.2.1 Cell viability and proliferation

Live/dead assay of BM-MSCs cultured under reduced serum indicated that majority of cells stained green (viable) with only few red stained (dead) cells (Figure 4.3.7).

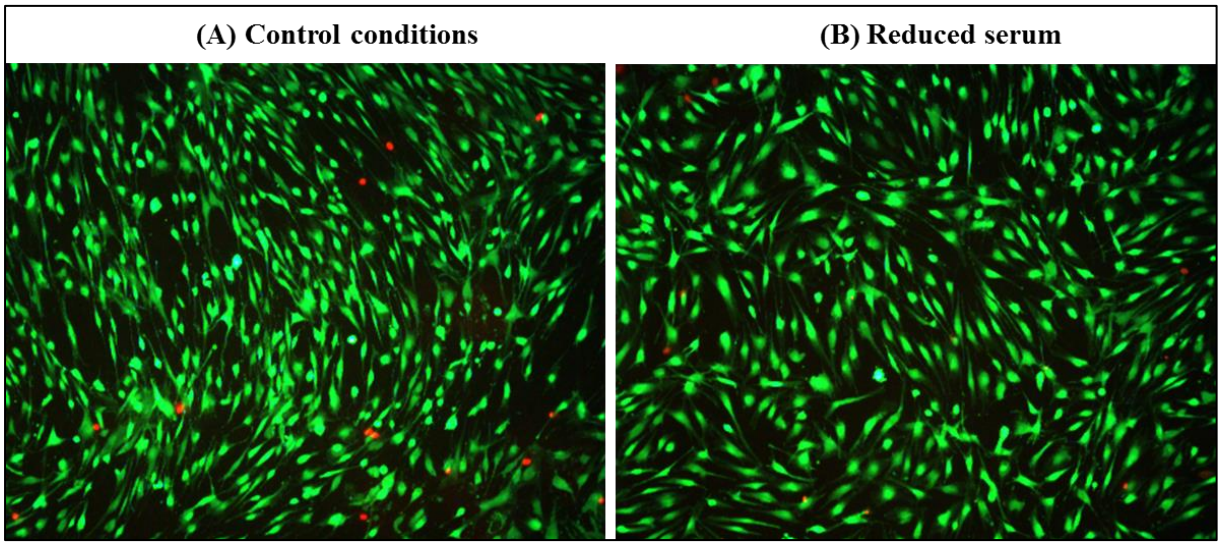

Figure 4.3.7 Effect of reduced serum on BM-MSCs viability. BM-MSCs (n=3) were cultured under (A) control conditions and (B) reduced serum for 7 days and labelled with live-dead stain. Representative fluorescence microscope images indicate viable (stained green) and dead (stained red) cell populations under both conditions (magnification x100).

Proliferation analysis showed that at day 7 the increase in cell number under reduced serum was significantly less compared to control conditions (2314±347 versus 8299±882, $p<0.05$) (Figure 4.3.8).

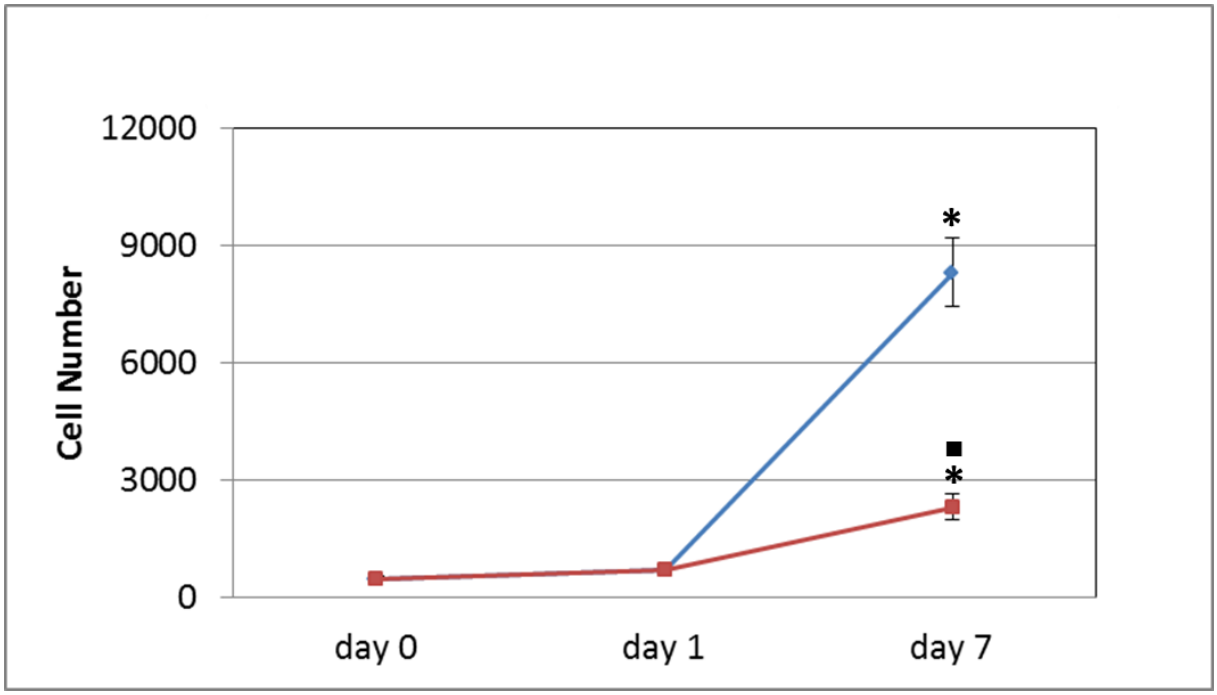

Figure 4.3.8 Effect of reduced serum on BM-MSCs (n=3) proliferation over the course of 7 days. Total cell number was determined for BM-MSCs cultured under reduced serum (red line) compared to control conditions (blue line). Day 0 cell number was used as baseline for each condition. Data was expressed as mean ± SEM of triplicates of 3 patient samples. Significant differences ($p \leq 0.05$) * compared to day 0 and ■ day 7 control conditions.

4.3.2.2 Gene expression

BM-MSCs cultured under reduced serum showed no change in expression for any of the genes investigated compared to BM-MSCs cultured under control conditions (Figure 4.3.9).

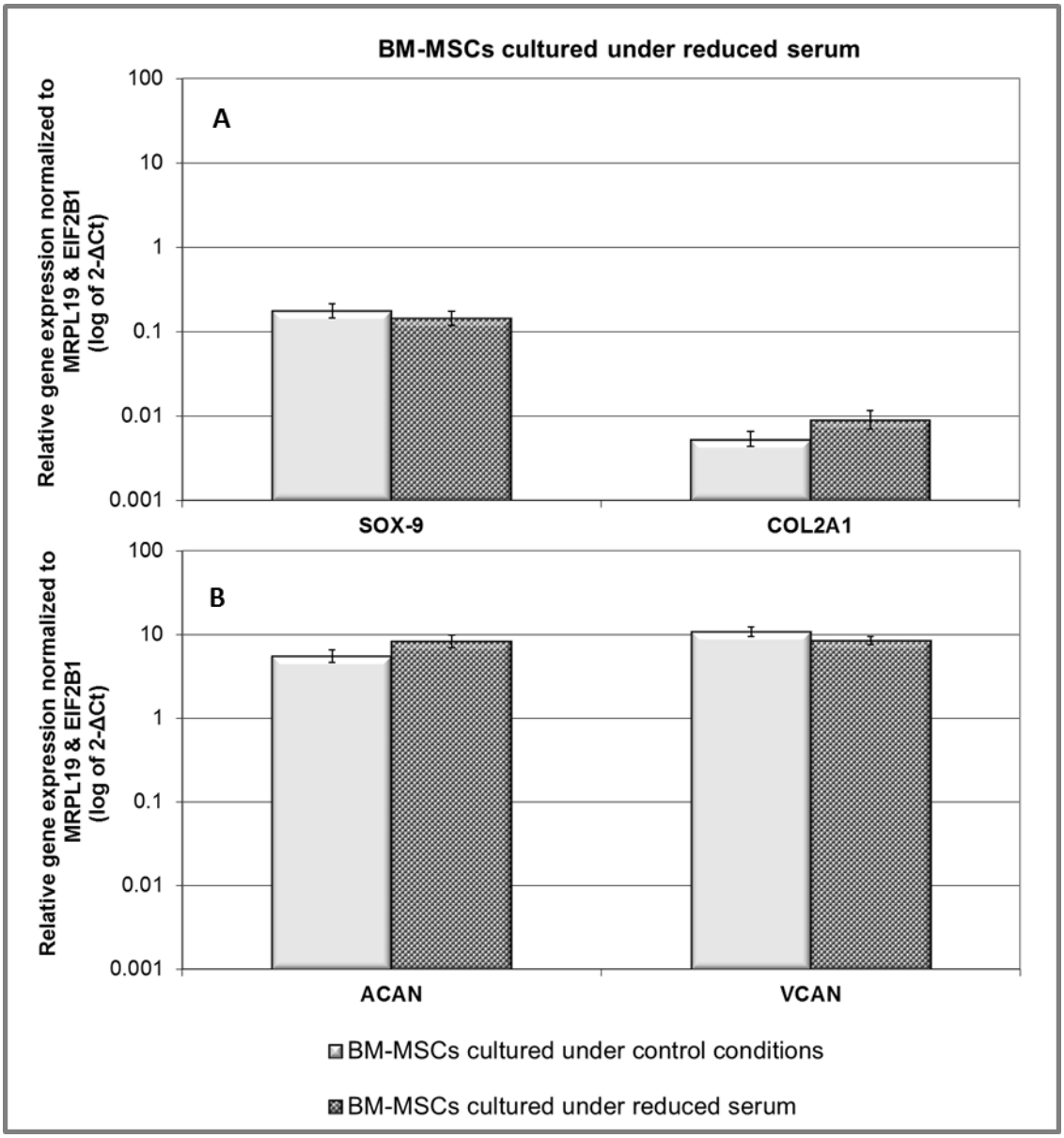

Figure 4.3.9 Relative gene expression (**A**) SOX-9, COL2A1 and (**B**) ACAN, VCAN in BM-MSCs cultured under reduced serum (n=3) compared to control conditions. Gene expression normalized to average of HK genes MRPL19 and EIF2B1 and plotted on a log scale. * Statistical significance ($p \leq 0.05$) compared to culture under control conditions.

4.3.2.3 ECM protein expression

BM-MSCs cultured under reduced serum stained positively for both aggrecan and versican protein (Figure 4.3.10 & Figure 4.3.11). Staining intensity appeared decreased under reduced serum conditions although cell number was also decreased.

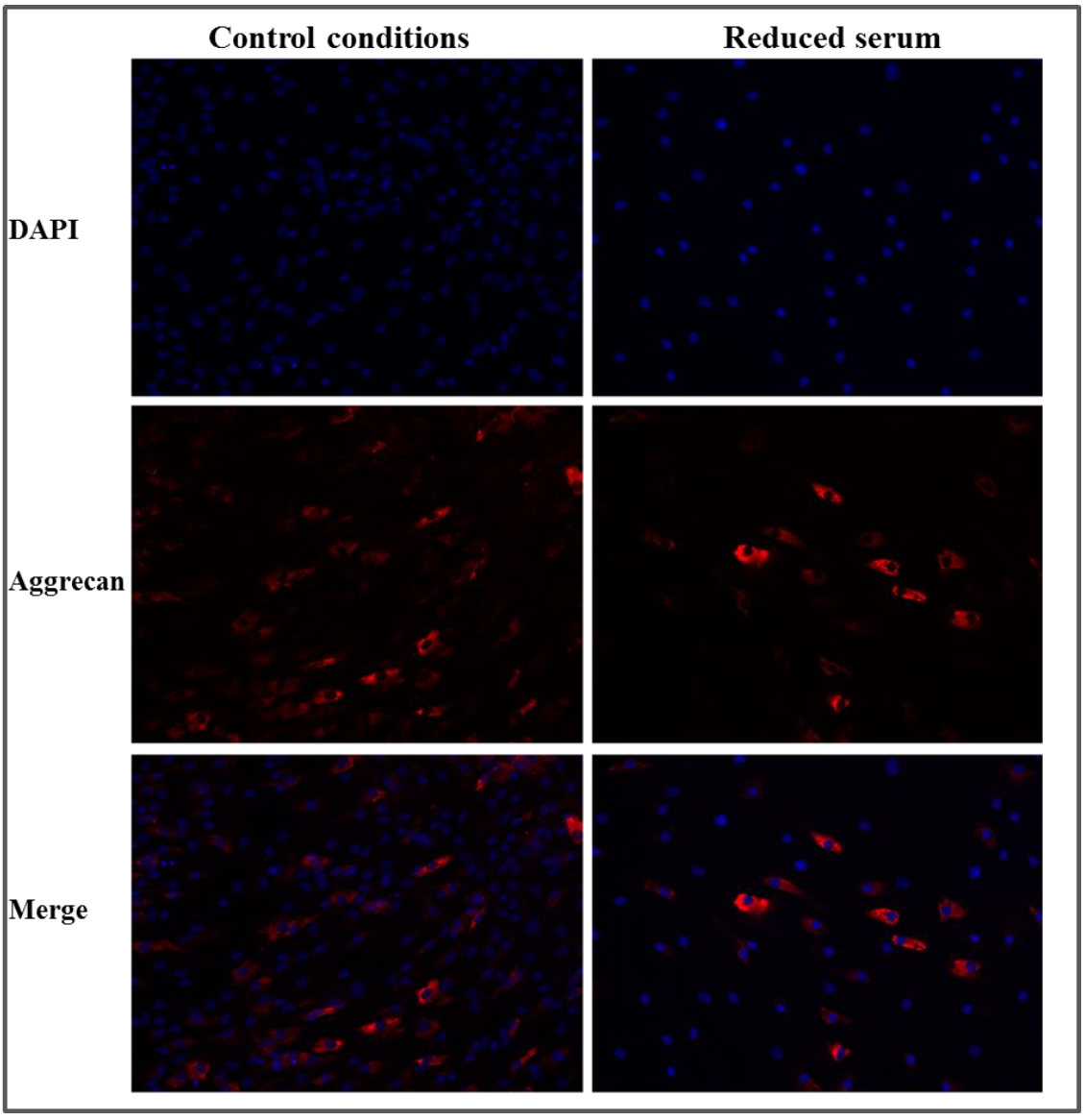

..

Figure 4.3.10 Representative images of aggrecan immunofluorescence staining of BM-MSCs (n=3) cultured under control conditions (left panels) and reduced serum (right panels) for 7 days. Immunofluorescence staining was performed using anti-aggrecan primary antibody followed by Alexa Fluor 555 conjugated secondary antibody (red). DAPI (blue) was used for nucleus staining Top row: DAPI, middle row: same field of view with aggrecan staining, bottom row: merge of above two rows (magnification x200).

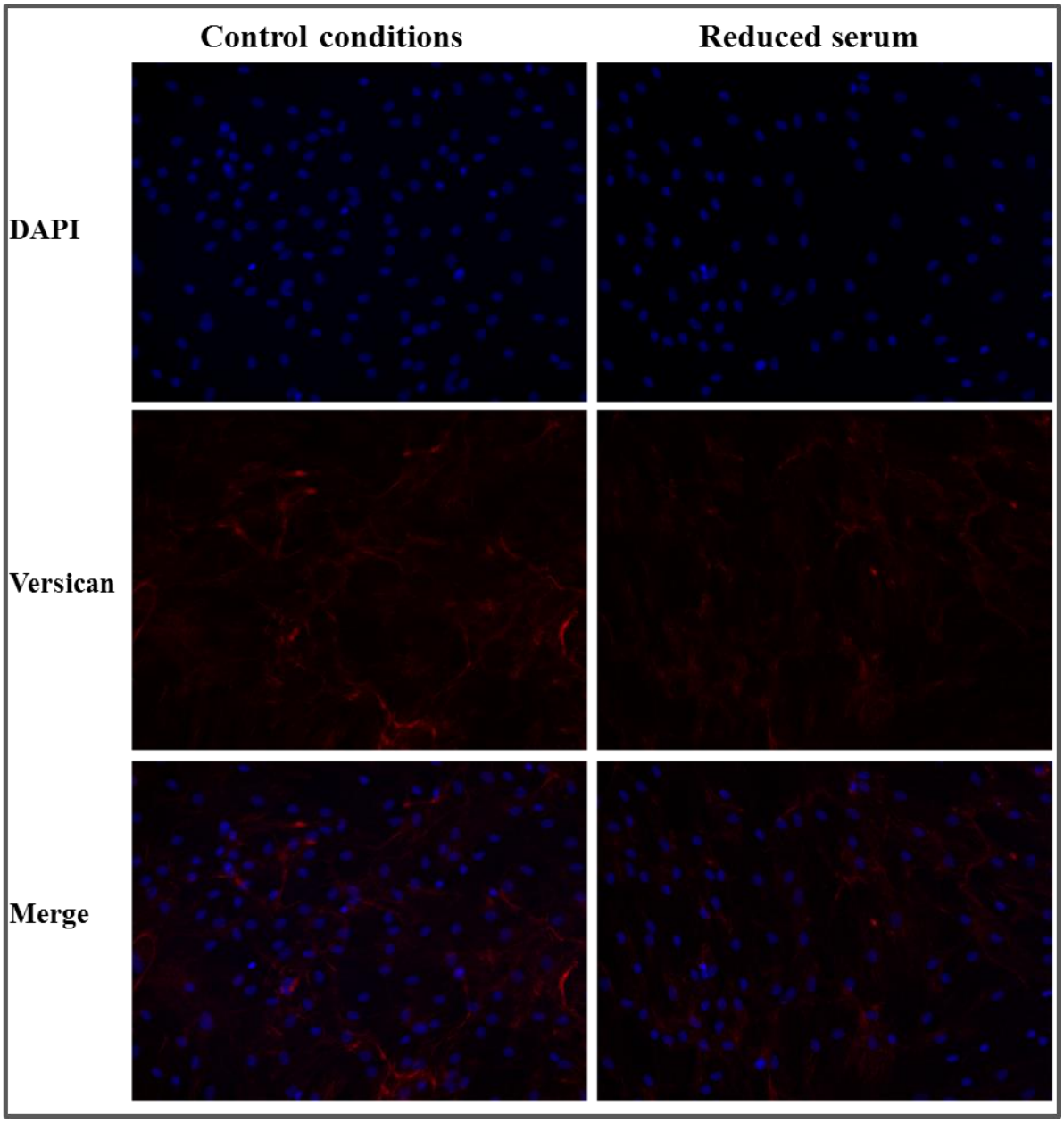

Figure 4.3.11 Representative images of versican immunofluorescence staining of BM-MSCs (n=3) cultured under control conditions (left panels) and reduced serum (right panels) for 7 days. Immunofluorescence staining was performed using anti-versican primary antibody followed by Alexa Fluor 555 conjugated secondary antibody (red). DAPI (blue) was used for nucleus staining Top row: DAPI, middle row: same field of view with versican staining, bottom row: merge of above two rows (magnification x200).

4.3.3 Influence of reduced glucose on BM-MSC behaviour

4.3.3.1 Cell viability

Live/dead staining of BM-MSCs cultured under reduced glucose showed similar staining to control conditions i.e. majority of cells stained green (viable) with few red stained (dead) cells (Figure 4.3.12).

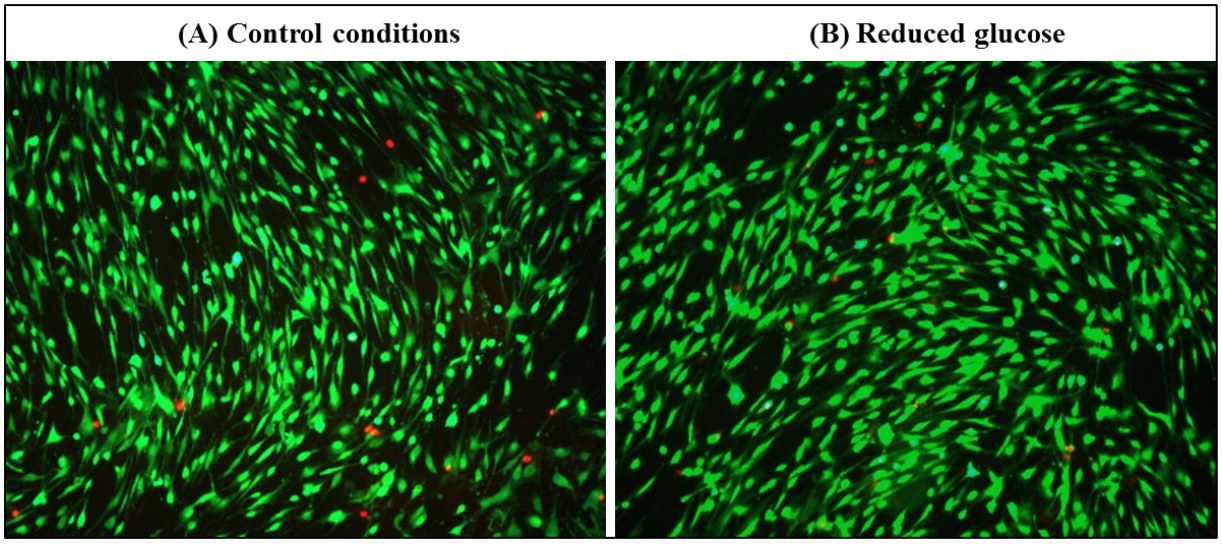

Figure 4.3.12 Effect of reduced glucose on BM-MSCs viability. BM-MSCs (n=3) were cultured under (A) control conditions and (B) reduced glucose for 7 days and labelled with live-dead stain. Representative fluorescence microscope images indicate viable (stained green) and dead (stained red) cell populations under both conditions (magnification x100).

Proliferation analysis showed that the increase in cell number under reduced glucose was significantly less compared to control conditions (5769±605 versus 8299±882, $p<0.05$) (Figure 4.3.13).

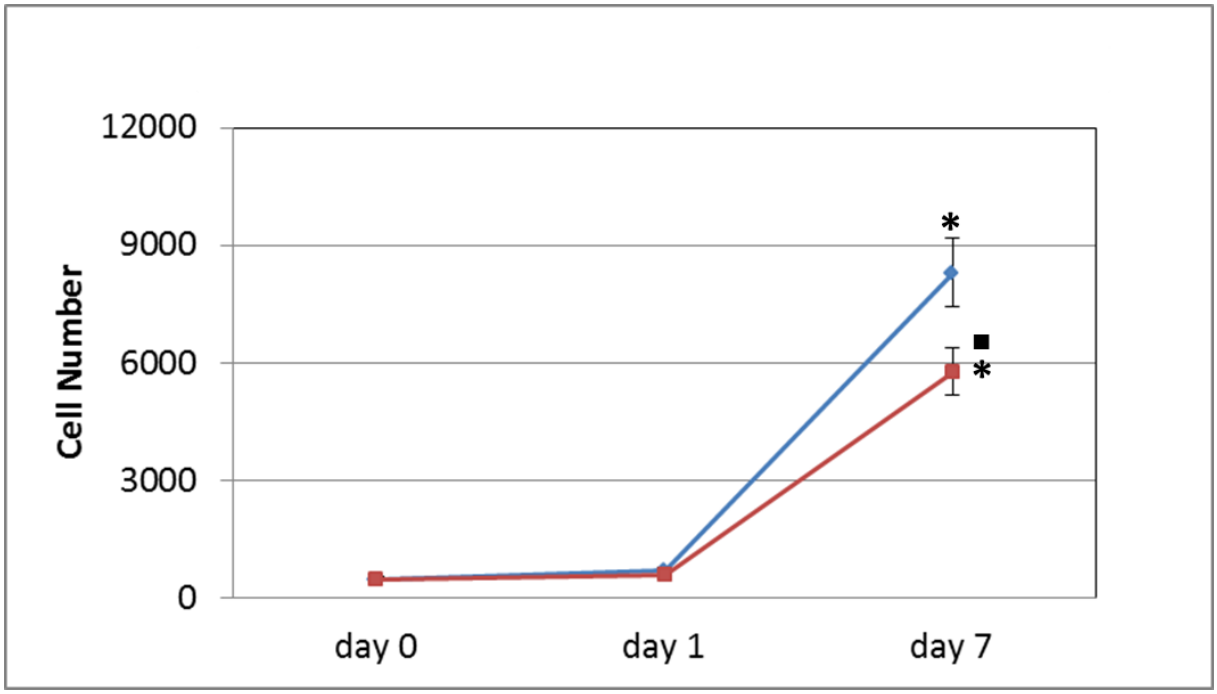

Figure 4.3.13 Effect of reduced glucose on BM-MSCs (n=3) proliferation over the course of 7 days. Total cell number was determined for BM-MSCs cultured under reduced glucose (red line) and control conditions (blue line). Day 0 cell number was used as baseline for each condition. Data was expressed as mean ±SEM of triplicates of 3 patient samples. Significant differences ($p \leq 0.05$) * compared to day 0 and ■ day 7 control conditions.

4.3.3.2 Gene expression

BM-MSCs cultured under reduced glucose showed no changes in SOX-9, COL2A1 and ACAN but significant decrease in VCAN expression ($p<0.05$) when compared to BM-MSCs cultured under control conditions (Figure 4.3.14 A & B).

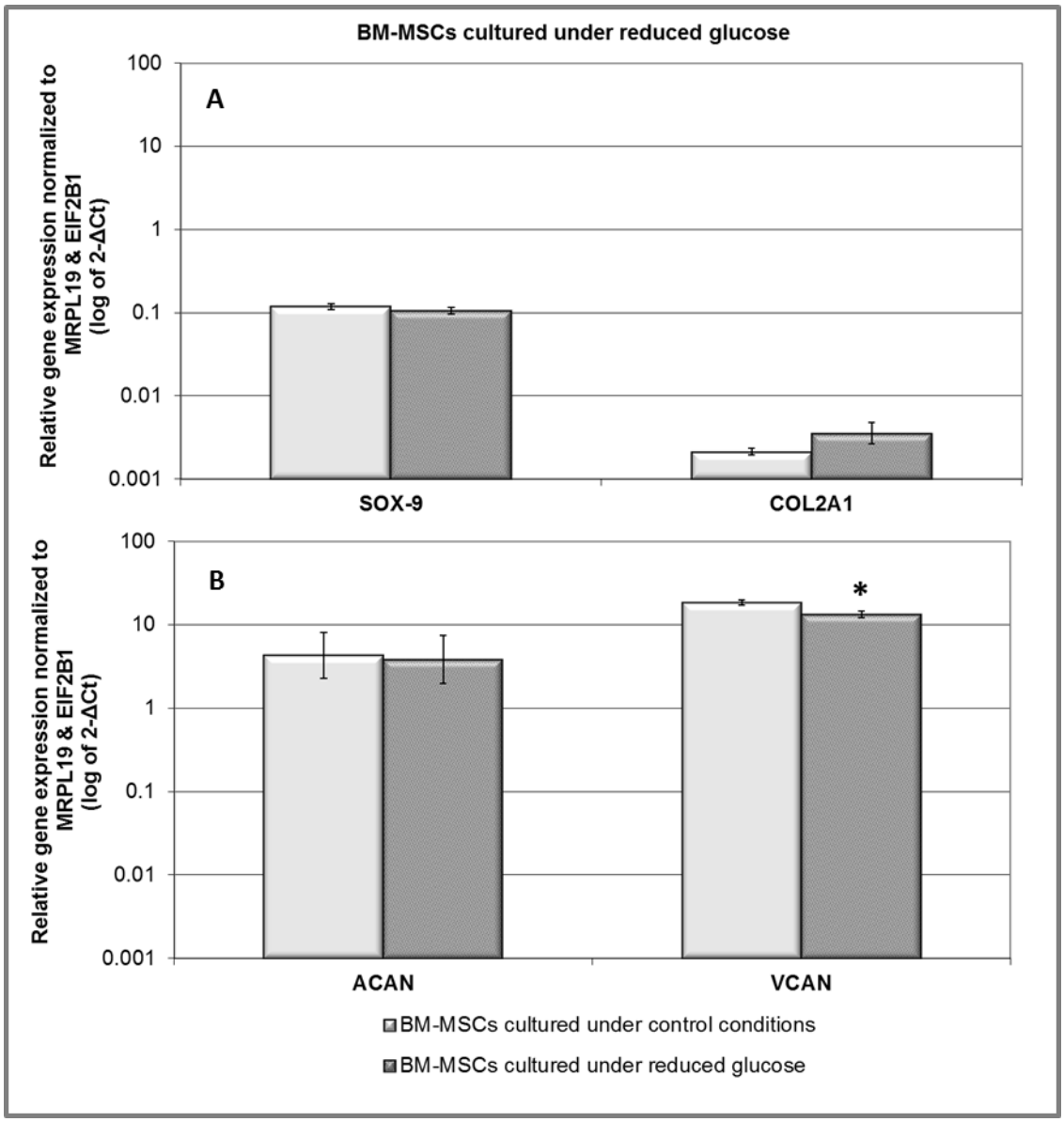

Figure 4.3.14 Relative gene expression of (**A**) SOX-9, COL2A1 and (**B**) ACAN, VCAN in BM-MSCs cultured under reduced glucose (n=3). Gene expression normalized to average of HK genes MRPL19 and EIF2B1 and plotted on a log scale. * Statistical significance ($p\leq0.05$) compared to culture under control conditions.

4.3.3.3 ECM protein expression

BM-MSCs cultured under reduced glucose showed a small increase in staining intensity for aggrecan protein compared to control conditions (Figure 4.3.15). Staining intensity for versican protein was comparable to control condition (Figure 4.3.16).

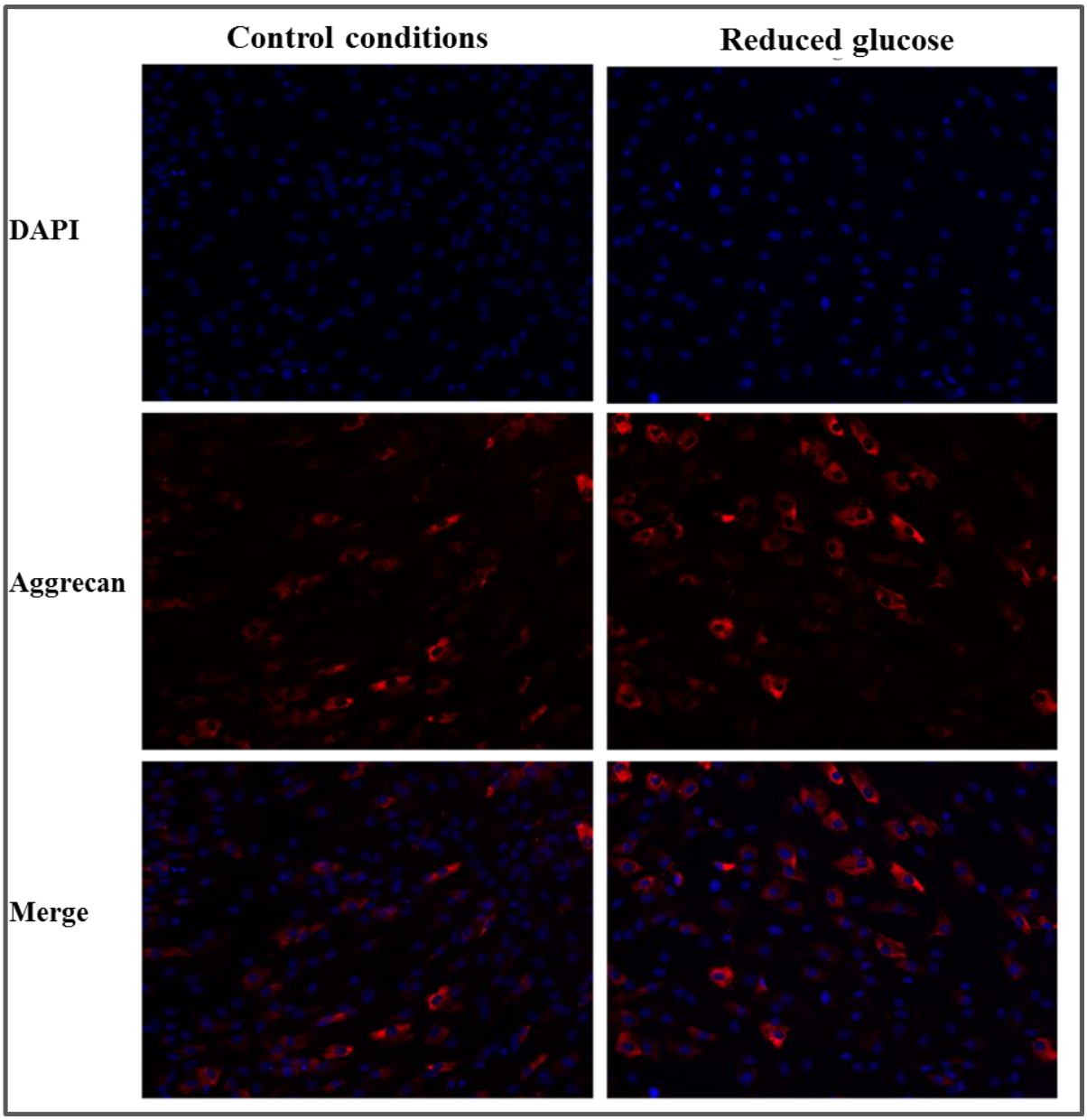

Figure 4.3.15 Representative images of aggrecan immunofluorescence staining of BM-MSCs (n=3) cultured under control conditions (left panels) and reduced glucose (right panels) for 7 days. Immunofluorescence staining was performed using anti-aggrecan primary antibody followed by Alexa Fluor 555 conjugated secondary antibody (red). DAPI (blue) was used for nucleus staining. Top row: DAPI, middle row: same field of view with aggrecan staining, bottom row: merge of above two rows (magnification x200).

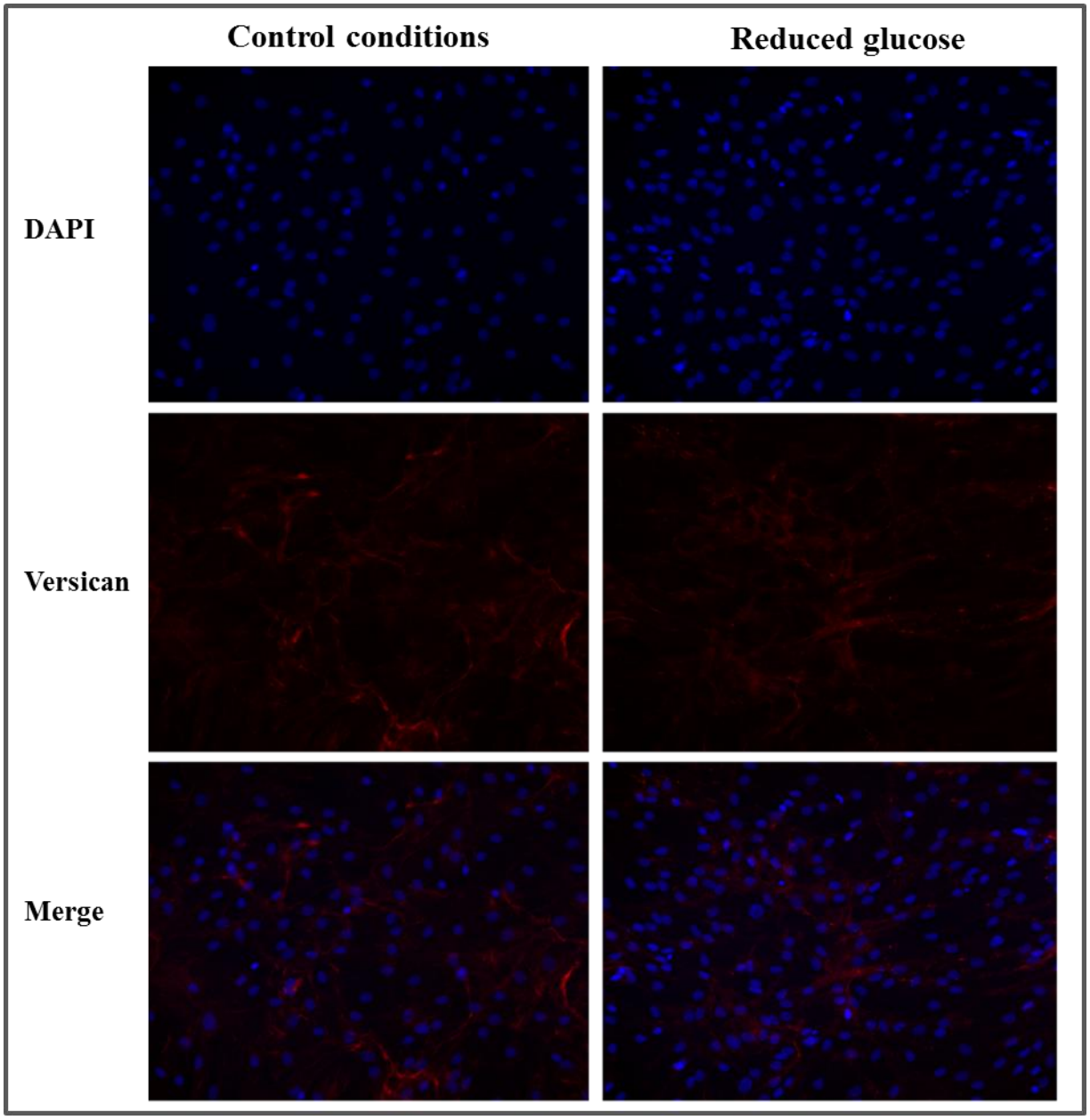

Figure 4.3.16 Representative images of versican immunofluorescence staining of BM-MSCs (n=3) cultured under control conditions (left panels) and reduced glucose (right panels) for 7 days. Immunofluorescence staining was performed using anti-versican primary antibody followed by Alexa Fluor 555 conjugated secondary antibody (red). DAPI (blue) was used for nucleus staining. Top row: DAPI, middle row: same field of view with versican staining, bottom row: merge of above two rows (magnification x200).

4.3.4 Influence of reduced serum and reduced glucose on BM-MSC behaviour

4.3.4.1 Cell viability and proliferation

Live/dead staining of BM-MSCs cultured under reduced serum and reduced glucose showed that majority of cells stained green (viable) with few red stained (dead) cells (Figure 4.3.17).

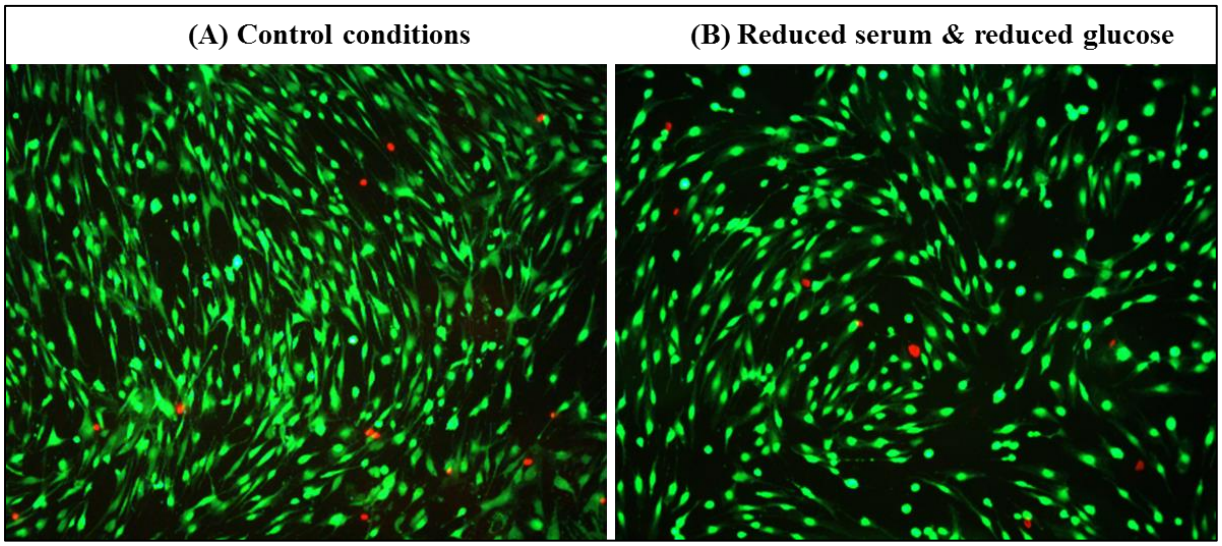

Figure 4.3.17 Effect of reduced serum and reduced glucose on BM-MSC viability. BM-MSCs (n=3) were cultured under (A) control conditions and (B) reduced serum and reduced glucose for 7 days and labelled with live-dead stain. Representative fluorescence microscope images indicate viable (stained green) and dead (stained red) cell populations under both conditions (magnification x100).

Proliferation analysis showed that at day 7 the increase in cell number under reduced serum and reduced glucose was significantly less compared to control conditions (3228±538 versus 8299±882, $p<0.05$) (Figure 4.3.18).

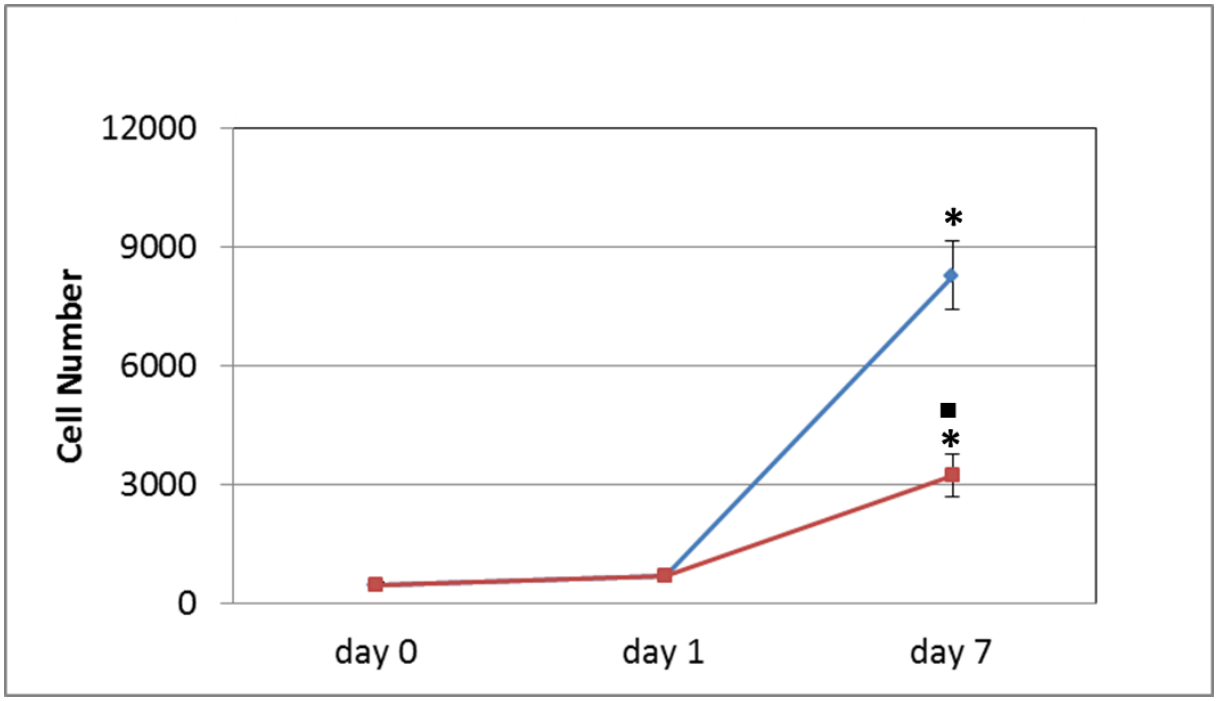

Figure 4.3.18 Effect of reduced serum and reduced glucose on BM-MSCs (n=3) proliferation over the course of 7 days. Total cell number was determined for BM-MSCs cultured under reduced serum and reduced glucose (red line) compared to control conditions (blue line). Day 0 cell number was used as baseline for each condition. Data was expressed as mean ±SEM of triplicates of 3 patient samples. Significant differences ($p \leq 0.05$) * compared to day 0 and ■ day 7 control conditions.

4.3.4.2 Gene expression

BM-MSCs cultured under reduced serum and reduced glucose showed no significant changes in, SOX-9, COL2A1 and ACAN expression. A significant decrease in VCAN expression (p<0.05) was observed compared to control conditions (Figure 4.3.19 A & B).

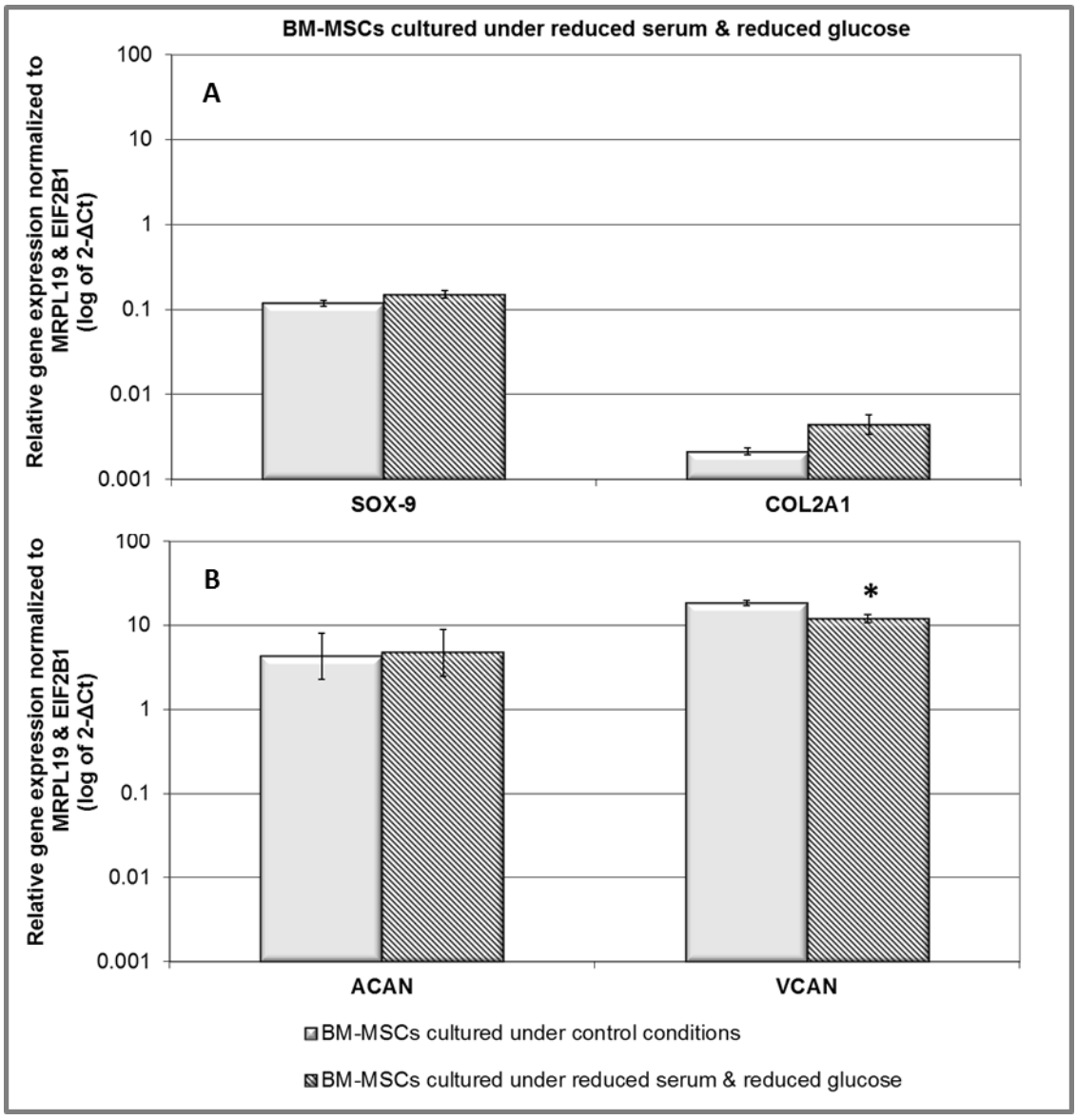

Figure 4.3.19 Relative gene expression of (**A**) SOX-9, COL2A1and (**B**) ACAN, VCAN in BM-MSCs cultured under reduced serum and reduced glucose (n=3). Gene expression normalized to average of HK genes MRPL19 and EIF2B1 and plotted on a log scale. * Statistical significance (p≤0.05) compared to culture under control conditions.

4.3.4.3 ECM protein expression

BM-MSCs cultured under reduced serum and reduced glucose showed staining intensity of aggrecan protein comparable to control conditions (Figure 4.3.20). BM-MSCs cultured under reduced serum and reduced glucose also showed positive staining for versican but the intensity appeared to be reduced and diffused without fibril pattern (Figure 4.3.21).

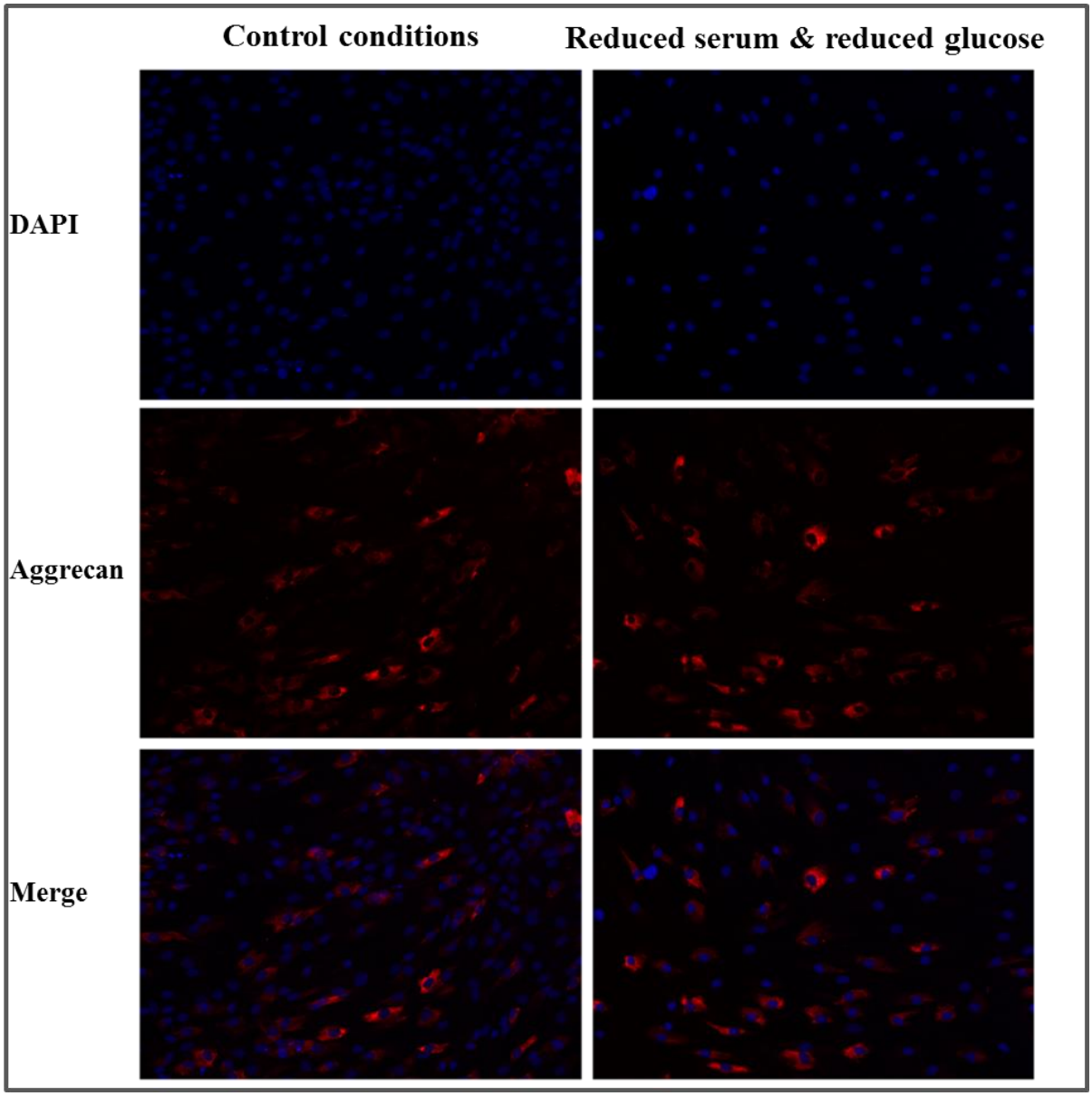

Figure 4.3.20 Representative images of aggrecan immunofluorescence staining of BM-MSCs (n=3) cultured under control conditions (left panels) and reduced serum and reduced glucose (right panels) for 7 days. Immunofluorescence staining was performed using anti-aggrecan primary antibody followed by Alexa Fluor 555 conjugated secondary antibody (red). DAPI (blue) was used for nucleus staining. Top row: DAPI, middle row: same field of view with aggrecan staining, bottom row: merge of above two rows (magnification x200).

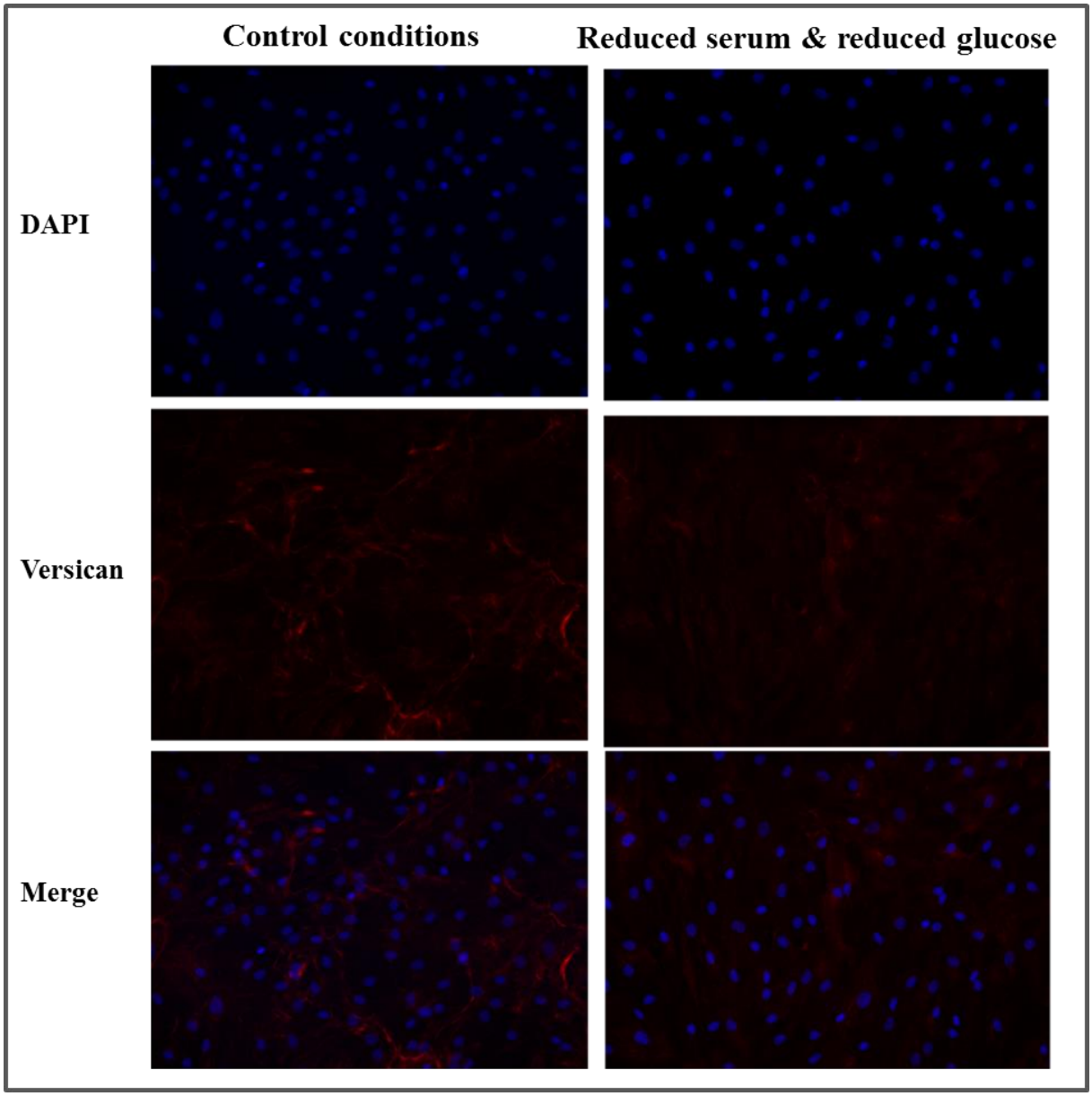

Figure 4.3.21 Representative images of versican immunofluorescence staining of BM-MSCs (n=3) cultured under control conditions (left panels) and reduced serum and reduced glucose (right panels) for 7 days. Immunofluorescence staining was performed using anti-versican primary antibody followed by Alexa Fluor 555 conjugated secondary antibody (red). DAPI (blue) was used for nucleus staining. Top row: DAPI, middle row: same field of view with versican staining, bottom row: merge of above two rows (magnification x200).

4.3.5 Influence of reduced serum and hypoxia on BM-MSC behaviour

4.3.5.1 Cell viability and proliferation

Live/dead staining of BM-MSCs cultured under reduced serum combined with hypoxia showed that majority of cells stained green (viable) with few red stained cells (dead) (Figure 4.3.22).

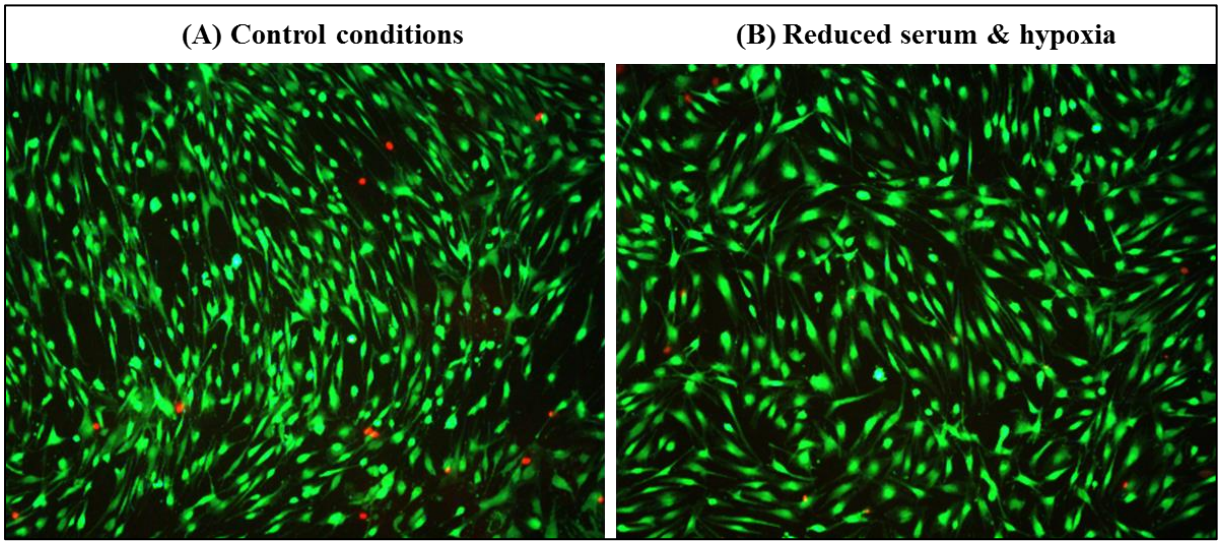

Figure 4.3.22 Effect of reduced serum and hypoxia on BM-MSCs viability. BM-MSCs (n=3) were cultured under (A) control conditions and (B) reduced serum and hypoxia (right) for 7 days and labelled with live-dead stain. Representative fluorescence microscope images indicate viable (stained green) and dead (stained red) cell populations under both conditions (magnification x100).

Proliferation analysis showed that at day 7 the increase in cell number under reduced serum and hypoxia was significantly less compared to control conditions (4750±334 versus 8299±882, $p<0.05$).

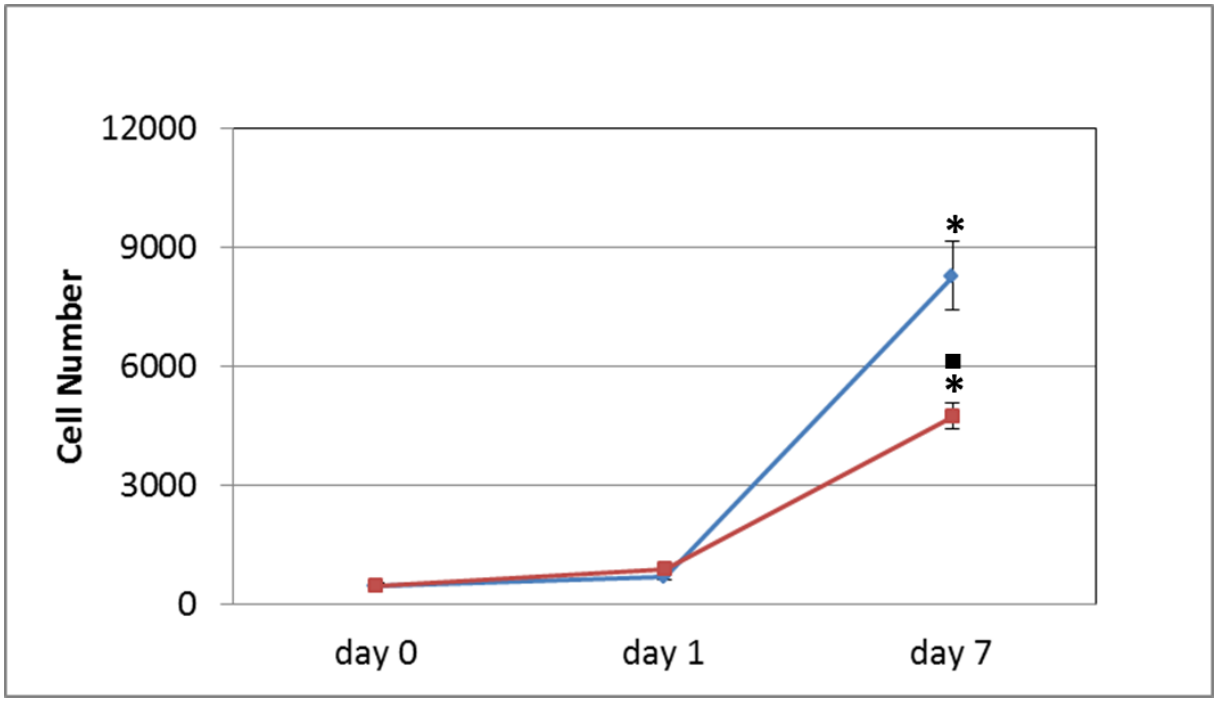

Figure 4.3.23 Effect of reduced serum and hypoxia combination on BM-MSCs (n=3) proliferation over the course of 7 days. Total cell number was determined for BM-MSCs cultured under reduced serum combined with hypoxia (red line) compared to control conditions (blue line). Cell number was also compared to BM-MSCs cultured under reduced serum alone (red line). Day 0 cell number was used as baseline for each condition. Data was expressed as mean ± SEM of triplicates of 3 patient samples. Significant differences ($p \leq 0.05$) * compared to day 0 and day 7 ■ control.

4.3.5.2 Gene expression

BM-MSCs cultured under reduced serum combined with hypoxia showed a significant decrease in SOX-9 expression (p=0.05) with no change in COL2A1 expression compared to BM-MSCs cultured under control conditions (Figure 4.3.24 A). ACAN and VCAN were significantly increased (p=0.05 & p<0.05 respectively) under reduced serum and hypoxic conditions (Figure 4.3.24 B).

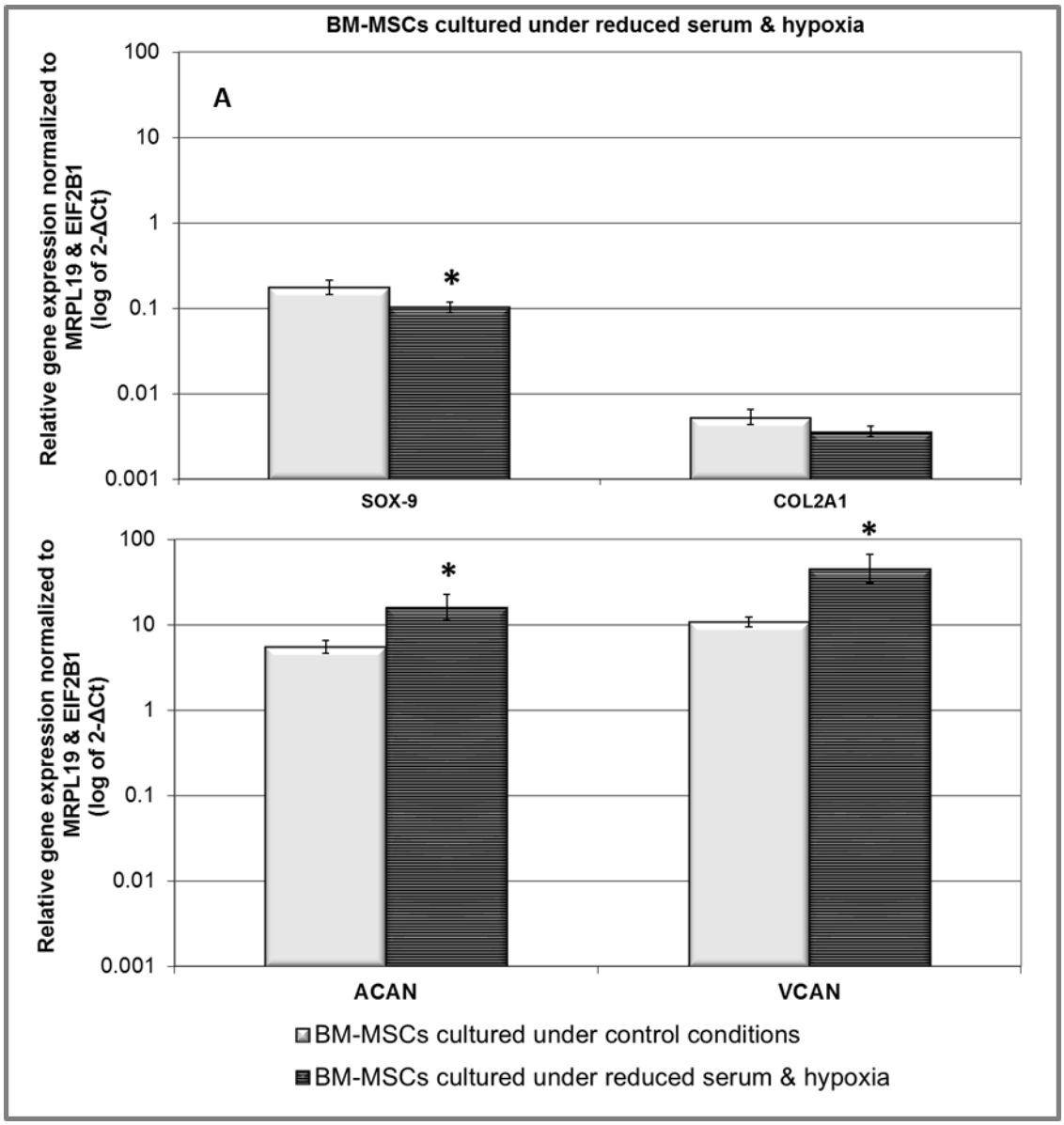

Figure 4.3.24 Relative gene expression of (**A**) SOX-9, COL2A1 and (**B**) ACAN, VCAN in BM-MSCs cultured under reduced serum and hypoxia (n=3). Gene expression normalized to average of HK genes MRPL19 and EIF2B1 and plotted on a log scale. * Statistical significance (p≤0.05) compared to culture under control conditions.

4.3.5.3 ECM protein expression

BM-MSCs cultured under reduced serum and hypoxia showed decreased aggrecan protein staining intensity. BM-MSCs showed no prominent change in versican staining intensity compared to control conditions (Figure 4.3.25 & 4.3.26).

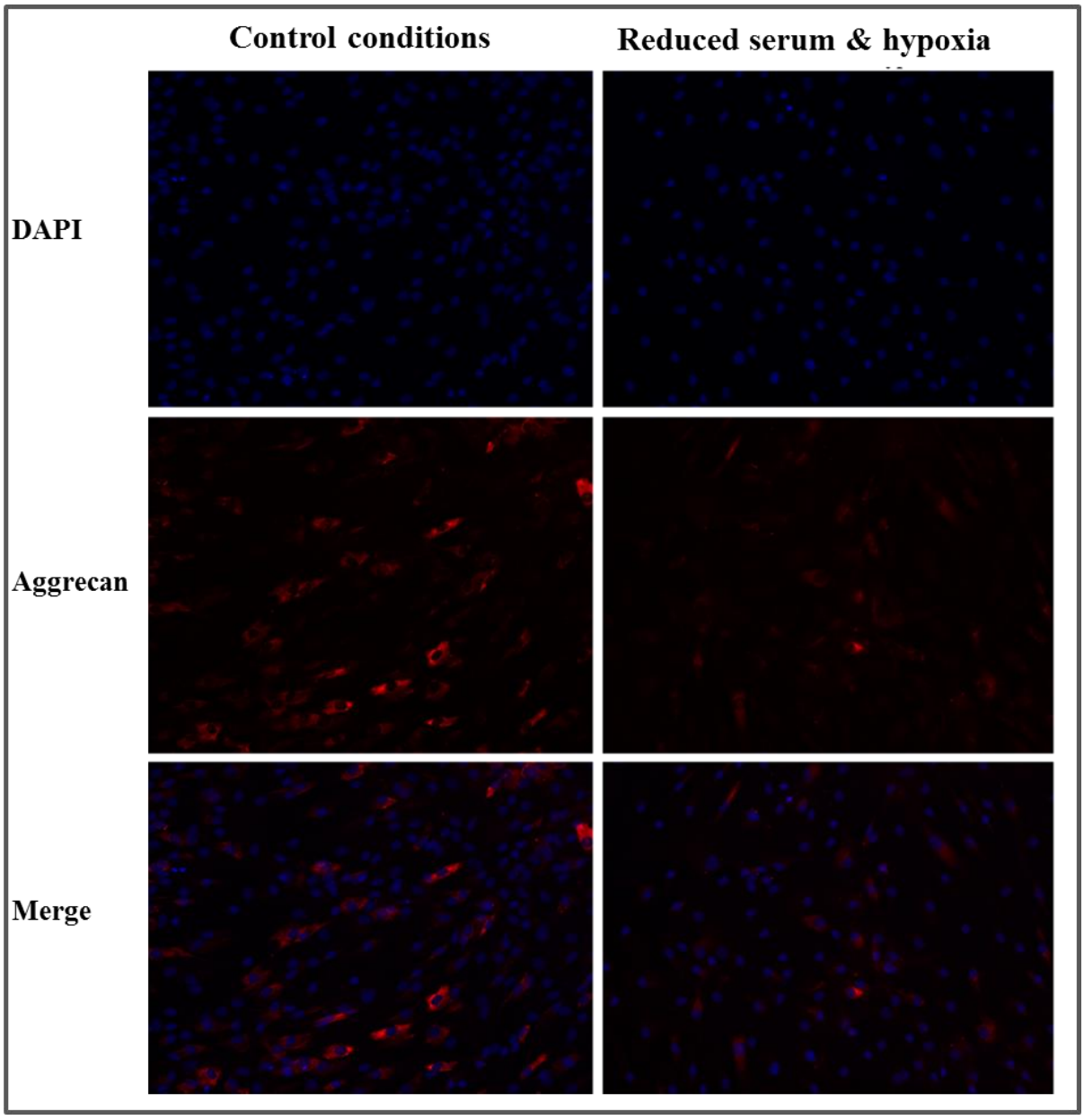

Figure 4.3.25 Representative images of aggrecan immunofluorescence staining of BM-MSCs (n=3) cultured under control conditions (left panels) and reduced serum combined with hypoxia (right panels) for 7 days. Immunofluorescence staining was performed using anti-aggrecan primary antibody followed by Alexa Fluor 555 conjugated secondary antibody (red). DAPI (blue) was used for nucleus staining. Top row: DAPI, middle row: same field of view with aggrecan staining, bottom row: merge of above two rows (magnification x200).

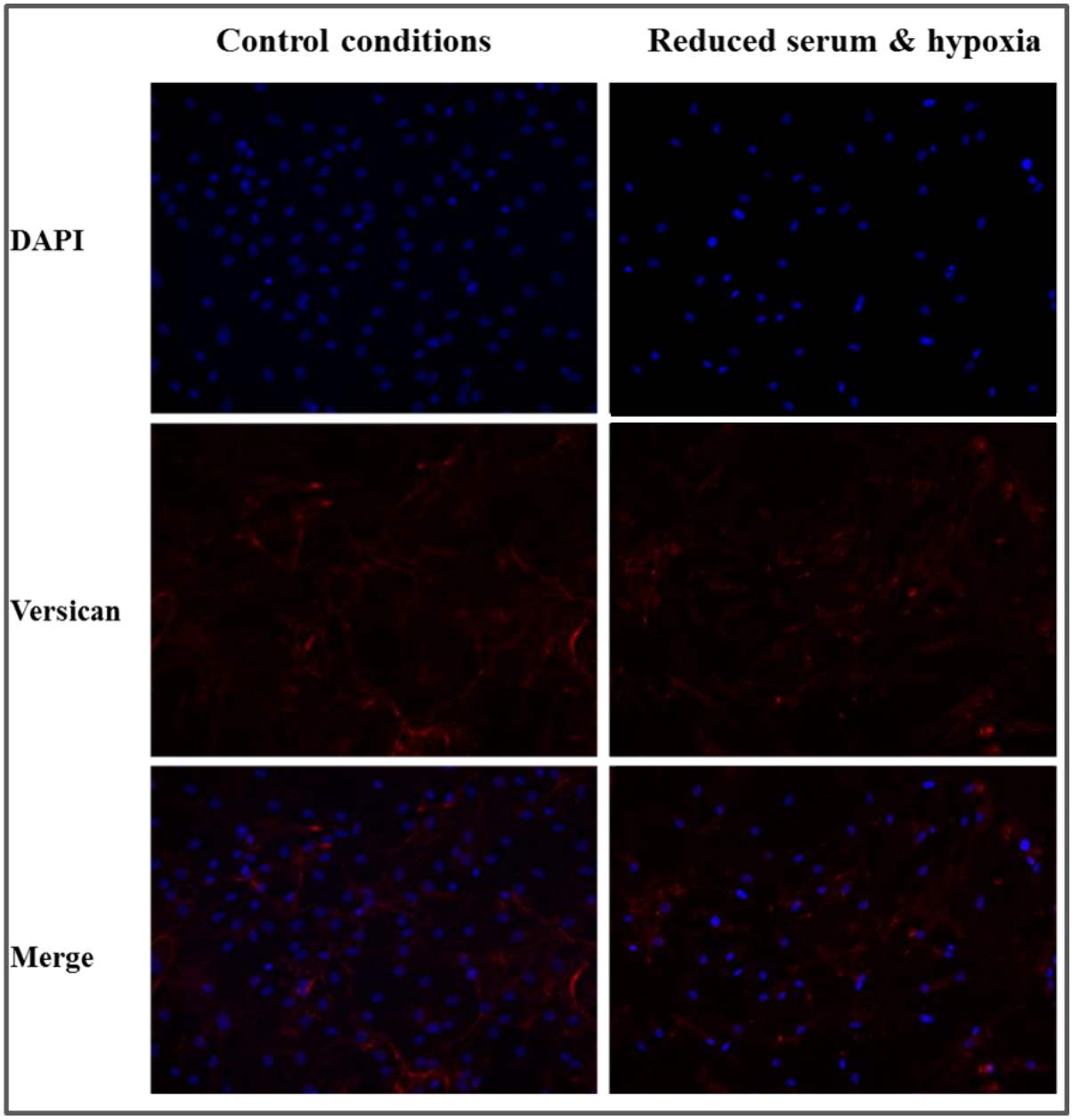

Figure 4.3.26 Representative images of versican immunofluorescence staining of BM-MSCs (n=3) culture under control conditions (left panels) and reduced serum combined with hypoxia (right panels) for 7 days. Immunofluorescence staining was performed using anti-versican primary antibody followed by Alexa Fluor 555 conjugated secondary antibody (red). DAPI (blue) was used for nucleus staining. Top row: DAPI, middle row: same field of view with versican staining, bottom row: merge of above two rows (magnification x200).

4.3.6 Influence of reduced glucose and hypoxia on BM-MSC behaviour

4.3.6.1 Cell viability and proliferation

Live/dead staining of BM-MSCs cultured under reduced glucose combined with hypoxia showed that majority of cells stained green (viable) with few red stained (dead) cells (Figure 4.3.27).

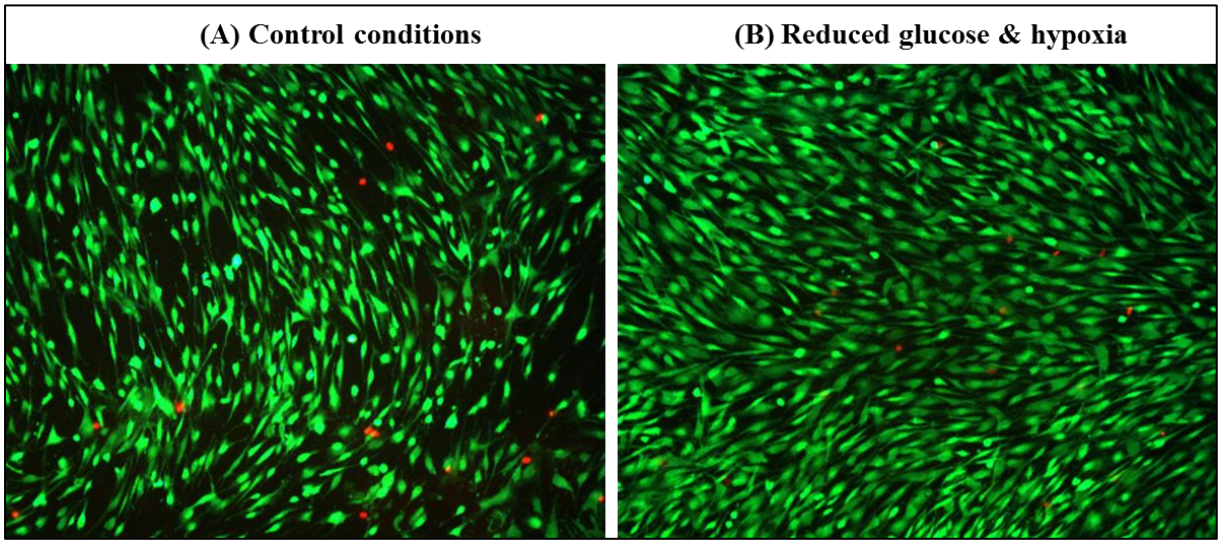

Figure 4.3.27 Effect of reduced glucose and hypoxia on BM-MSCs viability. BM-MSCs (n=3) were cultured under (A) control conditions and (B) reduced glucose combined with hypoxia for 7 days and labelled with live-dead stain. Representative fluorescence microscope images indicate viable (stained green) and dead (stained red) cell populations under both conditions (magnification x100).

Proliferation analysis showed that at day 7 the increase in cell number under reduced glucose and hypoxic conditions was not significantly different compared to control conditions (10167±433 versus 8299±882) (Figure 4.3.28).

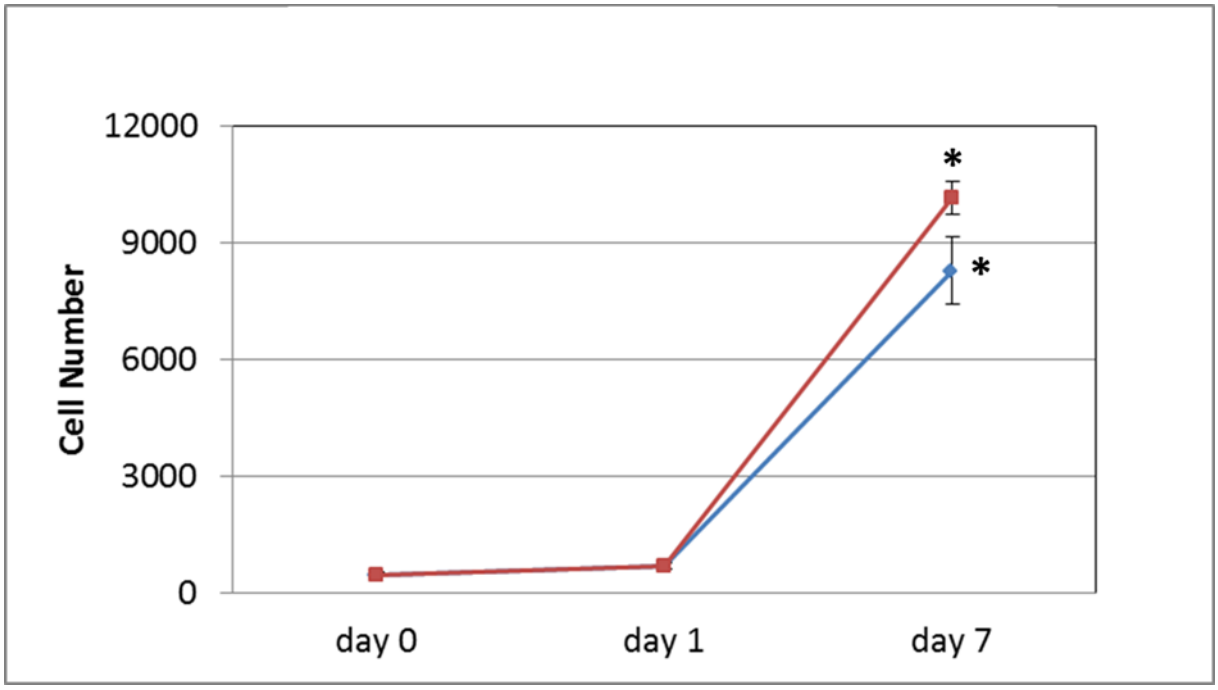

Figure 4.3.28 Effect of reduced glucose and hypoxia combination on BM-MSCs (n=3) proliferation over the course of 7 days. Total cell number was determined for BM-MSCs cultured under reduced glucose combined with hypoxia (red line) compared to control conditions (blue line). Day 0 cell number was used as baseline for each condition. Data was expressed as mean ± SEM of triplicates of 3 patient samples. Significant differences ($p \leq 0.05$) * compared to day 0.

4.3.6.2 Gene expression

BM-MSCs cultured under reduced glucose combined with hypoxia showed significant increase in SOX-9 (p<0.05) and COL2A1 (p<0.05) expression compared to BM-MSCs cultured under control conditions (Figure 4.3.29 A). ACAN expression was not changed while VCAN was significantly increased (p=0.05) (Figure 4.3.29 B).

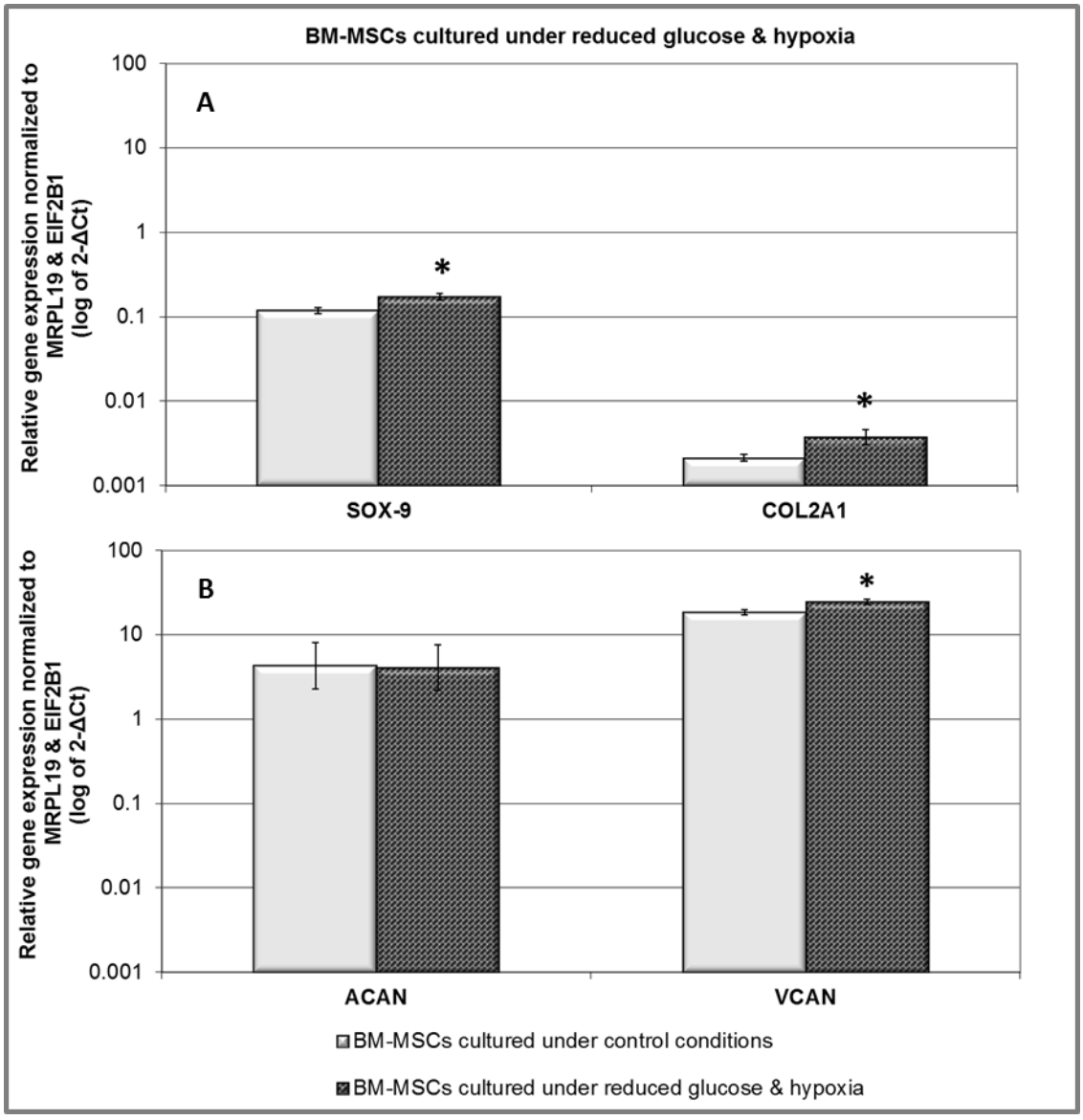

Figure 4.3.29 Relative gene expression of (**A**) SOX-9, COL2A1 and (**B**) ACAN, VCAN in BM-MSCs cultured under reduced glucose and hypoxia (n=3). Gene expression normalized to average of HK genes MRPL19 and EIF2B1 and plotted on a log scale. * Statistical significance ($p \leq 0.05$) compared to culture under control conditions.

4.3.6.3 ECM protein expression

BM-MSCs cultured under reduced glucose combined with hypoxia showed increased staining intensity of aggrecan and versican protein compared to BM-MSCs cultured under control conditions (Figure 4.3.30 & 4.3.31). BM-MSC culture showed a dense versican matrix deposit under reduced glucose and hypoxic conditions.

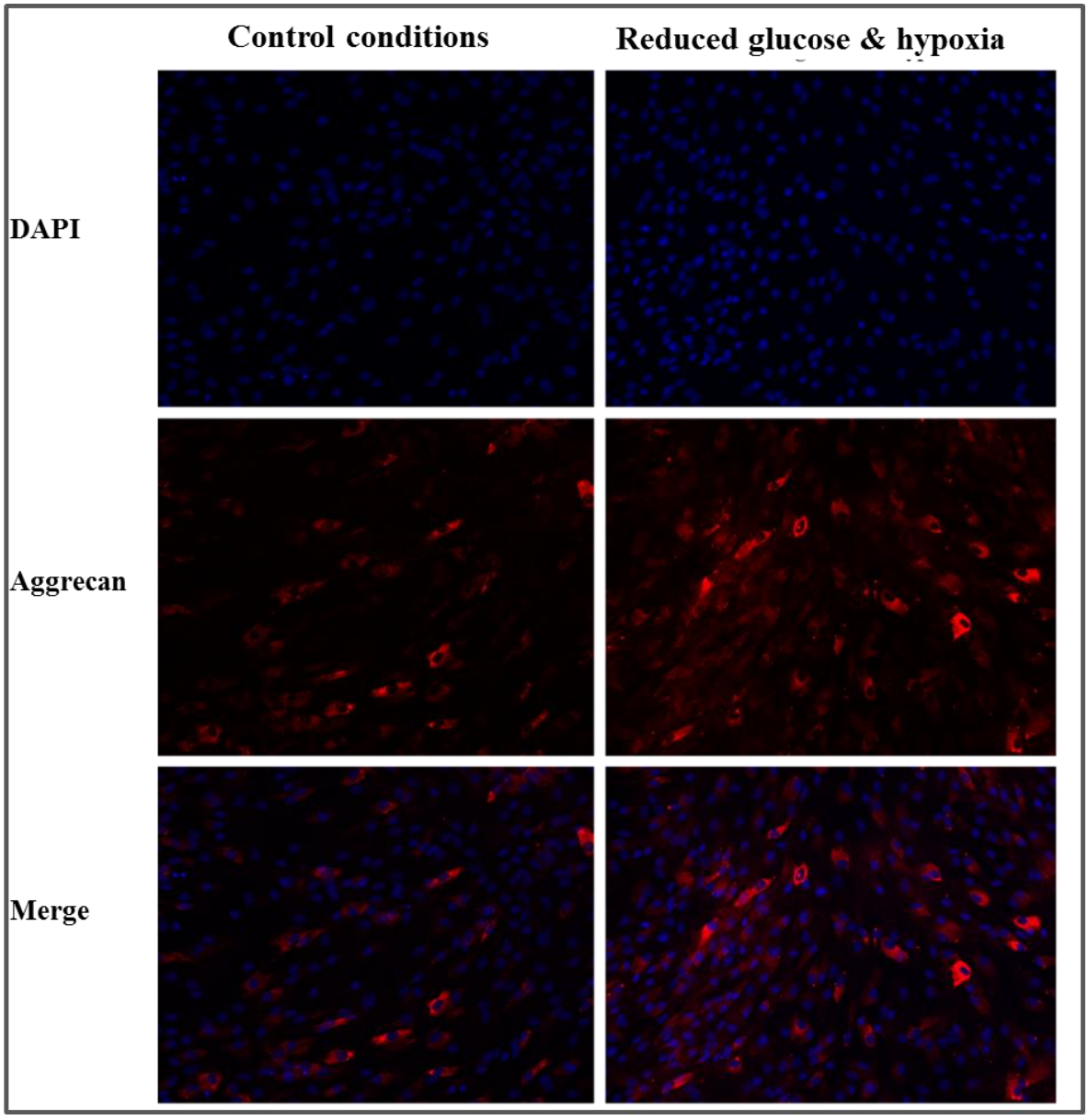

Figure 4.3.30 Representative images of aggrecan immunofluorescence staining of BM-MSCs (n=3) cultured under control conditions (left panels) and reduced glucose combined with hypoxia (right panels) for 7 days. Immunofluorescence staining was performed using anti-aggrecan primary antibody followed by Alexa Fluor 555 conjugated secondary antibody (red). DAPI (blue) was used for nucleus staining. Top row: DAPI, middle row: same field of view with aggrecan staining, bottom row: merge of above two rows (magnification x200).

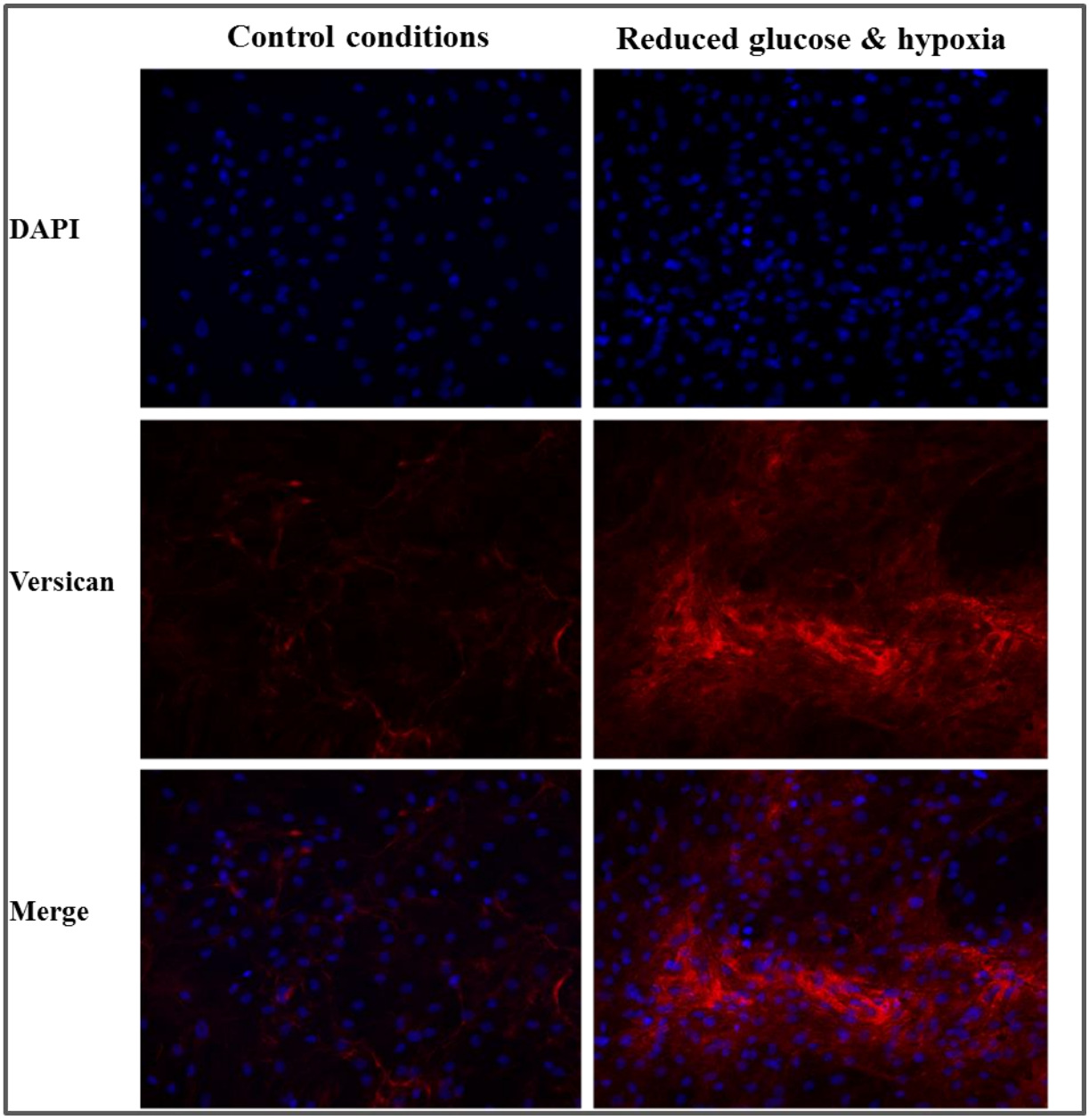

Figure 4.3.31 Representative images of versican immunofluorescence staining of BM-MSCs (n=3) cultured under control conditions (left panel) and reduced glucose combined with hypoxia (right panel) for 7 days. Immunofluorescence staining was performed using anti-versican primary antibody followed by Alexa Fluor 555 conjugated secondary antibody (red). DAPI (blue) was used for nucleus staining. Top row: DAPI, middle row: same field of view with versican staining, bottom row: merge of above two rows (magnification x200).

4.3.7 Influence of reduced serum, reduced glucose and hypoxia on BM-MSC behaviour

4.3.7.1 Cell viability and proliferation

Live/dead staining of BM-MSCs cultured under reduced serum, reduced glucose combined with hypoxia showed that majority of cells stained green (viable) with few cells in red staining (dead) (Figure 4.3.32).

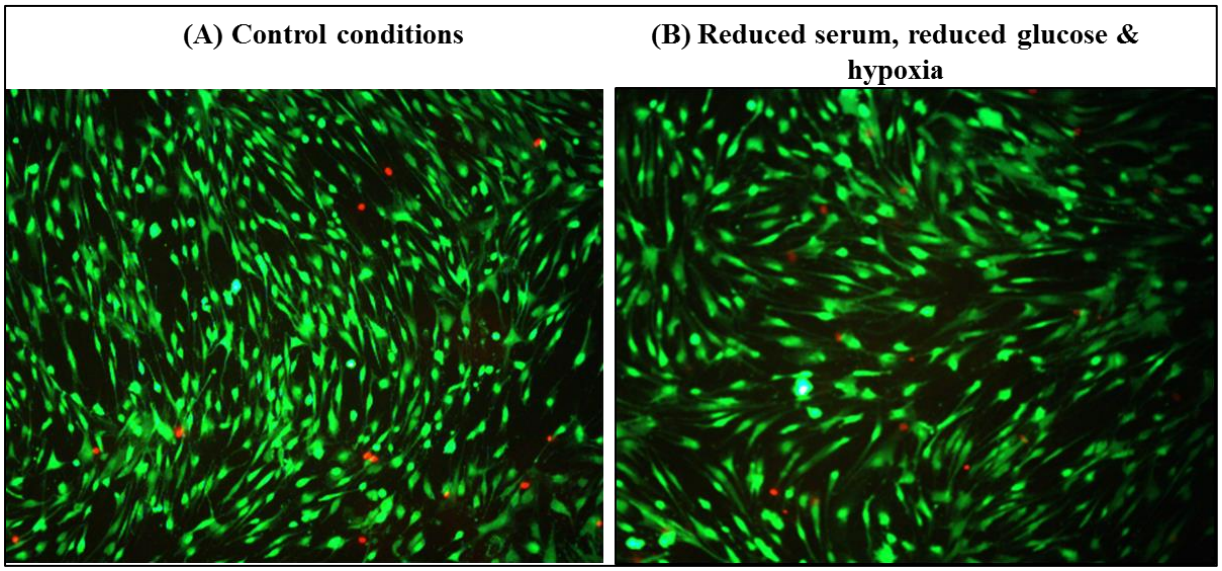

Figure 4.3.32 Effect of reduced serum, reduced glucose and hypoxia on BM-MSCs viability. BM-MSCs (n=3) were cultured under (A) control conditions and (B) reduced serum, reduced glucose and hypoxia for 7 days and labelled with live-dead stain. Representative fluorescence microscope images indicate viable (stained green) and dead (stained red) cell populations under both conditions (magnification x100).

Proliferation analysis showed that at day 7 the increase in cell number under reduced serum, reduced glucose combined with hypoxia had no significant difference compared to control conditions (7466±635 versus 8299±882) (Figure 4.3.33).

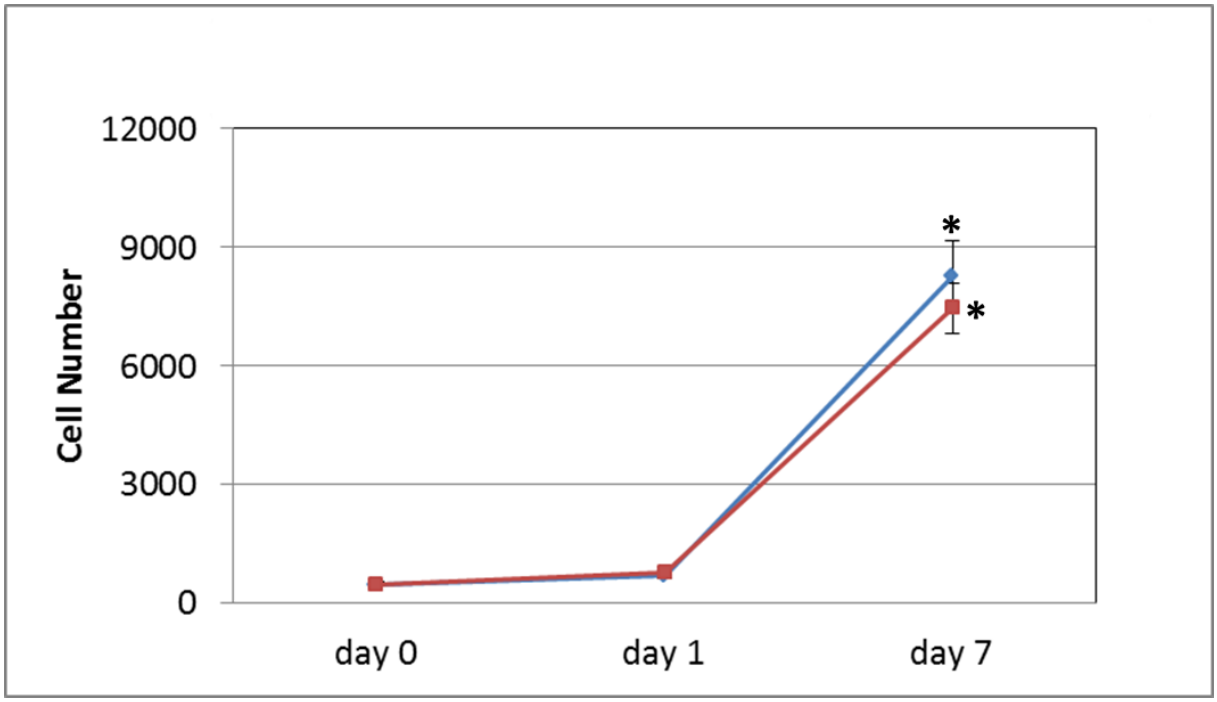

Figure 4.3.33 Effect of reduced serum, reduced glucose and hypoxia on BM-MSCs (n=3) proliferation over the course of 7 days. Total cell number was determined for BM-MSCs cultured under reduced serum, reduced glucose and hypoxia (red line) compared to control conditions (blue line). Day 0 cell number was used as baseline for each condition. Data was expressed as mean ± SEM of triplicates of 3 patient samples. Significant differences ($p \leq 0.05$) * compared to day 0.

4.3.7.2 Gene expression

BM-MSCs cultured under reduced serum, reduced glucose combined with hypoxia showed a significant increase in SOX-9 and COL2A1 expression (p<0.05 for each) (Figure 4.3.34 A). There was no change in ACAN and VCAN expression (Figure 4.3.34 B).

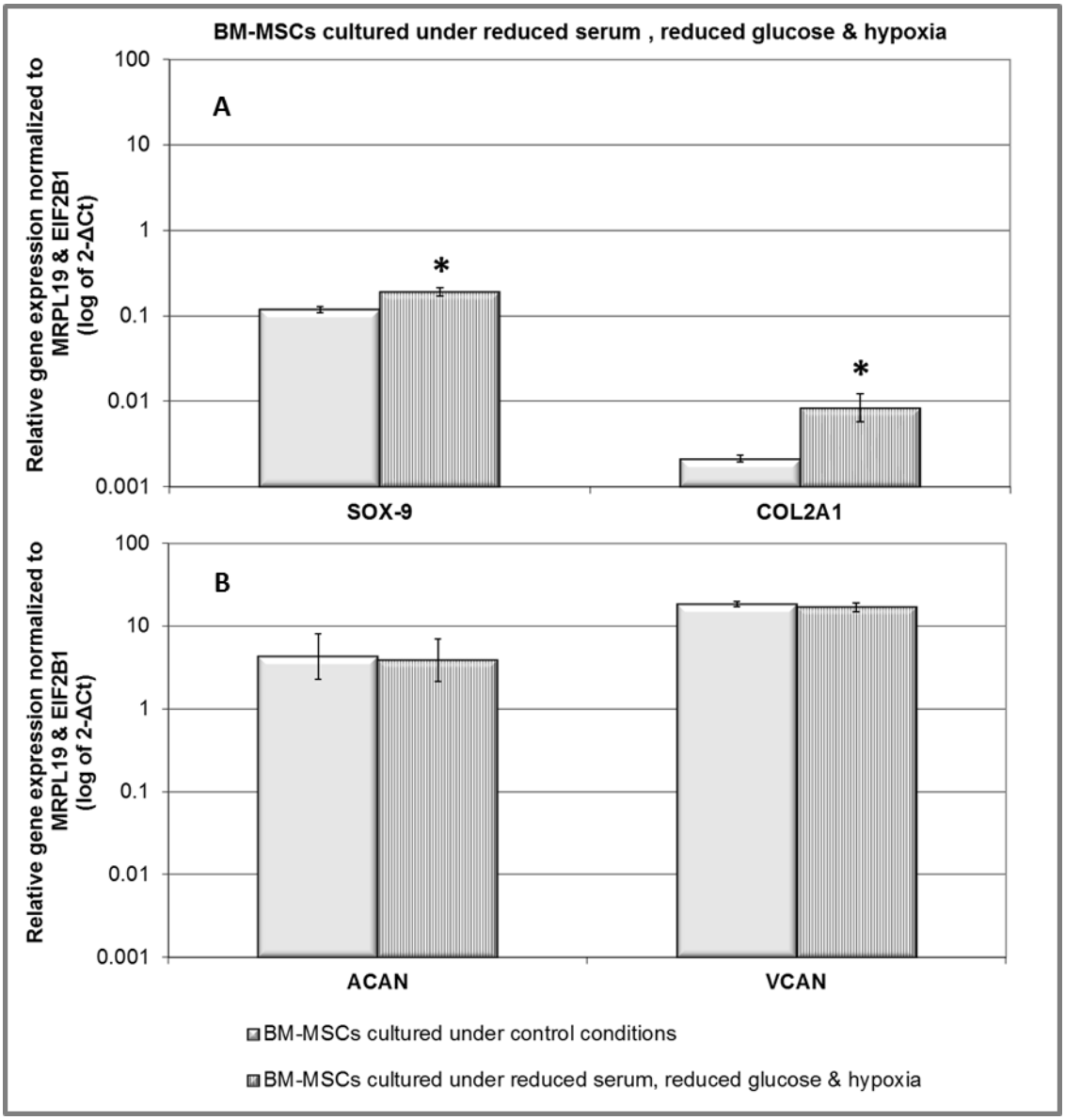

Figure 4.3.34 Relative gene expression of (**A**) SOX-9, COL2A1 and (**B**) ACAN, VCAN in BM-MSCs cultured under reduced serum, reduced glucose and hypoxia (n=3). Gene expression normalized to average of HK genes MRPL19 and EIF2B1 and plotted on a log scale. * Statistical significance ($p \leq 0.05$) compared to culture under control conditions.

4.3.7.3 ECM protein expression

BM-MSCs cultured under reduced serum, reduced glucose and hypoxia showed a decreased staining intensity for aggrecan compared to BM-MSCs cultured under control conditions (Figure 4.3.35). However, BM-MSCs cultured under reduced serum, reduced glucose and hypoxia showed versican staining intensity comparable to control conditions (Figure 4.3.36).

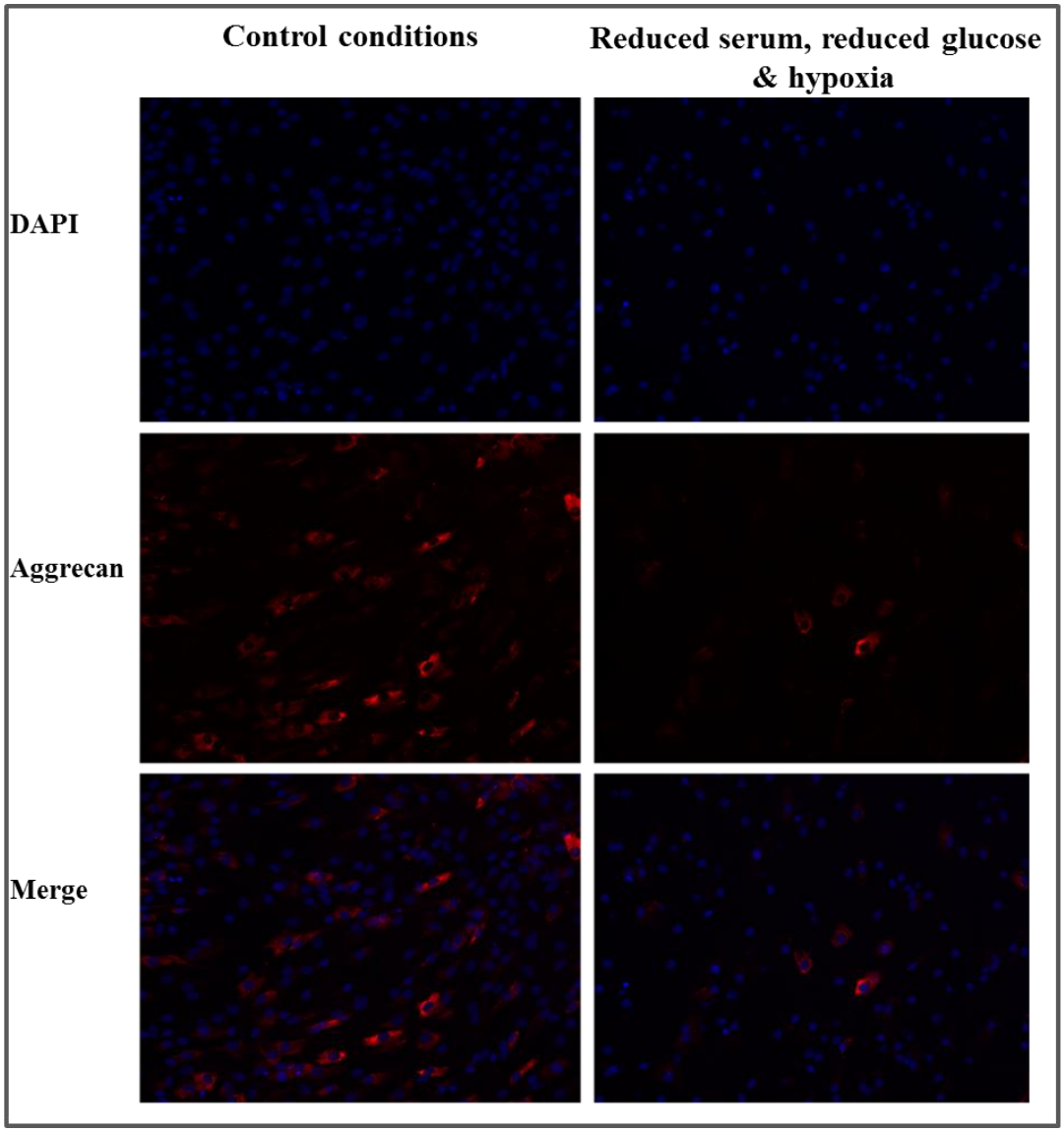

Figure 4.3.35 Representative images of aggrecan immunofluorescence staining of BM-MSCs (n=3) cultured under control conditions (left panels) and reduced serum, reduced glucose and hypoxia (right panels) for 7 days. Immunofluorescence staining was performed using anti-aggrecan primary antibody followed by Alexa Fluor 555 conjugated secondary antibody (red). DAPI (blue) was used for nucleus staining. Top row: DAPI, middle row: same field of view with aggrecan staining, bottom row: merge of above two rows (magnification x200).

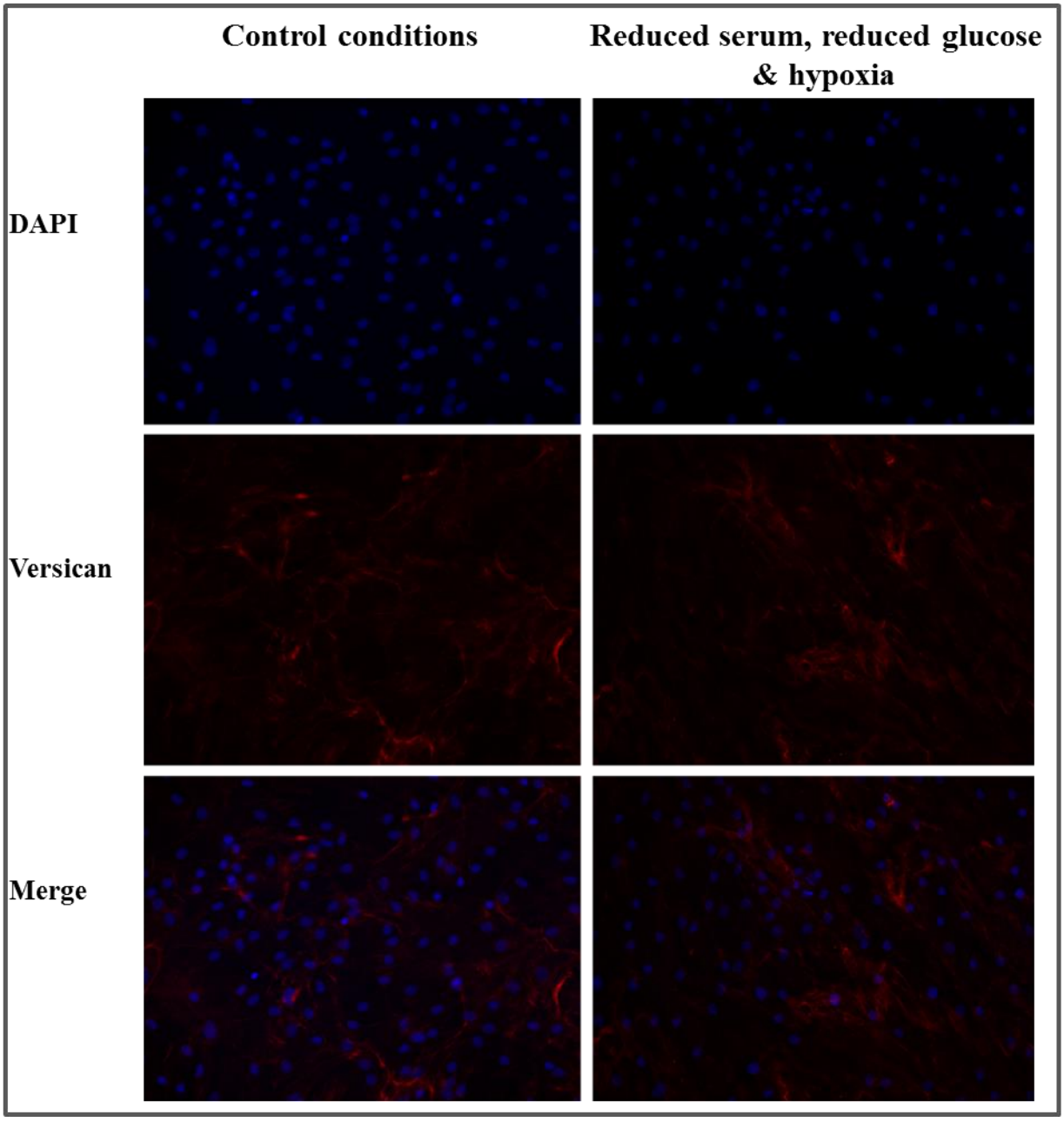

Figure 4.3.36 Representative images of versican immunofluorescence staining of BM-MSCs (n=3) cultured under control conditions (left panel) and reduced serum, reduced glucose and hypoxia (right panel) for 7 days. Immunofluorescence staining was performed using anti-versican primary antibody followed by Alexa Fluor 555 conjugated secondary antibody (red). DAPI (blue) was used for nucleus staining. Top row: DAPI, middle row: same field of view with versican staining, bottom row: merge of above two rows (magnification x200).

4.3.8 Influence of reduced pH on BM-MSC behaviour

4.3.8.1 Cell viability and proliferation

Live/dead staining of BM-MSCs cultured under pH 6.8 and 6.5 showed that the majority of cells stained green (viable) with few red stained (dead) cells (Figure 4.3.37). In control conditions cells appeared to have large cytoskeleton architecture that showed an obvious decrease with gradual pH decrease; cells were narrower and had a spindle shape morphology shown by arrow in pH 6.8 and 6.5 (Figure 4.3.37).

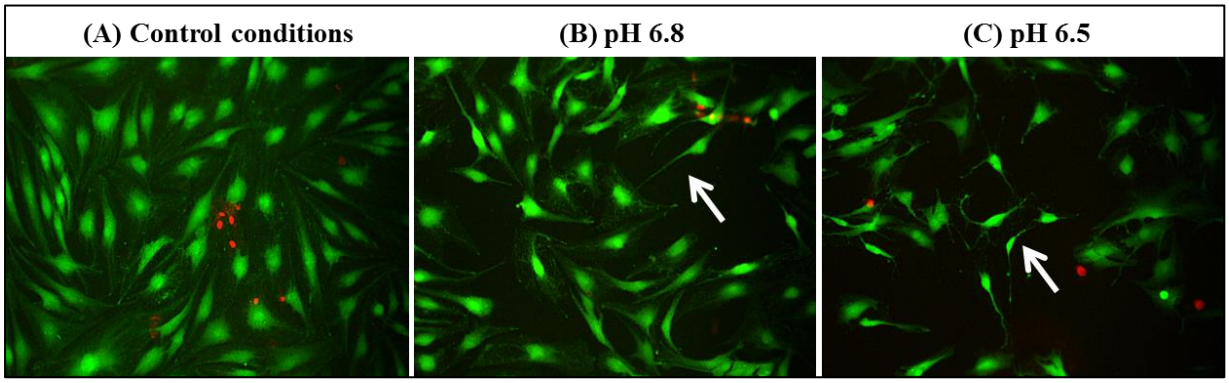

Figure 4.3.37 Effect of reduced pH (6.8 and 6.5) on BM-MSCs viability. BM-MSCs (n=3) were cultured under (A) control conditions (left), (B), pH 6.8 (middle) and (C) pH 6.5 (right) for 7 days and labelled with live-dead stain. Representative fluorescence microscope images indicate viable (stained green) and dead (stained red) cell populations under both conditions. White arrow indicates change in cell morphology compared to control condition (magnification x200).

Proliferation analysis showed that at day 7 the increase in cell number under pH 6.8 was significantly less compared to control conditions (23889±450 versus 47969±599, $p<0.05$) (Figure 4.3.38). At day 7 BM-MSCs cultured under pH 6.5 also showed significantly less increase in cell number compare to both control (7522±385 versus 47969±599, $p<0.05$) and pH 6.8 (7522±385 versus 23889±450, $p< 0.05$) conditions (Figure 4.3.38).

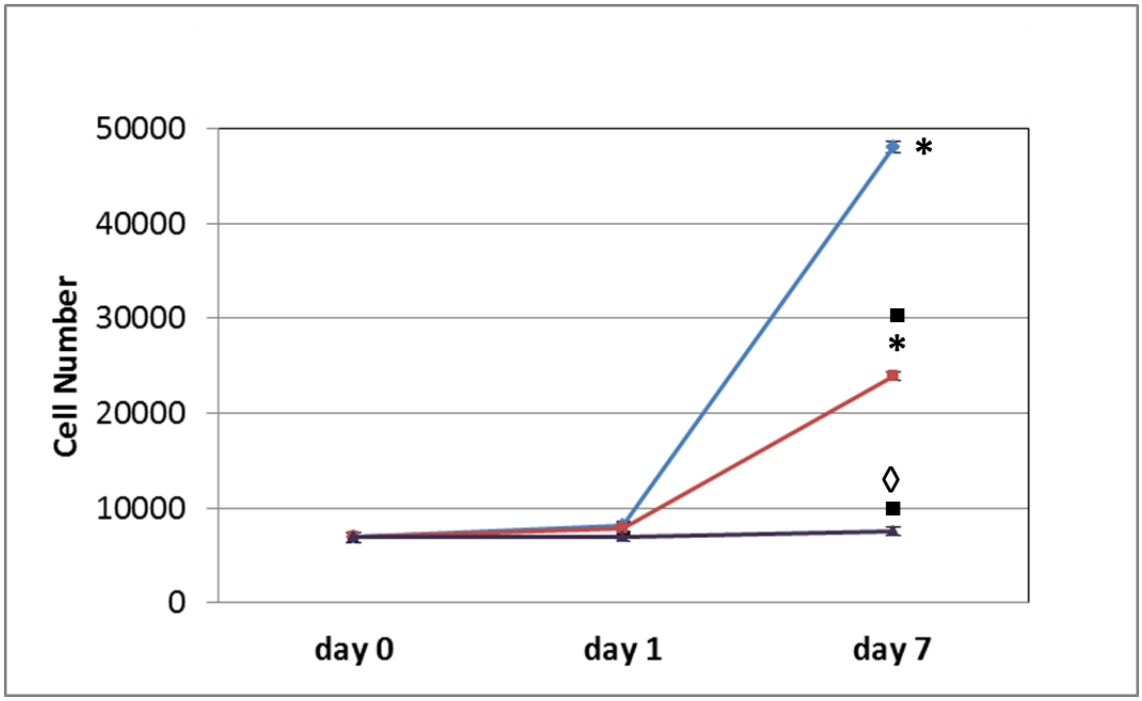

Figure 4.3.38 Effect of reduced pH 6.8 and 6.5 on BM-MSCs (n=3) proliferation over the course of 7 days. Total cell number was determined for BM-MSCs cultured under pH 6.8 (red line), pH 6.5 (purple line) and control conditions (blue line). Day 0 cell number was used as baseline for each condition. Data was expressed as mean ± SEM of triplicates of 3 patient samples. Significant differences ($p \leq 0.05$) * compared to day 0 and day 7 ■ control and ◊ pH 6.8 conditions.

4.3.8.2 Gene expression

BM-MSCs showed a significant decrease in SOX-9 expression under pH 6.8. A larger significant decrease was seen in SOX-9 expression under pH 6.5 compared to control conditions and pH 6.8 ($p<0.05$ for both). There was no change in COL2A1 expression at pH 6.8 but a significant increase ($p<0.05$) at pH 6.5 was seen compared to control conditions (Figure 4.3.39 A). At pH 6.8 no change in ACAN and VCAN expression was observed but both were significantly decreased under pH 6.5 compared to control conditions and pH 6.8 ($p<0.05$ for both) (Figure 4.3.39 B). A significant increase in CA9 expression was seen under both pH 6.8 and 6.5 ($p<0.05$) with a larger increase seen at pH 6.5 ($p<0.05$) compared to pH 6.8. There was no difference in CA12 expression with change in pH conditions (Figure 4.3.39 C).

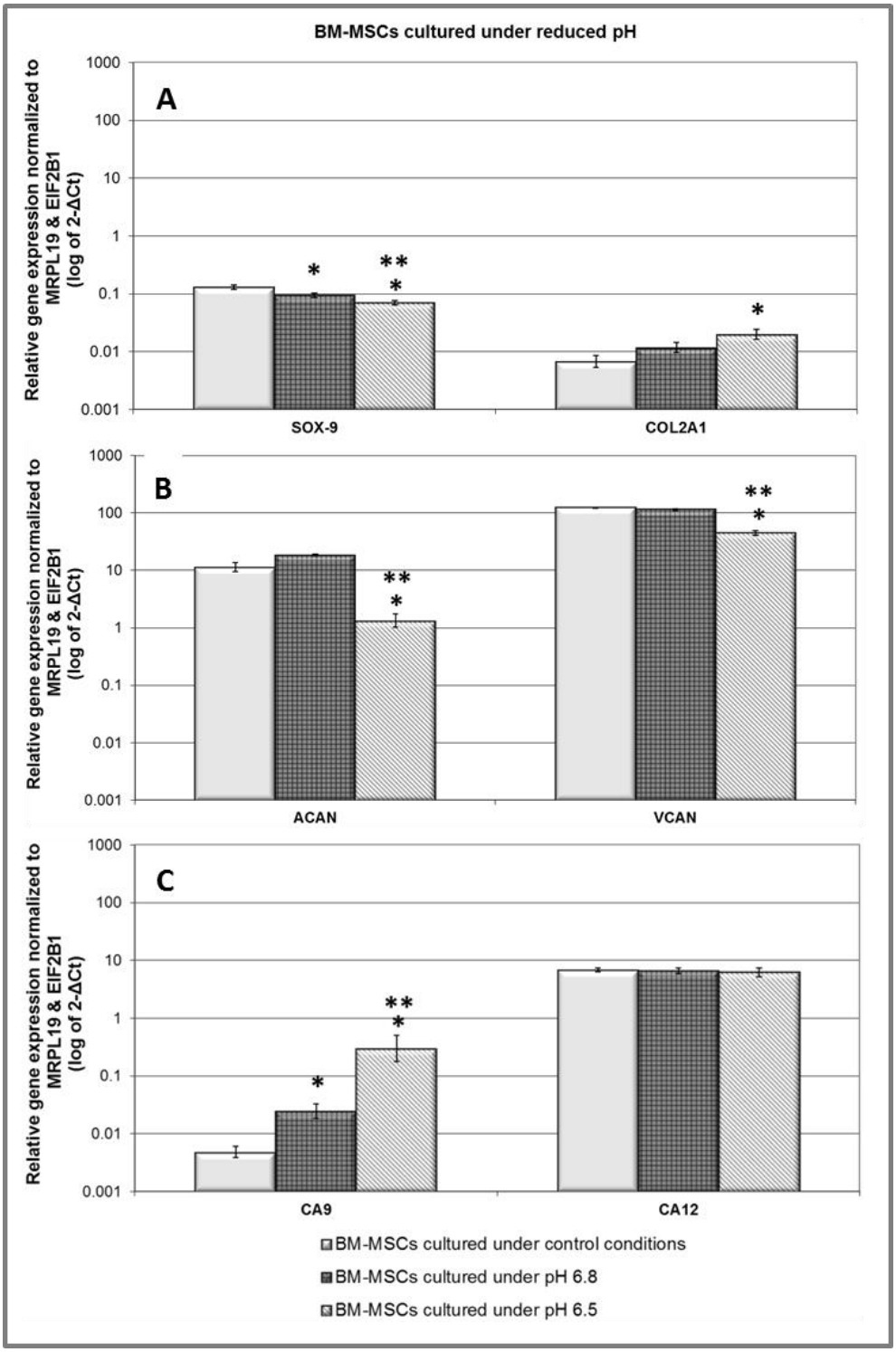

Figure 4.3.39 Relative gene expression of (**A**) SOX-9, COL2A1 (**B**) ACAN, VCAN and (**C**) CA9, CA12 in BM-MSCs cultured under reduced pH 6.8 and 6.5 (n=3). Gene expression normalized to average of HK genes MRPL19 and EIF2B1 and plotted on a log scale. * Statistical significance ($p \leq 0.05$) compared to culture under control conditions and ** culture under pH 6.8.

4.3.9 Influence of reduced pH 6.8 and hypoxia on BM-MSC behaviour

4.3.9.1 Cell viability proliferation

Live/dead staining of BM-MSCs cultured under pH 6.8 combined with hypoxia showed that majority of cells stained green (viable) as seen in control conditions. Under these conditions a change in cell morphology was observed; cells appeared more spindle shaped than cells in control conditions. As live/dead staining showed no evidence of cell death, reduced cell numbers suggest that cell proliferation may be affected under these conditions (Figure 4.3.40).

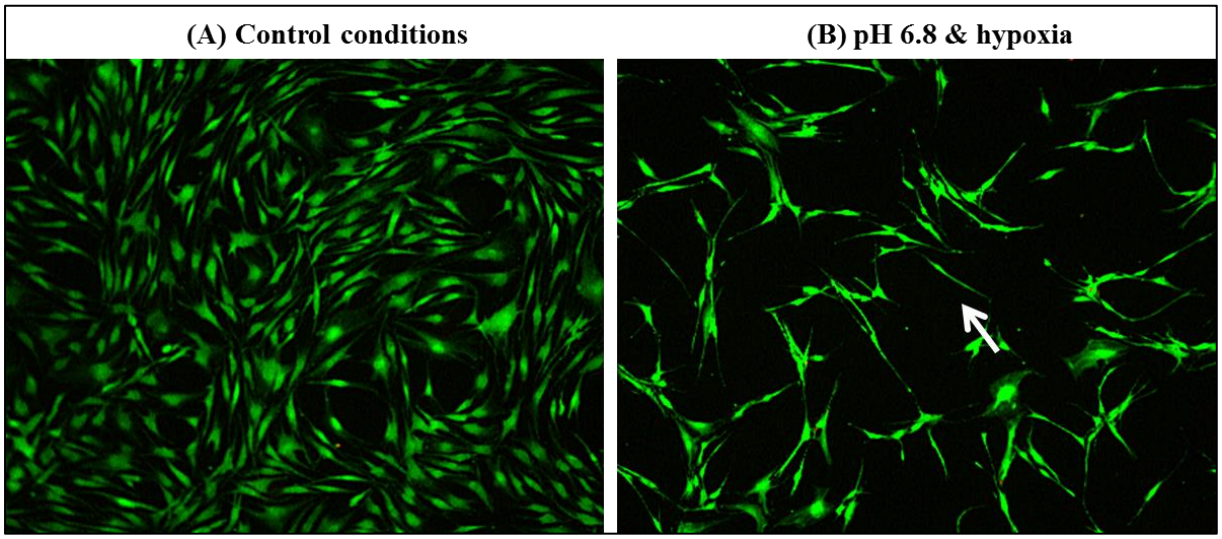

Figure 4.3.40 Effect of reduced pH 6.8 and hypoxia on BM-MSCs viability. BM-MSCs (n=3) were cultured under (A) control conditions (B) pH 6.8 and hypoxia for 7 days and labelled with live-dead stain. Representative fluorescence microscope images indicate viable (stained green) and dead (stained red) cell populations under both conditions. White arrow indicates change in cell morphology compare to control condition (magnification x100).

Proliferation analysis showed that at day 7 BM-MSCs cultured under pH 6.8 combined with hypoxia had a significant less increase in cell number compared to control conditions (30171±547 versus 47969±599, $p<0.05$) (Figure 4.3.41).

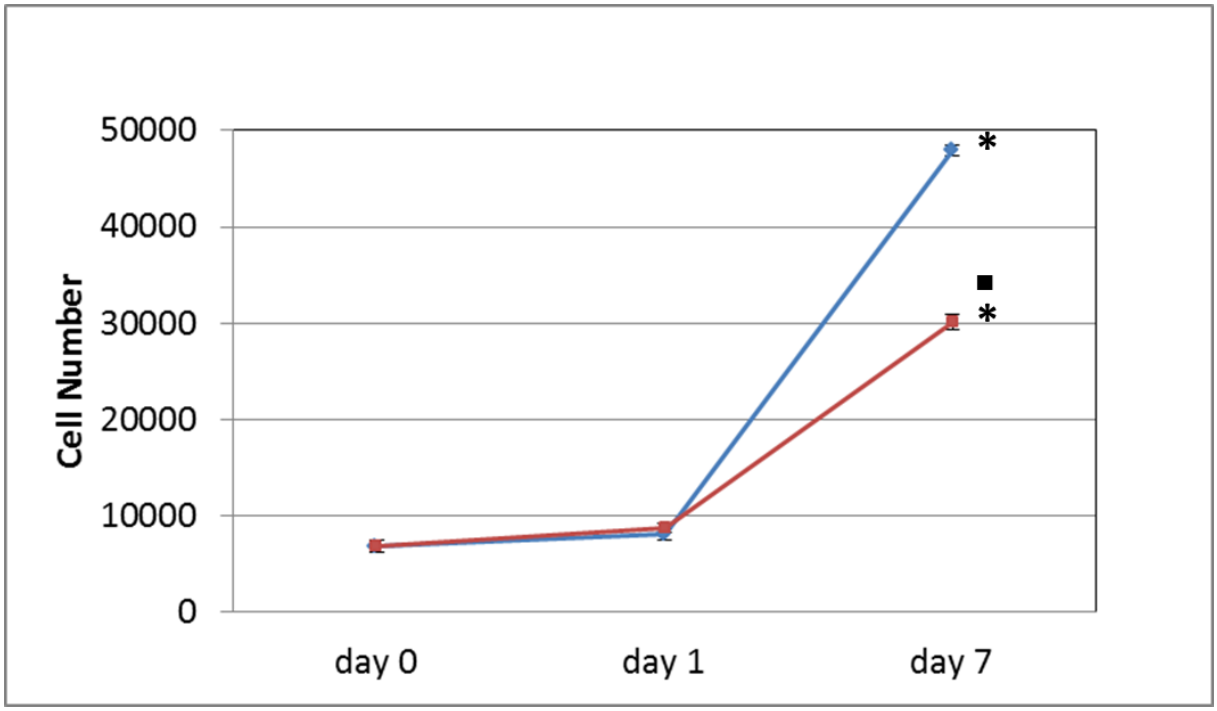

Figure 4.3.41 Effect of reduced pH 6.8 and hypoxia combination on BM-MSCs (n=3) proliferation over the course of 7 days. Total cell number was determined for BM-MSCs cultured under pH 6.8 combined with hypoxia (red line) and control conditions (blue line). Day 0 cell number was used as baseline for each condition. Data was expressed as mean ± SEM of triplicates of 3 patient samples. Significant differences ($p \leq 0.05$) * compared to day 0 and ■ day 7 control conditions.

4.3.9.2 Gene expression

BM-MSCs cultured under reduced pH 6.8 and hypoxia showed a significant decrease in SOX-9 expression ($p<0.05$) with no change in COL2A1 expression (Figure 4.3.42 A). There was no change in ACAN expression while VCAN expression was significantly up regulated ($p=0.05$) under reduced pH 6.8 and hypoxia compare to control conditions (Figure 4.3.42 B). CA9 expression was significantly increased ($p<0.05$) but CA12 showed no change compared to control conditions (Figure 4.3.42 C).

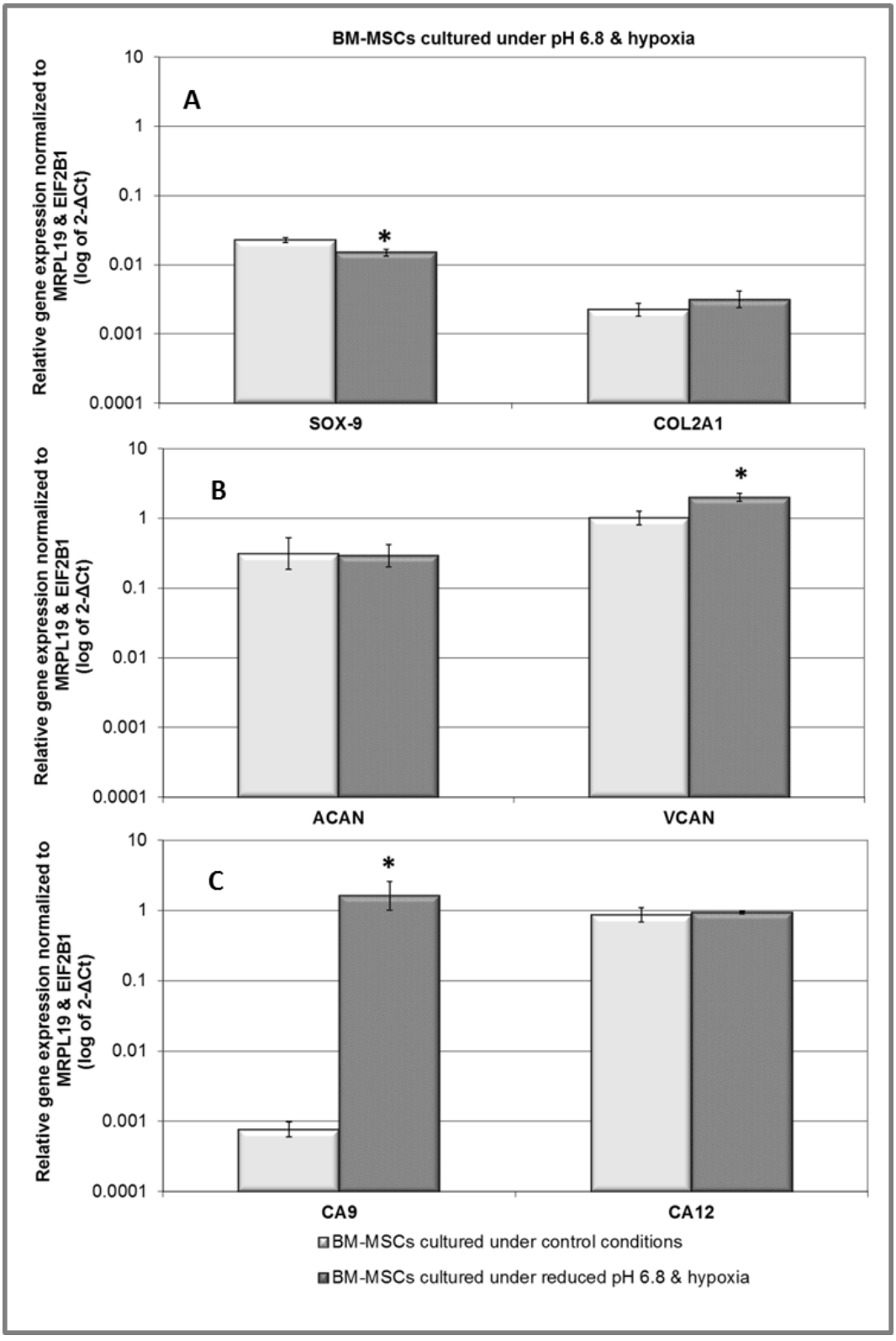

Figure 4.3.42 Relative gene expression of (**A**) SOX-9, COL2A1 (**B**) ACAN, VCAN and (**C**) CA9, CA12 in BM-MSCs cultured under reduced pH 6.8 and hypoxia (n=3). Gene expression normalized to average of HK genes MRPL19 and EIF2B1 and plotted on a log scale. * Statistical significance ($p \leq 0.05$) compared to culture under control conditions.

4.3.10 Influence of all IVD-like physio-chemical microenvironmental conditions (hypoxia, reduced serum, reduced glucose and pH 6.8) on BM-MSC behaviour

4.3.10.1 Cell viability and proliferation

Live/dead staining of BM-MSCs cultured under all IVD-like physio-chemical microenvironmental conditions showed that majority of cells stained green (viable) with few red stained (dead) cells (Figure 4.3.43). Cellular morphology was comparable to that seen under pH 6.8 and hypoxia combined conditions. Decreased cell numbers were due to reduced cell proliferation under these conditions.

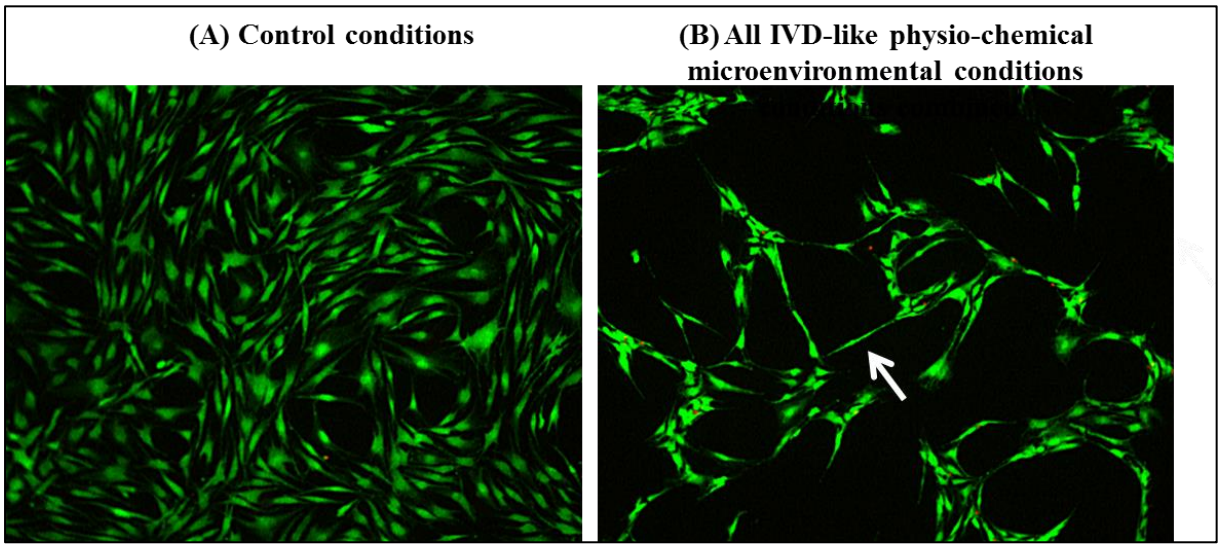

Figure 4.3.43 Effect of all IVD-like physio-chemical microenvironmental conditions on BM-MSCs viability. BM-MSCs (n=3) were cultured under control conditions (left) and all IVD-like physio-chemical microenvironmental conditions (right) for 7 days and labelled with live-dead stain. Representative fluorescence microscope images indicate viable (stained green) and dead (stained red) cell populations under both conditions. White arrow indicates change in cell morphology compare to control condition (magnification x100).

Proliferation analysis showed that at day 7 BM-MSCs cultured under all IVD-like physio-chemical microenvironmental conditions had a significantly less increase in cell number compared to control conditions (15148±590 versus 47969±599, $p< 0.05$) (Figure 4.3.44).

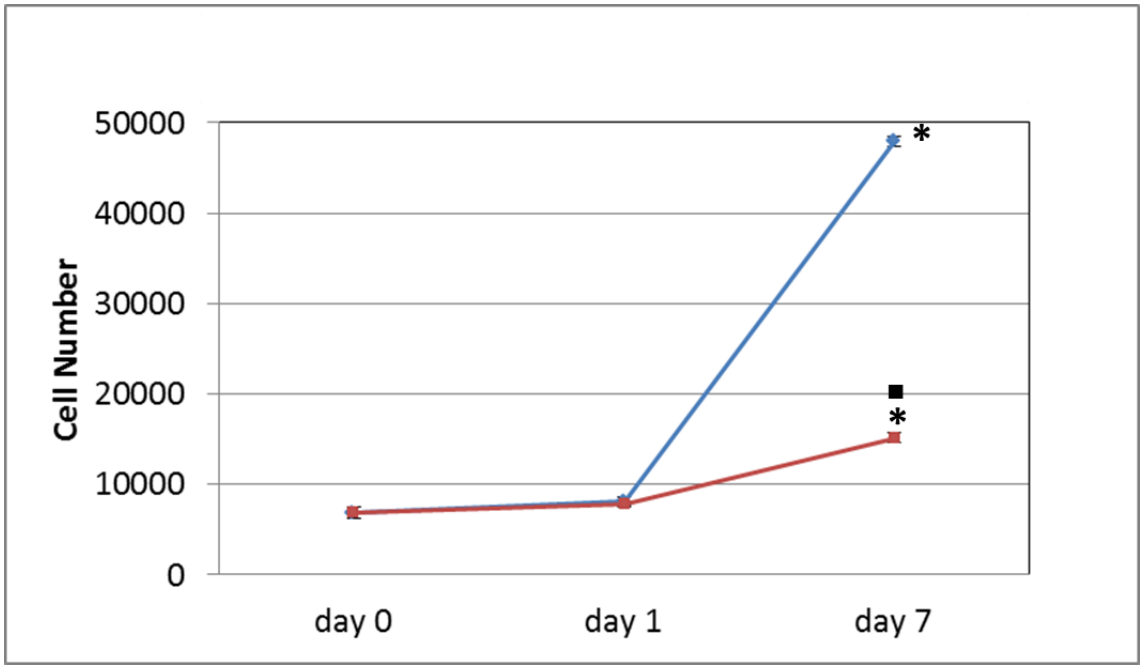

Figure 4.3.44 Effect of all IVD-like physio-chemical microenvironmental conditions on BM-MSCs (n=3) proliferation over the course of 7 days. Total cell number was determined for BM-MSCs cultured under all IVD-like physio-chemical microenvironmental conditions (red line) and control conditions (blue line). Day 0 cell numbers were used as baseline for each condition. Data was expressed as mean ± SEM of triplicates of 3 patient samples. Significant differences ($p \leq 0.05$) * compared to day 0 and ■ day 7 control conditions.

4.3.10.2 Gene expression

BM-MSCs cultured under all IVD-like physio-chemical microenvironmental conditions combined showed a significant decrease in SOX-9 expression ($p<0.05$) with no change in Col2A1 expression compared to BM-MSCs cultured under control conditions (Figure 4.3.45 A). There were no significant changes in ACAN and VCAN expression (Figure 4.3.45 B). CA9 expression was significantly increased ($p<0.05$) with no change in CA12 expression compare to control conditions (Figure 4.3.45 C).

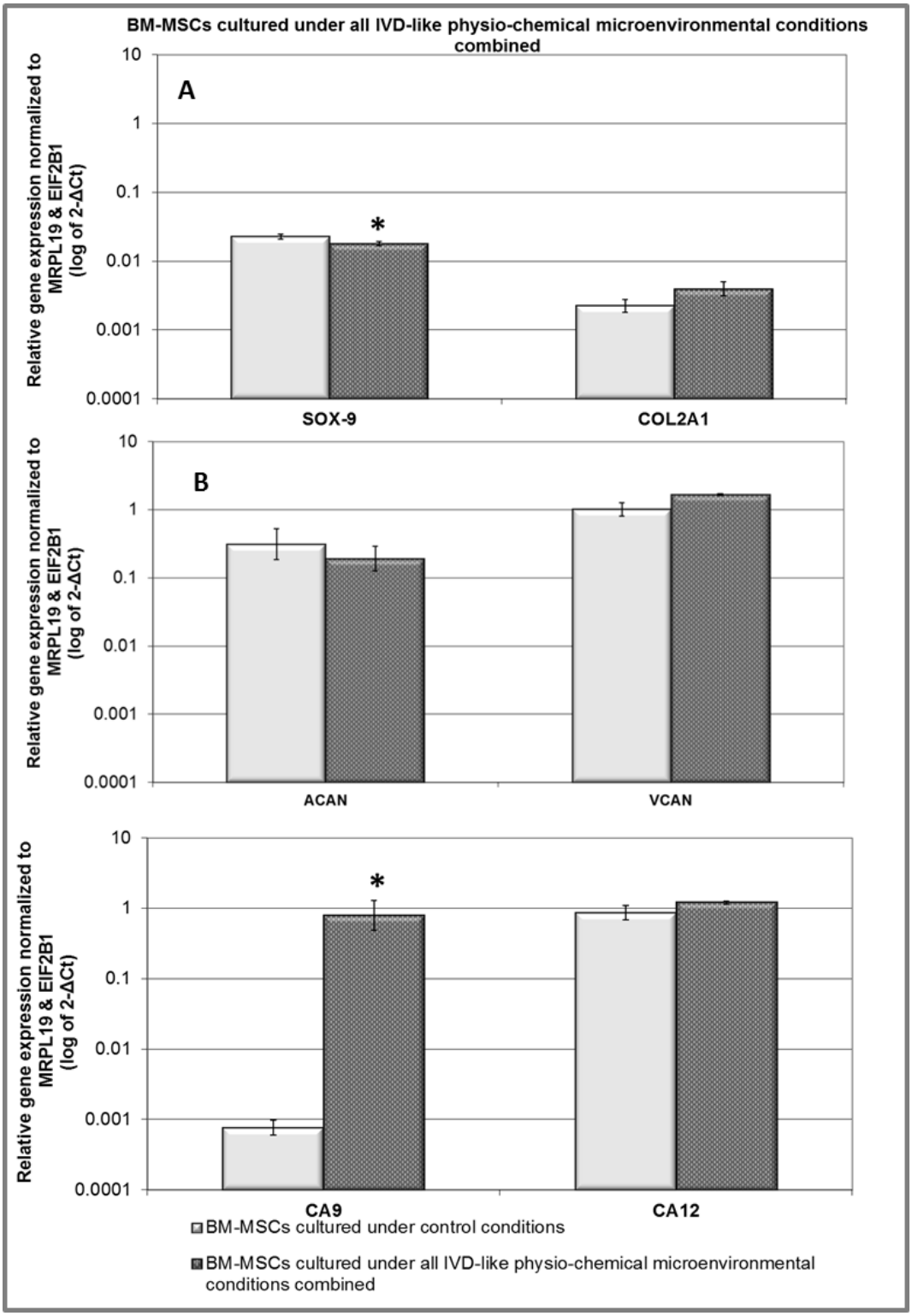

Figure 4.3.45 Relative gene expression of (**A**) SOX-9, COL2A1 (**B**) ACAN, VCAN and (**C**) CA9, CA12 in BM-MSCs cultured under all IVD-like physio-chemical microenvironmental conditions. (n=3). Gene expression normalized to average of HK genes MRPL19 and EIF2B1 and plotted on a log scale. * Statistical significance ($P \leq 0.05$) compared to culture under control conditions.

Table 4.4 Summary of changes in gene expression in BM-MSC under all test conditions compared to BM-MSC cultured under control conditions

Condition / Genes	Hyp	Nutrient limited conditions			Nutrient limited & hypoxic conditions			Acidic conditions		Acidic & hypoxic conditions	All
		RS	RG	RS+ RG	RS +H	RG +H	RS+ RG+ H	pH 6.8	pH 6.5	pH 6.8+ H	
SOX-9	↔	↔	↔	↔	↓	↑	↑	↓	↓	↓	↓
COL2A1	↔	↔	↔	↔	↔	↑	↑	↔	↑	↔	↔
ACAN	↔	↔	↔	↔	↑	↔	↔	↔	↓	↔	↔
VCAN	↑	↔	↓	↓	↑	↑	↔	↔	↓	↑	↔
CA9	−−	−−	−−	−−	−−	−−	−−	↑	↑	↑	↑
CA12	−−	−−	−−	−−	−−	−−	−−	↔	↔	↔	↔

↔ = no significant change

↑= significant increase

↓= significant decrease

−− = expression was not studied

Hyp= Hypoxia**, RS**= Reduced serum**, RG**= Reduced glucose**, RS+RG**= Reduced serum, reduced glucose**, RS+H**= Reduced serum & hypoxia, **RG+ H**= Reduced glucose & hypoxia**, RS+RG+H**= Reduced serum, reduced glucose & hypoxia**, pH 6.8 + H**= pH 6.8 & hypoxia**, All** = All IVD-like physio-chemical microenvironmental conditions combined.

Table 4.5 Summary of changes in ECM protein expression in BM-MSC under all test conditions compared to BM-MSC cultured under control conditions

Condition / Genes	Hyp	Nutrient limited conditions			Nutrient limited & hypoxic conditions			Acidic conditions		Acidic & hypoxic conditions
		RS	RG	RS+ RG	RS +H	RG +H	RS+ RG+ H	pH 6.8	pH 6.5	pH 6.8+ H
Aggrecan staining intensity	↑	↔	↑	↔	↓	↑	↓	––	––	––
Versican staining intensity	↑	↔	↔	↓	↔	↑	↔	––	––	––

↔ = no change

↑= increase

↓= decrease

–– = expression was not studied

Hyp= Hypoxia**, RS**= Reduced serum**, RG**= Reduced glucose**, RS+RG**= Reduced serum, reduced glucose**, RS+H**= Reduced serum & hypoxia, **RG+ H**= Reduced glucose & hypoxia**, RS+RG+H**= Reduced serum, reduced glucose & hypoxia**, pH 6.8 + H**= pH 6.8 & hypoxia**, All** = All IVD-like physio-chemical microenvironmental conditions combined.

.

Table 4.6 Summary of changes in BM-MSC number under all test conditions at day 7 compared to BM-MSC cultured under control conditions

Condition		Day-7 cell number	Significant difference compared to control at day 7 ($p \leq 0.05$)
Control Conditions (Day-0 cell number = 4484±63)		8299±882	N/A
Hypoxia		9718±1064	No
Nutrient limited conditions	Reduced serum	2314±347	Yes
	Reduced glucose	5769±605	Yes
	Reduced serum & reduced glucose	3228±538	Yes [(1)]
Nutrient limited & hypoxic conditions	Reduced serum & hypoxia	4750±334	Yes [(2)]
	Reduced glucose & hypoxia	10167±433	No [(3)]
	Reduced serum, reduced glucose & hypoxia	7466±635	No [(4)]
Control for pH conditions (Day-0 cell number =6874±573)		47969±599	N/A
pH 6.8		23889±450	Yes
pH 6.5		7522±385	Yes
pH 6.8 & hypoxia		30171±547	Yes [(5)]
All		15148±590	Yes

[(1)] Total cell number in reduced serum and reduced glucose combined was significantly reduced compared to reduced glucose alone, but demonstrated no significant difference compared to reduced serum alone.

[(2)] Total cell number in reduced serum and hypoxia combined was significantly higher compared to reduced serum alone but significantly low compared to hypoxia.

[(3)] Total cell number in reduced glucose and hypoxia combined condition was significantly higher compared to reduced glucose alone with no difference compared to hypoxia.

[(4)] Total cell number in reduced serum, reduced glucose and hypoxia combined condition was significantly higher compared to reduced serum and reduced glucose combined with no difference compared to hypoxia.

[5)] Total cell number in reduced pH 6.8 and hypoxia combined was significantly higher compared to reduced pH 6.8 alone. Comparison of pH 6.8 and hypoxia with hypoxia alone was not performed due to difference in samples and cell numbers used to conduct these experiments.

4.4 Discussion

MSCs have gained widespread attention for stem cell based IVD repair and regeneration therapies. However, the harsh microenvironmental conditions of the IVD may pose a significant challenge for implantation strategies. The hostile IVD microenvironment may have detrimental effects on implanted MSCs and thus maintaining the viability and functioning of MSCs after implantation in the harsh microenvironment of the degenerated disc is significantly important for regeneration purposes.

A limited number of studies have investigated the influences of IVD-like microenvironmental conditions on rat BM-MSCs and human AD-MSCs behaviour (i.e. viability, proliferation and biosynthesis of IVD matrix constituents) (Wuertz et al., 2008, Wuertz et al., 2009a, Liang et al., 2012a, Li et al., 2012). These studies showed a significant effect of IVD-like microenvironmental conditions on the behaviour of rat BM-MSCs and human AD-MSCs. However, knowledge of human BM-MSCs behaviour in IVD-like microenvironment remains largely unknown. Therefore, the goal of this study was to evaluate the behaviour of human BM-MSCs under culture conditions mimicking specific aspects of the *in vivo* physio-chemical microenvironment.

In this study human BM-MSCs were cultured in a monolayer culture system which has been utilized by many investigators (Wuertz et al., 2008, Wuertz et al., 2009a, Li et al., 2012, Liang et al., 2012a) under 2% $O_{2,}$ (Holm et al., 1981, Bartels et al., 1998), 2% FCS (chapter 3, section 3.4), 5mM glucose (Wuertz et al., 2008, Liang et al., 2012a) and pH 6.8/6.5 (Diamant et al., 1968, Wuertz et al., 2009a, Li et al., 2012) to represent the IVD hypoxic, limited nutritional and acidic microenvironment. As suggested in previous investigations (Wuertz et al., 2008, Wuertz et al., 2009a, Li et al., 2012, Liang et al., 2012a) cell survival, proliferation and gene and protein results were interpreted as general behaviour rather than specific phenotypic change.

4.4.1 The effect of IVD-like physio-chemical microenvironmental conditions on human BM-MSC viability

The potential of cell based IVD regeneration can be greatly hampered by the excessive death of administered cells in the harsh microenvironment. It can be hypothesized that if more cells survive after transplantation, there would be more cells to differentiate and restore tissue function. In this study it was found that IVD-like physio-chemical microenvironmental conditions alone or in different combinations were not detrimental to human BM-MSC

survival. Various previous independent investigations indicate that MSCs can survive under hypoxia (Fehrer et al., 2007) and nutrient deprived conditions i.e. reduced serum (Deorosan and Nauman, 2011), reduced glucose (Stolzing et al., 2006, Wuertz et al., 2008, Deorosan and Nauman, 2011, Liang et al., 2012a) and reduced serum combined with reduced glucose conditions (Deorosan and Nauman, 2011). However, a few previous reports suggest that pH 6.8, 6.5 and combination of different microenvironmental conditions may be critical for MSC viability. Significant cell death in rat BM-MSCs and human AD-MSCs cultures was observed under these conditions (Wuertz et al., 2008, Wuertz et al., 2009a, Li et al., 2012, Liang et al., 2012a). In contrast to those reports, in this study, pH 6.8, 6.5 and all conditions combined did not have a detrimental effect on human BM-MSC viability. Differences in cell survival in this study from those of Wuertz *et al* and Liang *et al* may be due to differences in MSCs species/source (human versus rat or BM versus adipose) or differences in combination of microenvironmental conditions (reduced serum, reduced glucose, hypoxia and pH 6.8 versus reduced glucose, reduced pH and hyper-osmolarity). Future studies are required to combine IVD-like osmolarity with all factors studied here to examine human BM-MSC survival. However, these results together with previous investigations suggest that human BM-MSCs may have better potential to survive in IVD-like hypoxic, nutrient limited and acidic conditions.

4.4.2 The effect of IVD-like physio-chemical microenvironmental conditions on human BM-MSC proliferation

This study showed that IVD-like physio-chemical microenvironmental conditions influence human BM-MSC proliferation. Hypoxia appeared to have no effect on proliferation. There are conflicting reports regarding proliferation of MSCs under hypoxia, with some studies reporting increases, and others showing decreases or no change (Grayson et al., 2007, Lee et al., 2009a, Nekanti et al., 2010, Valorani et al., 2012, Dos Santos et al., 2010, McCanless et al., 2011). Differences are mostly attributed to different sources and different species of MSCs and even differences in O_2 concentration.

It was found that nutrient deprived conditions (i.e. reduced serum or/and reduced glucose) decreased human BM-MSC proliferation. Deorosan and colleagues showed reduced proliferation of rat BM-MSCs under reduced serum (Deorosan and Nauman, 2011). Such results suggest that reduced serum may have a similar effect on the proliferation of MSCs isolated from different species. It was found here that reduced glucose decreased human BM-MSCs proliferation. These findings differ from previous studies where reduced glucose

maintained or increase proliferation of rat BM-MSCs and human AD-MSCs (Wuertz et al., 2008, Lo et al., 2011, Liang et al., 2012a). Again these differences may be attributed to different sources of MSCs.

Interestingly it was found that hypoxia prevented the negative influences of reduced glucose alone and reduced serum and reduced glucose combination on human BM-MSC proliferation. Although hypoxia in combination with reduced serum alone also increased proliferation it still remained significantly lower than the control suggesting that regardless of normoxia or hypoxia, reduced serum inhibits BM-MSCs proliferation. However, overall these results imply that in an *in vivo* hypoxic and both serum and glucose reduced microenvironment, hypoxia may be a protective factor to counteract the negative impact of limited nutritional conditions on proliferation of implanted BM-MSCs.

Adding to previous reports using rat BM-MSCs and human AD-MSCs (Wuertz et al., 2009a, Chen et al., 2009b, Li et al., 2012) this study demonstrated that decreasing pH also negatively influences human BM-MSCs proliferation. It can be hypothesized that in response to the severe acidic conditions (pH 6.5) cells may arrest into a pH dependent G1 phase of cell cycle (Taylor and Hodson, 1984, Musgrove et al., 1987) resulting in diminished or no proliferation. Under decreasing pH conditions, cell viability images displayed changes in cell morphology; from cells with a large cytoskeleton under control conditions to spindle shape cells with a shrunken cytoskeleton under reduced pH conditions as reported previously for rat BM-MSCs (Wuertz et al., 2009a). These changes in cytoskeleton may be due to changes in cell adhesion molecules (e.g. intercellular adhesion molecule-1 and vascular adhesion molecule-1) under reduced pHs as proposed previously for rat BM-MSCs (Wuertz et al., 2009a). Interestingly proliferation of human BM-MSCs also increased when pH 6.8 was combined with hypoxia indicating that similar to nutrient deprived conditions, hypoxia tends to protect human BM-MSC proliferation under acidic conditions. However, for conclusive results, comparison with hypoxia alone is important. Unfortunately, this could not be performed in this study due to different samples and cell numbers used to conduct hypoxia alone and pH 6.8 combined with hypoxia culture experiments.

It was found that all IVD-like physio-chemical microenvironmental combined conditions decreased human BM-MSC proliferation. Previous reports showed decreased proliferation of rat BM-MSCs and human AD-MSCs in a slightly different combination of microenvironmental conditions (i.e. reduce glucose, reduced pH and hyper-osmolarity)

(Wuertz et al., 2008, Liang et al., 2012a). This study together with previous reports suggests that the combination of different IVD-like microenvironmental conditions may also decrease human BM-MSC proliferation in a similar fashion.

Importantly, results of proliferation analysis showed that human BM-MSC number under any of the conditions tested did not decrease below the initial seeding density during the enitre culture period (especially at day 1). This supports cell viability results and suggests that the fewer cells observed under some microenvironment conditions during cell viability analysis may have been due to reduced proliferation. Overall these findings imply that *in vivo*, limited nutrients and acidic pH may decrease human BM-MSCs proliferation. However, interestingly under these harsh conditions, hypoxia may modulate proliferation indicating that hypoxia may be a protective factor. Improved proliferation under hypoxic conditions may be attributed to increased expression of genes encoding growth factors such as vascular endothelial growth factor (VEGF) and PDGF involved in MSC proliferation (Ohnishi et al., 2007, Rodrigues et al., 2010). An O_2 concentration of around 1%-7% is an integral component of the human BM-MSCs native BM microenvironment (Harrison et al., 2002, Mohyeldin et al., 2010). It is thus inferred that human BM-MSCs may inherently adapt to survive and proliferate in a hypoxic environment.

The significance of maintaining cellular proliferation after transplantation *in vivo* needs further investigation. It is possible that increased proliferation may provide sufficient cells to restore a functional extracellular matrix. With slow proliferating cells it can be hypothesised that transplantation of higher cell numbers may help to regenerate the tissue, although this would impact on nutritional requirements. It is important to consider the increased metabolic demands of larger numbers of transplanted cells, which may be detrimental in the existing harsh microenvironment. The optimal number of transplanted cells to achieve IVD regeneration is still the topic of investigation (Serigano et al., 2010, McCanless et al., 2011).

4.4.3 The effect of IVD-like physio-chemical microenvironmental conditions on human BM-MSC gene and protein biosynthesis

Investigation of influences of IVD-like physio-chemical microenvironmental condition on IVD matrix gene and protein biosynthesis is an important aspect of human BM-MSC based tissue repair. Previous investigations have shown expression of IVD matrix gene/proteins (i.e. COL1, II and ACAN) in rat BM-MSCs and human AD-MSCs under standard culture

condition without the addition of growth factors (Wuertz et al., 2008, Wuertz et al., 2009a, Li et al., 2012, Liang et al., 2012a). In this study, human BM-MSCs also demonstrated expression of COL2A1, SOX-9, ACAN, VCAN genes and aggrecan and versican protein under standard conditions without addition of growth factors. Thus, this study aimed to investigate the effect of IVD-like physio-chemical microenvironmental conditions on expression of these matrix constituents in human BM-MSCs. Influences in gene and protein expression were used as indicators of general biosynthesis as previously detailed instead of any phenotypic change (Wuertz et al., 2008, Wuertz et al., 2009a, Liang et al., 2012a, Li et al., 2012).

Results of this investigation demonstrated that hypoxia appeared to have limited influence on COL2A1, SOX-9 and ACAN gene expression but promoted VCAN gene expression and both aggrecan and versican protein synthesis. These findings suggest that *in vivo* hypoxia may maintain or increase expression of matrix genes and improve protein biosynthesis by human BM-MSCs. The beneficial effects of hypoxia on chondrogenic and discogenic differentiation of MSCs have been the subject of many studies (Felka et al., 2009, Stoyanov et al., 2011, McCanless et al., 2011, Duval et al., 2012). However, in the majority of these studies hypoxia was used along with either 3D culture and/or growth factors.

To the best of the candidate, no study has examined the effect of reduced serum alone or combined with reduced glucose on expression of ECM constituents in human BM-MSCs. This study has found that nutrient deprived conditions appeared to have minor effects on the expression of IVD matrix gene and protein expression in human BM-MSCs. Two studies have previously investigated the effect of reduced glucose on ACAN gene and protein biosynthesis in rat BM-MSCs and human AD-MSCs (Wuertz et al., 2008, Liang et al., 2012a). Here, reduced glucose increased aggrecan expression in human BM-MSCs. This finding adds to previous suggestions that reduced glucose, similar to rat BM-MSCs and human AD-MSCs (Wuertz et al., 2008, Liang et al., 2012a) may also promote aggrecan synthesis in human BM-MSCs. This study showed that reduced serum and reduced glucose combined conditions did not influence COL2A1, SOX-9 and ACAN gene and protein expression but inhibited VCAN gene and protein synthesis. Overall these results imply that *in vivo* complete nutrient deprived conditions may have limited effect on biosynthesis of most matrix components but these conditions clearly impair VCAN gene and protein synthesis in human BM-MSCs.

Noticeably it was found that the combination of hypoxia with nutrient deprived conditions increased synthesis of IVD matrix components in human BM-MSCs. Hypoxia combined with reduced serum promoted ACAN and VCAN gene expression. However, a reduced aggrecan immunopositivity showed that this combination may decrease aggrecan protein expression. Importantly, the combination of hypoxia and reduced glucose demonstrated an increase in most genes and protein biosynthesis. Increased aggrecan and versican immunopositivity suggests that these conditions may positively influence human BM-MSC matrix synthesis activity. Additionally reduced serum, reduced glucose and hypoxic conditions combined appeared to positively influence COL2A1 and SOX-9 with no detrimental effect on VCAN gene and protein expression. Although ACAN gene expression was unaffected, these conditions appeared to decrease aggrecan synthesis. Interestingly these results indicate that hypoxia which itself increased VCAN gene and protein expression also increased or restored VCAN gene and protein expression in nutrient deprived conditions. This finding indicates that hypoxia in addition to improving proliferation, may also play a direct role in influencing VCAN gene and protein biosynthesis under nutrient deprived condition. The hypoxia responsive element present in VCAN gene (Asplund et al., 2010) may be responsible for these changes. In contrast to versican, aggrecan expression was both increased and decreased under different reduced nutrient and hypoxic combinations. As hypoxia increased aggrecan expression these changes suggest that aggrecan synthesis may be sensitive to reduction of different nutrients under hypoxia.

Acidic pH conditions (pH 6.8 & 6.5) are reported to be critical for matrix biosynthesis in rat BM-MSCs and human AD-MSCs (Wuertz et al., 2008, Wuertz et al., 2009a, Li et al., 2012, Liang et al., 2012a). This study, in contrast to previous reports indicates that pH 6.8 appears to have minor effects on IVD matrix biosynthesis activity in human BM-MSCs but pH 6.5 is detrimental. Previously it was shown that pH 6.8 and 6.5 affected COL1, COL II and ACAN gene and protein expression in rat BM-MSCs and human AD-MSCs (Wuertz et al., 2008, Wuertz et al., 2009a, Li et al., 2012, Liang et al., 2012a). Here, human BM-MSCs showed overall maintained gene expression under pH 6.8. However further decrease in pH to severe acidic levels (pH 6.5) appeared detrimental for matrix gene expression. These findings imply that moderate acidic conditions may not be detrimental for expression of IVD matrix genes in human BM-MSCs but severe acidic conditions clearly seem to decrease their expression. However it is important to confirm these responses at protein level. Increased expression of CA9 suggests that human BM-MSCs have the ability to regulate CA9 according to severity

of acidic environment to regulate intracellular pH. No change in CA12 expression may suggest minor effect of acidic pH on expression of this gene in human BM-MSCs.

The combination of acidic pH and hypoxia was not detrimental to human BM-MSCs gene expression biosynthesis. Interestingly VCAN expression was increased under pH 6.8 combined with hypoxia. This suggests that similar to nutrient deprived conditions, hypoxia continues to influence VCAN gene expression even under moderate acidic conditions. In contrast to CA12, increased expression of CA9 under acidic hypoxic environment suggests that its expression may be regulated by acidic hypoxic conditions. Again aggrecan and versican protein expression was not studied under this combination which requires further investigation.

Finally this study found that a combination of hypoxic, nutrient deprived and moderate acidic conditions (pH 6.8) may not impair matrix biosynthesis activity in human BM-MSCs. Previously it was demonstrated that a combination of reduced glucose, pH 6.8 and hyper-osmolarity induced deleterious effects on expression of COL I and ACAN genes in rat BM-MSCs and genes and proteins in human AD-MSCs (Wuertz et al., 2008, Liang et al., 2012a). In those reports it was shown that reduced glucose alone increased, whereas pH 6.8 or hyper-osmolarity, decreased gene and protein expression. They suggested that when the three conditions were combined, pH (6.8) and hyper-osmolarity appeared to dominate the positive effect of reduced glucose and were considered critical factors for biosynthesis of IVD matrix. In contrast this study found no prominent deleterious effects on IVD matrix gene synthesis when all physio-chemical microenvironmental conditions (hypoxia, reduced serum/glucose and pH 6.8) were studied alone or in combinations. Unfortunately it was not possible to examine effects of these conditions on matrix protein synthesis when all conditions were combined. However, these results overall suggest that IVD-like physio-chemical microenvironment may not be detrimental to IVD main matrix gene expression in human BM-MSCs. However, it is important to mention that in common with previous investigations, although this study investigated reduced glucose and pH 6.8, it did not include IVD-like osmolarity. Therefore future studies are encouraged to combined IVD-like osmolarity with other conditions and explore its effect on human BM-MSC behaviour.

4.5 Conclusion

In conclusion to the best of the candidate knowledge, this is the first study to investigate the effect of IVD-like physio-chemical microenvironment conditions (hypoxia, reduced serum, reduced glucose, moderate (6.8) and severe (6.5) pH) on cell viability, proliferation and synthesis of IVD matrix constituents in human BM-MSCs. Importantly this study found that no IVD-like physio-chemical microenvironmental condition alone or in different combinations impaired BM-MSCs survival. Nutrient deprived (i.e. reduced serum or/and reduced glucose), moderate and severe acidic conditions decreased human BM-MSCs proliferation. Hypoxia maintained cell proliferation and appeared to induce protective influences on affected proliferation under harsh nutritional and moderate acidic conditions. A hypoxic microenvironment promoted aggrecan and versican biosynthesis in human BM-MSCs. Nutrient deprived conditions had a minor effect on the levels of most matrix gene and protein expression but these conditions impaired VCAN gene and protein synthesis in human BM-MSCs which was increased or restored with hypoxic combination. This finding indicates that hypoxia in addition to improving proliferation, may also play a direct role in influencing VCAN gene and protein biosynthesis under nutrient deprived conditions. It was identified that hypoxia combined with reduced glucose most prominently increased expression of all matrix constituents at gene and noticeably at protein level. These results imply that *in vivo* a reduced glucose and hypoxic microenvironment may elicit a prominent positive effect on implanted human BM-MSCs. Increasingly severe acidic conditions inhibited proliferation and matrix gene expression of human BM-MSCs adding to previous suggestions that extreme acidic conditions in degenerated discs may hamper the regenerative potential of MSCs (Wuertz et al., 2009a, Li et al., 2012). Similar to nutrient deprived conditions, hypoxia also increased VCAN gene expression under moderate acidic conditions. Importantly all IVD-like physio-chemical conditions combined closely reflecting *in vivo* hypoxic, limited nutritional and moderate acidic conditions showed no detrimental effects on human BM-MSCs matrix gene expression, strengthening the argument for the proposed efficacy of clinical application of human BM-MSC in treatment of IVD degeneration. Additionally based on the results observed for moderate and severe acidic conditions it can be suggested that human BM-MSC implantation for disc regeneration may be successful at early stages of degeneration where pH levels are 6.8 or above. The results of this study highlight the importance of studying the behaviour of cells under conditions predicted *in vivo* to ensure proper functioning of cells following implantation.

5 Chapter 5 Impact of an intervertebral disc-like physio-chemical microenvironment on co-culture of human bone marrow derived mesenchymal stem cells with degenerate nucleus pulposus cells: Implication for disc regeneration

5.1 Introduction

Cell based tissue engineering and regenerative medicine aims to provide patients with minimally invasive treatments that repair or replace dysfunctional musculoskeletal tissue. The objective of tissue engineering approaches for IVD repair is to re-establish the tissue architecture and function to that of the original NP matrix. Numerous *in vitro* and *in vivo* studies suggest that MSC implantation has the potential to repair degenerated disc tissue (Risbud et al., 2004a, Steck et al., 2005, Sakai et al., 2006). Different investigators are trying to understand how this repair is achieved.

It has been shown that MSCs contribute to tissue repair and regeneration by differentiating into the cell phenotype of the host tissue. However, it is also becoming evident that MSCs do more than just respond to different stimuli and differentiate (Caplan and Dennis, 2006). For instance, sometimes MSCs express no or low differentiation capabilities but there is often a measurable therapeutic effect (Li et al., 2005b, Tang et al., 2005, Wu et al., 2012). It is the trophic effect of MSCs that may likely be the primary cause of the observed positive therapeutic effects. Based on MSC dual functionality for damage tissue repair, studies are needed to understand their proper contribution in disc repair which may be due to either (1) discogenic differentiation of MSCs triggered by signals from NP cells or (2) modulated activity of degenerated NP cells stimulated by MSCs or (3) a combined effect.

The *in vitro* co-culture model system of MSCs and NP cells could serve to elucidate the mechanisms of disc repair (Richardson et al., 2006, Vadala et al., 2008b, Strassburg et al., 2010). To date a number of different *in vitro* co-culture systems of MSCs with disc explants or isolated cells have been utilized. 3D direct co-cultures of MSCs and NP cells demonstrates beneficial effects on matrix production but this system does not indicate that increased matrix production is either due to differentiation of MSCs toward NP-like cells or due to a stimulatory effect exerted by MSCs on the NP cells (Vadala et al., 2008b, Vadala et al., 2008a, Sobajima et al., 2008, Chen et al., 2009a, Svanvik et al., 2010).

For mechanistic studies, distinct quantitative analysis of MSCs and NP cells after co-culture is particularly important that principally depends on the successful separation of cells following co-culture. Vadala *et al* performed 3D direct co-culture of MSCs and NP cells specifically to investigate the mechanism of repair (Vadala et al., 2008b). Adenoviral transduction of MSCs and NP cells with vectors encoding the red (RFP) and green (GFP) fluorescent proteins respectively and fluorescent activated cell sorting (FACS) allowed separation and quantitative analysis of changes in the gene expression profile of MSC and NP cells after co-culture. Co-culturing was found to have a dominate effect on the differentiation of MSCs with only a partial trophic effect of MSCs on NP cells. It was suggested that MSC differentiation may be more responsible for increased matrix production during repair process.

Mechanistic studies have also been increasingly performed in monolayer and 3D configurations using a semi-permeable membrane to keep MSCs and NP cells/tissue separated (Li et al., 2005a). Two approaches have been used; conventional indirect co-culture in which one cell type is cultured on top of the insert membrane and the other on the culture plate (Li et al., 2005a, Lu et al., 2007, Yang et al., 2008) and novel direct co-culture in which one cell type is cultured on top of the insert membrane with the other cell type on the reverse side of the insert (Yamamoto et al., 2004, Watanabe et al., 2010). Using the conventional indirect co-culture system an increase in NP cell proliferation and gene expression (Yang et al., 2008, Umeda et al., 2009) and MSC differentiation (Li et al., 2005a, Lu et al., 2007, Yang et al., 2008) has been shown. Yamamoto *et al* and Watanabe *et al*, in addition, to conventional indirect co-culture system, also used the novel direct co-culture system of MSCs and NP cells separated by a membrane insert (Yamamoto et al., 2004, Watanabe et al., 2010). Scanning electron microscopy showed that in the novel direct co-culture group, MSCs and NP cells were in direct cell to cell contact through cytoplasmic processes passing through 0.4μm pores in the membrane. NP cells were isolated from both direct and indirect co-culture groups to assess proliferation. NP cells showed increased proliferation after being isolated from direct co-culture groups. PG synthesis was also determined in both co-cultures groups but without cell separation. Increase PG synthesis was seen in direct co-culture group compared to indirect co-culture group. Although both authors suggest that MSCs were stimulating NP cells matrix production in direct co-culture system, one fundamental flaw in these studies was that cells were not separated after direct co-culture for this analysis.

Therefore contribution of both cells towards observed positive effects was arguable in these studies.

Richardson *et al* and Strassburg *et al* performed direct co-culture of MSCs and NP cells with the aim of clearly separating and understanding phenotypic changes in each cell type (Richardson et al., 2006, Strassburg et al., 2010). They used a model monolayer co-culture system incorporating fluorescent labelling of cells and high speed cell sorting approaches to distinctly separate and examine cells after direct co-culture (Richardson et al., 2006, Strassburg et al., 2010). They showed that direct co-culture of MSCs and NP cells induces MSC discogenic differentiation (Richardson et al., 2006, Strassburg et al., 2010). Interestingly co-culture of MSCs and degenerate NP cells not only induced MSC discogenic differentiation but also increased expression of matrix associated genes in degenerate cells to the similar levels seen in non-degenerate NP cells (Strassburg et al., 2010). MSC differentiation along with modulation of degenerate NP cells in co-culture reinforced the idea that MSC not only differentiate in response to certain stimuli but also provide stimuli (trophic effects) to neighbouring cells to influence regeneration (Caplan and Dennis, 2006, Strassburg et al., 2010).

Findings from such studies imply that MSCs when implanted, may contribute to tissue repair and regeneration both by discogenic differentiation and through trophic effects on native NP cells, thereby influencing self-repair. It has been proposed that cellular communication mediated by growth factors, cytokines and/or membranous components between MSCs and degenerate NP cells may regulate MSC differentiation and stimulation of degenerate NP cells (Yamamoto et al., 2004, Yang et al., 2008, Strassburg et al., 2012).

To date the majority of MSC and NP cell co-culture model studies have been performed under standard culture conditions. Data presented in chapters 3 and 4 of this thesis, together with previous investigations, recognise that the harsh IVD microenvironment has a strong impact on both MSC behaviour and NP cell phenotype (Risbud et al., 2004a, Bibby and Urban, 2004, Wuertz et al., 2008, Mwale et al., 2011, Neidlinger-Wilke et al., 2012, Liang et al., 2012a). Based on these findings, it is assumed that IVD-like microenvironmental conditions may also affect co-culture influences in both MSC and degenerate NP cells.

In addition to mimicking the cellular conditions, co-culture systems can be modified to incorporate the effects of non-cellular conditions (e.g., disc harsh nutritional, hypoxic and acidic conditions). To date, only two research groups have incorporated disc microenvironmental conditions in their co-culture model systems. Kim *et al* were the first to incorporate IVD-like mechanical stimulation in their study to investigate its potential effect on MSC differentiation during 3D conventional indirect co-culture with NP cells. They reported that mechanical stimulation enhances MSC differentiation into NP like phenotype during co-culture (Kim et al., 2009a). Recently Tao *et al* conducted a direct co-culture of rat NP cells and MSCs in monolayer under different osmolarity conditions (400mOsm – defined in their paper as hyper-osmolarity compared to 280mOsm in control conditions). Although, they did not separate cells after co-culture, it was reported that hyper-osmolarity decreased proliferation, SOX-9, ACAN and COL2A1 gene and protein synthesis in co-cultured cells (Tao et al., 2013). These studies indicate that the disc microenvironment conditions can also influence cells in co-culture.

It is important to investigate MSC and NP cell co-culture responses under all the possible physical and chemical conditions akin to the *in vivo* IVD microenvironment. This will increase our understanding about the impact of disc microenvironmental conditions on MSC discogenic differentiation and modulation of degenerate NP cell phenotype.

5.1.1 Aims

This study aimed to incorporate IVD-like physio-chemical microenvironmental conditions characterized by hypoxia (2% O_2), reduced serum (2%FCS), reduced glucose (5mM) and acidic (moderate (6.8 and severe (6.5) pH) conditions alone and in combination into the previously described monolayer co-culture model system (Richardson et al., 2006, Strassburg et al., 2010) to evaluate their impact on BM-MSC differentiation and modulation of degenerate NP cell phenotype during direct co-culture.

For this work it was hypothesized that the IVD-like physio-chemical microenvironmental conditions will influence BM-MSCs discogenic differentiation and modulation of degenerate NP cells phenotype in a direct monolayer co-culture model system.

The specific aims of this study were to:

1. Evaluate the stimulatory or inhibitory effects of IVD-like physio-chemical microenvironmental conditions on BM-MSC discogenic differentiation during co-culture with degenerate NP cells.
2. Assess the stimulatory or inhibitory effects of IVD-like physio-chemical microenvironmental conditions on modulation of degenerate NP cell phenotype during co-culture with BM-MSC.

5.2 Materials and methods

5.2.1 Direct co-culture of BM-MSCs and degenerate NP cells

Degenerate NP cells and human BM-MSCs used in this study were isolated from tissue samples listed in Table 5.1 and 5.2 respectively.

Table 5.1 Details of degenerate NP samples used in co-culture study

Sample number	Tissue ID	Sex	Age (years)	Disc Level	Histological grade
1	HH0446	M	31	L5/S1	6
2	HH0454	F	78	L4/5	Unable to score
3	HH0447	F	41	L5/S1	8
4	HH0373	F	33	L4/5	9
5	HH0360	F	26	L5/S1	6
6	HH0445	F	37	L5/S1	7
7	HH0482	F	42	L4/5	8
8	HH0440	M	31	L4/5	9
10	HH0098	M	52	L4/5	9
11	HH0513	M	54	L4/5	7
12	HH0515	M	45	L5/S1	7
13	HH0389	F	46	L5/S1	7
14	HH0416	M	46	L5/S1	8
15	HH0363	F	35	L5/S1	7
16	HH0070	M	59	L4/5	7
17	HH0345	M	44	L4/5	10
18	HH0391	F	39	L5/S1	6
19	HH0397	M	37	L4/5	5
20	HH0403	M	53	L5/S1	5
21	HH0489	F	60	L4/5	8

Table 5.2 Detail of human BM samples used in co-culture study

Sample number	Tissue ID	Sex	Age (years)	Operation site	Reason for surgery
1	TH090	F	62	Knee	OA
2	TH092	M	77	Hip	OA
3	TH094	M	55	Knee	OA
4	TH109	M	41	Hip	OA
5	TH148	M	41	Hip	OA
6	TH107	F	73	Hip	OA
7	WH023	M	40	unknown	OA
8	WH027	F	54	Hip	OA
9	WH028	M	50	Hip	OA
10	TH106	M	64	Knee	OA
11	TH108	M	63	Knee	OA
12	TH110	F	76	Hip	OA
13	WH047	M	47	Hip	OA
14	WH051	M	71	Hip	OA
15	WH053	F	24	Hip	OA
16	TH180	F	89	Hip	OA
17	WH042	M	51	Hip	OA
18	WH046	F	27	Hip	AVN

OA= Osteoarthritis

AVN= Avascular necrosis

5.2.2 CFDA-SE labelling of BM-MSCs

The co-culture protocol was based on a previously established method (Richardson et al., 2006, Strassburg et al., 2010). Prior to co-culture BM-MSCs were fluorescently labelled with caboxyfluorescein diactetae, succinimidyl ester (CFDA-SE) (Invitrogen) to allow separation of the two cell populations after co-culture by FACS. CFDA-SE is a lipophilic, non-fluorescent molecule until it is transported inside the cells, where it is cleaved by intracellular

esterases to CFDA which is a cell permanent green fluorescent molecule that binds covalently to intracellular proteins (Parish, 1999). It has been shown to be suitable for labelling BM-MSCs during co-culture with NP cells without affecting BM-MSC expression level of discogenic genes (Richardson et al., 2006).

A stock solution of 10mM CFDA-SE was prepared by dissolving 500µg of CFDA-SE (component A) in 90 µl of DMSO (component B). Confluent cultures of BM-MSCs were trypsinised and centrifuged at 300g for 5 minutes. Cell pellets were re-suspended in an appropriate volume of α-MEM standard medium (chapter 2, section 2A.1) and counted using a haemocytometer. Five hundred thousand ($5x10^5$) cells were re-suspended in 1ml PBS, 0.1% (w/v) BSA with a final concentration of 10µM CFDA-SE. Cells were incubated for 30 minutes at 37°C in the dark. After incubation cells were centrifuged, re-suspended in fresh pre-warmed DMEM standard medium (chapter 2, section 2A.1) and incubated for another 30 minutes at 37°C in the dark. Cells were then centrifuged and washed with PBS. Finally the cell pellet was re-suspended in an adequate volume of DMEM standard medium and counted for required cell seeding.

5.2.3 Direct co-culture under IVD-like physio-chemical microenvironmental conditions

CFDA-labelled BM-MSCs and unlabelled degenerate NP cells were seeded in 50:50 ratios at a combined final density of 1.2×10^4 cells/cm^2. Co-culture under IVD-like physio-chemical microenvironmental conditions was performed using different media formulations (Table 2.1) and methodology as previously detailed in chapter 2, section 2A.3.

5.2.4 Cell separation of CFDA labelled BM-MSCs and degenerate NP cells following direct co-culture

CFDA-labelled BM-MSCs were separated from unlabelled degenerate NP cells after 7 days of co-culture with direct cell-to-cell contact using FACS. Co-cultured cells were harvested with trypsin-EDTA and centrifuged at 500g for 5 minutes. Cell pellets were washed in PBS and re-suspended in 300µl PBS. The cell suspension was then passed through a 50µm filter (BD Biosciences) to remove cell clumps and collected in a 5ml polypropylene tube (BD Biosciences). Samples were analysed and sorted based upon the fluorescent characteristics of each cell using an Aria FACS (BD Biosciences) with Diva 5 software (Figure 5.2.1). Fluorescent and non-fluorescent cell populations were sorted into separate microcentrifuge tubes.

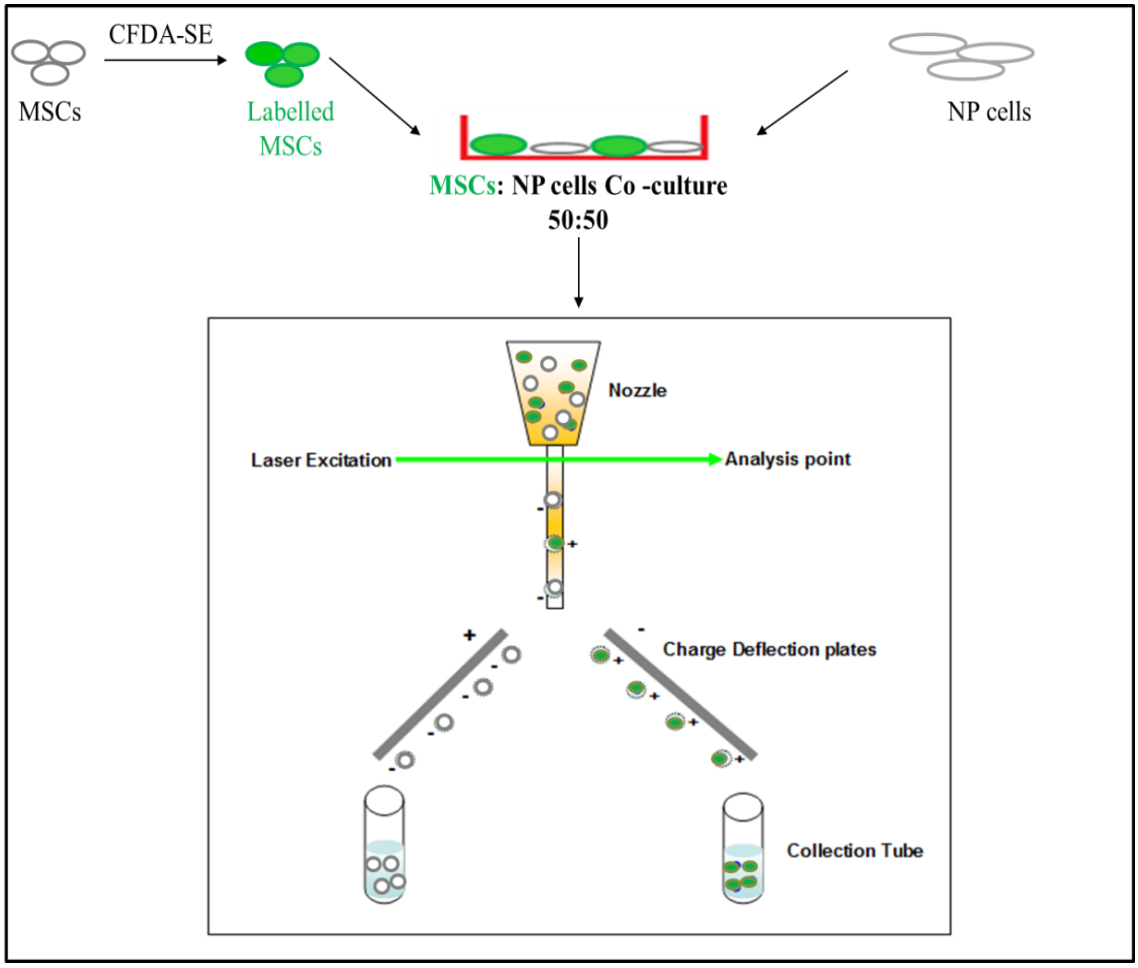

Figure 5.2.1 FACS separation of CFDA-labelled BM-MSCs and unlabelled degenerate NP cells. During FACS the cell suspension is directed into a thin stream of cells. A vibrating mechanism causes the stream of cells to break into discrete droplets. Just before the droplet formation a focused laser beam at 488 nanometers (nm) is directed at the cell stream. Cells scatter laser light and fluorescent molecules attached to, or within cells excite and fluoresce. Droplets containing cells are charged based on the fluorescence intensity measurement and sorted as they pass between constantly charged deflecting plates. Adapted from (Herzenberg et al., 2002).

5.2.5 Gene expression

For RNA extraction, FACS sorted CFDA-labelled BM-MSCs and unlabelled NP cells were pelleted at 500g for 5 minutes and lysed in 1ml of Trizol®. RNA was extracted and reverse transcribed as previously detailed (chapter 2, section 2A.7.1-7.5). QRT-PCR was then conducted for NP classical (COL2A1, SOX-9, ACAN, VCAN) and novel markers (PAX-1, FOXF1). CA9 and CA12 expression was also investigated under acidic pH conditions.

MRPL19 and EIF2B1 were used as HK genes and their values averaged for data normalisation. Details of primers and probes sequences used in this study are provided in Table 2.3 (chapter 2, section 2A.7.6-7.7). BM-MSCs and degenerate NP cell co-culture combinations used in gene expression analysis are listed in table 5.3.

Table 5.3 BM-MSC and degenerate NP cell co-culture combinations used for the separate experiments analysing gene expression following culture in the differing conditions.

IVD-like conditions	BM-MSCs and degenerate NP cells combination
1. Hypoxia (n=12)	TH092: HH0446
	TH092: HH0454
	TH092: HH0447
	TH094: HH0446
	TH094: HH0454
	TH094: HH0447
	TH090: HH0373
	TH090: HH0360
	TH109: HH0445
	TH109: HH0482
	TH148: HH0482
	TH107: HH0440
2. Reduced serum (n=8)	TH092: HH0446
	TH092: HH0454
	TH092: HH0447
	TH094: HH0446
	TH094: HH0454
	TH094: HH0447
	TH090: HH0373
	TH090: HH0360
3. Reduced Glucose (n=4)	TH109: HH0445
	TH109: HH0482
	TH148: HH0482
	TH107: HH0440
4. Reduced serum and reduced glucose (n=9)	WH023: HH098
	WH023: HH0513
	WH023: HH0515
	WH027 :HH0098
	WH027: HH0513

IVD-like conditions	BM-MSCs and degenerate NP cells combination
	WH027: HH0515
	WH028: HH098
	WH028: HH0513
	WH028: HH0515
5. Reduced serum and hypoxia (n=8)	Same combinations as in reduced serum
6. Reduced glucose & Hypoxia (n=4)	Same combinations as in reduced glucose
7. Reduced serum, reduced glucose and hypoxia (n=9)	Same combinations as in reduced serum
8. Reduced pH 6.8 & 6.5 (n=8)	TH106: HH0389
	TH106: HH0416
	TH106: HH0363
	TH108: HH0389
	TH108: HH0416
	TH108: HH0363
	TH110: HH0389
	TH110: HH0363
9. pH 6.8 & Hypoxia (n=9) 10. All IVD-like physio-chemical conditions combined (n=9)	WH047: HH0070
	WH047: HH0345
	WH047: HH0391
	WH051: HH0070
	WH051: HH0345
	WH051: HH0391
	WH053: HH0H70
	WH053: HH0345
	WH053: HH0391

5.2.6 Assessment of ECM protein synthesis by immunofluorescence in BM-MSC and degenerate NP cell co-culture under IVD-like physio-chemical microenvironment conditions

In order to investigate whether IVD-like physio-chemical conditions affect synthesis of aggrecan and versican protein in BM-MSCs and NP cells during co-culture, immunofluorescence was performed as previously reported in chapter 2, section 2A.4. Cells were co-cultured in 8-well chamber slides under IVD-like physio-chemical conditions (hypoxia, reduced serum, reduced glucose alone and in combination) using respective media formulations (Table 2.1, section 2A.3). Fluorescence intensity under all conditions was

assessed qualitatively. BM-MSC and degenerate NP cell co-culture combinations used in immunofluorescence analysis of aggrecan and versican are listed in table 5.4.

As mentioned previously in chapter 2 (section 2A.4) due to autofluorescence issues, images from all pH conditions were not analysed and included in this study.

Table 5.4 BM-MSC and degenerate NP cell co-culture combinations used for the separate experiments analysing aggrecan and versican expression by immunefluorescence analysis following culture in the differing conditions

IVD-like conditions	**BM-MSCs and degenerate NP cells combinations for aggrecan staining**	**BM-MSCs and degenerate NP cells combinations for versican staining**
1. Hypoxia 2. Reduced serum 3. Reduced glucose 4. Reduced serum and reduced glucose 5. Reduced serum and hypoxia 6. Reduced glucose and hypoxia	HH0397:TH180 HH0397: WH042 HH0397: WH046 HH0403:TH180 HH0403: WH042 HH0403: WH046	HH0397:TH180 HH0397: WH042 HH0397: WH046 HH0403:TH180 HH0403: WH042 HH0403: WH046 HH0489:TH180 HH0489: WH042 HH0489: WH046
7. Reduced serum, reduced glucose and hypoxia	HH0397:TH180 HH0397: WH042 HH0397: WH046	HH0397:TH180 HH0397: WH042 HH0397: WH046

5.3 Results

5.3.1 Fluorescence activated cell sorting (FACS)

For quantitative gene expression analysis of BM-MSCs and degenerate NP cells individually, co-cultured cells were separated by FACS. This facilitates clear discrimination between labelled BM-MSCs and unlabelled degenerate NP cells based on the light scatter and fluorescence characteristics of individual cells. During the separation process the co-cultured cell suspension was excited by a 488nm laser. Live single cells were identified by forward scatter (FSC) height (FSC-H) and area (FSC-A) parameters (figure 5.3.1A). When excited at 488nm CFDA has a green emission that was collected at 530nm. Data shown in a 2D plot suggested clear discrimination between cells fluorescing at 530nm gated as CFDA positive population (BM-MSCs) and non-fluorescent cells gated as NP cells (Figure 5.3.1).

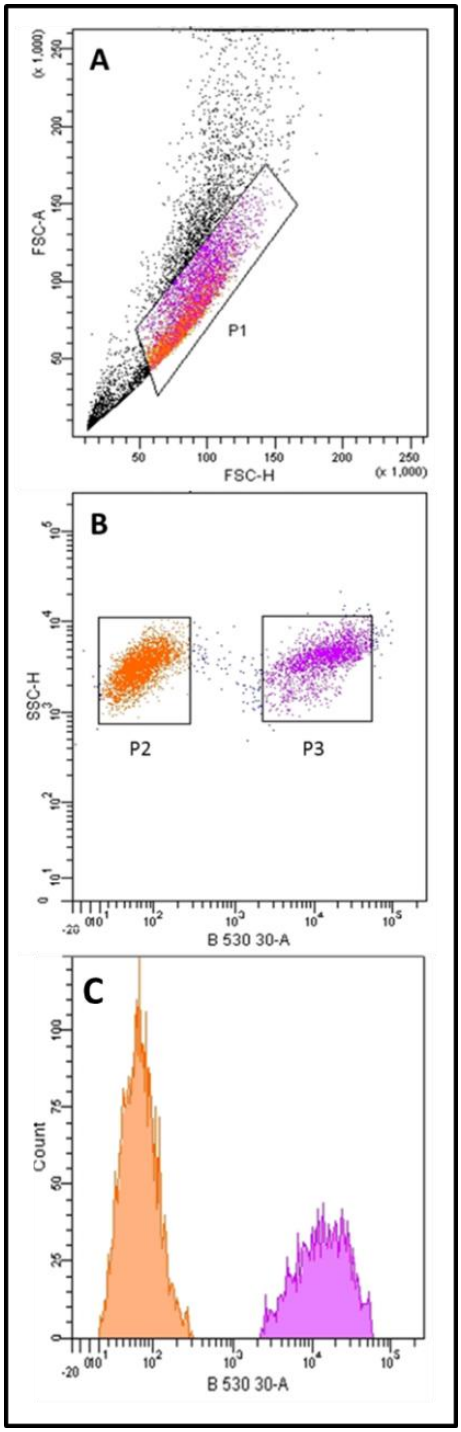

Figure 5.3.1: FACS process for separation of CFDA-labelled BM-MSCs and unlabelled degenerate NP cells following co-culture. Co-cultured cell suspension was passed through a 488nm laser beam and shown in (A) 2D dotplot. Gate P1 was drawn on FSC-H versus FSC-A to exclude dead cells and cell clumps from single live cells. (B) 2D dotplot showing gates P2 and P3 drawn based upon the CFDA fluorescence intensity of live cells to distinguish unlabelled degenerate NP cells from labelled BM-MSCs. (C) Histogram showing gate P2 (unlabelled degenerate NP cells) and gate P3 (labelled BM-MSCs).

5.3.2 Influence of hypoxia on BM-MSC and degenerate NP cell co-culture

5.3.2.1 Gene expression of BM-MSCs co-cultured with degenerate NP cells under hypoxia

BM-MSCs co-cultured with degenerate NP cells under hypoxia showed no change in SOX-9 expression but a significant increase in expression of COL2A1 (p=0.05) compared to BM-MSCs co-cultured with degenerate NP cells under control conditions (Figure 5.3.2 A). There was also a significant increase in both ACAN and VCAN expression (p<0.05 for each) under hypoxia (Figure 5.3.2 B). While PAX-1 expression was significantly increased (p<0.05), there was no change in FOXF1 expression in BM-MSCs co-cultured under hypoxia (Figure 5.3.2 C).

5.3.2.2 Gene expression in degenerate NP cells co-cultured with BM-MSCs under hypoxia

Degenerate NP cells co-cultured with BM-MSCs under hypoxia showed no changes in SOX-9 and COL2A1 expression compared to degenerate NP cells co-cultured with BM-MSCs under control conditions (Figure 5.3.3 A). There was no change in ACAN while a significant increase in VCAN expression (p<0.05) was seen under hypoxia (Figure 5.3.3 B). A significant increase in PAX-1 (p<0.05) but no change in FOXF1 expression was seen under hypoxia (Figure 5.3.3 C).

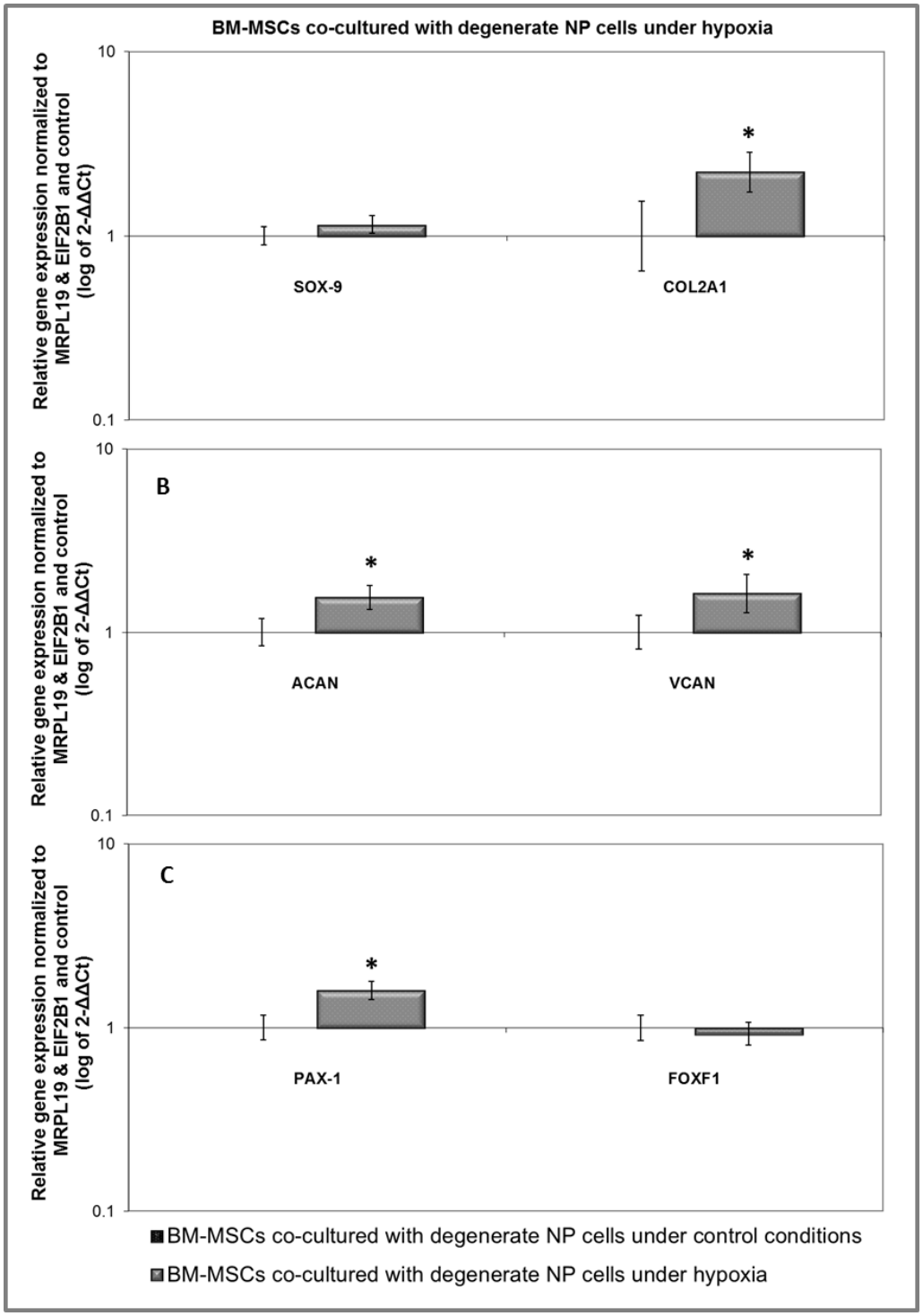

Figure 5.3.2 Relative gene expression of NP conventional markers (A) SOX-9, COL2A1 (B) ACAN, VCAN and NP novel markers (C) PAX-1 and FOXF-1 in BM-MSCs after co-culture with degenerate NP cells under hypoxia (n=12). Gene expression normalized to average of HK genes MRPL19 and EIF2B1 and BM-MSCs co-cultured with degenerate NP cells under control conditions (level expressed as 1) and plotted on a log scale. * Statistical significance ($p \leq 0.05$) compared to BM-MSCs co-cultured under control conditions.

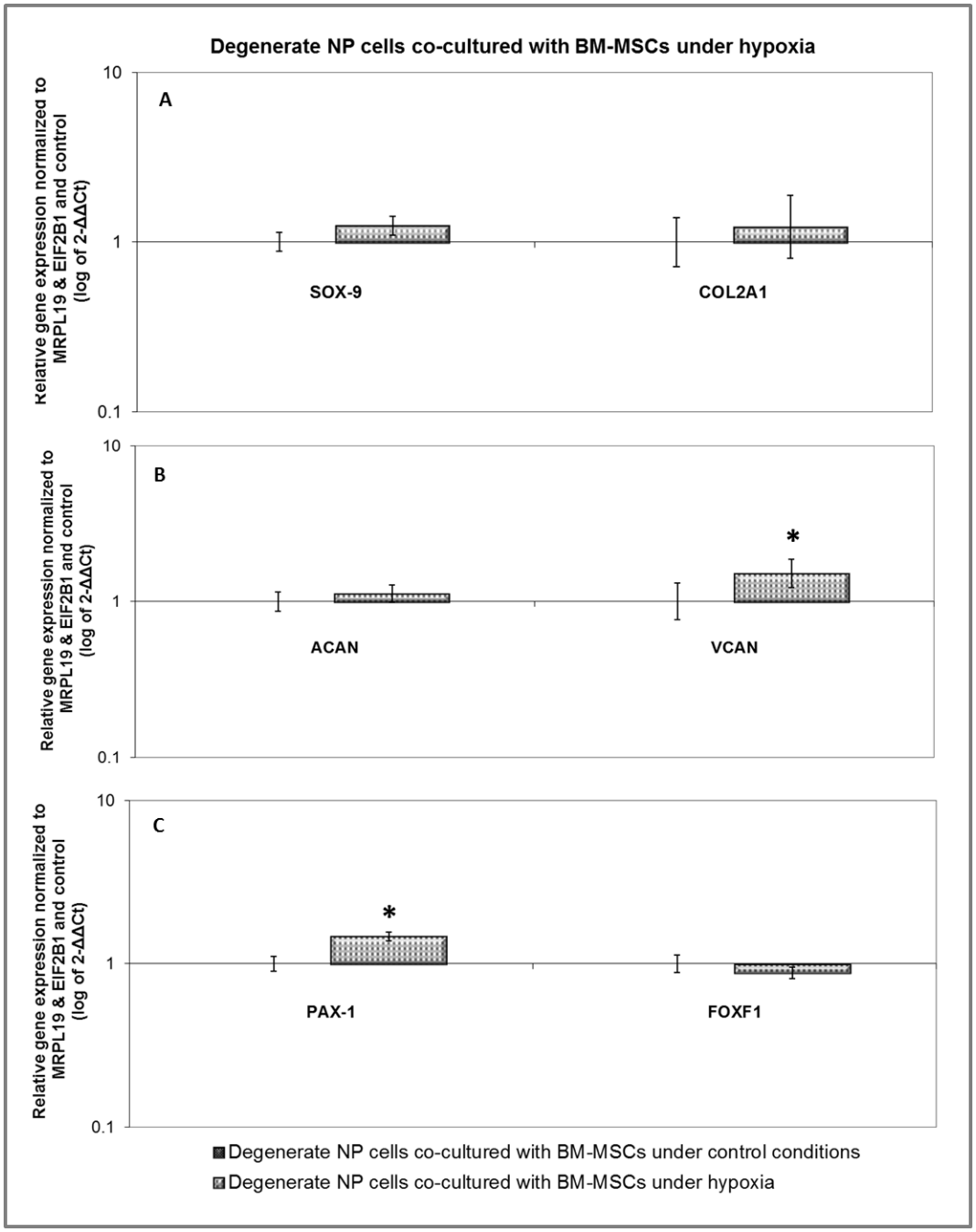

Figure 5.3.3 Relative gene expression of NP conventional markers (A) SOX-9, COL2A1 (B) ACAN, VCAN and NP novel markers (C) PAX-1 and FOXF-1 in degenerate NP cells co-cultured with BM-MSCs under hypoxia (n=12). Gene expression normalized to average of HK genes MRPL19 and EIF2B1 and degenerate NP cells co-cultured with BM-MSCs under control conditions (level expressed as 1) and plotted on a log scale. * Statistical significance ($p \leq 0.05$) compared to degenerate NP cells co-cultured under control conditions.

5.3.2.3 ECM protein expression in BM-MSC and degenerate NP cell co-culture under hypoxia

BM-MSC and degenerate NP cell co-culture under hypoxia showed increased staining intensity of aggrecan protein under hypoxia compared to control conditions (Figure 5.3.4). Co-culture of BM-MSCs and NP cells also showed high staining intensity of versican protein compared to control conditions (Figure 5.3.5). Distinct differences in aggrecan and versican staining were identified, with aggrecan staining predominantly localised intracellularly in the cytoplasm around the nucleus, whereas versican staining appeared to be both intra and extracellular. Representative primary antibody IgG controls (both for aggrecan and versican) of BM-MSC and degenerate NP cell co-culture were negative (Figure 5.3.6).

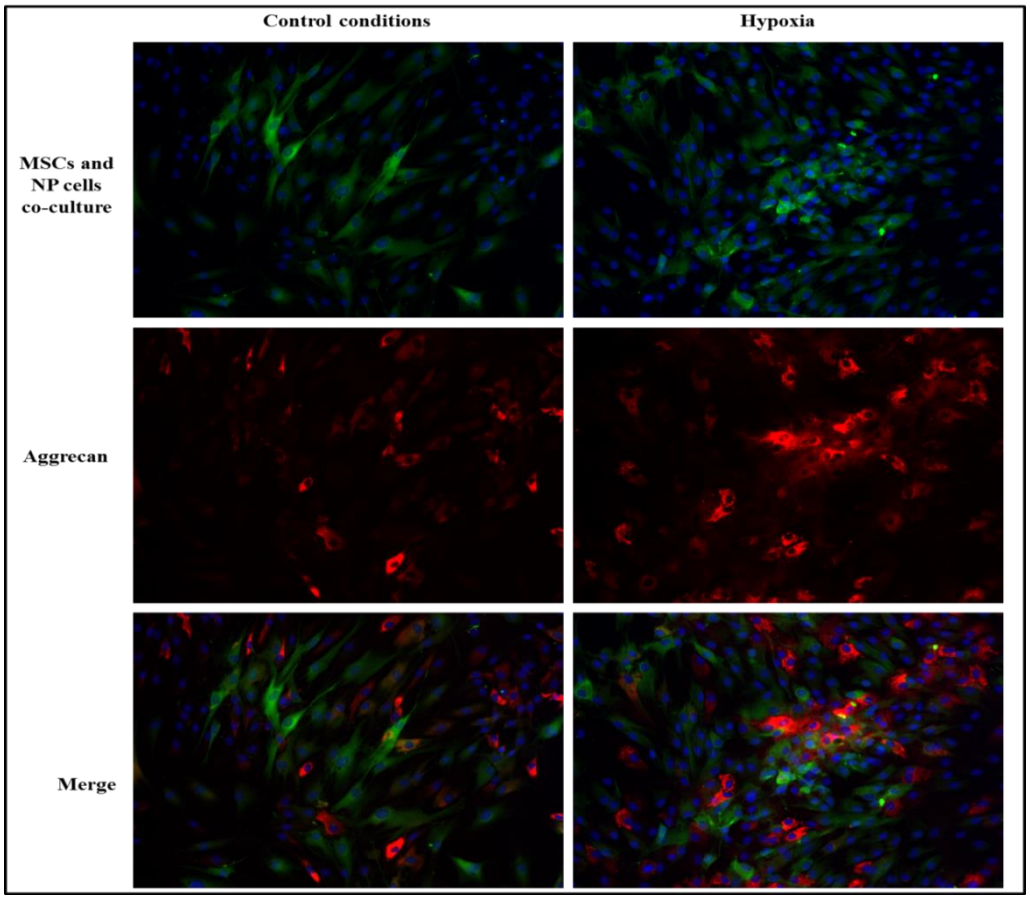

Figure 5.3.4 Representative images of aggrecan immunofluorescence staining of BM-MSC and degenerate NP cell co-culture (n=6) under control conditions (left panels) and hypoxia (right panels). Immunofluorescence staining was performed after 7 days of co-culture using anti-aggrecan primary antibody followed by Alexa Fluor 555 conjugated secondary antibody (red). DAPI (blue) was used for nucleus staining. Top row: DAPI and CFDA (green), middle row: same field of view with aggrecan staining, bottom row: merge of above two rows (magnification x200).

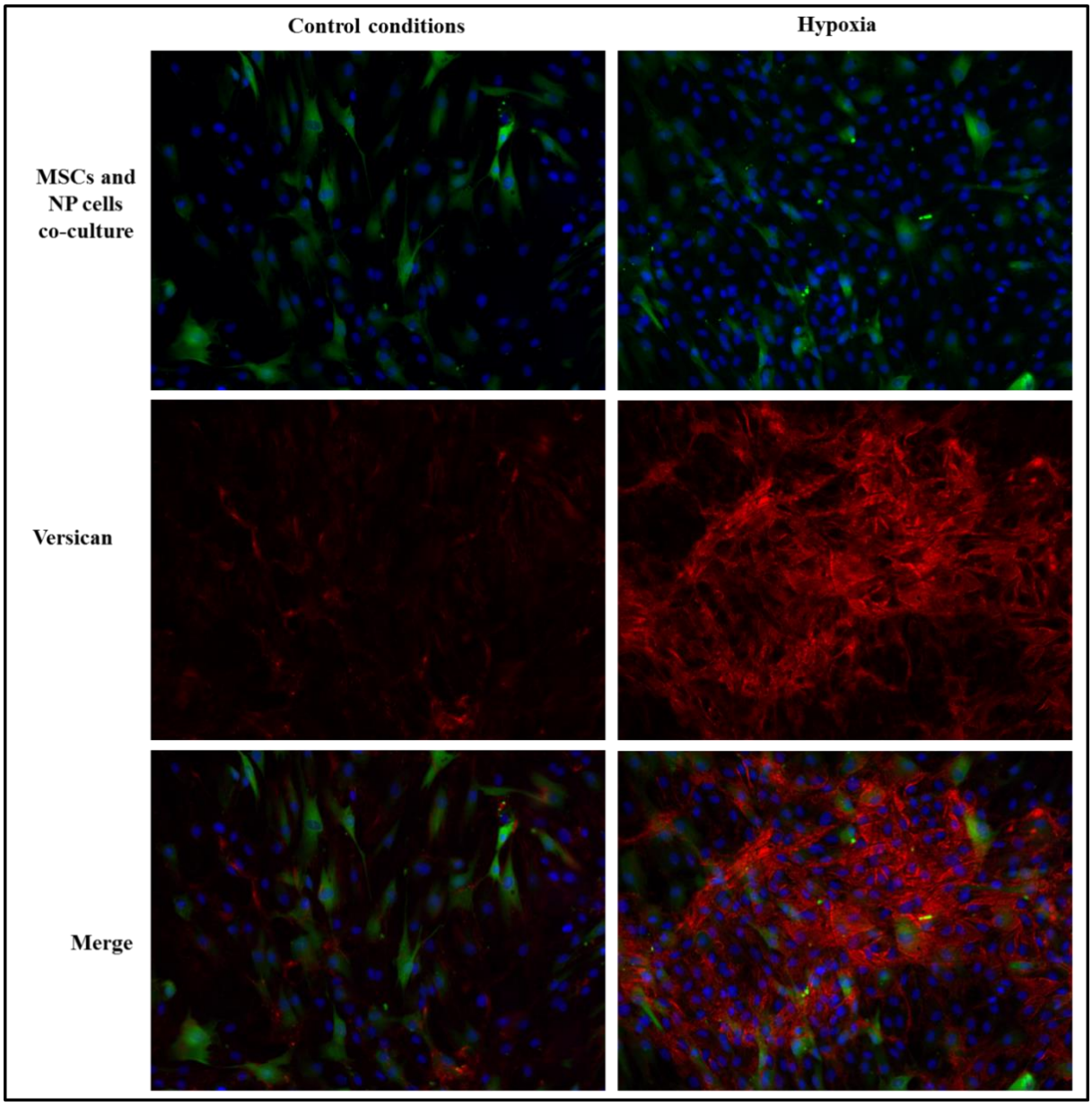

Figure 5.3.5 Representative images of versican immunofluorescence staining of BM-MSC and degenerate NP cell co-culture (n=9) under control conditions (left panels) and hypoxia (right panels). Immunofluorescence staining was performed after 7 days of co-culture using anti-versican primary antibody followed by Alexa Fluor 555 conjugated secondary antibody (red). DAPI (blue) was used for nucleus staining. Top row: DAPI and CFDA (green), middle row: same field of view with versican staining, bottom row: merge of above two rows (magnification x200).

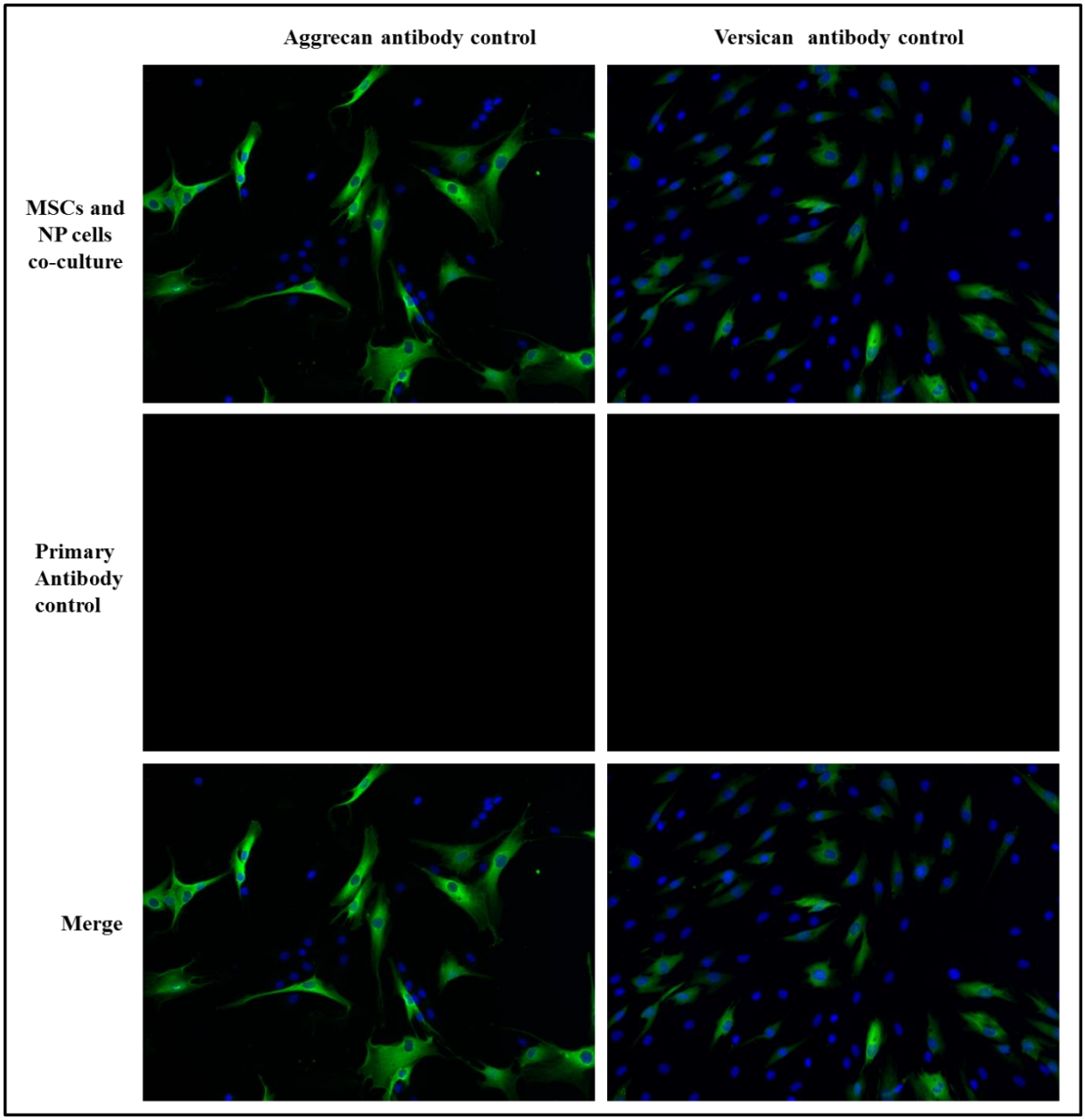

Figure 5.3.6 Representative primary antibody IgG controls for aggrecan (left panels) and versican (right panels) in BM-MSC and degenerate NP cell co-culture. Immunofluorescence staining was performed using IgG control primary antibody followed by Alexa Fluor 555 conjugated secondary antibody (red). IgG controls showed no non-specific IgG staining. DAPI (blue) was used for nucleus staining Top row: DAPI and CFDA (green), middle row: same field of view with IgG staining, bottom row: merge of above two rows (magnification x200).

5.3.3 Influence of reduced serum on BM-MSC and degenerate NP cell co-culture

5.3.3.1 Gene expression in MSCs co-cultured with degenerate NP cells under reduced serum

MSCs co-cultured with degenerate NP cells under reduced serum showed a significant decrease ($p<0.05$) in SOX-9 expression but no change in COL2A1 expression compared to MSCs co-cultured under control conditions (Figure 5.3.7 A). A significant increase ($p<0.05$) in ACAN was observed with no change in VCAN expression under reduced serum (Figure 5.3.7 B). There was no significant changes in PAX-1 and FOXF1 expression under reduced serum (Figure 5.3.7 C).

5.3.3.2 Gene expression in degenerate NP cells co-cultured with BM-MSCs under reduced serum

Degenerate NP cells co-cultured with MSCs under reduced serum showed no change in COL2A1 but a significant increase in SOX-9, ACAN and VCAN expression ($p<0.05$ for each) compared to degenerate NP cells co-cultured with MSCs under control conditions (Figure 5.3.8 A). A significant increase in PAX-1 ($p<0.05$) with no change in FOXF1 expression was seen under reduced serum compared with control conditions (Figure 5.3.8 B & C).

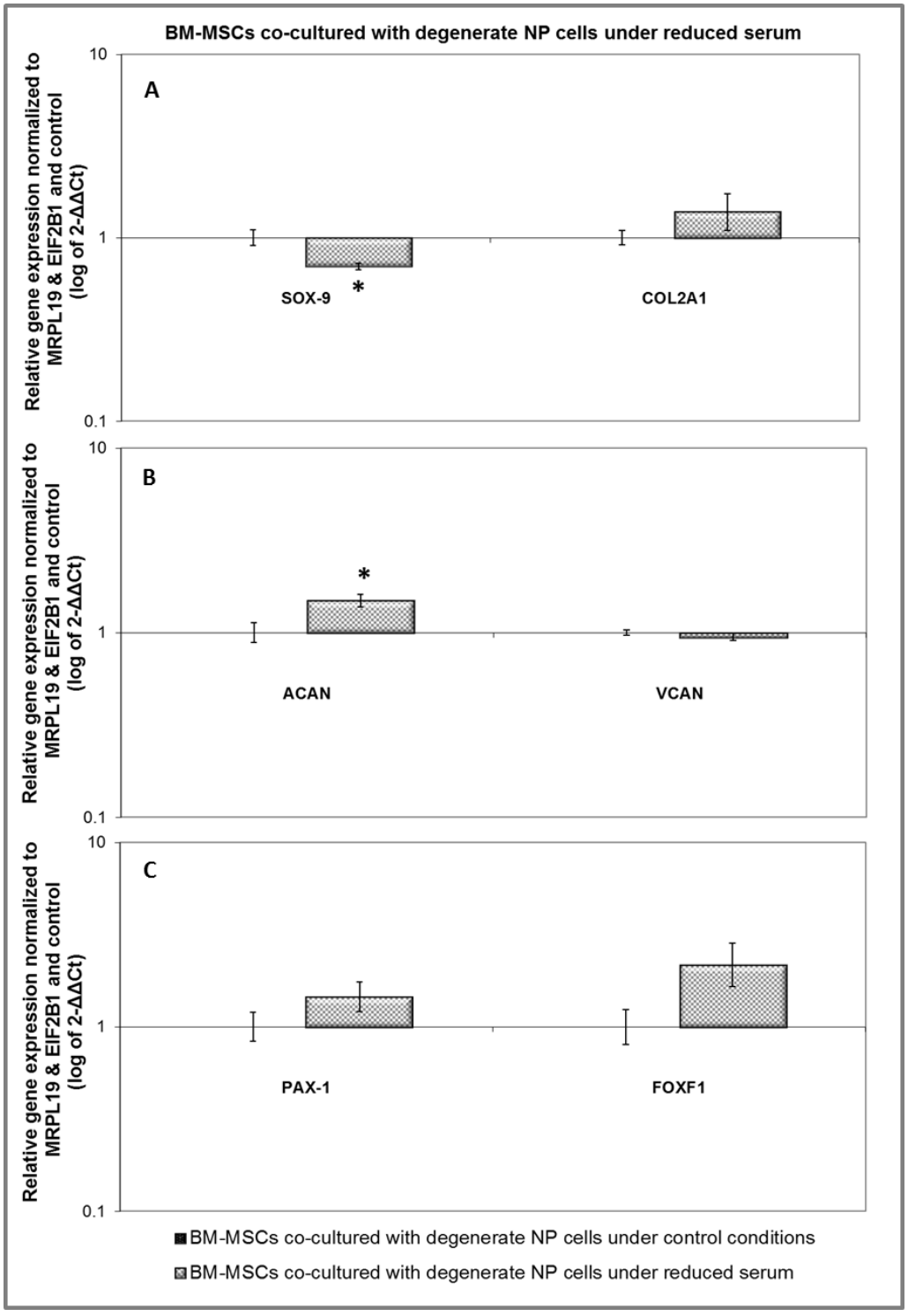

Figure 5.3.7 Relative gene expression of NP conventional markers (A) SOX-9, COL2A1 (B) ACAN, VCAN and NP novel markers (C) PAX-1 and FOXF-1 in BM-MSCs co-cultured with degenerate NP cells under reduced serum (n=8). Gene expression normalized to average of housekeeping genes MRPL19 and EIF2B1 and BM-MSCs co-cultured with degenerate NP cells under control conditions (level expressed as 1) and plotted on a log scale. * Statistical significance ($p \leq 0.05$) compared to BM-MSCs co-cultured under control conditions.

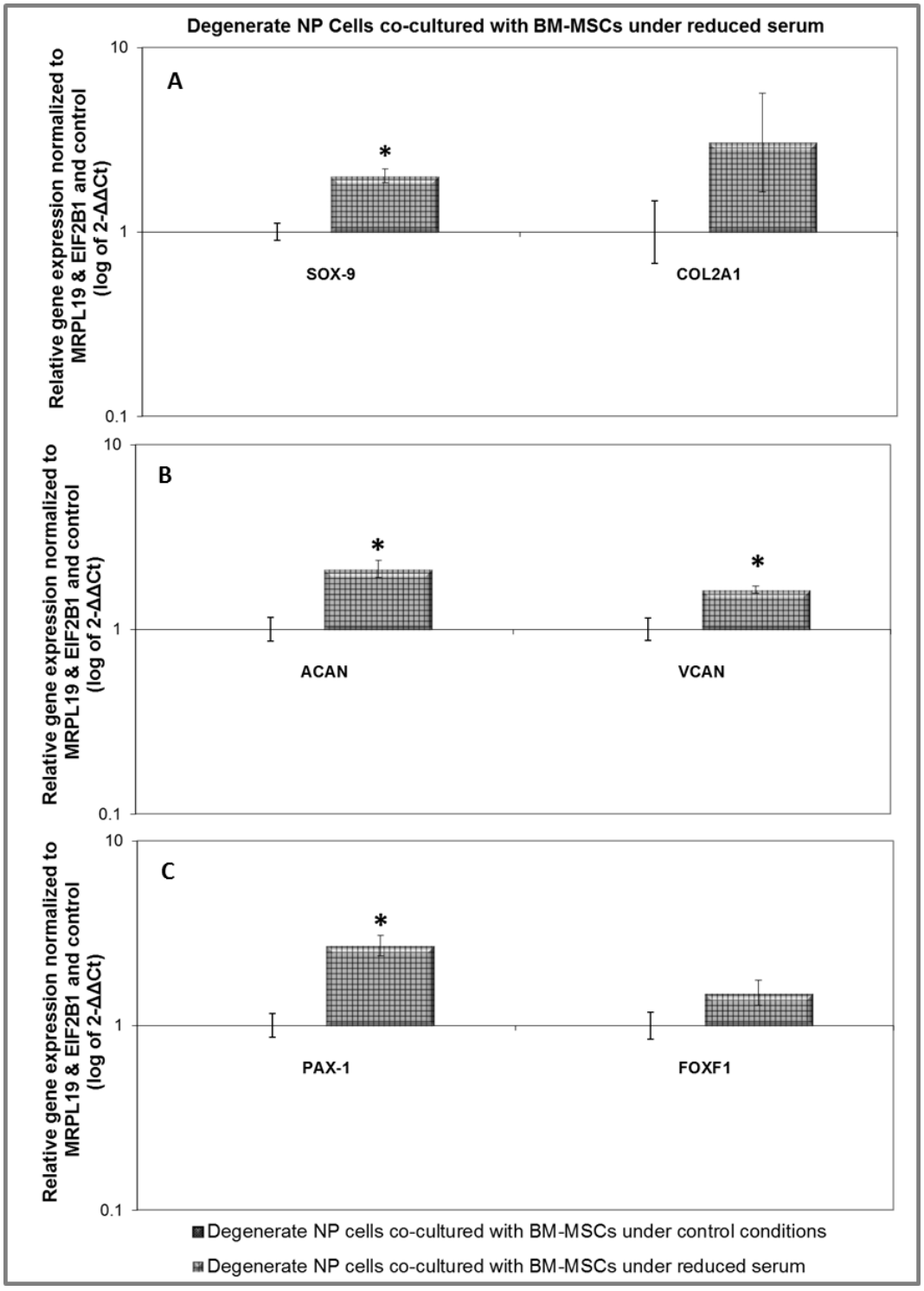

Figure 5.3.8 Relative gene expression of NP conventional markers (A) SOX-9, COL2A1 B) ACAN, VCAN and NP novel markers (C) PAX-1 and FOXF-1 in degenerate NP cells co-cultured with BM-MSCs under reduced serum (n=8). Gene expression normalized to average of HK genes MRPL19 and EIF2B1 and degenerate NP cells co-cultured with BM-MSCs under control conditions (level expressed as 1) and plotted on a log scale. * Statistical significance ($p \leq 0.05$) compared to degenerate NP cells co-cultured under control conditions.

5.3.3.3 ECM protein expression in BM-MSC and degenerate NP cell co-culture under reduced serum

BM-MSC and degenerate NP cell co-culture under reduced serum stained positively for aggrecan protein. Although staining intensity appeared to decrease, cell number under reduced serum was also decreased (Figure 5.3.9), thus the proportion of cells positive for aggrecan staining under reduced serum appeared comparable to control condition. Increased staining intensity of versican protein was seen in BM-MSC and degenerate NP cell co-culture under reduced serum compared to control conditions (Figure 5.3.10).

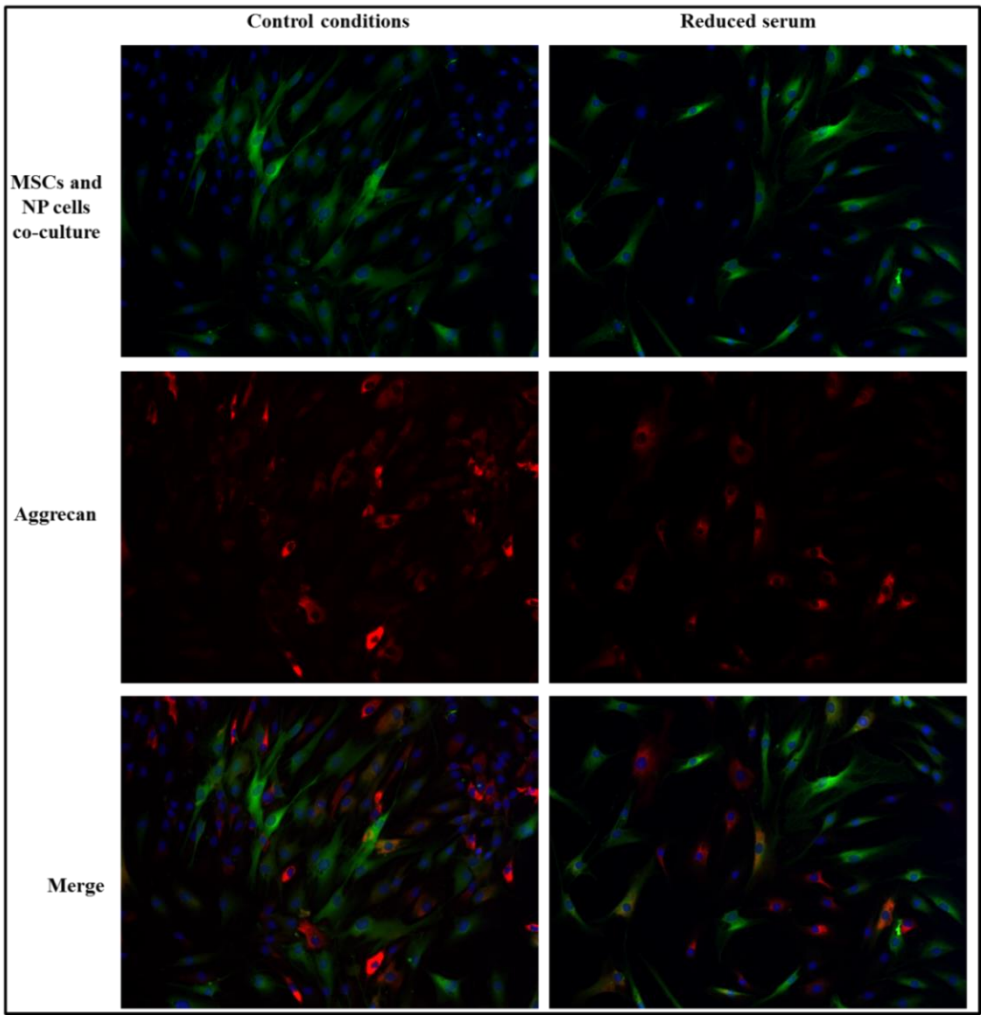

Figure 5.3.9 Representative images of aggrecan immunofluorescence staining of BM-MSC and degenerate NP cell co-culture (n=6) under control conditions (left panels) and reduced serum (right panels). Immunofluorescence staining was performed after 7 days of co-culture using anti-aggrecan primary antibody followed by Alexa Fluor 555 conjugated secondary antibody (red). DAPI (blue) was used for nucleus staining. Top row: DAPI and CFDA (green), middle row: same field of view with aggrecan staining, bottom row: merge of above two rows (magnification x200).

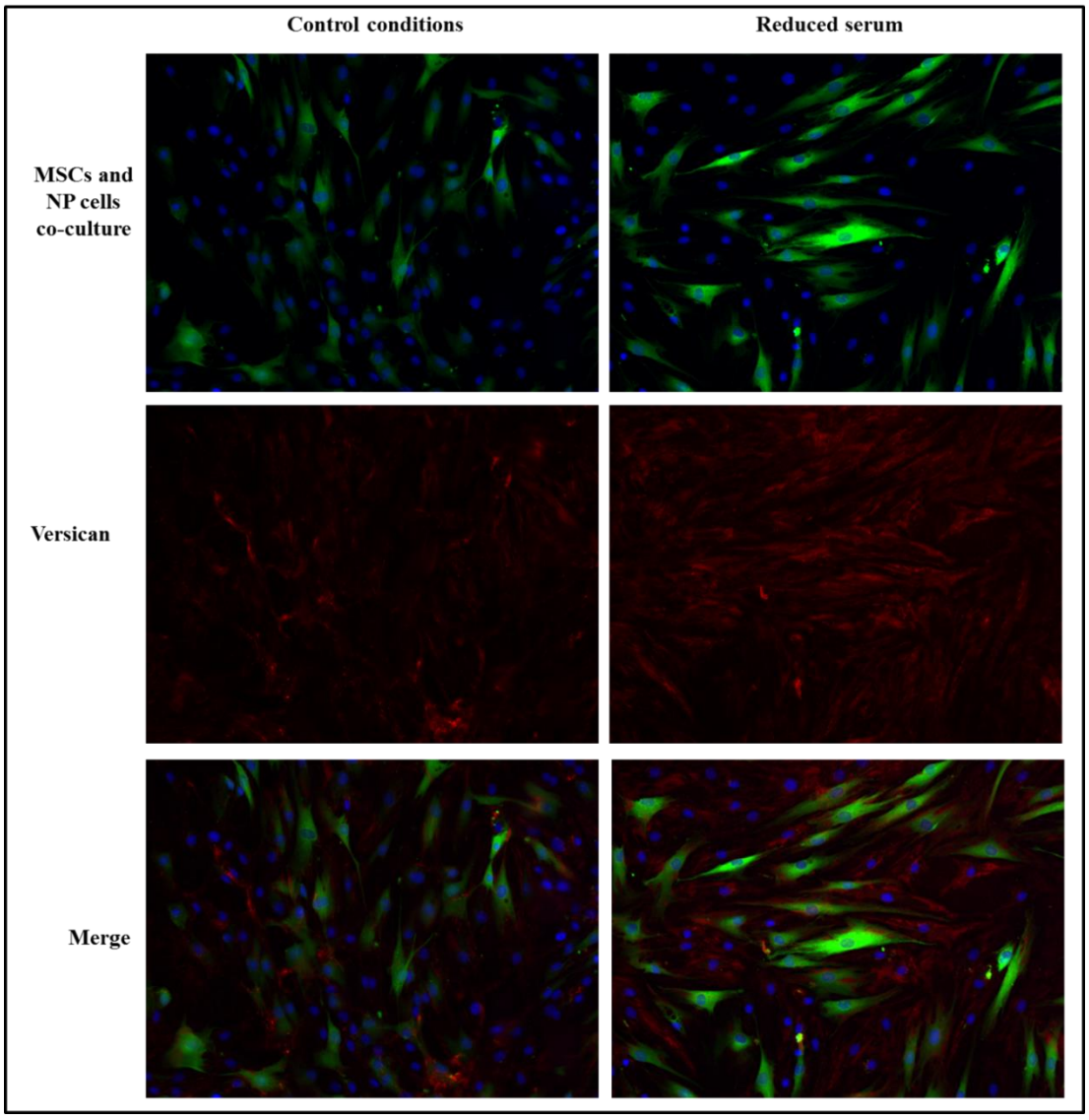

Figure 5.3.10 Representative images of versican immunofluorescence staining of BM-MSC and degenerate NP cell co-culture (n=9) under control conditions (left panels) and reduced serum (right panels). Immunofluorescence staining was performed after 7 days of co-culture using anti-versican primary antibody followed by Alexa Fluor 555 conjugated secondary antibody (red). DAPI (blue) was used for nucleus staining. Top row: DAPI and CFDA (green), middle row: same field of view with versican staining, bottom row: merge of above two rows (magnification x200).

5.3.4 Influence of reduced glucose on BM-MSC and degenerate NP cell co-culture

5.3.4.1 Gene expression in BM-MSCs co-cultured with degenerate NP cells under reduced glucose

BM-MSCs co-cultured with degenerate NP cells under reduced glucose showed no change in SOX-9 and COL2A1 (Figure 5.3.11 A). There was a significant increase in ACAN (p=0.05) while VCAN showed no significant change (Figure 5.3.11 B). There was no change in expression of novel marker genes under reduced glucose compared to control conditions (Figure 5.3.11 C).

5.3.4.2 Gene expression in degenerate NP cells co-cultured with BM-MSCs under reduced glucose

Degenerate NP cells co-cultured with BM-MSCs under reduced glucose showed no changes in SOX-9 and COL2A1 expression compared to degenerate NP cells co-cultured with MSCs under control conditions (Figure 5.3.12 A). There was a significant increase in ACAN (p<0.05) with no change in VCAN expression under reduced glucose (Figure 5.3.12 B). Degenerate NP cells co-cultured with BM-MSCs under reduced glucose showed no change in PAX-1 and FOXF1 expression compared to control conditions (Figure 5.3.12 C).

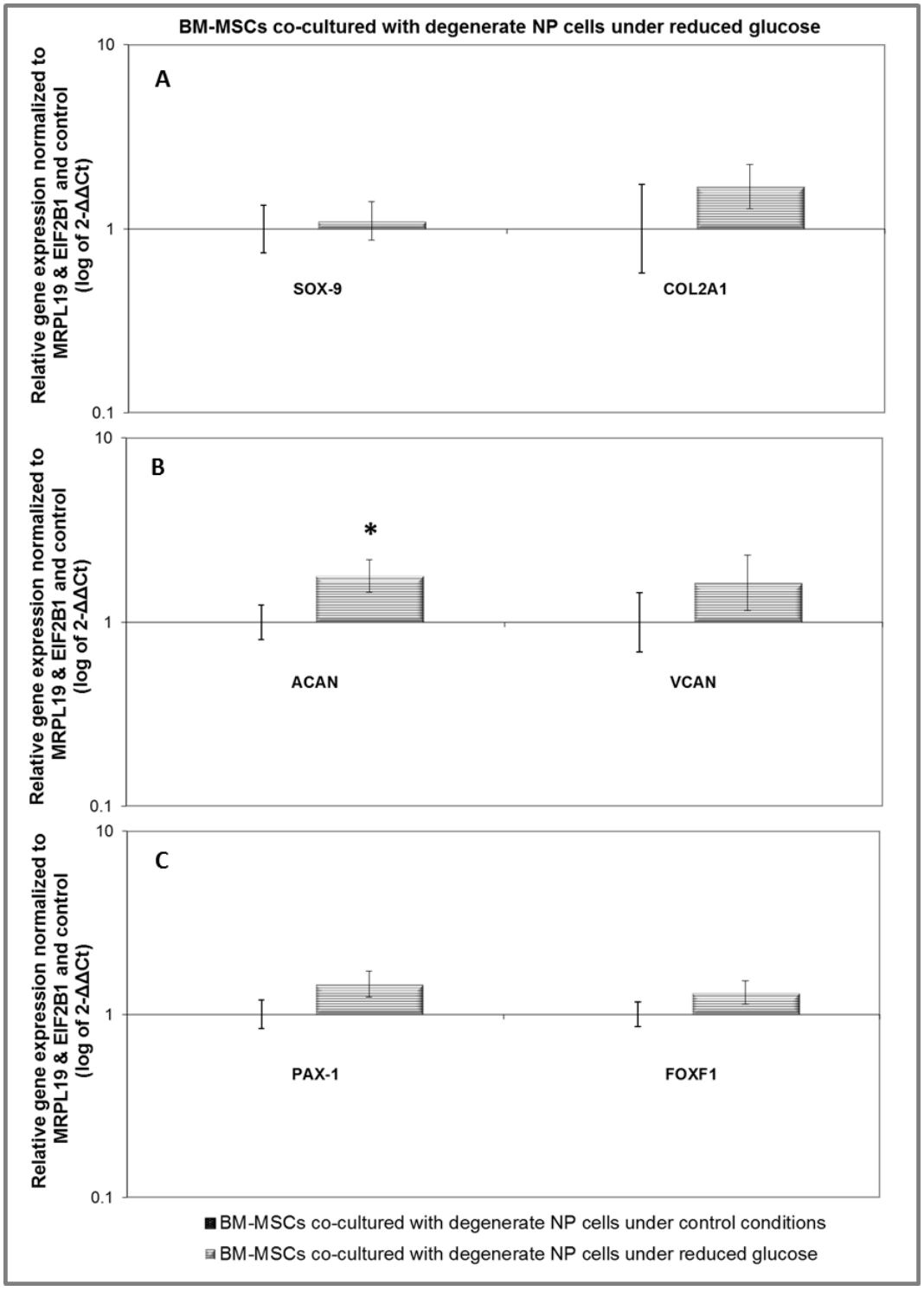

Figure 5.3.11 Relative gene expression of NP conventional markers (A) SOX-9, COL2A1 (B) ACAN, VCAN and NP novel markers (C) PAX-1 and FOXF-1 in BM-MSCs co-cultured with degenerate NP cells under reduced glucose (n=4). Gene expression normalized to average of HK genes MRPL19 and EIF2B1 and BM-MSCs co-cultured with degenerate NP cells under control conditions (level expressed as 1) and plotted on a log scale. * Statistical significance ($p \leq 0.05$) compared to BM-MSCs co-cultured under control conditions.

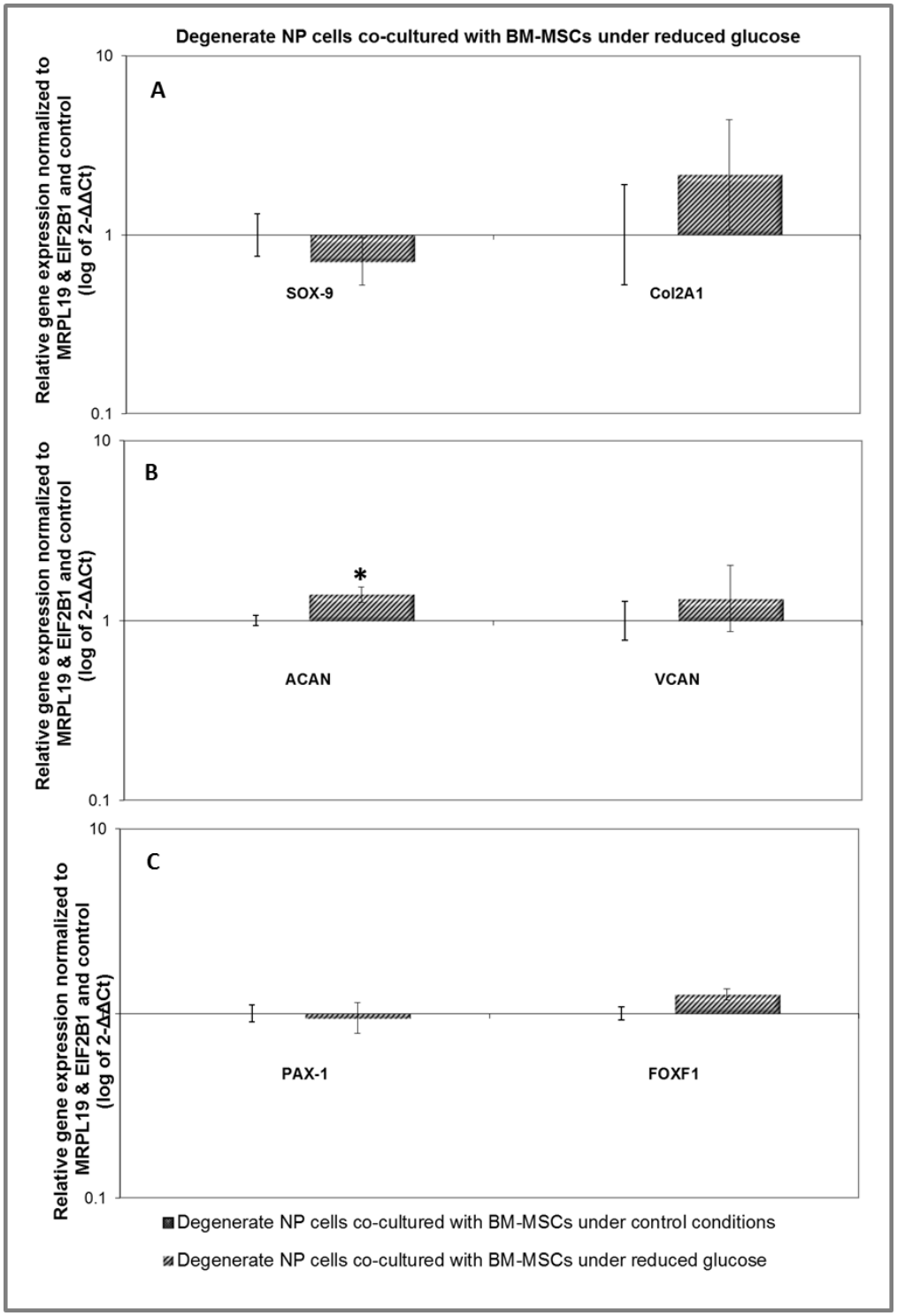

Figure 5.3.12 Relative gene expression of NP conventional markers (A) SOX-9, COL2A1 (B) ACAN, VCAN and NP novel markers (C) PAX-1 and FOXF-1 in degenerate NP cells co-cultured with BM-MSCs under reduced glucose (n=4). Gene expression normalized to average of HK genes MRPL19 and EIF2B1 and degenerate NP cells co-cultured with BM-MSCs under control conditions (level expressed as 1) and plotted on a log scale. * Statistical significance ($p \leq 0.05$) compared to degenerate NP cells co-cultured under control conditions

5.3.4.3 ECM protein expression in BM-MSCs and degenerate NP cell co-culture under reduced glucose

BM-MSC and degenerate NP cell co-culture under reduced glucose showed increased staining intensity of aggrecan protein compared to control conditions (Figure 5.3.13). A slight increase staining intensity of versican protein was also seen compared to control conditions (Figure 5.3.14).

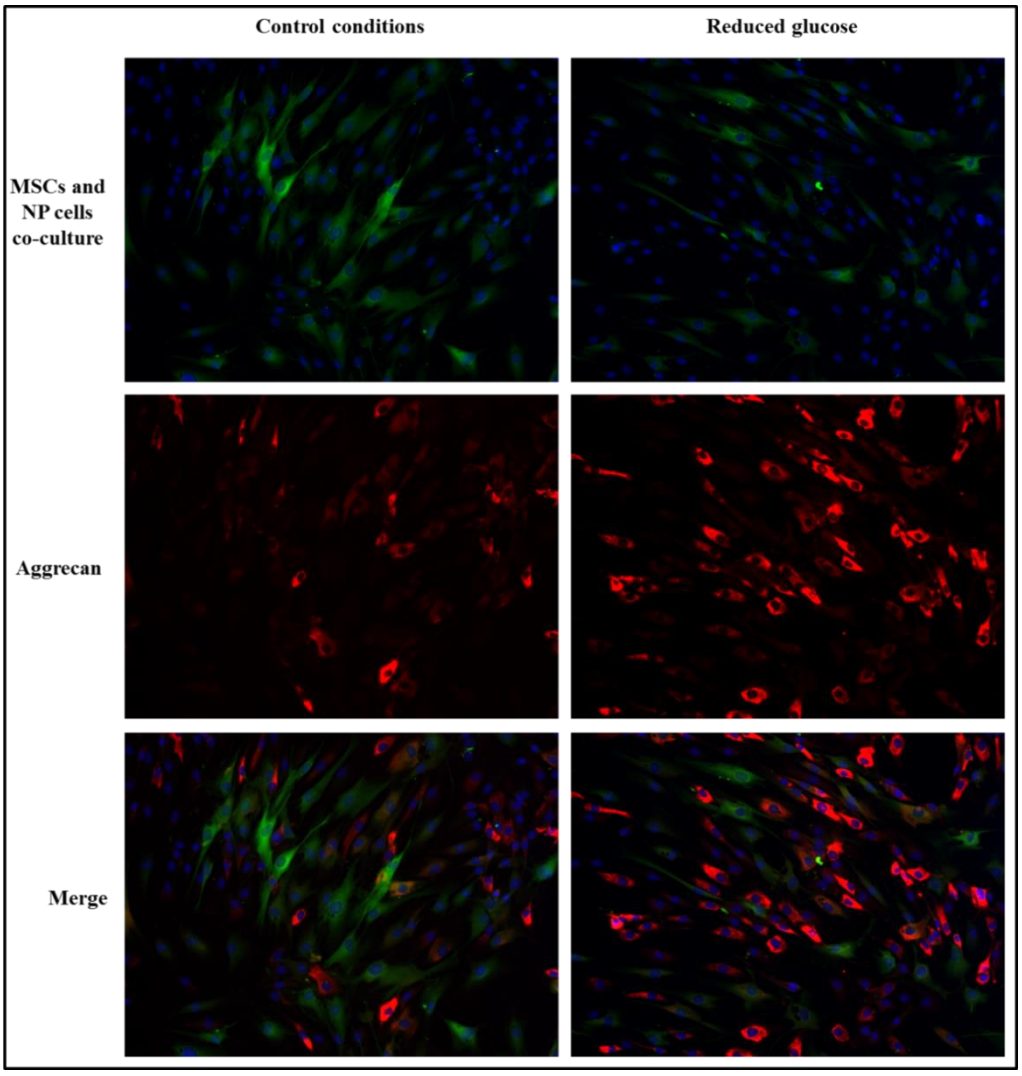

Figure 5.3.13 Representative images of aggrecan immunofluorescence staining of BM-MSC and degenerate NP cell co-culture (n=6) under control conditions (left panels) and reduced glucose (right panels). Immunofluorescence staining was performed after 7 days of co-culture using anti-aggrecan primary antibody followed by Alexa Fluor 555 conjugated secondary antibody (red). DAPI (blue) was used for nucleus staining. Top row: DAPI and CFDA (green), middle row: same field of view with aggrecan staining, bottom row: merge of above two rows (magnification x200).

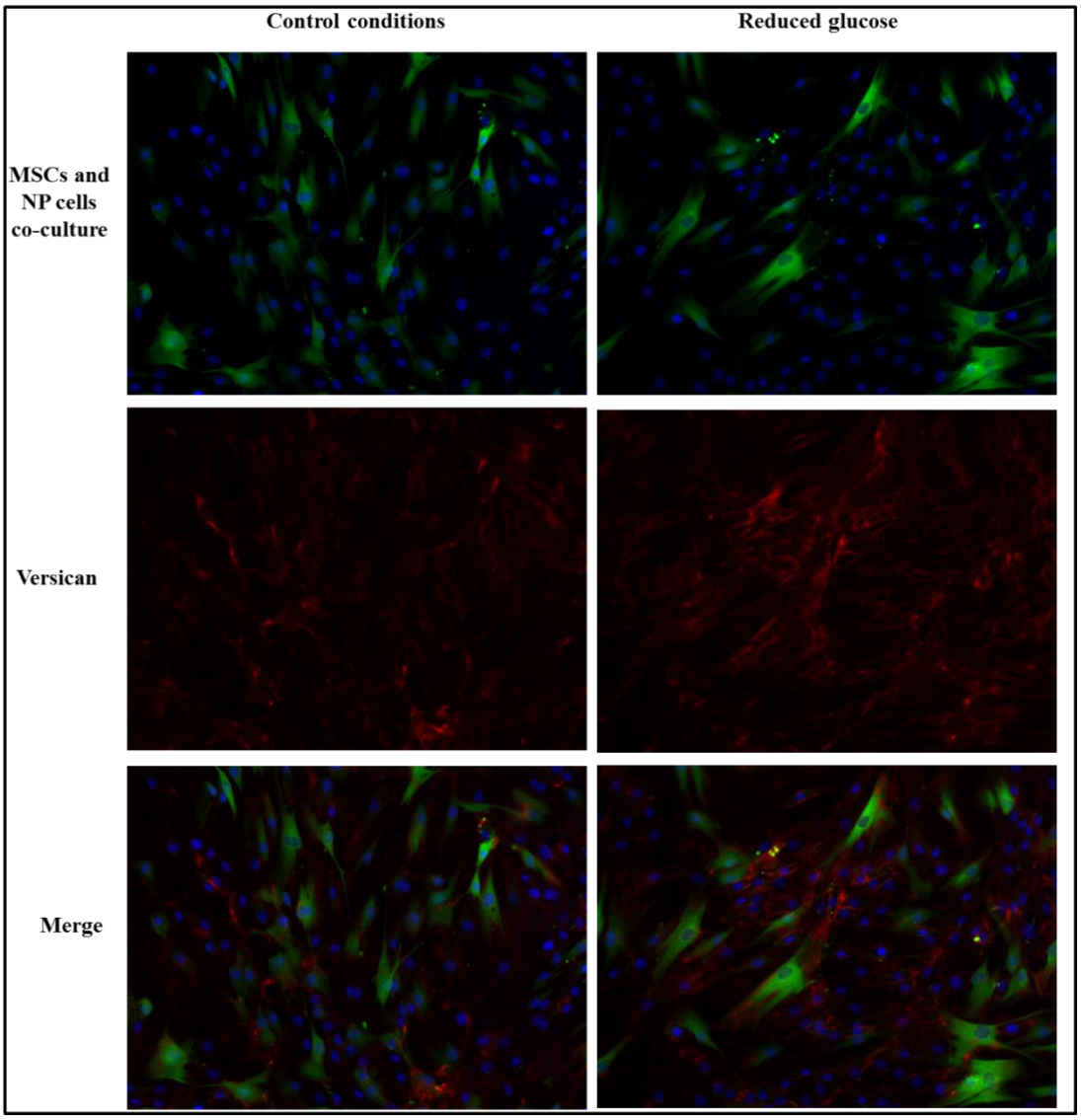

Figure 5.3.14 Representative images of versican immunofluorescence staining of BM-MSC and degenerate NP cell co-culture (n=9) under control conditions (left panels) and reduced glucose (right panels). Immunofluorescence staining was performed after 7 days of co-culture using anti-versican primary antibody followed by Alexa Fluor 555 conjugated secondary antibody (red). DAPI (blue) was used for nucleus staining. Top row: DAPI and CFDA (green), middle row: same field of view with versican staining, bottom row: merge of above two rows (magnification x200).

5.3.5 Influence of reduced serum and reduced glucose on BM-MSC and degenerate NP cell co-culture

5.3.5.1 Gene expression in BM-MSCs co-cultured with degenerate NP cells under reduced serum and reduced glucose

BM-MSCs co-cultured with degenerate NP cells under reduced serum and reduced glucose showed a significant decrease in SOX-9 ($p<0.05$) expression but no significant change in COL2A1 expression compared to control conditions (Figure 5.3.15 A). ACAN expression was significantly increased ($p<0.05$) while VCAN expression showed significant decrease ($p<0.05$) under reduced serum combined with reduced glucose (Figure 5.3.15 B). There was no change in PAX-1 and FOXF1 expression compared to control conditions (Figure 5.3.15 C).

5.3.5.2 Gene expression in degenerate NP cells co-cultured with BM-MSCs under reduced serum and reduced glucose

Degenerate NP cells co-cultured with BM-MSCs under reduced serum and reduced glucose showed no difference in expression of SOX-9, COL2A1, ACAN and VCAN (Figure 5.3.16 A & B). There was also no difference in PAX-1 gene expression under reduced serum and reduced glucose. FOXF1 expression however, was significantly decreased ($p<0.05$) compared to degenerate NP co-cultured with BM-MSCs under control conditions (Figure 5.3.16 C).

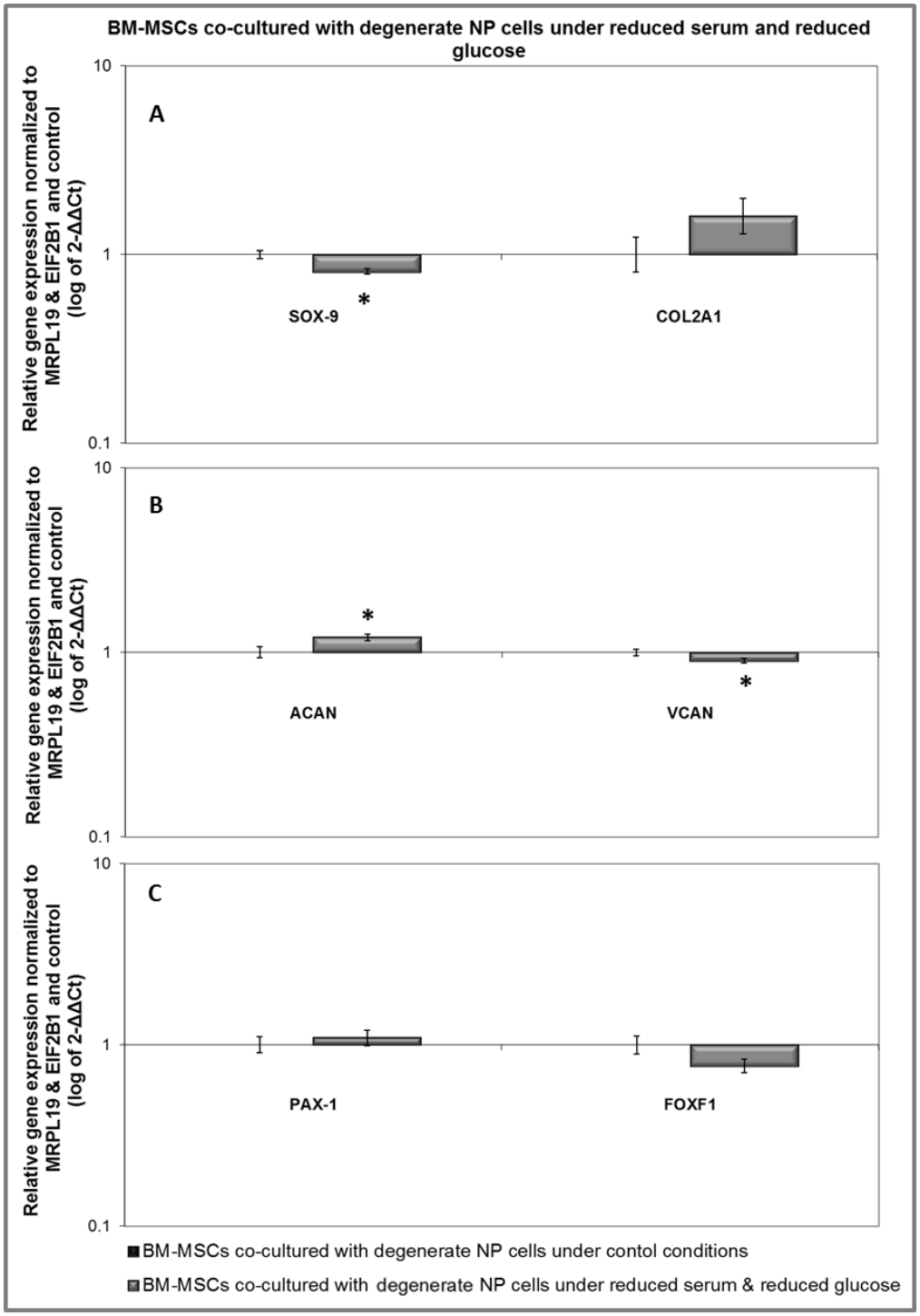

Figure 5.3.15 Relative gene expression of NP conventional markers (A) SOX-9, COL2A1 (B) ACAN, VCAN and NP novel markers (C) PAX-1 and FOXF-1 in BM-MSCs co-cultured with degenerate NP cells under reduced serum and reduced glucose (n=9). Gene expression normalized to average of HK genes MRPL19 and EIF2B1 and BM-MSCs co-cultured with degenerate NP cells under control conditions (level expressed as 1) and plotted on a log scale. * Statistical significance ($p \leq 0.05$) compared to BM-MSCs co-cultured under control conditions.

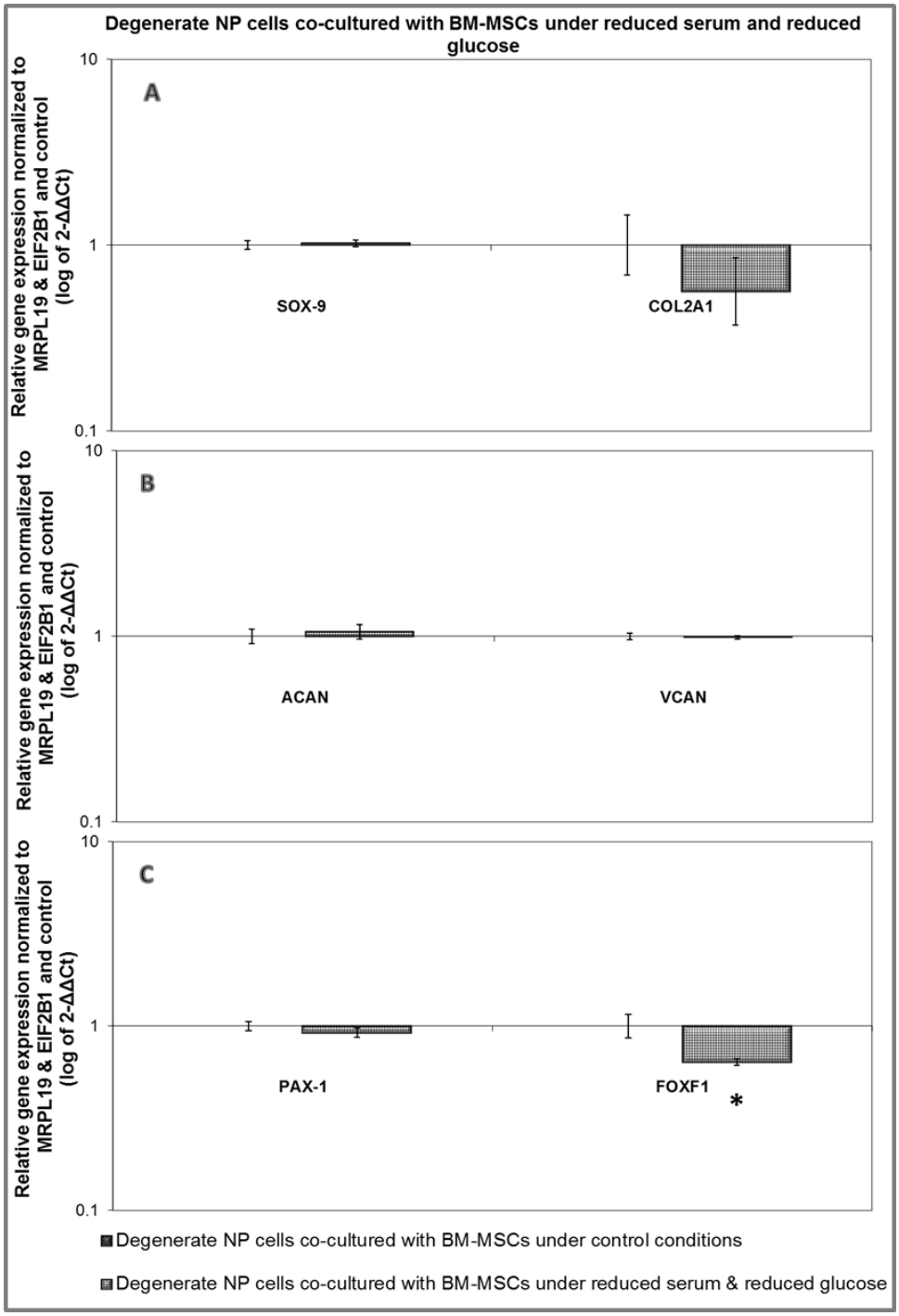

Figure 5.3.16 Relative gene expression of NP conventional markers (A) SOX-9, COL2A1 (B) ACAN, VCAN and NP novel markers (C) PAX-1 and FOXF-1 in degenerate NP cells co-cultured with BM-MSCs under reduced serum and reduced glucose (n=9). Gene expression normalized to average of HK genes MRPL19 and EIF2B1 and degenerate NP cells co-cultured with BM-MSCs under control conditions (level expressed as 1) and plotted on a log scale. * Statistical significance ($p \leq 0.05$) compared to degenerate NP cells co-cultured under control conditions.

5.3.5.3 ECM protein expression in BM-MSC and degenerate NP cell co-culture under reduced serum and reduced glucose

BM-MSC and degenerate NP cell co-culture under reduced serum and reduced glucose showed positive staining for aggrecan protein comparable to control conditions (Figure 5.3.17). BM-MSC and degenerate NP cell co-culture under reduced serum and reduced glucose showed a slight increase in staining intensity of versican protein compared to control conditions (Figure 5.3.18).

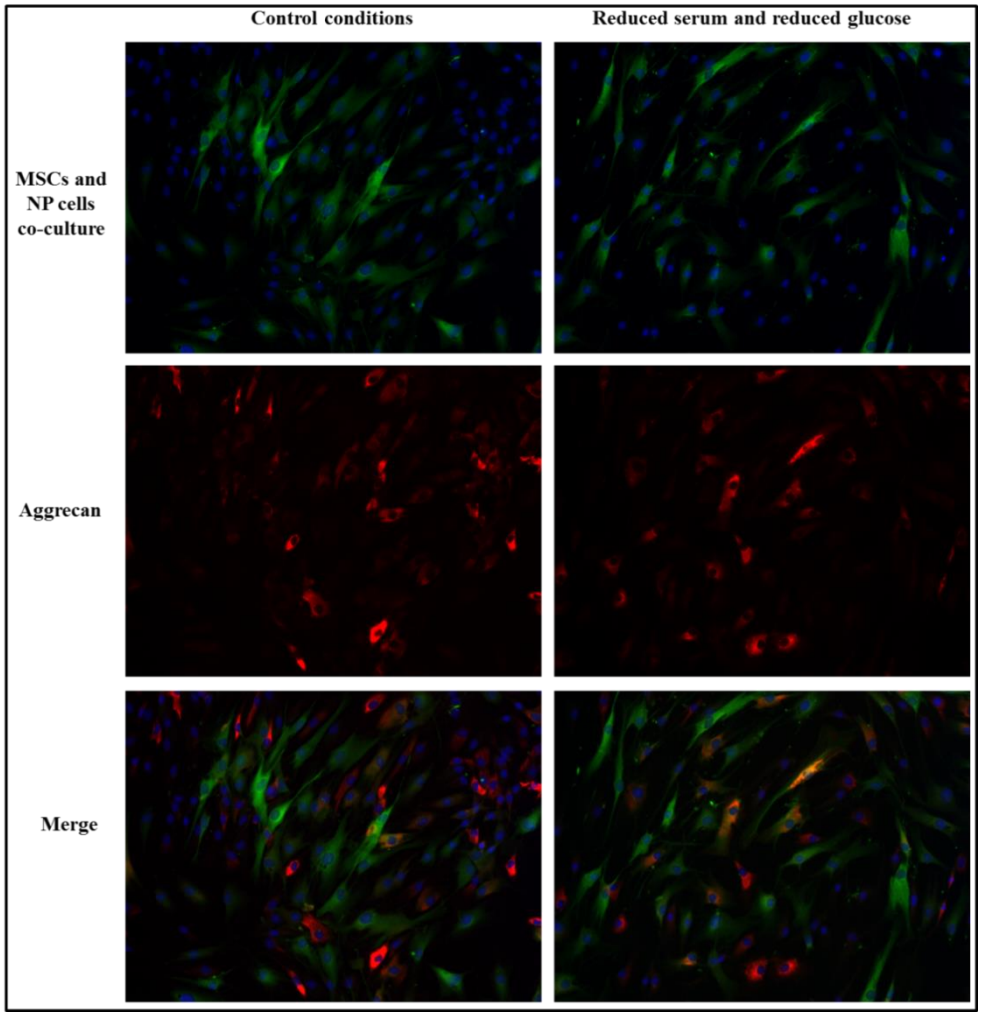

Figure 5.3.17 Representative images of aggrecan immunofluorescence staining of BM-MSC and degenerate NP cell co-culture (n=6) under control conditions (left panels) and reduced serum and reduced glucose (right panels). Immunofluorescence staining was performed after 7 days of co-culture using anti-aggrecan primary antibody followed by Alexa Fluor 555 conjugated secondary antibody (red). DAPI (blue) was used for nucleus staining. Top row: DAPI and CFDA (green), middle row: same field of view with aggrecan staining, bottom row: merge of above two rows (magnification x200).

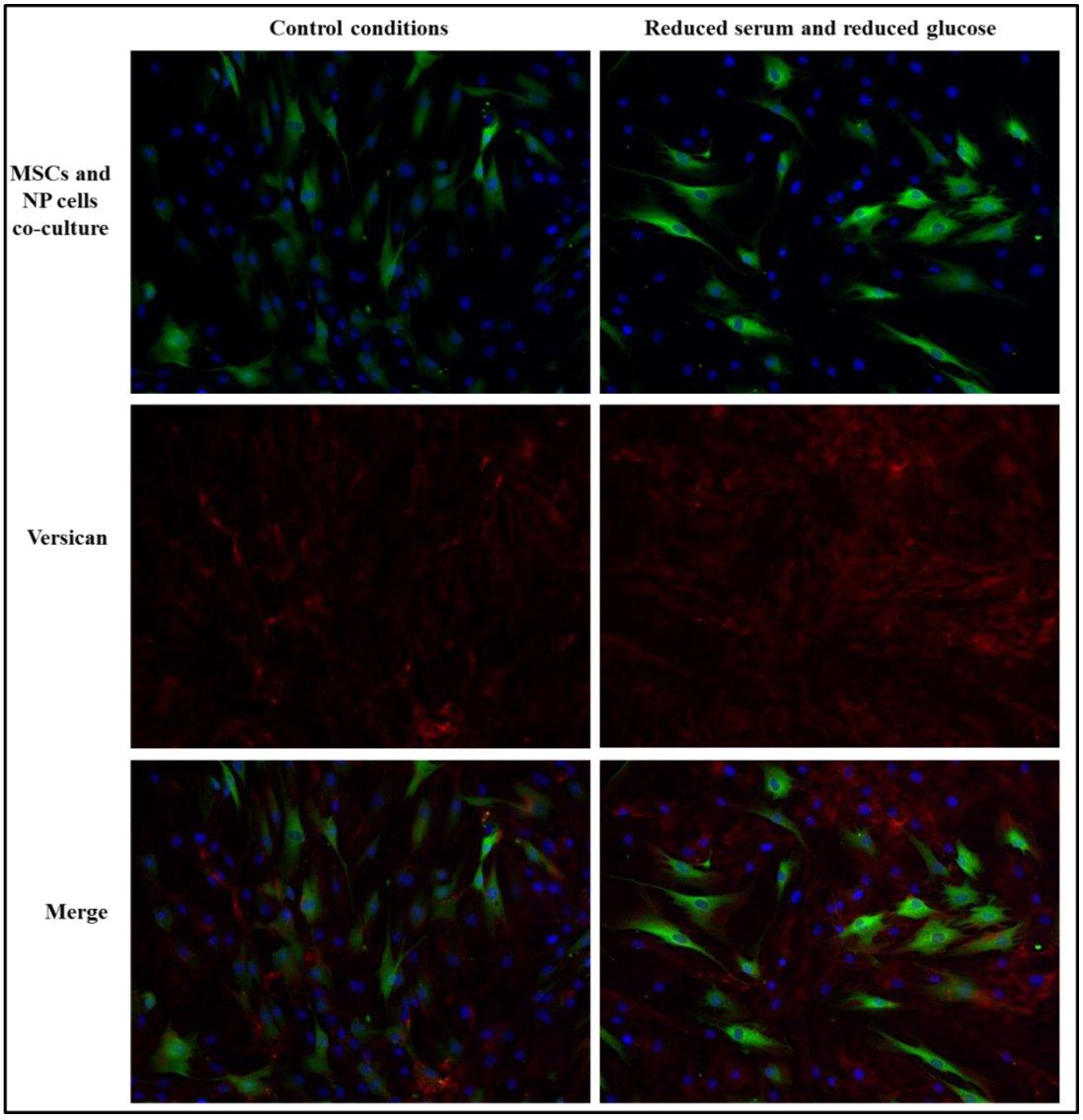

Figure 5.3.18 Representative images of versican immunofluorescence staining of BM-MSC and degenerate NP cell co-culture (n=9) under control conditions (left panels) and reduced serum and reduced glucose (right panels). Immunofluorescence staining was performed after 7 days of co-culture using anti-versican primary antibody followed by Alexa Fluor 555 conjugated secondary antibody (red). DAPI (blue) was used for nucleus staining. Top row: DAPI and CFDA (green), middle row: same field of view with versican staining, bottom row: merge of above two rows (magnification x200).

5.3.6 Influence of reduced serum and hypoxia on BM-MSC and degenerate NP cell co-culture

5.3.6.1 Gene expression in BM-MSCs co-cultured with degenerate NP cells under reduced serum and hypoxia

BM-MSCs co-cultured with degenerate NP cells under reduced serum combined with hypoxia showed no change in SOX-9 expression but a significant increase in COL2A1 (p=0.05) expression compared to BM-MSCs co-cultured with degenerate NP cells under control conditions (Figure 5.3.19 A). ACAN and VCAN showed no change in expression (Figure 5.3.19 B). Significant increases in PAX-1 and FOXF1 expression (p<0.05 for both) were observed under reduced serum combined with hypoxia compared to BM-MSCs co-cultured with degenerate NP cells under control conditions (Figure 5.3.19 C).

5.3.6.2 Gene expression in degenerate NP cells co-cultured with BM-MSCs under reduced serum and hypoxia

Degenerate NP cells co-cultured with BM-MSCs under reduced serum combined with hypoxia showed significant up regulation in all NP conventional (SOX-9, COL2A1, ACAN, VCAN) and novel markers (PAX-1, FOXF1) (p<0.05 for each) compared with degenerate NP cells co-cultured with MSCs under control conditions (Figure 5.3.20).

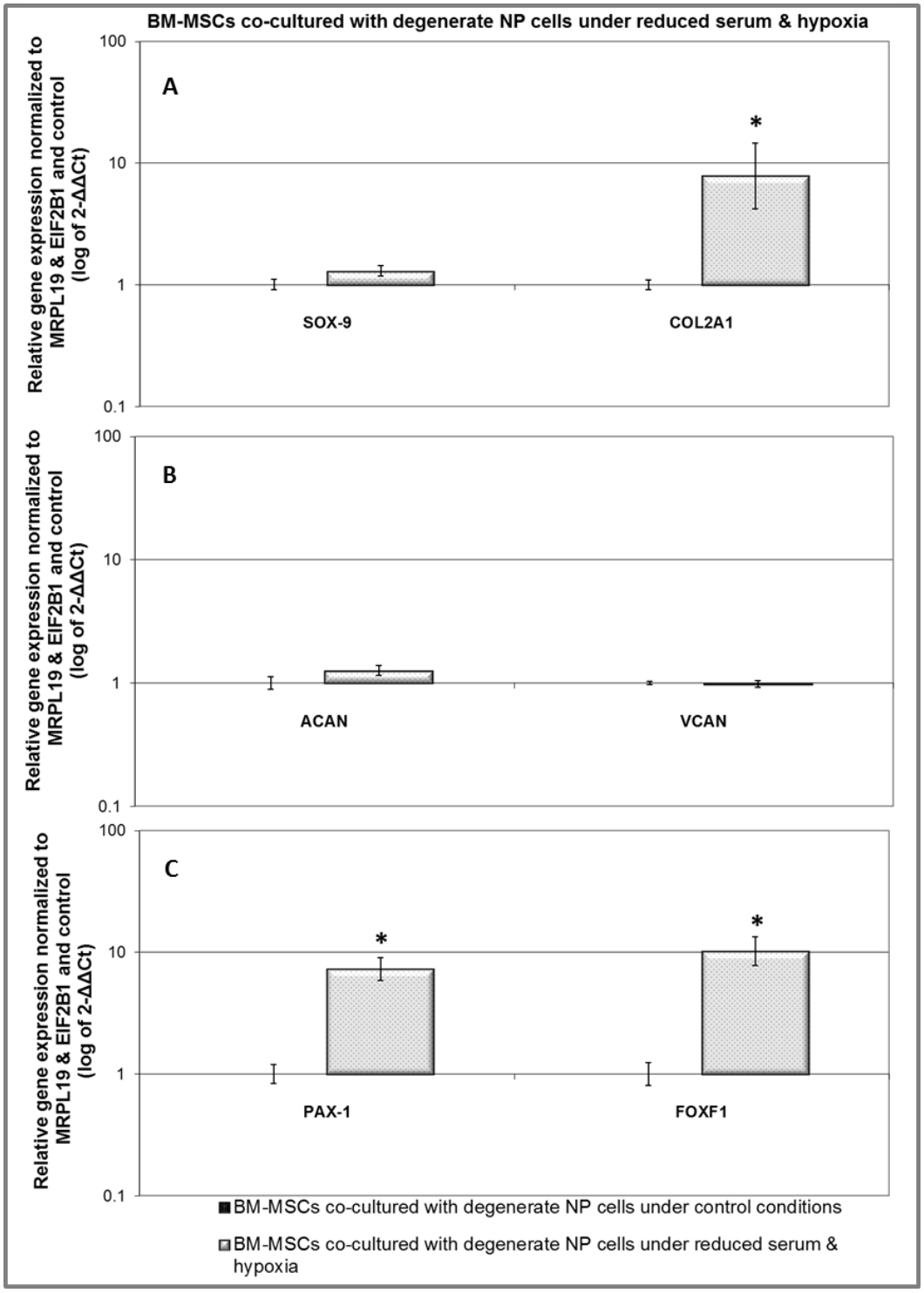

Figure 5.3.19 Relative gene expression of NP conventional markers (A) SOX-9, COL2A1 (B) ACAN, VCAN and NP novel markers (C) PAX-1 and FOXF-1 in BM-MSCs co-cultured with degenerate NP cells under reduced serum and hypoxia (n=8). Gene expression normalized to average of HK genes MRPL19 and EIF2B1 and BM-MSCs co-cultured with degenerate NP cells under control conditions (level expressed as 1) and plotted on a log scale. * Statistical significance ($p \leq 0.05$) compared to BM-MSCs co-cultured under control conditions.

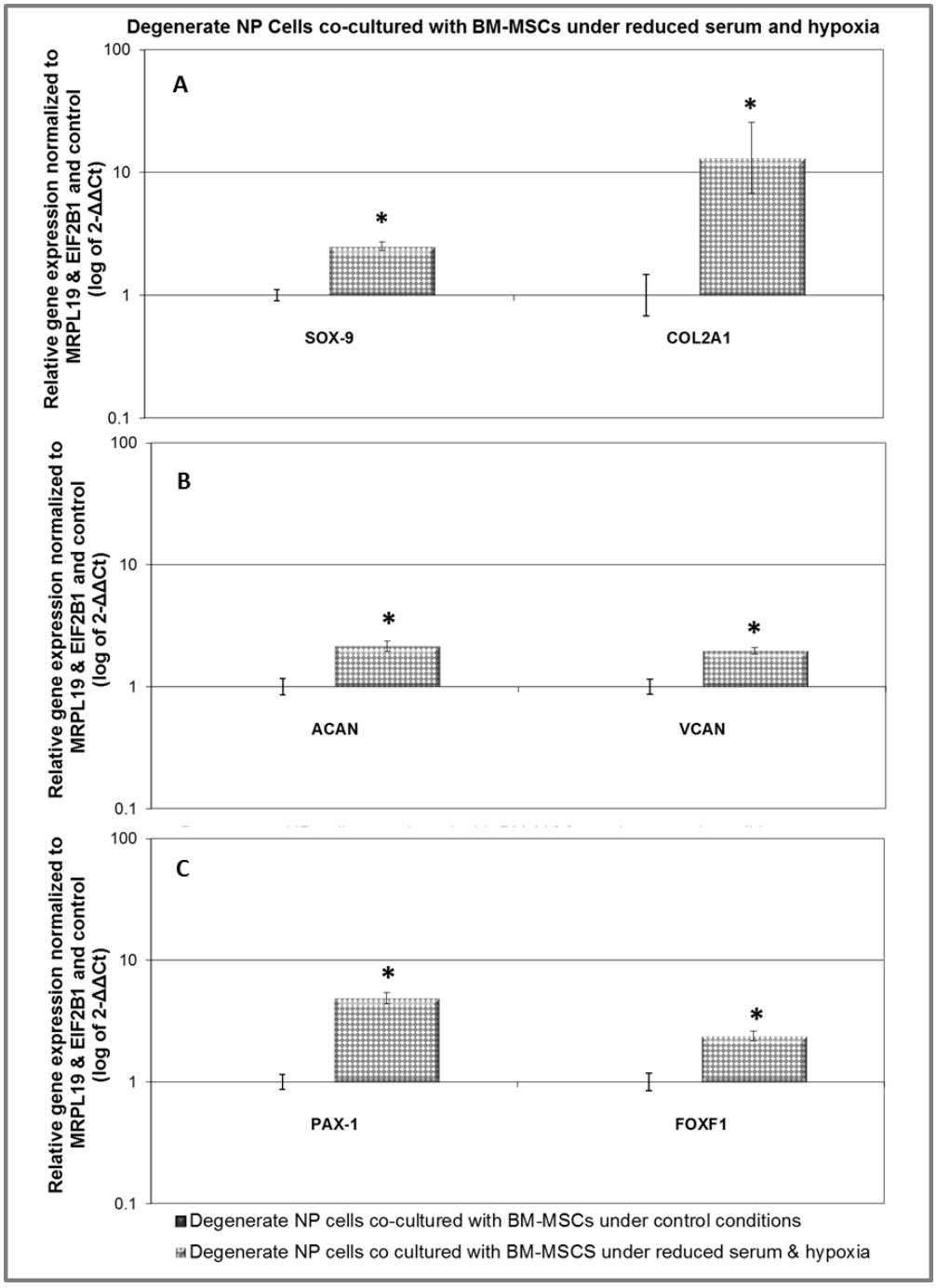

Figure 5.3.20 Relative gene expression of NP conventional markers (A) SOX-9. COL2A1 (B) ACAN, VCAN and NP novel markers (C) PAX-1 and FOXF-1 in degenerate NP cells co-cultured with BM-MSCs under reduced serum and hypoxia (n=8). Gene expression normalized to average of HK genes MRPL19 and EIF2B1 and degenerate NP cells co-cultured with BM-MSCs under control conditions (level expressed as 1) and plotted on a log scale. * Statistical significance ($p \leq 0.05$) compared to degenerate NP cells co-cultured under control conditions.

5.3.6.3 ECM protein expression in BM-MSC and degenerate NP cell co-culture under reduced serum and hypoxia

BM-MSC and degenerate NP cell co-culture under reduced serum and hypoxia showed positive staining of both aggrecan and versican protein comparable to co-culture under control conditions (Figure 5.3.21 & 5.3.22).

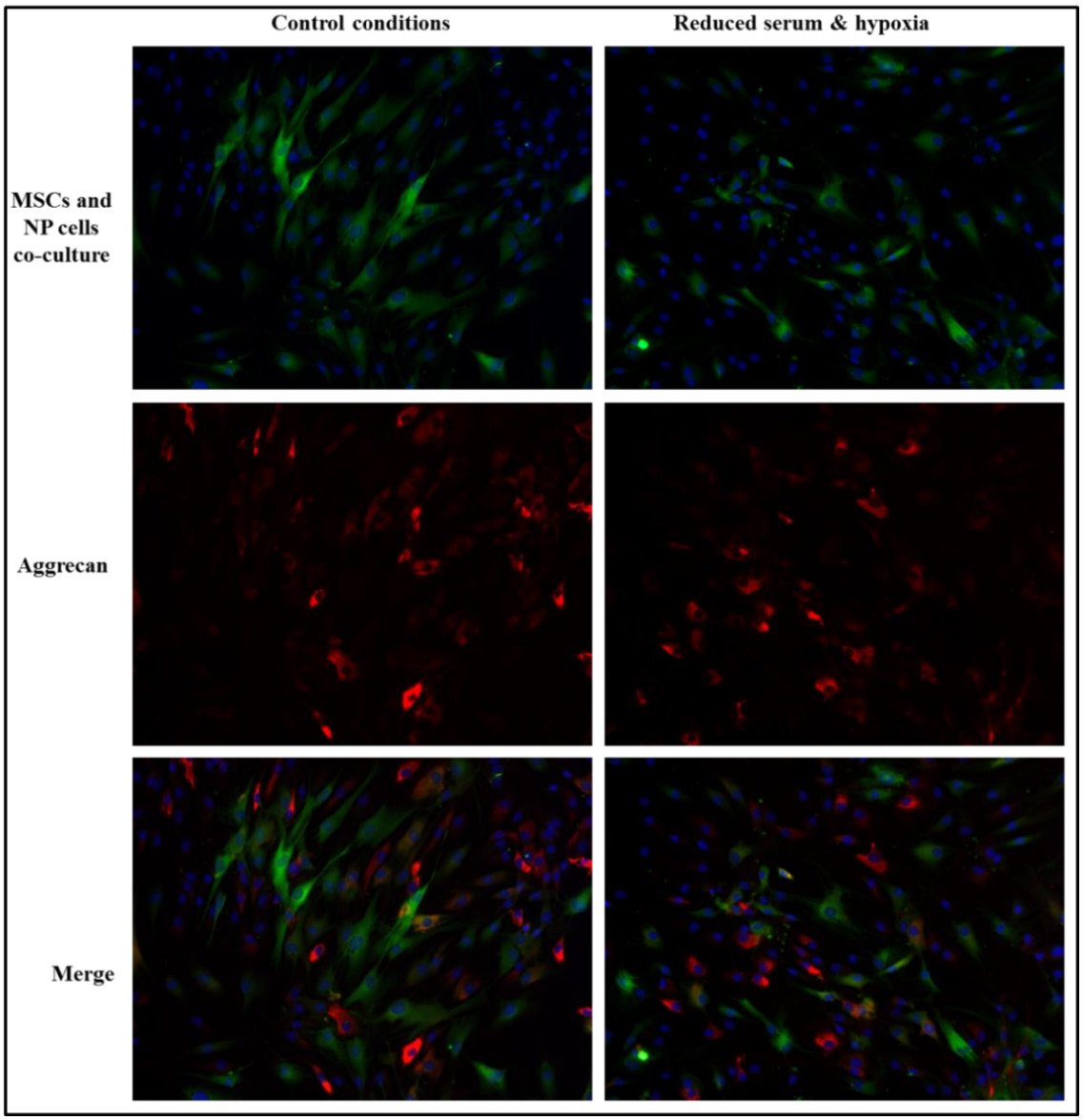

Figure 5.3.21 Representative images of aggrecan immunofluorescence staining of BM-MSC and degenerate NP cell co-culture (n=6) under control conditions (left panels) and reduced serum and hypoxia (right panels). Immunofluorescence staining was performed after 7 days of co-culture using anti-aggrecan primary antibody followed by Alexa Fluor 555 conjugated secondary antibody (red). DAPI (blue) was used for nucleus staining. Top row: DAPI and CFDA (green), middle row: same field of view with aggrecan staining, bottom row: merge of above two rows (magnification x200).

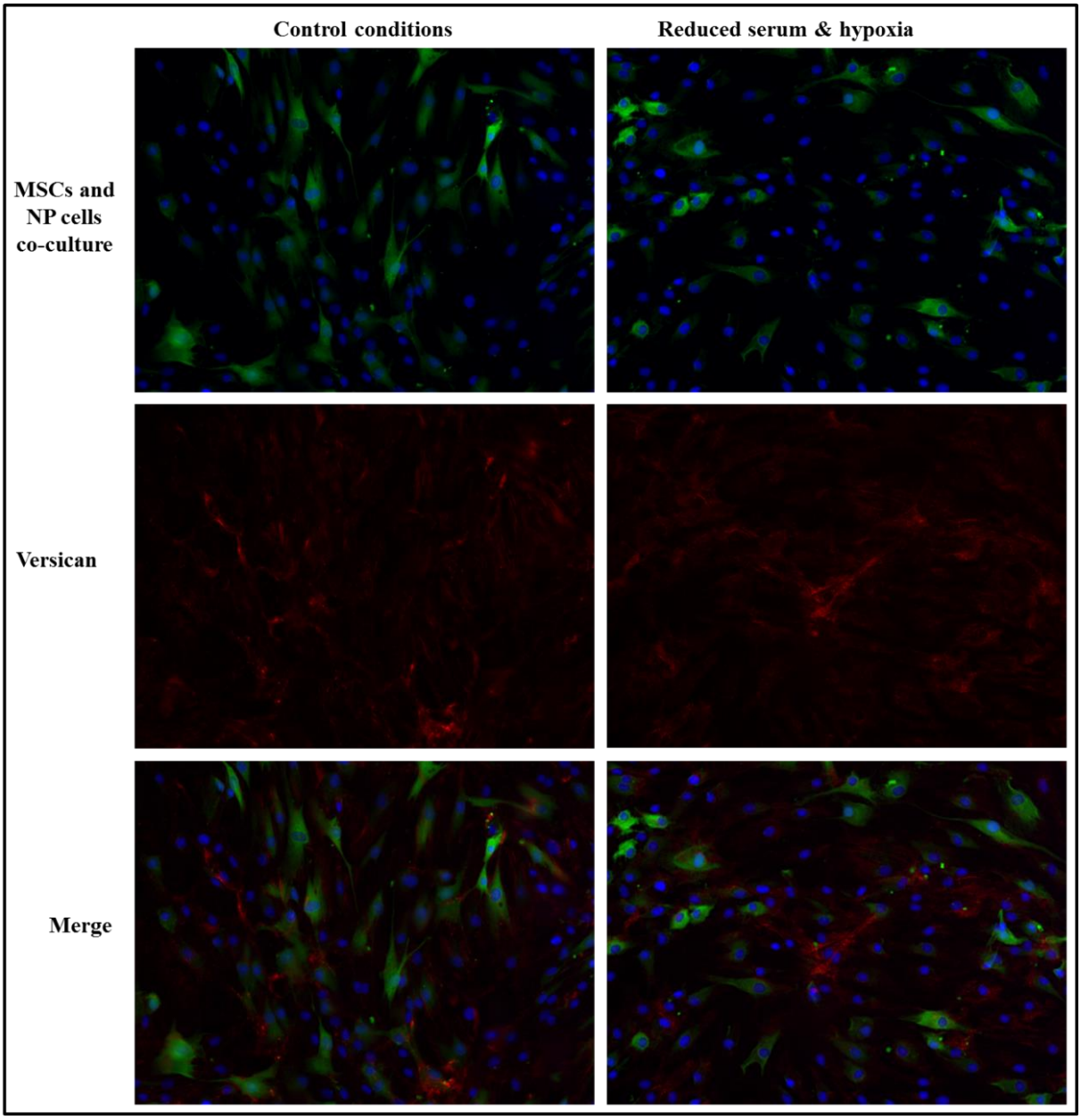

Figure 5.3.22 Representative images of versican immunofluorescence staining of BM-MSC and degenerate NP cell co-culture (n=9) under control conditions (left panels) and reduced serum and hypoxia (right panels). Immunofluorescence staining was performed after 7 days of co-culture using anti-versican primary antibody followed by Alexa Fluor 555 conjugated secondary antibody (red). DAPI (blue) was used for nucleus staining. Top row: DAPI and CFDA (green), middle row: same field of view with versican staining, bottom row: merge of above two rows (magnification x200).

5.3.7 Influence of reduced glucose and hypoxia on BM-MSC and degenerate NP cell co-culture

5.3.7.1 Gene expression in BM-MSCs co-cultured with degenerate NP cells under reduced glucose and hypoxia

BM-MSCs co-cultured with degenerate NP cells showed no changes in SOX-9 and COL2A1 expression under reduced glucose combined with hypoxia compared to BM-MSCs co-cultured with degenerate NP cells under control conditions (Figure 5.3.23 A). ACAN showed no significant change while VCAN had a significant increase in expression ($p<0.05$) under reduced glucose combined with hypoxia (Figure 5.3.23 B). There was no change in PAX-1 and FOXF1 expression compared to control conditions (Figure 5.3.23 C).

5.3.7.2 Gene expression in degenerate NP cells co-cultured with BM-MSCs under reduced glucose and hypoxia

Degenerate NP cells co-cultured with BM-MSCs under reduced glucose combined with hypoxia showed no difference in expression of all NP conventional (SOX-9, COL2A1, ACAN, VCAN) and novel markers (PAX-1, FOXF1) compared with degenerate NP co-cultured with MSCs under control conditions (Figure 5.3.24).

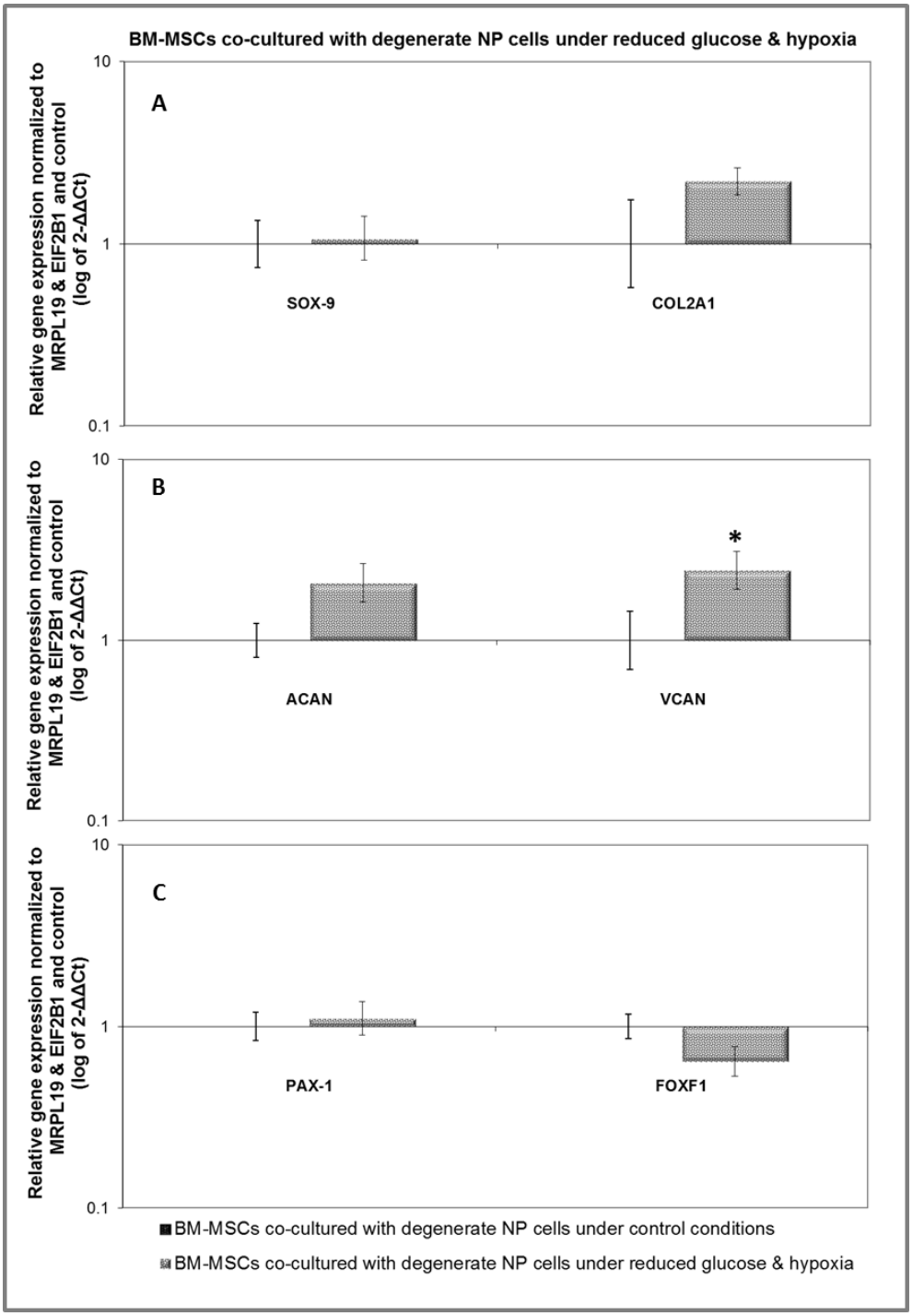

Figure 5.3.23 Relative gene expression of NP conventional markers (A) SOX-9, COL2A1 (B) ACAN, VCAN and NP novel markers (C) PAX-1 and FOXF-1 in BM-MSCs co-cultured with degenerate NP cells under reduced glucose and hypoxia (n=4). Gene expression normalized to average of HK genes MRPL19 and EIF2B1 and BM-MSCs co-cultured with degenerate NP cells under control conditions (level expressed as 1) and plotted on a log scale. * Statistical significance ($p \leq 0.05$) compared to BM-MSCs co-cultured under control conditions.

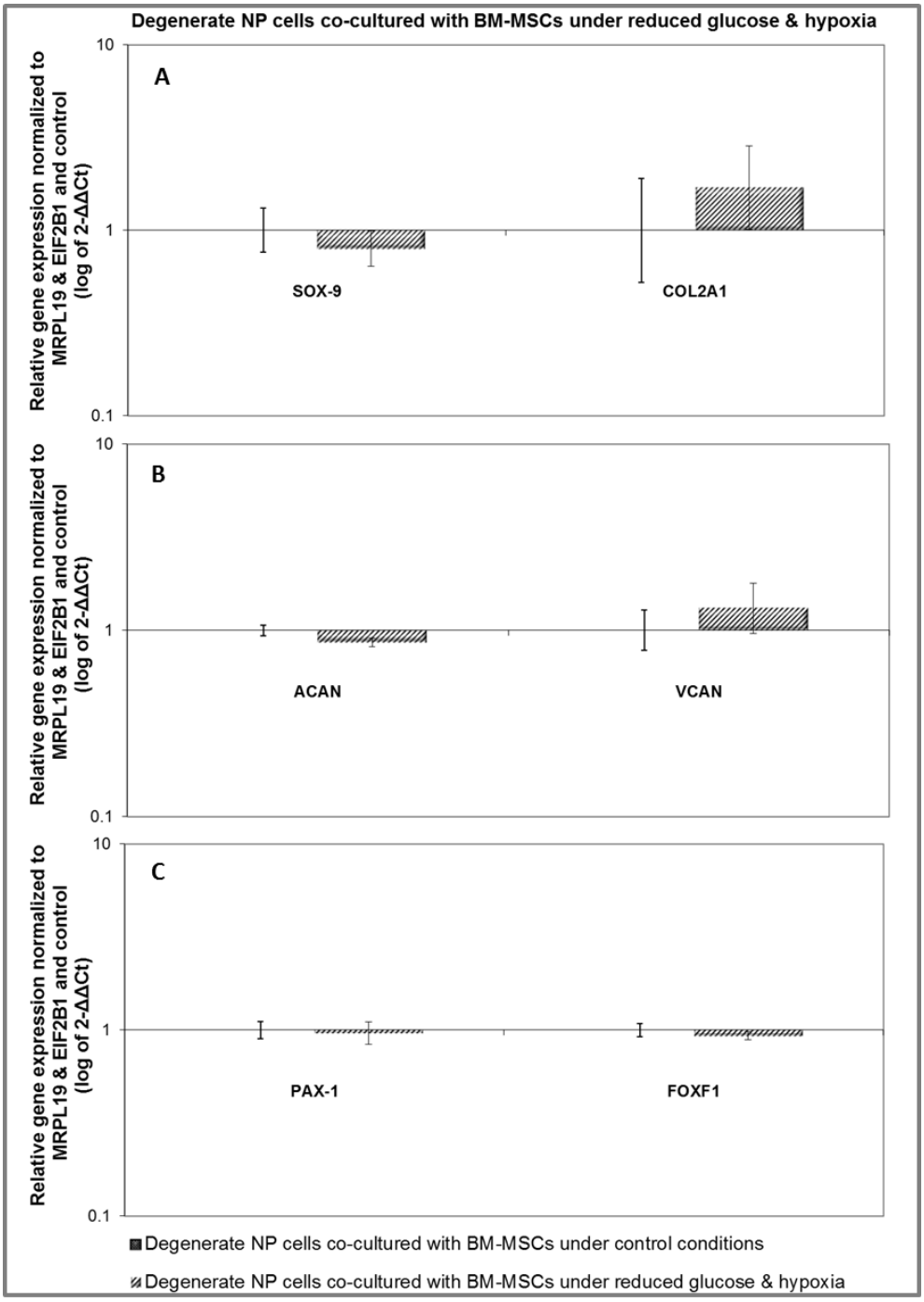

Figure 5.3.24 Relative gene expression of NP conventional markers (A) SOX-9, COL2A1 (B) ACAN, VCAN and NP novel markers (C) PAX-1 and FOXF-1 in degenerate NP cells co-cultured with BM-MSCs under reduced glucose and hypoxia (n=4). Gene expression normalized to average of HK genes MRPL19 and EIF2B1 and degenerate NP cells co-cultured with BM-MSCs under control conditions (level expressed as 1) and plotted on a log scale. * Statistical significance ($p \leq 0.05$) compared to degenerate NP cells co-cultured under control conditions.

5.3.7.3 ECM protein expression in BM-MSC and degenerate NP cell co-culture under reduced glucose and hypoxia

BM-MSC and degenerate NP cell co-culture under reduced glucose combined with hypoxia showed slight increase staining intensity of aggrecan protein compared to control conditions (Figure 5.3.25). Substantially more intense staining of versican protein was seen in BM-MSC and degenerate NP cell co-culture under reduced glucose combined with hypoxia compared to control conditions (Figure 5.3.26).

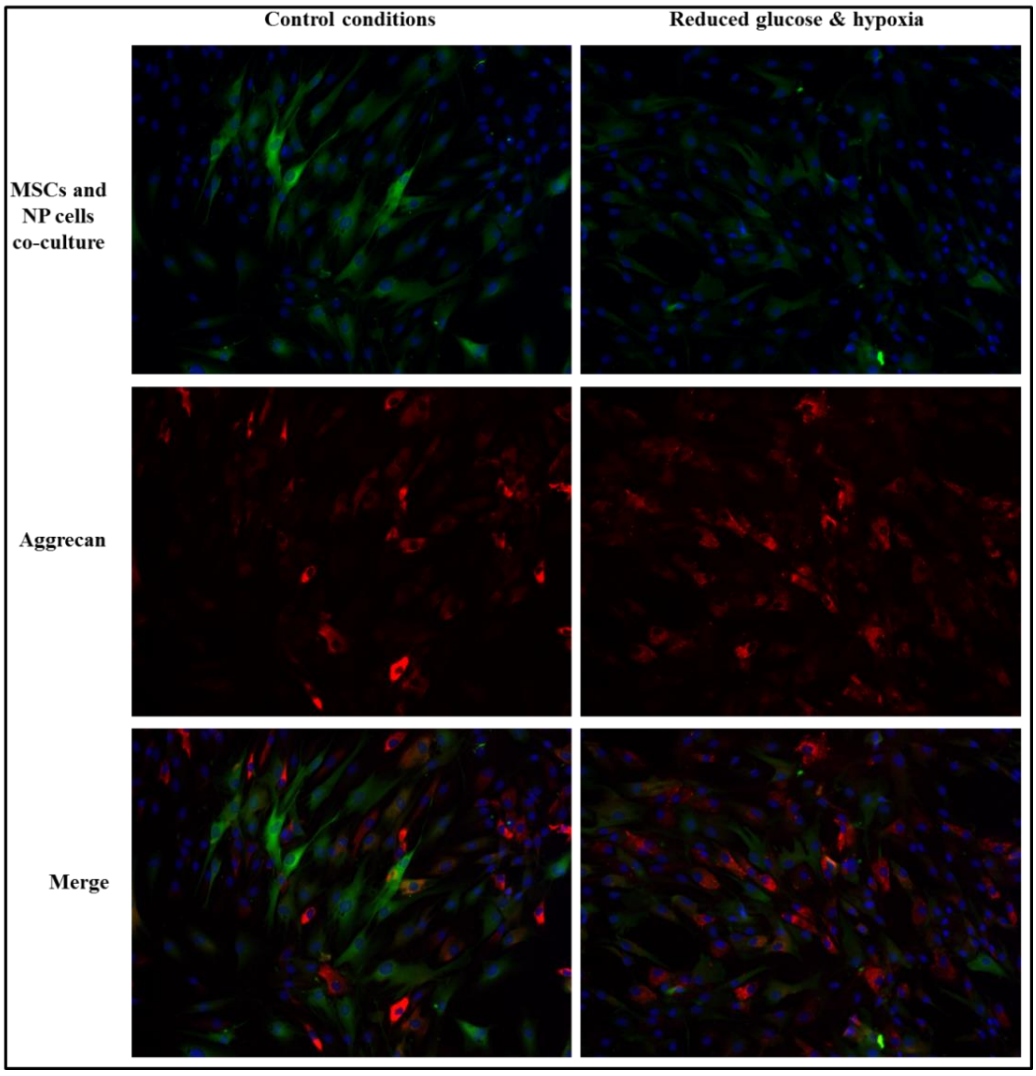

Figure 5.3.25 Representative images of aggrecan immunofluorescence staining of BM-MSC and degenerate NP cell co-culture (n=6) under control conditions (left panels) and reduced glucose and hypoxia (right panels). Immunofluorescence staining was performed after 7 days of co-culture using anti-aggrecan primary antibody followed by Alexa Fluor 555 conjugated secondary antibody (red). DAPI (blue) was used for nucleus staining. Top row: DAPI and CFDA (green), middle row: same field of view with aggrecan staining, bottom row: merge of above two rows (magnification x200).

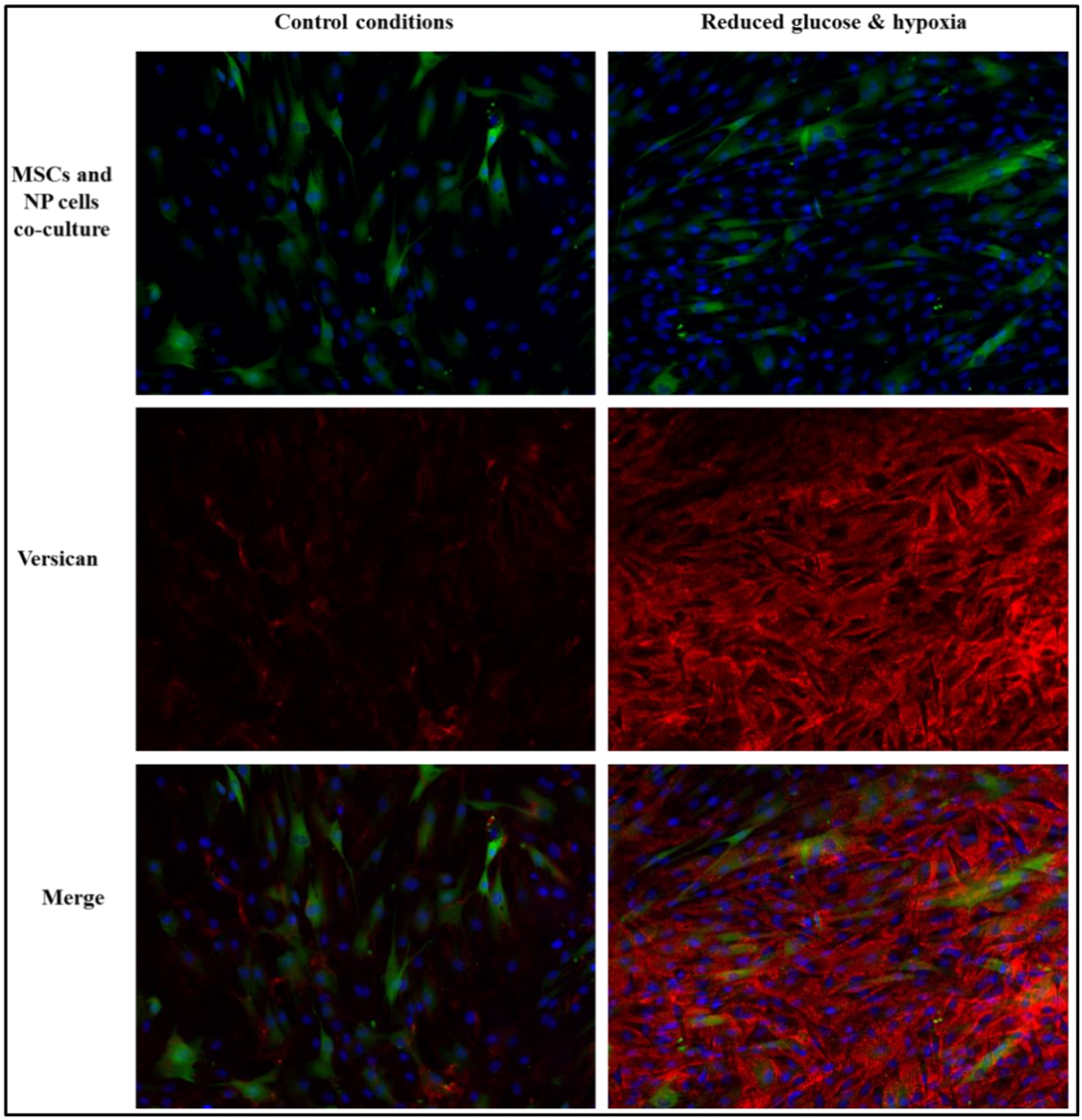

Figure 5.3.26 Representative images of versican immunofluorescence staining of BM-MSC and degenerate NP cell co-culture (n=9) under control conditions (left panels) and reduced glucose and hypoxia (right panels). Immunofluorescence staining was performed after 7 days of co-culture using anti-versican primary antibody followed by Alexa Fluor 555 conjugated secondary antibody (red). DAPI (blue) was used for nucleus staining. Top row: DAPI and CFDA (green), middle row: same field of view with versican staining, bottom row: merge of above two rows (magnification x200).

5.3.8 Influence of reduced serum, reduced glucose and hypoxia on BM-MSC and degenerate NP cell co-culture

5.3.8.1 Gene expression in BM-MSCs co-cultured with degenerate NP cells under reduced serum, reduced glucose and hypoxia

BM-MSCs co-cultured with degenerate NP cells under reduced serum, reduced glucose and hypoxia showed no significant changes in expression of all NP conventional markers (Figure 5.3.27 A & B). A significant decrease in PAX-1 expression ($p<0.05$) was seen under reduced serum and reduced glucose combined with hypoxia. FOXF1 expression however, was significantly increased ($p<0.05$) compared to BM-MSCs co-cultured with degenerate NP cells under control conditions (Figure 5.3.27 C).

5.3.8.2 Gene expression in degenerate NP cells co-cultured with BM-MSCs under reduced serum, reduced glucose and hypoxia

Degenerate NP cells co-cultured with BM-MSCs under reduced serum, reduced glucose and hypoxia showed a significant increase in SOX-9 expression with a significant decrease in COL2A1 expression ($p<0.05$ for each) compared to degenerate NP cells co-cultured with BM-MSCs under control conditions (Figure 5.3.28 A). ACAN and VCAN expression showed no difference in expression compared to control conditions (Figure 5.3.28 B). PAX-1 expression was significantly decreased ($p<0.05$) while FOXF1 expression was significantly increased ($p<0.05$) under reduced serum, reduced glucose and hypoxia Figure 5.3.28 C).

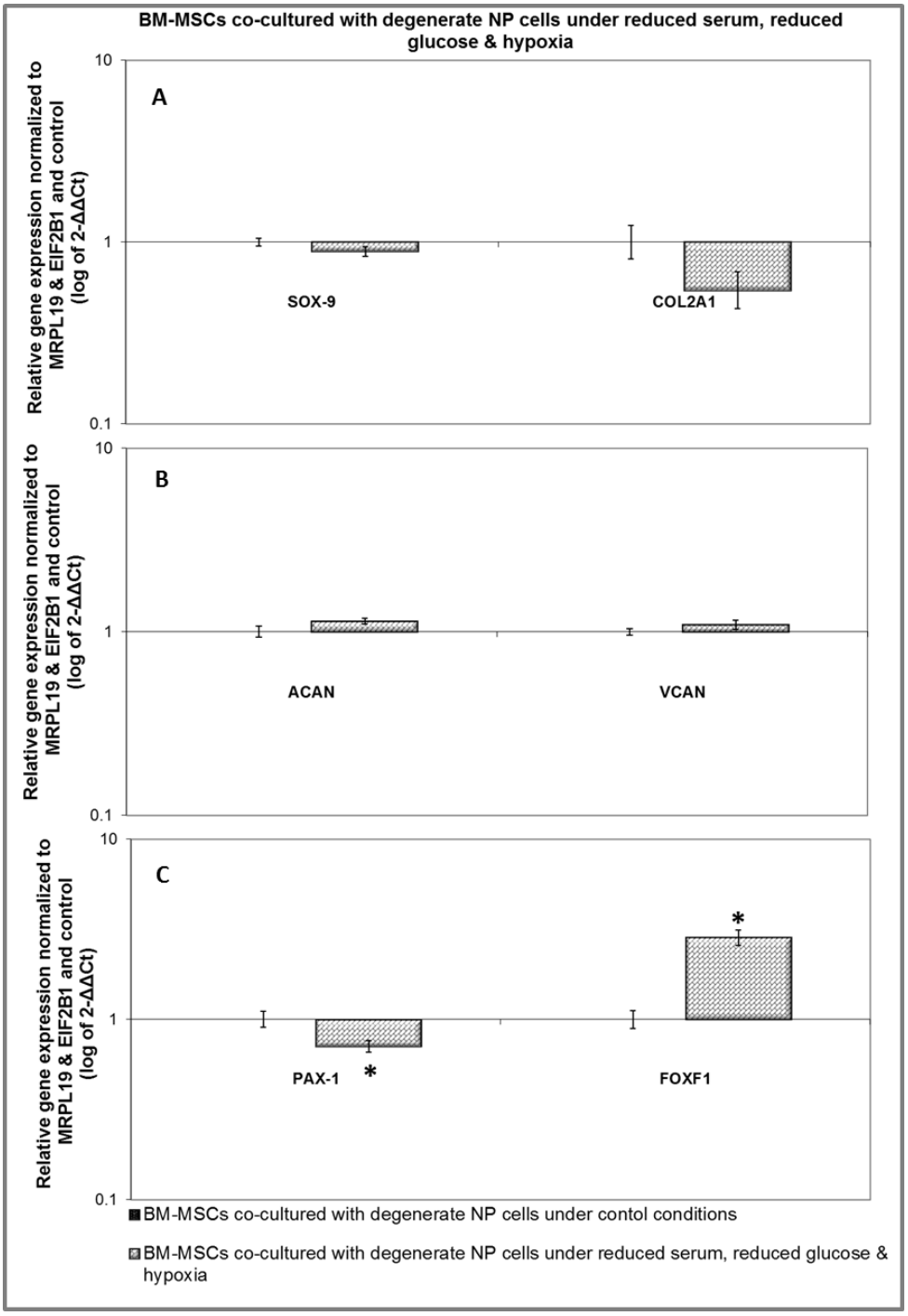

Figure 5.3.27 Relative gene expression of NP conventional markers (A) SOX-9, COL2A1 (B) ACAN, VCAN and NP novel markers (C) PAX-1 and FOXF-1 in BM-MSCs co-cultured with degenerate NP cells under reduced serum, reduced glucose and hypoxia (n=9). Gene expression normalized to average of HK genes MRPL19 and EIF2B1 and BM-MSCs co-cultured with degenerate NP cells under control conditions (level expressed as 1) and plotted on a log scale. * Statistical significance ($p \leq 0.05$) compared to BM-MSCs co-cultured under control conditions.

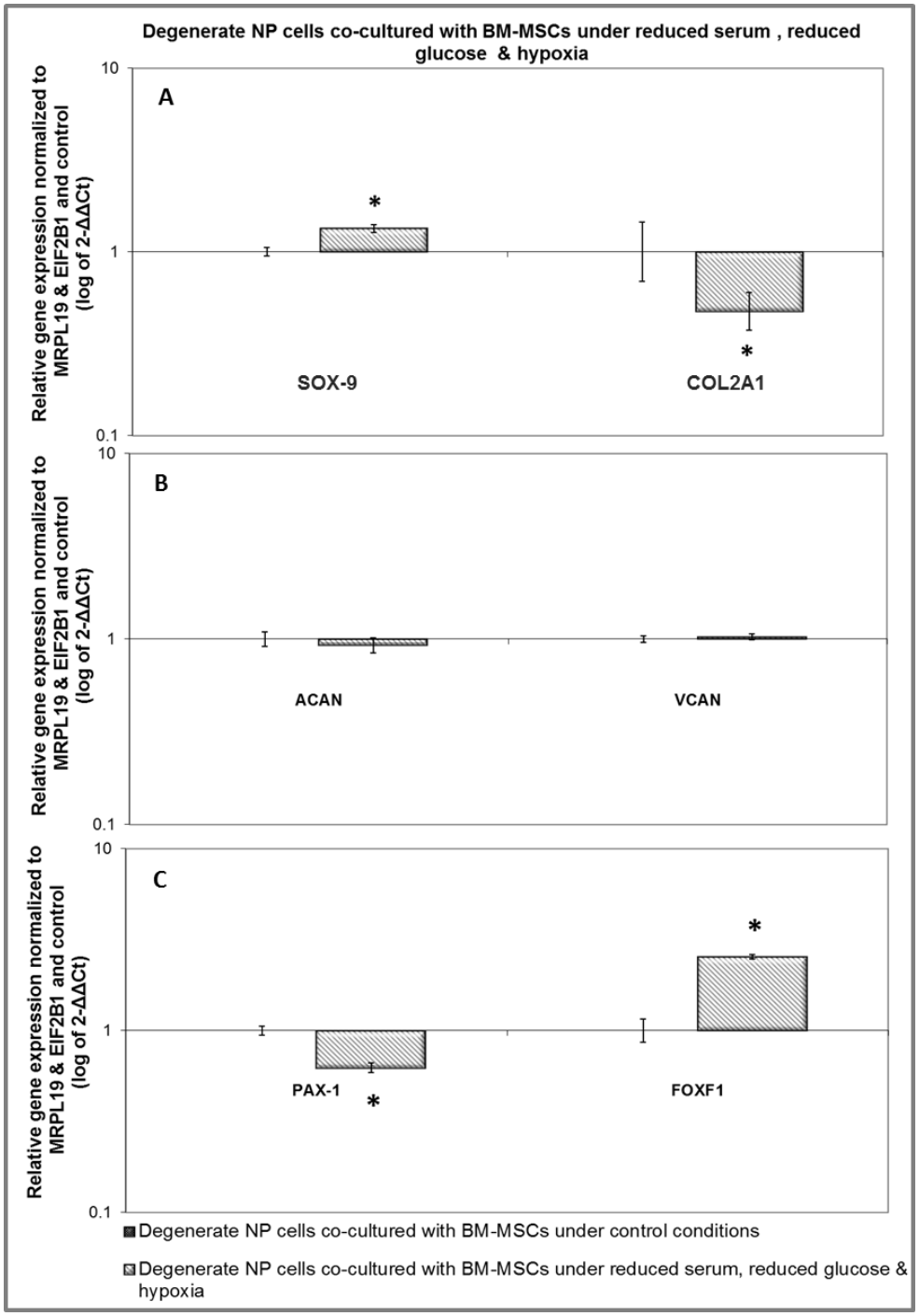

Figure 5.3.28 Relative gene expression of NP conventional markers (A) SOX-9, COL2A1 (B) ACAN, VCAN and NP novel markers (C) PAX-1 and FOXF-1 in degenerate NP cells co-cultured with BM-MSCs under reduced serum, reduced glucose and hypoxia (n=9). Gene expression normalized to average of HK genes MRPL19 and EIF2B1 and degenerate NP cells co-cultured with BM-MSCs under control conditions (level expressed as 1) and plotted on a log scale. * Statistical significance ($p \leq 0.05$) compared to degenerate NP cells co-cultured under control conditions.

5.3.8.3 ECM protein expression in BM-MSC and degenerate NP cell co-culture under reduced serum, reduced glucose and hypoxia

BM-MSC and degenerate NP cell co-culture under reduced serum and reduced glucose both combined with hypoxia showed decreased staining intensity of aggrecan protein compared to control conditions (Figure 5.3.29). However, BM-MSC and degenerate NP cell co-culture under reduced serum, reduced glucose and hypoxia showed staining intensity of versican protein comparable to co-culture under control conditions (Figure 5.3.30).

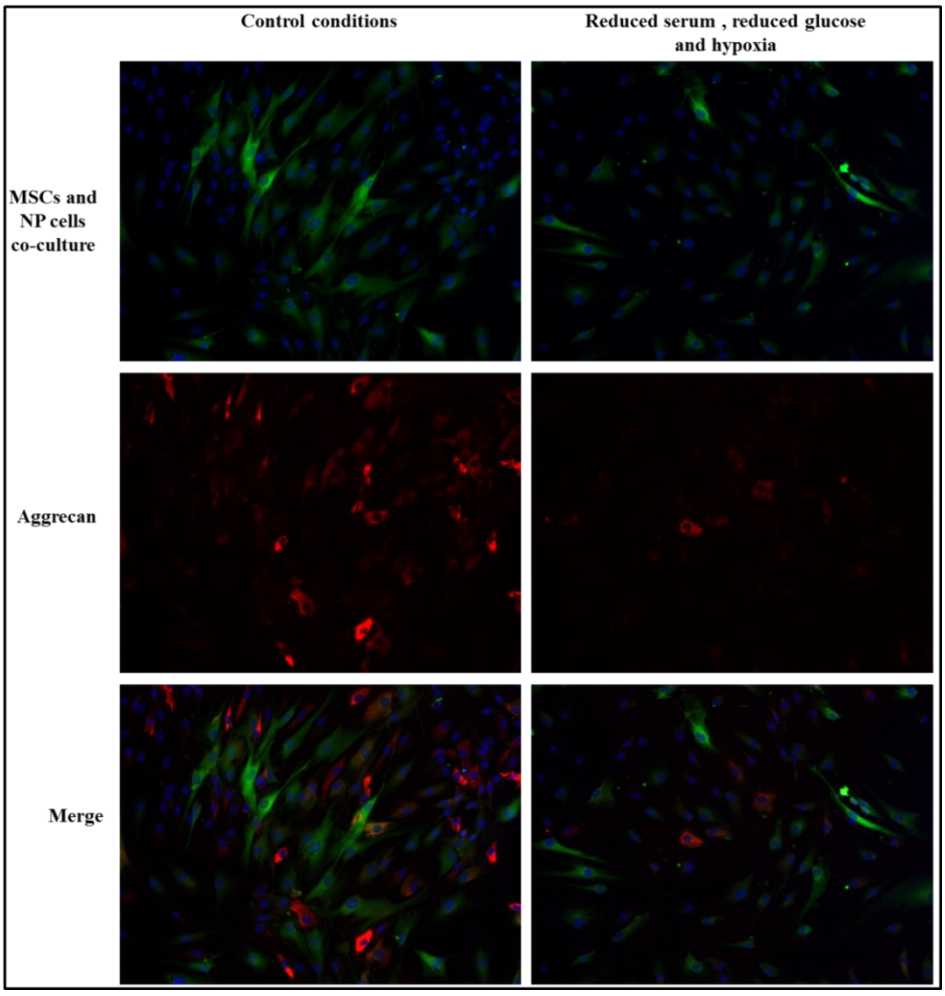

Figure 5.3.29 Representative images of aggrecan immunofluorescence staining of BM-MSC and degenerate NP cell co-culture (n=3) under control conditions (left panels) and reduced serum, reduced glucose and hypoxia (right panels). Immunofluorescence staining was performed after 7 days of co-culture using anti-aggrecan primary antibody followed by Alexa Fluor 555 conjugated secondary antibody (red). DAPI (blue) was used for nucleus staining. Top row: DAPI and CFDA (green), middle row: same field of view with aggrecan staining, bottom row: merge of above two rows (magnification x200).

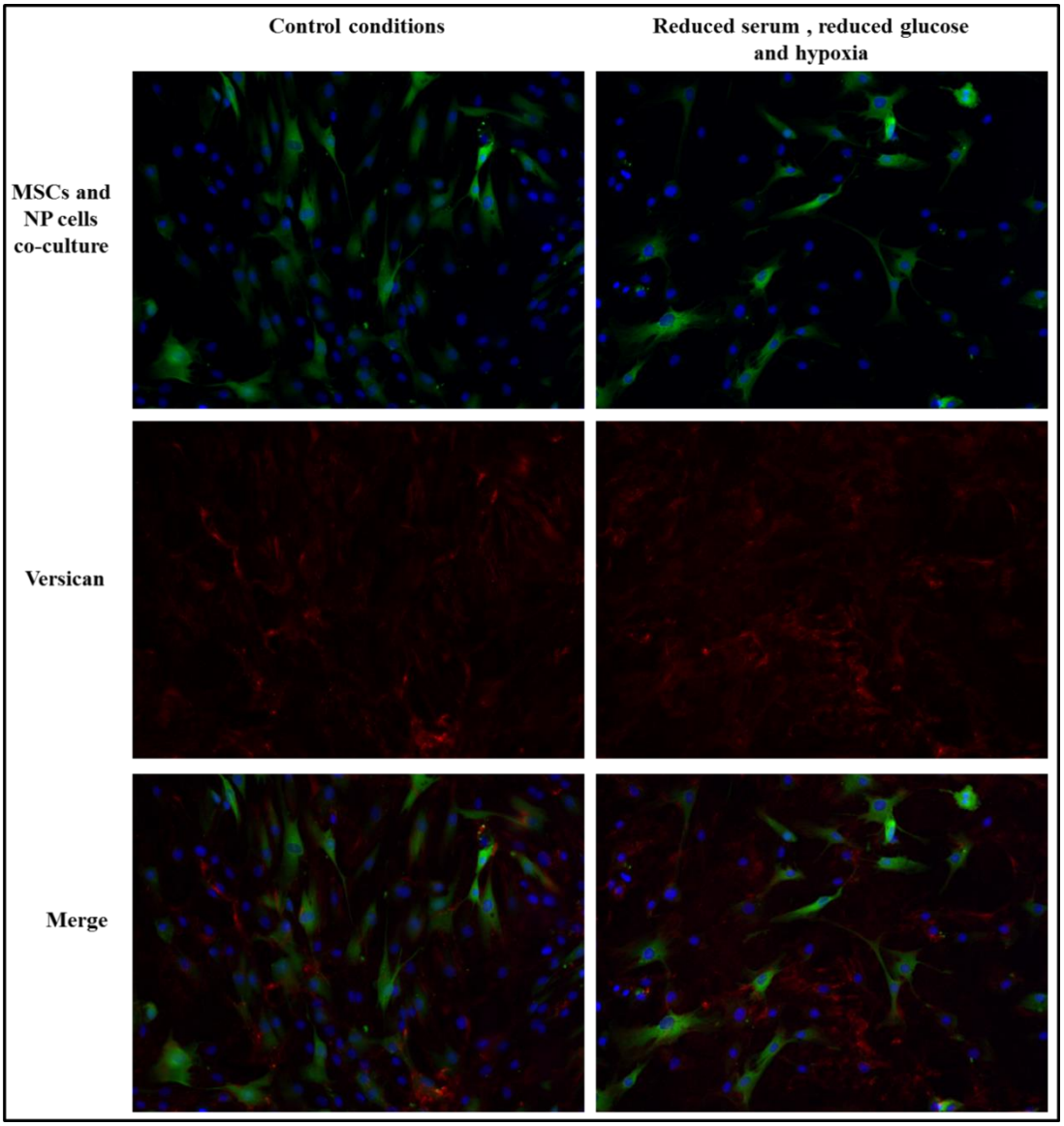

Figure 5.3.30 Representative images of versican immunofluorescence staining of BM-MSC and degenerate NP cell co-culture (n=3) under control conditions (left panels) and reduced serum and reduced glucose and hypoxia (right panels). Immunofluorescence staining was performed after 7 days of co-culture using anti-versican primary antibody followed by Alexa Fluor 555 conjugated secondary antibody (red). DAPI (blue) was used for nucleus staining. Top row: DAPI and CFDA (green), middle row: same field of view with versican staining, bottom row: merge of above two rows (magnification x200).

5.3.9 Influence of reduced pH on BM-MSC and degenerate NP cell co-culture

5.3.9.1 Gene expression in BM-MSCs co-cultured with degenerate NP cells under reduced pH

BM-MSCs co-cultured with degenerate NP cells both under pH 6.8 and 6.5 showed a significant increase ($p<0.05$) in SOX-9 expression with no change in COL2A1 expression compared to BM-MSCs co-cultured with degenerate NP cells under control conditions (Figure 5.3.31 A). A significant decrease in ACAN gene expression was observed under both pH 6.8 ($p<0.05$) and pH 6.5 ($p<0.05$). There was no difference in VCAN gene expression at pH 6.8 although a significant decrease ($p<0.05$) was seen following culture at pH 6.5 (Figure 5.3.31 B). Gene expression for both genes was significantly ($p<0.05$) decreased at pH 6.5 compared to pH 6.8. PAX-1 expression did not change at pH 6.8 but it was significantly down regulated ($p<0.05$) at pH 6.5 compared to control and pH 6.8. A significant increase in FOXF1 expression ($p<0.05$) was observed under both pH 6.8 and pH 6.5 with larger increase under pH 6.5 (Figure 5.3.31 C). BM-MSCs co-cultured with degenerate NP cells under both pH 6.8 and 6.5 showed a significant up regulation ($p<0.05$) in both CA9 and CA12 (Figure 5.3.31 D). CA9 expression showed larger increase ($p<0.05$) under pH 6.5 compared to pH 6.8.

5.3.9.2 Gene expression in degenerate NP cells co-cultured with BM-MSCs under reduced pH

Degenerate NP cells co-cultured with BM-MSCs showed a significant decrease ($p<0.05$) in SOX-9 under pH 6.8 and a significant increase under pH 6.5 ($p<0.05$) compared to degenerate NP cells co-cultured with BM-MSCs under control conditions and pH 6.8 (Figure 5.3.32 A). There was no change in COL2A1 expression both under pH 6.8 and 6.5 (Figure 5.3.32 A). A significant decrease in ACAN and VCAN gene expression ($p<0.05$ for both) was observed under both pH 6.8 and pH 6.5 (Figure 5.3.32 B). ACAN gene expression was also significantly decreased ($p<0.05$) at pH 6.5 compared to pH 6.8. PAX-1 expression was significantly down regulated ($p<0.05$) in co-cultured NP cells under pH 6.8 but remained unaffected at pH 6.5. No significant difference was seen in FOXF1 expression under pH 6.8 but a significant increase ($p<0.05$) was seen at pH 6.5 compared to control conditions (Figure 5.3.32 C). Under pH 6.5 both PAX-1 and FOXF1 showed significant increase ($p<0.05$) expression compared to pH 6.8. Degenerate NP cells co-cultured with BM-MSCs under pH 6.8 showed a significant increase in CA9 ($p<0.05$) while CA12 expression showed no difference. CA9 and CA12 expression was significantly increased ($p<0.05$) at pH 6.5 compared to both control and pH 6.8 (Figure 5.3.32 D).

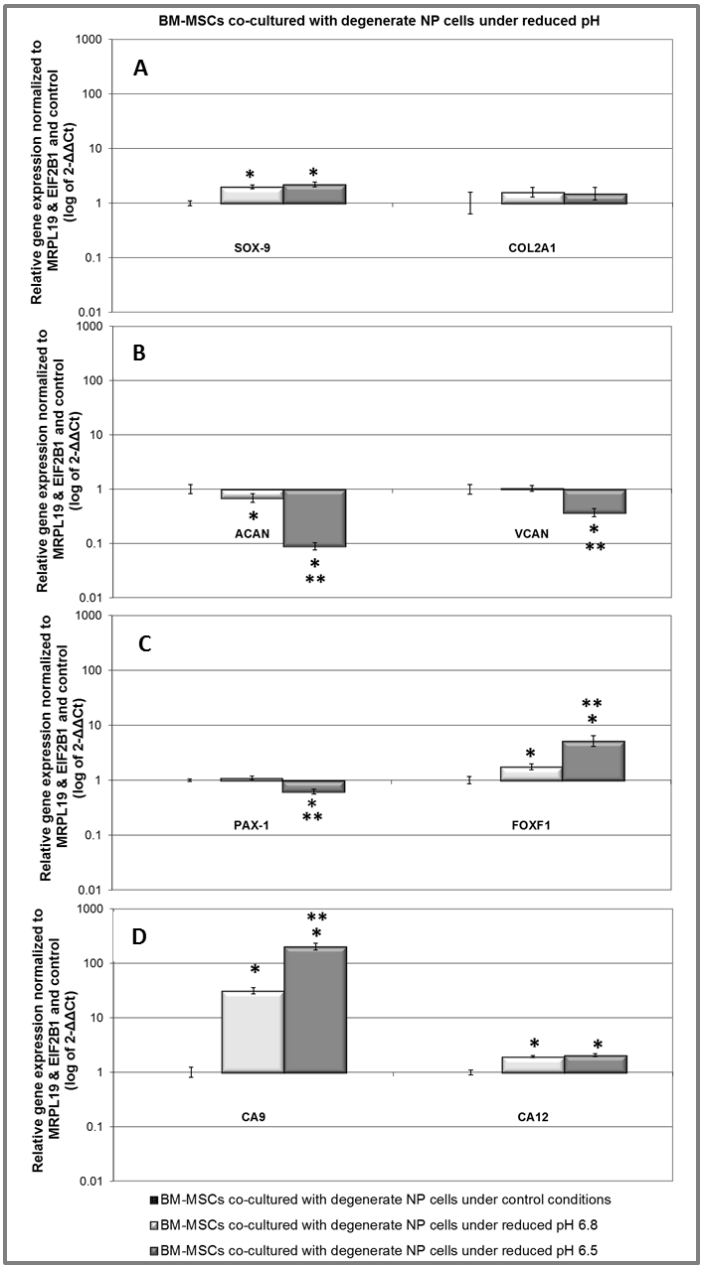

Figure 5.3.31 Relative gene expression of NP conventional markers (A) SOX-9, COL2A1 (B) ACAN, VCAN and NP novel markers (C) PAX-1 and FOXF-1 and (D) carbonic anhydrases CA9, CA12 in BM-MSCs co-cultured with degenerate NP cells under reduced pH 6.8 and 6.5 (n=8). Gene expression normalized to average of HK genes MRPL19 and EIF2B1 and BM-MSCs co-cultured with degenerate NP cells under control conditions (level expressed as 1) and plotted on a log scale. * Statistical significance ($p \leq 0.05$) compared to BM-MSCs co-cultured under control conditions.

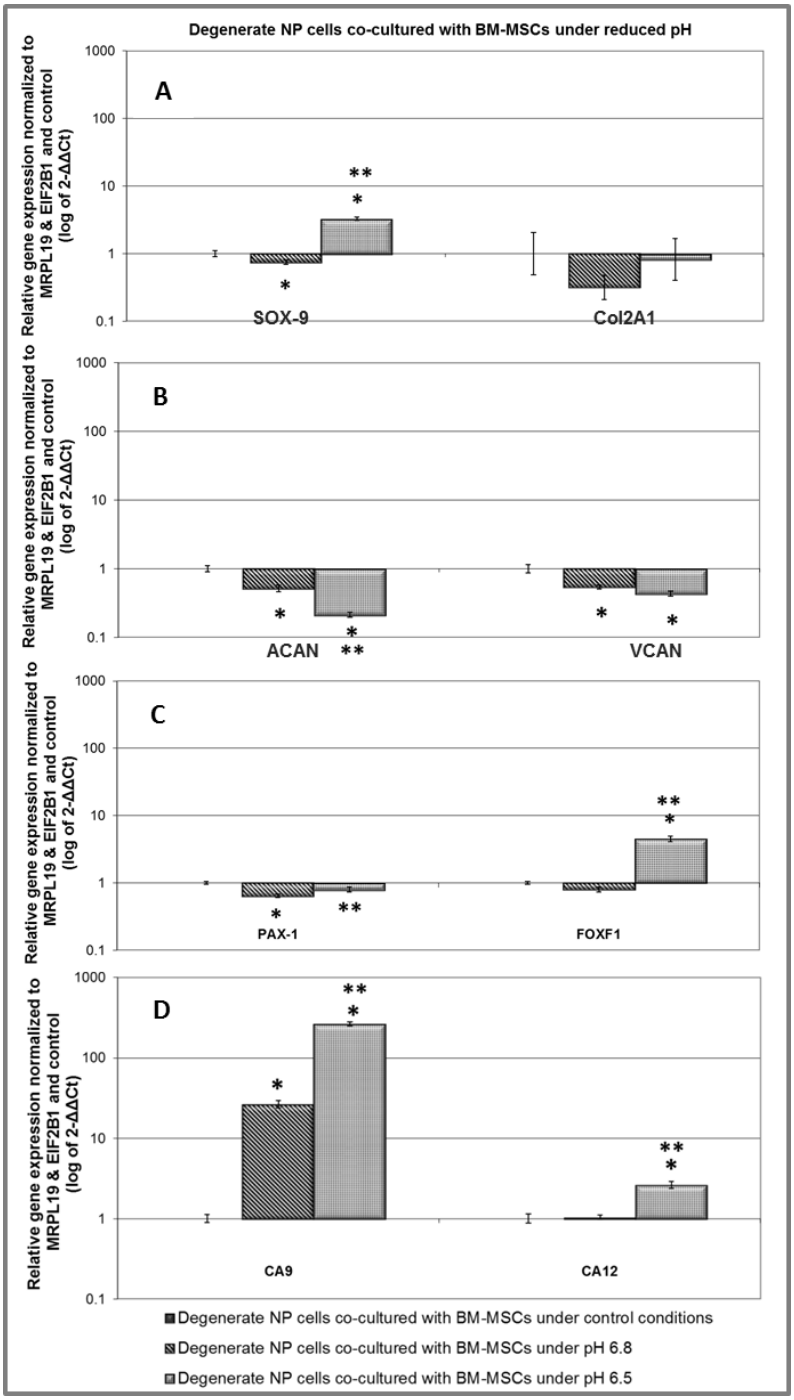

Figure 5.3.32 Relative gene expression of NP conventional markers (A) SOX-9, COL2A1 (B) ACAN, VCAN and NP novel markers (C) PAX-1 and FOXF-1 and (D) carbonic anhydrases CA9, CA12 in degenerate NP cells co-cultured with BM-MSCs under reduced pH 6.8 and 6.5 (n=8). Gene expression normalized to average of HK genes MRPL19 and EIF2B1 and degenerate NP cells co-cultured with BM-MSCs under control conditions (level expressed as 1) and plotted on a log scale. * Statistical significance ($p \leq 0.05$) compared to degenerate NP cells co-cultured under control conditions.

5.3.10 Influence of reduced pH (pH 6.8) and hypoxia on BM-MSC and degenerate NP cell co-culture

5.3.10.1 Gene expression in BM-MSCs co-cultured with degenerate NP cells under reduced pH 6.8 and hypoxia

BM-MSCs co-cultured with degenerate NP cells under reduced pH 6.8 and hypoxia showed a significant decrease in SOX-9 expression ($p<0.05$) and a significant increase ($p<0.05$) in COL2A1 expression (Figure 5.3.33 A). ACAN and VCAN expression were significantly down regulated ($p<0.05$ for each) under reduced pH 6.8 and hypoxia (Figure 5.3.33 B). Significant decreases in both PAX-1 and FOXF1 expression ($p<0.05$ for each) were also observed (Figure 5.3.33 C). BM-MSCs co-cultured with degenerate NP cells under reduced pH 6.8 and hypoxia showed significant increases in CA9 ($p<0.05$) and CA12 ($p<0.05$) expression compared to BM-MSCs co-cultured with degenerate NP cells under control conditions.

5.3.10.2 Gene expression in degenerate NP cells co-cultured with BM-MSCs under reduced pH 6.8 and hypoxia

Degenerate NP cells co-cultured with BM-MSCs under reduced pH 6.8 combined with hypoxia showed a significant increase in SOX-9 expression and no change in COL2A1 expression compared to degenerate NP cells co-cultured with BM-MSCs under control conditions (Figure 5.3.34 A). ACAN and VCAN expression was significantly decreased ($p<0.05$ for both) under reduced pH 6.8 and hypoxia (Figure 5.3.34 B). PAX-1 expression was significantly increased ($p<0.05$) while FOXF1 expression was significantly decreased ($p<0.05$) under reduced pH and hypoxia (Figure 5.3.34 C). There was a significant up regulation in CA9 expression ($p<0.05$) with a small significant decrease ($p<0.05$) in CA12 seen under reduced pH and hypoxia compared to control conditions (Figure 5.3.34 D).

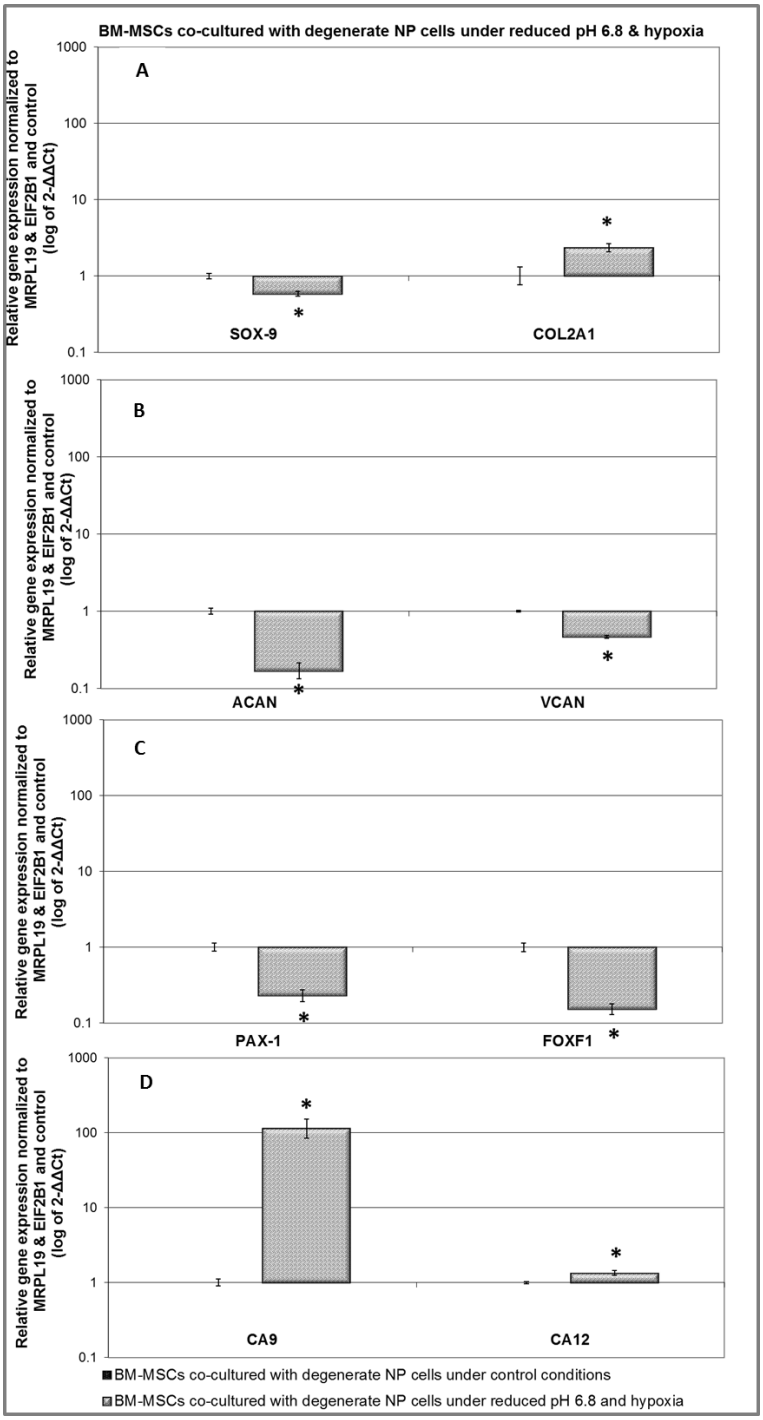

Figure 5.3.33 Relative gene expression of NP conventional markers (A) SOX-9, COL2A1 (B) ACAN, VCAN and NP novel markers (C) PAX-1 and FOXF-1 and (D) carbonic anhydrases CA9, CA12 in BM-MSCs co-cultured with degenerate NP cells under reduced pH 6.8 and hypoxia (n=9). Gene expression normalized to average of HK genes MRPL19 and EIF2B1 and BM-MSCs co-cultured with degenerate NP cells under control conditions (level expressed as 1) and plotted on a log scale. * Statistical significance ($p \leq 0.05$) compared to BM-MSCs co-cultured under control conditions.

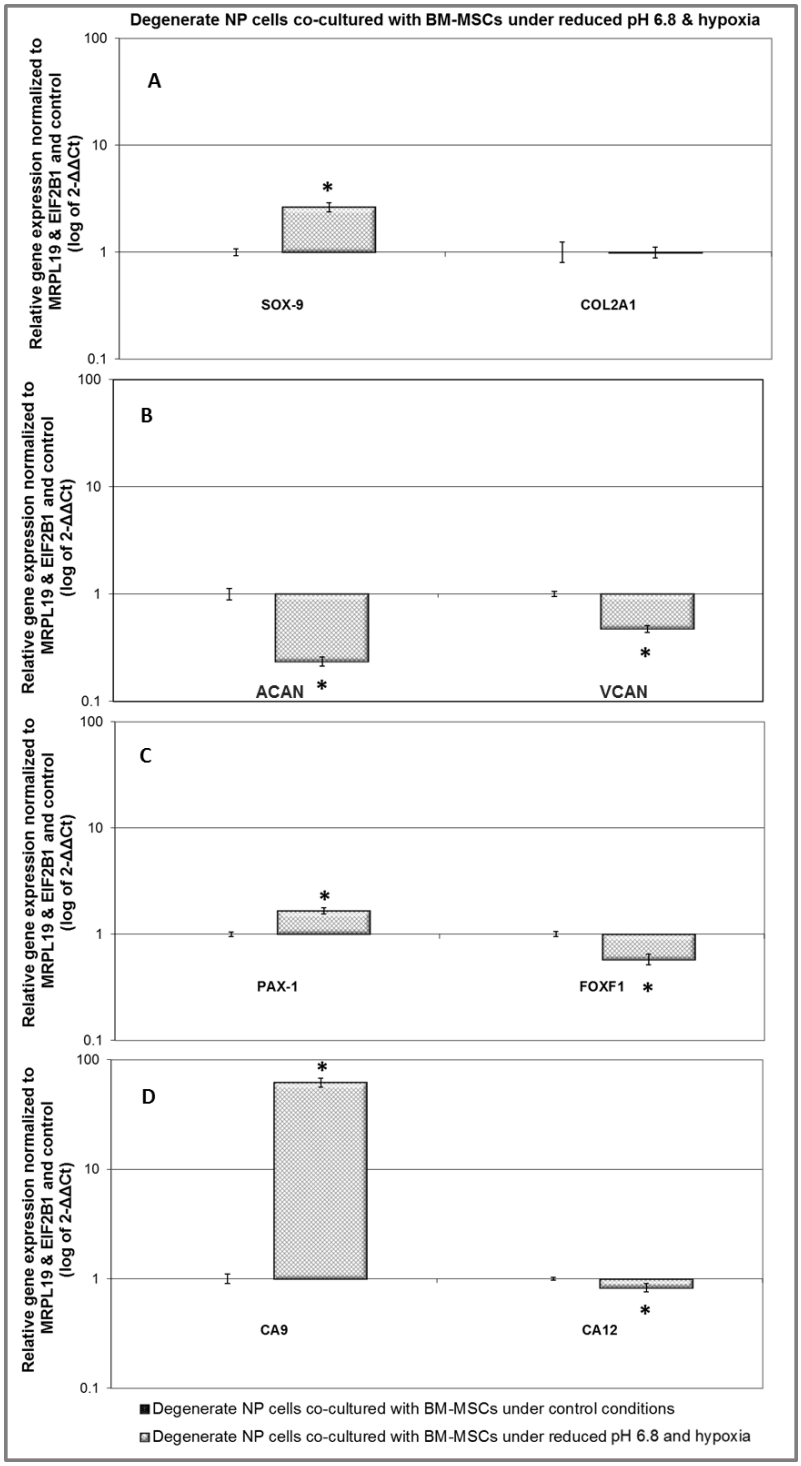

Figure 5.3.34 Relative gene expression of NP conventional markers (A) SOX-9, COL2A1 (B) ACAN, VCAN and NP novel markers (C) PAX-1 and FOXF-1 and (D) carbonic anhydrases CA9, CA12 in degenerate NP cells co-cultured with BM-MSCs under reduced pH 6.8 and hypoxia (n=9). Gene expression normalized to average of HK genes MRPL19 and EIF2B1 and degenerate NP cells co-cultured with BM-MSCs under control conditions (level expressed as 1) and plotted on a log scale. * Statistical significance ($p \leq 0.05$) compared to degenerate NP cells co-cultured under control conditions.

5.3.11 Influence of all IVD-like physio-chemical microenvironmental conditions (hypoxia, reduced serum, reduced glucose and pH 6.8) on BM-MSC and degenerate NP cell co-culture

5.3.11.1 Gene expression in BM-MSCs co-cultured with degenerate NP cells under all IVD-like physio-chemical microenvironmental conditions (hypoxia, reduced serum, reduced glucose and pH 6.8)

BM-MSCs co-cultured with degenerate NP cells under all IVD-like physio-chemical microenvironmental conditions combined showed a significant decrease in SOX-9 expression ($p<0.05$) and a significant increase in ($p<0.05$) COL2A1 compared to BM-MSCs co-cultured with degenerate NP cells under control conditions (Figure 5.3.35 A). ACAN and VCAN expression was significantly decreased (Figure 5.3.35 B). There was a significant down regulation in PAX-1 and FOXF1 ($p<0.05$ for each) compared to control conditions (Figure 5.3.35 C). CA9 showed significant increase ($p<0.05$) while no change in CA12 expression (Figure 5.3.35 D) was observed.

5.3.11.2 Gene expression in degenerate NP cells co-cultured with BM-MSCs under all IVD-like physio-chemical microenvironmental conditions (hypoxia, reduced serum, reduced glucose and pH 6.8)

Degenerate NP cells co-cultured with BM-MSCs under all IVD-like physio-chemical microenvironmental conditions combined showed a significant increase in SOX-9 expression ($p<0.05$) with no change in COL2A1 expression (Figure 5.3.36 A). ACAN and VCAN expression was significantly decreased ($p<0.05$ for each) compared to control conditions (Figure 5.3.36 B). PAX-1 was significantly increased ($p<0.05$) while FOXF1 showed a significant decrease ($p<0.05$) in expression (Figure 5.3.36 C). Significant increases in CA9 and CA12 ($p<0.05$ for each) were observed in degenerate NP cells co-cultured with BM-MSCs under all IVD-like physio-chemical microenvironmental conditions compared to degenerate NP cells co-cultured with BM-MSCs under control conditions (Figure 5.3.36 D).

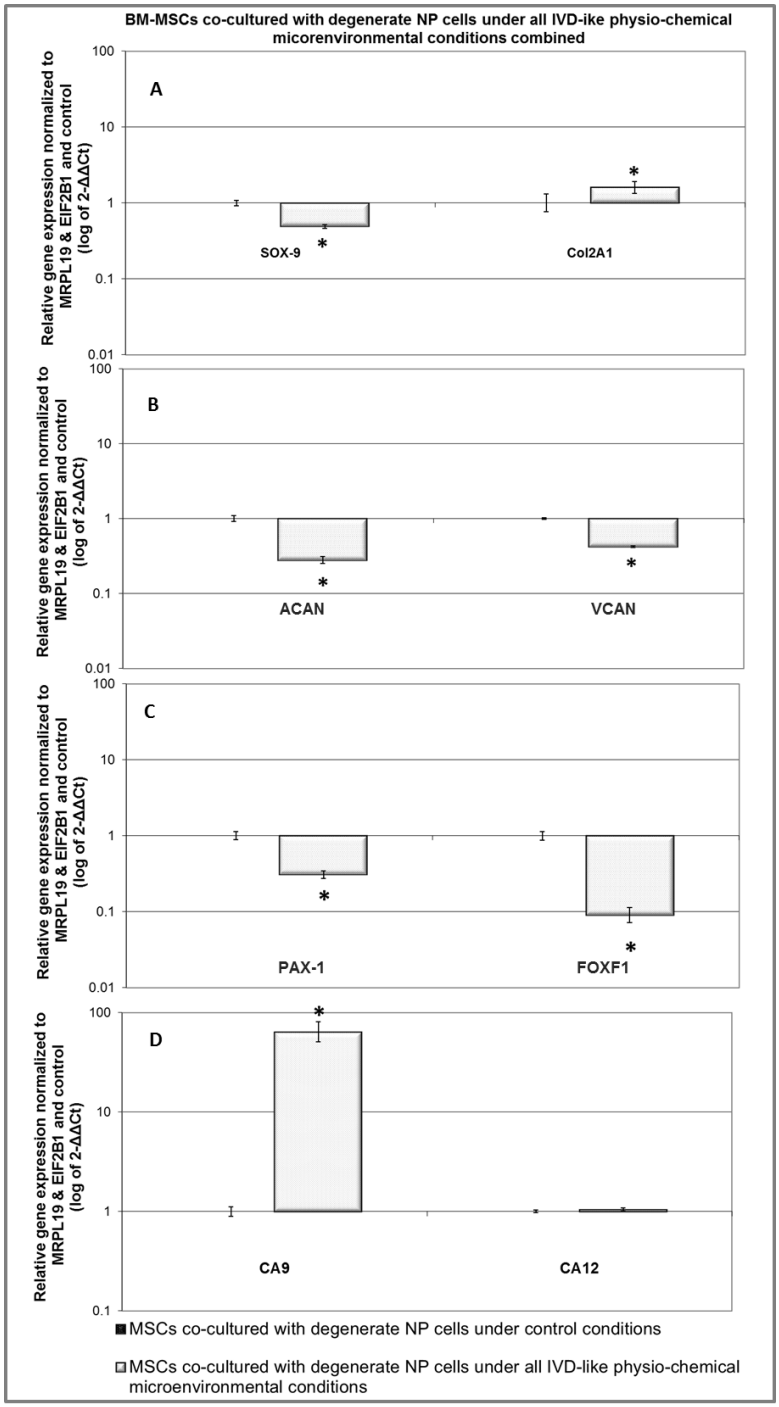

Figure 5.3.35 Relative gene expression of NP conventional markers (A) SOX-9, COL2A1 (B) ACAN, VCAN and NP novel markers (C) PAX-1, FOXF-1 and (D) carbonic anhydrases CA9, CA12 in BM-MSCs co-cultured with degenerate NP cells under all IVD-like physio-chemical microenvironmental conditions (n=9). Gene expression normalized to average of HK genes MRPL19 and EIF2B1 and BM-MSCs co-cultured with degenerate NP cells under control conditions (level expressed as 1) and plotted on a log scale. * Statistical significance ($p \leq 0.05$) compared to BM-MSCs co-cultured under control conditions.

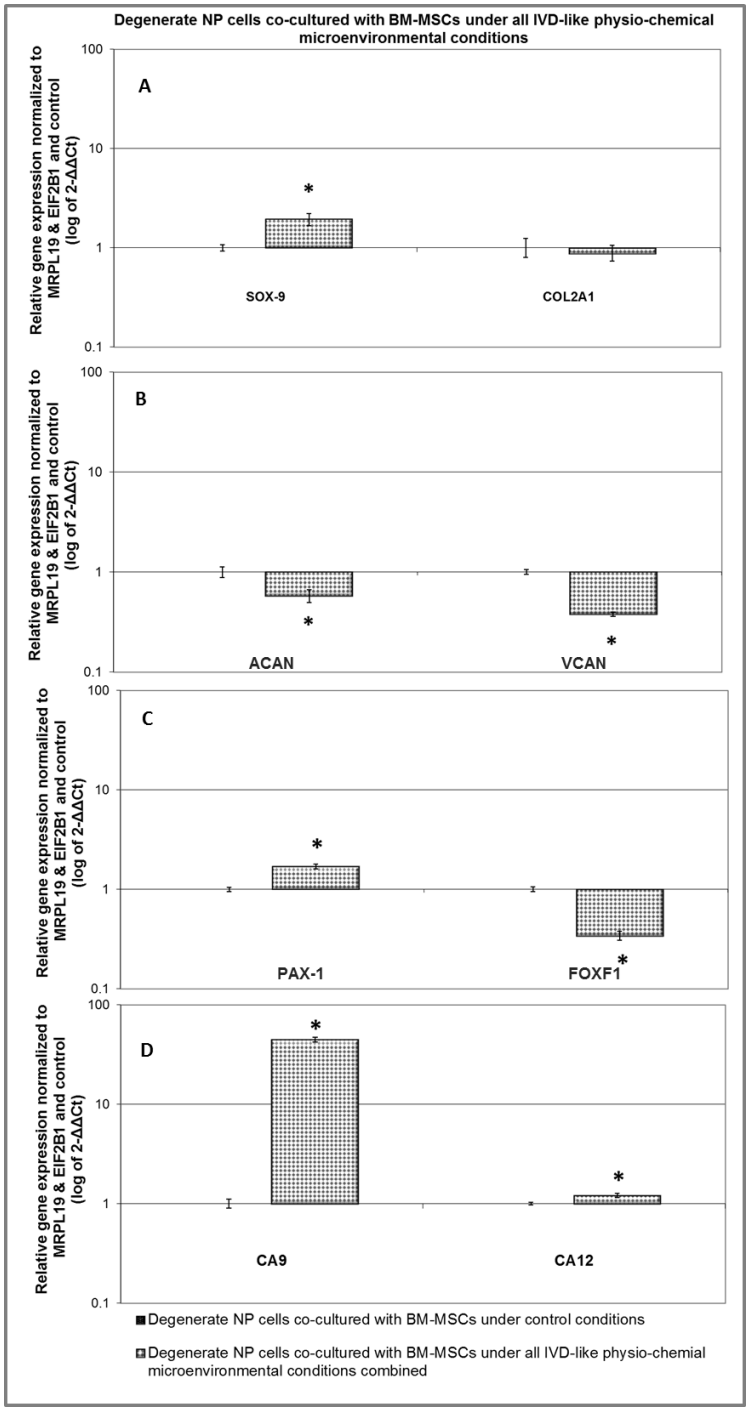

Figure 5.3.36 Relative gene expression of NP conventional markers (A) SOX-9, COL2A1 (B) ACAN, VCAN and NP novel markers (C) PAX-1 and FOXF-1 and (D) carbonic anhydrases CA9, CA12 in degenerate NP cells co-cultured with BM-MSCs under all IVD-like physio-chemical microenvironmental conditions (n=9). Gene expression normalized to average of HK genes MRPL19 and EIF2B1 and degenerate NP cells co-cultured with BM-MSCs under control conditions (level expressed as 1) and plotted on a log scale. * Statistical significance ($p \leq 0.05$) compared to degenerate NP cells co-cultured under control conditions.

Table 5.5 Summary of changes in gene expression in BM-MSCs co-cultured with degenerate NP cells under all test conditions compared to BM-MSCs co-cultured under control conditions.

Condition / Genes	Hyp	Nutrient limited conditions			Nutrient limited & hypoxic conditions			Acidic conditions		Acidic & hypoxic conditions	All
		RS	RG	RS+ RG	RS +H	RG +H	RS+ RG+ H	pH 6.8	pH 6.5	pH 6.8+ H	
SOX-9	↔	↓	↔	↓	↔	↔	↔	↑	↑	↓	↓
COL2A1	↑	↔	↔	↔	↑	↔	↔	↔	↔	↑	↑
ACAN	↑	↑	↑	↑	↔	↔	↔	↓	↓	↓	↓
VCAN	↑	↔	↔	↓	↔	↑	↔	↔	↓	↓	↓
PAX-1	↑	↔	↔	↔	↑	↔	↓	↔	↓	↓	↓
FOXF1	↔	↔	↔	↔	↑	↔	↑	↑	↑	↓	↓
CA9	−−	−−	−−	−−	−−	−−	−−	↑	↑	↑	↑
CA12	−−	−−	−−	−−	−−	−−	−−	↑	↑	↑	↔

↔ = no significant change

↑= significant increase

↓= significant decrease

−− = expression was not studied

Hyp= Hypoxia**,** **RS**= Reduced serum**,** **RG**= Reduced glucose**,** **RS+RG**= Reduced serum, reduced glucose**,** **RS+H**= Reduced serum & hypoxia, **RG+ H**= Reduced glucose & hypoxia**,** **RS+RG+H**= Reduced serum, reduced glucose& hypoxia**, pH 6.8 + H**= pH 6.8 & hypoxia**,** **All** = All IVD-like physio-chemical microenvironmental conditions combined

Table 5.6 Summary of changes in gene expression in degenerate NP cells co-cultured with BM-MSCs under all test conditions compared to degenerate NP cells co-cultured under control conditions.

Condition / Genes	Hyp	Nutrient limited conditions			Nutrient limited & hypoxic conditions			Acidic conditions		Acidic & hypoxic conditions	All
		RS	RG	RS+ RG	RS +H	RG +H	RS+ RG+ H	pH 6.8	pH 6.5	pH 6.8+ H	
SOX-9	↔	↑	↔	↔	↑	↔	↑	↓	↑	↑	↑
COL2A1	↔	↔	↔	↔	↑	↔	↓	↔	↔	↔	↔
ACAN	↔	↑	↑	↔	↑	↔	↔	↓	↓	↓	↓
VCAN	↑	↑	↔	↔	↑	↔	↔	↓	↓	↓	↓
PAX-1	↑	↑	↔	↔	↑	↔	↓	↓	↔	↑	↑
FOXF1	↔	↔	↔	↓	↑	↔	↑	↔	↑	↓	↓
CA9	−−	−−	−−	−−	−−	−−	−−	↑	↑	↑	↑
CA12	−−	−−	−−	−−	−−	−−	−−	↔	↑	↓	↑

↔ = no significant change

↑= significant increase

↓= significant decrease

−− = expression was not studied

Hyp= Hypoxia**,** **RS**= Reduced serum**,** **RG**= Reduced glucose**,** **RS+RG**= Reduced serum, reduced glucose**,** **RS+H**= Reduced serum & hypoxia, **RG+ H**= Reduced glucose & hypoxia**,** **RS+RG+H**= Reduced serum, reduced glucose& hypoxia**,** **pH 6.8 + H**= pH 6.8 & hypoxia**,** **All** = All IVD-like physio-chemical microenvironmental conditions combined

Table 5.7 Summary of changes in ECM protein expression in BM-MSC and degenerate NP cell co-culture under all test conditions compared to co-culture under control conditions.

Condition / Genes	Hyp	Nutrient limited conditions			Nutrient limited & hypoxic conditions			Acidic conditions		Acidic & hypoxic conditions	All
		RS	RG	RS+ RG	RS +H	RG +H	RS+ RG+ H	pH 6.8	pH 6.5	pH 6.8+ H	
Aggrecan staining intensity	↑	↔	↑	↔	↔	↑	↓	––	––	––	––
Versican staining intensity	↑	↑	↑	↑	↔	↑	↔	––	––	––	––

↔ = no change

↑= increase

↓= decrease

–– = expression was not studied

Hyp= Hypoxia**, RS**= Reduced serum**, RG**= Reduced glucose**, RS+RG**= Reduced serum, reduced glucose**, RS+H**= Reduced serum & hypoxia, **RG+ H**= Reduced glucose & hypoxia**, RS+RG+H**= Reduced serum, reduced glucose& hypoxia**, pH 6.8 + H**= pH 6.8 & hypoxia**, All** = All IVD-like physio-chemical microenvironmental conditions combined

5.4 Discussion

Various investigators have utilized *in vitro* co-culture model systems to understand the mechanism of MSC based disc repair. Using these model systems it has been suggested that regeneration of degenerated tissue after MSC implantation *in vivo* may result from interactions between MSCs and native disc cells (Richardson et al., 2006, Sobajima et al., 2008, Vadala et al., 2008b, Yang et al., 2008, Strassburg et al., 2010, Svanvik et al., 2010). It was shown that interaction of MSCs and NP cells not only induces discogenic differentiation of MSCs (Richardson et al., 2006, Vadala et al., 2008b, Yang et al., 2008) but also exerts stimulatory effects on degenerated NP cells (Strassburg et al., 2010). However, to date the majority of co-cultures have been conducted in standard culture conditions. It is essential to conduct these co-cultures in all possible conditions akin to the *in vivo* physio-chemical microenvironment to understand their influence on MSCs differentiation and modulation of the degenerate NP cell phenotype.

Based on previous investigations 2% $O_{2,}$ (Holm et al., 1981, Bartels et al., 1998), 2% FCS (chapter 3, section 3.4), 5mM glucose (Wuertz et al., 2008, Liang et al., 2012a) and pH 6.8/6.5 (Diamant et al., 1968, Wuertz et al., 2009a, Li et al., 2012) were chosen to represent IVD hypoxic, limited nutritional (reduce serum and reduced glucose) and moderate/severe acidic microenvironment respectively. Co-culture was conducted under each condition alone and in combination. Apart from the co-culture method, another feature of the current study was that no additional reagents to induce gene expression or differentiation were used. Therefore, the additive or inhibitory effects of IVD-like physiochemical conditions on previously reported positive effects of co-culture on both BM-MSC and degenerate NP cell can be confirmed throughout this study.

5.4.1 The effect of hypoxia on BM-MSC and degenerate NP cell direct co-culture

A hypoxic microenvironment appeared to increase BM-MSC differentiation and also modulated the degenerate NP cell phenotype during co-culture. BM-MSCs demonstrated significant increases in expression of the majority of discogenic genes following co-culture. Degenerate NP cells also showed increased expression of VCAN and PAX-1. Importantly hypoxia promoted aggrecan and versican matrix production in BM-MSC and degenerate NP cell co-culture. However, further study is needed to conclusively demonstrate contribution of each cell population in the overall increased PG synthesis seen during co-culture. Nevertheless increased expression of aggrecan and versican is desirable in the disc where

these structural macromolecules play important biological and mechanical roles (Melrose et al., 2001). The positive effects of hypoxia on induction of MSC discogenic differentiation (Risbud et al., 2004a, Khan et al., 2007, Stoyanov et al., 2011, Muller et al., 2011) and increased synthesis of matrix by NP cells (Mwale et al., 2011) have been previously reported; however, most of these studies were performed in 3D culture system with addition of chondrogenic growth factors. BM-MSCs and NP cells cultured alone (chapter 3 and 4 of this thesis respectively) also showed increase matrix synthesis under hypoxia. Adding to these reports, this study demonstrates that hypoxia also has beneficial effects on both BM-MSCs and degenerate NP cells during direct co-culture.

Several reports have shown that hypoxia increases expression of a variety of growth factors and cytokines in several cell types (Helfman and Falanga, 1993, Sahai et al., 1999, Lee et al., 2009b, Hung et al., 2012). Studies have also demonstrated that co-culture increases the release of various growth factors (e.g TGF-β, PDGF and IGF) implicated in the discogenic differentiation of MSCs and anabolic regulation of NP cells (Yamamoto et al., 2004, Strassburg et al., 2010). It can therefore be proposed that hypoxia may enhance production of growth factors by BM-MSCs and degenerate NP cells in co-culture that may account for responses observed in this study.

5.4.2 The effect of reduced nutrient microenvironment on BM-MSC and degenerate NP cell co-culture

A nutrient reduced microenvironment (reduced serum and/or reduced glucose) appeared to have a minor impact on BM-MSC differentiation and degenerate NP cell discogenic gene expression during co-culture. Only reduced serum increased expression of most discogenic genes in degenerate NP cells indicating that this condition may exert positive effects on BM-MSC and degenerate NP cell co-culture interaction to predominantly modulate degenerate NP cell phenotype. This nutrient limited microenvironment appeared to influence ACAN and VCAN gene and protein expression in BM-MSC and degenerate NP cell co-culture. Reduced glucose appeared to favour ACAN gene and protein expression in BM-MSC and NP cell co-culture. Previous investigations have demonstrated increased ACAN gene and protein expression in MSCs (e.g. rat BM-MSCs and human AD-MSCs) cultured alone under reduced glucose (Wuertz et al., 2008, Liang et al., 2012a). Results presented in chapter 4 of this thesis also showed increased aggrecan expression in BM-MSCs cultured alone under reduced glucose. Data from this thesis combined with previous reports suggests that reduced glucose

also promotes ACAN expression in BM-MSCs during co-culture. Mietsch *et al* recently found that bovine NP cells cultured alone in 5mM glucose showed no improvement in ACAN expression (Mietsch et al., 2012). In agreement with this, NP cells cultured alone under reduced glucose (chapter 3 of this thesis) also showed no changes in ACAN expression. However, the increased ACAN expression in NP cells during co-culture seen here indicates that these cells may behave differently to reduced glucose under different culture conditions i.e. co-culturing with BM-MSCs under reduce glucose may up regulate ACAN expression in NP cells. Increased versican expression observed in BM-MSC and degenerate NP cell co-culture, in contrast with BM-MSC and degenerate NP cells cultured alone under all nutrient limited microenvironmental conditions (chapter 3 and 4 of this thesis respectively), also suggests that cross-talk between BM-MSCs and degenerate NP cells may indeed positively influence versican expression.

5.4.3 The effect of hypoxia and reduced nutrient microenvironment on BM-MSC and degenerate NP cell co-culture

The combination of hypoxia with nutrient deprived conditions appeared to improve or recover BM-MSC and degenerate NP cell co-culture responses. When hypoxia was combined with reduced serum, BM-MSCs and particularly degenerate NP cells showed significant improvement in their gene expression profile indicating a synergistic effect of hypoxia and reduced serum microenvironment on co-culture interaction to enhance MSC differentiation and promote modulation in degenerate NP cell phenotype. The combination of hypoxia with reduced glucose noticeably increased both aggrecan and versican protein staining suggesting that these conditions promote ECM protein synthesis in BM-MSC and NP cell co-culture. The combination of hypoxia with reduced serum and reduced glucose appeared to abolish the reduced serum and reduced glucose associated reduction of FOXF1 in NP cells and SOX-9 and ACAN in BM-MSCs during co-culture. However, at protein level, co-culture showed decreased aggrecan protein staining. These findings overall indicate that hypoxia and limited nutrient (reduced serum and reduced glucose combine) conditions may not be critical for either discogenic differentiation of BM-MSCs or stimulation of NP cell phenotype in co-culture at gene expression level. But similar to human degenerate NP cells and BM-MSCs (chapter 3 and 4 of this thesis respectively), hypoxia together with a reduced serum and glucose reduced microenvironment may also impair aggrecan matrix production by BM-MSCs and degenerate NP cells during co-culture.

5.4.4 The effect of reduced pH (6.8 & 6.5) on BM-MSC and degenerate NP cell co-culture

Moderate acidic conditions (pH 6.8) seemed to have limited impact on BM-MSC discogenic differentiation but clearly inhibited modulation of degenerate NP cells during co-culture. However, severe acidic conditions (pH 6.5) were detrimental for both BM-MSC differentiation and degenerate NP cells phenotype. It was noteworthy that both pH 6.8 and 6.5 acidic conditions were particularly deleterious for ACAN and VCAN gene expression in degenerate NP cells during co-culture. Degenerate NP cells cultured alone (chapter 3) showed maintained ACAN and VCAN gene expression at pH 6.8 that significantly decreased at pH 6.5. Results from this chapter combined with chapter 3 findings suggest that pH 6.8 may negatively influence ACAN and VCAN expression in degenerate NP cells in co-culture conditions. In contrast pH 6.5 may inhibit ACAN and VCAN gene expression in degenerate NP cells both in alone and co-culture conditions.

BM-MSCs co-cultured with degenerate NP cells showed a gradual decrease in ACAN gene expression with acidification. Decreases in ACAN gene and protein expression in MSCs (BM-MSCs and AD-MSCs) cultured alone at both pH 6.8 and pH 6.5 have been shown previously (Wuertz et al., 2008, Wuertz et al., 2009a, Li et al., 2012, Liang et al., 2012a). However, in contrast BM-MSCs cultured alone in this thesis (chapter 4) under pH 6.8 showed maintained ACAN expression that decreased at pH 6.5. Differences in ACAN expression in BM-MSCs cultured alone and co-cultured in this thesis and in previous investigations may be due to differences in culture conditions (alone vs co-culture in this study) or differences in MSCs species (rat BM-MSCs or human AD-MSCs versus human BM-MSCs in this study). No study has previously investigated expression of VCAN in MSCs under acidic pH. It appeared that moderate acidic pH (6.8) had limited influence on VCAN expression in co-cultured BM-MSC but severe pH (6.5) conditions significantly compromised its expression in co-culture BM-MSC.

Expression of NP novel gene markers in co-cultured BM-MSCs and NP cells also appeared to be regulated by increasing acidic pH. BM-MSCs and degenerate NP cells co-cultured in this study showed that acidic conditions significantly increased expression of CA9 and CA12 genes. Increased expression of CA12 in co-cultured BM-MSCs, in contrast to BM-MSCs cultured alone (chapter 4) suggest that co-culture may promote CA12 expression in BM-MSCs. Stoyanov *et al* have suggested that indirect co-culture with NP cells promote CA12

expression in BM-MSCs (Stoyanov et al., 2011). Interestingly severe acidic conditions (pH 6.5) showed increased expression of CAs compared to moderate acidic conditions (pH 6.8). This suggests that cells during co-culture can sense pH shift and up-regulate CA expression according to severity of acidic conditions. It is possible that increased CAs expression may work in conjunction with other known acid extrusion mechanisms for maintenance of a constant intracellular pH in degenerate NP cells (Razaq et al., 2000, Uchiyama et al., 2007) and BM-MSCs for maintaining cell survival under acidic conditions.

5.4.5 The effect of hypoxia and reduced pH on BM-MSC and degenerate NP cell co-culture

Combination of hypoxia with reduced pH (6.8) compromised BM-MSCs discogenic differentiation and modulation of degenerate NP cell in co-culture system. Unlike the positive effects of a combined hypoxic and reduced nutrient microenvironment, combination of pH 6.8 with hypoxia appeared to diminish the positive effects of hypoxia observed on ACAN and VCAN gene expression in co-cultured BM-MSCs and degenerate NP cells. It can be suggested that increased lactic acid production under hypoxic conditions **(**Holm et al**.,** 1981**,** Ishihara and Urban**,** 1999**)** may contribute to worsen the already acidic conditions and result in the observed effects. However, this assumption needs to be confirmed. Increased expression of CA9 in BM-MSCs and degenerate NP cells during co-culture under these conditions reinforces the suggestion of hypoxic acidic induction of CA9 (Chiche et al., 2009). The compromised response of co-cultured cells under reduced pH 6.8 and hypoxia, in contrast to observed responses of degenerate NP cells and BM-MSCs (chapter 3 and 4 of this thesis respectively) cultured alone suggest that co-culture interaction may be negatively influenced by this combined microenvironment. Future studies are required to understand mechanisms of communication during co-culture under these conditions.

5.4.6 The effect of all IVD-like physio-chemical microenvironmental conditions (hypoxia, reduced serum, reduced glucose and pH 6.8) on BM-MSC and degenerate NP cell co-culture

Combination of all IVD-like physio-chemical microenvironmental conditions (reduced serum and reduced glucose, hypoxia and pH 6.8) demonstrated comparable effects on BM-MSC and degenerate NP cell co-culture responses as seen under pH 6.8 and hypoxia. These results indicate that when all conditions are combined, pH 6.8 and hypoxia combination may be the major limiting factors affecting BM-MSC differentiation and modulation of degenerate NP cell phenotype.

Overall these results indicate that a hypoxic and limited nutrient microenvironment may protect and enhance BM-MSC discogenic differentiation during co-culture with stimulatory effects on degenerate NP cells. However, acidic and hypoxic conditions combined may severely compromise these responses. As hypoxia promoted BM-MSC differentiation and modulation of degenerate NP cells in co-culture, acidic pH may be the key limiting factor when all conditions are combined. Determining the window of degenerative stage for the best efficacy appears to be an essential step. As detailed in chapter 4 it can be envisaged that early cellular intervention when pH is still higher than 6.8 (Wuertz et al., 2009a) might be an effective approach to prevent the possible deleterious impacts of acidic pH on implanted MSC differentiation and endogenous degenerate NP cell phenotype. Future studies are required to investigate the mechanisms of cross-talk between MSCs and degenerate NP cells under different microenvironmental conditions.

5.5 Conclusion

In conclusion, this study demonstrates for the first time that previously reported BM-MSC and degenerate NP cell co-culture responses i.e. differentiation of BM-MSC and modulation of degenerate NP cell phenotype, are sensitive to changes in IVD-like physio-chemical microenvironmental conditions. Results showed that hypoxia, reduced serum and reduced glucose (limited nutrients) are stimulatory conditions for BM-MSC differentiation and modulation in degenerate NP cell phenotype in co-culture. This study also found additive or inhibitory effects of different combinations. Hypoxia appeared to improve or recover changes at gene expression level in both BM-MSCs and degenerate NP cells under nutrient deprived (reduced serum or/and reduced glucose) conditions during co-culture. However, the combination of hypoxia with both reduced serum and reduced glucose together (complete nutrient deprived conditions) appeared to decrease aggrecan matrix synthesis. Hypoxia showed synergistic interaction with reduced glucose condition for additive influences on matrix synthesis. Severe pH (6.5) condition alone and moderate pH 6.8 in combination with hypoxia was deleterious for both BM-MSC discogenic differentiation and improvement in degenerated NP cell phenotype during co-culture. Finally co-culture responses observed under all IVD-like physio-chemical microenvironment conditions were comparable to pH 6.8 and hypoxic combined conditions. It can be inferred that *in vivo* hypoxic and limited nutrient microenvironment as such and in interaction may maintain and enhance BM-MSC discogenic differentiation during co-culture with stimulatory effects on degenerate NP cell phenotype. But the combination of moderate acidic conditions with hypoxia may severely compromise

regenerative responses. This study emphasized that that *in vitro* model systems for studying cell based regenerative mechanisms should mimic the *in vivo* situation as closely as possible to ensure appropriate cellular responses following implantation.

6 Chapter 6: Conclusions and future work

LBP affects millions of individuals each year, resulting in high medical costs. Degeneration of the IVD has been linked with LBP. The IVD microenvironment which is characterised by hypoxia together with reduced nutritional and acidic conditions is thought to be one of the etiological factors implicated in disc degeneration. *In vitro* studies using animal disc and isolated NP cells have attempted to establish the link between the harsh disc microenvironment and NP cellular behaviour. The first aim of this study was to investigate the effect of IVD-like physiochemical microenvironment characterized by hypoxia (2%O2), limited nutrition (2% FCS and/or 5mM glucose) and acidic (moderate 6.8 or severe 6.5 pH) conditions on human degenerate NP cell behaviour.

The growing field of cell based regenerative medicine focuses on the use of the MSC in the treatment of disc disease. A considerable amount of literature has been published on improving the differentiation potential of MSCs into NP-like cells. However, few investigations have studied the behaviour of MSCs in an IVD-like inhospitable microenvironment. The second aim of this study was to investigate survival and functioning of human BM-MSCs under IVD-like physio-chemical microenvironmental conditions.

MSCs and NP cells co-culture model systems have been used to study MSC based disc repair mechanisms. These models propose that disc regeneration, may be due to MSC differentiation and modulation of the degenerate NP cell phenotype. As the importance of disc microenvironment is increasingly highlighted, it is essential to incorporate these conditions into these co-culture model systems. The third aim of this project was to incorporate IVD-like physio-chemical microenvironmental conditions into BM-MSC and degenerate NP cell co-culture to study their stimulatory or inhibitory effects on MSCs differentiation and modulation of degenerate NP cells phenotype.

This study found that IVD-like physio-chemical microenvironmental conditions influence human degenerate NP cell/BM-MSC behaviour (especially proliferation and matrix synthesis) and their co-culture responses. Importantly the results of this project indicate that 1) hypoxia may be a positive factor for both modulating degenerate NP cell phenotype and improving behaviour of implanted BM-MSCs; 2) Nutrient deprived and moderate acidic (pH

6.8) conditions alone may have minimal impact on cellular behaviour; 3) hypoxia and reduced glucose combination may promote matrix synthesis by degenerate NP cells and BM-MSCs; 4) hypoxia and complete nutrient deprived (both reduced serum and reduced glucose) microenvironment may accelerate degenerate processes in degenerate NP cells; 5) a severe acidic microenvironment may exacerbate the degenerative phenotype of NP cells and hamper the behaviour of BM-MSCs and finally 6) hypoxia; a complete nutrient deprived and moderate acidic microenvironment of the disc together may not promote degenerative changes or affect survival and functioning of implanted BM-MSCs.

Differentiation of BM-MSCs and modulation of degenerate NP cell phenotype seen during co-culture were also found to be sensitive to the conditions simulating the disc microenvironment. The results imply that; 1) the hypoxia, reduced serum and reduced glucose conditions of the disc may enhance cell based regenerative processes; 2) hypoxia and moderate acidic pH (6.8) together may compromise those responses; 3) severe acidic pH (6.5) also compromised co-culture responses.

This study has generated informative data about influences of IVD-like physiochemical microenvironment in modulating or accelerating disc degeneration. It also generated useful information about the factors of the hostile disc microenvironment which affect BM-MSCs (potential cell population for disc regeneration) behaviour. Finally this study emphasized that *in vitro* model systems for studying cell based regenerative mechanisms should mimic the *in vivo* situation as closely as possible to ensure appropriate cellular responses following implantation.

The severe acidic condition (pH 6.5) was critical for all responses studied in this thesis. Results from chapter 4 and chapter 5 combined corroborate previous reports that the acidic pH in severely degenerated discs may impede the behaviour and regenerative abilities of MSCs (Wuertz et al., 2009a, Li et al., 2012). Differences between moderate and severe acidic conditions demonstrate that MSC-based cell therapies to repair the degenerate disc should be only offered to patients with pH levels of 6.8 or above, unless the native disc pH can be altered prior to implantation. As the decrease in the EP permeability is implicated in ineffective removal of lactic acid leading to a more acidic pH in the degenerated disc, increasing its permeability may improve nutrient supply and thus help to balance pH levels

thereby, decreasing the degenerative processes. However, strategies for increasing the EP permeability still need to be developed.

Previously it was proposed that differentiated end stage cells (i.e. disc cells) may be better adapted to survive harsh conditions particular the low pH than undifferentiated stem cells. It was further suggested that MSCs gradual acclimatisation to the altered pH prior to implantation may be a way to increase MSCs survival and regeneration potential (Wuertz et al., 2008, Wuertz et al., 2009a). However, the similar behaviour of undifferentiated BM-MSCs cultured alone in this study (especially under changing acidic conditions) to that of differentiated degenerate NP cells suggest that even pre-differentiation may not benefit cells in escaping the detrimental effects of severe pH.

The results from this study concerning the choice of HK gene show that there is no ideal and universal HK gene that can be applied to all experimental conditions. Importantly, it illustrates that a number of HK genes should be validated for each experimental condition so that the most optimal HK gene is selected (i.e where basal levels of HK gene do not change across experimental conditions applied). This study identified that MRPL19 and EIF2B1 are two novel HK genes that could be used for normalization of gene expression in both NP cells and MSCs under different IVD like microenvironmental culture condition. MRPL19 encodes mitochondrial 39S ribosome subunit protein. EIF2B1 encodes one of five subunits of eukaryotic translation initiation factor 2B (EIF2B), a GTP exchange factor for eukaryotic initiation factor 2 and an essential regulator for protein synthesis (NCB1-Gene).

Occasionally during this study expression of matrix genes did not correlate with the protein expression in terms of the fact that sometimes there was an increase in gene with no change in protein expression or, alternatively a decrease in gene with increase in protein expression. These differences could be attributed to post-transcriptional or /translational regulation or differences in timing of mRNA synthesis versus protein synthesis (Maier et al., 2009). Importantly, gene and protein expression in this study were essentially a snapshot of only one time point (day 7); investigating their expression at more additional time points (e.g. day 0, day 3, 7 or 12) may help to explain these disparities and provide a clear view of any changes in their expression with time.

Future work

Studies described in this thesis have increased our understanding about the influences of the disc microenvironmental conditions on degeneration and regeneration responses. However, these studies have a few limitations and point to a number of avenues in future work to fully understand the relationship between the disc microenvironment with degeneration and regeneration.

Since this study clearly indicated that the IVD-like increasing acidic conditions may contribute to the processes associated with disc degeneration and hinder regenerative strategies, it is important to study the underlying pathways responsible for observed effects. It is suggested that extracellular acidity exerts its effect through changes in the intracellular pH. Animal NP cells have been shown to possess an effective buffering capacity and expression of acid sensitive ion channels to regulate steady state intracellular pH (Uchiyama et al., 2007, Razaq et al., 2000). Studying the regulation of the intracellular pH in human NP cells and MSCs under severe extracellular acidic conditions would be an interesting avenue. Changes in catabolic genes and proteins expression (e.g. MMPs, ADAMTSs) in animal NP cells and rat BM-MSCs under disc microenvironmental conditions especially under acidic pH is well documented (Razaq et al., 2003, Wuertz et al., 2009a, Neidlinger-Wilke et al., 2012, Rinkler et al., 2010). Determining catabolic expression in human NP cells and BM-MSCs under IVD-like physio-chemical microenvironmental conditions especially under acidic pH would increase our understanding about the implication of disc acidity in matrix turnover. It has been shown that a drop in pH can stimulate IL-8 production (Bischoff et al., 2008). High levels of IL-8 has been seen in IVD tissues from patients with LBP (Burke et al., 2002). It is possible that reduced pH increases production of certain cytokines in the disc which are known to influence matrix synthesis.

The co-culture model system employed in this study modelled the direct cell to cell interaction of BM-MSCs with degenerate NP cells. However, it is possible that BM-MSCs after implantation have less direct cell to cell contact with sparse NP cell population and have more interaction with NP cell secreted ECM. Future work is needed to modify the co-culture model system to limit the influence of direct cell contact and study the role of ECM in possible regeneration responses.

Compared with animal tissues (which are more readily available), the use of human tissues always remains a valuable commodity. Due to the limited availability of normal NP cells, degenerated cells were used in chapter 3 of this study. Though this work has established the causal relationship between the disc microenvironment and degenerative changes, use of normal human NP cells in future investigations will clearly establish the link between disc harsh microenvironment and degenerative changes.

Due to the use of one degenerate NP cell sample for proliferation analysis in chapter 3 statistical significance was not achieved. In future, use of a small sample number of at least n=3 is desirable for statistical significant outcomes.

In addition to hypoxia, reduced nutrient and acidic pH, disc microenvironment is also a combination of other conditions such as hypo-osmolality, a high level of inflammatory cytokines and high mechanical loading. It would be interesting to conduct similar experiments under all possible physio-chemical conditions simulating the *in vivo* microenvironment to understand the complete influence of disc microenvironment on degeneration and regeneration responses.

In this study the influence of disc microenvironmental conditions on protein synthesis was studied qualitatively using immunofluorescence analysis. Within the time frame of this PhD quantitative analysis was not achieved but would further enhance our understanding. During immunofluorescence analysis of co-culture, attempts to discriminate between degenerate NP cell and BM-MSC were made but were not successful. At the end of immunofluorescence staining, the co-culture was labelled with Alexa Fluor 647 Phalloidin (Invitrogen) to fluorescently stain the cytoskeleton. It was anticipated that with this step, the CFDA labelled MSCs would be stained both green and red and NP cells would be stained red. Unfortunately the fluorescence signal of this dye was quickly lost (photobleached), therefore, images were not acquired. Finding a suitable dye and optimizing labelling in future work will help to discriminate MSCs and NP cells during immunofluorescence to understand their contribution towards matrix synthesis during co-culture. Transduction or transfection of MSCs and NP cells with different fluorescent proteins could also aid to discriminate cells after co-culture.

7 Appendix I

Published Abstract

Khan S, Richardson SM, Hoyland JA. Interactions between mesenchymal stem cells and nucleus pulposus cells: implications for intervertebral disc regeneration. European Cells and Materials. 2012;23:S4

Interactions between mesenchymal stem cells and nucleus pulposus cells: Implications for intervertebral disc regeneration

S Khan[1], SM Richardson[1], JA Hoyland [1]

[1]University of Manchester, Manchester, UK,

INTRODUCTION: Intervertebral disc (IVD) degeneration is a major cause of low back pain. Mesenchymal stem cells (MSCs) are a promising cell population for regeneration of the degenerate IVD. We have previously shown that direct cell-cell interaction between MSCs and nucleus pulposus (NP) cells stimulates the differentiation of MSCs towards NP like cells and enhances matrix gene expression within NP cells[1,2] suggesting restoration of a non-degenerate phenotype. However, these studies did not consider the harsh microenvironmental "niche" of the degenerate IVD characterized by reduced oxygen and nutrients[3]. Therefore the purpose of this study was to use an in vitro co-culture model system to investigate MSC: NP cell interactions under IVD-like microenvironmental niche (low oxygen and reduced serum) conditions.

METHODS: Human bone marrow MSCs (n=3) were fluorescently labelled and co-cultured with degenerate NP cells (n=5) in monolayer with cell-cell contact at 50:50 ratio in either normoxia (20% O2) supplemented with 10% fetal calf serum (FCS) or hypoxia (2% O2) supplemented with 10% or 2% FCS for 7 days. Following co-culture, cells were separated using fluorescence activated cell sorting. Labelled MSCs and unlabelled NP cells were also cultured alone under identical conditions. QRT-PCR analysis of NP markers genes (Col II, SOX-9, ACAN, VCAN, PAX-1 and FOXF1) was performed to compare the effect of degenerate IVD-like microenvironmental conditions on alone and co-cultured cell phenotypes.

RESULTS: NP cells and MSCs cultured alone under IVD-like microenvironment niche did not demonstrate phenotype changes. Following co-culture under hypoxia degenerate NP cells showed significant increases in VCAN and PAX-1 gene expression levels. Serum reduction under hypoxia significantly increased expression of all NP marker gene expression (Figure 1A). MSCs co-cultured with degenerate NP cells under hypoxia showed significant increases in ACAN and VCAN. Co-cultured MSCs under hypoxia with reduced serum demonstrated significant increases in expression of PAX-1 and FOXF1 (Figure 1B).

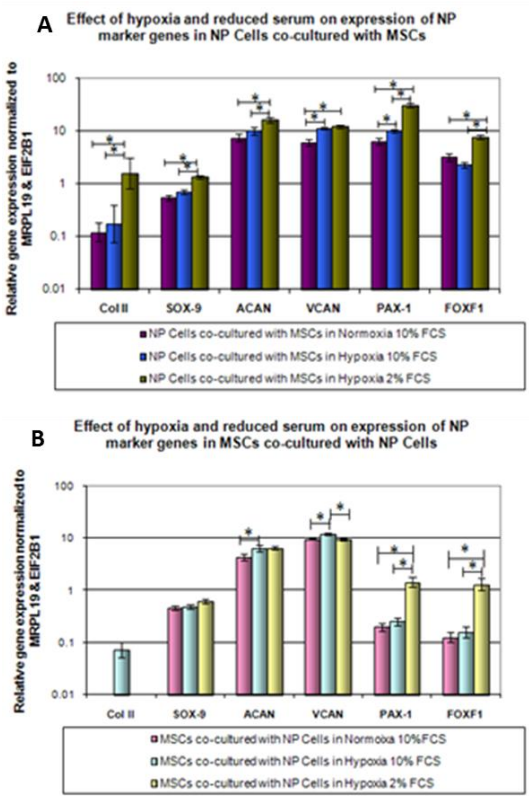

Figure 1: QRT-PCR analysis of NP markers genes in co-cultured NPCs (A) and MSCs (B).

DISCUSSION & CONCLUSIONS: The results demonstrate that IVD-like microenvironmental factors had minor effects on degenerate NP cell phenotype and MSC differentiation when cells were cultured alone. Importantly co-culture under conditions which mimic the IVD niche resulted in significant increases in NP marker gene expression in both NP cells and MSCs. This suggests that cellular communication between MSCs and NP cells under hypoxic and reduced serum may favour the release of bidirectional stimulatory signals that restore a more normal NP cell phenotype and initiate MSCs differentiation. This study demonstrates that MSCs and NP cells are able to interact in an environment similar to that of the degenerate IVD "niche". Importantly it highlights the fact that model systems should

mimic the in vivo situation as closely as possible to ensure that cells will function appropriately following implantation.

REFERENCES: [1]S.M. Richardson, R.V. Walker, S. Parker, et al (2006) Stem Cells 24: 707-16. [2]S. Strassburg, S.M. Richardson, A.J. Freemont, et al (2010) Regenerative Medicine 5:701-11.[3]W.E. Johnson, S. Stephan, S. Roberts (2008) Arthritis Res Ther, 10:R46.

8 References

ABBOTT, R. D., PURMESSUR, D., MONSEY, R. D. & IATRIDIS, J. C. 2012. Regenerative potential of TGFbeta3 + Dex and notochordal cell conditioned media on degenerated human intervertebral disc cells. *J Orthop Res,* 30**,** 482-8.

ACOSTA, F. L., JR., METZ, L., ADKISSON, H. D., LIU, J., CARRUTHERS-LIEBENBERG, E., MILLIMAN, C., MALONEY, M. & LOTZ, J. C. 2011. Porcine intervertebral disc disc repair using allogeneic juvenile articular chondrocytes or mesenchymal stem cells. *Tissue Eng Part A,* 17**,** 3045-55.

ADAMS, D. S., KELLER, R. & KOEHL, M. A. 1990. The mechanics of notochord elongation, straightening and stiffening in the embryo of Xenopus laevis. *Development,* 110**,** 115-30.

ADAMS, M. A., MCNALLY, D. S. & DOLAN, P. 1996. 'Stress' distributions inside intervertebral discs. The effects of age and degeneration. *J Bone Joint Surg Br,* 78**,** 965-72.

ADAMS, M. A. & ROUGHLEY, P. J. 2006. What is intervertebral disc degeneration, and what causes it? *Spine (Phila Pa 1976),* 31**,** 2151-61.

AGRAWAL, A., GAJGHATE, S., SMITH, H., ANDERSON, D. G., ALBERT, T. J., SHAPIRO, I. M. & RISBUD, M. V. 2008. Cited2 modulates hypoxia-inducible factor-dependent expression of vascular endothelial growth factor in nucleus pulposus cells of the rat intervertebral disc. *Arthritis Rheum,* 58**,** 3798-808.

AGRAWAL, A., GUTTAPALLI, A., NARAYAN, S., ALBERT, T. J., SHAPIRO, I. M. & RISBUD, M. V. 2007. Normoxic stabilization of HIF-1alpha drives glycolytic metabolism and regulates aggrecan gene expression in nucleus pulposus cells of the rat intervertebral disk. *Am J Physiol Cell Physiol,* 293**,** 621-31.

AGUIAR, D. J., JOHNSON, S. L. & OEGEMA, T. R. 1999. Notochordal cells interact with nucleus pulposus cells: regulation of proteoglycan synthesis. *Exp Cell Res,* 246**,** 129-37.

ALLON, A. A., BUTCHER, K., SCHNEIDER, R. A. & LOTZ, J. C. 2012. Structured bilaminar coculture outperforms stem cells and disc cells in a simulated degenerate disc environment. *Spine (Phila Pa 1976),* 37**,** 813-8.

ANDERSEN, C., GUNDESEN, C. & ADOLFMDL, K. 2010. Documentation for Normfinder Version 20-2004-2010.

ANDERSEN, C. L., JENSEN, J. L. & ORNTOFT, T. F. 2004. Normalization of real-time quantitative reverse transcription-PCR data: a model-based variance estimation approach to identify genes suited for normalization, applied to bladder and colon cancer data set. *Cancer Res,* 64**,** 5245-50.

ARTEEL, G. E., THURMAN, R. G. & RALEIGH, J. A. 1998. Reductive metabolism of the hypoxia marker pimonidazole is regulated by oxygen tension independent of the pyridine nucleotide redox state. *Eur J Biochem,* 253**,** 743-50.

ARTEEL, G. E., THURMAN, R. G., YATES, J. M. & RALEIGH, J. A. 1995. Evidence that hypoxia markers detect oxygen gradients in liver: pimonidazole and retrograde perfusion of rat liver. *Br J Cancer,* 72**,** 889-95.

ASPLUND, A., STILLEMARK-BILLTON, P., LARSSON, E., RYDBERG, E. K., MOSES, J., HULTEN, L. M., FAGERBERG, B., CAMEJO, G. & BONDJERS, G. 2010. Hypoxic regulation of secreted proteoglycans in macrophages. *Glycobiology,* 20**,** 33-40.

ASZODI, A., CHAN, D., HUNZIKER, E., BATEMAN, J. F. & FASSLER, R. 1998. Collagen II is essential for the removal of the notochord and the formation of intervertebral discs. *J Cell Biol,* 143**,** 1399-412.

BARTELS, E. M., FAIRBANK, J. C., WINLOVE, C. P. & URBAN, J. P. 1998. Oxygen and lactate concentrations measured in vivo in the intervertebral discs of patients with scoliosis and back pain. *Spine (Phila Pa 1976),* 23**,** 1-8.

BATTIE, M. C., VIDEMAN, T., KAPRIO, J., GIBBONS, L. E., GILL, K., MANNINEN, H., SAARELA, J. & PELTONEN, L. 2009. The Twin Spine Study: contributions to a changing view of disc degeneration. *Spine J,* 9**,** 47-59.

BATTIE, M. C., VIDEMAN, T., LEVALAHTI, E., GILL, K. & KAPRIO, J. 2007. Heritability of low back pain and the role of disc degeneration. *Pain,* 131**,** 272-80.

BENNEKER, L. M., HEINI, P. F., ALINI, M., ANDERSON, S. E. & ITO, K. 2005. 2004 Young Investigator Award Winner: vertebral endplate marrow contact channel occlusions and intervertebral disc degeneration. *Spine (Phila Pa 1976),* 30**,** 167-73.

BERTRAM, H., NERLICH, A., OMLOR, G., GEIGER, F., ZIMMERMANN, G. & FELLENBERG, J. 2009. Expression of TRAIL and the death receptors DR4 and DR5 correlates with progression of degeneration in human intervertebral disks. *Mod Pathol,* 22**,** 895-905.

BIBBY, S. R., FAIRBANK, J. C., URBAN, M. R. & URBAN, J. P. 2002. Cell viability in scoliotic discs in relation to disc deformity and nutrient levels. *Spine (Phila Pa 1976),* 27**,** 2220-8.

BIBBY, S. R., JONES, D. A., LEE, R. B., YU, J. & URBAN, J. P. G. 2001. The pathophysiology of the intervertebral disc. *Joint Bone Spine,* 68**,** 537-42.

BIBBY, S. R., JONES, D. A., RIPLEY, R. M. & URBAN, J. P. 2005. Metabolism of the intervertebral disc: effects of low levels of oxygen, glucose, and pH on rates of energy metabolism of bovine nucleus pulposus cells. *Spine (Phila Pa 1976),* 30**,** 487-96.

BIBBY, S. R. & URBAN, J. P. 2004. Effect of nutrient deprivation on the viability of intervertebral disc cells. *Eur Spine J,* 13**,** 695-701.

BISCHOFF, D. S., ZHU, J. H., MAKHIJANI, N. S. & YAMAGUCHI, D. T. 2008. Acidic pH stimulates the production of the angiogenic CXC chemokine, CXCL8 (interleukin-8), in human adult mesenchymal stem cells via the extracellular signal-regulated kinase, p38 mitogen-activated protein kinase, and NF-kappaB pathways. *J Cell Biochem,* 104**,** 1378-92.

BLANCO, J. F., GRACIANI, I. F., SANCHEZ-GUIJO, F. M., MUNTION, S., HERNANDEZ-CAMPO, P., SANTAMARIA, C., CARRANCIO, S., BARBADO, M. V., CRUZ, G., GUTIERREZ-COSIO, S., HERRERO, C., SAN MIGUEL, J. F., BRINON, J. G. & DEL CANIZO, M. C. 2010. Isolation and characterization of mesenchymal stromal cells from human degenerated nucleus pulposus: comparison with bone marrow mesenchymal stromal cells from the same subjects. *Spine (Phila Pa 1976),* 35**,** 2259-65.

BOOS, N., NERLICH, A. G., WIEST, I., VON DER MARK, K. & AEBI, M. 1997. Immunolocalization of type X collagen in human lumbar intervertebral discs during ageing and degeneration. *Histochem Cell Biol,* 108**,** 471-80.

BOOS, N., WEISSBACH, S., ROHRBACH, H., WEILER, C., SPRATT, K. F. & NERLICH, A. G. 2002. Classification of age-related changes in lumbar intervertebral discs: 2002 Volvo Award in basic science. *Spine (Phila Pa 1976),* 27**,** 2631-44.

BOSCH, P., MUSGRAVE, D. S., LEE, J. Y., CUMMINS, J., SHULER, T., GHIVIZZANI, T. C., EVANS, T., ROBBINS, T. D. & HUARD 2000. Osteoprogenitor cells within skeletal muscle. *J Orthop Res,* 18**,** 933-44.

BRISBY, H., PAPADIMITRIOU, N., BRANTSING, C., BERGH, P., LINDAHL, A. & BARRETO HENRIKSSON, H. 2013. The presence of local mesenchymal progenitor cells in human degenerated intervertebral discs and possibilities to influence these in vitro: a descriptive study in humans. *Stem Cells Dev,* 22**,** 804-14.

BRODIN, H. 1955. Paths of nutrition in articular cartilage and intervertebral discs. *Acta Orthop Scand,* 24**,** 177-83.

BRON, J. L., HELDER, M. N., MEISEL, H. J., VAN ROYEN, B. J. & SMIT, T. H. 2009. Repair, regenerative and supportive therapies of the annulus fibrosus: achievements and challenges. *Eur Spine J,* 18**,** 301-13.

BROX, J. I., NYGAARD, O. P., HOLM, I., KELLER, A., INGEBRIGTSEN, T. & REIKERAS, O. 2010. Four-year follow-up of surgical versus non-surgical therapy for chronic low back pain. *Ann Rheum Dis,* 69**,** 1643-8.

BUCKWALTER, J. A. 1995. Aging and degeneration of the human intervertebral disc. *Spine (Phila Pa 1976),* 20**,** 1307-14.

BURKE, J. G., WATSON, R. W., MCCORMACK, D., DOWLING, F. E., WALSH, M. G. & FITZPATRICK, J. M. 2002. Intervertebral discs which cause low back pain secrete high levels of proinflammatory mediators. *J Bone Joint Surg Br,* 84**,** 196-201.

BUSTIN, S. A. 2000. Absolute quantification of mRNA using real-time reverse transcription polymerase chain reaction assays. *J Mol Endocrinol,* 25**,** 169-93.

CAMPISI, J. 1997. The biology of replicative senescence. *Eur J Cancer,* 33**,** 703-9.

CAPLAN, A. I. 1991. Mesenchymal stem cells. *J Orthop Res,* 9**,** 641-50.

CAPLAN, A. I. & DENNIS, J. E. 2006. Mesenchymal stem cells as trophic mediators. *J Cell Biochem,* 98**,** 1076-84.

CHELBERG, M. K., BANKS, G. M., GEIGER, D. F. & OEGEMA, T. R., JR. 1995. Identification of heterogeneous cell populations in normal human intervertebral disc. *J Anat,* 186 (Pt 1)**,** 43-53.

CHEN, J., YAN, W. & SETTON, L. A. 2006. Molecular phenotypes of notochordal cells purified from immature nucleus pulposus. *Eur Spine J,* 15 Suppl 3**,** S303-11.

CHEN, S., EMERY, S. E. & PEI, M. 2009a. Coculture of synovium-derived stem cells and nucleus pulposus cells in serum-free defined medium with supplementation of transforming growth factor-beta1: a potential application of tissue-specific stem cells in disc regeneration. *Spine (Phila Pa 1976),* 34**,** 1272-80.

CHEN, T., ZHOU, Y. & TAN, W. S. 2009b. Influence of lactic acid on the proliferation, metabolism, and differentiation of rabbit mesenchymal stem cells. *Cell Biol Toxicol,* 25**,** 573-86.

CHICHE, J., ILC, K., LAFERRIERE, J., TROTTIER, E., DAYAN, F., MAZURE, N. M., BRAHIMI-HORN, M. C. & POUYSSEGUR, J. 2009. Hypoxia-inducible carbonic anhydrase IX and XII promote tumor cell growth by counteracting acidosis through the regulation of the intracellular pH. *Cancer Res,* 69**,** 358-68.

CHO, H., LEE, S., PARK, S. H., HUANG, J., HASTY, K. A. & KIM, S. J. 2013. Synergistic effect of combined growth factors in porcine intervertebral disc degeneration. *Connect Tissue Res,* 54**,** 181-6.

CHOI, K. S., COHN, M. J. & HARFE, B. D. 2008. Identification of nucleus pulposus precursor cells and notochordal remnants in the mouse: implications for disk degeneration and chordoma formation. *Dev Dyn,* 237**,** 3953-8.

CHOI, K. S. & HARFE, B. D. 2011. Hedgehog signaling is required for formation of the notochord sheath and patterning of nuclei pulposi within the intervertebral discs. *Proc Natl Acad Sci U S A,* 108**,** 9484-9.

CHOI, Y. S. 2009. Pathophysiology of degenerative disc disease. *Asian Spine J,* 3**,** 39-44.

CHUJO, T., AN, H. S., AKEDA, K., MIYAMOTO, K., MUEHLEMAN, C., ATTAWIA, M., ANDERSSON, G. & MASUDA, K. 2006. Effects of growth differentiation factor-5 on the intervertebral disc--in vitro bovine study and in vivo rabbit disc degeneration model study. *Spine (Phila Pa 1976),* 31**,** 2909-17.

CIAPETTI, G., GRANCHI, D., DEVESCOVI, V., LEONARDI, E., GREGGI, T., DI SILVESTRE, M. & BALDINI, N. 2012. Ex vivo observation of human intervertebral disc tissue and cells isolated from degenerated intervertebral discs. *Eur Spine J,* 21 Suppl 1**,** S10-9.

CREVENSTEN, G., WALSH, A. J., ANANTHAKRISHNAN, D., PAGE, P., WAHBA, G. M., LOTZ, J. C. & BERVEN, S. 2004. Intervertebral disc cell therapy for regeneration: mesenchymal stem cell implantation in rat intervertebral discs. *Ann Biomed Eng,* 32**,** 430-4.

DAGENAIS, S., CARO, J. & HALDEMAN, S. 2008. A systematic review of low back pain cost of illness studies in the United States and internationally. *Spine J,* 8**,** 8-20.

DEOROSAN, B. & NAUMAN, E. A. 2011. The role of glucose, serum, and three-dimensional cell culture on the metabolism of bone marrow-derived mesenchymal stem cells. *Stem Cells Int,* 2011**,** 429187.

DEYO, R. A., GRAY, D. T., KREUTER, W., MIRZA, S. & MARTIN, B. I. 2005. United States trends in lumbar fusion surgery for degenerative conditions. *Spine (Phila Pa 1976),* 30**,** 1441-5; discussion 1446-7.

DIAMANT, B., KARLSSON, J. & NACHEMSON, A. 1968. Correlation between lactate levels and pH in discs of patients with lumbar rhizopathies. *Experientia,* 24**,** 1195-6.

DOMINICI, M., LE BLANC, K., MUELLER, I., SLAPER-CORTENBACH, I., MARINI, F., KRAUSE, D., DEANS, R., KEATING, A., PROCKOP, D. & HORWITZ, E. 2006. Minimal criteria for defining multipotent mesenchymal stromal cells. The International Society for Cellular Therapy position statement. *Cytotherapy,* 8**,** 315-7.

DOS SANTOS, F., ANDRADE, P. Z., BOURA, J. S., ABECASIS, M. M., DA SILVA, C. L. & CABRAL, J. M. 2010. Ex vivo expansion of human mesenchymal stem cells: a more effective cell proliferation kinetics and metabolism under hypoxia. *J Cell Physiol,* 223**,** 27-35.

DRAZIN, D., ROSNER, J., AVALOS, P. & ACOSTA, F. 2012. Stem cell therapy for degenerative disc disease. *Adv Orthop,* 2012**,** 961052.

DUVAL, E., BAUGE, C., ANDRIAMANALIJAONA, R., BENATEAU, H., LECLERCQ, S., DUTOIT, S., POULAIN, L., GALERA, P. & BOUMEDIENE, K. 2012. Molecular mechanism of hypoxia-induced chondrogenesis and its application in in. *Biomaterials,* 33**,** 6042-51.

ERWIN, W. M., ISLAM, D., EFTEKARPOUR, E., INMAN, R. D., KARIM, M. Z. & FEHLINGS, M. G. 2013. Intervertebral disc-derived stem cells: implications for regenerative medicine and neural repair. *Spine (Phila Pa 1976),* 38**,** 211-6.

ERWIN, W. M., ISLAM, D., INMAN, R. D., FEHLINGS, M. G. & TSUI, F. W. 2011. Notochordal cells protect nucleus pulposus cells from degradation and apoptosis: implications for the mechanisms of intervertebral disc degeneration. *Arthritis Res Ther,* 13**,** R215.

ESSER, P. 2010. pH and pressure in closed tissue culture vessel. Thermo Fisher Scientific Technical Bulletin-05.

EYRE, D. R., MATSUI, Y. & WU, J. J. 2002. Collagen polymorphisms of the intervertebral disc. *Biochem Soc Trans,* 30**,** 844-8.

EYRE, D. R. & MUIR, H. 1976. Types I and II collagens in intervertebral disc. Interchanging radial distributions in annulus fibrosus. *Biochem J,* 157**,** 267-70.

FAIRBANK, J., FROST, H., WILSON-MACDONALD, J., YU, L. M., BARKER, K. & COLLINS, R. 2005. Randomised controlled trial to compare surgical stabilisation of the lumbar spine with an intensive rehabilitation programme for patients with chronic low back pain: the MRC spine stabilisation trial. *Bmj,* 330**,** 1233.

FANG, Z., YANG, Q., LUO, W., LI, G. H., XIAO, J., LI, F. & XIONG, W. 2013. Differentiation of GFP-Bcl-2-engineered mesenchymal stem cells towards a nucleus pulposus-like phenotype under hypoxia in vitro. *Biochem Biophys Res Commun,* 432**,** 444-50.

FEHRER, C., BRUNAUER, R., LASCHOBER, G., UNTERLUGGAUER, H., REITINGER, S., KLOSS, F., GULLY, C., GASSNER, R. & LEPPERDINGER, G. 2007. Reduced oxygen tension attenuates differentiation capacity of human mesenchymal stem cells and prolongs their lifespan. *Aging Cell,* 6**,** 745-57.

FELKA, T., SCHAFER, R., SCHEWE, B., BENZ, K. & AICHER, W. K. 2009. Hypoxia reduces the inhibitory effect of IL-1beta on chondrogenic differentiation. *Osteoarthritis Cartilage,* 17**,** 1368-76.

FENG, G., LI, L., LIU, H., SONG, Y., HUANG, F., TU, C., SHEN, B., GONG, Q., LI, T., LIU, L., ZENG, J., KONG, Q., YI, M., GUPTE, M., MA, P. X. & PEI, F. 2013. Hypoxia differentially regulates human nucleus pulposus and annulus fibrosus cell extracellular matrix. *Osteoarthritis Cartilage,* 21**,** 582-8.

FENG, G., ZHAO, X., LIU, H., ZHANG, H., CHEN, X., SHI, R., LIU, X., ZHANG, W. & WANG, B. 2011. Transplantation of mesenchymal stem cells and nucleus pulposus cells in a degenerative disc model in rabbits: a comparison of 2 cell types as potential candidates for disc regeneration. *J Neurosurg Spine,* 14**,** 322-9.

FENG, H., DANFELTER, M., STROMQVIST, B. & HEINEGARD, D. 2006. Extracellular matrix in disc degeneration. *J Bone Joint Surg Am,* 88 Suppl 2**,** 25-9.

FERGUSON, S. J., ITO, K. & NOLTE, L. P. 2004. Fluid flow and convective transport of solutes within the intervertebral disc. *J Biomech,* 37**,** 213-21.

FREEMONT, A. J. 2009. The cellular pathobiology of the degenerate intervertebral disc and discogenic back pain. *Rheumatology (Oxford),* 48**,** 5-10.

FREEMONT, A. J., PEACOCK, T. E., GOUPILLE, P., HOYLAND, J. A., O'BRIEN, J. & JAYSON, M. I. 1997. Nerve ingrowth into diseased intervertebral disc in chronic back pain. *Lancet,* 350**,** 178-81.

FREEMONT, A. J., WATKINS, A., LE MAITRE, C., BAIRD, P., JEZIORSKA, M., KNIGHT, M. T., ROSS, E. R., O'BRIEN, J. P. & HOYLAND, J. A. 2002. Nerve growth factor expression and innervation of the painful intervertebral disc. *J Pathol,* 197**,** 286-92.

FREIMARK, D. & CZERMAK, P. 2009. Cell-based regeneration of intervertebral disc defects: review and concepts. *Int J Artif Organs,* 32**,** 197-203.

FRIEDENSTEIN, A. J., PETRAKOVA, K. V., KUROLESOVA, A. I. & FROLOVA, G. P. 1968. Heterotopic of bone marrow. Analysis of precursor cells for osteogenic and hematopoietic tissues. *Transplantation,* 6**,** 230-47.

FRITZELL, P., HAGG, O., WESSBERG, P. & NORDWALL, A. 2002. Chronic low back pain and fusion: a comparison of three surgical techniques: a prospective multicenter randomized study from the Swedish lumbar spine study group. *Spine (Phila Pa 1976),* 27**,** 1131-41.

GANEY, T., HUTTON, W. C., MOSELEY, T., HEDRICK, M. & MEISEL, H. J. 2009. Intervertebral disc repair using adipose tissue-derived stem and regenerative cells: experiments in a canine model. *Spine (Phila Pa 1976),* 34**,** 2297-304.

GAWRI, R., MWALE, F., OUELLET, J., ROUGHLEY, P. J., STEFFEN, T., ANTONIOU, J. & HAGLUND, L. 2011. Development of an organ culture system for long-term survival of the intact human intervertebral disc. *Spine (Phila Pa 1976),* 36**,** 1835-42.

GILBERT, H. T., HOYLAND, J. A. & MILLWARD-SADLER, S. J. 2010. The response of human anulus fibrosus cells to cyclic tensile strain is frequency-dependent and altered with disc degeneration. *Arthritis Rheum,* 62**,** 3385-94.

GIMBLE, J. & GUILAK, F. 2003. Adipose-derived adult stem cells: isolation, characterization, and differentiation potential. *Cytotherapy,* 5**,** 362-9.

GIRISH, V. & VIJAYALAKSHMI, A. 2004. Affordable image analysis using NIH Image/ImageJ. *Indian J Cancer,* 41**,** 47.

GRAYSON, W. L., ZHAO, F., BUNNELL, B. & MA, T. 2007. Hypoxia enhances proliferation and tissue formation of human mesenchymal stem cell. *Biochem Biophys Res Commun,* 358**,** 948-53.

GRUBER, H. E., FISHER, E. C., JR., DESAI, B., STASKY, A. A., HOELSCHER, G. & HANLEY, E. N., JR. 1997. Human intervertebral disc cells from the annulus: three-dimensional culture in agarose or alginate and responsiveness to TGF-beta1. *Exp Cell Res,* 235**,** 13-21.

GRUBER, H. E. & HANLEY, E. N., JR. 1998. Analysis of aging and degeneration of the human intervertebral disc. Comparison of surgical specimens with normal controls. *Spine (Phila Pa 1976),* 23**,** 751-7.

GRUBER, H. E., INGRAM, J. A., NORTON, H. J. & HANLEY, E. N., JR. 2007. Senescence in cells of the aging and degenerating intervertebral disc: immunolocalization of senescence-associated beta-galactosidase in human and sand rat discs. *Spine (Phila Pa 1976),* 32**,** 321-7.

GRUBER, H. E., NORTON, H. J. & HANLEY, E. N., JR. 2000. Anti-apoptotic effects of IGF-1 and PDGF on human intervertebral disc cells in vitro. *Spine (Phila Pa 1976),* 25**,** 2153-7.

GRUNHAGEN, T., WILDE, G., SOUKANE, D. M., SHIRAZI-ADL, S. A. & URBAN, J. P. 2006. Nutrient supply and intervertebral disc metabolism. *J Bone Joint Surg Am,* 88 Suppl 2**,** 30-5.

HANCOCK, M. J., BATTIE, M. C., VIDEMAN, T. & GIBBONS, L. 2010. The role of back injury or trauma in lumbar disc degeneration: an exposure-discordant twin study. *Spine (Phila Pa 1976),* 35**,** 1925-9.

HANDA, T., ISHIHARA, H., OHSHIMA, H., OSADA, R., TSUJI, H. & OBATA, K. 1997. Effects of hydrostatic pressure on matrix synthesis and matrix metalloproteinase production in the human lumbar intervertebral disc. *Spine (Phila Pa 1976),* 22**,** 1085-91.

HARRISON, J. S., RAMESHWAR, P., CHANG, V. & BANDARI, P. 2002. Oxygen saturation in the bone marrow of healthy volunteers. *Blood,* 99**,** 394.

HASCHTMANN, D., STOYANOV, J. V., GEDET, P. & FERGUSON, S. J. 2008. Vertebral endplate trauma induces disc cell apoptosis and promotes organ degeneration in vitro. *Eur Spine J,* 17**,** 289-99.

HASSLER, O. 1969. The human intervertebral disc. A micro-angiographical study on its vascular supply at various ages. *Acta Orthop Scand,* 40**,** 765-72.

HEDBOM, E. & HEINEGARD, D. 1993. Binding of fibromodulin and decorin to separate sites on fibrillar collagens. *J Biol Chem,* 268**,** 27307-12.

HELFMAN, T. & FALANGA, V. 1993. Gene expression in low oxygen tension. *Am J Med Sci,* 306**,** 37-41.

HENRIKSSON, H., THORNEMO, M., KARLSSON, C., HAGG, O., JUNEVIK, K., LINDAHL, A. & BRISBY, H. 2009a. Identification of cell proliferation zones, progenitor cells and a potential stem cell niche in the intervertebral disc region: a study in four species. *Spine (Phila Pa 1976),* 34**,** 2278-87.

HENRIKSSON, H. B., SVANVIK, T., JONSSON, M., HAGMAN, M., HORN, M., LINDAHL, A. & BRISBY, H. 2009b. Transplantation of human mesenchymal stems cells into intervertebral discs in a xenogeneic porcine model. *Spine (Phila Pa 1976),* 34**,** 141-8.

HERZENBERG, L. A., PARKS, D., SAHAF, B., PEREZ, O. & ROEDERER, M. 2002. The history and future of the fluorescence activated cell sorter and flow cytometry: a view from Stanford. *Clin Chem,* 48**,** 1819-27.

HEYWOOD, H. K., BADER, D. L. & LEE, D. A. 2006. Rate of oxygen consumption by isolated articular chondrocytes is sensitive to medium glucose concentration. *J Cell Physiol,* 206**,** 402-10.

HIYAMA, A., MOCHIDA, J., IWASHINA, T., OMI, H., WATANABE, T., SERIGANO, K., TAMURA, F. & SAKAI, D. 2008. Transplantation of mesenchymal stem cells in a canine disc degeneration model. *J Orthop Res,* 26**,** 589-600.

HIYAMA, A., SKUBUTYTE, R., MARKOVA, D., ANDERSON, D. G., YADLA, S., SAKAI, D., MOCHIDA, J., ALBERT, T. J., SHAPIRO, I. M. & RISBUD, M. V. 2011. Hypoxia activates the notch signaling pathway in cells of the intervertebral disc: implications in degenerative disc disease. *Arthritis Rheum,* 63**,** 1355-64.

HOHAUS, C., GANEY, T. M., MINKUS, Y. & MEISEL, H. J. 2008. Cell transplantation in lumbar spine disc degeneration disease. *Eur Spine J,* 17 Suppl 4**,** 492-503.

HOLM, S., MAROUDAS, A., URBAN, J. P., SELSTAM, G. & NACHEMSON, A. 1981. Nutrition of the intervertebral disc: solute transport and metabolism. *Connect Tissue Res,* 8**,** 101-19.

HOLM, S. & NACHEMSON, A. 1988. Nutrition of the intervertebral disc: acute effects of cigarette smoking. An experimental animal study. *Ups J Med Sci,* 93**,** 91-9.

HOLM, S., SELSTAM, G. & NACHEMSON, A. 1982. Carbohydrate metabolism and concentration profiles of solutes in the canine lumbar intervertebral disc. *Acta Physiol Scand,* 115**,** 147-56.

HORNER, H. A. & URBAN, J. P. 2001. 2001 Volvo Award Winner in Basic Science Studies: Effect of nutrient supply on the viability of cells from the nucleus pulposus of the intervertebral disc. *Spine (Phila Pa 1976),* 26**,** 2543-9.

HOY, D., BROOKS, P., BLYTH, F. & BUCHBINDER, R. 2010. The Epidemiology of low back pain. *Best Pract Res Clin Rheumatol,* 24**,** 769-81.

HUANG, C. Y., YUAN, T. Y., JACKSON, A. R., HAZBUN, L., FRAKER, C. & GU, W. Y. 2007. Effects of low glucose concentrations on oxygen consumption rates of intervertebral disc cells. *Spine (Phila Pa 1976),* 32**,** 2063-9.

HUGHES, S. P., FREEMONT, A. J., HUKINS, D. W., MCGREGOR, A. H. & ROBERTS, S. 2012. The pathogenesis of degeneration of the intervertebral disc and emerging therapies in the management of back pain. *J Bone Joint Surg Br,* 94**,** 1298-304.

HUNG, S. P., YANG, M. H., TSENG, K. F. & LEE, O. K. 2012. Hypoxia-induced Secretion of TGF-beta 1 in Mesenchymal Stem Cell Promotes Breast Cancer Cell Progression. *Cell Transplant,* 21**,** Epub ahead of print.

ILLIEN-JUNGER, S., GANTENBEIN-RITTER, B., GRAD, S., LEZUO, P., FERGUSON, S. J., ALINI, M. & ITO, K. 2010. The combined effects of limited nutrition and high-frequency loading on intervertebral discs with endplates. *Spine (Phila Pa 1976),* 35**,** 1744-52.

IMAI, Y., MIYAMOTO, K., AN, H. S., THONAR, E. J., ANDERSSON, G. B. & MASUDA, K. 2007. Recombinant human osteogenic protein-1 upregulates proteoglycan metabolism of human anulus fibrosus and nucleus pulposus cells. *Spine (Phila Pa 1976),* 32**,** 1303-9; discussion 1310.

INOUE, H. & TAKEDA, T. 1975. Three-dimensional observation of collagen framework of lumbar intervertebral discs. *Acta Orthop Scand,* 46**,** 949-56.

IOZZO, R. V. 1997. The family of the small leucine-rich proteoglycans: key regulators of matrix assembly and cellular growth. *Crit Rev Biochem Mol Biol,* 32**,** 141-74.

IOZZO, R. V. & MURDOCH, A. D. 1996. Proteoglycans of the extracellular environment: clues from the gene and protein side offer novel perspectives in molecular diversity and function. *Faseb J,* 10**,** 598-614.

ISHIHARA, H. & URBAN, J. P. 1999. Effects of low oxygen concentrations and metabolic inhibitors on proteoglycan and protein synthesis rates in the intervertebral disc. *J Orthop Res,* 17**,** 829-35.

ISHII, Y., THOMAS, A. O., GUO, X. E., HUNG, C. T. & CHEN, F. H. 2006. Localization and distribution of cartilage oligomeric matrix protein in the rat intervertebral disc. *Spine (Phila Pa 1976),* 31**,** 1539-46.

IWAHASHI, M., MATSUZAKI, H., TOKUHASHI, Y., WAKABAYASHI, K. & UEMATSU, Y. 2002. Mechanism of intervertebral disc degeneration caused by nicotine in rabbits to explicate intervertebral disc disorders caused by smoking. *Spine (Phila Pa 1976),* 27**,** 1396-401.

JACKSON, A. R., HUANG, C. Y., BROWN, M. D. & GU, W. Y. 2011a. 3D finite element analysis of nutrient distributions and cell viability in the intervertebral disc: effects of deformation and degeneration. *J Biomech Eng,* 133**,** 091006.

JACKSON, A. R., HUANG, C. Y. & GU, W. Y. 2011b. Effect of endplate calcification and mechanical deformation on the distribution of glucose in intervertebral disc: a 3D finite element study. *Comput Methods Biomech Biomed Engin,* 14**,** 195-204.

JEONG, J. H., JIN, E. S., MIN, J. K., JEON, S. R., PARK, C. S., KIM, H. S. & CHOI, K. H. 2009. Human mesenchymal stem cells implantation into the degenerated coccygeal disc of the rat. *Cytotechnology,* 59**,** 55-64.

JIM, J. J., NOPONEN-HIETALA, N., CHEUNG, K. M., OTT, J., KARPPINEN, J., SAHRARAVAND, A., LUK, K. D., YIP, S. P., SHAM, P. C., SONG, Y. Q., LEONG, J. C., CHEAH, K. S., ALA-KOKKO, L. & CHAN, D. 2005. The TRP2 allele of COL9A2 is an age-dependent risk factor for the development and severity of intervertebral disc degeneration. *Spine (Phila Pa 1976),* 30**,** 2735-42.

JOHNSON, W. E., CATERSON, B., EISENSTEIN, S. M., HYNDS, D. L., SNOW, D. M. & ROBERTS, S. 2002. Human intervertebral disc aggrecan inhibits nerve growth in vitro. *Arthritis Rheum,* 46**,** 2658-64.

JOHNSON, W. E., CATERSON, B., EISENSTEIN, S. M. & ROBERTS, S. 2005. Human intervertebral disc aggrecan inhibits endothelial cell adhesion and cell migration in vitro. *Spine (Phila Pa 1976),* 30**,** 1139-47.

JOHNSON, W. E., EISENSTEIN, S. M. & ROBERTS, S. 2001. Cell cluster formation in degenerate lumbar intervertebral discs is associated with increased disc cell proliferation. *Connect Tissue Res,* 42**,** 197-207.

JOHNSON, W. E., STEPHAN, S. & ROBERTS, S. 2008. The influence of serum, glucose and oxygen on intervertebral disc cell growth in vitro: implications for degenerative disc disease. *Arthritis Res Ther,* 10**,** R46.

JUNG, S., PANCHALINGAM, K. M., ROSENBERG, L. & BEHIE, L. A. 2012. Ex vivo expansion of human mesenchymal stem cells in defined serum-free media. *Stem Cells Int,* 2012**,** 123030.

JUNGER, S., GANTENBEIN-RITTER, B., LEZUO, P., ALINI, M., FERGUSON, S. J. & ITO, K. 2009. Effect of limited nutrition on in situ intervertebral disc cells under simulated-physiological loading. *Spine (Phila Pa 1976),* 34**,** 1264-71.

KAPLAN, K. M., SPIVAK, J. M. & BENDO, J. A. 2005. Embryology of the spine and associated congenital abnormalities. *Spine J,* 5**,** 564-76.

KARP, G. 1996. Aerobic respiration and metabolism. *Cell and molecular biology. John Wiley & Sons,* Inc.

KASHIWAGI, M., TORTORELLA, M., NAGASE, H. & BREW, K. 2001. TIMP-3 is a potent inhibitor of aggrecanase 1 (ADAM-TS4) and aggrecanase 2 (ADAM-TS5). *J Biol Chem,* 276**,** 12501-4.

KATZ, M. M., HARGENS, A. R. & GARFIN, S. R. 1986. Intervertebral disc nutrition. Diffusion versus convection. *Clin Orthop Relat Res***,** 243-5.

KAUPPILA, L. I. 1995. Ingrowth of blood vessels in disc degeneration. Angiographic and histological studies of cadaveric spines. *J Bone Joint Surg Am,* 77**,** 26-31.

KAUPPILA, L. I. 1997. Prevalence of stenotic changes in arteries supplying the lumbar spine. A postmortem angiographic study on 140 subjects. *Ann Rheum Dis,* 56**,** 591-5.

KAUPPILA, L. I., MIKKONEN, R., MANKINEN, P., PELTO-VASENIUS, K. & MAENPAA, I. 2004. MR aortography and serum cholesterol levels in patients with long-term nonspecific lower back pain. *Spine (Phila Pa 1976),* 29**,** 2147-52.

KAUPPILA, L. I., PENTTILA, A., KARHUNEN, P. J., LALU, K. & HANNIKAINEN, P. 1994. Lumbar disc degeneration and atherosclerosis of the abdominal aorta. *Spine (Phila Pa 1976),* 19**,** 923-9.

KEPLER, C. K., PONNAPPAN, R. K., TANNOURY, C. A., RISBUD, M. V. & ANDERSON, D. G. 2013. The molecular basis of intervertebral disc degeneration. *Spine J,* 13**,** 318-30.

KHAN, W. S., ADESIDA, A. B. & HARDINGHAM, T. E. 2007. Hypoxic conditions increase hypoxia-inducible transcription factor 2alpha and enhance chondrogenesis in stem cells from the infrapatellar fat pad of osteoarthritis patients. *Arthritis Res Ther,* 9**,** R55.

KIM, D. H., KIM, S. H., HEO, S. J., SHIN, J. W., LEE, S. W. & PARK, S. A. 2009a. Enhanced differentiation of mesenchymal stem cells into NP-like cells via 3D co-culturing with mechanical stimulation. *J Biosci Bioeng,* 108**,** 63-7.

KIM, K. W., HA, K. Y., LEE, J. S., NAM, S. W., WOO, Y. K., LIM, T. H. & AN, H. S. 2009b. Notochordal cells stimulate migration of cartilage end plate chondrocytes of the intervertebral disc in in vitro cell migration assays. *Spine J,* 9**,** 323-9.

KIM, K. W., LIM, T. H., KIM, J. G., JEONG, S. T., MASUDA, K. & AN, H. S. 2003. The origin of chondrocytes in the nucleus pulposus and histologic findings associated with the transition of a notochordal nucleus pulposus to a fibrocartilaginous nucleus pulposus in intact rabbit intervertebral discs. *Spine (Phila Pa 1976),* 28**,** 982-90.

KIM, N. K., SHIN, D. A., HAN, I. B., YOO, E. H., KIM, S. H. & CHUNG, S. S. 2011. The association of aggrecan gene polymorphism with the risk of intervertebral disc degeneration. *Acta Neurochir (Wien),* 153**,** 129-33.

KLUBA, T., NIEMEYER, T., GAISSMAIER, C. & GRUNDER, T. 2005. Human anulus fibrosis and nucleus pulposus cells of the intervertebral disc: effect of degeneration and culture system on cell phenotype. *Spine (Phila Pa 1976),* 30**,** 2743-8.

KREBS, S., FISCHALECK, M. & BLUM, H. 2009. A simple and loss-free method to remove TRIzol contaminations from minute RNA samples. *Anal Biochem,* 387**,** 136-8.

KUH, S. U., ZHU, Y., LI, J., TSAI, K. J., FEI, Q., HUTTON, W. C. & YOON, S. T. 2008. The AdLMP-1 transfection in two different cells; AF cells, chondrocytes as potential cell therapy candidates for disc degeneration. *Acta Neurochir (Wien),* 150**,** 803-10.

LE MAITRE, C. L., FREEMONT, A. J. & HOYLAND, J. A. 2004. Localization of degradative enzymes and their inhibitors in the degenerate human intervertebral disc. *J Pathol,* 204**,** 47-54.

LE MAITRE, C. L., FREEMONT, A. J. & HOYLAND, J. A. 2005. The role of interleukin-1 in the pathogenesis of human intervertebral disc degeneration. *Arthritis Res Ther,* 7**,** R732-45.

LE MAITRE, C. L., FREEMONT, A. J. & HOYLAND, J. A. 2006. A preliminary in vitro study into the use of IL-1Ra gene therapy for the inhibition of intervertebral disc degeneration. *Int J Exp Pathol,* 87**,** 17-28.

LE MAITRE, C. L., FREEMONT, A. J. & HOYLAND, J. A. 2007a. Accelerated cellular senescence in degenerate intervertebral discs: a possible role in the pathogenesis of intervertebral disc degeneration. *Arthritis Res Ther,* 9**,** R45.

LE MAITRE, C. L., HOYLAND, J. A. & FREEMONT, A. J. 2007b. Catabolic cytokine expression in degenerate and herniated human intervertebral discs: IL-1beta and TNFalpha expression profile. *Arthritis Res Ther,* 9**,** R77.

LE MAITRE, C. L., HOYLAND, J. A. & FREEMONT, A. J. 2007c. Interleukin-1 receptor antagonist delivered directly and by gene therapy inhibits matrix degradation in the intact degenerate human intervertebral disc: an in situ zymographic and gene therapy study. *Arthritis Res Ther,* 9**,** R83.

LE MAITRE, C. L., POCKERT, A., BUTTLE, D. J., FREEMONT, A. J. & HOYLAND, J. A. 2007d. Matrix synthesis and degradation in human intervertebral disc degeneration. *Biochem Soc Trans,* 35**,** 652-5.

LEE, E. Y., XIA, Y., KIM, W. S., KIM, M. H., KIM, T. H., KIM, K. J., PARK, B. S. & SUNG, J. H. 2009a. Hypoxia-enhanced wound-healing function of adipose-derived stem cells: increase in stem cell proliferation and up-regulation of VEGF and bFGF. *Wound Repair Regen,* 17**,** 540-7.

LEE, R. B., WILKINS, R. J., RAZAQ, S. & URBAN, J. P. 2002. The effect of mechanical stress on cartilage energy metabolism. *Biorheology,* 39**,** 133-43.

LEE, Y. K., KIM, E. J., LEE, J. E., NOH, J. W. & KIM, Y. G. 2009b. Hypoxia induces connective tissue growth factor mRNA expression. *J Korean Med Sci,* 24 Suppl**,** S176-82.

LEVIN, D. A., HALE, J. J. & BENDO, J. A. 2007. Adjacent segment degeneration following spinal fusion for degenerative disc disease. *Bull NYU Hosp Jt Dis,* 65**,** 29-36.

LEWIS, G. 2012. Nucleus pulposus replacement and regeneration/repair technologies: present status and future prospects. *J Biomed Mater Res B Appl Biomater,* 100**,** 1702-20.

LI, H., LIANG, C., TAO, Y., ZHOU, X., LI, F., CHEN, G. & CHEN, Q. X. 2012. Acidic pH conditions mimicking degenerative intervertebral discs impair the survival and biological behavior of human adipose-derived mesenchymal stem cells. *Exp Biol Med (Maywood),* 237**,** 845-52.

LI, X., LEE, J. P., BALIAN, G. & GREG ANDERSON, D. 2005a. Modulation of chondrocytic properties of fat-derived mesenchymal cells in co-cultures with nucleus pulposus. *Connect Tissue Res,* 46**,** 75-82.

LI, Y., CHEN, J., ZHANG, C. L., WANG, L., LU, D., KATAKOWSKI, M., GAO, Q., SHEN, L. H., ZHANG, J., LU, M. & CHOPP, M. 2005b. Gliosis and brain remodeling after treatment of stroke in rats with marrow stromal cells. *Glia,* 49**,** 407-17.

LIANG, C., LI, H., TAO, Y., ZHOU, X., LI, F., CHEN, G. & CHEN, Q. 2012a. Responses of human adipose-derived mesenchymal stem cells to chemical microenvironment of the intervertebral disc. *J Transl Med,* 10**,** 49.

LIANG, C. Z., LI, H., TAO, Y. Q., ZHOU, X. P., YANG, Z. R., XIAO, Y. X., LI, F. C., HAN, B. & CHEN, Q. X. 2012b. Dual delivery for stem cell differentiation using dexamethasone and bFGF in/on polymeric microspheres as a cell carrier for nucleus pulposus regeneration. *J Mater Sci Mater Med,* 23**,** 1097-107.

LIANG, W., YE, D., DAI, L., SHEN, Y. & XU, J. 2012c. Overexpression of hTERT extends replicative capacity of human nucleus pulposus cells, and protects against serum starvation-induced apoptosis and cell cycle arrest. *J Cell Biochem,* 113**,** 2112-21.

LIAO, S. Y., LERMAN, M. I. & STANBRIDGE, E. J. 2009. Expression of transmembrane carbonic anhydrases, CAIX and CAXII, in human development. *BMC Dev Biol,* 9**,** 22.

LIEBSCHER, T., HAEFELI, M., WUERTZ, K., NERLICH, A. G. & BOOS, N. 2011. Age-related variation in cell density of human lumbar intervertebral disc. *Spine (Phila Pa 1976),* 36**,** 153-9.

LIU, L. T., HUANG, B., LI, C. Q., ZHUANG, Y., WANG, J. & ZHOU, Y. 2011. Characteristics of stem cells derived from the degenerated human intervertebral disc cartilage endplate. *PLoS One,* 6**,** e26285.

LIVAK, K. J. & SCHMITTGEN, T. D. 2001. Analysis of relative gene expression data using real-time quantitative PCR and the 2(-Delta Delta C(T)) Method. *Methods,* 25**,** 402-8.

LO, T., HO, J. H., YANG, M. H. & LEE, O. K. 2011. Glucose reduction prevents replicative senescence and increases mitochondrial respiration in human mesenchymal stem cells. *Cell Transplant,* 20**,** 813-25.

LONGO, U. G., PAPAPIETRO, N., PETRILLO, S., FRANCESCHETTI, E., MAFFULLI, N. & DENARO, V. 2012. Mesenchymal stem cell for prevention and management of intervertebral disc degeneration. *Stem Cells Int,* 2012**,** 921053.

LOTZ, J. C., COLLIOU, O. K., CHIN, J. R., DUNCAN, N. A. & LIEBENBERG, E. 1998. Compression-induced degeneration of the intervertebral disc: an in vivo mouse model and finite-element study. *Spine (Phila Pa 1976),* 23**,** 2493-506.

LU, Z. F., ZANDIEH DOULABI, B., WUISMAN, P. I., BANK, R. A. & HELDER, M. N. 2007. Differentiation of adipose stem cells by nucleus pulposus cells: configuration effect. *Biochem Biophys Res Commun,* 359**,** 991-6.

LUDWINSKI, F. E., GNANALINGHAM, K., RICHARDSON, S. M. & HOYLAND, J. A. 2013. Understanding the native nucleus pulposus cell phenotype has important implications for intervertebral disc regeneration strategies. *Regen Med,* 8**,** 75-87.

MACLEAN, J. J., LEE, C. R., ALINI, M. & IATRIDIS, J. C. 2004. Anabolic and catabolic mRNA levels of the intervertebral disc vary with the magnitude and frequency of in vivo dynamic compression. *J Orthop Res,* 22**,** 1193-200.

MAERZ, T., HERKOWITZ, H. & BAKER, K. 2013. Molecular and genetic advances in the regeneration of the intervertebral disc. *Surg Neurol Int,* 4**,** S94-s105.

MAIDHOF, R., ALIPUI, D. O., RAFIUDDIN, A., LEVINE, M., GRANDE, D. A. & CHAHINE, N. O. 2012. Emerging trends in biological therapy for intervertebral disc degeneration. *Discov Med,* 14**,** 401-11.

MAIER, T., GUELL, M. & SERRANO, L. 2009. Correlation of mRNA and protein in complex biological samples. *FEBS Lett,* 583**,** 3966-73.

MARCHAND, F. & AHMED, A. M. 1990. Investigation of the laminate structure of lumbar disc anulus fibrosus. *Spine (Phila Pa 1976),* 15**,** 402-10.

MAROUDAS, A., STOCKWELL, R. A., NACHEMSON, A. & URBAN, J. 1975. Factors involved in the nutrition of the human lumbar intervertebral disc: cellularity and diffusion of glucose in vitro. *J Anat,* 120**,** 113-30.

MATSUI, H., KANAMORI, M., ISHIHARA, H., YUDOH, K., NARUSE, Y. & TSUJI, H. 1998. Familial predisposition for lumbar degenerative disc disease. A case-control study. *Spine (Phila Pa 1976),* 23**,** 1029-34.

MAVROGONATOU, E. & KLETSAS, D. 2010. Effect of varying osmotic conditions on the response of bovine nucleus pulposus cells to growth factors and the activation of the ERK and Akt pathways. *J Orthop Res,* 28**,** 1276-82.

MCCANLESS, J. D., COLE, J. A., SLACK, S. M., BUMGARDNER, J. D., ZAMORA, P. O. & HAGGARD, W. O. 2011. Modeling nucleus pulposus regeneration in vitro: mesenchymal stem cells, alginate beads, hypoxia, bone morphogenetic protein-2, and synthetic peptide B2A. *Spine (Phila Pa 1976),* 36**,** 2275-85.

MEISEL, H. J., SIODLA, V., GANEY, T., MINKUS, Y., HUTTON, W. C. & ALASEVIC, O. J. 2007. Clinical experience in cell-based therapeutics: disc chondrocyte transplantation A treatment for degenerated or damaged intervertebral disc. *Biomol Eng,* 24**,** 5-21.

MELROSE, J., GHOSH, P. & TAYLOR, T. K. 2001. A comparative analysis of the differential spatial and temporal distributions of the large (aggrecan, versican) and small (decorin, biglycan, fibromodulin) proteoglycans of the intervertebral disc. *J Anat,* 198**,** 3-15.

MIETSCH, A., IGNATIUS, A., CARSTENS, C., BRAYDA-BRUNO, M. & NEIDLINGER-WILKE, C. 2012. Differentiation of Nucleus Pulposus Cells Alters Their Responsivity to Mechanics and Glucose Reduction. *Global Spine J,* 02**,** P82.

MINOGUE, B. M., RICHARDSON, S. M., ZEEF, L. A., FREEMONT, A. J. & HOYLAND, J. A. 2010a. Characterization of the human nucleus pulposus cell phenotype and evaluation of novel marker gene expression to define adult stem cell differentiation. *Arthritis Rheum,* 62**,** 3695-705.

MINOGUE, B. M., RICHARDSON, S. M., ZEEF, L. A., FREEMONT, A. J. & HOYLAND, J. A. 2010b. Transcriptional profiling of bovine intervertebral disc cells: implications for identification of normal and degenerate human intervertebral disc cell phenotypes. *Arthritis Res Ther,* 12**,** R22.

MIYAMOTO, K., MASUDA, K., KIM, J. G., INOUE, N., AKEDA, K., ANDERSSON, G. B. & AN, H. S. 2006. Intradiscal injections of osteogenic protein-1 restore the viscoelastic properties of degenerated intervertebral discs. *Spine J,* 6**,** 692-703.

MIYAMOTO, T., MUNETA, T., TABUCHI, T., MATSUMOTO, K., SAITO, H., TSUJI, K. & SEKIYA, I. 2010. Intradiscal transplantation of synovial mesenchymal stem cells prevents intervertebral disc degeneration through suppression of matrix metalloproteinase-related genes in nucleus pulposus cells in rabbits. *Arthritis Res Ther,* 12**,** R206.

MOHYELDIN, A., GARZON-MUVDI, T. & QUINONES-HINOJOSA, A. 2010. Oxygen in stem cell biology: a critical component of the stem cell niche. *Cell Stem Cell,* 7**,** 150-61.

MOKHBI SOUKANE, D., SHIRAZI-ADL, A. & URBAN, J. P. 2009. Investigation of solute concentrations in a 3D model of intervertebral disc. *Eur Spine J,* 18**,** 254-62.

MULLER, J., BENZ, K., AHLERS, M., GAISSMAIER, C. & MOLLENHAUER, J. 2011. Hypoxic conditions during expansion culture prime human mesenchymal stromal precursor cells for chondrogenic differentiation in three-dimensional cultures. *Cell Transplant,* 20**,** 1589-602.

MURAKAMI, H., YOON, S. T., ATTALLAH-WASIF, E. S., TSAI, K. J., FEI, Q. & HUTTON, W. C. 2006. The expression of anabolic cytokines in intervertebral discs in age-related degeneration. *Spine (Phila Pa 1976),* 31**,** 1770-4.

MUSGROVE, E., SEAMAN, M. & HEDLEY, D. 1987. Relationship between cytoplasmic pH and proliferation during exponential growth and cellular quiescence. *Exp Cell Res,* 172**,** 65-75.

MWALE, F., ClOBANU, I., GIANNITSIOS, D., ROUGHLEY, P., STEFFEN, T. & ANTONIOU, J. 2011. Effect of oxygen levels on proteoglycan synthesis by intervertebral disc cells. *Spine (Phila Pa 1976),* 36**,** E131-8.

NACHEMSON, A. 1969. Intradiscal measurements of pH in patients with lumbar rhizopathies. *Acta Orthop Scand,* 40**,** 23-42.

NACHEMSON, A., LEWIN, T., MAROUDAS, A. & FREEMAN, M. A. 1970. In vitro diffusion of dye through the end-plates and the annulus fibrosus of human lumbar inter-vertebral discs. *Acta Orthop Scand,* 41**,** 589-607.

NCB1-GENE http://www.ncbi.nlm.nih.gov/gene/1967 and

http://www.ncbi.nlm.nih.gov/gene/9801.

NEIDLINGER-WILKE, C., MIETSCH, A., RINKLER, C., WILKE, H. J., IGNATIUS, A. & URBAN, J. 2012. Interactions of environmental conditions and mechanical loads have influence on matrix turnover by nucleus pulposus cells. *J Orthop Res,* 30**,** 112-21.

NEIDLINGER-WILKE, C., WURTZ, K., URBAN, J. P., BORM, W., ARAND, M., IGNATIUS, A., WILKE, H. J. & CLAES, L. E. 2006. Regulation of gene expression in intervertebral disc cells by low and high hydrostatic pressure. *Eur Spine J,* 15 Suppl 3**,** S372-8.

NEKANTI, U., DASTIDAR, S., VENUGOPAL, P., TOTEY, S. & TA, M. 2010. Increased proliferation and analysis of differential gene expression in human Wharton's jelly-derived mesenchymal stromal cells under hypoxia. *Int J Biol Sci,* 6**,** 499-512.

NERLICH, A. G., SCHLEICHER, E. D. & BOOS, N. 1997. 1997 Volvo Award winner in basic science studies. Immunohistologic markers for age-related changes of human lumbar intervertebral discs. *Spine (Phila Pa 1976),* 22**,** 2781-95.

NGUYEN, C., POIRAUDEAU, S. & RANNOU, F. 2012. Vertebral subchondral bone. *Osteoporos Int,* 23 Suppl 8**,** S857-60.

NISHIDA, K., KANG, J. D., GILBERTSON, L. G., MOON, S. H., SUH, J. K., VOGT, M. T., ROBBINS, P. D. & EVANS, C. H. 1999. Modulation of the biologic activity of the rabbit intervertebral disc by gene therapy: an in vivo study of adenovirus-mediated transfer of the human transforming growth factor beta 1 encoding gene. *Spine (Phila Pa 1976),* 24**,** 2419-25.

NOMURA, T., MOCHIDA, J., OKUMA, M., NISHIMURA, K. & SAKABE, K. 2001. Nucleus pulposus allograft retards intervertebral disc degeneration. *Clin Orthop Relat Res***,** 94-101.

O'HARA, B. P., URBAN, J. P. & MAROUDAS, A. 1990. Influence of cyclic loading on the nutrition of articular cartilage. *Ann Rheum Dis,* 49**,** 536-9.

OGATA, K. & WHITESIDE, L. A. 1981. 1980 Volvo award winner in basic science. Nutritional pathways of the intervertebral disc. An experimental study using hydrogen washout technique. *Spine (Phila Pa 1976),* 6**,** 211-6.

OHNISHI, S., YASUDA, T., KITAMURA, S. & NAGAYA, N. 2007. Effect of hypoxia on gene expression of bone marrow-derived mesenchymal stem cells and mononuclear cells. *Stem Cells,* 25**,** 1166-77.

OHSHIMA, H. & URBAN, J. P. 1992. The effect of lactate and pH on proteoglycan and protein synthesis rates in the intervertebral disc. *Spine (Phila Pa 1976),* 17**,** 1079-82.

OKUMA, M., MOCHIDA, J., NISHIMURA, K., SAKABE, K. & SEIKI, K. 2000. Reinsertion of stimulated nucleus pulposus cells retards intervertebral disc degeneration: an in vitro and in vivo experimental study. *J Orthop Res,* 18**,** 988-97.

OROZCO, L., SOLER, R., MORERA, C., ALBERCA, M., SANCHEZ, A. & GARCIA-SANCHO, J. 2011. Intervertebral disc repair by autologous mesenchymal bone marrow cells: a pilot study. *Transplantation,* 92**,** 822-8.

PAASSILTA, P., LOHINIVA, J., GORING, H. H., PERALA, M., RAINA, S. S., KARPPINEN, J., HAKALA, M., PALM, T., KROGER, H., KAITILA, I., VANHARANTA, H., OTT, J. & ALA-KOKKO, L. 2001. Identification of a novel common genetic risk factor for lumbar disk disease. *Jama,* 285**,** 1843-9.

PARISH, C. R. 1999. Fluorescent dyes for lymphocyte migration and proliferation studies. *Immunol Cell Biol,* 77**,** 499-508.

PATTAPPA, G., LI, Z., PEROGLIO, M., WISMER, N., ALINI, M. & GRAD, S. 2012. Diversity of intervertebral disc cells: phenotype and function. *J Anat,* 221**,** 480-96.

PAUL, C. P., SCHOORL, T., ZUIDERBAAN, H. A., ZANDIEH DOULABI, B., VAN DER VEEN, A. J., VAN DE VEN, P. M., SMIT, T. H., VAN ROYEN, B. J., HELDER, M. N. & MULLENDER, M. G. 2013. Dynamic and static overloading induce early degenerative processes in caprine lumbar intervertebral discs. *PLoS One,* 8**,** e62411.

PAUL, R., HAYDON, R. C., CHENG, H., ISHIKAWA, A., NENADOVICH, N., JIANG, W., ZHOU, L., BREYER, B., FENG, T., GUPTA, P., HE, T. C. & PHILLIPS, F. M. 2003. Potential use of Sox9 gene therapy for intervertebral degenerative disc disease. *Spine (Phila Pa 1976),* 28**,** 755-63.

PEACOCK, A. 1951. Observations on the prenatal development of the intervertebral disc in man. *J Anat,* 85**,** 260-74.

PEI, M., SHOUKRY, M., LI, J., DAFFNER, S. D., FRANCE, J. C. & EMERY, S. E. 2012. Modulation of in vitro microenvironment facilitates synovium-derived stem cell-based nucleus pulposus tissue regeneration. *Spine (Phila Pa 1976),* 37**,** 1538-47.

PITTENGER, M. F., MACKAY, A. M., BECK, S. C., JAISWAL, R. K., DOUGLAS, R., MOSCA, J. D., MOORMAN, M. A., SIMONETTI, D. W., CRAIG, S. & MARSHAK, D. R. 1999. Multilineage potential of adult human mesenchymal stem cells. *Science,* 284**,** 143-7.

POCKERT, A. J., RICHARDSON, S. M., LE MAITRE, C. L., LYON, M., DEAKIN, J. A., BUTTLE, D. J., FREEMONT, A. J. & HOYLAND, J. A. 2009. Modified expression of the ADAMTS enzymes and tissue inhibitor of metalloproteinases 3 during human intervertebral disc degeneration. *Arthritis Rheum,* 60**,** 482-91.

PONNAPPAN, R. K., MARKOVA, D. Z., ANTONIO, P. J., MURRAY, H. B., VACCARO, A. R., SHAPIRO, I. M., ANDERSON, D. G., ALBERT, T. J. & RISBUD, M. V. 2011. An organ culture system to model early degenerative changes of the intervertebral disc. *Arthritis Res Ther,* 13**,** R171.

PORTER, S., CLARK, I. M., KEVORKIAN, L. & EDWARDS, D. R. 2005. The ADAMTS metalloproteinases. *Biochem J,* 386**,** 15-27.

POTTER, C. P. & HARRIS, A. L. 2003. Diagnostic, prognostic and therapeutic implications of carbonic anhydrases in cancer. *Br J Cancer,* 89**,** 2-7.

POURQUIE, O. 2000. Segmentation of Paraxial Mesoderm and vertebrate somitogenesis. *Curr Top Dev Biol,* 47**,** 81-105.

POWER, K. A., GRAD, S., RUTGES, J. P., CREEMERS, L. B., VAN RIJEN, M. H., O'GAORA, P., WALL, J. G., ALINI, M., PANDIT, A. & GALLAGHER, W. M. 2011. Identification of cell surface-specific markers to target human nucleus pulposus cells: expression of carbonic anhydrase XII varies with age and degeneration. *Arthritis Rheum,* 63**,** 3876-86.

PRATSINIS, H. & KLETSAS, D. 2007. PDGF, bFGF and IGF-I stimulate the proliferation of intervertebral disc cells in vitro via the activation of the ERK and Akt signaling pathways. *Eur Spine J,* 16**,** 1858-66.

PRERADOVIC, A., KLEINPETER, G., FEICHTINGER, H., BALAUN, E. & KRUGLUGER, W. 2005. Quantitation of collagen I, collagen II and aggrecan mRNA and expression of the corresponding proteins in human nucleus pulposus cells in monolayer cultures. *Cell Tissue Res,* 321**,** 459-64.

PURMESSUR, D., FREEMONT, A. J. & HOYLAND, J. A. 2008. Expression and regulation of neurotrophins in the nondegenerate and degenerate human intervertebral disc. *Arthritis Res Ther,* 10**,** R99.

RADONIC, A., THULKE, S., MACKAY, I. M., LANDT, O., SIEGERT, W. & NITSCHE, A. 2004. Guideline to reference gene selection for quantitative real-time PCR. *Biochem Biophys Res Commun,* 313**,** 856-62.

RAJ, P. P. 2008. Intervertebral disc: anatomy-physiology-pathophysiology-treatment. *Pain Pract,* 8**,** 18-44.

RAJASEKARAN, S., BABU, J. N., ARUN, R., ARMSTRONG, B. R., SHETTY, A. P. & MURUGAN, S. 2004. ISSLS prize winner: A study of diffusion in human lumbar discs: a serial magnetic resonance imaging study documenting the influence of the endplate on diffusion in normal and degenerate discs. *Spine (Phila Pa 1976),* 29**,** 2654-67.

RATSEP, T., MINAJEVA, A. & ASSER, T. 2013. Relationship between neovascularization and degenerative changes in herniated lumbar intervertebral discs. *Eur Spine J,* 22**,** Epub ahead of print.

RAWLS, A. & FISHER, R. E. 2010. Development and functional anatomy of the spine. *In:* KUSUMI, K. & DUNWOODIE, S. L. (eds.) *The genetics and development of scoliosis.*: S. L. *Springer*, 2, 30-33.

RAZAQ, S., URBAN, J. P. & WILKINS, R. J. 2000. Regulation of intracellular pH by bovine intervertebral disc cells. *Cell Physiol Biochem,* 10**,** 109-15.

RAZAQ, S., WILKINS, R. J. & URBAN, J. P. 2003. The effect of extracellular pH on matrix turnover by cells of the bovine nucleus pulposus. *Eur Spine J,* 12**,** 341-9.

RICHARDSON, S. M., DOYLE, P., MINOGUE, B. M., GNANALINGHAM, K. & HOYLAND, J. A. 2009. Increased expression of matrix metalloproteinase-10, nerve growth factor and substance P in the painful degenerate intervertebral disc. *Arthritis Res Ther,* 11**,** R126.

RICHARDSON, S. M., HOYLAND, J. A., MOBASHERI, R., CSAKI, C., SHAKIBAEI, M. & MOBASHERI, A. 2010. Mesenchymal stem cells in regenerative medicine: opportunities and challenges for articular cartilage and intervertebral disc tissue engineering. *J Cell Physiol,* 222**,** 23-32.

RICHARDSON, S. M., HUGHES, N., HUNT, J. A., FREEMONT, A. J. & HOYLAND, J. A. 2008. Human mesenchymal stem cell differentiation to NP-like cells in chitosan-glycerophosphate hydrogels. *Biomaterials,* 29**,** 85-93.

RICHARDSON, S. M., WALKER, R. V., PARKER, S., RHODES, N. P., HUNT, J. A., FREEMONT, A. J. & HOYLAND, J. A. 2006. Intervertebral disc cell-mediated mesenchymal stem cell differentiation. *Stem Cells,* 24**,** 707-16.

RINKLER, C., HEUER, F., PEDRO, M. T., MAUER, U. M., IGNATIUS, A. & NEIDLINGER-WILKE, C. 2010. Influence of low glucose supply on the regulation of gene expression by nucleus pulposus cells and their responsiveness to mechanical loading. *J Neurosurg Spine,* 13**,** 535-42.

RISBUD, M. V., ALBERT, T. J., GUTTAPALLI, A., VRESILOVIC, E. J., HILLIBRAND, A. S., VACCARO, A. R. & SHAPIRO, I. M. 2004a. Differentiation of mesenchymal stem cells towards a nucleus pulposus-like phenotype in vitro: implications for cell-based transplantation therapy. *Spine (Phila Pa 1976),* 29**,** 2627-32.

RISBUD, M. V., FERTALA, J., VRESILOVIC, E. J., ALBERT, T. J. & SHAPIRO, I. M. 2005. Nucleus pulposus cells upregulate PI3K/Akt and MEK/ERK signaling pathways under hypoxic conditions and resist apoptosis induced by serum withdrawal. *Spine (Phila Pa 1976),* 30**,** 882-9.

RISBUD, M. V., GUTTAPALLI, A., TSAI, T. T., LEE, J. Y., DANIELSON, K. G., VACCARO, A. R., ALBERT, T. J., GAZIT, Z., GAZIT, D. & SHAPIRO, I. M. 2007. Evidence for skeletal progenitor cells in the degenerate human intervertebral disc. *Spine (Phila Pa 1976),* 32**,** 2537-44.

RISBUD, M. V., SCHAER, T. P. & SHAPIRO, I. M. 2010a. Toward an understanding of the role of notochordal cells in the adult intervertebral disc: from discord to accord. *Dev Dyn,* 239**,** 2141-8.

RISBUD, M. V., SCHIPANI, E. & SHAPIRO, I. M. 2010b. Hypoxic regulation of Nucleus pulposus cell survival. *Am J Pathol,* 176**,** 1-7.

RISBUD, M. V. & SHAPIRO, I. M. 2011. Notochordal cells in the adult intervertebral disc: new perspective on an old question. *Crit Rev Eukaryot Gene Expr,* 21**,** 29-41.

RISBUD, M. V., SHAPIRO, I. M., VACCARO, A. R. & ALBERT, T. J. 2004b. Stem cell regeneration of the nucleus pulposus. *Spine J,* 4**,** 348s-353s.

ROBERTS, S., CATERSON, B., MENAGE, J., EVANS, E. H., JAFFRAY, D. C. & EISENSTEIN, S. M. 2000. Matrix metalloproteinases and aggrecanase: their role in disorders of the human intervertebral disc. *Spine (Phila Pa 1976),* 25**,** 3005-13.

ROBERTS, S., EVANS, E. H., KLETSAS, D., JAFFRAY, D. C. & EISENSTEIN, S. M. 2006a. Senescence in human intervertebral discs. *Eur Spine J,* 15 Suppl 3**,** S312-6.

ROBERTS, S., EVANS, H., TRIVEDI, J. & MENAGE, J. 2006b. Histology and pathology of the human intervertebral disc. *J Bone Joint Surg Am,* 88 Suppl 2**,** 10-4.

ROBERTS, S., MENAGE, J., DUANCE, V., WOTTON, S. & AYAD, S. 1991. 1991 Volvo Award in basic sciences. Collagen types around the cells of the intervertebral disc and cartilage end plate: an immunolocalization study. *Spine (Phila Pa 1976),* 16**,** 1030-8.

ROBERTS, S., MENAGE, J. & URBAN, J. P. 1989. Biochemical and structural properties of the cartilage end-plate and its relation to the intervertebral disc. *Spine (Phila Pa 1976),* 14**,** 166-74.

ROBERTS, S., URBAN, J. P., EVANS, H. & EISENSTEIN, S. M. 1996. Transport properties of the human cartilage endplate in relation to its composition and calcification. *Spine (Phila Pa 1976),* 21**,** 415-20.

RODRIGUES, M., GRIFFITH, L. G. & WELLS, A. 2010. Growth factor regulation of proliferation and survival of multipotential stromal cells. *Stem Cell Res Ther,* 1**,** 32.

RODRIGUES-PINTO, R., RICHARDSON, S. M. & HOYLAND, J. A. 2013. Identification of novel nucleus pulposus markers: Interspecies variations and implications for cell-based therapiesfor intervertebral disc degeneration. *Bone Joint Res,* 2**,** 169-78.

SAHAI, A., MEI, C., SCHRIER, R. W. & TANNEN, R. L. 1999. Mechanisms of chronic hypoxia-induced renal cell growth. *Kidney Int,* 56**,** 1277-81.

SAKAI, D., MOCHIDA, J., IWASHINA, T., HIYAMA, A., OMI, H., IMAI, M., NAKAI, T., ANDO, K. & HOTTA, T. 2006. Regenerative effects of transplanting mesenchymal stem cells embedded in atelocollagen to the degenerated intervertebral disc. *Biomaterials,* 27**,** 335-45.

SAKAI, D., MOCHIDA, J., IWASHINA, T., WATANABE, T., NAKAI, T., ANDO, K. & HOTTA, T. 2005. Differentiation of mesenchymal stem cells transplanted to a rabbit degenerative disc model: potential and limitations for stem cell therapy in disc regeneration. *Spine (Phila Pa 1976),* 30**,** 2379-87.

SAKAI, D., MOCHIDA, J., YAMAMOTO, Y., NOMURA, T., OKUMA, M., NISHIMURA, K., NAKAI, T., ANDO, K. & HOTTA, T. 2003. Transplantation of mesenchymal stem cells embedded in Atelocollagen gel to the intervertebral disc: a potential therapeutic model for disc degeneration. *Biomaterials,* 24**,** 3531-41.

SCHMITTGEN, T. D. & ZAKRAJSEK, B. A. 2000. Effect of experimental treatment on housekeeping gene expression: validation by real-time, quantitative RT-PCR. *J Biochem Biophys Methods,* 46**,** 69-81.

SCOTT, J. E., BOSWORTH, T. R., CRIBB, A. M. & TAYLOR, J. R. 1994. The chemical morphology of age-related changes in human intervertebral disc glycosaminoglycans from cervical, thoracic and lumbar nucleus pulposus and annulus fibrosus. *J Anat,* 184 (Pt 1)**,** 73-82.

SELARD, E., SHIRAZI-ADL, A. & URBAN, J. P. 2003. Finite element study of nutrient diffusion in the human intervertebral disc. *Spine (Phila Pa 1976),* 28**,** 1945-53; discussion 1953.

SEOL, D., CHOE, H., ZHENG, H., JANG, K., RAMAKRISHNAN, P. S., LIM, T. H. & MARTIN, J. A. 2011. Selection of reference genes for normalization of quantitative real-time PCR in organ culture of the rat and rabbit intervertebral disc. *BMC Res Notes,* 4**,** 162.

SERIGANO, K., SAKAI, D., HIYAMA, A., TAMURA, F., TANAKA, M. & MOCHIDA, J. 2010. Effect of cell number on mesenchymal stem cell transplantation in a canine degeneration model. *J Orthop Res,* 28**,** 1267-75.

SETTON, L. A. & CHEN, J. 2006. Mechanobiology of the intervertebral disc and relevance to disc degeneration. *J Bone Joint Surg Am,* 88 Suppl 2**,** 52-7.

SHEN, F. H., SAMARTZIS, D. & ANDERSSON, G. B. 2006. Nonsurgical management of acute and chronic low back pain. *J Am Acad Orthop Surg,* 14**,** 477-87.

SINGH, K., MASUDA, K., THONAR, E. J., AN, H. S. & CS-SZABO, G. 2009. Age-related changes in the extracellular matrix of nucleus pulposus and anulus fibrosus of human intervertebral disc. *Spine (Phila Pa 1976),* 34**,** 10-6.

SITTE, I., KATHREIN, A., PFALLER, K., PEDROSS, F. & ROBERTS, S. 2009. Intervertebral disc cell death in the porcine and human injured cervical spine after trauma: a histological and ultrastructural study. *Spine (Phila Pa 1976),* 34**,** 131-40.

SIVAN, S. S., HAYES, A. J., WACHTEL, E., CATERSON, B., MERKHER, Y., MAROUDAS, A., BROWN, S. & ROBERTS, S. 2013. Biochemical composition and turnover of the extracellular matrix of the normal and degenerate intervertebral disc. *Eur Spine J,* 22**,** Epub ahead of print.

SIVE, J. I., BAIRD, P., JEZIORSK, M., WATKINS, A., HOYLAND, J. A. & FREEMONT, A. J. 2002. Expression of chondrocyte markers by cells of normal and degenerate intervertebral discs. *Mol Pathol,* 55**,** 91-7.

SMITH, L. J., NERURKAR, N. L., CHOI, K. S., HARFE, B. D. & ELLIOTT, D. M. 2011. Degeneration and regeneration of the intervertebral disc: lessons from development. *Dis Model Mech,* 4**,** 31-41.

SOBAJIMA, S., VADALA, G., SHIMER, A., KIM, J. S., GILBERTSON, L. G. & KANG, J. D. 2008. Feasibility of a stem cell therapy for intervertebral disc degeneration. *Spine J,* 8**,** 888-96.

SOUKANE, D. M., SHIRAZI-ADL, A. & URBAN, J. P. 2007. Computation of coupled diffusion of oxygen, glucose and lactic acid in an intervertebral disc. *J Biomech,* 40**,** 2645-54.

SOWA, G. A., COELHO, J. P., BELL, K. M., ZORN, A. S., VO, N. V., SMOLINSKI, P., NIYONKURU, C., HARTMAN, R., STUDER, R. K. & KANG, J. D. 2011. Alterations in gene expression in response to compression of nucleus pulposus cells. *Spine J,* 11**,** 36-43.

STAIRMAND, J. W., HOLM, S. & URBAN, J. P. 1991. Factors influencing oxygen concentration gradients in the intervertebral disc. A theoretical analysis. *Spine (Phila Pa 1976),* 16**,** 444-9.

STECK, E., BERTRAM, H., ABEL, R., CHEN, B., WINTER, A. & RICHTER, W. 2005. Induction of intervertebral disc-like cells from adult mesenchymal stem cells. *Stem Cells,* 23**,** 403-11.

STEPHAN, S., JOHNSON, W. E. & ROBERTS, S. 2011. The influence of nutrient supply and cell density on the growth and survival of intervertebral disc cells in 3D culture. *Eur Cell Mater,* 22**,** 97-108.

STOLZING, A., COLEMAN, N. & SCUTT, A. 2006. Glucose-induced replicative senescence in mesenchymal stem cells. *Rejuvenation Res,* 9**,** 31-5.

STOYANOV, J. V., GANTENBEIN-RITTER, B., BERTOLO, A., AEBLI, N., BAUR, M., ALINI, M. & GRAD, S. 2011. Role of hypoxia and growth and differentiation factor-5 on differentiation of human mesenchymal stem cells towards intervertebral nucleus pulposus-like cells. *Eur Cell Mater,* 21**,** 533-47.

STRASSBURG, S., HODSON, N. W., HILL, P. I., RICHARDSON, S. M. & HOYLAND, J. A. 2012. Bi-directional exchange of membrane components occurs during co-culture of mesenchymal stem cells and nucleus pulposus cells. *PLoS One,* 7**,** e33739.

STRASSBURG, S., RICHARDSON, S. M., FREEMONT, A. J. & HOYLAND, J. A. 2010. Co-culture induces mesenchymal stem cell differentiation and modulation of the degenerate human nucleus pulposus cell phenotype. *Regen Med,* 5**,** 701-11.

STUDER, R. K., ABOKA, A. M., GILBERTSON, L. G., GEORGESCU, H., SOWA, G., VO, N. & KANG, J. D. 2007. p38 MAPK inhibition in nucleus pulposus cells: a potential target for treating intervertebral disc degeneration. *Spine (Phila Pa 1976),* 32**,** 2827-33.

SUDO, H., YAMADA, K., IWASAKI, K., HIGASHI, H., ITO, M., MINAMI, A. & IWASAKI, N. 2013. Global identification of genes related to nutrient deficiency in intervertebral disc cells in an experimental nutrient deprivation model. *PLoS One,* 8**,** e58806.

SVANVIK, T., HENRIKSSON, H. B., KARLSSON, C., HAGMAN, M., LINDAHL, A. & BRISBY, H. 2010. Human disk cells from degenerated disks and mesenchymal stem cells in co-culture result in increased matrix production. *Cells Tissues Organs,* 191**,** 2-11.

SVASTOVA, E., HULIKOVA, A., RAFAJOVA, M., ZAT'OVICOVA, M., GIBADULINOVA, A., CASINI, A., CECCHI, A., SCOZZAFAVA, A., SUPURAN, C. T., PASTOREK, J. & PASTOREKOVA, S. 2004. Hypoxia activates the capacity of tumor-associated carbonic anhydrase IX to acidify extracellular pH. *FEBS Lett,* 577**,** 439-45.

SWIETACH, P., VAUGHAN-JONES, R. D. & HARRIS, A. L. 2007. Regulation of tumor pH and the role of carbonic anhydrase 9. *Cancer Metastasis Rev,* 26**,** 299-310.

SZTROLOVICS, R., ALINI, M., MORT, J. S. & ROUGHLEY, P. J. 1999. Age-related changes in fibromodulin and lumican in human intervertebral discs. *Spine (Phila Pa 1976),* 24**,** 1765-71.

SZTROLOVICS, R., ALINI, M., ROUGHLEY, P. J. & MORT, J. S. 1997. Aggrecan degradation in human intervertebral disc and articular cartilage. *Biochem J,* 326 (Pt 1)**,** 235-41.

TAKAHASHI, M., HARO, H., WAKABAYASHI, Y., KAWA-UCHI, T., KOMORI, H. & SHINOMIYA, K. 2001. The association of degeneration of the intervertebral disc with 5a/6a polymorphism in the promoter of the human matrix metalloproteinase-3 gene. *J Bone Joint Surg Br,* 83**,** 491-5.

TAKENO, K., KOBAYASHI, S., NEGORO, K., UCHIDA, K., MIYAZAKI, T., YAYAMA, T., SHIMADA, S. & BABA, H. 2007. Physical limitations to tissue engineering of intervertebral disc cells: effect of extracellular osmotic change on glycosaminoglycan production and cell metabolism. Laboratory investigation. *J Neurosurg Spine,* 7**,** 637-44.

TANG, Y. L., ZHAO, Q., QIN, X., SHEN, L., CHENG, L., GE, J. & PHILLIPS, M. I. 2005. Paracrine action enhances the effects of autologous mesenchymal stem cell transplantation on vascular regeneration in rat model of myocardial infarction. *Ann Thorac Surg,* 80**,** 229-36; discussion 236-7.

TAO, Y. Q., LIANG, C. Z., LI, H., ZHANG, Y. J., LI, F. C., CHEN, G. & CHEN, Q. X. 2013. Potential of co-culture of nucleus pulposus mesenchymal stem cells and nucleus pulposus cells in

hyperosmotic microenvironment for intervertebral disc regeneration. *Cell Biol Int,* 37**,** 826-34.

TAYLOR, I. W. & HODSON, P. J. 1984. Cell cycle regulation by environmental pH. *J Cell Physiol,* 121**,** 517-25.

TRIVANOVIC, D., KOCIC, J., MOJSILOVIC, S., KRSTIC, A., ILIC, V., DJORDJEVIC, I. O., SANTIBANEZ, J. F., JOVCIC, G., TERZIC, M. & BUGARSKI, D. 2013. Mesenchymal stem cells isolated from peripheral blood and umbilical cord Wharton's jelly. *Srp Arh Celok Lek,* 141**,** 178-86.

TROUT, J. J., BUCKWALTER, J. A. & MOORE, K. C. 1982. Ultrastructure of the human intervertebral disc: II. Cells of the nucleus pulposus. *Anat Rec,* 204**,** 307-14.

TUAN, R. S., BOLAND, G. & TULI, R. 2003. Adult mesenchymal stem cells and cell-based tissue engineering. *Arthritis Res Ther,* 5**,** 32-45.

UCHIYAMA, Y., CHENG, C. C., DANIELSON, K. G., MOCHIDA, J., ALBERT, T. J., SHAPIRO, I. M. & RISBUD, M. V. 2007. Expression of acid-sensing ion channel 3 (ASIC3) in nucleus pulposus cells of the intervertebral disc is regulated by p75NTR and ERK signaling. *J Bone Miner Res,* 22**,** 1996-2006.

UMEDA, M., KUSHIDA, T., SASAI, K., ASADA, T., OE, K., SAKAI, D., MOCHIDA, J., IKEHARA, S. & IIDA, H. 2009. Activation of rat nucleus pulposus cells by coculture with whole bone marrow cells collected by the perfusion method. *J Orthop Res,* 27**,** 222-8.

URBAN, J. P., HOLM, S., MAROUDAS, A. & NACHEMSON, A. 1977. Nutrition of the intervertebral disk. An in vivo study of solute transport. *Clin Orthop Relat Res***,** 101-14.

URBAN, J. P., HOLM, S., MAROUDAS, A. & NACHEMSON, A. 1982. Nutrition of the intervertebral disc: effect of fluid flow on solute transport. *Clin Orthop Relat Res***,** 296-302.

URBAN, J. P., SMITH, S. & FAIRBANK, J. C. 2004. Nutrition of the intervertebral disc. *Spine (Phila Pa 1976),* 29**,** 2700-9.

URBAN, M. R., FAIRBANK, J. C., ETHERINGTON, P. J., LOH, F. L., WINLOVE, C. P. & URBAN, J. P. 2001. Electrochemical measurement of transport into scoliotic intervertebral discs in vivo using nitrous oxide as a tracer. *Spine (Phila Pa 1976),* 26**,** 984-90.

VADALA, G., SOBAJIMA, S., LEE, J. Y., HUARD, J., DENARO, V., KANG, J. D. & GILBERTSON, L. G. 2008a. In vitro interaction between muscle-derived stem cells and nucleus pulposus cell. *Spine J,* 8**,** 804-9.

VADALA, G., STUDER, R. K., SOWA, G., SPIEZIA, F., IUCU, C., DENARO, V., GILBERTSON, L. G. & KANG, J. D. 2008b. Coculture of bone marrow mesenchymal stem cells and nucleus pulposus cells modulate gene expression profile without cell fusion. *Spine (Phila Pa 1976),* 33**,** 870-6.

VALORANI, M. G., MONTELATICI, E., GERMANI, A., BIDDLE, A., D'ALESSANDRO, D., STROLLO, R., PATRIZI, M. P., LAZZARI, L., NYE, E., OTTO, W. R., POZZILLI, P. & ALISON, M. R. 2012. Pre-culturing human adipose tissue mesenchymal stem cells under hypoxia increases their adipogenic and osteogenic differentiation potentials. *Cell Prolif,* 45**,** 225-38.

VAN DEN EERENBEEMT, K. D., OSTELO, R. W., VAN ROYEN, B. J., PEUL, W. C. & VAN TULDER, M. W. 2010. Total disc replacement surgery for symptomatic degenerative lumbar disc disease: a systematic review of the literature. *Eur Spine J,* 19**,** 1262-80.

VAN DER WERF, M., LEZUO, P., MAISSEN, O., VAN DONKELAAR, C. C. & ITO, K. 2007. Inhibition of vertebral endplate perfusion results in decreased intervertebral disc intranuclear diffusive transport. *J Anat,* 211**,** 769-74.

VARLOTTA, G. P., BROWN, M. D., KELSEY, J. L. & GOLDEN, A. L. 1991. Familial predisposition for herniation of a lumbar disc in patients who are less than twenty-one years old. *J Bone Joint Surg Am,* 73**,** 124-8.

VIDEMAN, T., LEPPAVUORI, J., KAPRIO, J., BATTIE, M. C., GIBBONS, L. E., PELTONEN, L. & KOSKENVUO, M. 1998. Intragenic polymorphisms of the vitamin D receptor gene associated with intervertebral disc degeneration. *Spine (Phila Pa 1976),* 23**,** 2477-85.

VIDEMAN, T., SAARELA, J., KAPRIO, J., NAKKI, A., LEVALAHTI, E., GILL, K., PELTONEN, L. & BATTIE, M. C. 2009. Associations of 25 structural, degradative, and inflammatory candidate genes with lumbar disc desiccation, bulging, and height narrowing. *Arthritis Rheum,* 60**,** 470-81.

VO, N. V., HARTMAN, R. A., YURUBE, T., JACOBS, L. J., SOWA, G. A. & KANG, J. D. 2013. Expression and regulation of metalloproteinases and their inhibitors in intervertebral disc aging and degeneration. *Spine J,* 13**,** 331-41.

WALLACH, C. J., KIM, J. S., SOBAJIMA, S., LATTERMANN, C., OXNER, W. M., MCFADDEN, K., ROBBINS, P. D., GILBERTSON, L. G. & KANG, J. D. 2006. Safety assessment of intradiscal gene transfer: a pilot study. *Spine J,* 6**,** 107-12.

WALLACH, C. J., SOBAJIMA, S., WATANABE, Y., KIM, J. S., GEORGESCU, H. I., ROBBINS, P., GILBERTSON, L. G. & KANG, J. D. 2003. Gene transfer of the catabolic inhibitor TIMP-1 increases measured proteoglycans in cells from degenerated human intervertebral discs. *Spine (Phila Pa 1976),* 28**,** 2331-7.

WALSH, A. J. & LOTZ, J. C. 2004. Biological response of the intervertebral disc to dynamic loading. *J Biomech,* 37**,** 329-37.

WATANABE, K., MOCHIDA, J., NOMURA, T., OKUMA, M., SAKABE, K. & SEIKI, K. 2003. Effect of reinsertion of activated nucleus pulposus on disc degeneration: an experimental study on various types of collagen in degenerative discs. *Connect Tissue Res,* 44**,** 104-8.

WATANABE, T., SAKAI, D., YAMAMOTO, Y., IWASHINA, T., SERIGANO, K., TAMURA, F. & MOCHIDA, J. 2010. Human nucleus pulposus cells significantly enhanced biological properties in a coculture system with direct cell-to-cell contact with autologous mesenchymal stem cells. *J Orthop Res,* 28**,** 623-30.

WEI, A., TAO, H., CHUNG, S. A., BRISBY, H., MA, D. D. & DIWAN, A. D. 2009. The fate of transplanted xenogeneic bone marrow-derived stem cells in rat intervertebral discs. *J Orthop Res,* 27**,** 374-9.

WEILER, C., NERLICH, A. G., BACHMEIER, B. E. & BOOS, N. 2005. Expression and distribution of tumor necrosis factor alpha in human lumbar intervertebral discs: a study in surgical specimen and autopsy controls. *Spine (Phila Pa 1976),* 30**,** 44-53; discussion 54.

WEILER, C., NERLICH, A. G., SCHAAF, R., BACHMEIER, B. E., WUERTZ, K. & BOOS, N. 2010. Immunohistochemical identification of notochordal markers in cells in the aging human lumbar intervertebral disc. *Eur Spine J,* 19**,** 1761-70.

WIBERG, C., HEINEGARD, D., WENGLEN, C., TIMPL, R. & MORGELIN, M. 2002. Biglycan organizes collagen VI into hexagonal-like networks resembling tissue structures. *J Biol Chem,* 277**,** 49120-6.

WOJTKOWIAK, J. W., ROTHBERG, J. M., KUMAR, V., SCHRAMM, K. J., HALLER, E., PROEMSEY, J. B., LLOYD, M. C., SLOANE, B. F. & GILLIES, R. J. 2012. Chronic autophagy is a cellular adaptation to tumor acidic pH microenvironments. *Cancer Res,* 72**,** 3938-47.

WONG, M. L. & MEDRANO, J. F. 2005. Real-time PCR for mRNA quantitation. *Biotechniques,* 39**,** 75-85.

WU, L., PRINS, H. J., HELDER, M. N., VAN BLITTERSWIJK, C. A. & KARPERIEN, M. 2012. Trophic effects of mesenchymal stem cells in chondrocyte co-cultures are independent of culture conditions and cell sources. *Tissue Eng Part A,* 18**,** 1542-51.

WU, Y. J., LA PIERRE, D. P., WU, J., YEE, A. J. & YANG, B. B. 2005. The interaction of versican with its binding partners. *Cell Res,* 15**,** 483-94.

WUERTZ, K., GODBURN, K. & IATRIDIS, J. C. 2009a. MSC response to pH levels found in degenerating intervertebral discs. *Biochem Biophys Res Commun,* 379**,** 824-9.

WUERTZ, K., GODBURN, K., MACLEAN, J. J., BARBIR, A., DONNELLY, J. S., ROUGHLEY, P. J., ALINI, M. & IATRIDIS, J. C. 2009b. In vivo remodeling of intervertebral discs in response to short- and long-term dynamic compression. *J Orthop Res,* 27**,** 1235-42.

WUERTZ, K., GODBURN, K., NEIDLINGER-WILKE, C., URBAN, J. & IATRIDIS, J. C. 2008. Behavior of mesenchymal stem cells in the chemical microenvironment of the intervertebral disc. *Spine (Phila Pa 1976),* 33**,** 1843-9.

WUERTZ, K., URBAN, J. P., KLASEN, J., IGNATIUS, A., WILKE, H. J., CLAES, L. & NEIDLINGER-WILKE, C. 2007. Influence of extracellular osmolarity and mechanical stimulation on gene expression of intervertebral disc cells. *J Orthop Res,* 25**,** 1513-22.

YAMAMOTO, Y., MOCHIDA, J., SAKAI, D., NAKAI, T., NISHIMURA, K., KAWADA, H. & HOTTA, T. 2004. Upregulation of the viability of nucleus pulposus cells by bone marrow-derived stromal cells: significance of direct cell-to-cell contact in coculture system. *Spine (Phila Pa 1976),* 29**,** 1508-14.

YANG, F., LEUNG, V. Y., LUK, K. D., CHAN, D. & CHEUNG, K. M. 2009. Mesenchymal stem cells arrest intervertebral disc degeneration through chondrocytic differentiation and stimulation of endogenous cells. *Mol Ther,* 17**,** 1959-66.

YANG, H., WU, J., LIU, J., EBRAHEIM, M., CASTILLO, S., LIU, X., TANG, T. & EBRAHEIM, N. A. 2010. Transplanted mesenchymal stem cells with pure fibrinous gelatin-transforming growth factor-beta1 decrease rabbit intervertebral disc degeneration. *Spine J,* 10**,** 802-10.

YANG, S. H., HU, M. H., SUN, Y. H. & LIN, F. H. 2013. Differential phenotypic behaviors of human degenerative nucleus pulposus cells under normoxic and hypoxic conditions: influence of oxygen concentration during isolation, expansion, and cultivation. *Spine J,,* 13**,** Epub ahead of print.

YANG, S. H., WU, C. C., SHIH, T. T., SUN, Y. H. & LIN, F. H. 2008. In vitro study on interaction between human pulposus cells and mesenchymal stem cells through paracrine stimulation. *Spine (Phila Pa 1976),* 33**,** 1951-7.

YUAN, M., LEONG, K. W. & CHAN, B. P. 2011. Three-dimensional culture of rabbit nucleus pulposus cells in collagen microspheres. *Spine J,* 11**,** 947-60.

YURUBE, T., TAKADA, T., HIRATA, H., KAKUTANI, K., MAENO, K., ZHANG, Z., YAMAMOTO, J., DOITA, M., KUROSAKA, M. & NISHIDA, K. 2011. Modified house-keeping gene expression in a rat tail compression loading-induced disc degeneration model. *J Orthop Res,* 29**,** 1284-90.

ZHANG, L., NIU, T., YANG, S. Y., LU, Z. & CHEN, B. 2008. The occurrence and regional distribution of DR4 on herniated disc cells: a potential apoptosis pathway in lumbar intervertebral disc. *Spine (Phila Pa 1976),* 33**,** 422-7.

ZHANG, R., RUAN, D. & ZHANG, C. 2006a. Effects of TGF-beta1 and IGF-1 on proliferation of human nucleus pulposus cells in medium with different serum concentrations. *J Orthop Surg Res,* 1**,** 9.

ZHANG, Y., AN, H. S., THONAR, E. J., CHUBINSKAYA, S., HE, T. C. & PHILLIPS, F. M. 2006b. Comparative effects of bone morphogenetic proteins and sox9 overexpression on extracellular matrix metabolism of bovine nucleus pulposus cells. *Spine (Phila Pa 1976),* 31**,** 2173-9.

ZHANG, Y., CHEE, A., THONAR, E. J. & AN, H. S. 2011. Intervertebral disk repair by protein, gene, or cell injection: a framework for rehabilitation-focused biologics in the spine. *Pm r,* 3**,** S88-94.

ZHANG, Y. G., GUO, X., XU, P., KANG, L. L. & LI, J. 2005. Bone mesenchymal stem cells transplanted into rabbit intervertebral discs can increase proteoglycans. *Clin Orthop Relat Res***,** 219-26.

ZHANG, Y. G., SUN, Z. M., LIU, J. T., WANG, S. J., REN, F. L. & GUO, X. 2009. Features of intervertebral disc degeneration in rat's aging process. *J Zhejiang Univ Sci B,* 10**,** 522-7.

ZHAO, C. Q., WANG, L. M., JIANG, L. S. & DAI, L. Y. 2007. The cell biology of intervertebral disc aging and degeneration. *Ageing Res Rev,* 6**,** 247-61.

ZONG, Z., LI, N., RAN, X., SU, Y., SHEN, Y., SHI, C. M. & CHENG, T. M. 2012. Isolation and characterization of two kinds of stem cells from the same human skin back sample with therapeutic potential in spinal cord injury. *PLoS One,* 7**,** e50222.